قطب علمی مهندسی معدن برگزار می کند:

کارگاه آموزشی رویکردهای طراحی مهندسی سنگ و چالش‌ها در فضاهای زیرزمینی عمیق

(با رویکرد خاص به معادن زیرزمینی عمیق)

Rock Engineering Design Approaches and challenges in Deep Hard Rock Mining Engineering"

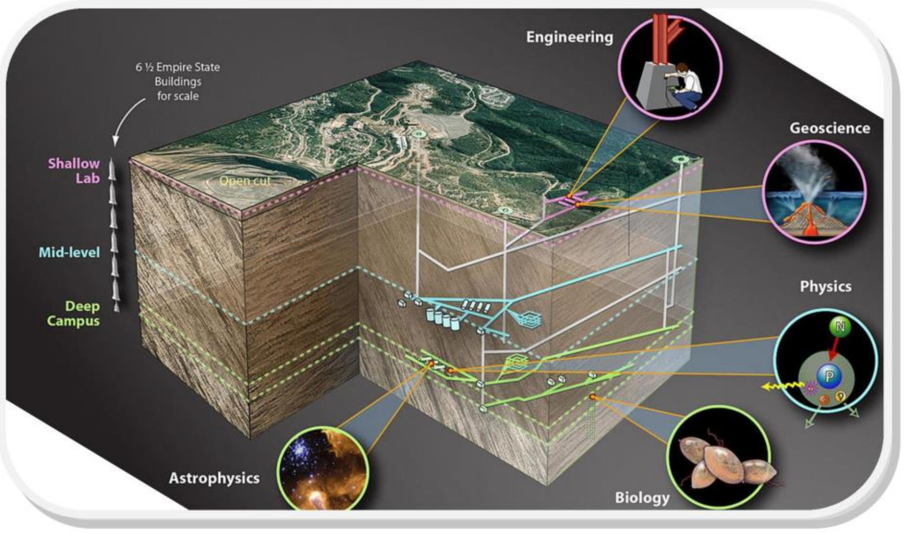

هدف از برگزاری این کارگاه آموزشی بحث و تبادل نظر در خصوص چالش‌های ژئومکانیکی در فضاهای زیرزمینی عمیق (بویژه معادن با اعماق بسیار زیاد) با ارائه نتایج و دستاوردهای روز دنیا است. چالش‌های متعدد در خصوص نحوه تعیین پارامترهای معرف توده‌سنگ و نحوه تعامل با عدم قطعیت های مهندسی زمین با رویکرد کارآیی طراحی در این کارگاه آموزشی بحث شده و نهایتاً تجارب مختلفی از سرتاسر جهان ارائه خواهد شد.

Main Topics:

Introduction to Rock Mechanics application in deep underground Mining
Challenges in determining reliable design input parameters
Comprehension of ground behaviour and selection of suitable design strategy
Support system, reinforcement and stabilisation design and verification
Real time monitoring (conventional–seismic) and design update (forensic study)
Case studies from Australia, China, Iran and South America,…
Concluding remarks, discussion and future prospects.

یکشنبه
۲۴آذر ۱۳۹۸
۸:۳۰ الی ۱۶:۳۰

دانشگاه صنعتی شاهرود
دانشکده مهندسی معدن، نفت و ژئوفیزیک
سالن آمفی تئاتر دانشکده (طبقه سوم)

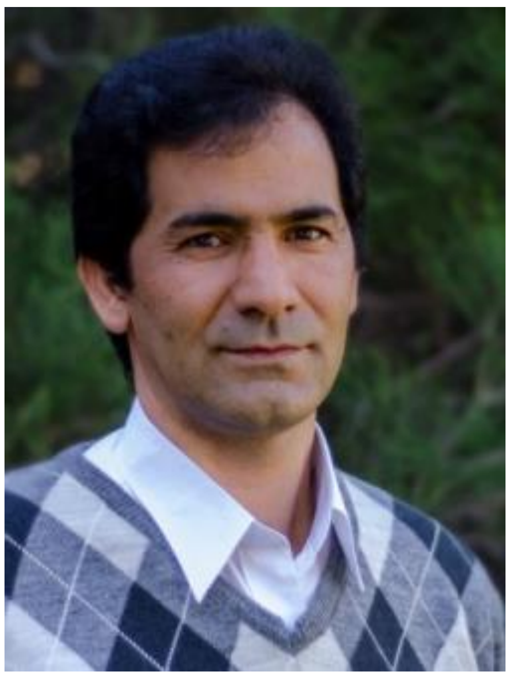

Summery:
The rapid-growing trend of resource extraction in the world, results in increases depth of underground mines. Eventually deep underground mines will face an increasing magnitude of stress, temperature, water pressure and seismicity. On the other hand, geoengineering deals with huge uncertainty in geomaterial properties, in-situ stresses, testing, and modelling, which leads to great challenges in design. Knowledge of ground, mine and operational factors and their variability leads the designer to better estimation of geomechanical behaviour and safe design optimisation. This workshop is designed to develop audience knowledge in geomechanical design of deep underground hard rock mines, which will enhance their competencies and prepares them for better and more effective contributions in their future career. This is designed to introduce from basic to advanced topics of geomechanical design aspects on deep underground mine excavation. Attendees from mining, civil and engineering geology or other related fields and professionals who work on this area would also benefit from this course.

Mostafa Sharifzadeh
Western Australian School of Mine (WASM)
Curtin University, Perth, Australia

سخنران: جناب آقای دکتر مصطفی شریف‌زاده
(استاد دانشگاه کرتین استرالیا)

Shahrood University of Technology

Curtin University

Introduction to Rock Mechanics application in deep underground Mining,

Mostafa Sharifzadeh
Western Australian School of Mines (WASM)

1

PRESENTATION OUTLINE

1. Introduction
2. Underground mine design procedure
3. Application of rock mechanics in underground mining
4. Concluding summary

2

Mining Status in Goldfields – Western Australia

3

Mining Status in Goldfields – Western Australia

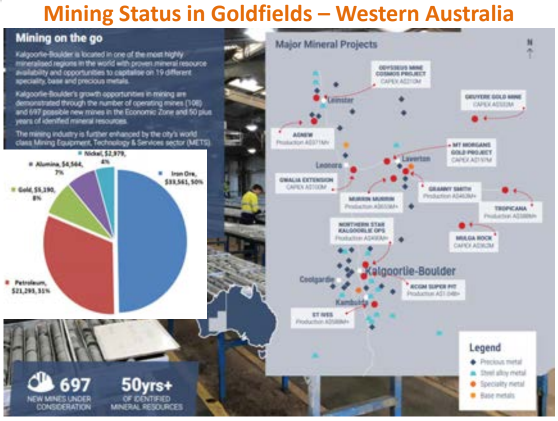

4

Gwalia Underground Gold Mine in Western Australia

5

Design procedure : Components and logic of a rock mechanics programme for mining engineering design.

Site characterisation
definition of hydromechanical properties of the host rock mass for mining

Mine model formulation
conceptualisation of site characterisation data

Design analysis
selection and application of mathematical and computational schemes for study of various mining layouts and strategies

Rock performance monitoring
measurement of the operational response to mining of the host rock mass

Retrospective analysis
quantification of *in-situ* rock mass properties, and identification of dominant modes of response of mine structure

Brady & Brown, 2004

6

Simplified geotechnical Design methodology for deep underground mine excavation

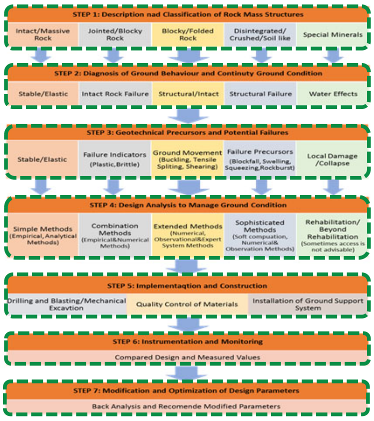

Rahimi, Sharifzadeh, Feng, 2019

7

7

Rock Engineering Design Approaches and challenges in Deep Hard Rock Mining Engineering – Dec. 15th, 2019 – Shahrood UT

Interaction between technical groups involved in mine engineering.

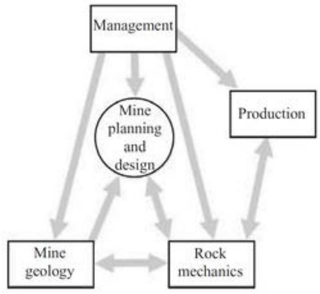

Brady & Brown, 2004

8

8

Rock Engineering Design Approaches and challenges in Deep Hard Rock Mining Engineering – Dec. 15th, 2019 – Shahrood UT

Definition of geomechanics

Geomechanics discusses about the **earth crust mechanics** which is mostly formed from **soil, rock** and affected by **structural forces and tectonics**.

Since most engineering activities take place in earth crust, **geomechanics** help us to study their **in situ condition** and predict its **behaviour under the new condition.**

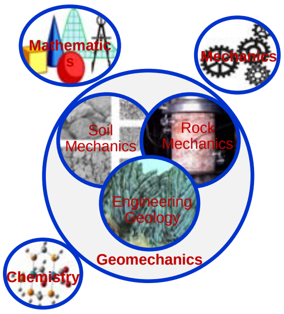

9

9

Rock Engineering Design Approaches and challenges in Deep Hard Rock Mining Engineering – Dec. 15th, 2019 – Shahrood UT

Figure (a) Pre-mining conditions around an orebody, and (b) mechanical consequences of mining excavations in the orebody.

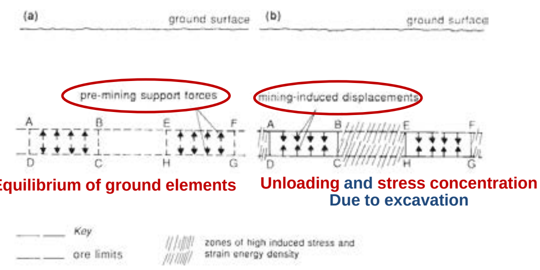

Adapted from Brady and Brown, 2004

10

10

Rock Engineering Design Approaches and challenges in Deep Hard Rock Mining Engineering – Dec. 15th, 2019 – Shahrood UT

Application of rock mechanics in underground Mining

- **Shaft, pillar, draft and stope design;**
- **Drilling and blasting; fragmentation;**
- **Cavability of rock and ore; improvement of rockbursts; mechanized excavation; in situ recovery.**

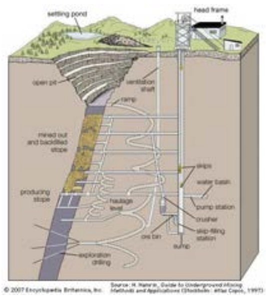

11

11

Rock Engineering Design Approaches and challenges in Deep Hard Rock Mining Engineering – Dec. 15th, 2019 – Shahrood UT

Common Mining Practice in Western Australia

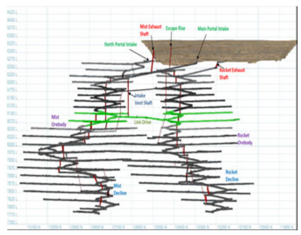

Frog's Leg Gold Mine, operated by Evolution Mining Western Australia (600m)

world largest open pit gold mine (Super pit) in WA

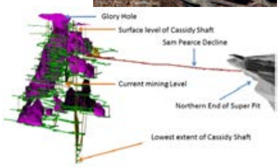

Underground Operations – Mt Charlotte shaft – KCGM – Western Australia (1200m)

12

12

Common Mining Practice in Western Australia

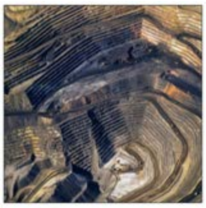

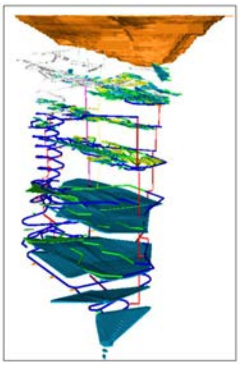

13

13

Rock Engineering Design Approaches and challenges in Deep Hard Rock Mining Engineering – Dec. 15th, 2019 – Shahrood UT

Common Rock Mechanics Objectives In Mining Structure:

1, Ensure The Overall Stability Of The whole Mine Structure,

2, Protect The Major Service Openings in Duty Life time,

3, Provide Secure Access To Safe Working Places,

4, Preserve The Mineable Condition Of Unmined Ore Reserves.

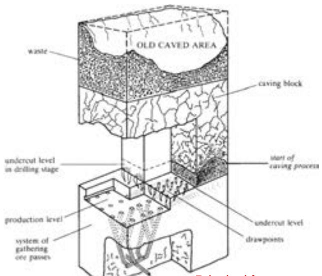

Principal features of caving operation

Adapted from Brady and Brown, 2004

14

14

Rock Engineering Design Approaches and challenges in Deep Hard Rock Mining Engineering – Dec. 15th, 2019 – Shahrood UT

Examples of rock mechanics applications

Underground opening:

Shaft and/or decline stability analysis and design

Adapted from MEA course materials

15

15

Rock Engineering Design Approaches and challenges in Deep Hard Rock Mining Engineering – Dec. 15th, 2019 – Shahrood UT

Examples of rock mechanics applications

- Stope design
- Stope Span Design
- Stoping sequence design
- Support system design

Adapted from MEA course materials

16

16

Rock Engineering Design Approaches and challenges in Deep Hard Rock Mining Engineering – Dec. 15th, 2019 – Shahrood UT

Examples of rock mechanics applications

- Rock reinforcement and support design

Adapted from MEA course materials 17

17

Rock Engineering Design Approaches and challenges in Deep Hard Rock Mining Engineering – Dec. 15th, 2019 – Shahrood UT

Examples of consequences of poor rock mechanics design

- Collapse of rock in underground excavation

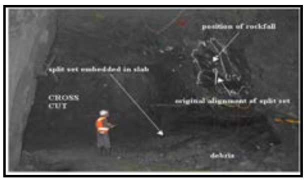

Adapted from MEA course materials

18

18

Examples of rock mechanics applications

- Foundations
- Room and pillar mine design
- Longwall mine design

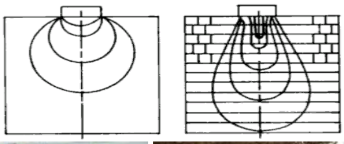

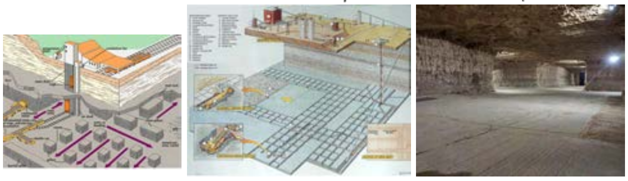

19

Blast hole and firing pattern for optimum fragmentation and less dilution

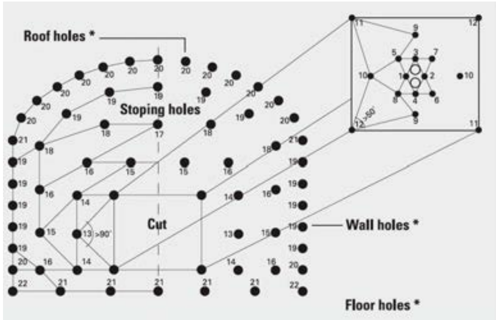

20

Examples of underground mining in Western Australia

Underground Operations – Mt Charlotte shaft – KCGM – Western Australia

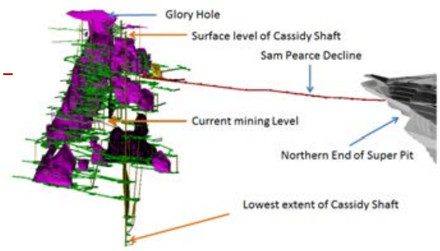

21

Examples of underground mining in Western Australia

Underground excavation – Decline-shaft network – Mt Charlotte shaft – KCGM – Western Australia

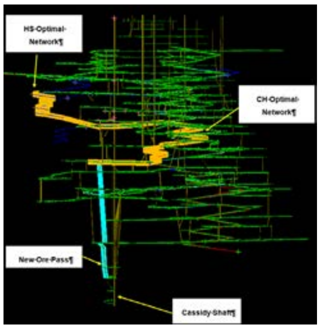

22

Examples of underground mining in Western Australia
Murchison Underground Mines – Western Australia

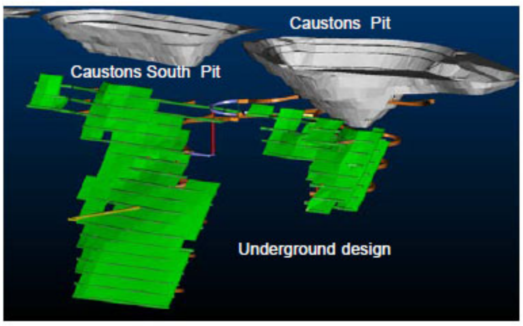

23

Examples of underground mining in Western Australia

Agnico Eagle's Suurikuusiko gold mining project showing both surface and underground mining.

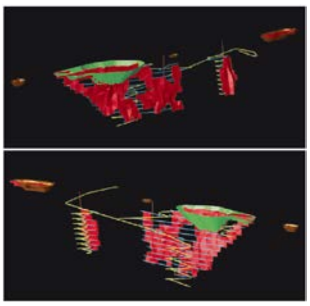

24

Rock Engineering Design Approaches and challenges in Deep Hard Rock Mining Engineering – Dec. 15th, 2019 – Shahrood UT

Examples of underground mining in Western Australia

Frog's Leg Gold Mine, owned and operated by Evolution Mining makes use of underground mining techniques. The mine is located 20 km West of Kalgoorlie. Two declines access the Rocket (Southern) and Mist (Northern) ore lodes. Current capital development is about 530 m below surface elevation.

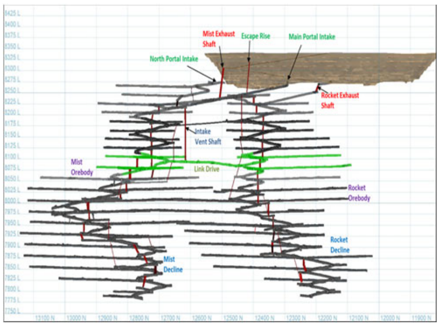

25

25

Rock Engineering Design Approaches and challenges in Deep Hard Rock Mining Engineering – Dec. 15th, 2019 – Shahrood UT

Introduction – Mining at depth

Conditions often become difficult beyond a 1000m or so

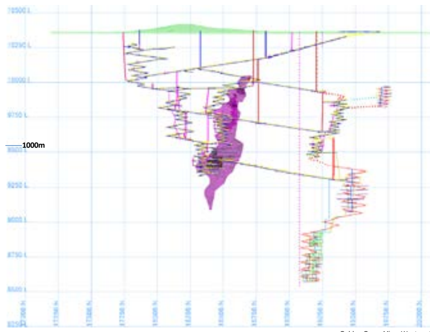

Golden Grove Mine, Western Australia (Thompson, 2011)

26

26

Rock Engineering Design Approaches and challenges in Deep Hard Rock Mining Engineering – Dec. 15th, 2019 – Shahrood UT

Maximum recovery – minimal dilution

Continuous extraction sequence required to avoid pillars

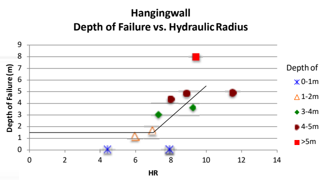

Golden Grove Mine, Western Australia (Thompson, 2011)

27

27

Rock Engineering Design Approaches and challenges in Deep Hard Rock Mining Engineering – Dec. 15th, 2019 – Shahrood UT

Geotechnical monitoring requirements

A need to understand the overall failure process and instability

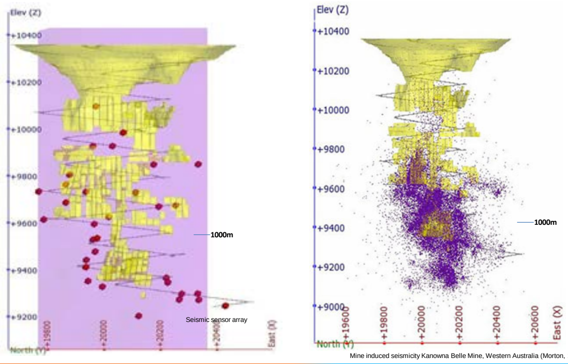

Mine induced seismicity Kanowna Belle Mine, Western Australia (Morton, 2013)

28

28

Rock Engineering Design Approaches and challenges in Deep Hard Rock Mining Engineering – Dec. 15th, 2019 – Shahrood UT

Large scale geological structures (discontinuities)

The global stability may be controlled by large scale structures and the structures may become seismically active or seismic source

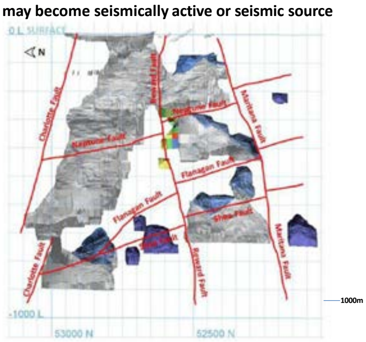

Mount Charlotte Mine, Western Australia (Corskie, 2013)

29

29

Rock Engineering Design Approaches and challenges in Deep Hard Rock Mining Engineering – Dec. 15th, 2019 – Shahrood UT

Seismic response of large scale structures

The structures may become seismically active

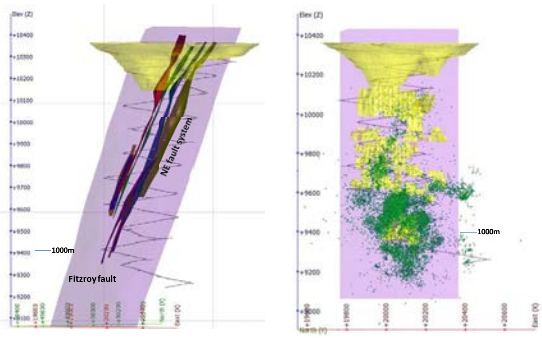

Kanowna Belle Mine, Western Australia (Morton, 2013)

30

30

In-situ stress measurements- a key requirement

Acoustic Emission from oriented core samples –
No access required – only deep core

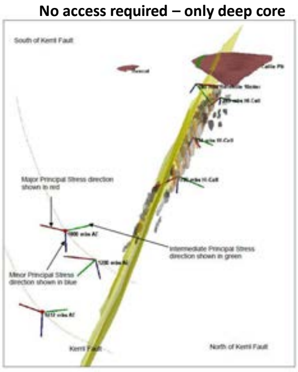

Callie Mine, NT Australia (Graf, 2013)

31

31

Joint condition determination

From development exposure and diamond drilled core

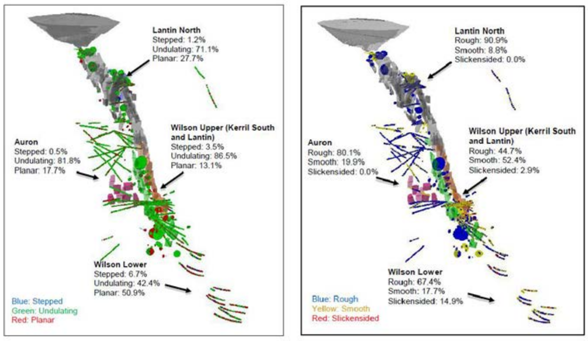

Callie Mine, NT Australia (Graf, 2013)

32

32

Primary and secondary stope extraction sequence for a shallow plunging orebody.

P1, primary stope

cemented fill;

S1, secondary stope

unconsolidated fill.

The numbers show the

sequence of stope

extraction.

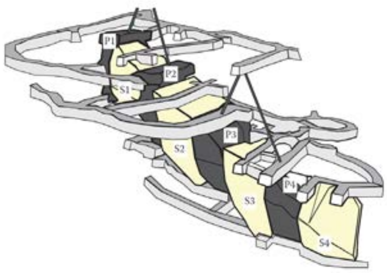

Villaescusa, 2014

33

33

Stoping sequence

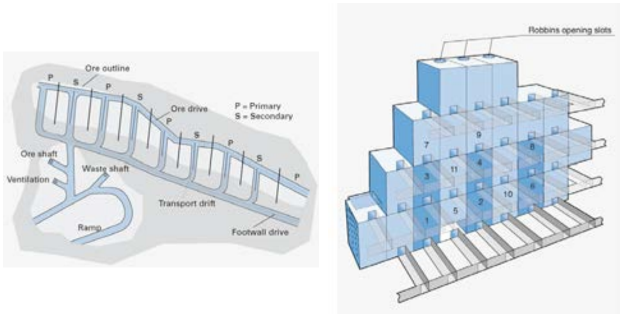

34

34

Longitudinal view of a top-down extraction sequence, permanent pillars, and retreat to a central crosscut

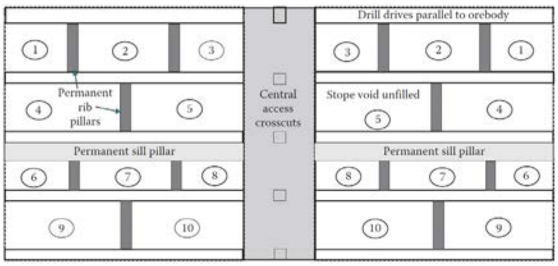

Villaescusa, 2014 35

35

Longitudinal view of Kanowna Belle Mine—Stoping Block A

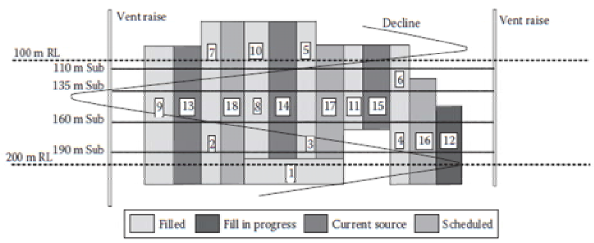

Villaescusa, 2014 36

36

What we deliver in Geomechanical design

- Understanding of earth structure, and associated Hazards,
- Understanding of the nature of mining engineering activity and its disturbance level,
- Risks associated with earth-engineering activities composition (Diagnosis mechanisms and problems),
- Selecting right tools to solve the problem (Design),
- Implement the design and monitor the effectiveness,
- Retrospective analysis and design update.

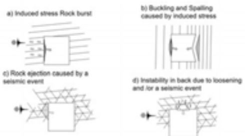

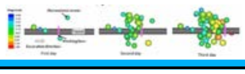

37

37

Table 4 : Typical problems, critical parameters, methods of analysis and acceptability criteria for underground hard rock mining excavations.

STRUCTURE	TYPICAL PROBLEMS	CRITICAL PARAMETERS	ANALYSIS METHODS	ACCEPTABILITY CRITERIA
Pillars.	Progressive spalling and slabbing of the rock mass leading to eventual pillar collapse or rockbursting.	• Strength of the rock mass forming the pillars. • Presence of unfavourably oriented structural features. • Pillar geometry, particularly width to height ratio. • Overall mine geometry including extraction ratio.	For horizontally bedded deposits, pillar strength from empirical relationships based upon width to height ratios and average pillar stress based on tributary area calculations are compared to give a factor of safety. For more complex mining geometry, numerical analyses including progressive pillar failure may be required.	Factor of safety for simple pillar layouts in horizontally bedded deposits should exceed 1.6 for "permanent" pillars. In cases where progressive failure of complex pillar layouts is modelled, individual pillar failures can be tolerated provided that they do not initiate "domino" failure of adjacent pillars.
Crown pillars.	Caving of surface crown pillars for which the ratio of pillar depth to stope span is inadequate. Rockbursting or gradual spalling of overstressed internal crown pillars.	• Strength of the rock mass forming the pillars. • Depth of weathering and presence of steeply dipping structural features in the case of surface crown pillars. • In situ stress levels and geometry of internal crown pillars.	Rock mass classification and limit equilibrium analyses can give useful guidance on surface crown pillar dimensions for different rock masses. Numerical analyses, including discrete element studies, can give approximate stress levels and indications of zones of potential failure.	Surface crown pillar depth to span ratio should be large enough to ensure very low probability of failure. Internal crown pillars may require extensive support to ensure stability during mining of adjacent stopes. Careful planning of mining sequence may be necessary to avoid high stress levels and rockburst problems.
Cut and fill stopes.	Falls of structurally defined wedges and blocks from stope backs and hanging walls. Stress induced failures and rockbursting in high stress environments.	• Orientation, inclination and shear strength of structural features in the rock mass. • In situ stresses in the rock mass. • Shape and orientation of stope. • Quality, placement and drainage of fill.	Numerical analyses of stresses and displacements for each excavation stage will give some indication of potential problems. Some of the more sophisticated numerical models will permit inclusion of the support provided by fill or the reinforcement of the rock by means of grouted cables.	Local instability should be controlled by the installation of rockbolts or grouted cables to improve safety and to minimize dilution. Overall stability is controlled by the geometry and excavation sequence of the stopes and the quality and sequence of filling. Acceptable mining conditions are achieved when all the ore is recovered safely.
Non-entry stopes.	Ore dilution resulting from rockfalls from stope back and walls. Rockbursting or progressive failure induced by high stresses in pillars between stopes.	• Quality and strength of the rock. • In situ and induced stresses in the rock surrounding the excavations. • Quality of drilling and blasting in excavation of the stope.	Some empirical rules, based on rock mass classification, are available for estimating safe stope dimensions. Numerical analyses of stope layout and mining sequence, using three-dimensional analyses for complex orebody shapes, will provide indications of potential problems and estimates of support requirements.	A design of this type can be considered acceptable when safe and low cost recovery of a large proportion of the orebody has been achieved. Rockfalls in shafts and haulages are an unacceptable safety hazard and pattern support may be required. In high stress environments, local destressing may be used to reduce rockbursting.
Drawpoints and orepasses.	Local rock mass failure resulting from abrasion and wear of poorly supported drawpoints or orepasses. In extreme cases this may lead to loss of stopes or orepasses.	• Quality and strength of the rock. • In situ and induced stresses and stress changes in the rock surrounding the excavations. • Selection and installation sequence of support.	Limit equilibrium or numerical analyses are not particularly useful since the processes of wear and abrasion are not included in these models. Empirical designs based upon previous experience or trial and error methods are generally used.	The shape of the opening should be maintained for the design life of the drawpoint or orepass. Loss of control can result in serious dilution of the ore or abandonment of the excavation. Wear resistant flexible reinforcement such as grouted cables, installed during excavation of the opening, may be successful in controlling instability.

38

38

Scope of rock mechanics application in Underground

Site characterisation
definition of hydromechanical properties of the host rock mass for mining

Mine model formulation
conceptualisation of site characterisation data

Design analysis
selection and application of mathematical and computational schemes for study of various mining layouts and strategies

Rock performance monitoring
measurement of the operational response to mining of the host rock mass

Retrospective analysis
quantification of *in-situ* rock mass properties, and identification of dominant modes of response of mine structure

Brady & Brown, 2004

39

39

Rock Mechanics Application in Mining

– **Development layouts**
– **Support types & sequencing**
– **Mining sequence**
– **Mine Planning**

40

40

Recommended References:

- Hudson, J A and Harrison, J P (1997). Engineering Rock Mechanics, An Introduction to the Principles, Pergamon, Elsevier S41cience, UK. ISBN 0-080-419-12-7. http://lib.myilibrary.com.dbgw.lis.curtin.edu.au/Open.aspx?id=105874
- Das, Braja M, Advanced Soil Mechanics, 3rd ed Hoboken: Taylor and Francis 2007. ISBN: 9780415420266. http://www.curtin.eblib.com.au.dbgw.lis.curtin.edu.au/patron/FullRecord.aspx?p=325531
- B H G Brady and E T Brown, (2004) *Rock Mechanics for Underground Mining (3rd Ed.)*, Springer, Netherlands. ISBN 10-1-4020-2064-3 (PB). http://web.a.ebscohost.com.dbgw.lis.curtin.edu.au/ehost/detail?sid=3e8b1a97-d8da-476c-97db-f6997cbfa378%40sessionmgr4005&vid=1&hid=4109&bdata=JnNpdGU9ZWhvc3QtbGl2ZQ%3d%3d#db=nlebk&AN=135236
- Zhang, Lianyang, (2005) Engineering Properties of Rocks, Elsevier, app.knovel.com/web/toc.v/cid:kpEPR00001/viewerType:toc/root_ slug:engineering-properties/url_slug:engineering-properties/?2005
- Hoek, Evert, Practical Rock Engineering, available from http://www.rocscience.com/education/hoeks_corner
- The ISRM Suggested Methods for Rock Characterization, Testing and Monitoring: 2007–2014, Editor R. Ulusay, P.292. Springer International Publishing Switzerland 2015, ISBN 978-3-319-07712-3.
- Villaescusa, Ernesto, (2014). Geotechnical Design for Sublevel Open Stoping, CRC Press, ISBN:9781482211887. http://link.library.curtin.edu.au/p?cur_aleph001151473

41

41

End of presentation
Any questions ?

42

42

Challenges in Determining Reliable Design Input Parameters

Mostafa Sharifzadeh
Western Australian School of Mines (WASM)

Shahrood University of Technology

Curtin University

1

Presentation layout

1. Introduction
2. Variability in rock type and rock mass structure
3. Effect of scale in rock behaviour
4. Estimation of rock mass properties using statistical analysis
5. Estimation of in-situ stresses
6. Summary

2

Presentation layout

1. **Introduction**
2. Variability in rock type and rock mass structure
3. Effect of scale in rock behaviour
4. Estimation of rock mass properties using statistical analysis
5. Estimation of in-situ stresses
6. Summary

3

Engineering Activities In Earth Crust

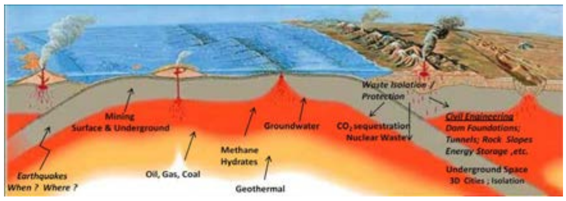

- **Deepest borehole is 12 km. Deepest mine is 4 km.**
- **Rock temperature increases approx. 25̊ C/km depth.**
- **Vertical rock pressure σv increases ~ 27MPa/km.**
- **Horizontal pressure σh~ (0.5-3) σv.**

Magma, heat convection, tectonic movement controls the overall earth structure.

Modified after NEU, 2010

4

Presentation layout

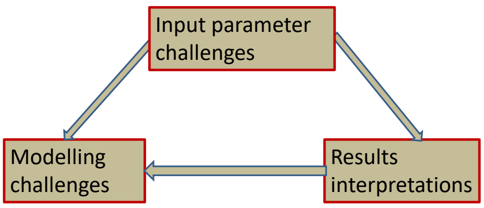

- **Input Data Challenges of Rock Engineering**
- **Rock Strength**
- **Analysis of Data and Estimation of Parameters**
- **The reliability of results must be verified by judgement and experience**

5

Presentation layout

1. Introduction
2. **Variability in rock type and rock mass structure**
3. Effect of scale in rock behaviour
4. Estimation of rock mass properties using statistical analysis
5. Estimation of in-situ stresses
6. Summary

6

Introduction - How rock forms

- Recall: Atom, molecule, cell, crystal, lattice
- Minerals are building blocks of rocks.
- Mineral combines to each other to form a rock
- Crystal formation is slow and it needs geological time.
- Crystals size and shape depend on temperature, and pressure of the medium(room).

7

7

MICRO-SCALE ROCK STRUCTURE

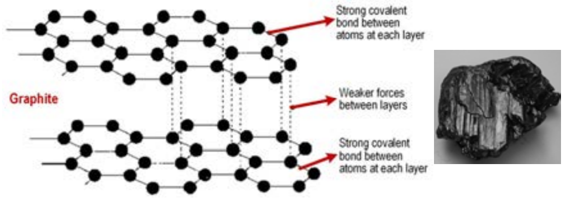

Two dimensional covalent network bonding structure with weak Van Der Waals bonds between layers in foliated rocks (example of Graphite).

Sharifzadeh et al., 2017 8

8

Atomic Bonding Structure and SEM Image of Three Typical Rocks

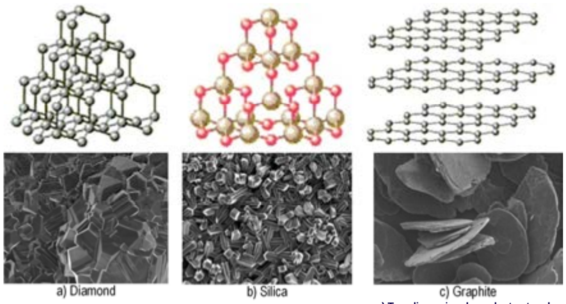

a) Three-dimensional covalent network homogenous bonding structure in Diamond

b) Three-dimensional covalent network heterogeneous bonding structure in Silica

c) Two dimensional covalent network bonding structure with weak Van Der Waals bonds between layers in Graphite

Sharifzadeh et al., 2017 9

9

Rock Micro-Structural Deficiencies:

- Atomic disorder and dislocations in pure and homogenous rocks,
- Crystal lattice boundaries in crystalline and foliated rocks due to two dimensional covalent network,
- Heterogeneity (adjacency of weak and strong particles),
- Pore spaces during generation mainly due to gas escape in volcanic rocks,
- Cleavages due to overtime deformation and residual stresses,
- Micro-crack or structural defects due to stresses.

10

10

Weakness planes at different rock types

- Crystals or small particles forms the soil and rocks and forms the earth crust.
- Weakness plane in materials and applied forces from the ground caused the separation in rocks and forming plates (Continents). The plate tectonic cause to movement and deformation of plates and producing geological structures such as faulting and folding.
- In geo-engineering design it is necessary to consider the effect of soil and rock material type and geological structures on project performance.

11

11

The main variables/features influencing rock properties and behaviour

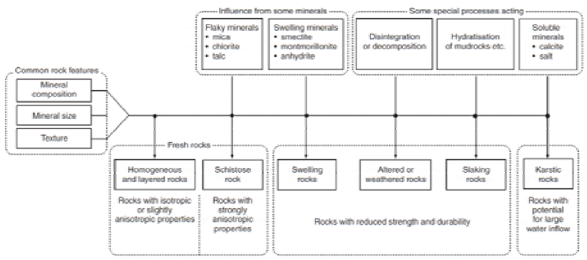

Rock engineering, Palmstrom&Stille, 2010 12

12

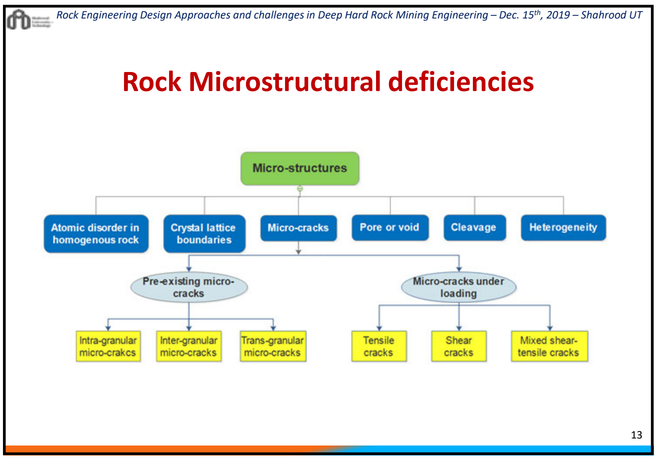

13

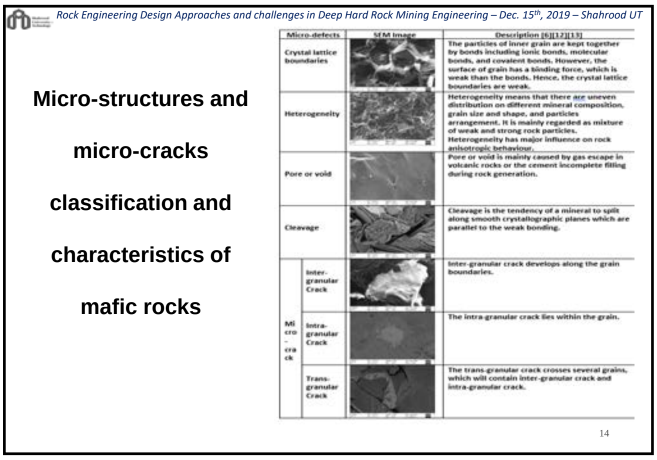

14

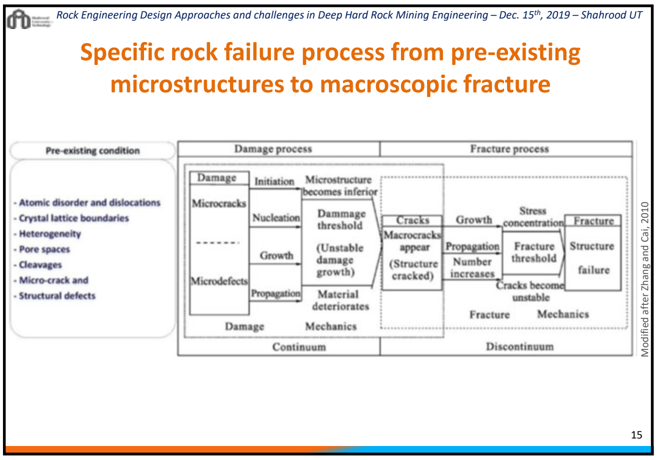

15

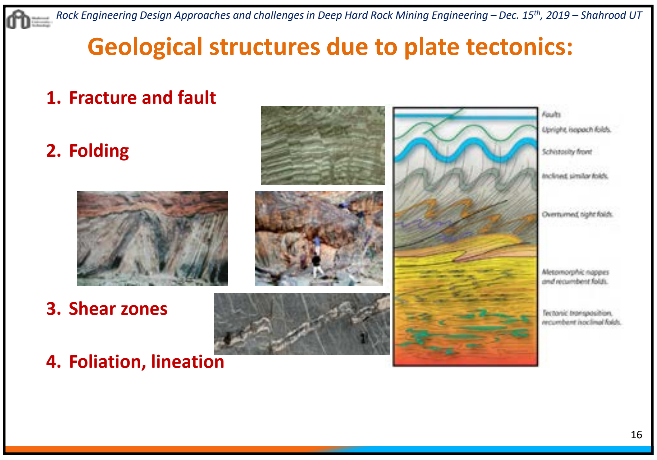

16

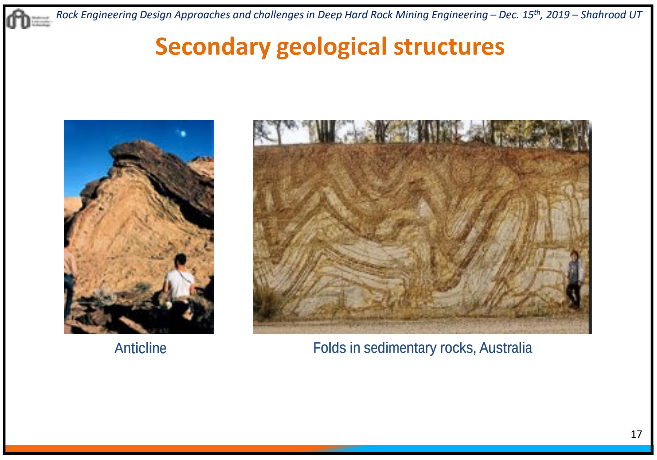

17

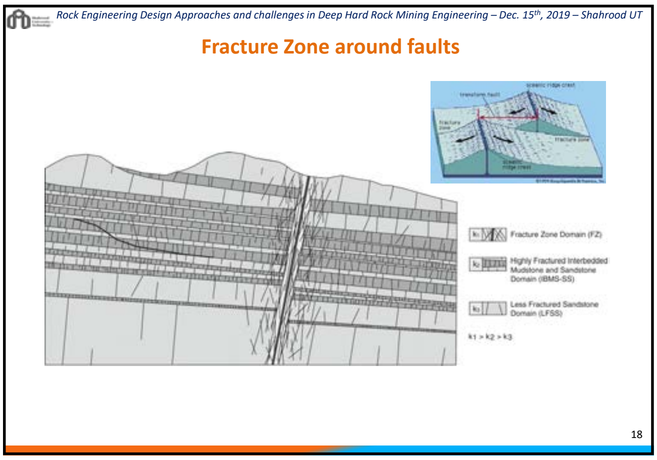

18

Typical fracture patterns

- The upper picture shows 4th order discontinuities in rhombohedral arrangement with a spacing of 5-10 m.
- The central is the basic 4th order pattern with 3rd order zones integrated (spacing 30-50 m).
- The lower picture shows the basic pattern with a 2nd order discontinuity

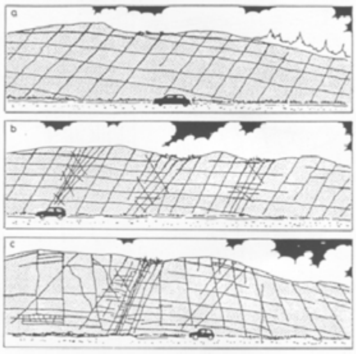

19

19

Examples of block shapes or the jointing pattern

Barton,2009

20

20

Discontinuities in rock mass have profound effect on deformation, strength, stress-strain relation and failure of rock mass

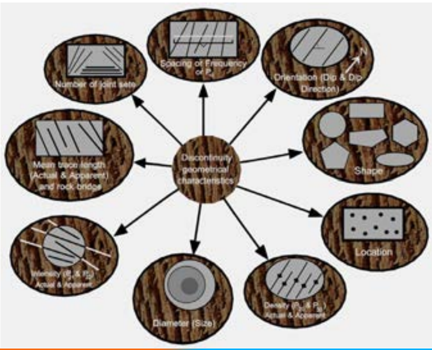

Kamali et al. 2018

21

21

Common Statistical Distribution of Rock Mass Parameters

Discontinuity Parameter	Function or distribution
Persistence	Normal
	Lognormal
	Exponential
	Gamma
	Power-law
Spacing	Lognormal
	Weibull
	Power-law
	Exponential
Aperture	Power-law
	Gamma
	Lognormal
	Exponential

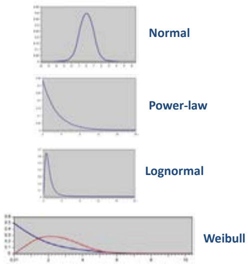

Kamali et al. 2018

22

22

Discontinuities mapping and representation

- Types of mapping
- Scanline
- Window
- Discrete
- Borehole logging
  - Oriented core
  - Televiewers
    - Acoustic
    - Optical

- Stereographic Representation

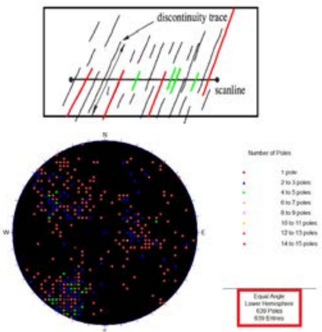

Kamali et al. 2018

23

23

Role of linear and areal mapping on rock mass parameters

Kamali et al, 2016

24

24

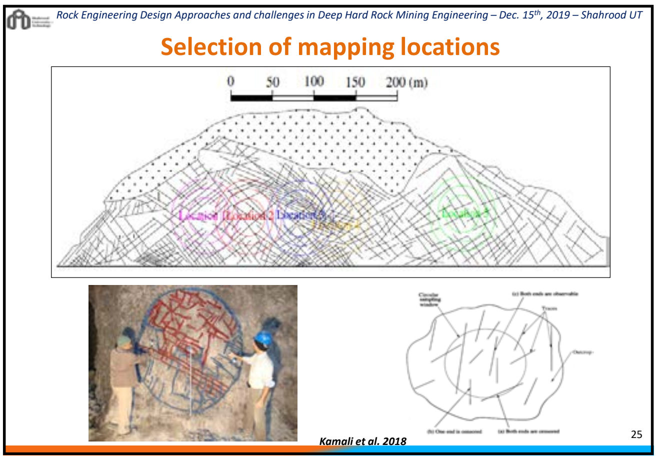

25

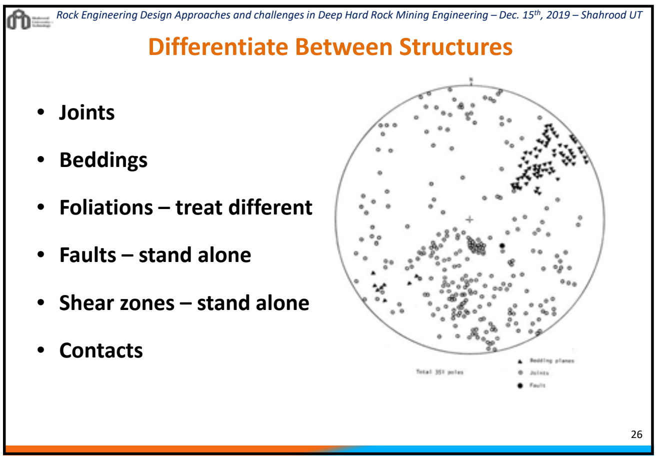

26

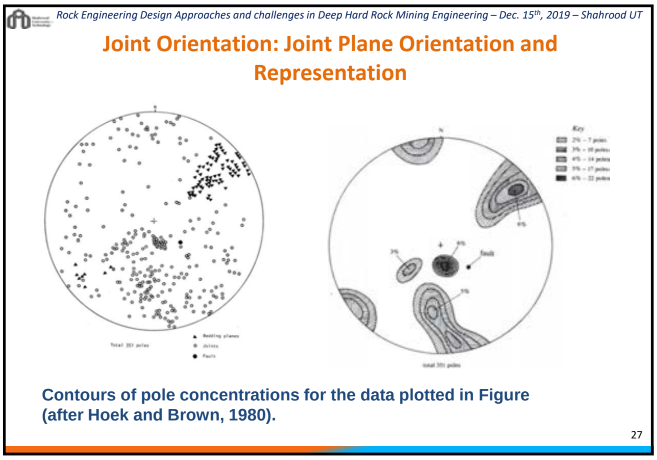

27

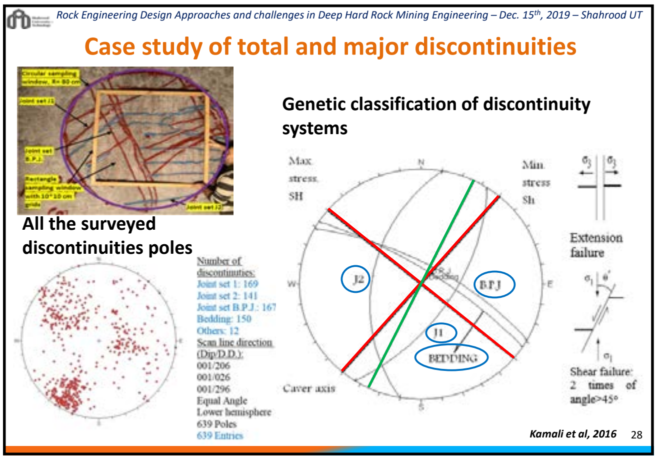

28

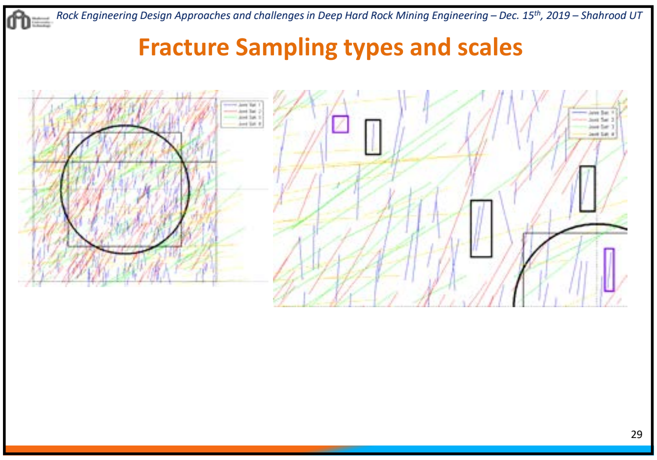

29

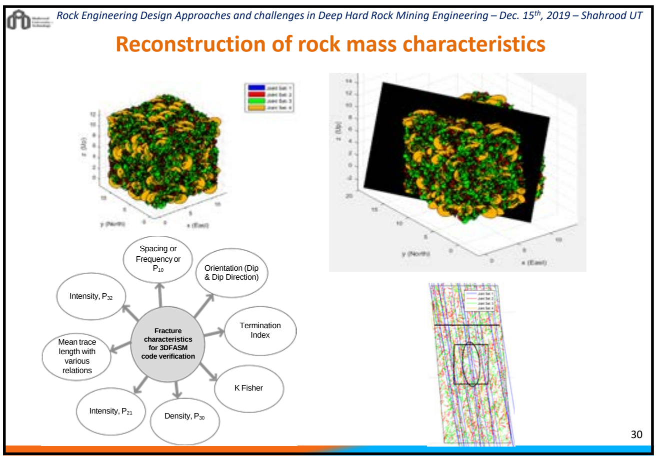

30

Rock Engineering Design Approaches and challenges in Deep Hard Rock Mining Engineering – Dec. 15th, 2019 – Shahrood UT

Verification of rock mass model

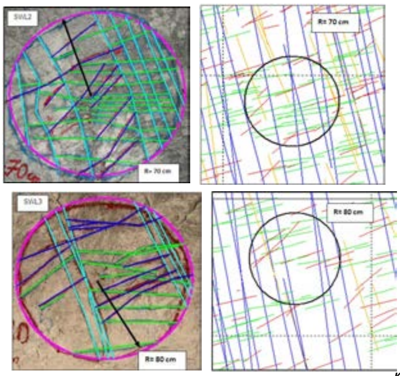

Kamali et al, 2016 31

31

Rock Engineering Design Approaches and challenges in Deep Hard Rock Mining Engineering – Dec. 15th, 2019 – Shahrood UT

Geological Strength Index

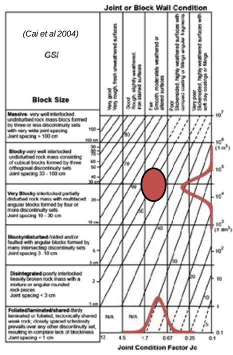

Value based on blockiness & joint condition

Selected in one of two ways:

Qualitatively: repeated observations based on experience (bias present)

Quantitatively: through calculation of a block size (Vb) & joint/block wall condition (Vc) parameters

32

32

Rock Engineering Design Approaches and challenges in Deep Hard Rock Mining Engineering – Dec. 15th, 2019 – Shahrood UT

GSI classification of GSI for different rock types in geological structures

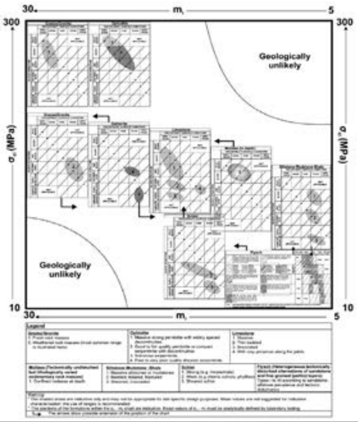

T.G. Carter & Marinos, 2014 33

33

Rock Engineering Design Approaches and challenges in Deep Hard Rock Mining Engineering – Dec. 15th, 2019 – Shahrood UT

GSI and UCS probability density function

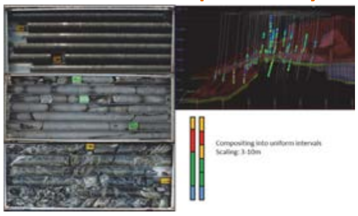

Determining the variability of GSI

GSI and UCS probability density function

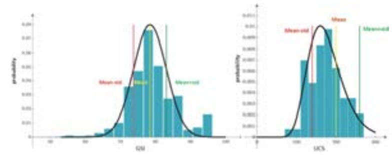

Joughin, 2017 34

34

Rock Engineering Design Approaches and challenges in Deep Hard Rock Mining Engineering – Dec. 15th, 2019 – Shahrood UT

Rock mass characterization :Persistance

- **Persistence:**

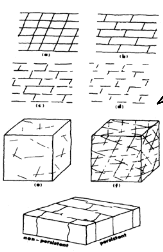

The relative persistence of various sets of discontinuities.
a) Persistent
b,c) Sub persistent
d) non-persistent
e,f,g) three-dimensional view

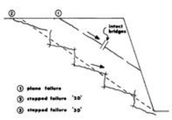

Idealized examples of potential failure planes showing the importance of "intact rock bridges" in slope failure.

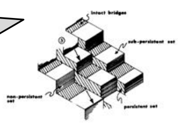

ISRM suggested methods, 2007 35

35

Rock Engineering Design Approaches and challenges in Deep Hard Rock Mining Engineering – Dec. 15th, 2019 – Shahrood UT

Data processing and rock mass model

The three main sources of uncertainty in geotechnical design

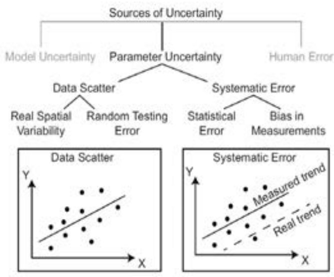

Uncertainty analysis of Rock mass characteristics and properties

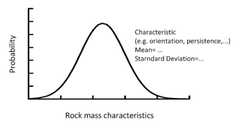

After Macciotta et al., 2014 36

36

Recommendation on Data processing and rock mass model

Transferring data from the measured condition to the application location:

At the preliminary stages of study when data obtained from surface mapping and it will be used for underground excavation design, it is required to adjust data considering the depth of tunnel.

Basically rock mass quality improves with depth increasing. Comparison of the surface mapping and mapping after the excavation of tunnel proves this statement.

Study on 28 tunnel shows that the rock mass quality increases about one class in RMR and GSI scale with an increasing of 200m depth.

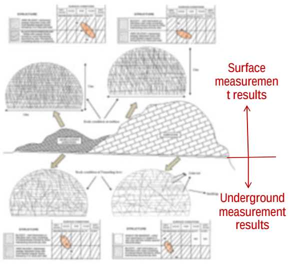

Moosavi & Sharifzadeh, 2010 37

37

Rock Engineering Design Approaches and challenges in Deep Hard Rock Mining Engineering – Dec. 15th, 2019 – Shahrood UT

Recommendation on Data processing and rock mass model

Rock mass characteristics Interrelation matrix.

DE: Depth.
AP: Aperture,
PE: Persistence,
SP: Spacing,
UCS: Uniaxial Compressive Strength,
EM: Elastic Modulus,
COFA: Continuity Factor, DEMO: Deformation Modulus, RMST: Rock Mass Strength, BRMR: Basic RMR, JCR: Joint Condition Rating,
RQD: Rock Quality Designation,

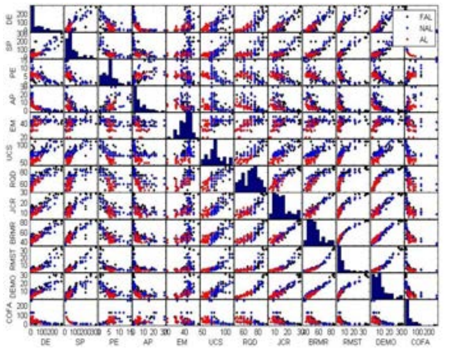

Moosavi & Sharifzadeh, 2010 38

38

Rock Engineering Design Approaches and challenges in Deep Hard Rock Mining Engineering – Dec. 15th, 2019 – Shahrood UT

Example of geomechanical parameters selection for tunnel design

Contents lists available at ScienceDirect

Tunnelling and Underground Space Technology

journal homepage: www.elsevier.com/locate/tust

Evaluation of rock mass engineering geological properties using statistical analysis and selecting proper tunnel design approach in Qazvin–Rasht railway tunnel

Behrooz Rahimi[a,*], Kourosh Shahriar[a], Mostafa Sharifzadeh[a,b]

"… inadequacies in site characterisation of geological data probably present the major weakness to the design, construction and operation of excavations in rock. Improvements in site characterisation methodology and techniques, and in the interpretation of the data are of primary research requirements for all forms of rock engineering." (E.T. Brown, 1986)

39

39

Rock Engineering Design Approaches and challenges in Deep Hard Rock Mining Engineering – Dec. 15th, 2019 – Shahrood UT

Example of geomechanical parameters selection for tunnel design: Tunnel cross section and structural geology

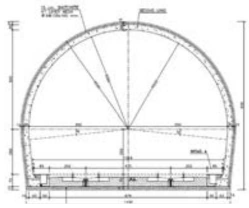

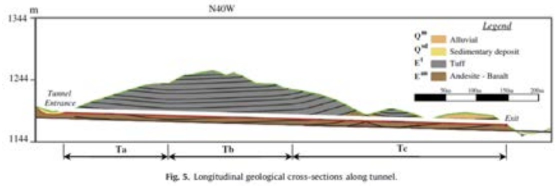

Fig. 5. Longitudinal geological cross-sections along tunnel.

40

40

Rock Engineering Design Approaches and challenges in Deep Hard Rock Mining Engineering – Dec. 15th, 2019 – Shahrood UT

Example of geomechanical parameters selection for tunnel design: Rock mass characteristics along tunnel route

Table 2
Engineering properties of discontinuities in first and second parts of the tunnel.

Joint sets	dip / dip direction	rang of dip direction / range of dip	Length(m)	Spacing* (cm)	Aperture (mm)	Percent of infilling	Roughness	Weathering	Water condition
Bedding	039/17	±11/±8	>20	40 – 100/70	0.1-2	soft < 5	Slightly rough	Moderately to highly	Humid
J_1	084/83	±9/±7	10-20	10 – 60/35	0.1-1	soft < 5	Slightly rough	Moderately to highly	Humid
J_2	160/74	±20/±8	3-10	10 – 50/30	0.1-1	soft < 5	Slightly rough	Moderately to highly	Humid
J_3	309/63	±6/±6	3-10	30 – 70/50	0.1-1	soft < 5	Slightly rough	Moderately to highly	Humid

Columns Length, Spacing and Aperture are under "Properties of joint sets and bedding surfaces".

Table 3
Engineering properties of discontinuities in third parts of the tunnel.

Joint sets	dip / dip direction	rang of dip direction / range of dip	Length(m)	Spacing* (cm)	Aperture(mm)	Percent of infilling	Roughness	Weathering	Water condition
Bedding	014/18	±10/±8	3-10	70 – 150/100	0.1-5	Soft < 5	Slightly rough	Moderately to highly	Humid
J_1	105/83	±13/±6	3-15	30 – 60/40	0.1-3	Soft < 5	Slightly rough	Moderately to highly	Humid
J_2	199/71	±10/±9	3-10	30 – 60/40	0.1-2	Soft < 5	Slightly rough	Moderately to highly	Humid

41

41

Rock Engineering Design Approaches and challenges in Deep Hard Rock Mining Engineering – Dec. 15th, 2019 – Shahrood UT

Example of geomechanical parameters selection for tunnel design: Clusters of Major discontinuity sets in Ta and Tb (a) and Tc (b) of the tunnel.

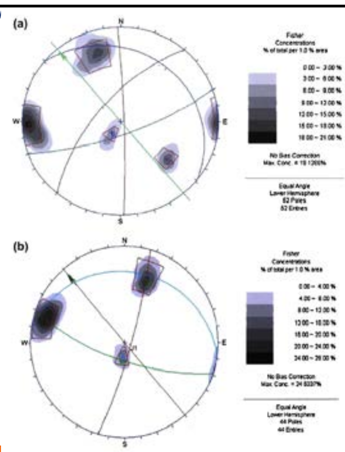

42

42

Example of geomechanical parameters selection for tunnel design: Laboratory test results and rock mass classes

Table 4
Physical and mechanical properties of rocks obtained from the laboratory tests.

Properties, symbol (unit)	Maximum of overburden, H (m)	Poisson's ratio, v	Unit weight, γ (t/m^3)	Young modulus, E_i (GPa)	Uniaxial compressive strength, σ_c (MPa)
Ta	48	0.27	2.2	15	20
Tb	71	0.25	2.2	20	30
Tc	45	0.25	2.2	20	30

Table 6
The estimated rock mass classification systems.

Parts of the tunnel	Rock mass classification (description, rate)				
	RMR	Q	SRC	GSI	Support weight
Ta	Weak, 40	Very weak, 0.55	Weak, 25	48–58	4.1
Tb	Good, 43	Weak, 1.21	Weak, 28	45–55	4.5
Tc	Good, 47	Weak, 1.65	Weak, 30	50–60	5.6

43

43

Rock Engineering Design Approaches and challenges in Deep Hard Rock Mining Engineering – Dec. 15th, 2019 – Shahrood UT

Presentation layout

1. Introduction
2. Variability in rock type and rock mass structure
3. **Effect of scale in rock behaviour**
4. Estimation of rock mass properties using statistical analysis
5. Estimation of in-situ stresses
6. Summary

44

44

Rock Engineering Design Approaches and challenges in Deep Hard Rock Mining Engineering – Dec. 15th, 2019 – Shahrood UT

Scale Dependent Rock Behaviour

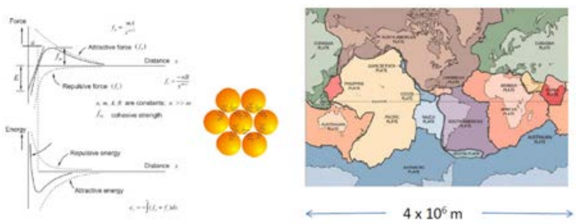

Inter-atomic spacing, 10^{-9} m

Plate tectonics 10^6 m

Length Scale - Range 10 powered by15

Fairharst, 2010 45

45

Rock Engineering Design Approaches and challenges in Deep Hard Rock Mining Engineering – Dec. 15th, 2019 – Shahrood UT

Material discontinuity at different scales

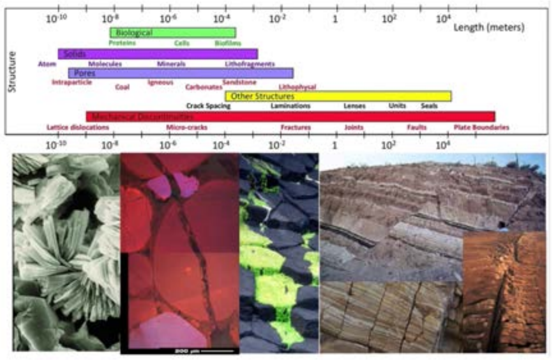

Pyrak Nolte, 2018 46

46

Rock Engineering Design Approaches and challenges in Deep Hard Rock Mining Engineering – Dec. 15th, 2019 – Shahrood UT

Scale Dependent Rock Behaviour:

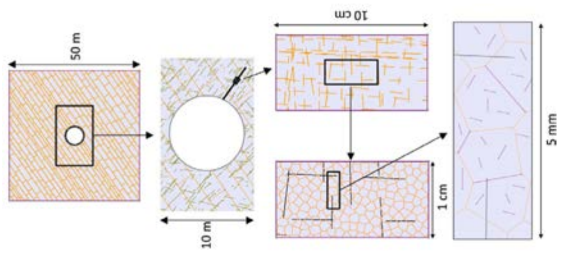

Heterogeneity Observed From Rockmass Scale To Down To Grain-scale

Hamdi, 2015 47

47

Rock Engineering Design Approaches and challenges in Deep Hard Rock Mining Engineering – Dec. 15th, 2019 – Shahrood UT

The difference in size between the main types of discontinuities

Discontinuities also could be divided to: Large scale and small scale.

- Large discontinuities have low shear strength and seismically active.
- Small scale discontinuities are stochastically distributed and should be studied using sampling techniques.

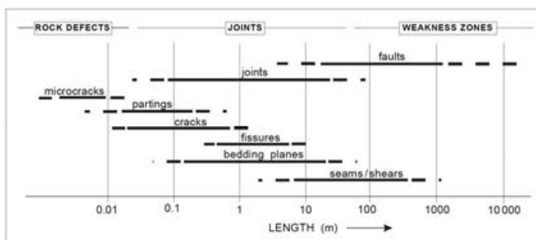

48

48

Rock Engineering Design Approaches and challenges in Deep Hard Rock Mining Engineering – Dec. 15th, 2019 – Shahrood UT

Scale-dependency of rockmass properties and the concept of Representative Elementary Volume (REV).

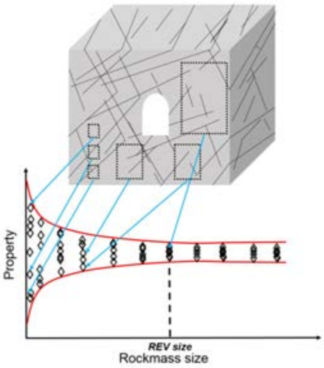

49

49

Rock Engineering Design Approaches and challenges in Deep Hard Rock Mining Engineering – Dec. 15th, 2019 – Shahrood UT

Rock Fracture - Size/Scale Effects

Larger Excavation ⇨ increased potential for blocky fall-out

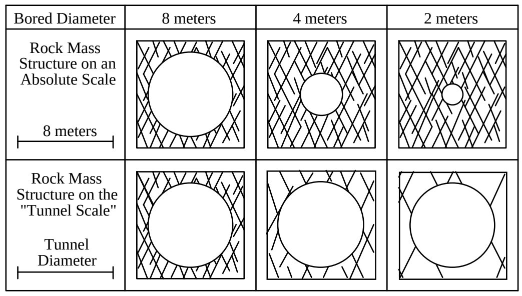

(www.phy.bnl.gov/~dwan)

50

50

Rock Engineering Design Approaches and challenges in Deep Hard Rock Mining Engineering – Dec. 15th, 2019 – Shahrood UT

Presentation layout

1. Introduction
2. Variability in rock type and rock mass structure
3. Effect of scale in rock behaviour
4. **Estimation of rock mass properties using statistical analysis**
5. Estimation of in-situ stresses
6. Summary

51

51

Rock Engineering Design Approaches and challenges in Deep Hard Rock Mining Engineering – Dec. 15th, 2019 – Shahrood UT

Natural variability of intact rock

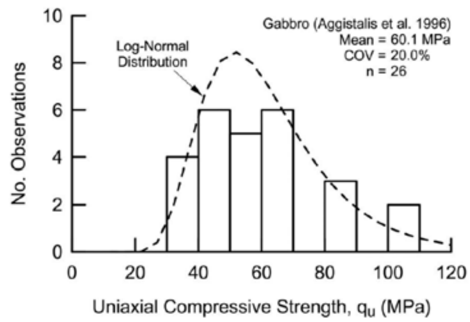

distributions of intact rock properties.

52

52

Rock Engineering Design Approaches and challenges in Deep Hard Rock Mining Engineering – Dec. 15th, 2019 – Shahrood UT

Covariance (COV) of intact rock properties

		Coefficient of Variation (%)			
Test Type	*Property*	*Number of data groups*	*Mean*	*S.D.*	*Range*
Index	γ, γ_d	79	1.0	1.2	0.1–8.6
	n	30	24.2	18.6	3.0–71
	R	54	8.7	5.4	1.4–26
	S_h	59	11.1	8.5	1.4–38
Strength	q_u	174	14.0	11.7	0.8–61
	$q_{t\text{-Brazilian}}$	54	19.4	12.9	3.8–61
	I_s	66	20.5	14.3	2.8–59
Stiffness	$E_{t\text{-}50}$	72	20.5	16.9	1.4–69

(Prakoso 2002)

53

53

Rock Engineering Design Approaches and challenges in Deep Hard Rock Mining Engineering – Dec. 15th, 2019 – Shahrood UT

Estimate uniaxial compressive strength (UCS) using textural characteristics: Correlation of rock mass strength with texture parameters

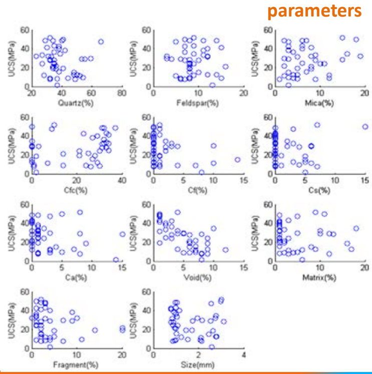

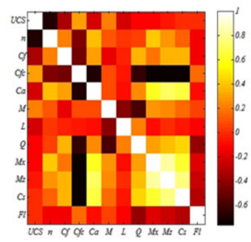

$$UCS = 3680void^2 - 711.6void + 49.19$$
$$UCS = 4401Cfc^3 - 2121Cfc^2 + 268Cfc + 18.66$$

Cf : ferruginous cement,
Cfc: ferroan calcitic cement,
Ca : argillaceous cement.

Manouchehrian A., Sharifzadeh M., Hamidzadeh H., (2012)

54

54

Estimate uniaxial compressive strength (UCS) using textural characteristics

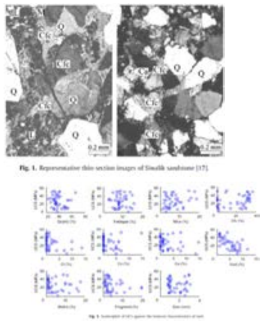

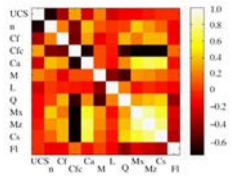

Fig. 4. Correlation matrix for original data set.

$$UCS = 3680void^2 - 711.6void + 49.19$$
$$UCS = 4401Cfc^3 - 2121Cfc^2 + 268Cfc + 18.66$$

Cf : ferruginous cement,
Cfc: ferroan calcitic cement,
Ca : argillaceous cement.

Manouchehrian A., Sharifzadeh M., Hamidzadeh H., (2012) 55

55

Rock Engineering Design Approaches and challenges in Deep Hard Rock Mining Engineering – Dec. 15th, 2019 – Shahrood UT

Uncertainty in material properties

- Complex history of formation & continual modification leads to a high degree of variability in geomaterials & in situ stress
- Need to consider uncertainty as it can have a significant impact on ground response & support performance

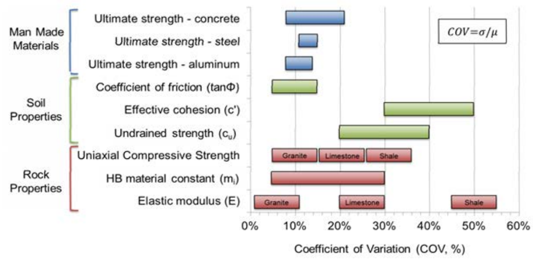

(with data from Bond & Harris 2008, Ruffolo & Shakoor 2009, Marinos & Hoek 2000) 56

56

Rock Engineering Design Approaches and challenges in Deep Hard Rock Mining Engineering – Dec. 15th, 2019 – Shahrood UT

Hoek-Brown $m_{i\text{-}GSI}$ parameters

Rock type	Number of data groups	Mean, $m_{mi\text{-}GSI}$	Range, $r_{mi\text{-}GSI}$	$COV_{mi\text{-}GSI}$ (%)
Granite	18	25.3	8–43	37.7
Dolerite	4	13.2	11–15	14.7
Granodiorite	4	26.0	16–35	31.4
Sandstone	57	16.0	3–42	53.8
Mudstone	7	19.2	9–47	75.8
Shale	3	14.6	3–29	91.9
Chalk	2	7.2	–	–
Limestone	25	9.6	4–26	47.3
Dolostone	8	11.4	5–18	37.7
Carnallitite	5	20.8	3–46	94.7
Amphibolite	3	27.8	24–33	16.7
Quartzite	6	20.4	15–28	24.9
Marble	14	8.1	5–16	39.5
			Mean =	47.2
			S.D. =	27.1

(Hoek-Brown $m_{i\text{-}GSI}$ parameter)

Doruk, 1991 57

57

Rock Engineering Design Approaches and challenges in Deep Hard Rock Mining Engineering – Dec. 15th, 2019 – Shahrood UT

HB Material Constant

- **Given expense of triaxial tests, empirical estimates sometimes used**
- **Values contain both aleatory & epistemic uncertainty**
- **Should be used for**
- **initial estimates only!**

Rock type	Class	Group	Texture: Coarse	Medium	Fine	Very fine
SEDIMENTARY	Clastic		Conglomerate* (22±3) Breccias (19±5)	Sandstone 17±4	Siltstone 7±2 Greywacke (18±3)	Claystone 4±2 Shales (6±2) Marls (7±2)
	Non-Clastic	Organic				Chalk 7±2
		Carbonates	Crystalline Limestone (12±3)	Spartic Limestone (10±2)	Micritic Limestone (9±2)	Dolomites (9±3)
		Evaporites		Gypsum 8±2	Anhydrite 12±2	
METAMORPHIC	Non Foliated		Marble 9±3	Hornfels (19±4) Metasandstones 26±6	Quartzites 20±3	
	Slightly foliated		Migmatite (29±3)	Amphibolites 26±6		
	Foliated*		Gneiss 28±5	Schists 12±3	Phyllites (7±3)	Slates 7±4
IGNEOUS	Plutonic	Light	Granite 32±3	Diorite 25±5		
			Granodiorite (29±3)			
		Dark	Gabbro 27±3	Dolerite (16±5)		
			Norite 20±5			
	Hypabyssal		Porphyries (20±5)		Diabase (15±5)	Peridotite (25±5)
	Volcanic	Lava		Rhyolite (25±5) Andesite 25±5	Dacite (25±3) Basalt (25±5)	Obsidian (19±3)
		Pyroclastic	Agglomerate (19±3)	Breccia (19±5)	Tuff (13±5)	

Hoek 2007 58

58

Rock Engineering Design Approaches and challenges in Deep Hard Rock Mining Engineering – Dec. 15th, 2019 – Shahrood UT

Variation of rock strength with changing scale

Properties of rock discontinuities govern the overall behavior of the rock masses. This lecture addresses properties of rock discontinuities.

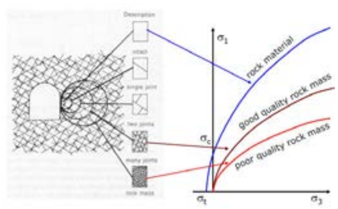

- Properties of rock discontinuities govern the overall behaviour of the rock masses. This lecture addresses properties of rock discontinuities.
- Accurate evaluation of rock mass strength in engineering activities leads us to safe and economic design.

59

59

Rock Engineering Design Approaches and challenges in Deep Hard Rock Mining Engineering – Dec. 15th, 2019 – Shahrood UT

Uniaxial Compressive Strength (UCS)

- **Determined through repeated**
  - **laboratory testing of intact samples**
- **Natural variability (aleatory) due to changes in:**
  - **Index properties (density, porosity)**
  - **Petrographic characteristics (grain**
  - **size/shape, nature of cement)**
- **Changes in petrographic characteristics result in micro defects**
  - **Leads to different modes of sample**
  - **failure for intact rock**
  - **Analyze each mode separately**

(Szwedzicki 2007)

60

60

Uniaxial Compressive Strength (UCS)

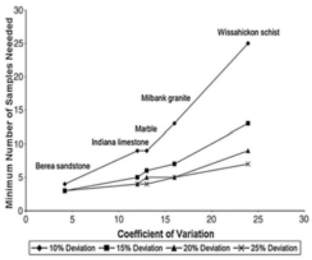

- Epistemic uncertainty due to measurement & statistical estimation errors
  - Measurement errors
    - limited with QA/QC
  - Statistical estimation error reduced by performing adequate number of tests

61

61

Example of geomechanical parameters selection for tunnel design:
Estimation of Rock Mass Properties Using Statistical Analysis (1)

- **The rock mass properties such as Hoek–Brown constants, deformation modulus (Emass) and rock mass strength (σcmass) are important input parameters in any analysis of rock mass, such as designing the primary support and final lining in a tunnel.**
- **The usual methods for determining rock mass properties and in situ stresses are empirical methods, back analysis, field tests and mathematical modeling. Field tests to determine these parameters directly are time consuming, expensive and the reliability of the results of these tests is sometimes questionable.**

62

62

Example of geomechanical parameters selection for tunnel design:
Estimation of Rock Mass Properties Using Statistical Analysis(2)

- **Statistical analysis is a branch of mathematics dealing with gathering, analyzing, and making inferences from data.**
- **The method is used to predict the characteristics of certain applicable real properties in all science.**
- **Statistical tools not only summarize past data through such indicators as the mean, medium, mode and the standard deviation but can predict future events using frequency distribution functions. Statistics provides ways to design efficient experiments that eliminate time-consuming trial and error.**

63

63

Example of geomechanical parameters selection for tunnel design:
Estimation of Rock Mass Properties Using Statistical Analysis(3)

- **The estimation of rock mass parameters using statistical analysis methods is carried out as following steps:**

1. **Selection of several empirical equation or classification system for estimation of rock mass properties.**
2. **Statistical analysis of obtained data from empirical equations. Generally, average, maximum, minimum, and standard deviation data are calculated. According to condition and requirement project may be calculated other statistical parameters.**
3. **Omit high deviation data.**
4. **Re-statistical analysis of data without high deviation data and estimation of rock mass properties.**

64

64

Example of geomechanical parameters selection for tunnel design: Estimation of Rock Mass Strength (σ_{cmass})

Researcher (year)	Equation
Rock – Lab software	$\sigma_{cmass} = \sigma_{ci} s^a \ (MPa)$
singh (1971)	$\sigma_{cmass} = 7\gamma Q^{1/3} \ (MPa), \sigma_{ci} > 2MPa, Q < 10$
Hoek and Brown(1980)	$\sigma_{cmass} = \sigma_{ci}\sqrt{e^{(\frac{RMR-100}{9})}} \ (MPa)$
Yudhbir(1983)	$\sigma_{cmass} = \sigma_{ci} e^{7.65(\frac{RMR-100}{100})} \ (MPa)$
Ramamurthy (1985)	$\sigma_{cmass} = \sigma_{ci}[\frac{E_m}{E_i}]^{0.7} \ (MPa)$
Ramamurthy (1986)	$\sigma_{cmass} = \sigma_{ci} e^{\frac{RMR-100}{18/75}} \ (MPa)$
Goel (1994)	$\sigma_{cmass} = \frac{5.5\gamma {Q_N}^{1/3}}{\sigma_{ci} B^{0.1}}, Q_N = \left(\frac{RQD}{J_n}\right)(\frac{J_r}{J_a})J_w$
Goel (1994)	$\sigma_{cmass} = \frac{5.5\gamma \acute{Q}^{1/3}}{B^{0.1}} \ (\mathrm{MPa}), \quad \acute{Q} = \left(\frac{RQD}{J_n}\right)(\frac{J_r}{J_a})$
Kalamaris and Bieniawski (1995)	$\sigma_{cmass} = \sigma_{ci} e^{\frac{RMR-100}{24}} \ (MPa)$
Bhasin and Grimstad (1996)	$\sigma_{cmass} = \left(\frac{\sigma_{ci}}{100}\right) \times 7\gamma Q^{1/3}, \sigma_{ci} > 100MPa, Q > 10$
Singh(1997)	$\sigma_{cmass} = \sigma_{ci} s_m^n \ (MPa)$
Sheorey (1997)	$\sigma_{cmass} = \sigma_{ci} e^{\frac{RMR-100}{20}} \ (MPa)$
Trueman (1998)	$\sigma_{cmass} = 0.5e^{0.06\mathrm{RMR}}$
Aydan and Dalgic (1998)	$\sigma_{cmass} = \frac{RMR}{RMR + \beta(100 - RMR)}\sigma_{ci}(MPa), \beta = 6$
Barton (2000)	$\sigma_{cmass} = 5\gamma(Q\frac{\sigma_{ci}}{100})^{1/3} \ (MPa)$
Palm srotm (2000)	$\sigma_{cmass} = RMi = \sigma_{ci} J_p \ (MPa)$
Hoek (2002)	$\sigma_{cmass} = \frac{\sigma_{ci}\left(m_b + 4s - a(m_b - 8s)\right)(m_b/4 + s)^{a-1}}{2(1+a)(2+a)} \ (MPa)$
Barton (2002)	$\sigma_{cmass} = 5\gamma Q_c^{1/3}, Q_c = \mathrm{Q}\frac{\sigma_c}{100}$

σ_{ci}: uniaxial compressive strength of intact rock (MPa)
Jv: coefficient of strength decrease in RMi
E_i: deformation modulus of intact rock (MPa)
B: width tunnel (m)
a, s, m_b: Hoek and Brown constants for rock mass
γ: rock mass density (t/m³)

65

65

Example of geomechanical parameters selection for tunnel design: Estimation of rock mass strength along tunnel using the proposed empirical equations

Researcher (year)	Equation	Equation number	Ta (MPa)	Tb (MPa)	Tc (MPa)
Rock-Lab software	$\sigma_{cmass} = \sigma_{ci} s^a (MPa)$	(4)	1.4	1.8	2.4
Singh et al. (1997)	$\sigma_{cmass} = 7\gamma Q^{1/3} (MPa), \sigma_{ci} > 2MPa, Q < 10$	(5)	12.60	16.40	18.2
Hoek and Brown (1980)	$\sigma_{cmass} = \sigma_{ci}\sqrt{e^{(\frac{RMR-100}{9})}} (MPa)$	(6)	0.7	1.3	1.6
Yudhbir et al. (1983)	$\sigma_{cmass} = \sigma_{ci} e^{7.65(\frac{RMR-100}{100})} (MPa)$	(7)	0.3	0.4	0.5
Ramamurthy (1985)	$\sigma_{cmass} = \sigma_{ci}\left[\frac{E_m}{E_i}\right]^{0.7} (MPa)$	(8)	10.2	14.2	16.3
Ramamurthy (1986)	$\sigma_{cmass} = \sigma_{ci} e^{\frac{RMR-100}{18.75}} (MPa)$	(9)	1.2	1.4	1.8
Goel (1994)	$\sigma_{cmass} = \frac{5.5\gamma Q_N^{1/3}}{\sigma_{ci} B^{0.1}}, Q_N = \left(\frac{RQD}{J_n}\right)\left(\frac{J_r}{J_a}\right)J_w$	(10)	–	–	–
Goel (1994)	$\sigma_{cmass} = \frac{5.5\gamma Q^{1/3}}{B^{0.1}} (MPa), Q = \left(\frac{RQD}{J_n}\right)\left(\frac{J_r}{J_a}\right)$	(11)	17.1	17.3	24.7
Kalamaris and Bieniawski (1995)	$\sigma_{cmass} = \sigma_{ci} e^{\frac{RMR-100}{24}} (MPa)$	(12)	2.5	2.8	3.3
Bhasin and Grimstad (1996)	$\sigma_{cmass} = \left(\frac{\sigma_{ci}}{100}\right) \times 7\gamma Q^{1/3}, \sigma_{ci} > 100MPa, Q > 10$	(13)	–	–	–
Singh et al. (1997)	$\sigma_{cmass} = \sigma_{ci} s_m^n (MPa)$	(14)	1.4	1.7	2.1
Sheorey (1997)	$\sigma_{cmass} = \sigma_{ci} e^{\frac{RMR-100}{20}} (MPa)$	(15)	1	1.7	2.1
Trueman (1998)	$\sigma_{cmass} = 0.5e^{0.06RMR}$	(16)	5.5	6.6	8.4
Aydan and Dalgic (1998)	$\sigma_{cmass} = \frac{RMR}{RMR+\beta(100-RMR)}\sigma_{ci} (MPa), \beta = 6$	(17)	1.9	3.4	3.9
Barton (2000)	$\sigma_{cmass} = 5\gamma(Q\frac{\sigma_{ci}}{100})^{1/3} (MPa)$	(18)	5.3	7.8	8.7
Palmstrom (2000)	$\sigma_{cmass} = RMi = \sigma_{ci} J_p (MPa)$	(19)	–	–	–
Hoek et al. (2002)	$\sigma_{cmass} = \frac{\sigma_{ci}(m_b+4s-a(m_b-8s))(m_b/4+s)^{a-1}}{2(1+a)(2+a)} (MPa)$	(20)	5.2	6.3	7.9
Barton (2002)	$\sigma_{cmass} = 5\gamma Q_c^{1/3}, Q_c = Q\frac{\sigma_c}{100}$	(21)	6	8.9	9.9

σ_{ci}: Uniaxial compressive strength of intact rock (MPa).
Jv: Coefficient of strength decrease in RMi.
E_i: deformation modulus of intact rock (MPa).
B: width tunnel (m).
a, *s*, m_b: Hoek and Brown constants for rock mass.
γ: Rock mass density (t/m³).

66

66

Example of geomechanical parameters selection for tunnel design:

Statistical approach to estimate rock mass strength along tunnel using the proposed empirical equations

Table 8
Statistical analysis results obtained from estimated rock mass strength (σ_{cmass}) along the tunnel.

	Parts of tunnel	Minimum	Maximum	Average	Standard deviation	Average with 95% confidence level	$\frac{\sigma_{ci}}{\sigma_{cmass}}$
First step: considering all data	Ta	0.3	17.10	4.82	4.96	4.82 ± 2.95	4.15
	Tb	0.4	17.70	6.16	5.8	6.16 ± 3	4.87
	Tc	0.5	24.7	7.45	7.21	7.45 ± 3.72	4.03
Second step: without considering of equation values 5, 8 and 11	Ta	0.3	6	2.7	2.15	2.7 ± 1.24	7.41
	Tb	0.4	8.9	3.68	2.91	3.68 ± 1.68	8.15
	Tc	0.5	9.9	4.38	3.34	4.38 ± 1.93	6.85

67

67

Example of geomechanical parameters selection for tunnel design:

Estimation of Deformation Modulus of rock mass (E_{mass})

Researcher (year)	Equation
Bieniawski (1978)	$E_{mass} = 2RMR - 100\ (GPa),\ RMR > 50$
Serafim and Pereira (1983)	$E_{mass} = 10^{\left(\frac{RMR-10}{40}\right)}\ (GPa),\ RMR < 50$
Grimstad and Barton (1993)	$E_{mass} = 25\log Q\ \ (GPa), Q > 1$
Verman (1993)	$E_{mass} = 0.3H^{\alpha}10^{\left(\frac{RMR_{1979}-20}{38}\right)}\ (GPa), H > 50m$
Mitri (1994)	$E_{mass} = E_i\left[0.5\left(1-\left\{\cos\pi\frac{RMR}{100}\right\}\right)\right]\ (GPa)$
Palm Strom (1995)	$E_{mass} = 5.6RMi^{0.375}\ \ (GPa)\ ,RMi > 0.1$
Singh(1997)	$E_{mass} = E_i(s_m)^{1/1.4}\ \ (GPa)$
Hoek and Brown (1998)	$E_{mass} = \sqrt{\frac{\sigma_{ci}}{100}}10^{\left(\frac{GSI-10}{40}\right)}\ \ (GPa)\ ,\sigma_{ci} < 100MPa)$
Read (1999)	$E_{mass} = 0.1(\frac{RMR}{10})^3\ (GPa)$
Ramamurthy (2001)	$E_{mass} = \frac{E_i\exp[(RMR-100)]}{17.4}\ (GPa)$
Ramamurthy (2001)	$E_{mass} = E_i\exp(0/8625\log Q - 2/875)\ (GPa)$
Hoek (2002)	$E_{mass} = \left(1-\frac{D}{2}\right)\sqrt{\frac{\sigma_{ci}}{100}}10^{\left(\frac{GSI-10}{40}\right)}(GPa)$
Barton (2002)	$E_{mass} = 10Q_c^{1/3}\ \ (GPa),\ \ Q_c = Q\frac{\sigma_c}{100}$
Barton (2002)	$E_{mass} = 10^{\left(\frac{15\log Q+40}{40}\right)}\ \ (GPa)\ \ ,Q < 1, RMR < 50$
Ramamurthy (2004)	$E_{mass} = E_i\exp - 00035[5(100 - RMR)](GPa)$
Ramamurthy (2004)	$E_{mass} = E_i\exp - 0.0035[250(1 - 0.3\log Q)](GPa)$
Hoek and Diederiches (2006)	$E_{mass} = E_i\left(0.02 + \frac{1}{1+e^{(60+15D-GSI)/11}}\right)(GPa)$

σ_{ci}: uniaxial compressive strength of intact rock (MPa)
E_i: deformation modulus of intact rock (GPa)
GSi: ground strength index
D: disturbance degree factor
m_m: Hoek and Brown constant
α: 0.16 for hard rocks and 0.35 for weak rocks

68

68

Example of geomechanical parameters selection for tunnel design:

Estimation of rock mass deformation modulus (E_{mass}) along tunnel using the proposed empirical equations

Researcher (year)	Equation	Equation number	Ta (GPa)	Tb (GPa)	Tc (GPa)
Bieniawski (1978)	$E_{mass} = 2RMR - 100(GPa), RMR > 50$	(22)	–	–	–
Serafim and Pereira (1983)	$E_{mass} = 10^{\left(\frac{RMR-10}{40}\right)}(GPa), RMR < 50$	(23)	5.6	6.7	8.4
Grimstad and Barton (1993)	$E_{mass} = 25\log Q(GPa), Q > 1$	(24)	–	2.1	5.4
Verman (1993)	$E_{mass} = 0.3H^{\alpha}10^{\left(\frac{RMR_{1979}-20}{38}\right)}(GPa), H > 50m$	(25)	–	–	–
Mitri et al. (1994)	$E_{mass} = E_i[0.5(1-(\cos\pi\frac{RMR}{100}))](GPa)$	(26)	5.2	7.8	9.1
Palmstrom (1995)	$E_{mass} = 5.6RMi^{0.375}(GPa), RMi > 0.1$	(27)	–	–	–
Singh et al. (1997)	$E_{mass} = E_i(s_m)^{1/1.4}(GPa)$	(28)	0.3	0.3	0.4
Hoek and Brown (1998)	$E_{mass} = \sqrt{\frac{\sigma_{ci}}{100}}10^{\left(\frac{GSI-10}{40}\right)}(GPa), \sigma_{ci} < 100MPa$	(29)	5.3	5.5	7.3
Read et al. (1999)	$E_{mass} = 0.1(\frac{RMR}{10})^3(GPa)$	(30)	6.4	8	10.4
Ramamurthy (2001)	$E_{mass} = \frac{E_i\exp[(RMR-100)]}{17.4}(GPa)$	(31)	0.48	0.76	0.95
Ramamurthy (2001)	$E_{mass} = E_i\exp(0/8625\log Q - 2/875)(GPa)$	(32)	–	1.21	1.54
Hoek et al. (2002)	$E_{mass} = (1-\frac{D}{2})\sqrt{\frac{\sigma_{ci}}{100}}10^{\left(\frac{GSI-10}{40}\right)}(GPa)$	(33)	5.3	5.5	7.3
Barton (2002)	$E_{mass} = 10Q_c^{1/3}(GPa), Q_c = Q\frac{\sigma_c}{100}$	(34)	4.8	7.1	7.9
Barton (2002)	$E_{mass} = 10^{\left(\frac{15\log Q+40}{40}\right)}(GPa), Q < 1, RMR < 50$	(35)	8	10.7	11.8
Ramamurthy (2004)	$E_{mass} = E_i\exp -00035[5(100 - RMR)](GPa)$	(36)	5.3	7.4	2.9
Ramamurthy (2004)	$E_{mass} = E_i\exp -0.0035[250(1 - 0.3\log Q)](GPa)$	(37)	5.8	8.5	8.8
Hoek and Diederichs (2006)	$E_{mass} = E_i\left(0.02 + \frac{1}{1+e^{(60+15D-GSI)/11}}\right)(GPa)$	(38)	5.5	6.1	8.2

σ_{ci}: Uniaxial compressive strength of intact rock (MPa).
E_i: deformation modulus of intact rock (GPa).
GSI: ground strength index.
D: disturbance degree factor.
m_m: Hoek and Brown constant.
α: 0.16 for hard rocks and 0.35 for weak rocks.

69

69

Example of geomechanical parameters selection for tunnel design:

Statistical approach to estimate rock mass deformation modulus (E_{mass}) along tunnel using the proposed empirical equations

Table 10
Statistical analysis results for determination of deformation modulus of rock mass (E_{mass}) in the tunnel.

	Parts of tunnel	Minimum	Maximum	Average	Standard deviation	Standard deviation	Average with 95% confidence level	$\frac{E_i}{E_{mass}}$
First step: considering all data	Ta	0.30	8.00	4.83	4.98	2.23	4.83 ± 1.28	3.10
	Tb	0.30	10.70	5.55	10.38	3.22	5.55 ± 1.72	3.60
	Tc	0.40	11.80	6.81	12.27	3.5	6.81 ± 1.87	2.94
Second step: without considering of equation values 28, 31 and 32	Ta	4.80	8.00	5.72	0.82	0.91	5.72 ± 0.58	2.62
	Tb	2.10	10.70	6.85	4.69	2.17	6.85 ± 1.3	2.92
	Tc	5.40	11.80	8.41	2.82	1.68	8.41 ± 1.00	2.38

70

70

Example of geomechanical parameters selection for tunnel design:

Estimation of Hoek–Brown and Mohr–Coulomb constants of rock mass

Researcher (year)	Equation
Singh(1993)	$s_m = 0.002Q_N\ ,\ \ Q_N = \left(\frac{RQD}{J_n}\right)\left(\frac{J_r}{J_a}\right)J_w$ $\frac{m_m}{m_i} = 0.135{Q_N}^{1/3}$
Hoek (2002)	$m_m = m_i\exp\left(\frac{GSI-100}{28-14D}\right)$ $s_m = \exp\left(\frac{GSI-100}{9-3D}\right)$ $a = \frac{1}{2}+\frac{1}{6}\left(e^{-\frac{GSI}{15}} - e^{-\frac{20}{3}}\right)$
Singh(1997)	$\frac{m_m}{m_i} = s_m^{1/3}\ ,\ \ GSI > 25$ $s_m^n = \frac{7\gamma Q^{1/3}}{\sigma_{ci}}\quad ,Q < 10\ ,J_w = 1\ ,\sigma_{ci} < 100MPa$ $\begin{cases} n = 0.5 & ,if\ \ GSI \geq 25 \\ n = 0.65 - \frac{GSI}{200} \leq 0.6 & ,if\ \ GSI < 25 \end{cases}$
Ramamurthy (1985)	$s_m = e^{\left(\frac{1}{40}(0.0564RMR-5.64)\right)}$
Palm Strom (1995)	$s_m = J_p^2$ $m_m = m_i{J_p}^{0.64}$

GSi: ground strength index
D: disturbance degree factor of rock types of rock mass
a, s_m and m_m: Hoek and Brown constant
m_i: Hoek and Brown constant for intact rock
Jp: coefficient of strength decrease in RMi
γ: rock mass density (t/m3)

71

71

Example of geomechanical parameters selection for tunnel design: Calculated Hoek–Brown and Mohr–Coulomb parameters values.

Method	Parameter	Ta	Tb	Tc
(1) empirical equations (based on Table 10)	m_m	4.6	2.73	3.90
	s_m	0.0047	0.0034	0.0048
	a	0.505	0.506	0.504
(2) rock mass rating classification (RMR)	c(MPa)	0.2–0.3	0.2–0.3	0.2–0.3
	φ (degree)	25–35	25–35	25–35
(3) Rock-lab software	m_m	3.733	2.515	4.009
	s_m	0.0054	0.0039	0.0067
	a	0.505	0.506	0.504
	c(MPa)	0.31	0.41	0.39
	φ (degree)	55	52	58
Estimation of Hoek–Brown and Mohr–Coulomb parameters values	m_m	4.17	2.62	3.95
	s_m	0.0051	0.0037	0.0058
	a	0.505	0.506	0.504
	c(MPa)	0.28	0.33	0.32
	φ (degree)	43	41	44

72

72

Presentation layout

1. Introduction
2. Variability in rock type and rock mass structure
3. Effect of scale in rock behaviour
4. Estimation of rock mass properties using statistical analysis
5. **Estimation of in-situ stresses**
6. Summary

73

73

Methods of stress determination

1. **Theoretical methods of stress estimation**
2. **Field measurements methods**
3. **Stress estimation using world data and stress map**
4. **Geological structural evidences (Faulting type, folding,…)**
5. **Core disking**
6. **Failure location in underground excavations**

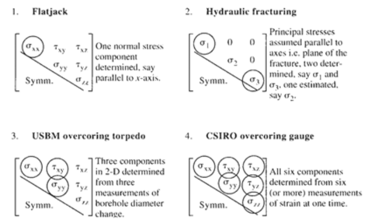

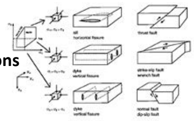

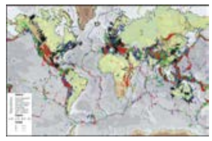

74

74

Variation of vertical stress with depth(after Amadei & Stephansson, 1997;Yokoyam, 2003).

Reference	Variation of vertical stress σ_v (MPa) with depth z (m)	Location and depth range (m)
Herget (1974)	$(1.9 \pm 1.26) + (0.0266 \pm 0.0028)z$	World data (0–2,400)
Lindner & Halpern (1977)	$(0.942 \pm 1.1.31) + (0.0339 \pm 0.0067)z$	North American (0–1,500)
McGarr & Gay (1978)	$0.0265z$	World data (100–3,000)
Hoek & Brown (1980a)	$0.027z$	World data (0–3,000)
Herget (1987)	$(0.026–0.0324)z$	Canadian Shield (0–2,200)
Arjang (1989)	$(0.0266 \pm 0.008)z$	Canadian Shield (0–2,000)
Baumgärtner et al. (1993)	$(0.0275–0.0284)z$	KTP pilot hole (800–3,000)
Herget (1993)	$0.0285z$	Canadian Shield (0–2,300)
Sugawara & Obara (1993)	$0.027z$	Japanese Islands (0–1,200)
Te Kamp et al. (1995)	$(0.0275–0.0284)z$	KTP hole (0–9,000)
Lim and Lee (1995)	$0.233 + 0.024z$	South Korea (0–850)
Yokoyam, T. (2003)	$0.0255z$ (Crystalline rock) $0.0249z$ (Sedimentary rock)	Japan (0–1,600)

75

Variation of horizontal stress with depth

…ansson, 1997; Rummel, 2002; Yokoyam, 2003).

Reference	Variation of σ_{have}, σ_{hmax}, σ_{hmin} (MPa) or k, k_{max}, k_{min} with depth z (m)	Location and depth range (m)
Voight (1966)	$\sigma_{have} = 8.0 + 0.043z$	World data (0–1,000)
Herget (1974)	$\sigma_{have} = (8.3 \pm 0.5) + (0.0407 \pm 0.0023)z$	World data (0–800)
Van Heerden (1976)	$k = 0.448 + 248/z$ $(r = 0.85)$	South Africa (0–2,500)
Worotnicki & Denham (1976)	$\sigma_{have} = 7.7 + (0.021 \pm 0.002)z$ $(r = 0.85)$	Australia (0–1,500)
Haimson (1977)	$\sigma_{hmax} = 4.6 + 0.025z$ $\sigma_{hmin} = 1.4 + 0.018z$ $(r = 0.95)$	Michigan Basin (0–5,000)
Lindner & Halpern (1977)	$\sigma_{have} = (4.36 \pm 0.815) + (0.039 \pm 0.0072)z$	North American (0–1,500)
Hoek & Brown (1980a)	$0.3 + 100/z < k < 0.5 + 1500/z$	World data (0–3,000)
Aytmatov (1986)	$5.0 + 0.058z < (\sigma_{hmax} + \sigma_{hmin}) < 9.5 + 0.075z$	World data (mostly former USSR) (0–1,000)
Li (1986)	$\sigma_{have} = 0.72 + 0.041z$ $0.3 + 100/z < k < 0.5 + 440/z$	China (0–500)
Rummel (1986)	$k_{max} = 0.98 + 250/z$ $k_{min} = 0.5 + 150/z$	World data (500–3,000)
Herget (1987)	$\sigma_{have} = 9.86 + 0.0371z$ $\sigma_{have} = 33.41 + 0.0111z$ $k = 1.25 + 267/z$ $k_{max} = 1.46 + 357/z$ $k_{min} = 1.10 + 167/z$	Canadian Shield (0–900) (990–2,200) (0–2,200)
Pine & Kwakwa (1989)	$\sigma_{hmax} = 15 + 0.028z$ $\sigma_{hmin} = 6 + 0.012z$	Cammenellis granite Cornwall, UK (0–2,000)
Arjang (1989)	$\sigma_{hmax} = 8.8 + 0.0422z$ $\sigma_{hmin} = 3.64 + 0.0276z$ $\sigma_{have} = 5.91 + 0.0349z$	Canadian Shield (0–2,000)
Baumgärtner et al. (1993)	$\sigma_{hmax} = 30.4 + 0.023z$ $\sigma_{hmin} = 16.0 + 0.011z$ $\sigma_{hmin} = 1.75 + 0.0133z$	KTP pilot hole (800–3,000) Cajon pass hole (800–3,000)
Sugawara & Obara (1993)	$\sigma_{have} = 2.5 + 0.013z$	Japanese Islands (0–1,200)

Reference	Variation of σ_{have}, σ_{hmax}, σ_{hmin} (MPa) or k, k_{max}, k_{min} with depth z (m)	Location and depth range (m)
Hast (in Stephansson, 1993)	$\sigma_{hmax} = 9.1 + 0.0724z$ $(r = 0.78)$ $\sigma_{hmin} = 5.3 + 0.0542z$ $(r = 0.83)$	Fennoscandia, overcoring (0–1,000)
Stephansson (1993)	$\sigma_{hmax} = 10.4 + 0.0446z$ $(r = 0.61)$ $\sigma_{hmin} = 5.0 + 0.0286z$ $(r = 0.58)$ $\sigma_{hmax} = 6.7 + 0.0444z$ $(r = 0.61)$ $\sigma_{hmin} = 0.8 + 0.0329z$ $(r = 0.91)$ $\sigma_{hmax} = 2.8 + 0.0399z$ $(r = 0.79)$ $\sigma_{hmin} = 2.2 + 0.0240z$ $(r = 0.81)$	Fennoscandia Leeman-Hiltscher overcoring (0–700) Leeman-type overcoring (0–1,000) Hydraulic fracturing (0–1,000)
Te Kamp et al. (1995)	$\sigma_{hmax} = 15.83 + 0.0303z$ $\sigma_{hmin} = 6.52 + 0.0157z$	KTP hole (0–9,000)
Lim and Lee (1995)	$\sigma_{have} = 1.858 + 0.018z$ $(r = 0.869)$ $\sigma_{have} = 2.657 + 0.032z$ $(r = 0.606)$	South Korea overcoring (0–850) Hydraulic fracturing (0–500)
Rummel (2002)	$k_{max} = 1.30 + 110/z$ $k_{min} = 0.66 + 72/z$	Hong Kong (0–200)
Yokoyama, et al. (2003)	Crystalline rock: $\sigma_{hmax} = -21.9 + 0.0301z$ $\sigma_{hmin} = 33.7 + 0.0219z$ Sedimentary rock: $\sigma_{hmax} = 23.5 + 0.0340z$ $\sigma_{hmin} = 47.5 + 0.0281z$	Japan (0–1,600)

Notes: $k = \sigma_{have}/\sigma_v$; $k_{max} = \sigma_{hmax}/\sigma_v$; $k_{min} = \sigma_{hmin}/\sigma_v$; and r is the correlation coefficient.

76

76

Estimation of in situ stresses (1)

- **Determination of in situ stresses is very difficult and expensive, for this reason, many projects are carried out in which the stress field has been estimated using compilations of measurement data from nearby or regional tunnels.**
- **Sheorey (1994) developed an elasto – static thermal model which accounted for the crust curvature, changes in density, elastic constants and coefficients of thermal expansion. He suggested the following relationship for horizontal to vertical stress ratio K :**

$$\mathrm{K} = 0.25 + 7E_h\left[0.001 + \frac{1}{H}\right]$$

77

77

Estimation of in situ stresses (2)

- **Stephensson (1993) has suggested the following relation between horizontal stress and vertical stress based on hydraulic fracturing tests.**

$$\sigma_h = 2.8 + 1.48\sigma_v \quad (H < 1000m)$$

- **Sengupta (1998) used σ_v in his equation to calculate horizontal stress as**

$$\sigma_h = 1.5 + 1.2\sigma_v$$

78

78

Estimation of in situ stresses (3)

- The horizontal stress was determined from the following equation based on results of in–situ tests in Canada, Australia, USA, Scandinavia, South Africa and other regions in the world.

$$\sigma_h = \frac{12.60}{\sqrt[3]{z}}\sigma_v$$

- Sheorey (2001) proposed the below equation for calculating σ_h:

$$\sigma_h = \frac{\nu}{1-\nu}\sigma_v + \frac{\beta E_{mass} G}{1-\nu}(H+100)$$

Where $\beta = 8 \times 10^{-6}$ /°C is the coefficient of linear thermal, $G = 0.024$ °C/m that is geothermal gradient, ν is Poisson's ratio and E_{mass} deformation modulus of rock mass (MPa).

Calculated in situ stress (σ_h, σ_v and K).

	Ta	Tb	Tc
σ_v (MPa)	1.06	1.56	0.99
σ_h (MPa)	1.52	1.91	1.65
K	1.43	1.22	1.67

79

79

Presentation layout

1. Introduction
2. Variability in rock type and rock mass structure
3. Effect of scale in rock behaviour
4. Estimation of rock mass properties using statistical analysis
5. Estimation of in-situ stresses
6. **Summary**

80

80

Presentation layout

Input parameter challenges

Modelling challenges

Results interpretations

- **Input Data Challenges of Rock Engineering**
- **Rock Strength**
- **Analysis of Data and Estimation of Parameters**
- **The reliability of results must be verified by judgement and experience**

81

81

Geotechnical Model

Input

Geological Model
- Lithology
- Alteration
- Mineral zones
- Seismic coefficient
- Stress state

Structural Model
- Major Structures
  - Bedding
  - Folds
  - Faults
- Minor structures
  - Minor faults
  - Joints

Rockmass Model
- Intact rock strength
- Strength of structures
- Rockmass classification
- Rockmass strength

Hydrogeological Model
- Hydrogeological units
- Hydraulic conductivities
- Flow regimes
- Phreatic surfaces
- Pore pressure distribution

output

Geotechnical Model
- Geotechnical domains and associated properties, including:
  - Material distribution
  - Structural anisotropy
  - Strength parameters
  - Hydrogeological factors (drainability)

82

82

Precision vs. Accuracy

High Accuracy High Precision | Low Accuracy High Precision | High Accuracy Low Precision | Low Accuracy Low Precision

- Precision--Precision is a measure of the repeatability of a set of measurements. When a set of measurements of the same quantity are all close together then the data are precise. If a set of measurements vary widely then they are imprecise.
- Accuracy --Accuracy is a measure of the truth of an experimental result. It must be measured against a known and trusted standard.

83

83

Garbage in – Garbage out Paradigm

Garbage In -> Garbage Out Paradigm

Garbage Data →	Good Model →	Garbage Results
Good Data →	Garbage Model →	Garbage Results
Garbage Data →	Garbage Model →	Disaster
Good Data →	Good Model →	Good Results

84

84

Approaches to reduce data uncertainty

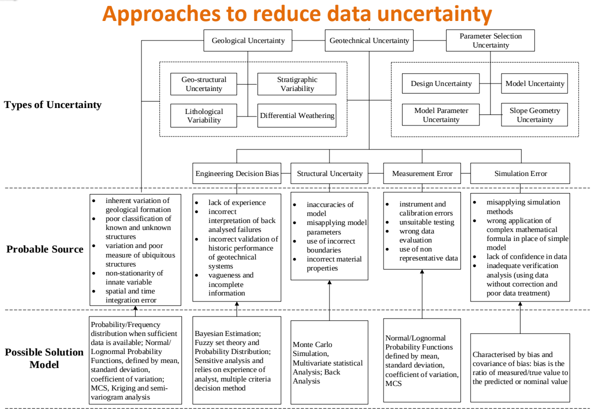

Abdulai, Sharifzadeh, 2018

Garbage in garbage out (GIGO) paradigm

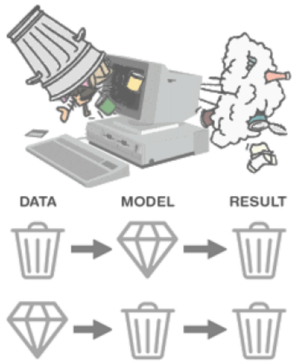

Levels of geotechnical investigation effort by mining project Stages

	PROJECT STAGE				
Project level status	Conceptual	Pre-feasibility	Feasibility	Design and Construction	Operations
Geotechnical level status	Level 1	Level 2	Level 3	Level 4	Level 5
Geological model	Regional literature; advanced exploration mapping and core logging; database established; initial country rock model	Mine scale outcrop mapping and core logging; enhancement of geological database; initial 3D geological model	Infill drilling and mapping; further enhancement of geological database and 3D model	Targeted drilling and mapping; refinement of geological database and 3D model	Ongoing pit/underground mapping and drilling; further refinement of geological database and 3D model
Structural model (major features)	Aerial photos and initial ground proofing	Mine scale outcrop mapping; targeted oriented drilling; initial structural model	Trench or exploration mapping; infill oriented drilling; 3D structural model	Refined interpretation of 3D structural model	Structural mapping on all pit benches / working levels; further refinement of 3D model
Structural model (fabric)	Regional outcrop mapping	Mine scale outcrop mapping; targeted oriented drilling; database established; initial stereographic assessment of fabric data; initial structural domains established	Infill trench mapping and oriented drilling; enhancement of database; advanced stereographic assessment of fabric data; confirmation of structural domains	Refined interpretation of fabric data and structural domains	Structural mapping on all pits, benches / Underground excavations, drifts, cross cuts, ore drive; further refinement of fabric data and structural domains
Hydrogeological model	Regional groundwater survey	Mine scale airlift, pumping and packer testing to establish initial hydrogeological parameters; initial hydrogeological database and model stablished	Targeted pumping and airlift testing; piezometer installation; enhancement of hydrogeological database and 3D model; initial assessment of depressurisation and dewatering requirements	Installation of piezometers and dewatering wells; refinement of hydrogeological database, 3D model, depressurisation and dewatering requirements	Ongoing management of piezometer and dewatering well network; continued refinement of hydrogeological database and 3D model
Intact rock strength	Literature values supplemented by index tests on core from geological drilling	Index and laboratory testing on samples selected from targeted mine scale drilling; database established; initial assessment of lithological domains	Targeted drilling and detailed sampling and laboratory testing; enhancement of database; detailed assessment and establishment of geotechnical units for 3D geotechnical model	Infill drilling, sampling and laboratory testing; refinement of database and 3D geotechnical model	Ongoing maintenance of database and 3D geotechnical model
Strength of structural defects	Literature values supplemented by index tests on core from geological drilling	Laboratory direct shear tests of saw cut and defect samples selected from targeted mine scale drill holes and outcrops; database established; assessment of defect strength within initial structural domains	Targeted sampling and laboratory testing; enhancement of database; detailed assessment and establishment of defect strengths within structural domains	Selected sampling and laboratory testing and refinement of database	Ongoing maintenance of database
Geotechnical characterisation	Pertinent regional information geotechnical assessment of advanced exploration data	Assessment and compilation of initial mine scale geotechnical data; preparation of initial geotechnical database and 3D model	Ongoing assessment and compilation of all new mine scale geotechnical data; enhancement of geotechnical database and 3D model	Refinement of geotechnical database and 3D model	Ongoing maintenance of geotechnical database and 3D model

(Modified after Stacy, 2009)

Geotechnical model components and minimum contents at each component and target level of data confidence by mining project Stages

		PROJECT STAGE / LEVEL OF CONFIDENCE				
Project level status		Conceptual	Pre-feasibility	Feasibility	Design and Construction	Operations
Component/level	Description	Level 1: Based on assumed and factored data (Analogy & Synthesis)	Level 2: Based on some engineering investigation and test (Synthesis & Experience)	Level 3: Based on sound engineering investigation and test (Fully supported synthesis)	Level 4: Based on sound engineering investigation, test and additional investigation (comprehensively supported by synthesis)	Level 5: Based on during operation measurements, tests and back analysis (synthesis verified by monitoring)
Geological model	The geological model generally consists of the lithology, alteration, weathering, mineralised zones and the in situ stress state. The reliability of boundaries between zones is a key issue.	>50%	50-70%	65-85%	80-90%	>90%
Structural model	Consists of the major structures (large faults, bedding and folds) and minor structures or fabric (joints and minor faults). The reliability of the location of major structures is a key issue as these often play a significant role in controlling instability.	>20%	40-50%	45-70%	60-75%	>75%
Hydrogeological model	The hydrogeological model consists of hydrogeological units, hydraulic conductivities, flow regimes, phreatic surfaces and the pore pressure distribution, and water quality distribution.	>20%	30-50%	40-65%	60-75%	>75%
Rock mass model	The rock mass model consists of the intact rock strength, defect shear strength, rock mass strength and rock mass classification. These are used to determine the input parameters for geotechnical analyses thus having an understanding of their variability and reliability is	>30%	40-65%	60-75%	70-80%	>80%
Geotechnical domains	Geotechnical or geomechanical domains that exhibit similar rock mass and structural characteristics. Geotechnical domains form the basis of geotechnical design sectors or areas.	>30%	40-60%	50-75%	65-85%	>80%

Thank you for your attention and

Questions are welcome!

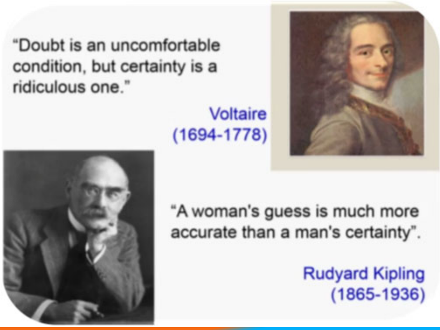

References

1. Wawersik WR and C Fairhurst 1970. A study of brittle rock fracture in laboratory compression experiments. Int. J. of Rock Mechanics and Mining Sciences, 7(5): 561–575.
2. Grand Challenges and Earth Resources Engineering, 2010. National academy of engineering, USA.
3. Farahmand K. 2017. Characterization Of Rockmass Properties And Excavation Damage Zone (Edz) Using A Synthetic Rock Mass (Srm) Approach, PhD Thesis, Queen's University.
4. Abdulai M., Sharifzadeh M., (2018) Uncertainty and Reliability Analysis of Open Pit Rock Slopes: A Critical Review of Methods of Analysis, Geotech Geol Eng (2018).
5. Rahimi B, Shahriar K., Sharifzadeh M., (2014). "Evaluation of Rock Mass Engineering Geological Properties Using Statistical Analysis and Selecting Proper Tunnel Design Approach in Qazvin–Rasht Railway Tunnel", Tunnelling and Underground Space Technology 41 (2014) 206–222,
6. Manuchehrian A., Sharifzadeh M., Hamidzadeh M. R. (2012) "Application Of Artificial Neural Networks And Multivariate Statistics To Estimate UCS Using Textural Characteristics", International Journal of Mining Science and Technology 22 (2012
7. Sharifzadeh M., Feng XT, Zhang X., Qiao L., Zhang Y., (2017) Challenges in multi-scale hard rock behaviour evaluation at deep underground excavations P18, Keynote lecture in 12th Iranian and 3rd regional tunneling conference, Tunnelling and Climate Change, 27-29 NOV, 2017, Tehran Iran.
8. Hoek E. & Bieniawski Z.T. 1965. Brittle rock fracture propagation in rock under compression. International Journal of Fracture Mechanics, 1: 137-155.
9. Kaiser P.K. & Kim B. 2008. Rock mechanics challenges in underground construction and mining, In: Proc. 1st Southern Hemisphere International Rock Mechanics Symposium, 1: 3-38.
10. Ortlepp, W.D., and Stacey, T.R. 1994. Rockburst mechanisms in tunnels and shafts. Tunnelling and Underground Space Technology, 9(1): 59–65. doi:10. 1016/0886-7798(94)90010-8.
11. Kamali B. A., Shahriar K., Sharifzadeh M. & Marefvand P.(2018) Validation of 3D discrete fracture network model focusing on areal sampling methods-a case study on the powerhouse cavern of rudbar lorestan pumped storage power plant, Iran, Geomechanics and Engineering, Vol. 16, No. 1 (2018) 21-34,

References

15. Vakili, A., Sandy, M., & Albrecht, J. 2013. Interpretation of non-linear numerical models in Geomechanics – a Case Study in the Application of numerical modelling for Raise Bored Shaft Design in a Highly Stressed and Foliated Rock Mass. Yet to be published.
16. Sandy, M., Sharrock, G., Albrecht, J., Vakili, A. 2010. Managing the Transition from low Stress to High Stress Conditions. Proceedings from Second Australasian Ground Control in Mining Conference, Sydney.
17. Capes, G. W., Sharrock, G. B. and Lowther, R. J. 2012. Methodology for Understanding Drive Deformation and Damage in Variable Rock Types in a High Stress, Advanced Undercut. MassMIN 2012 Conference Proceedings. MassMin 2012: 6th International Conference and Exhibition on Mass Mining, Sudbury, Ontario, Canada.
18. Lowther, R. J., Capes, G. W., Sharrock, G. B. 2010. A deformation monitoring plan for extraction level drives at Ridgeway Deeps block cave mine. Proceedings of the Second International Symposium on Block and Sublevel Caving. Edited by Y. Potvin. Australian Centre for Geomechanics, Perth, ISBN: 978-0-9806154-1-8.
19. Cho, N. Martin, C.D. Sego, D.C. 2007. A clumped particle model for rock. Int. J. Rock Mech. Min. Sci. 44, 997-1010.
20. Potyondy, D.O. Cundall, D.O. 2004. A bonded-particle model for rock. Int. J. Rock Mech. Min. Sci. 41, 1329-1364.
21. Perras, M.A. Diederichs, M.S. Lam, T. 2010. A review of excavation damage zone in sedimentary rocks with emphasis on numerical modelling for EDZ definition. Proc. 63rd Canadian Geotechnical Conference, Calgary, Canada.
22. Ghazvinian, E. Diederichs, M.S. 2010a. A comparison between application of two and three dimensional bonded-particle models for simulation of damage accumulation in rock. Proc. Eurock 2010, Lausanne, Switzerland.
23. Ghazvinian, E. Diederichs, M.S. 2010b. Effect of clumping and clustering on more realistic behaviour of bonded-particle model. Proc. 63rd Canadian Geotechnical Conference, Calgary, Canada.
24. Diederichs, M.S. Carvalho, J.L. Carter, T.G. 2007. A modified approach for prediction of strength and post yield behaviour for high GSI rockmasses in strong, brittle ground. Proc. 1st Can-US Rock Symposium. Meeting Society's Challenges and Demands. Vancouver. pp. 277-298.
25. Aglawe J. P. 1999. Unstable and Violent Failure around Underground Openings in Highly Stressed Ground. PhD Thesis, Queen's University, Canada.

End of presentation:
Diagnosis of problem and selecting right tools to solve

International Journal of Mining Science and Technology 22 (2012) 229–236

Contents lists available at SciVerse ScienceDirect

International Journal of Mining Science and Technology

journal homepage: www.elsevier.com/locate/ijmst

Application of artificial neural networks and multivariate statistics to estimate UCS using textural characteristics

Amin Manouchehrian [a], Mostafa Sharifzadeh [b,*], Rasoul Hamidzadeh Moghadam [a]

[a] Department of Mining Engineering, Sahand University of Technology, Tabriz, Iran
[b] Department of Mining, Metallurgy and Petroleum Engineering, Amirkabir University of Technology, Tehran, Iran

A R T I C L E   I N F O

Article history:
Received 2 July 2011
Received in revised form 24 July 2011
Accepted 21 August 2011
Available online 23 March 2012

Keywords:
Textural characteristics
Uniaxial compressive strength
Predictive models
Artificial neural networks
Multivariate statistics

A B S T R A C T

Before any rock engineering project, mechanical parameters of rocks such as uniaxial compressive strength and young modulus of intact rock get measured using laboratory or in-situ tests, but in some situations preparing the required specimens is impossible. By this time, several models have been established to evaluate UCS and *E* from rock substantial properties. Artificial neural networks are powerful tools which are employed to establish predictive models and results have shown the priority of this technique compared to classic statistical techniques. In this paper, ANN and multivariate statistical models considering rock textural characteristics have been established to estimate UCS of rock and to validate the responses of the established models, they were compared with laboratory results. For this purpose a data set for 44 samples of sandstone was prepared and for each sample some textural characteristics such as void, mineral content and grain size as well as UCS were determined. To select the best predictors as inputs of the UCS models, this data set was subjected to statistical analyses comprising basic descriptive statistics, bivariate correlation, curve fitting and principal component analyses. Results of such analyses have shown that void, ferroan calcitic cement, argillaceous cement and mica percentage have the most effect on USC. Two predictive models for UCS were developed using these variables by ANN and linear multivariate regression. Results have shown that by using simple textural characteristics such as mineral content, cement type and void, strength of studied sandstone can be estimated with acceptable accuracy. ANN and multivariate statistical UCS models, revealed responses with 0.87 and 0.76 regressions, respectively which proves higher potential of ANN model for predicting UCS compared to classic statistical models.

1. Introduction

In many rock engineering projects, the uniaxial compressive strength of intact rock (UCS) is not measured by laboratory tests, because performing such tests needs high quality samples and sophisticated equipments. In many situations it is too difficult to prepare standard core samples from weak, stratified (thinly bedded), highly fractured and block-in-matrix rocks. For solving this problem which arises during the core sample preparation, some predictive models considering simple index parameters such as Schmidt hammer, point load, block punch, and physical and petrographical properties were developed by many researchers [1–8], because these index tests require relatively small samples when compared with the uniaxial compressive strength test samples. Despite some deficiencies, index tests, when coupled with experienced judgment, can provide initial estimate of rock properties required at the feasibility and design stage.

As view of structural point, rock is the combination of some minerals and the cement exist between them which various combinations of them forms rocks with various properties (physical properties, chemical properties, mechanical properties, magnetic properties, etc). Mechanical properties of rocks are a function of its structure such as mineral content, porosity, number of weak planes and texture of itself. In fact, mineral content and porosity explain the genus of forming materials and their packing density, quality of structural materials will be explained by considering the number of micro cracks exist in the body of rock and configuration of forming materials and their linkage will be explained by texture of rock. By knowing these three parameters, mechanical properties of every composite material will be recognized more accurately.

In recent years, many researchers have focused on the relationship between textural and mechanical properties [1,5,9–13]. Results have shown that mechanical properties of rocks are a function of the

* Corresponding author. Tel.: +98 (21) 6454 2952.
E-mail address: sharifzadeh@aut.ac.ir (M. Sharifzadeh).

2095-2686/$ - see front matter © 2012 Published by Elsevier B.V. on behalf of China University of Mining & Technology.
doi:10.1016/j.ijmst.2011.08.013

textural properties. These research results show that mechanical properties of rock depends on its textural characteristics and most effective parameters are mineral content, grain size, grain shape and porosity. Thus some researchers by using classic statistical methods and recently by developing intelligent techniques, by using them have established models based on textural characteristics to estimate mechanical parameters of rock [1,14–19]. In these models textural characteristics were chosen as inputs of models which were not easy to determine. So these models didn't become popular ones.

Singh et al. (2001) employed ANN to estimate mechanical parameters of rock. In their studies they used parameters as inputs of predictive models which were not simple to determine and needed to use up much time and use specific equipments [16]. Also Tamrakar et al. (2007) established models to estimate mechanical parameters of sandstone which their studies suffered from the above problem [17].

In this paper, two ANN and multivariate statistical models are presented which have potential of predicting UCS with acceptable accuracy using some simple textural parameters. This ease of use can cause popularity of this method for estimating different parameters of rocks such as mechanical properties, physical properties, magnetic properties, etc.

2. Siwalik sandstone

Analyses that were carried out in this study on the relationships between UCS and rock textural characteristics have been based on the data obtained by Tamrakar et al. (2007) [17]. They tried to find relationships among mechanical, physical and petrographic properties of Siwalik sandstones, central Nepal sub-Himalayas by performing statistical analyses. Textural configurations and UCS of studied samples are summarized in Table 1. Also two representative thin-section images of studied samples are shown in Fig. 1.

Petrographic analyses have shown that quartz, feldspar and lithic fragments vary from 32% to 66%, 3% to 16% and 0 to 24%, respectively in these samples (Table 1). Quartz is mostly undulosed monocrystalline to polycrystalline, and some are non-undulosed. Feldspar is both K-feldspar and plagioclase. Lithic fragments are often quartz-mica tectonite, quartz-mica aggregate, quartz-mica-feldspar aggregate, and argillite-shale. Among the micas, biotite and muscovite are substantial whilst chlorite is minor. Heavy minerals form minor constituents in sandstones. Matrix forms 0% to 18% and occurs as primary and secondary alteration products. Total cement ranges between 6% and 41%. Ferroan calcitic cement occurs as pore occluding, replacing and fracture-filling cements. Besides, ferruginous and argillaceous cements occur as grain coats and

Table 1
Some properties of the rock samples.[17]

No.	Q (%)	Fl (%)	Cfc (%)	Cf (%)	Cs (%)	Ca (%)	M (%)	n (%)	Mx (%)	L (%)	Mz (mm)	UCS (MPa)
1	49	6	1	0	7	8	1	9	12	7	2.13	7.9
2	52	5	7	10	6	3	2	7	3	4	2.11	11.2
3	48	14	0	1	3	3	4	4	17	5	2.8	12.6
4	32	9	10	1	7	8	15	4	9	2	3.01	51.6
5	55	4	3	3	2	1	3	4	12	9	1.74	28.8
6	41	7	0	0	15	5	18	1	11	1	2.97	49.8
7	66	5	9	1	3	3	3	1	5	3	2.55	47.5
8	59	3	0	10	6	3	2	5	5	7	2.15	29.4
9	32	8	0	2	4	15	15	8	13	2	3.12	28.7
10	36	8	2	1	5	9	8	9	16	5	2.64	18.5
11	50	12	0	0	5	7	5	9	9	2	2.77	12.6
12	39	9	0	2	2	2	16	10	18	1	2.76	34.8
13	53	6	0	4	6	8	3	5	10	4	2.54	29.3
14	48	10	0	14	5	4	3	6	8	2	2.44	15.2
15	37	13	2	8	5	14	3	8	6	4	2.58	1.29
16	54	8	1	1	4	5	3	7	5	11	1.53	9.57
17	41	8	21	1	0	1	5	6	2	14	1.44	19
18	31	12	32	0	0	0	8	4	1	10	1.96	32.2
19	44	6	24	4	1	3	4	6	4	4	2.07	9
20	34	8	28	1	1	0	5	1	1	20	1.72	19.2
21	36	8	25	0	0	0	2	7	1	20	0.95	21.8
22	23	3	34	3	3	1	19	4	10	0	2.74	31.9
23	38	7	23	0	0	0	3	3	1	1	0.78	42.7
24	32	15	14	7	0	1	12	5	2	1	0.99	9.8
25	34	16	14	0	0	0	8	6	2	2	0.99	21.4
26	27	9	21	2	0	2	11	9	3	1	1.08	24
27	28	9	29	0	0	0	12	12	6	3	1.22	11.7
28	40	8	31	0	0	0	2	1	1	2	1.05	48.4
29	38	8	27	0	0	0	7	7	1	2	1.01	15.4
30	27	11	33	0	0	1	9	2	2	1	1.05	33.4
31	35	7	32	0	0	1	4	3	1	1	0.99	36.4
32	35	8	30	0	0	1	10	3	1	2	1.07	24
33	37	8	30	0	0	1	5	8	1	3	0.94	8.2
34	29	14	37	0	0	1	7	1	1	2	1.05	48.4
35	35	8	34	0	0	1	6	2	1	1	0.87	25
36	35	7	31	0	0	0	9	6	1	1	0.77	27.8
37	32	10	33	0	0	1	9	3	1	1	0.88	27.9
38	30	15	34	1	0	0	8	1	1	2	0.77	41.4
39	38	12	29	0	0	0	6	2	1	4	1.16	40.4
40	33	12	31	0	0	1	5	1	1	3	0.84	31.6
41	42	11	27	0	0	1	3	2	1	9	0.91	38.5
42	34	11	32	0	0	0	6	1	1	3	0.96	48.4
43	35	9	33	0	0	0	6	1	3	3	0.99	43.2
44	32	7	26	1	0	1	9	8	3	2	0.86	7.9

Note: Q, Quartz; Fl, Feldspar; M, Mica; Cfc, Ferroan calcitic cement; Cf, Ferruginous cement (brown to reddish brown iron hydroxides); Cs, Siliceous cement; Ca, Argillaceous cement; n, Void; Mx, Matrix; L, Lithic fragments; Mz, Mean grain size; UCS, Uniaxial compression strength.

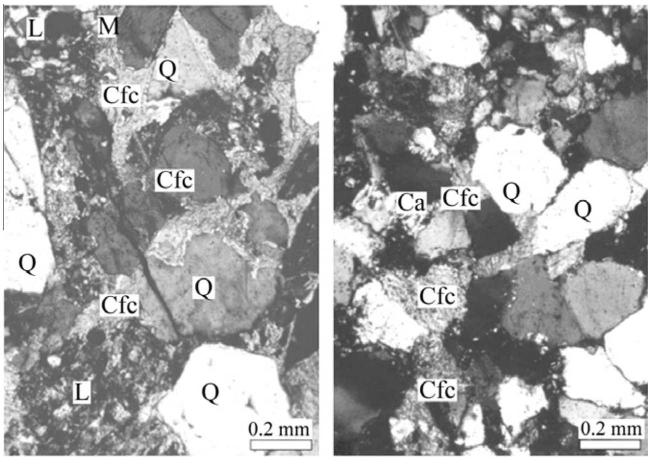

Fig. 1. Representative thin-section images of Siwalik sandstone [17].

isolated patches in some sandstone. Optical void (hereafter-void) ranges between 1% and 12% of the modal composition. Voids are mainly intergranular and rarely intragranular. Besides, secondary voids are also found; grain fracture, rock fracture and dissolution [17].

3. Statistical analyses on experimental data

There are many textural characteristics which can be determined in petrographical studies but for establishing predictive models it's needed to define dominant independent variables on the target dependant variables. For this purpose, statistical analyses can be helpful. Statistical analyses which were done in this study on the relationships between mechanical properties of rock and textural characteristics of rock have been based on the data obtained from analyzing Siwalik sandstone.

In this study, just textural characteristics are used which have easy determining technique. Thus considered textural parameters here consist of mineral content, void and grain size for evaluating UCS. A data matrix has been built using observations belonging to 44 rocks (Table 1).

In this study some data analyses including basic descriptive statistics, bivariate correlation, curve fitting and principal component analyses has been applied to data set.

Original data set was subjected to bivariate correlation. This analysis was aimed to determine the independent variables affecting UCS more than the others do, for recognizing the relationships between UCS and other textural characteristics of rock. After selecting the model parameters, two ANN and statistical models of UCS were built in following section of artificial neural networks and multivariate statistics in this paper.

Domains of measurements variation in the original data set are shown in Fig. 2. The boxplot of the original data set which is shown in Fig. 2 shows that for the most of the data groups, the median is not in the center of the box, which indicates that data for most of measurements are not symmetric.

To visualize relationship between USC and each measured textural characteristics and its trend, scatterplot of UCS against each of them were plotted (Fig. 3). Fig. 3 indicates that USC of studied sandstone have more relationship with void and Cfc than the others.

Bivariate correlation analysis was carried out to recognize relation between every single parameter (Table 2 and Fig. 4). Results of bivariate correlation analysis show that UCS is most correlated with void, Cf (ferruginous cement), Cfc (ferroan calcitic cement), Ca (argillaceous cement), mica and lithic fragments. The other variables do not have any significant correlation with UCS. It means these six textural characteristics affect UCS more than the others do.

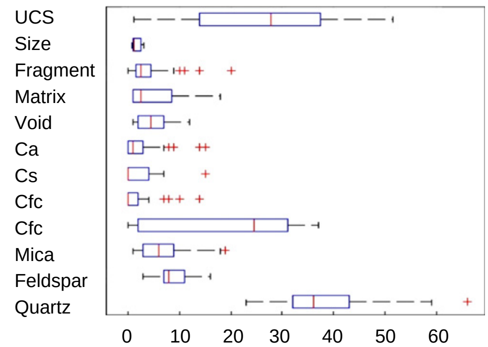

Fig 2. Boxplot of variation of measured data.

Beside, to recognize potential of predicting UCS by each single textural parameter, curve fitting was applied to data set. For this purpose, all the nonlinear models along with the linear model were tried to fit the data to establish bivariate regression models for UCS using each independent variable, so the goodness of fit statistics have been used. Sum of squares due to error (SSE), root mean squared error (RMSE), the coefficient of determination (R^2), and the adjusted R^2 were used as the numerical measures of the goodness of the fit for bivariate regression models. R^2 is the square of the correlation between the response values and the predicted response values. A value closer to 1 indicates that a greater proportion of variance is accounted for by the model. Adj-R^2 is the degrees of freedom adjusted R-square. A value closer to 1 indicates a better fit. SSE measures the total deviation of the response values from the fitted values of the response values. It is also called the summed square of residuals. A SSE value closer to zero indicates a better fit. RMSE is also known as the fit standard error and the standard error of the regression. An RMSE value closer to zero indicates a better fit [20]. Models fitting the data best for the predictions of UCS are given in Table 3.

Measurements collected in a series of variables in a data set may be strongly correlated. Such measurements may also be regarded as expressing two or more fundamental aspects of a single parameter. Principal components analysis is an effective method to check if a data set is suffering from the above problem. It is also a quantitatively rigorous method for achieving necessary simplification of the data sets having that problem. The method generates a new set of variables, called principal components. Each principal component is a linear combination of the original variables. All the principal components are orthogonal to each other, so there is no redundant information. The full set of principal components is as large as the original set of variables. However, it is commonplace for the sum of the variances of the first few principal components to exceed 80% of the total variance of the original data [20].

A principal components analysis has been applied on the original data set. The coefficients for twelve principal components are given in Table 4. The columns in Table 4 are in order of decreasing component variance. The absolute largest coefficients in the first principal component are mainly Cfc, Ca, matrix, grain size and Cs. This means that the principal component with the highest variance is mainly weighted on Cfc, Ca, matrix, grain size and Cs. All coefficients of the first principal component have proper signs, making it a weighted average of all the original variables. The second principal component is mainly weighted on mica, third component is weighted on UCS and void and fourth component is weighted on Cf and lithic fragments.

The variance explained by each principal component is given in Table 5. It shows that the most of the variance (78%) in data set can

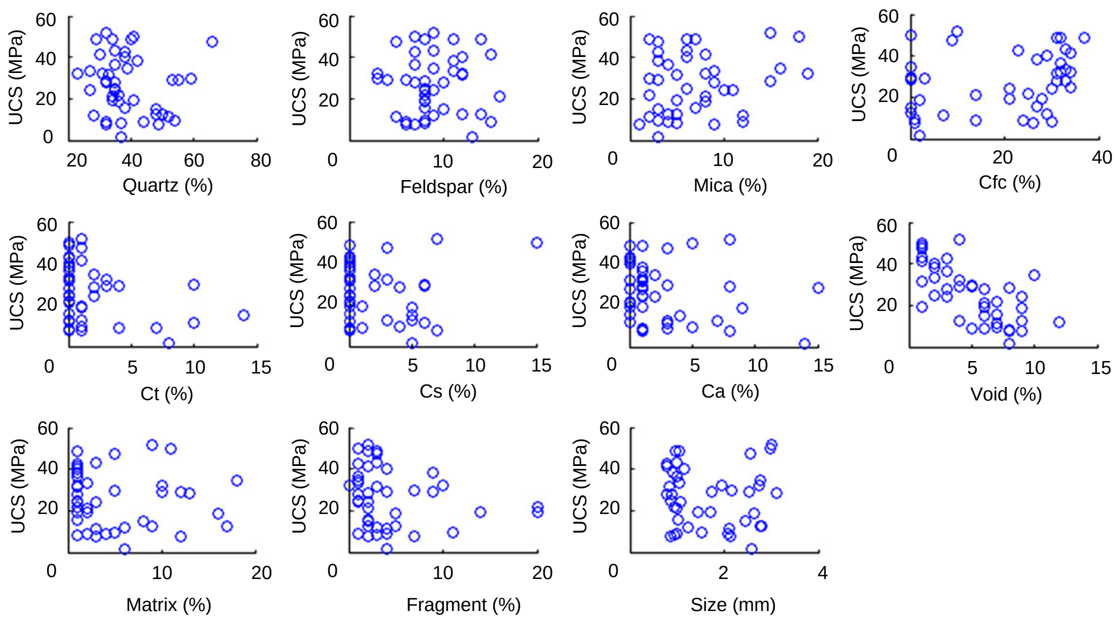

Fig. 3. Scatterplots of UCS against the textural characteristics of rock.

Table 2
Correlation coefficients for original data set.

Parameter	UCS	Void	Cf	Cfc	Ca	Mica	Fragment	Quartz	Matrix	Size	Cs	Feldspar
UCS	1	−0.7	−0.34	0.29	−0.24	0.22	−0.21	−0.13	−0.12	−0.07	0	0
Void	−0.7	1	0.22	−0.44	0.39	0.1	0.02	0.05	0.41	0.27	0.14	−0.14
Cf	−0.34	0.22	1	−0.48	0.29	−0.18	−0.04	0.36	0.18	0.37	0.35	−0.15
Cfc	0.29	−0.44	−0.48	1	−0.7	0.07	−0.06	−0.65	−0.76	−0.76	−0.75	0.16
Ca	−0.24	0.39	0.29	−0.7	1	0.07	−0.07	0.23	0.6	0.72	0.64	−0.07
Mica	0.22	0.1	−0.18	0.07	0.07	1	−0.42	−0.59	0.28	0.24	0.16	0.06
Fragment	−0.21	0.02	−0.04	−0.06	−0.07	−0.42	1	0.22	−0.09	−0.01	−0.05	−0.12
Quartz	−0.13	0.05	0.36	−0.65	0.23	−0.59	0.22	1	0.3	0.39	0.44	−0.39
Matrix	−0.12	0.41	0.18	−0.76	0.6	0.28	−0.09	0.3	1	0.82	0.62	−0.19
Size	−0.07	0.27	0.37	−0.76	0.72	0.24	−0.01	0.39	0.82	1	0.77	−0.25
Cs	0	0.14	0.35	−0.75	0.64	0.16	−0.05	0.44	0.62	0.77	1	−0.3
Feldspar	0	−0.14	−0.15	0.16	−0.07	0.06	−0.12	−0.39	−0.19	−0.25	−0.3	1

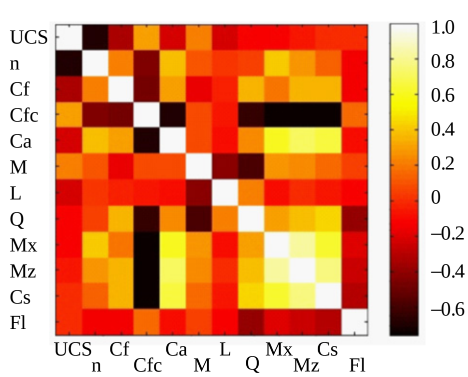

Fig. 4. Correlation matrix for original data set.

be explained by only four principal components with three first principal components account for the highest percent of the total variance (70%) (Fig. 5). This indicates that data set is mainly driven by independent variables of void, Ca, matrix, grain size, Cs, mica, UCS and void. Therefore, it was decided to consider void, Cfc, Ca and mica percentages as the predictors in the ANN and statistical models for UCS, also considering the scatterplots and correlation analyses.

4. Analysis using artificial neural networks

A neural network is a massively parallel-distributed processor that has a natural propensity for storing experiential knowledge and making it available for use. Because of its ability to learn and generalize interactions among many variables, artificial neural

Table 3
Best bivariate regressions for UCS.

Predictor	R^2	Adj-R^2	RMSE	Regression model
Void	0.54	0.52	9.613	UCS = 3680void^2 − 711.6void + 49.19
Cfc	0.203	0.143	12.92	UCS = 4401Cfc^3 − 2121Cfc^2 + 268Cfc + 18.66

Table 4
Coefficients for the principal components.

Parameter	Principal component											
	1st	2nd	3rd	4th	5th	6th	7th	8th	9th	10th	11th	12th
UCS	0.15	−0.3	0.6	−0.01	0.06	−0.02	0.05	−0.27	0.64	−0.07	0.18	−0.05
Void	−0.23	0.05	−0.59	0.25	−0.12	−0.22	0.04	0.02	0.55	0.04	0.39	−0.12
Cf	−0.24	0.19	−0.06	−0.49	−0.46	0.56	0.16	−0.22	0.14	−0.11	−0.02	−0.15
Cfc	0.43	−0.05	−0.02	0.12	−0.14	0.12	−0.2	−0.15	−0.3	0.05	0.44	−0.64
Ca	−0.36	−0.13	−0.08	−0.13	0.22	−0.03	−0.74	−0.29	0.08	0.08	−0.29	−0.23
Mica	−0.01	−0.62	−0.13	0.21	−0.13	0.29	0.22	0.24	0.08	0.37	−0.39	−0.23
Fragment	−0.01	0.43	0.03	0.43	0.52	0.55	0.08	−0.02	0.15	−0.01	−0.08	−0.12
Quartz	−0.27	0.4	0.34	−0.08	−0.05	−0.37	0.22	0.15	0.02	0.46	−0.12	−0.46
Matrix	−0.38	−0.23	−0.01	0.17	0.15	−0.19	0.42	−0.35	−0.26	−0.51	−0.07	−0.29
Size	−0.41	−0.18	0.12	0.05	0.12	0.18	0.07	−0.25	−0.28	0.5	0.5	0.3
Cs	−0.38	−0.14	0.25	−0.02	0.02	0.16	−0.21	0.7	−0.03	−0.34	0.3	−0.13
Feldspar	0.15	−0.14	−0.25	−0.63	0.61	−0.01	0.23	0.13	0.06	0.08	0.14	−0.16

Table 5
Variance explained by each principal component.

Principal component	Variance	Variance explained (%)
1	4.7	38.9
2	2.1	17.3
3	1.6	13.4
4	1	8
5	0.9	7.5
6	0.6	5
7	0.4	3.7
8	0.3	2.4
9	0.2	1.7
10	0.1	1.1
11	0.1	0.9
12	0	0.2

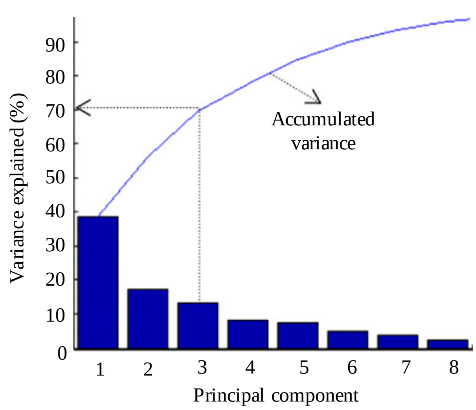

Fig. 5. Percent variability explained by the first eight principal components.

networks technology has been reported to be very useful in modeling the rock material behavior by many researchers [21,22].

Meulenkamp and Alvarez Grima (1999) investigated the possibility of predicting UCS by ANN from rock hardness information using Equotip hardness tester and other intact rock properties. Their study indicated that ANN technology was more powerful than conventional statistical techniques in predicting UCS from intact rock properties [23]. Studies of Singh et al. (2001) in developing predictive models for UTS, UCS, and axial point load strength from the intrinsic rock properties revealed that using ANN in building these models was more accurate than using conventional statistical techniques [16].

Feed-forward back propagation network was chosen to build the prediction models for UCS in this study, which is a two-layer network with tangent sigmoid transfer function neurons in the hidden layer and a pure linear transfer function neuron corresponding to UCS in the output layer. Also, the input layer had four neurons corresponding to four independent variables of void, Cfc, Ca and mica percentage. This network architecture is shown in Fig. 6.

Above network architecture is known as a useful neural network structure for function approximation or regression problems. Back propagation was created by generalizing the Widrow-Hoff learning rule to multiple-layer networks and nonlinear differentiable transfer functions. Standard back propagation is a gradient descent algorithm, as is the Widrow-Hoff learning rule, in which the network weights are moved along the negative of the gradient of the performance function. The term back propagation refers to the manner in which the gradient is computed for nonlinear multilayer networks. Properly trained back propagation networks were reported to tend to give reasonable answers when presented with inputs that they have never seen [20].

The multilayer feed-forward network is the most commonly used network architecture with the back propagation algorithm. Feed-forward networks often have one or more hidden layers of sigmoid neurons followed by an output layer of linear neurons. Multiple layers of neurons with nonlinear transfer functions allow the network to learn nonlinear and linear relationships between input and output vectors. Tangent sigmoid nonlinear transfer function is known useful for neural networks where speed is important and the exact shape of the transfer function is not. The linear output layer lets the network produce values outside the range −1 to +1. If the last layer of a multilayer network has sigmoid neurons, then the outputs of the network are limited to a small range. If linear output neurons are used, the network outputs can take any value. Moreover, in back propagation, it is important to be able to calculate the derivatives of any transfer functions used. Each of the transfer functions mentioned above has a corresponding derivative function [20].

Determining the number of hidden layers and the appropriate number of neurons for each hidden layer are very important in architecting neural networks. Researches in this area have shown that one or two hidden layers with an adequate number of neurons are sufficient to model any solution surface of practical interest.

Previous studies in this area have also shown that the number of neurons to include in the hidden layer is a function of the

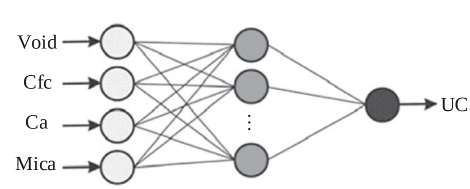

Fig. 6. Architecture of designed network.

number of training pairs available [24]. A large number of hidden layer nodes have large number of associated undetermined parameters, and if the number of training pairs is small, the network will then tend to memorize rather than generalize. Seibi and Al-Alawi (1997) pointed out that an overdetermined network should be used in order to have a good approximation over the region of interest. They suggested the following formula for calculating the appropriate number of hidden neurons to be used in a single hidden layer if the number of training pairs is known:

$$n = \theta \times (N_h \times (m+1) + p \times (N_h + 1)) \quad (1)$$

where n is the number of training pairs available; θ a constant greater than 1.0 (i.e., $\theta = 1.25$ would give a 25% overdetermined approximation); N_h the number of hidden neurons to be used in a network that has only one hidden layer; m the number of input nodes; and p the number of output nodes [24].

Using the above formula, 3.16 was obtained for N_h in this study. Thus, two ANN models with 3 and 4 neurons in the hidden layer were built. The data set was subdivided into training, validation, and test subsets. The one fourth of the data was taken for the validation set, one fourth for the test set, and one half for the training set. The sets were picked as equally spaced points throughout the data set. ANN then were trained and implemented by using MATLAB neural network toolbox using back propagation with Levenberg-Marquardt algorithm. This algorithm was chosen because it is known to be the fastest method for training moderate-sized feed-forward neural networks.

Training, validation, and test errors are shown for two ANN models in Fig. 7. The results for two model is reasonable, since the test set errors and the validation set errors have similar characteristics, and it does not appear that any significant overfitting has occurred. The network response was also analyzed for two ANN models as given in Fig. 8. It was understood from Fig. 8 that two ANN models for UCS have given predicted UCS values close to the measured ones. The correlation coefficients between observed and predicted UCS values based on 3 and 4 neuron in hidden layer ANN models are 0.82 and 0.87, respectively. Due to minute better correlation coefficient of 4 neurons in hidden layer ANN model, it's selected for the entire of the studies.

5. Analysis using multivariate statistics

For establishing multivariate statistics model, the same Input variables which were used as inputs of neural network models consist of void, Cfc, Ca and mica were used. The obtained results were used to check out the efficiency of ANN model by comparing the results.

Results of linear multivariate regression analysis resulted in an equation with the general form as shown below:

$$Y' = c + b_1x_1 + b_2x_2 + \cdots + b_nx_n \quad (2)$$

where Y' is the dependent variable, c a constant, x_1 to x_n are variables and b_1 to b_n are partial regression coefficients for x_1 to x_n.

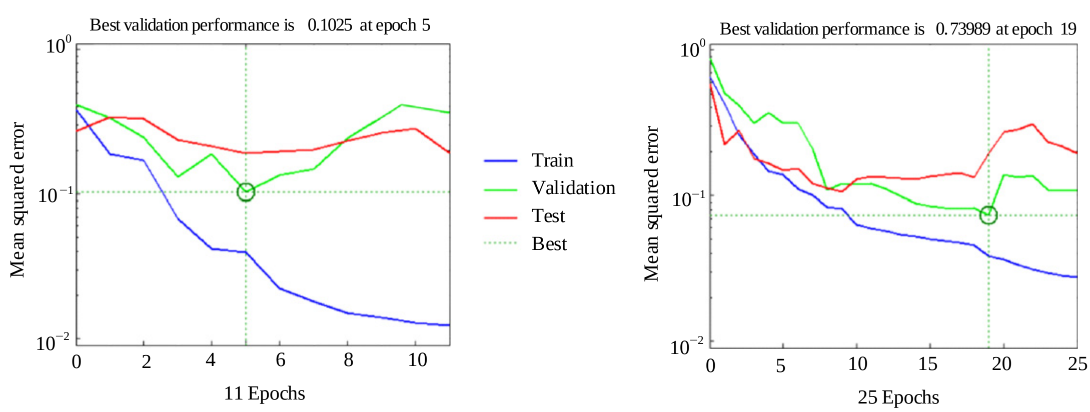

(a) Three-hidden-neuron (b) Four-hidden-neuron

Fig. 7. Network errors for three and four-hidden-neuron neural network.

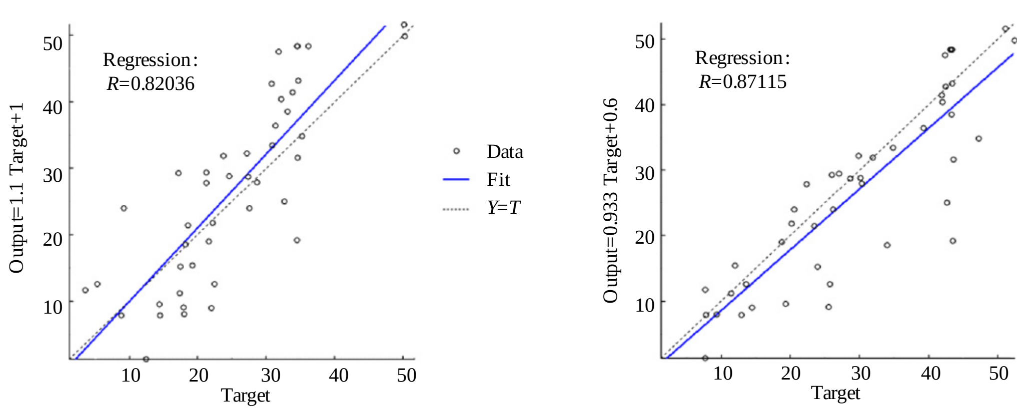

(a) Three hidden neurons (b) Four hidden neurons

Fig. 8. Scatterplot for ANN model using four hidden neurons versus observed UCS.

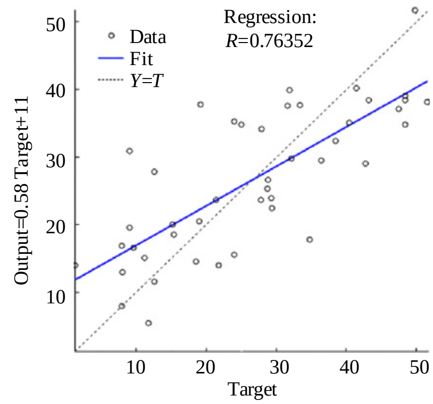

Fig. 9. Scatterplot of statistical model versus observed UCS.

Derived equation for statistical UCS model in this study is in the below form:

$$UCS = 38 - 352.26n - 5.3Cfc + 10.67Cf + 93.15M \quad (3)$$

where n is void percent, Cfc the percent ferroan calcitic cement, Cf the ferruginous cement percent and M the mica percent.

Scatterplot of estimated UCS from statistical model against observed UCS is plotted in Fig. 9. It may be noted that the incorporated independent variables might introduce multicollinearity into the model. Although multicollinearity causes problems in interpreting the regression coefficients, it does not affect the usefulness of a regression equation for prediction of new observation [25].

6. Results and discussion

In this paper artificial neural networks along with multivariate statistics were used to establish UCS models. According to the results of statistical analyses, there are statistically meaningful relationships between UCS and void, ferroan calcitic cement (Cfc), ferruginous cement (Cf) and mica percentage. The models of ANN and multivariate statistics for the prediction of the UCS were then constructed using four inputs and one output. Investigation of revealed results indicates that ANN models are more powerful than statistical models. Results of two ANN and statistical models are shown in Table. 6.

Tamrakar et al. (2007) performed statistical analyses to find relationship among mechanical, physical and petrographic properties of same samples which were used in this study. In spite of using complex input variables which are not easy to determine in their models, their results had lower accuracy in comparison with results obtained here.

In this study the textural characteristics were chosen as input of neural networks which can be determined so easier than ones used in previous models based on textural characteristics. This convenience and acceptable accuracy can increase the use of this method for evaluating mechanical properties of rock.

Considering ease of use and low expense of such studies, employing this method for evaluating mechanical properties of rock in preliminary phase of rock engineering projects will save money and time intensively.

Table 6
Comparison of results of established models in this study.

Model	R	R^2	Adj-R^2	RMSE	SSE
ANN	0.87	0.7663	0.7498	6.23	1846
Multiple linear regression	0.76	0.5692	0.5587	7.039	2031

7. Conclusions

In this study artificial neural networks along with multivariate statistics have been employed to predict UCS from textural properties of rocks. The following results and conclusions can be drawn from the present study of building predictive models of UCS:

(1) Principal components analysis has shown that principal component with the highest variance is weighted on void, ferroan calcitic cement, argillaceous cement, siliceous cement, mica, grain size, matrix and UCS. Also bivariate correlation analysis and scatterplots revealed that void, ferroan calcitic cement, Ferruginous cement, argillaceous cement, rock fragments and mica percentage are the most correlated independent variables with UCS. Thus void, ferroan calcitic cement, argillaceous cement and mica percentage were chosen as input of the established neural networks.
(2) In previous UCS models, textural characteristics were used as input of model which determination of them is difficult and needs more expensive equipments. This study have shown by carrying out proper statistical analyses, simple textural characteristics but dominant ones on the UCS which predict UCS with acceptable accuracy can be defined. This can reduce popularity of this technique for evaluating mechanical properties of rock from textural characteristics.
(3) A large number of hidden layer nodes have large number of associated undetermined parameters, and if the number of training pairs is small, the network will then tend to memorize rather than generalize. An over determined network could be used in order to have a good approximation over the region of interest.
(4) Bivariate correlation, bivariate linear regression, and curve fitting analyses revealed that void percentage was the most reliable indirect test to estimate UCS for the sandstone that was employed in this study.
(5) Evaluation of the graphical and numerical measures of the goodness of the fit statistics has clearly indicated that respective ANN models of UCS are more acceptable than multiple linear regression models of UCS in predicting actual UCS values.

References

[1] Fahy MP, Guccione MJ. Estimating strength of sandstone using petrographic thin-section data. Bull Assoc Eng Geol 1979;16:467–85.

[2] Shakoor A, Bonelli RE. Relationship between petrographic characteristics, engineering index properties and mechanical properties of selected sandstones. Bull Assoc Eng Geol 1991;28:55–71.
[3] Edet A. Physical properties and indirect estimation of microfractures using Nigerian carbonate rocks as examples. Eng Geol 1992;33:71–80.
[4] Ulusay R, Tureli K, Ider MH. Prediction of engineering properties of a selected litharenite sandstone from its petrographic characteristics using correlation and multivariate statistical techniques. Eng Geol 1994;37:135–57.
[5] Howarth DF, Rowlands JC. Development of an index to quantify rock texture for qualitative assessment of intact rock properties. Geotech Testing J 1986;9:169–79.
[6] Howarth DF, Rowlands JC. Quantitative assessment of rock texture and correlation with drillability and strength properties. Rock Mech Rock Eng 1987;20:57–85.
[7] Alvarez Grima M, Babuska R. Fuzzy model for the prediction of unconfined compressive strength of rock samples. Int J Rock Mech Min Sci 1999;36:339–49.
[8] Gokceoglu CA. Fuzzy triangular chart to predict the uniaxial compressive strength of the Ankara agglomerates from their petrographic composition. Eng Geol 2002;66:39–51.
[9] Brace WF. Dependence of fracture strength of rocks on grain size. Bulletin of Mineral Industries Experiment Station, Mining Engineering Series. Rock Mech 1961;76:99–103.
[10] Mendes FM, Aires-Barros L, Rodrigues FP. The use of modal analysis in the mechanical characterization of rock masses. In: Proceedings of the 1st International Congress Rock Mechanics, Lisbon, 1966; 1:217–23.
[11] Olsson WA. Grain size dependence of yield stress in marble. J Geophys Res 1974;79(32):4859–62.
[12] Onodera TF, Asoka KHM. Relationship between texture and mechanical properties of crystalline rocks. Bull Int Assoc Eng Geol 1980;22:173–7.
[13] Tugrul A, Zarif IH. Correlation of mineralogical and textural characteristics with engineering properties of selected granitic rocks from Turkey. Eng Geol 1999;51:303–17.
[14] Vernik L, Nur A. Petrophysical classification of siliciclastics for lithology and porosity prediction from seismic velocity. Am Assoc Pet Geol Bull 1992;9:1295–309.
[15] Vernik L, Buno M, Bovberg C. Empirical relations between compressive strength and porosity of siliciclastic rocks. Int J Rock Mech Min Sci Geomech Abstr 1993;30(7):677–80.
[16] Singh VK, Singh D, Singh TN. Prediction of strength properties of some schistose rocks from petrographic properties using artificial neural networks. Int J Rock Mech Min Sci 2001;38:269–84.
[17] Tamrakar KT, Yokota S, Shrestha SD. Relationships among mechanical, physical and petrographic properties of Siwalik sandstones, Central Nepal Sub-Himalayas. Eng Geol 2007;90:105–23.
[18] Tiryaki B. Predicting intact rock strength for mechanical excavation using multivariate statistics, artificial neural networks, and regression trees. Eng Geol 2008;99:51–60.
[19] Tiryaki B, Dikmen AC. Effects of rock properties on specific cutting energy in linear cutting of sandstones by picks. Rock Mech Rock Eng 2006;39(2):89–120.
[20] MATLAB. Statistics Toolbox for Use with MATLAB, User's Guide. The MathWorks, Inc. 2009.
[21] Ghabousi J, Garret Jr JH, Wu X. Knowledge based modeling of material behaviour with neural networks. J Eng Mech ASCE 1991;117(1):132–53.
[22] Ellis GW, Yao C, Zhao R. Neural network modelling of the mechanical behaviour of sand. In: Proceedings of the Ninth Conference on ASCE Engineering Mechanics ASCE, New York, 1992. p. 421–24.
[23] Meulenkamp F, Alvarez Grima M. Application of neural networks for the prediction of the unconfined compressive strength (UCS) from Equotip hardness. Int J Rock Mech Min Sci 1999;36:29–39.
[24] Seibi A, Al-Alawi SM. Prediction of fracture toughness using artificial neural networks (ANNs). Eng Fract Mech 1997;56:311–9.
[25] Glantz SA, Slinker BK. Primer for applied regression and analysis of variance. New York: McGraw-Hill; 1992.

Geotech Geol Eng
https://doi.org/10.1007/s10706-018-0680-y

ORIGINAL PAPER

Uncertainty and Reliability Analysis of Open Pit Rock Slopes: A Critical Review of Methods of Analysis

Musah Abdulai · Mostafa Sharifzadeh

Received: 23 March 2018 / Accepted: 27 August 2018

Abstract The stability analyses of slope excavations in rock mass require reliable geomechanical input parameters such as rock mass strength, friction angle and cohesion of sliding surface. These parameters are naturally uncertain and their exact values cannot be known, therefore, their variability must be properly accounted for in the stability analyses. Deterministic approaches such as the limit equilibrium methods, numerical methods and kinematic analysis methods do not account for the variability in any of the input parameter. This paper therefore provides a review of uncertainty and uncertainty analysis methods, problems and developments in geotechnical modelling of rock slope stability. The review is motivated by the availability of qualitative and number of methods for uncertainty analysis. The paper examines the various definitions and description of uncertainty and the different vocabularies that are used, and also summarises and categorises the different sources of uncertainty as well as integrating uncertainty for rock slope assessment problems. The paper discussed a simple survey of probability-based reliability methods that have been used for rock slope stability analysis in the past 3 decades.

M. Abdulai · M. Sharifzadeh (✉)
Western Australian School of Mines, Curtin University, Kalgoorlie, WA 6845, Australia
e-mail: M.Sharifzadeh@curtin.edu.au

M. Abdulai
e-mail: Musah.abdulai@postgrad.curtin.edu.au

Keywords Rock slope stability · Uncertainty · Rock variability property · Probabilistic-based reliability

1 Introduction

Rock slope stability study is one of the most challenging issues in geotechnical engineering. It has both economic and safety implications for open pit mines. The analysis and design of open pit rock slope is a key aspect of mine design as it generally seeks to optimise the overall slope angle in order to maximise the extraction of ore while maintaining the stability of the individual bench slopes. The knowledge of the rock shear strength and the determination of the required safety factor are the most key parts of slope design. The stability of slope is usually determined using conventional design methods such as the limit equilibrium methods. Conventional rock slope design methods comprise the calculation of the mean shear strength of rock and the estimation of the rock strength using empirical methods. Based on the shear stress and shear strength of the rock mass the factor of safety can be calculated. The factor of safety is the ratio of the rock strength at failure to the mobilised shear stress on the failure surface. When the factor of safety approaches one, failure is assumed to be imminent or the slope is assumed to be at stable equilibrium. The slope is considered safe or stable only if the calculated

Published online: 29 August 2018

factor of safety is greater than one and the slope fails when the ratio is less than one.

Even though the conventional methods are commonly used for rock slope design, many geotechnical investigators (e.g. McMahon 1985; Chowdhury 1986; Duzgun et al. 2003; Jimenez-Rodriguez et al. 2006) have expressed some concerns about the conventional approach for stability design of rock slope. They noted that the rock slope failure could not be properly explained by comparing rock shear strength with stresses induced on the rock masses by mining activities. They suggested that rock slope failure could be related to stress–strain behaviour. Hence either approaches of determining the factor of safety are basically deterministic and do not consider the inherent variability of the rock mass properties. In deterministic approach the mean values of the input parameters are generally assumed and represented with certainty by a single value. The results from the deterministic methods could be misleading depending on the distribution of the rock property variation. In order words deterministic methods do not account for variability in any of the input parameter. There have been cases where rock slopes failed even though the failed slope had been considered stable with factor of safety greater than one.

Therefore, for a reliable design and analysis of rock slope in open pit mine, appropriate methods which incorporate the variability in the rock mass properties must be used. The methods which consider this variability are known as probabilistic methods. In a probabilistic approach, the stability analysis can be considered as a random system, where the occurrence of a rock slope failure is a random event depending on the outcome of the random variables involved. Figure 1 shows a schematic diagram of the design approaches for rock slope.

A number of probabilistic studies on rock slope stability problems that treat the rock property as a random variable have been carried out (e.g. McMahon 1985; Chowdhury 1986; Low and Einstein 1992; Low 1997; Park and West 2001; Duzgun et al. 2003; Miller et al. 2004; Park et al. 2005, 2006; Low 2007, 2008; Jimenez-Rodriguez et al. 2006; Jimenez-Rodriguez and Sitar 2007; Duzgun and Bhasin 2009; Wattimena 2013; Gravanis et al. 2014). Low (1997) presented a closed-form equation for the calculations of a factor of safety of two-joint tetrahedral wedges in rock slopes with an inclined ground surface that dips in the same direction as the slope face. Low (2007) further investigated the system reliability of wedge in which four parameter beta distributions are used to describe the basic random variables in the rock wedge stability model. Miller et al. (2004) explored a point estimate method (Rosenblueth 1981) to analyse the stability of plane shear and rock wedge failures. Park et al. (2006) also presented a probabilistic approach for rock wedge failure analysis based on point estimate method where normal probabilistic distribution were assumed for the random variable and the safety margin. Based on Low (1997), Jimenez-Rodriguez et al. (2006) and Jimenez-Rodriguez and Sitar (2007) analysed the stability of rock slopes using the joint cut-set formulation models to model the system reliability of wedge in which each cut-set corresponds to a failure mode of the wedge. Duzgun and Bhasin (2009) applied the first order reliability method (FORM) for probabilistic modelling of rock plane failure. Gravanis et al. (2014) proposed an analytical solution for calculating the probability of failure of rock slopes against planar sliding based on the theory of random field where cohesion and friction coefficients along discontinuity were treated as Gaussian random field. In operational open pit mines, Duzgun et al. (2003) used the advanced first-order-second-moment (AFOSM) reliability method to account for rock variability in the probabilistic method for the design of plane failure mode. Abbaszadeh et al. (2011) presented a method which combines point estimate method and the Taylor series approximation methods in a case study at a copper mine. Wattimena (2013) utilised the logistic regression method to predict the probability of rock slope stability for a given rock mass strength parameters. Valerio et al. (2013) used the point estimation methods in combination with limit equilibrium methods to evaluate the factor of safety of a proposed open pit slope in a diamond mine. They use the Monte Carlo random sampling method to develop a simulated population to approximate a normal distribution, which in this case represents the probability of slope performance defined in terms of the factor of safety.

Generally the probabilistic assessment of rock slope stability is performed by: (1) quantifying the uncertainty in the rock properties in order to determine the basic statistical parameters (e.g. mean and variance) and probability density functions of the strength property of the rock mass; (2) the probability of failure is determined with respect to a particular failure

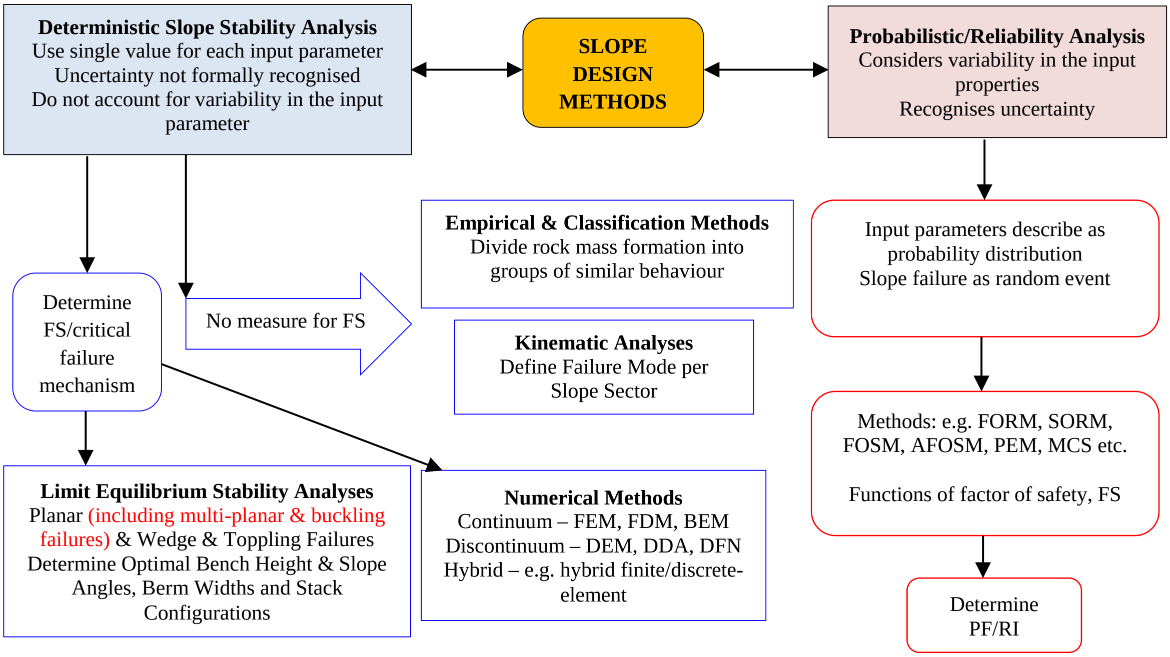

FS = Factor of Safety; PF = Probability of Failure; RI = Reliability Index; FEM = Finite Difference Method; BEM = Boundary Element Method; DEM = Distinct/Discrete Element Method; DDA = Discontinuous Deformation Analysis; FEM = Discrete Fracture Network; FORM = First Order Reliability Method; SORM = Second Order Reliability Method; FOSM = First Order Second Moment; AFOSM = Advanced First Order Second Moment; PEM = Point Estimate Method; MCS = Monte Carlo Simulation

Fig. 1 The design approaches for rock slope

criterion, which can either be the induced shear stress exceeding the rock mass strength, or the strain developing in the slope exceeding a defined threshold strain value for the rock mass. The failure of rock slope in this context is defined as the limit state when strength of the rock mass is violated or when the strain occurring in the rock is greater than the peak strain for the rock. In open pit excavations the limit state is not known explicitly, however numerical analysis using the finite element methods can be combined with function approximation tools to construct a closed-form expression for the limit state surface.

In recent years many approximation methods have been increasingly used in the analysis and design of rock slopes such as the first order reliability method (FORM), the second order reliability method (SORM), the first order-second moment (FOSM), the advance first order-second moment (AFSOM); the point estimate method (PEM), the advanced point estimate method (APEM) and the random set (RS) theory to model the relationship between non-linear multivariate variables. The probability and reliability analysis of rock slope have become popular because they provide a more realistic estimation of uncertainty. The use of probabilistic options in slope stability software like Slide, Swedge, Rocplane and RS2 (Rocscience Inc. 2006, 2001, 2015a, b) reveals the general acceptance of probability and reliability tools by geotechnical practioners; these software have built-in routines that employ probabilistic methods such as Monte Carlo (MC) simulations, Latin Hypercube (LH) simulation and Rosenblueth Point Estimate Method (PEM).

The objective of this paper is to present some basic concepts of geotechnical uncertainty modelling and analyses in addition to probabilistic concept of rock slope stability; understand the difference between uncertainty and variability; brief coverage to quantification of uncertainty and methods of quantifying uncertainty, and sources and types of uncertainty through understanding of various vocabulary that are used for uncertainty and briefly discussed the economics and safety aspect of slope instability in terms of on the consequence analysis. Based on existing knowledge, an integration of uncertainty for rock slope stability analysis is presented and in addition, appropriate possible solution models are also discussed. Finally the paper presents a review of the historical development and scope of probabilistic-reliability applications in rock slope design starting from 1985 to 2017.

1.1 Probability Concepts of Rock Slope Stability

For stability analysis of rock slope, geotechnical engineers cannot ignore the deterministic methods of analysing the possibility of structurally controlled failure. The analyses can range from empirical, kinematic, limit equilibrium and numerical methods (Fig. 1). For instance, kinematic analyses are carried out using mean joint orientations of discontinuity sets to analyse the stability of slope and benches against various structurally controlled failures (i.e. planar, wedge and toppling failures). Depending on whether possible structurally controlled failures exist or not regarding slope dimensions compared to say discontinuity spacing, the stability analysis of the slope may be carried out using appropriate limit equilibrium and/ or numerical approach to make informative decision from the output results (i.e. factor of safety). While the deterministic analysis do not take into account the variability in rock mass properties, probabilistic methods are generally used and aimed at statistical characterisation of factor of safety for a given input statistics of the rock mass properties. Here the stability of slope is defined in terms of probability of failure or reliability index instead of a factor of safety; this is necessary owing to the uncertainties in rock mass properties. The probability of failure concepts is shown in Fig. 2 (Steffen et al. 2008). There is a linear relationship between the probability of failure and the likelihood of failure, whereas none exists with factor safety. The assessment of stability of the slope may be carried out using two different types of probabilistic methods, i.e. by ignoring spatial variability and by considering spatial variability of rock mass properties.

1.1.1 Probabilistic Slope Stability Analysis by Ignoring Spatial Variability

In the traditional probability methods, the reliability index of slope is estimated by treating input parameters as random variables and does not consider spatial variability in rock mass properties. There are two approaches, namely the most probable point-based (MPP) and the sampling-based approaches. The MPP approach includes the first/second order reliability (FORM/SORM). They involve searching a design point in input space with an objective depending on the adopted method (Ang and Tang 1975; Pandit et al. 2018). Both the FORM/SORM approach divides the input space into safe region and failure region (Fig. 3). The factor of safety (FS) is used to calculate the slope stability where the FS is expressed by performance function, i.e. $F = g(X)$ where X is vector of input variables required to obtain the FS. The input space for which input values yield FS less than 1 is called failure region. It involves calculation of derivatives of performance function and hence generally adopted where an explicit expression of the performance function can easily be obtained.

The sampling-based approach uses Monte Carlo simulation (MC) and/or Latin hypercube sampling (LHS). It involves generating random input vectors ($X_1, X_2 \ldots X_k$) from input variable space and repeated calculation of the FS is carried out (Pandit et al. 2018). The sampling-based approach is easy to be applied in numerical programs but is computationally expensive and time consuming as it requires large number of runs.

1.1.2 Probabilistic Slope Stability Analysis Considering Spatial Variability

When the spatial variability of strength parameters of rock mass is neglected, it may lead to significant underestimation or overestimation of the probability of failure and reliability index, depending on amount of variability in rock mass properties. Random fields are usually adopted to model spatial variability in rock properties of the slope (Vanmarcke 1983). One of the significant components of random field characterisation is autocorrelation function (Vanmarcke 1983). The autocorrelation function provides the measure of correlation between same rock properties at two different spatial locations as function of distance. In 2-dimensional isotropic random field, correlation between two points depends on absolute distance between them and not on the orientation relative to each other. However this is not the usual case with many rock slope stability problems since correlation between strength properties is generally different in

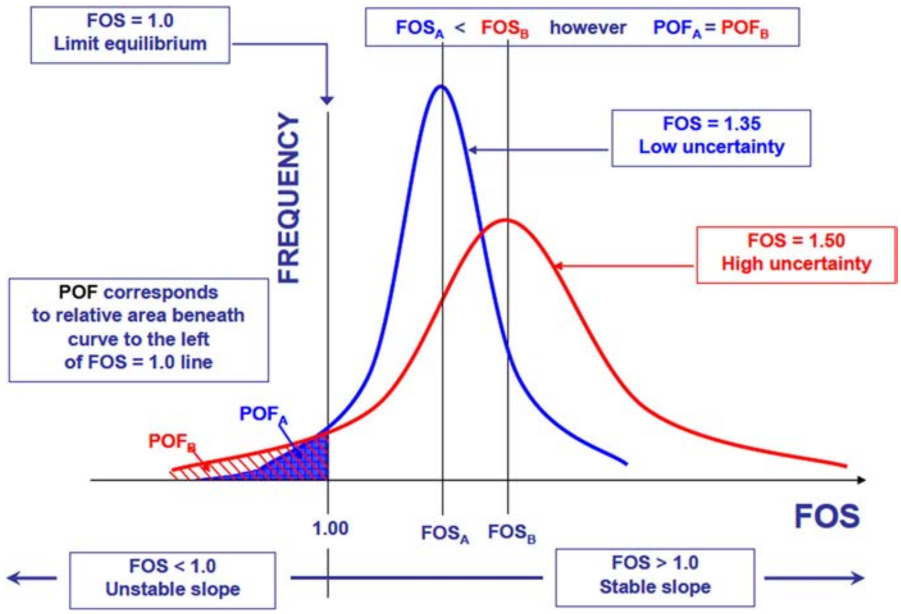

Fig. 2 Definition of probability of failure and relation with factor of safety based on the (Steffen et al. 2008)

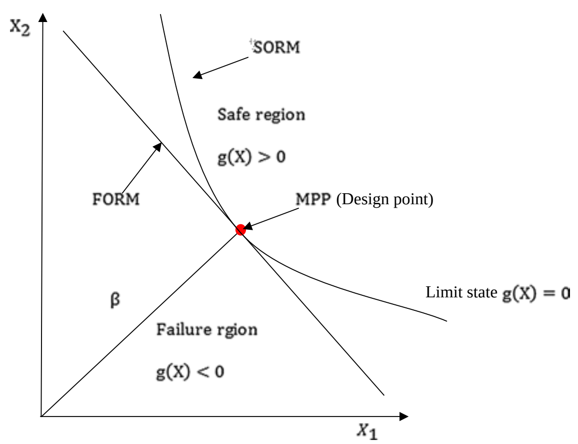

Fig. 3 The limit state function of FORM/SORM showing safe and failure regions

horizontal and vertical direction. Therefore, the anisotropic 2-dimensional stationary random field becomes an attractive alternatives and useful for the rock slope stability problems (Vanmarcke 1983; Pandit et al. 2018). In the anisotropic 2D stationary random field, the correlation between two locations is defined as (Pandit et al. 2018):

$$\rho_w(\Delta x, \Delta z) = \frac{COV[w(x,z), w(x+\Delta x, z+\Delta z)]}{VAR[w(x,z)]} \quad (1)$$

where $\rho_w(\Delta x, \Delta z)$ is autocorrelation function, $w(x,z)$ is the random field (i.e. a function in the horizontal and vertical coordinates (x,z), Δx, Δz are horizontal and vertical distances from (x,z), COV is covariance and VAR is variance. In general two correlation functions are widely used, namely the single exponential and squared exponential methods. For rock slopes, the single exponential 2D autocorrelation model is adopted and can be expressed as:

$$\rho_w(\Delta x, \Delta z) = exp\left(-\frac{2|\Delta x|}{\delta_x} - \frac{2|\Delta z|}{\delta_z}\right) \quad (2)$$

where δ_x and δ_z are horizontal and vertical scale of fluctuations (SOFs) respectively. The SOF is a measure of distance within which the rock properties are significantly correlated (Vanmarcke 1983). Equation 2 is also known as the separable Markov correlation model. The autocorrelation model (Eq. 2) is a function of the lag ($\tau_x = |\Delta x|$; $\tau_z = |\Delta z|$). A small values of δ_x and δ_z lead to domain being correlated until shorter distances result in rougher random fields, while the spatial distribution of rock property becomes smoother (i.e. less spatial variability) on increasing values of SOFs.

In literature there are two procedures for the estimation of SOF from the available data, the maximum likelihood method and the curve fitting method. The maximum likelihood method which involves assuming different sets of numerical values of parameters of proposed autocorrelation function (ACF) model, and the set of parameter values which maximises the maximum likelihood function are considered optimal (Pandit et al. 2018). The curve fitting method suggests that the parameters of ACF must be adjusted so as to best fit the actual sample correlation coefficients obtained from the measured data, i.e. fitting theoretical correlation model to the experimental correlation (Vanmarcke 1983). A variety of methods for generating realisations of random field exist, mainly the matrix decomposition method, Fast Fourier transform, moving average method, turning-band method (Matheron 1973), local average subdivision (Fenton and Griffiths 2008; Gravanis et al. 2014; Pantelidis et al. 2015), midpoint method (Vanmarcke and Grigoriu 1983), Karhunen–Loève expansion (Phoon et al. 2002a, b, 2005; Galal 2013).

2 Uncertainty and Variability for Rock Slope Stability: Concepts and Definitions

The term uncertainty is used in every day engineering discussion to express a sense of not knowing or being unsure (Begg et al. 2014). It is important that geotechnical engineers know if they are to estimate for variability and uncertainty ranges and also identify if they are to build models of variability or uncertainty and their relationship. Both uncertainty and variability contribute to imprecision and unpredictability of a geotechnical parameter or system especially when limited information is used to characterise the properties of the parameter or system. Hence having a clear understanding of uncertainty and how to quantity uncertainty aid in differentiating uncertainty from variability.

2.1 Uncertainty and Variability

In geotechnical engineering the term uncertainty is used to define the total unpredictability of a parameter or system (Bedi and Harrison 2013). Unpredictability characterises all deficiencies and inabilities to correctly predict the value of a parameter such as key geomechanical properties like rock stresses, or rock strength. A measurement of such properties involves some error due to the sampling process, sample preparation or sensitivity and calibration of the measuring devices.

Variability refers to the multiple values a quantity has at different locations (Begg et al. 2014); example is the range of permeability at different location within a rock mass. Variability is a function of the inherent randomness of a system and it is a characteristic of the real world which needs to be measured, analysed and where appropriate explained (Bedi and Harrison 2013). In rock slope engineering, variability arises from the formation and transformation process of rock and rock masses which have a local influence on their mechanical properties. Variability therefore leads to uncertainty. For instance the unit weight of rock at a particular location will be unknown unless it is measured at the location. Thus uncertainty arises because the unit weight varies from point to point in the rock mass.

In order to carry out useful uncertainty analysis there is the need to increase data collection and apply statistical and probability models. Probability is how uncertainty is quantified and it is applied when data is severely limited and when it is difficult to assign a single parameter value to a particular rock structure or lithology (e.g. Einstein 2003; Carter 1992). On the other hand the collection of all the true values at all locations within a domain of interest is called a population (e.g. the permeability of all rock types forming open pit slope). Therefore, to quantify variability, data is acquired by measuring the values of the quantity in question from different location. It is possible to ignore measurement error during such data collection on assumption that the error in each measurement is either negligible or has been reduced to an acceptable level by repeated measurement. From these data the variability of the sample is quantified by calculating the frequency of occurrence of each known values of the quantity. However a frequency distribution which describes the known values of multiple instances of a particular quantity is not a probability distribution; probability distribution describes the uncertainty in the unknown value of a single instance of the quantity. Hence a frequency distribution is not a quantification of uncertainty (Begg et al. 2014).

2.2 Quantification of Uncertainty

The quantification of uncertainty involves the developing of framework that will focus on the effects of variability. This means the ability to attach a measure to something that may not be precise. Within computational mechanics the designed system is used to manufacture the real system using a mathematical-mechanical modelling process (Soize 2013). The main objective is the prediction of the responses of the real system in its environment. The real system, when presented to a given environment can exhibit variability in its responses due to fluctuations in the manufacturing process and due to small variations of the configuration associated with the designed system (Soize 2013). This means the computational model which results from a mathematical-mechanical modelling process of the design system has parameters which can be uncertain (Soize 2013). In other words the modelling process induces some modelling errors defined as modelling uncertainty. Therefore it is important to take into account both the uncertainties on the computational model parameters and the modelling uncertainties for credible predictions of computational models so that a computational model can be used to carry out robust optimization, robust design and robust updating with respect to uncertainties (Soize 2013). The role of uncertainty in computational mechanics is explained in three steps by Sudret and Blatman (2009) in Fig. 4. In step A, a mechanical model is built together with assessment criteria (failure criteria) for the behaviour of the system (Huber 2013); this step gathers and analyse all components used for classical deterministic analysis of the physical system. The quantification of sources of uncertainty is done in step B; in this step random variables or random fields are used for the representation of the different sources of uncertainties of the system. The response of the system with regard to the random input variables and fields is evaluated within the uncertainty propagation in step C. This step encloses the uncertainty of the system. There are numerous methods to carry out the task explained in Fig. 4. Sudret and Blatman (2009) noted that uncertainty propagation methods provide information on the impact of the random input parameters on the response randomness. They noted that a sensitivity analysis helps to identify the main sources of the response randomness and that this sensitivity analysis may sometimes be the unique goal of a probabilistic study (Huber 2013). Table 1 is from Honjo et al. (2009) and shows the different level of design accuracy in the quantification of uncertainty in geotechnical analysis. The first of these is the use of deterministic variables and partial safety factors to simulate random variables of geotechnical problem. By taking the mean and standard deviation of the random variables into account, the result of this analysis method is called the reliability index. Lastly the simulation of random variables can be done using probability density function which will make it possible to determine the probability of failure more precisely because more information is available as compared to the other levels of reliability based design and uncertainty quantification (Huber 2013).

2.3 Sources of Uncertainty in Rock Slope Parameter

2.3.1 Where Do Uncertainties Arise from?

The rock mass on which the slope is formed is a complex geological structure with strong heterogeneous behaviour; the heterogeneity exhibits considerable variation of rock property. Rock properties such as joint aperture, joint spacing, strength and deformational parameters vary in space and time. The variations can be introduced by stress, temperature, groundwater, decomposition, boundary conditions and rock structure (e.g. fault, shear zones, fractured dyke and discontinuities). The stability of slopes in rock masses could be dominated by these conditions. Research evidence has shown that reliable estimates of the ground condition are not always suitably assessed due to difficulty in obtaining information on every continuous and intermediate geological structures and incomplete interpretation. That is, the incomplete information and lack of knowledge about the ground condition are the essential sources of uncertainty. In the analysis and design of rock slope, field and/or laboratory investigation is performed to determine specific geotechnical design properties. Therefore to assess the safety of rock slope, there is the need to recognise the different sources of uncertainties related to the geotechnical design properties.

There are multiple sources of uncertainty such as statistical variation, linguistic imprecision, approximation, subjectivity in measurement techniques, disagreement, variability, practical unpredictability (Begg et al. 2014) (Fig. 5).

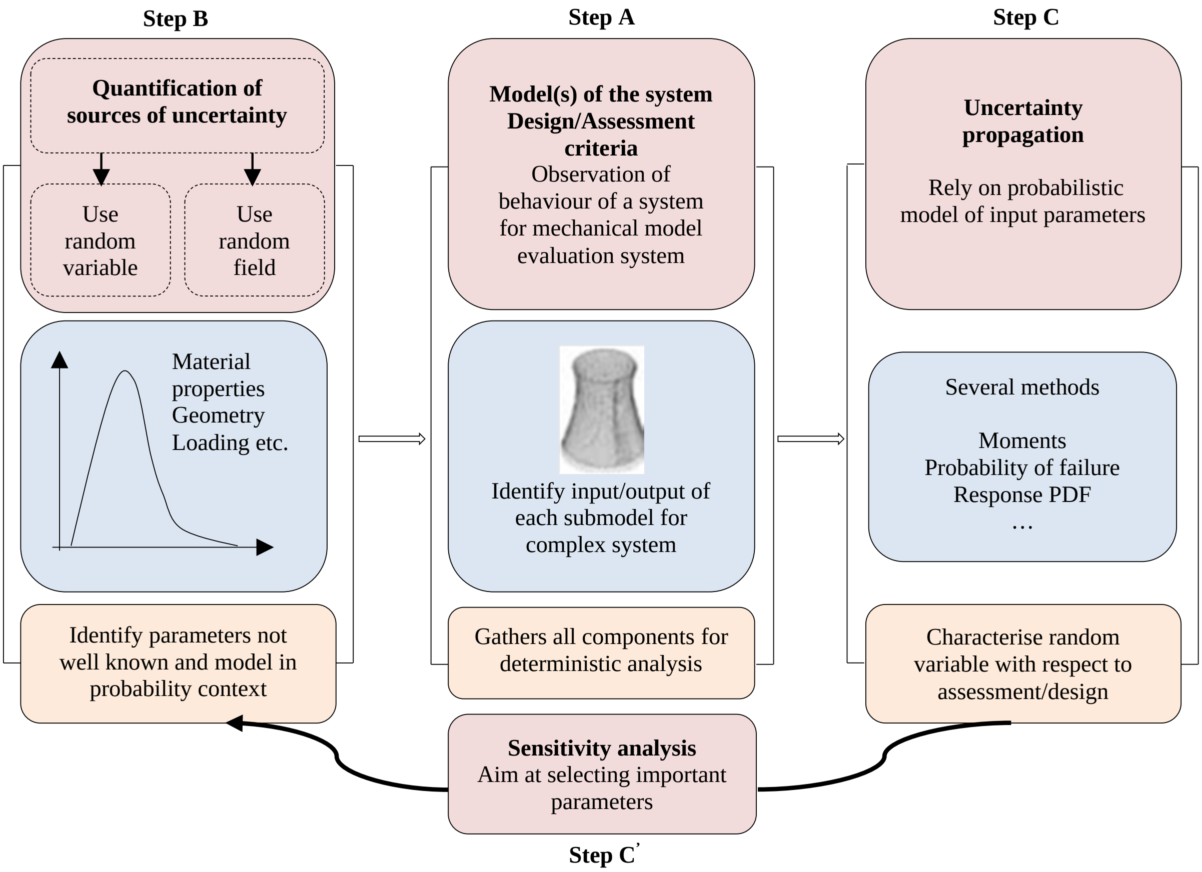

Fig. 4 A schematic illustration of uncertainty quantification in computational mechanics after Sudret and Blatman (2009)

Table 1 Reliability based design: different levels of accuracy from Honjo et al. (2009)

Level	Basic variables	Reliability	Verification
I	Deterministic variables	Partial safety factors	Verification formula
II	Random variables with mean and standard deviation	Reliability index	Target reliability index
III	Random variable and probability density function	Probability of failure	Acceptable level of reliability

- Statistical variation arises from random fluctuations or error in direct measurements of a quantity which can occur from imperfections in measuring devices.
- Linguistic imprecision is extremely common. Some precision is required for general communication. People often use imprecise terms and expressions in communication and when the terms are used with others who are not familiar with the intended meanings or in a setting where exactitude is important, this imprecision may result in uncertainty.
- Approximations include numerical (e.g. finite difference/element) approximations to equations and model reduction by approximation.
- Subjectivity in measurement technique is simply systematic error and subjective judgment; they arise from bias in measurement apparatus and experimental procedure as well as from key assumptions by the experimenter or analyst.

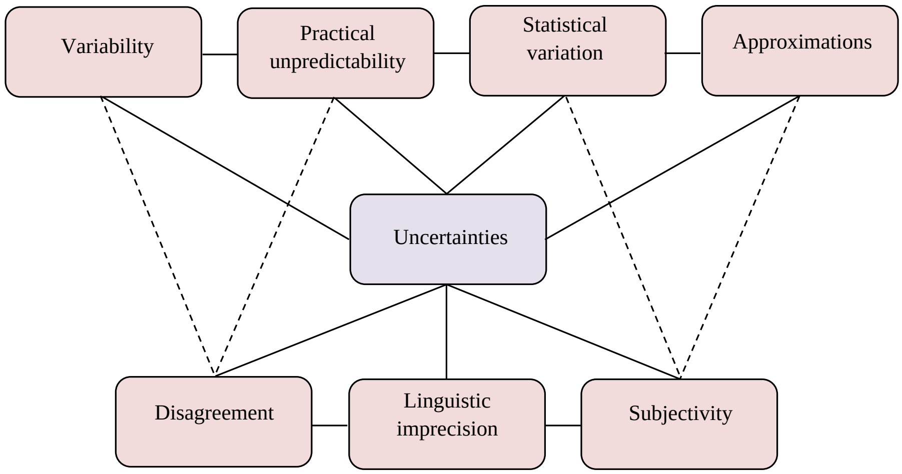

Fig. 5 Common sources of uncertainty

- Disagreement stems from different technical interpretations of same data, as well as from different stakeholder positions in the outcome.
- Variability is when there is a natural frequency distribution associated with a variable such as the frictional property of rock within a rock layer.
- Practical unpredictability justifies randomness; it describes quantities which must be viewed as random. Inherent randomness is as a result of not knowing the position and magnitude of a quantity or the quantity cannot be computed accurately.

Most problems of engineering interest involve one or more or combination of above types of uncertainties. Within the realms of computational mechanics the sources of uncertainties can be considered to be composed of (a) parametric uncertainty such as uncertainty in geometric parameters, friction coefficient, strength of the materials; (b) model inadequacy that stems from the lack of scientific knowledge about the model which is a priori unknown; (c) experimental error which relates to uncertain and unknown error that infiltrate into the model when they are calibrated against experimental results; (d) model uncertainty which relates to randomness in the model and (e) computational uncertainty involves things like machines precision, error tolerance.

2.3.2 Types of Uncertainties in Rock Slope Parameters

In geotechnical engineering, the field and laboratory data are often limited and are not known completely which leads to two forms of uncertainty namely the model uncertainty and parameter uncertainty. The model uncertainty depends on how well the applied mathematical model represents the reality (Spross 2014). Model uncertainty results from the mismatching of theory adopted in prediction models and reality on the basis of causal inference. Due to geological heterogeneity which contributes to spatial variations in rock mass property, the rock property will be subject to parameter uncertainty. Over the years most researchers and geotechnical practioners indicated that the sources of uncertainties affecting rock properties arise from three main aspects; they include: inherent variability, statistical uncertainty and systematic uncertainties (e.g. Baecher and Christian 2003; Phoon and Kulhawy 1999; Jimenez-Rodriguez et al. 2006). The inherent variability results from the spatial variation and random testing error; the rock properties exhibit variability by nature even in a homogeneous rock medium. Due to limited field sampling and laboratory testing, the statistics (i.e. mean and standard deviation) of a rock property will be subject to uncertainty; this type of uncertainty decreases with increasing number of samples. Systematic uncertainty stems from the inability of experimental test to produce the in situ property as a result of sample or test disturbance and limited specimen size; the discrepancies between the laboratory and in situ conditions are due to scale and anisotropy. Most investigators have used terms like data uncertainty to represent inherent variability of a measured quantity. They explained that no matter how carefully one measures such a quantity, there will still be variability among the measured values because it is inherent (Sari and Karpuz 2006). Furthermore, measurement errors and transformation uncertainty are considered among the sources of uncertainty. The causes of such uncertainties for rock slope engineering have been discussed in detail by Duzgun et al. (2002, 2003). Measurement error is related to how geotechnical field investigation is interpreted, and it includes systematic bias and random errors associated with measurements process. From Song et al. (2011), measurement error arises from equipment, test-operator and random test effect during measurements. On the other hand, transformation uncertainty occurs when the information of interest is not measured directly but estimated through transformation model and other measured information. It relates to the process in which field and laboratory measurements are transformed to an appropriate design property (Phoon and Kulhawy 1999). Example is when the rock core bearing angles (i.e. α-alpha and β-beta) measured during rock core logging is translated to dip and dip direction with respect to the azimuth of borehole. The transformation is often made by theoretical relationships or by empirical data fitting model (Phoon and Kulhawy 1999).

In line with the above descriptions and several definitions of sources of uncertainty, many researchers have grouped geotechnical uncertainties into aleatory and epistemic uncertainty (Baecher and Christian 2003; Der Kiureghian and Ditlevsen 2009; Oberkampf et al. 2001; Ayyub and McCuen 1997). The classification, as shown in Fig. 6, has been based on the combination of lack of knowledge and randomness (e.g. Baecher and Christian 2003; Christian 2004; Bea 2006; Read 2009; Oberkampf et al. 2001). Aleatory uncertainty is based on natural randomness in rock mass that results from geological formation and transformation processes. Epistemic uncertainty is associated with lack of information and limitation from measurements, sampling and testing methods and calculation procedures. By their nature several authors referred to epistemic uncertainty as reducible uncertainty, subjective uncertainty and cognitive uncertainty; while aleatory uncertainty has been referred to as irreducible uncertainty, inherent uncertainty, variability and stochastic uncertainty and noncognitive uncertainty (Roy and Oberkampf 2011; Ayyub and McCuen 1997).

Bea (2006) categorised epistemic uncertainty into unknown knowables and unknown unknowables events. The unknown knowables events are related to the conditions where information access is ignored, not used, not accessed or incorrectly handled (Bea 2006) and the term unknown unknowable refers to events that are not predictable by an observer at a point in time. In other words the unknown unknowable events are related to limitations in current knowledge or limitations in the ability to obtain it. This categorisation has been linked to the "predicament of evidence-based theory" where uncertainty is referred to as: known knowns, known unknowns and unknown unknowns. The known knowns refers to the things we know that we know. There are known unknowns; that is to say, there are things that we now know we don't know. The unknown unknowns are the things we do not know we don't know". These expressions have long been used by many geotechnical engineers in their classifications of uncertainty and have become popular in the geotechnical engineering group.

2.3.3 Epistemic Uncertainty

In geotechnical engineering, a lack of knowledge may arise from lack of field or laboratory investigation data. This reflects incompleteness of data or because the nature of the data is such that they cannot be accurately measured (Bedi and Harrison 2013). Therefore such data require subjectivity or expert opinion in their estimation, which leads to difference of opinion (Bedi and Harrison 2013). In spite of the advances in rock engineering, the source of many design parameters are empirical in nature and no physical measurements are made; that is, the parameters are derived from expert opinion. Sometimes design parameters are either based on an approximation, or are sought by the analyst. These situations, therefore, leave people with insufficient information to make a precise description; these situations have introduced what is called imprecision and inaccuracy. Therefore any geotechnical situation that is associated with lack of knowledge due to lack of data, subjective estimation and/or relying on the beliefs of the expert opinion is described as epistemic uncertainty. Since

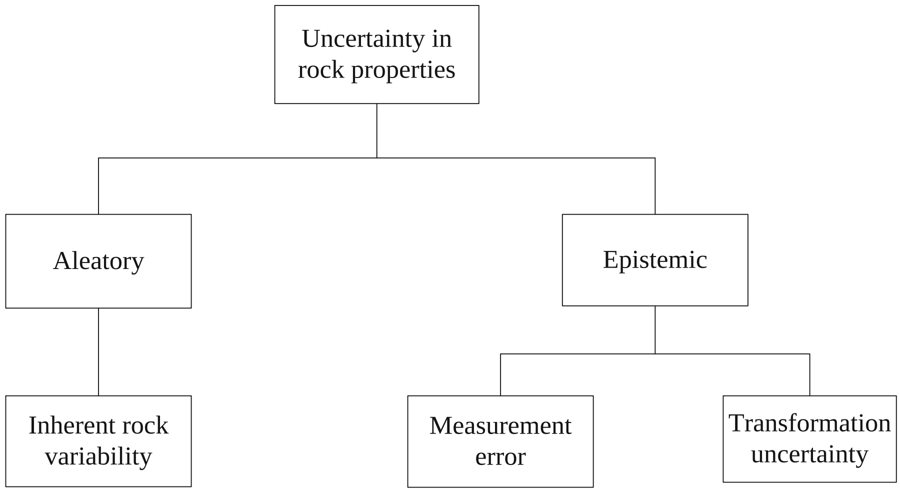

Fig. 6 Generic sources and types of uncertainty in geotechnical engineering

epistemic uncertainty is a function of available information, it implies that epistemic uncertainty can be reduced by obtaining additional information because it is a type of uncertainty associated with limited, insufficient or imprecise knowledge (Huber 2013). However, in case of direct-calculation approach, Baecher and Christian (2003) indicated that epistemic uncertainties enter the analysis as model and parameter uncertainties. As mentioned earlier, model uncertainties reflect the inability of a model or design technique to represent a system's true physical behaviour precisely (Baecher and Christian 2003; Abbaszadeh et al. 2011). That is the analyst's inability to identify the best simulation model, design technique or empirical formula (Abbaszadeh et al. 2011); or a model that may be changing in time in poorly known ways (Baecher and Christian 2003). Parameter uncertainties stem from the inability to accurately measure model input parameter exactly from test or calibration data due to limited numbers of observations and the statistical imprecision attendant (Abbaszadeh et al. 2011; Baecher and Christian 2003).

2.3.4 Aleatory Uncertainty

Aleatory uncertainty consists of physical uncertainty. Physical uncertainty is also known as inherent uncertainty and intrinsic uncertainty. Physical uncertainty is a natural randomness of a quantity such as the variability in the rock strength from point to point within a rock mass (Huber 2013). Such physical uncertainty or natural variability is a type of uncertainty which cannot be reduced on increasing site investigation (Huber 2013). Aleatory uncertainty is used to characterise any unpredictability that result from natural fluctuations of the property in question (Bedi and Harrison 2013). They referred to aleatory uncertainty as aleatory variability, because variability is a function of the inherent randomness of a system. This type of uncertainty can be quantified by measurements and using statistical estimations; however it is unpredictable and irreducible through collection of more experimental data or using refined models.

According to Bedi and Harrison (2013), if sufficient additional information is obtained in order to improve the state of information, it may be possible to recharacterise the uncertainty as variability. Therefore, in this concept of reducibility, the distinction between aleatory variability and epistemic uncertainty can be made through understanding of the existing level of knowledge, based on the available information (Bedi and Harrison 2013), as visualised in Fig. 7a. In this figure one can see how complete ignorance is one extreme of epistemic uncertainty, and as knowledge increases, it may be possible to recognise that aleatory variability exists. Figure 7b shows how this transition from epistemic uncertainty to aleatory variability occurs as knowledge, and/or information increases and a threshold is crossed (Bedi and Harrison 2013); the threshold represents the state of precise information. The state of precise information is achieved when there is sufficient data so that one can use established

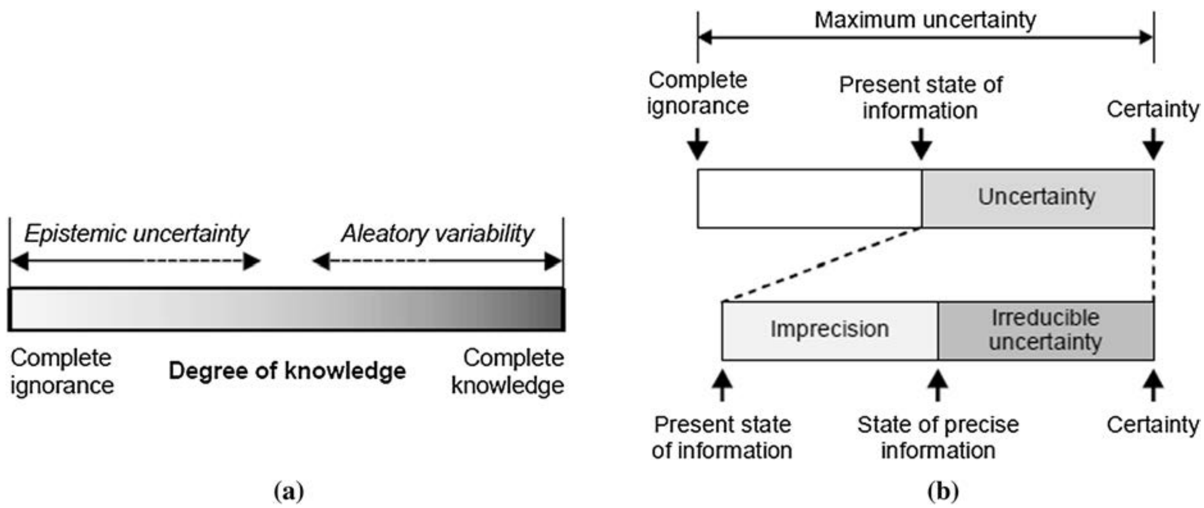

Fig. 7 **a** Uncertainty, variability and degree of knowledge; **b** uncertainty and information states (Bedi and Harrison 2013)

statistical methods to objectively fit a precise probability distribution function to characterise it, i.e. apply an aleatory model (Bedi and Harrison 2013). That is, the data can be measured with acceptable accuracy to allow a unique probability of occurrence to be given to each value of a variable. However once an acceptable aleatory model has been developed, additional investigation will not reduce the variability but may increase the precision of the parameters that describe it (Christian 2004); this is because the additional information to be obtained is inherent in the system and thus irreducible.

2.3.5 Methods for Uncertainty Quantification

In the literature, the nature of uncertainties and the way of dealing with them has been extensively discussed by many researchers (e.g. Lindley 2013; Der Kiureghian and Ditlevsen 2009). Recently, various mathematical frameworks have been developed for the general assessment of uncertainty and variability in rock slope stability analysis. They include the reliability analyses and non-deterministic methods. The non-deterministic methods consist of the probabilistic and non-probabilistic methods; the non-probabilistic methods are also called the imprecise methods. In the non-deterministic analysis, either probabilistic analysis or non-probabilistic analysis is combined with the deterministic slope stability analysis. However the non-deterministic slope stability analysis cannot be considered as an entirely new slope stability analysis method, but as an extension of the deterministic slope stability analysis. It is worth noting that the accuracy of non-deterministic analysis is not only depending on the selection of a suitable probabilistic or non-probabilistic analysis method, but also on a more rigorous deterministic analysis method (Shen 2012). From Huber (2013), a possible classification of probabilistic methods which can be utilised for uncertainty quantification is shown in Fig. 8. The classification is distinguished between probabilistic and non-probabilistic methods (Huber 2013).

Reading Huber (2013), the non-probabilistic approaches comprise interval analysis, fuzzy approaches, grey number theory, imprecise probability method based on p-box representation and random set approaches. According to Huber (2013), the probabilistic approaches aim to compute the probability of failure which is faster than the computationally time consuming Monte Carlo (MC) sampling approach. Each of the alternatives (in Fig. 8) to the MC method implies some loss of accuracy (Huber 2013). Hence, the MC approach is used for verification and calibration of these approaches. In uncertainty quantification, the Bayesian approach has been described in various publications as well as the standard reliability methods (e.g. FOSM, FORM, SORM). The point sampling methods like Taylor series, finite difference methods or the Point Estimate method can be found in several publications. According to Huber (2013), Fenton has worked in various publications (e.g. Fenton and Griffiths 2008) and

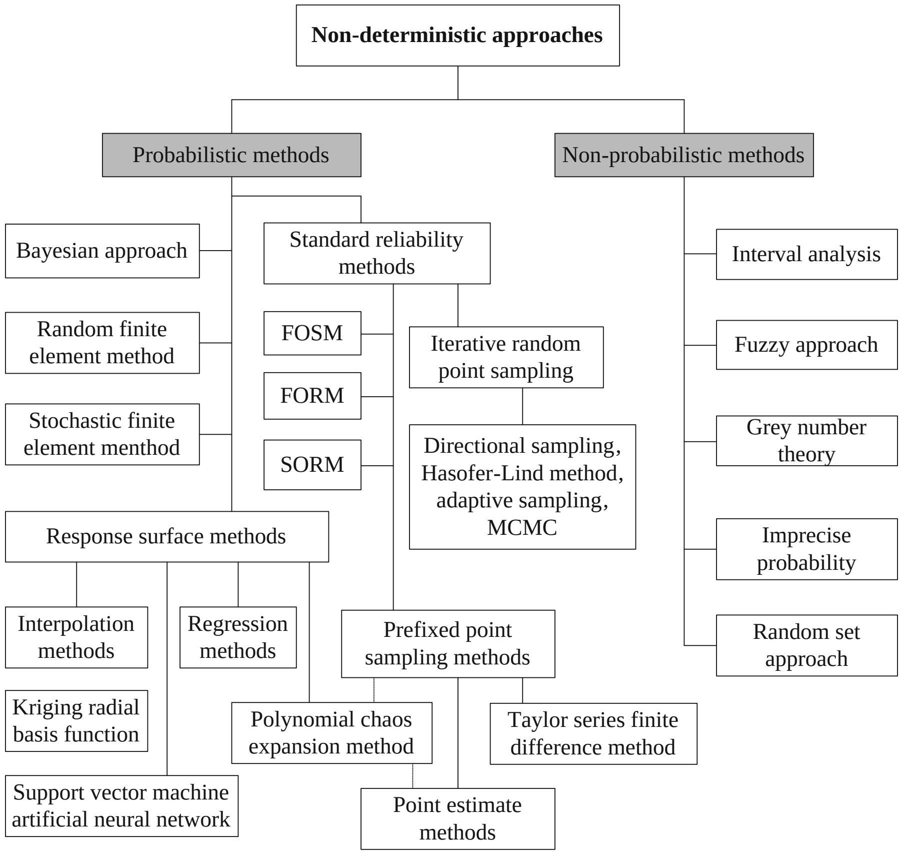

Fig. 8 Non-deterministic methods for uncertainty quantification (Huber 2013)

different applications in geotechnical engineering on the simulation of spatial variability using random fields within the Random Finite Element Method.

As pointed out in Shen and Abbas (2013), most cases of rock slope analysis do not have sufficient input data. In this condition the number of samples is not adequate to determine the probability distributions of the random variables. As a result people proposed many non-probabilistic methods termed the imprecise methods in geotechnical engineering. Examples of the imprecise methods are Interval Approach, Evidence Theory, Fuzzy Set Theory, Possibility Theory, Imprecise Probabilities and Random Set Theory.

The interval analysis was introduced by Moore (1966); it is used to describe the parameter uncertainties either in geometry and loadings or in geotechnical model parameters as interval quantities (Shen 2012). An interval number is interpreted as a random variable whose probability density function is unknown but non-zero in the range of the interval. It can also be interpreted as the intervals of confidence for α-cuts of fuzzy sets. In general, the interval concept serves as a basis of other non-probabilistic uncertainty models. For example, in the fuzzy set approach a continuous membership function of input parameters can be split into several α levels with corresponding intervals and the fuzzy set approach turns into several analyses on different α-cuts. Zadeh (1965) proposed the fuzzy set approach; the model parameters of geotechnical engineering, like geometrical, loading and rock model parameters are considered as fuzzy quantities in this method. The fuzzy set approach is applied in reliability analysis with different terminology and interpretations concerning the resulting reliability. For instance, Shrestha and Duckstein (1998) calculated the probability of a fuzzy failure based on the fuzzy reliability measure which satisfies the necessary properties of the probabilistic reliability measures, and they developed a kind of fuzzy reliability index. Dodagoudar and Venkatachalam (2000) computed the reliability of slopes using the term "fuzzy probability of failure". Kendall (1974) proposed the random set theory and was later developed by several authors. It is a mathematical model which can handle uncertainty of the system, while the exact values of input parameters are not available but only the interval of these values can be obtained. The method provides a general framework for dealing with set-based information and discrete probability distribution (Shen and Abbas 2013). In other words the worst and the best cases of the system are obtained through series of interval analyses based on the Cartesian product of focal elements of the systems input parameters. It has been widely applied in geotechnical engineering, but most of these are focused on the tunnelling (e.g. Tonon et al. 2000a, b; Peschl 2004; Schweiger et al. 2007). Recently, random set theory has seen wide application in rock slope stability analysis (e.g. Shen and Abbas 2013; Shen et al. 2013).

3 Integration of Uncertainty for Rock Slope Stability Analysis

There have been several categorisations of uncertainty in geomechanics such as the inherent variability, model uncertainty, data uncertainty, parameter uncertainty, statistical uncertainty, systematic uncertainty, measurements error and transformation uncertainty (e.g. Baecher and Christian 2003; Hadjigeorgiou and Harrison 2011; Read 2009). These and other sources of uncertainties have been reclassified as aleatory and epistemic uncertainty. However, the limits of aleatory and epistemic uncertainties are often not clear for the categorisation of uncertainty especially for rock slope stability problems. In addition, the stability of rock slope is clearly influenced by intrinsic rock factors (e.g. jointing or geological structures and rock formation which include rock type, strength and weathering) environmental factors (e.g. groundwater and blast induced stress), and geometric factors (e.g. slope orientation, slope angle, slope height and berm sizes). Also, the analysis of rock slope often involves the development of a model based on these factors, which the analyst must decide on which of these factors to include and which to leave out in the analysis. The ability to make such decision often leads the analyst to a state of confusion or uncertainty, which can make a model development difficult. Again, depending on the state of knowledge about these factors (i.e. intrinsic, environmental and geometric factors) and the experience of the analysts, some of these factors may not be known and few factors may be neglected. Therefore, an integration of uncertainty for rock slope stability analysis is presented and is shown in Fig. 9. This integration is based on existing knowledge and some criteria that has been set by several other authors (e.g. Baecher and Christian 2003; Hadjigeorgiou and Harrison 2011; Christian 2004; Bea 2006). The dotted arrows (Fig. 9) are added to direct the user to the 'unknown-neglected' factors for a more complete categorisation of uncertainty. In this way, the structure can lead the user to identify other factors or other types or sources of uncertainty in order to select appropriate models that can be used to model uncertainty.

Figure 9 shows the main types of uncertainties in rock slopes. Table 2 has been developed to show the relationship between the types of uncertainties and the appropriate methods that are used to model uncertainty. Three relevant types of uncertainty specific to the rock slope stability are clearly identified, they are; geological uncertainty, geotechnical uncertainty and design parameter-selection uncertainty and summarised below.

3.1 Geological Uncertainty

The various uncertainties (e.g. geo-structural uncertainty, stratigraphic variability, lithological variability and hydrogeological uncertainty) contained in geological uncertainty results in inherent variability. They basically comprise the uncertainties associated with geometry of geological structures and their relationships between lithologies, and those uncertainties associated with the boundaries of lithological units. It also includes uncertain properties of a given geological units due to incomplete or inaccurate sampling, data collection and calculation model. Often the geological structural models for slope design comprise faults, bedding, folds and joints. The location of these structures in relation to hydrogeological units, hydraulic conductivities, flow regime and pore pressure distributions vary in space and time and add to inherent spatial variability. However the spatial inherent variability is independent of state of knowledge and cannot be reduced as knowledge improves (Baecher and Christian 2003). While inherent spatial variability can be quantified by measurements and

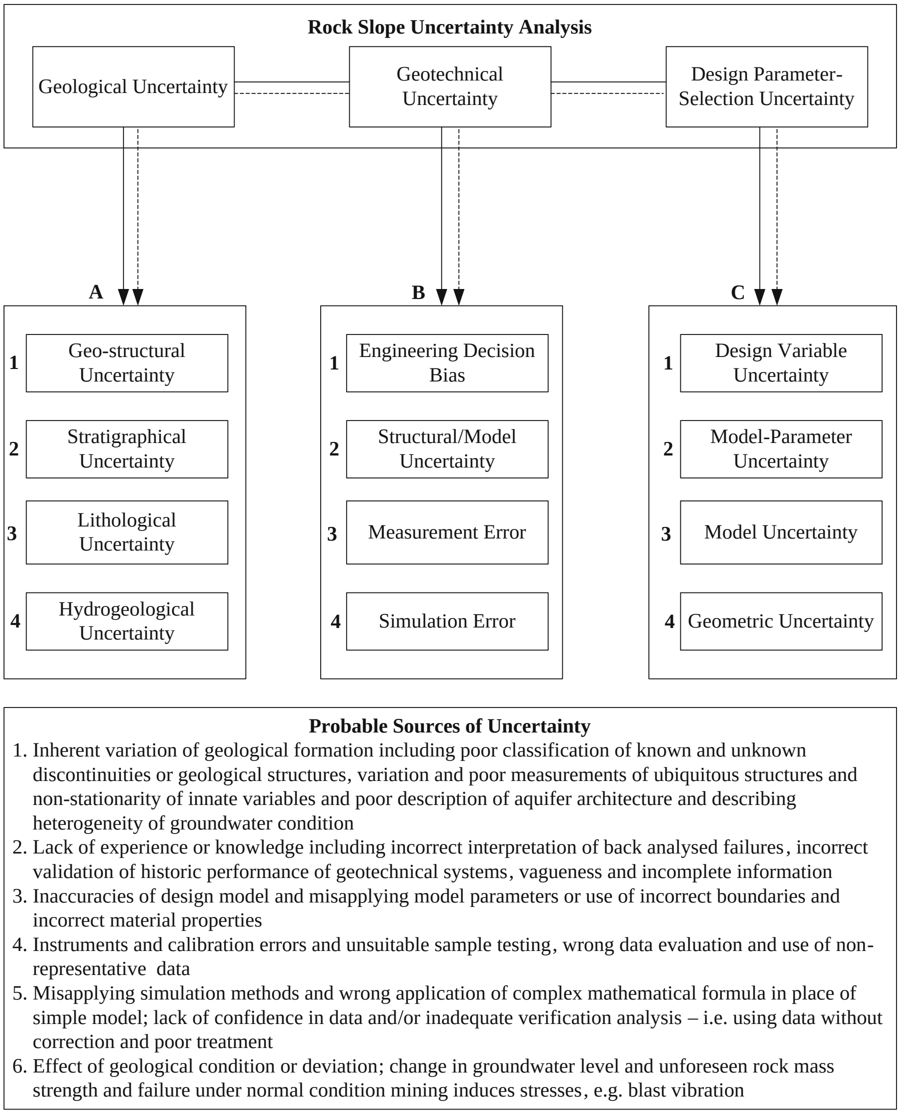

Fig. 9 Rock slope uncertainty classification along with probable sources and possible solutions

using statistical estimations, it adds up to model uncertainty which may stem from imperfect representation of reality.

3.2 Geotechnical Uncertainty

Geotechnical uncertainties have been studied and have wide range of definitions (e.g. Phoon and Kulhawy 1999; Baecher and Christian 2003; Bea 2006; Hadjigeorgiou and Harrison 2011). These past researches described geotechnical as subjective uncertainty. Subjective uncertainty arises from three sources of error; error in data collection, error in data processing and error in design analysis. Oberkampf et al. (2001), defined error as recognisable inaccuracy in any phase or activity of modelling and simulation that is not caused by lack of knowledge. They stressed that the inaccuracy is identifiable or knowable when examined. As an example, in an open pit rock slopes: (a) the combined type of errors in data collection and processing may include incorrect identification of joints and bedding planes specific to bench scales which are incorrectly assigned to overall slope; and also assigning faults, shear, dykes, bedding specific to

Table 2 Examples of probable sources of uncertainty and possible solution model

Group	Sources	Type of uncertainty	Possible solution
A1	1, 6	Aleatory, inherent or data variability	Probability/Frequency distribution when sufficient data is available; Normal/Lognormal Probability Functions, defined by mean, standard deviation, coefficient of variation; MCS, Kriging and semi-variogram analysis
A2	1	Aleatory, inherent or data variability	
A3	1	Aleatory, inherent or data variability	
A4	1, 6	Aleatory, inherent or data variability	
B1	2, 5	Epistemic, statistical uncertainty, model uncertainty, transformation uncertainty	Bayesian Estimation; Fuzzy set theory and Probability Distribution; Sensitive analysis and relies on experience of analyst, multiple criteria decision method
B2	3, 5	Epistemic, statistical uncertainty, model uncertainty	Monte Carlo Simulation, Multivariate statistical Analysis; Back Analysis
B3	4	Epistemic, measurement error, transformation uncertainty	Normal/Lognormal Probability Functions defined by mean, standard deviation, coefficient of variation, MCS
B4	3, 5	Epistemic	Characterised by bias and covariance of bias: bias is the ratio of measured/true value to the predicted or nominal value
C1	2, 3, 5	Epistemic	Probability/Frequency distribution when sufficient data is available; Normal/Lognormal Probability Functions, defined by mean, standard deviation, coefficient of variation; MCS
C2	5, 6	Epistemic, statistical uncertainty, model uncertainty	Monte Carlo simulation, point estimate method, random fields theory methods
C3	5, 6	Epistemic	Monte Carlo simulation, point estimate method, random fields theory methods
C4	3, 4	Epistemic	Sensitivity analysis, probability function

overall slope to bench scale; and (b) there are possible design errors in defining bench face angle, berm width, multiple bench stack angles, inter-ramp angles and overall slope angles. Such errors may arise during measurements of geometrical and mechanical parameters. These errors are reducible because they are essentially due to incorrectness rather than lack of knowledge; they can be reduced by applying correct slope design tools depending on the nature of data available. Here, the geotechnical uncertainty can be divided into engineering decision bias, structural or model uncertainty, measurement error, and simulation error. The engineering decision bias describes uncertainties that results from lack of knowledge of geotechnical data such that it is useful to obtain expert knowledge in the estimations of parameter of interest; but the expert knowledge include point estimates which lead to difference of opinion such as when the expert's uncertainty is strongly skewed. For example the experts involved in the interpretation of the geological model are geologist, engineering geologist or a geotechnical engineer. In their interpretation the geologist or engineer makes use of existing knowledge of the geological environments which they think to be present. The quality of this information which is essential in the interpretation cannot be quantified at present, however if the geotechnical engineer is well experienced there will be a good model, and if the geologist is not well experienced, a poor model will result; but how well experienced the expert nobody can measure.

Structural uncertainty is a function of model uncertainty which relates to the inability of simulation model, design method or empirical formula represents the true physical behaviour of a system under consideration. Measurement error is an inappropriate noise in rock property measurements. It is caused by operator or instrumental variations from one test to the other and not variations in rock properties. Simulation error can be caused by, for example wrong application of complex mathematical formula in place of simple model.

Geotechnical uncertainty in rock slope stability analysis are characterised by either an objective or a subjective modelling approach. The objective modelling involves the use of statistical and probabilistic methods on available data such as the Bayesian methods which are also been used to deal with gaining information of parameters (Ayyub and McCuen 1997). Subjective modelling is based on the expert's experience, belief and prior information or combination; this involves use of non-probabilistic or imprecise methods such as the fuzzy approximations. The theories of fuzzy sets and possibility have been successfully used in classification of rock masses and for rock slope stability analysis (e.g. Park et al. 2008, 2012a, b).

3.3 Design Parameter-Selection Uncertainty

The selection of design parameters must certainly satisfy all values within the range over which they vary. Design parameter-selection uncertainties can be caused by, for example, measuring limitations. There are parameters that can take on any possible value within a specified range, e.g. RMR or Q. Also, there can be parameters which must necessarily satisfy all values within the range over which they vary, e.g. cohesion and friction angle. The parameter types can be divided into design parameters and performance parameter. The design parameters are the parameters in the engineering model for which the engineer must select values, e.g. slope geometries because they are iteratively selected. The performance parameters are the values the engineer uses to indicate the design ability in order to satisfy the practical requirements, e.g. shear strength, shear stress which enters into the model. The performance parameter adds up to model parameter uncertainty which has been explained in Sect. 2.3.3, in accordance to Baecher and Christian (2003) and Abbaszadeh et al. (2011). Prior to slope stability analysis, the design parameter values are uncertain, such that the engineer does not know what values to use. Therefore, the performance parameter values are also uncertain, and as design process continues, values are determined more and more precisely in an iterative test. However every uncertainty form discussed shall be directly modelled. Many times, the initial design parameter uncertainties are modelled using the method of imprecision where each design parameter value is given a rank from zero to one to indicate degree of preference; this forms a preference function over each design parameter and performance parameter, indicating degree of preference for values. Probabilistic design parameters shall have their values ranked with degrees of probability. These uncertainties reflect different phenomena, and consequently will have different derived mathematics. A design parameter may have both a preference function and a probability density function.

4 Survey of Probability and Reliability Methods

In recent years, researchers as well as geotechnical engineers have been using probability and reliability methods to describe the stability of rock slopes. This is because, by using probability and reliability methods, it is possible to predict more precisely the rock property variability and getting more knowledge for geotechnical modelling. Therefore to track the growth of interest of geotechnical engineers in the application of probability and reliability methods in the field of rock slope stability analysis, a simple survey of rock slope stability publications that listed "uncertainty and reliability analysis" in their titles, abstracts or keywords was conducted. The survey focused mainly on publications from journal and conference papers including doctorate thesis and reports from engineering project works termed as "other source". Although there are several publications from other source as well as duplicating publications, only papers that were deemed relevant to rock slopes were considered. The search covered the period from 1985 to early 2017 and it found 91 such publications (41 journal papers, 26 conference papers and 24 other papers involving PhD thesis and engineering project reports). The outcome was sorted by year of publication and Fig. 10 shows histogram of the resulting table. The histogram indicates that from 1985, sufficient number of papers existed that listed its focus as uncertainty and reliability analysis of rock slope stability. Between 1996 and 2006 the interest seems to peak, and currently the interest appears to be at another high. A high trend is observed in journal papers than in conference papers even though the interest seems to rise steadily over the same period.

Table 3 provides a list of publications in the literature that applied probability and reliability methods to the stability analysis of rock slopes. The table lists the types of rock failure and the parameters employed as random variables. Figure 11 compares five major types of probability-based reliability methods. It is shown that the most popular methods that

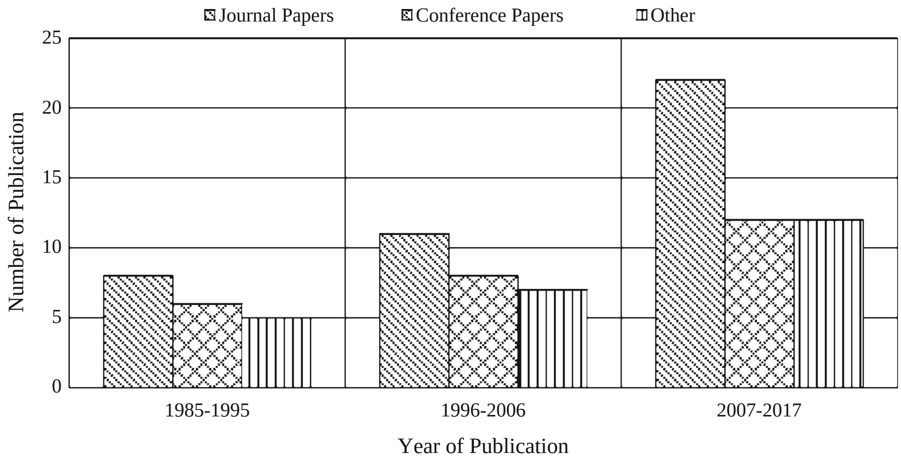

Fig. 10 A histogram plot of the frequency of rock slope stability publications on probability and reliability over the last 3 decades

Table 3 A summary of probabilistic reliability methods applied to rock slope stability

Failure type	Method	Random variable	References
Plane	FOSM, AFOSM, FORM, SORM, MCS, PEM, Fuzzy Set Theory, RS-DEM, Random Field Theory	c and ϕ, γ, j_c and j_ϕ,ϕ_r,β_f, JCS, JRC, discontinuity orientation, length, spacing, persistence, waviness, position of tension crack and depth of water in tension crack and FS; normal and shear stiffness (k_n and k_s)	Chowdhury (1986), Tamimi et al. (1989), Duzgun et al. (1995), Genske and Walz (1991), Park et al. (2005, 2008), Duzgun et al. (2003), Miller et al. (2004), Jimenez-Rodriguez et al. (2006), Duzgun and Bhasin (2009), Shen and Abbas (2013) and Gravanis et al. (2014)
Wedge	FOSM, FORM, MCS, PEM, Maximum Likelihood, Fuzzy Set Theory	c and ϕ, γ, waviness, FS, height of wedge and slope orientation, discontinuity orientation, length, spacing, persistence, position of tension crack, depth of water in tension crack and normalised water pressure	Genske and Walz (1991), Low (1997, 2007), Park and West (2001), Miller et al. (2004), Jimenez-Rodriguez and Sitar (2007) and Park et al. (2005, 2006, 2012a, b)
Toppling	MCS	dip of toppling discontinuity, basal discontinuities with direction close to that of slope face and spacing of discontinuities	Scavia et al. (1990), Genske and Walz (1991) and Tatone and Grasselli (2010)

FOSM First Order Second Moment, *AFOSM* Advanced First Order Second Moment, *FORM* First Order Reliability Method, *SORM* Second Order Reliability Method, *MCS* Monte Carlo Simulation, *PEM* Point Estimate Method, *RS-DEM* Random Set-Distinct Element Method, c cohesion, γ unit weight, j_c joint surface cohesion, j_ϕ joint friction angle, ϕ_r residual friction angle, β_f basic friction angle, *JCS* joint compressive strength, *JRC* joint roughness coefficient, *FS* factor of safety, *kn* normal stiffness, *ks* shear stiffness

have applied to all three rock failure types are Monte Carlo (MC) simulation and First Order Second Moment (FOSM) methods. The histogram indicates that Point Estimate Method (PEM) and First Order Reliability Method (FORM) have been applied to plane and wedge failure, and only plane failures were realised from Advanced First Order Second Moment (AFOSM). It is obvious that the MC method is the most used; it is possibly due its effectiveness to allow uncertain information and its ability to provide best tools for large number of simulations. Generally MC enables a relatively quick calculation of probability of failure. Several probability and reliability methods are in use and Figs. 10 and 11 may interpret differently where those missed in this survey are covered. The purpose of this comparison is to present how

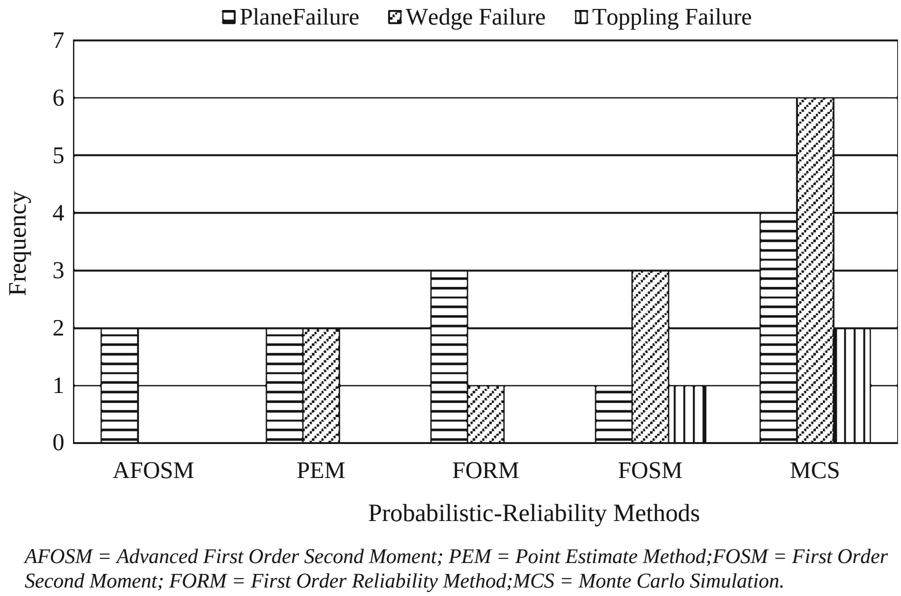

Fig. 11 Frequency histogram of probabilistic-reliability analysis method for different types

probability and reliability methods have advanced and what choice of design model was applied for the various types of rock failure.

There are several commercial software programs that can be used to carry out probabilistic-reliability computations; these include @Risk, SPSS (Statistical Package for the Social Science), MATLAB (Matrix Laboratory), STATISCA, and SAS (Statistical Analysis System).

- @Risk—a Microsoft add-in program; risk evaluation or sampling technique such as Monte Carlo simulation, Latin Hypercube and Point Estimate Method.
- SPSS—a window program; handles large amount of data and has scores of statistical and mathematical functions and statistical procedure such as simple linear regression and multivariate statistical analyses.
- MATLAB—handles descriptive statistics and plots for exploratory data analysis, and fit probability distributions to data; generates random numbers for Monte Carlo simulations, and performs hypothesis tests; preforms regression and classification analyses and builds predictive models such as stepwise regression, principal component analysis, regularisation, and other dimensionality reduction methods that let one identify variables or features that impact on the model.
- STATISCA—the suite includes range of data analysis, management and visualisation and data mining processes; can perform predictive modelling, clustering technique and classification.
- SAS—use for traditional analysis of variance and linear regression and Bayesian inferences; has high performance modelling tools for large data.

Apart from MATLAB software which has functions for FORM, SORM, FOSM, PEM, Fuzzy sets, the following software FERUM (Finite Element Reliability using Matlab); OpenSees (Open System for Earthquake Engineering Simulation); CalREL, and FSG (Floor Spectrum Generator) appear feasible for FORM, SORM and FOSM.

5 Consequences/Probabilistic Analysis: Economic and Safety Impact of Slope Instability

With the increasing demand of mineral deposits, geotechnical engineers are faced with the demands for steeper pit slopes. While it is normal for geotechnical engineers to define the appropriate slope design angles using deterministic and probabilistic methods, the analyses are generally based on the comparing the calculated factor of safety and probability of failure, with generic acceptability criteria not directly related to the impacts of failure. Therefore the high cost associated with the development of large open pit mine in complex geological condition including poor rock mass condition coupled with steep slope strategies have triggered the development of risk-based optimisation techniques. By utilising the risk-based method, there is potential for obtaining a better understanding on the conventional slope design methods. The risk-based approach therefore is used it to evaluate risks and failure consequences in terms of both safety and economics. The analysis provides valuable indication of optimum slope design configurations and thus becomes a great asset to surface mine design process (Steffen et al. 2008). To do so the probability of failure and potential consequences for various slope failure influencing factors must be quantified. The consequences of failure evaluates the overall slope design with the importance of personnel and equipment in high risk areas, related geological structures, loss of ore and production (Steffen et al. 2008; Contreras 2015).

Risk is defined as the probability of occurrence of an event combined with the consequence or potential loss associated with that event (Steffen et al. 2008; Contreras 2015):

$$\text{Risk} = \text{P}(_{\text{event}}) \times \text{Consequence of the event} \tag{3}$$

For slopes, the $\text{P}(_{\text{event}})$ is the probability of failure of the slope and the consequences can is the impact of failure to personnel and economics. The probability of failure is based on a slope stability model calculation and accounts only for part of the uncertainties of the slope. Because risk analysis sets the acceptability criteria on the consequences rather than on the likelihood of the event, a complete evaluation of the probability of slope is therefore required, incorporating other sources of uncertainty not accounted for with the slope stability model (Contreras 2015; Golestanifar et al. 2018). By comparing the calculated risk for various consequences with established threshold limits, decisions are made on the desirable design slope angle (Contreras et al. 2006). For the analysis of consequences of slope failure, engineering judgment and expert knowledge are integrated into the process with the aid of methods such as logic diagrams and event tree analysis (Golestanifar et al. 2018). Terbrugge et al. (2006) and Joughin (2017) presented a flow chart to illustrate the relationship between factor of safety (FS), probability of failure (PF) and risk as design acceptance criteria within the risk-based design process (Fig. 12).

The first step in performing any slope design is to estimate the FS. If the FS is low (i.e. FS < 1), the design may be deemed unacceptable and improvement on the design is required. In cases where other considerations dictate the design, a very high FS (FS > 1) may be sufficient to accept the design (Joughin 2017). Where potential for optimisation exists, the reliability of the design needs to be quantified. Likewise the FS, a low or high PF may be sufficient to consider the risk insignificant or unacceptably high. According to Joughin (2017), making decision based on FS or PF is often limited to the geotechnical team. He stressed that geotechnical team implicitly accepts a risk profile without quantification, however for some designs in the mine, this may not be acceptable and that the risk associated with a design should be quantified. In such cases the design acceptance criteria should be dictated by management through the company risk profile. In quantifying the economic impacts of slope failures of open pit mines, a risk-based design approach was proposed by SRK Consulting 2013. Figure 13 shows a flow chart of risk evaluation process depicting the main elements of the methodology. The flow chart follows the conventional geotechnical slope design process as described in several literatures and incorporates the additional elements required from the mine design process. The risk evaluation includes the following steps (SRK Consulting 2013; Contreras 2015):

- Definition of the set of slope sections to analyse key and critical pit areas during the mine life in order to provide representative cases of potential risks of slope failure within the mine plan.
- Calculation of the probability of failure (PF) of the slopes for areas selected in step 1 above.
- Estimate the economic impacts of slope failure with reference to the loss of annual profit or total project value as measured by the NPV (net present value).
- Create risk map to integrate the results of probability of failure and economic impact in order to identify the optimum slope angles, and comparison of the risk map with criteria to assess acceptability

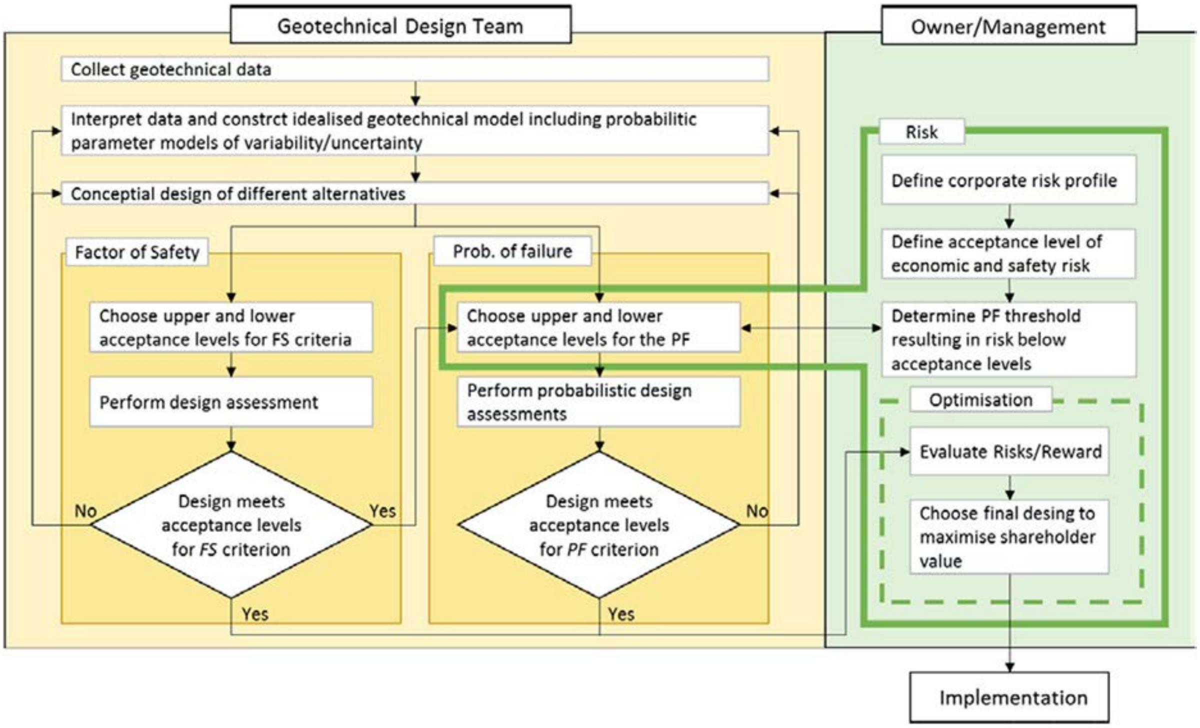

Fig. 12 Relationship between FS, PF and risk-based design acceptance criterion with the design process applicable to slope stability (Terbrugge et al. 2006; Joughin 2017)

Fig. 13 Risk-based slope design flow chart based on economic impact of slope failure (SRK Consulting 2013; Contreras 2015)

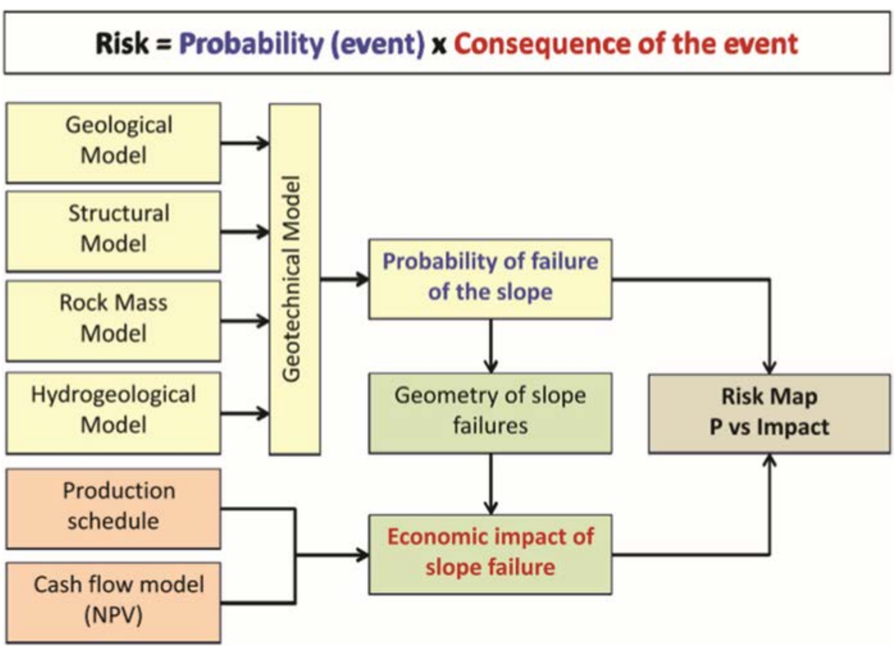

of the design and to define risk mitigation options as required.

- If the analysis is intended for the comparison of alternative slope design options, the process is repeated for each alternative pit layout and the results are collated in a graph of slope angle versus value and risk cost where the optimum slope angles can be defined.

For full understanding of the process the reader is referred to SRK Consulting (2013) and Contreras (2015).

6 Conclusion

The paper presents the advances and prospects of probability-based reliability methods for the stability analyses of rock slopes with the purpose of reducing uncertainty. Geotechnical engineers are usually asked to estimate ranges for uncertain quantities, it is important to know if they are to estimate for variability ranges or uncertainty ranges and also to know if they are to build models of variability or uncertainty. Therefore having a clear understanding of uncertainty and how to quantity uncertainty forms the basis to differentiate uncertainty from variability.

The review outlined in this article is intended to provide comprehensive guidelines to practicing geotechnical engineers and to promote the reliability methods in slope engineering designs. Based on existing knowledge, an integration of uncertainty for rock slopes stability analysis has been presented. The integration provides a logical structure that can be used to reduce several types of uncertainties in the design of rock slopes. This is useful when the engineer needs to create reliable geotechnical and geotechnical model in the design of open pit mine slopes. With due consideration for lack of adequate information during geotechnical investigations it is recommended that open pit mines should be designed to properly manage slope instability. Designing the mine slope using probability methods will characterise uncertainty and refine the range of parameters associated with slope stability models. It should be realised that model errors can be determined through probabilistic back analysis if information on the field performance of slopes in similar rock mass condition is available. This method can be used to update the probabilistic distribution of uncertain parameters based on field observations; the past performance of similar observed slopes can be used to reduce uncertainty and directly used for reliability update. Where the probability distribution of random variable cannot be determined accurately, using reliability-based method for optimisation can be important.

To track the growth of interest in the application of probability and reliability methods in the field of rock slope stability analysis, a simple survey of rock slope stability publications was conducted starting from 1985. From the result of this study, the interest peaked between 1996 and 2006 and currently appears to be at another high. The interest is confirmed by the use of probabilistic options in popular slope stability software such as Slide, Swedge, Rocplane and RS2. In studying the type of rock slope failure and what methods of probability-based reliability analysis were applied, the Monte Carlo and First Order Second Moment methods were found to have been used for planar, wedge and toppling failures analyses. The Point Estimate Method and First Order Reliability Method have been widely applied to plane and wedge failure. The most popular method was Monte Carlo probably due its effectiveness and its ability to provide best tools for large number of simulations.

While the deterministic approach attempts to give a dependable analysis which leads to cosmetic slope design recommendations, it does not allow for the optimisation of slope safety performance. The reliability based open pit slope stability gives insight in safety factor and risk of failure. The method can be used to select the optimal slope configurations based on the minimum acceptable risk of slope failure and also better understand the likelihood of slope failure hazards.

From the review study the stability of open pit mine rock slopes has been largely carried out using traditional probability (i.e. the sampling-based approach) whether the rock mass is moderately to heavily jointed and/or rock mass strength is nearly isotropic. Likewise the approximation methods (i.e. most probable point-based approach) have been used extensively in academic research for similar conditions of rock mass, but less used in mining industry due to the perceived mathematical complexity. However the complex nature of rock mass and whether the discontinuity spacing is large or small compared to the dimension of rock slope and/or the stability is governed by shear strength of individual discontinuity, lead to spatial variation of the rock mass strength parameters. It is therefore recommended that the concept of spatial variability which has been mostly applied to soils should be employed and emphasised in rock slope stability analysis.

References

Abbaszadeh M, Shahriar K, Sharifzadeh M, Heydari M (2011) Uncertainty and reliability analysis to slope stability: a case study from Sungun Copper Mine. Geotech Geol Eng 29(4):581–596

Ang AHS, Tang WH (1975) Probability concepts in engineering planning and design-basic principles. Wiley, New York

Ayyub BM, McCuen RH (1997) Probability statistics and reliability for engineers, 3rd edn. CRC Press LLC, Boca Raton

Baecher GB, Christian JT (2003) Reliability and statistics in geotechnical engineering. Wiley, London

Bea R (2006) Reliability and human factors in geotechnical engineering. J Geotech Geoenviron Eng ASCE 132:631

Bedi A, Harrison JP (2013) Characterisation and propagation of epistemic uncertainty in rock engineering: a slope stability example. In: Proceedings of international symposium of the ISRM, Eurock 2013, 21–26 September, Wroclaw, Poland

Begg SH, Bratvold RB, Welsh MB (2014) Uncertainty vs. variability: what's the difference and why is it important? In: SPE hydrocarbon economics and evaluation symposium held in Houston, Texas, USA, 19–20 May 2014. Copyright 2014, Society of Petroleum Engineers

Carter TG (1992) Prediction and uncertainties in geological engineering and rock mass characterization assessment. In: Proceedings of 4th Italian rock mechanics conference, Torino, pp 1.1–1.22

Chowdhury RN (1986) Geomechanics risk model for multiple failures along rock discontinuities. Int J Rock Mech Min Sci Geomech Abstr 23:337–346

Christian JT (2004) Geotechnical engineering reliability; how well do we know what we are doing? J Geotech Geoenviron Eng ASCE 130(10):985–1003

Contreras LF (2015) An economic risk evaluation approach for pit slope optimization. SRK Consulting, Johannesburg, The Southern African Institute of Mining and Metallurgy vol.115 n.7 Johannesburg Jul. 2015

Contreras LF, Le Sueur R, Maran J (2006) A case study of risk evaluation at Cerrejon Mine. In: Proceedings of the international symposium on stability of rock slopes in open pit mining and civil engineering situations, Cape Town, South Africa, 3–6 April 2006. Symposium Series S44. Southern African Institute of Mining and Metallurgy, Johannesburg

Der Kiureghian A, Ditlevsen O (2009) Aleatory or epistemic? Does it matter? Struct Saf 31(2):105–112

Dodagoudar GR, Venkatachalam G (2000) Reliability analysis of slopes using fuzzy sets theory. Comput Geotech 27(2000):101–115

Duzgun HSB, Bhasin RK (2009) Probabilistic stability evaluation of Oppstadhornet rock slope Norway. Rock Mech Rock Eng 42:724–749

Duzgun HSB, Yucemen MS, Pasamehmetoglu AG (1995) Plane failure analysis of rock slopes: a reliability approach. Int J Surf Min Rec 9:1–6

Duzgun HSB, Yucemen MS, Karpuz C (2002) A probabilistic model for the assessment of uncertainties in the shear strength of rock discontinuities. Int J Rock Mech Min Sci 39:743–754

Duzgun HS, Yucemen MS, Karpuz C (2003) A methodology for reliability-based design of rock slopes. Rock Mech Rock Eng 36(2):95–120

Einstein HH (2003) Uncertainty in rock mechanics and rock engineering-then and now. In: Proceedings of ISRM 2003, technology roadmap for rock mechanics. South African Institute of Mining and Metallurgy

Fenton GA, Griffiths DV (2008) Risk assessment in geotechnical engineering. Wiley, New Jersey

Galal OH (2013) A proposed stochastic finite difference approach based on homogeneous chaos expansion. J Appl Math 2013(2013), Article ID: 950469

Genske DD, Walz B (1991) Probabilistic assessment of the stability of rock slopes. Struct Saf 9(3):179–195

Golestanifar M, Ahangari K, Goshtasbi K, Dehkharghani AA, Terbrugge P (2018) Governing risk elements through open pit slope optimization. J SAIMM 118(1):47–56

Gravanis E, Pantelidis L, Griffiths DV (2014) An analytical solution in probabilistic rock slope stability assessment based on random fields. Int J Rock Mech Min Sci 71:19–24

Hadjigeorgiou J, Harrison JP (2011) Uncertainty and sources of error in rock engineering. In: Qian Q, Zhou X (eds) Proceedings, 12th ISRM international congress on rock mechanics, harmonising rock engineering and the environment, 18–21 October 2011, Beijing, China. CRC Press, Leiden, pp 2063–2067

Honjo Y, Hara T, Suzuki M, Shirato M, Le Kieu TC, Kikuchi Y (2009) Code calibration in reliability based design level I verification format for geotechnical structures. In: Proceedings of 2nd international symposium on geotechnical safety and risk, pp 435–452

Huber M (2013) Soil variability and its consequences in geotechnical engineering. PhD thesis, Institut für Geotechnik der Universität Stuttgart, Germany

Jimenez-Rodriguez R, Sitar N (2007) Rock wedge stability analysis using system reliability methods. Rock Mech Rock Eng 40(4):419–427

Jimenez-Rodriguez R, Sitar N, Chacon J (2006) System reliability approach to rock slope stability. Int J Rock Mech Min 43(6):847–859

Joughin WC (2017) Dealing with uncertainty and risk in the design of deep and high stress mining excavations. In: Wesseloo J (ed) Deep mining 2017: eighth international conference on deep and high stress. Mining Australian Centre for Geomechanics, Perth Australia

Kendall DG (1974) Foundations of a theory of random sets. In: Harding EF, Kendall DG (eds) Stochastic geometry. Wiley, New York

Lindley DV (2013) Understanding uncertainty. Wiley, New York

Low BK (1997) Reliability analysis of rock wedges. J Geotech Geoenviron Eng (ASCE) 123(6):498–505
Low BK (2007) Reliability analysis of rock slopes involving correlated non-normals. Int J Rock Mech Min 44(6):922–935
Low BK (2008) Efficient probabilistic algorithm illustrated for a rock slope. Rock Mech Rock Eng 2008(41):715–734
Low BK, Einstein HH (1992) Simplified reliability analysis for wedge mechanisms in rock slopes. In: Proceedings of 6th international symposium on landslides. A. A. Balkema, Rotterdam, pp 499–507
Matheron G (1973) The intrinsic random functions and their applications. Adv Appl Probab 5:439–468
McMahon BK (1985) Geotechnical design in the face of uncertainty. Australian Geomechanics Society, E.H. Davis Memorial Lecture
Miller SM, Whyatt JK, McHugh EL (2004) Applications of point estimate method for stochastic rock slope engineering. In: 6th North America rock mechanics symposium (NARMS), Houston, Texas Gulf Rocks 2004, pp 1–12
Moore RE (1966) Interval analysis. Englewood Cliffs, Prentice-Hall
Oberkampf WL, Sharon MD, Brian MR, Kathleen VD, Kenneth FA (2001) Error and uncertainty modeling and simulation. Reliab Eng Syst Saf 75:333–357
Pandit B, Tiwari G, Latha GM, Babu GLS (2018) Stability analysis of large gold mine open-pit slope using advanced probabilistic method. Rock Mech Rock Eng 51(7):2153–2174
Pantelidis L, Gravanis E, Griffiths DV (2015) Influence of spatial variability on rock slope reliability using 1-D random fields. Eng Geol Soc Territ. https://doi.org/10.1007/978-3-319-09057-3_216
Park H, West TR (2001) Development of a probabilistic approach for rock wedge failure. Eng Geol 59:233–251
Park HJ, West TR, Woo I (2005) Probabilistic analysis of rock slope stability and random properties of discontinuity parameters. Interstate Highway 40, Western North Caroline, USA. Eng Geol 79:230–250
Park HJ, Jeong UJ, Han BH, Ro BD, Shin KH, Kim JK (2006) The evaluation of the probability of rock wedge failure using the point estimate method and maximum likelihood estimation method. IAEG, Paper number 485
Park HJ, Um J, Woo I (2008) The evaluation of failure probability for rock slope based on fuzzy set theory and Monte Carlo simulation. In: Chen et al (eds) Landslides and engineered slopes. Taylor & Francis Group, London. ISBN 978-0-415-41196-7
Park HJ, Um JG, Woo I, Kim JW (2012a) Application of fuzzy set theory to evaluate the probability of failure in rock slopes. Eng Geol 125:92–101
Park HJ, Um JG, Woo I, Kim JW (2012b) The evaluation of the probability of rock wedge failure using the point estimate method. Environ Earth Sci 65:353–361
Peschl GM (2004) Reliability analyses in geotechnics with the random set finite element method. Ph.D. dissertation, Institute for Soil Mechanics and Foundation Engineering, Graz. University of Technology
Phoon KK, Kulhawy FH (1999) Evaluation of geotechnical property variability. Can Geotech J 36(4):625–639
Phoon KK, Huang SP, Quek ST (2002a) Implementation of karhunen-loève expansion for simulation using a wavelet-Galerkin scheme. Probab Eng Mech 17(3):293–303
Phoon KK, Huang SP, Quek ST (2002b) Simulation of second-order processes using Karhunen–Loève expansion. Comput Struct 80(2002):1049–1060
Phoon KK, Huang SP, Quek ST (2005) Simulation of strongly non-Gaussian processes using Karhunen–Loève expansion. Probab Eng Mech 20(2005):188–198
Read J (2009) Data uncertainty: guidelines for open pit slope design. In: Read J, Stacey P (eds) CSIRO Publishing, Collingwood, pp 214–220
Rocscience Inc. (2001) RocPlane Version 3.0—planar sliding stability analysis for rock slopes. www.rocscience.com. Toronto, Ontario, Canada. Accessed 7 June 2018
Rocscience Inc. (2006) Swedge Version 6.0—3D surface wedge analysis for slopes. www.rocscience.com. Toronto, Ontario, Canada. Accessed 7 June 2018
Rocscience Inc. (2015a) Slide Version 7.0—2D Limit equilibrium slope stability analysis. www.rocscience.com. Toronto, Ontario, Canada. Accessed 7 June 2018
Rocscience Inc. (2015b) RS2 Version 9.0—finite element analysis for excavations and slopes. www.rocscience.com. Toronto, Ontario, Canada. Accessed 7 June 2018
Rosenblueth E (1981) Two-point estimates in probabilities. Appl Math Model 5:5329–5335
Roy CJ, Oberkampf WL (2011) A comprehensive framework for verification, validation, and uncertainty quantification in scientific computing. Comput Methods Appl Mech Eng 200(25–28):2131–2144
Sari M, Karpuz C (2006) Rock variability and establishing confining pressure levels for triaxial tests on rocks. Int J Rock Mech Min Sci 43(2006):328–335
Scavia C, Barla G, Bernaudo V (1990) Probabilistic stability analysis of block toppling failure in rock slopes. Int J Rock Mech Min Sci Geo-mech Abstr 27:465–478
Schweiger HF, Pöttler R, Peschl GM (2007) Application of the random set finite element method for analysing tunnel excavation. Georisk 1:43–56
Shen H (2012) Non-Deterministic analysis of slope stability based on numerical simulation. PhD dissertation, TU Bergakademie Freiberg
Shen H, Abbas SM (2013) Rock slope reliability analysis based on distinct element method and random set theory. Int J Rock Mech Min Sci 61:15–22
Shen H, Widodo S, Klapperich H, Tamáskovics HN (2013) Reliability analysis of reinforced slope by random set theory. http://tu-freiberg.de. Accessed 21 Aug 2016
Shrestha B, Duckstein L (1998) A fuzzy reliability measure for engineering applications. In: Press CRC (ed) Uncertainty modeling and analysis in civil engineering. Ayyub LLC, Boca Raton, pp 121–135
Soize C (2013) Stochastic modeling of uncertainties in computational structural dynamics: recent theoretical advances. J Sound Vib 332(10):2379–2395
Song KI, Cho GC, Lee SW (2011) Effects of spatially variable weathered rock properties on tunnel behaviour. Probab Eng Mech 26:413–426
Spross J (2014) A critical review of the observational method. Licentiate thesis, Department of Civil and Architectural

Engineering Division of Soil and Rock Mechanics KTH Royal Institute of Technology Stockholm
SRK Consulting (2013) Pit slope risk study. SRK Consulting, Johannesburg
Steffen OKH, Terbrugge P, Venter J (2008) A risk evaluation approach for pit slope design. ARMA American Rock Mechanics Association, Johannesburg
Sudret B, Blatman G (2009) Advanced methods for FE-reliability analysis: adaptive polynomial chaos expansions. Partnership between Phimeca IFMA/LaMI and EDF R&D, JCSS workshop on semi-probabilistic FEM calculations December 2nd, 2009
Tamimi S, Amadei B, Frangopol DM (1989) Monte Carlo simulation of rock slope stability. Comput Struct 33(6):1495–1505
Tatone BSA, Grasselli G (2010) Rocktopple: a spreadsheet-based program for probabilistic block-toppling analysis. Comput Geosci 36:98–114
Terbrugge PJ, Wesseloo J, Venter J, Steffen OKH (2006) A risk consequence approach to open pit slope design. ARMA American Rock Mechanics Association, Johannesburg
Tonon F, Bernardini A, Mammino A (2000a) Determination of parameters range in rock engineering by means of random set theory. Reliab Eng Syst Saf 70:241–261
Tonon F, Bernardini A, Mammino A (2000b) Reliability analysis of rock mass response by means of random set theory. Reliab Eng Syst Saf 70(3):263–282
Valerio M, Clayton C, D'Ambra S, Yan C (2013) An application of a reliability based method to evaluate open pit slope stability. In: Dight PM (ed) Proceedings of the 2013 international symposium on slope stability in open pit mining and civil engineering. Australian Centre for Geomechanics, Perth, pp 457–471
Vanmarcke EH (1983) Random fields: analysis and synthesis. MIT Press, Cambridge
Vanmarcke EH, Grigoriu M (1983) Stochastic finite element analysis of simple beams. J Eng Mech 109:1203
Wattimena RK (2013) Predicting probability stability of rock slopes using logistic regression. Int J Jpn Comm Rock Mech (JCRM) 9:1–6
Zadeh LA (1965) Fuzzy sets. Inf Control 8:338–353

Tunnelling and Underground Space Technology 41 (2014) 206–222

Contents lists available at ScienceDirect

Tunnelling and Underground Space Technology

journal homepage: www.elsevier.com/locate/tust

Evaluation of rock mass engineering geological properties using statistical analysis and selecting proper tunnel design approach in Qazvin–Rasht railway tunnel

Behrooz Rahimi [a,*], Kourosh Shahriar [a], Mostafa Sharifzadeh [a,b]

[a] Department of Mining & Metallurgical Engineering, Amirkabir University of Technology, 424 Hafez Ave., Tehran, Iran
[b] Department of Mining Engineering, Western Australian School of Mines, Curtin University, Australia

ARTICLE INFO

Article history:
Received 2 February 2013
Received in revised form 5 December 2013
Accepted 27 December 2013
Available online 30 January 2014

Keywords:
Tunnel
Ground behavior
Statistical analysis
Empirical methods
Numerical modeling
Optimum support system

ABSTRACT

Various geological and geotechnical conditions at different project sites require different design, calculation and construction methods. Stability of underground openings depends on ground conditions with different modes of behavior. An essential step in the design procedure is to assess the ground behavior and continuity factor in the tunnel. The objective of this research is to give a methodology for selecting appropriate design approach based on ground behavior and continuity factor in tunnels. The common procedure for determining rock mass properties and in situ stresses are empirical methods, back analysis, field tests and mathematical modeling. In most cases, estimation of rock mass parameters and in situ stresses using empirical methods are not accurate enough. Therefore, rock mass properties are estimated using several empirical equations and statistical analysis were performed to estimation of these properties in order to obtain rational and reasonable results with acceptable accuracy. The Qazvin–Rasht railway tunnel are taken as case study. Behavior types along the tunnel assessed as stable with the potential of discontinuity controlled block failure, several blocks irregular failure, shallow shear failure, plastic behavior (initial), swelling of certain rocks and water inflow. Therefore, appropriate approach for the tunnel support design selected based on classification systems, numerical modelling, observation methods, and engineering judgment. In order to evaluation of tunnel stability, necessary support types and categories RMR, *Q*, support weight and SRC were employed as empirical tunnel support design methods. The performances of the proposed support systems were analyzed and verified by means of numerical analysis. According to results of empirical and numerical methods and engineering judgment, shotcrete 0.15–0.2 m with wire mesh and light ribs steel sets (IPE160) were proposed as support elements for the tunnel. We found that using proposed approach the optimum support system could be designed.

1. Introduction

The Qazvin–Rasht railway tunnel is located 50 km north of Qazvin city in North–West Iran (Fig. 1). The planned length of the tunnel is 693 m with horseshoe shape with excavated dimensions of 12 m width and 9.3 m height (Fig. 2). The tunnel will be driven in the west Alborz Mountains (Haraz Rah Consulting Company, 2006). Evaluation of stability is one of the most important concerns in the design of tunnels. For the purposes of rock engineering design, different types of design tool or design system can be applied to the available information on the ground conditions, such as numerical modelling, analytical calculation, empirical (classification) systems or observational methods (Shahriar et al., 2009).

The various types of behavior require different assessments or calculation methods (rock engineering tools) for a proper design that can be depend onto cover the actual case (Palmstrom and Stille, 2007). It is clear that finding a single solution for tunnel stability problems is not an easy task. Uncertainties in the rock material strength parameters and stress are main impediments. Rock mass geomechanical parameters such as Hoek & Brown constants, deformation modulus and uniaxial compressive strength are input data for numerical analysis. Estimation of such parameters is important because the result of numerical analysis depends on accuracy of input data (Sari and Pasamehmetoglu, 2004).

The stability of an underground opening depends on the behavior of the ground surrounding it. Therefore, it is necessary to understand the actual type of behavior, as a prerequisite for rock

* Corresponding author. Tel.: +98 (21) 64542972; fax: +98 (21) 640 5846.
E-mail address: behrooz.riran@gmail.com (B. Rahimi).

0886-7798/$ - see front matter © 2014 Elsevier Ltd. All rights reserved.
http://dx.doi.org/10.1016/j.tust.2013.12.010

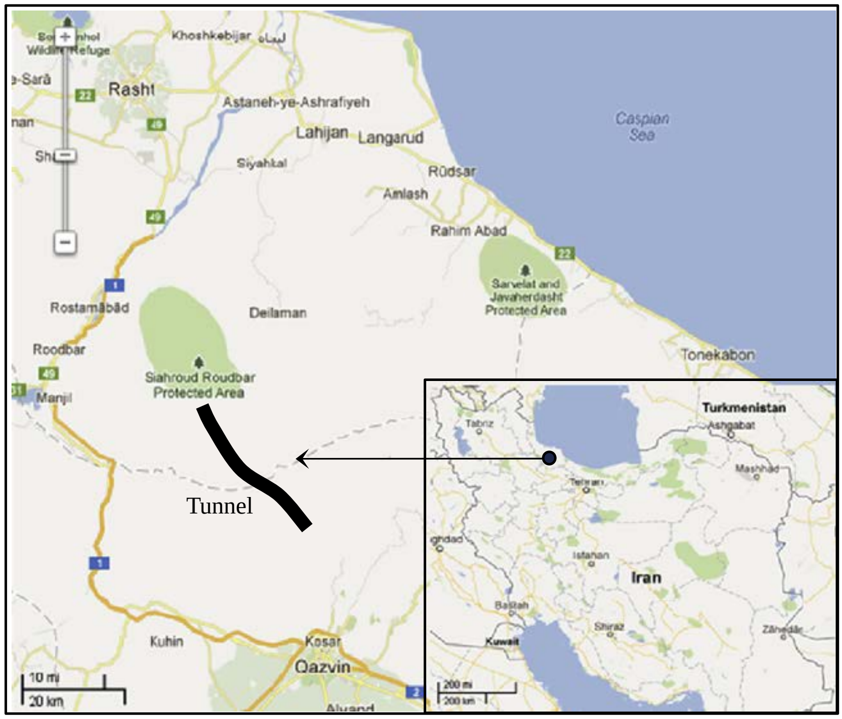

Fig. 1. Location of the study area Qazvin–Rasht railway tunnel.

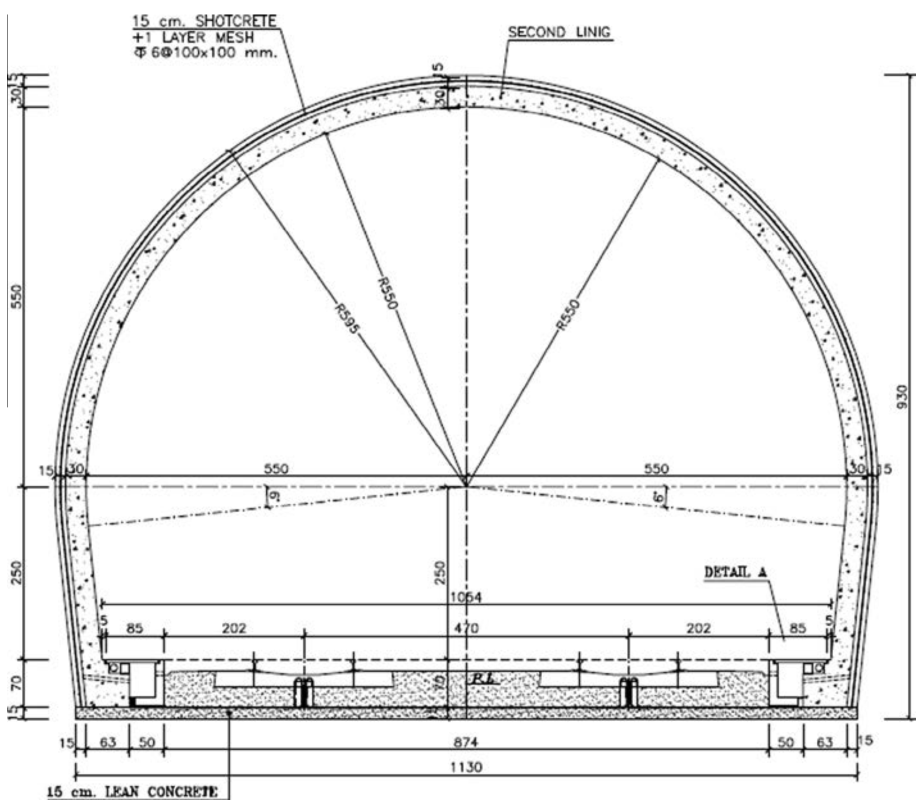

Fig. 2. The Qazvin–Rasht railway tunnel cross-section.

support and other evaluations. Ground behavior is the way the ground acts in response to the rock mass conditions, the forces acting and the project related features (Stille and Palmstrom, 2007). The objective of this research is to give a guideline for selecting proper design methods of tunnels, in order to increase in the quality of engineering assessments and design parameters, and realistic application of classification systems. An essential step in the design procedure is to assess the ground behavior. It is related to mode of failure or behavior type. Knowledge and understanding of the complexity of the ground are essential for a good geotechnical design of tunnel excavations. Therefore, guideline for selection of suitable design methods of tunnel is based on ground behavior. The usual methods for determining rock mass properties and in situ stresses are empirical methods, back analysis, field tests and mathematical modeling. Using of field tests are time and cost consuming often very difficult to control. Application of back analysis methods is not possible in the design stage and before the tunnel construction. Empirical methods are generally preferred by engineers and engineering geologists due to practicality, and in most cases, estimation of rock mass properties using these methods does not provide accurate enough. Statistical analysis methods are used to estimation of engineering geology properties. Using this method, determination of rock mass properties are obtained rational and reasonable results and decrease uncertainties. In this paper, selecting appropriate design methods and estimation of rock mass properties using statistical analysis methods carried out as a case study in the Qazvin–Rasht railway tunnel. Ground behavior types in the Qazvin–Rasht railway tunnel assessed as stable with the potential of discontinuity controlled block fall, block fall(s) of several blocks, shallow shear failure, plastic behavior (initial), swelling of certain rocks and water ingress. According to the ground behavior and continuity factor, appropriate methods for the tunnel support design have been selected classification systems, numerical modelling, observational methods, and engineering judgment.

The tunnel stability and the required support systems are evaluated by means of rock mass rating (RMR), rock mass quality (Q), support weight and surface rock classification (SRC).

Different empirical relationships have been used to estimate rock mass parameters and in situ stresses. In order to overcome some uncertainties of empirical relationships is used statistical analysis method for the results obtained from the empirical and range of parameters was estimated rather than just a single value.

Although classification systems are very useful during support design, they cannot adequately calculate stress distributions, support performance and deformations around the tunnel. Therefore empirical methods should be augmented by numerical methods and a 2D finite difference element program is utilized as numerical method to analyze the stability of tunnel and support performance. Consequently, suitable support system has been suggested for Qazvin–Rasht railway tunnel by using empirical, numerical modelling, engineering judgment and observational methods simultaneously.

2. Rock engineering and design methods

The rock engineer is generally needed to make a number of design decisions in which judgment and practical experience must play an important role. Prediction and/or evaluation of support requirements for tunnels are largely based on observations, experience and personal judgment of those involved in tunnel construction. The design of excavation and support systems for rock, although based on some scientific principles, has to meet practical requirements. The purpose is to select and combine the parameters of importance for stability in an underground opening the main features determining the stability are reviewed including various modes of failure. Underground openings design generally means designing support systems for such excavations. Various geological and geotechnical situations in different project sites required using different designing, calculations and execution methods and also made engineers pay more attention to prior experience and apply engineering principals, permanently.

In order to design an underground space, it is necessary to be able to evaluate the consequences of different design options to be able to predict what will happen. For this purpose, some form of predictive capability is required through modeling. Type of modeling will depend on the nature of the project and the 'risk' involved to what extent any failure can be tolerated (Hudson and Feng, 2007).

In rock engineering design, different types of design tool or can be applied to the available information. Usual rock engineering and design tools for tunnels are:

1. Empirical methods.
   - The Q system.
   - The rock mass rating (RMR) system.
   - The RMi rock support method.
   - The new Austrian tunneling method(NATM).
   - The geological strength index(GSI).
2. Calculated solutions.
   - Numerical modeling.
   - Analytical calculations.
3. Judgmental solutions.
   - Observational methods.
   - Engineering judgment.

The design of the tunnel lining requires the designer to use computational tools that are able to evaluate the underground and surface displacements, and the plasticized zones around the void, but also the forecast stresses acting inside the lining, to produce a structural design (Barpi and Peila, 2012). The British Tunneling Society clearly states that the most important goal of a tunnel design is to provide an understanding of the rock mass and lining behavior during tunneling, including the evaluation of risks. Risk analysis is the essential way for producing a robust and safe design. Finally the design process should provide the basis for interpreting the monitoring results during construction. The widely used design methods in tunneling practice are (Barpi et al., 2011):

1. empirical methods, usually based on rock mass classification;
2. analytical solutions, which are usually developed using:
   - continuum analytical models,
   - convergence-confinement,
   - limit equilibrium methods, to evaluate the stability of rock blocks around a tunnel and the stability of tunnel face,
   - bedded-beam-spring models, where the tunnel lining is modeled as a series of beams connected to each other and to the ground by radial and tangential springs that simulate the ground support interaction;
3. two and three-dimensional numerical analyses, which can be carried out using the finite element, the finite difference methods or the distinct element method with the ability to model complex geometrical, geological and geotechnical structures.

Tunnel designers should always take into account that every model could be affected by many error sources that could lead to poor predictions such as the theoretical shape of the tunnel, which can be different from the reality due to the construction method (Barpi and Peila, 2012).

3. Appropriate design method selection

The stability of a tunnel depends on the behavior of the ground surrounding it. The various types of behavior require different assessments or rock engineering tools for a suitable design that can be relied onto include the real case. It is very important to select proper design tools based on geological and geotechnical conditions. It should be emphasized that without adequate knowledge of the geology and ground conditions, as well as the site specific features, the ground behavior cannot be defined and, hence, appropriate design work cannot be carried out. The choice of suitable tools for the design is essentially an outcome of the actual ground behavior, such as an acceptable standard or some other requirement. It is necessary that appropriate engineering judgment to be used for weak zones such as shear zones. Therefore, it is necessary to understand the real type of behavior, as an essential for rock support and other evaluations. Palmstrom and Stille have presented the principle relationships between ground behavior and rock engineering and design. Fig. 3 shows the main geological and topographical features influencing on ground behavior and the application of rock engineering tools used for design. The choice of appropriate tools for the design is essentially a result of the real ground behavior (Palmstrom and Stille, 2007).

The first step in analyzing instability is the geotechnical and geological characterization of the site. For this purpose, field surveys are best suited. A critical interpretation of the survey results allow the development of a model to simulate the instability phenomenon, with the aim to ascertain the main causes that induced it. The same model can then be used for the verification of the predicted stabilization system. According to requirements and condition of projects, detailed geological and geotechnical surveys can be carried out as follows (Barbero and Barpi, 2011).

1. Geological structural survey.
2. Geomorphological survey.
3. Core drilling, and installation of inclinometer.
4. Seismic refraction and geo-electrical survey

Drilled core analysis and the geological and geomorphological data could be used to identify of the:

- complex structural and geological rock mass conditions,
- water infiltration in the rock mass fractures.

The relationship between various engineering design tools and ground behavior is presented in Table 1. It is intended to help in relating the fitness of some of the rock engineering tools that are appropriate to design studies. The assessment in Table 1 is based on the behavior of tunnel in various ground conditions. In addition, use of the table should lead to better use of classification systems, increase in the quality of engineering design evaluations, better relationship (Palmstrom and Stille, 2007).

All systems require training, experience and understanding of ground composition and behavior for proper use. The Q system considers all the aspects of behavior incorporated into one number and works best in ground conditions where wedge failure are likely. It also includes input parameters for slabbing, for which adequate rock support may be estimated. For weakness zones for which squeezing and/or swelling are likely, the system is not reliable. RMR is restricted to support design to counter wedge failure instability. As for the Q system, the influence of water on stability and therefore on rock support requirements is unclear. The NATM covers squeezing ground conditions. In the NATM, the ground behavior is the main item considered in the design. The qualitative ground descriptions used are associated with excavation techniques. Monitoring the behavior (displacements) of the tunnel during and after excavation plays a fundamental role in this method. The geological strength index (GSI) considers the rock structure in terms of blockiness and the surface condition of the discontinuities, as indicated by joint roughness and alteration (Rahimi, 2008).

The RMi system applies different approaches to rock support estimation in continuous and discontinuous ground, and it covers wedge failure as well as overstressed ground. For squeezing conditions, it makes an incomplete estimation, partly because of the relatively few case histories available, but also because tangential stresses in particulate ground are difficult to measure or calculate. This, of course, is the general case for all types of rock engineering tools. In addition, weakness zones are crudely included in the estimates (Palmstrom and Stille, 2007).

The numerical modelling is used mainly for the analysis of rock stresses and deformations and both continuum models and discrete block models are available. In many cases, and especially for highly fractured and massive ground, continuum models with appropriate material properties will be suitable. For blocky or jointed ground, where the rock mass is dominated by few dominate joints, discrete block models may be more appropriate.

Analytical calculations methods are used for simplified situations. For example, the behavior of a circular tunnel in an isotropic stress field can be ascertained directly. For such models, advanced analytical solutions allow both elastic–plastic and creep material

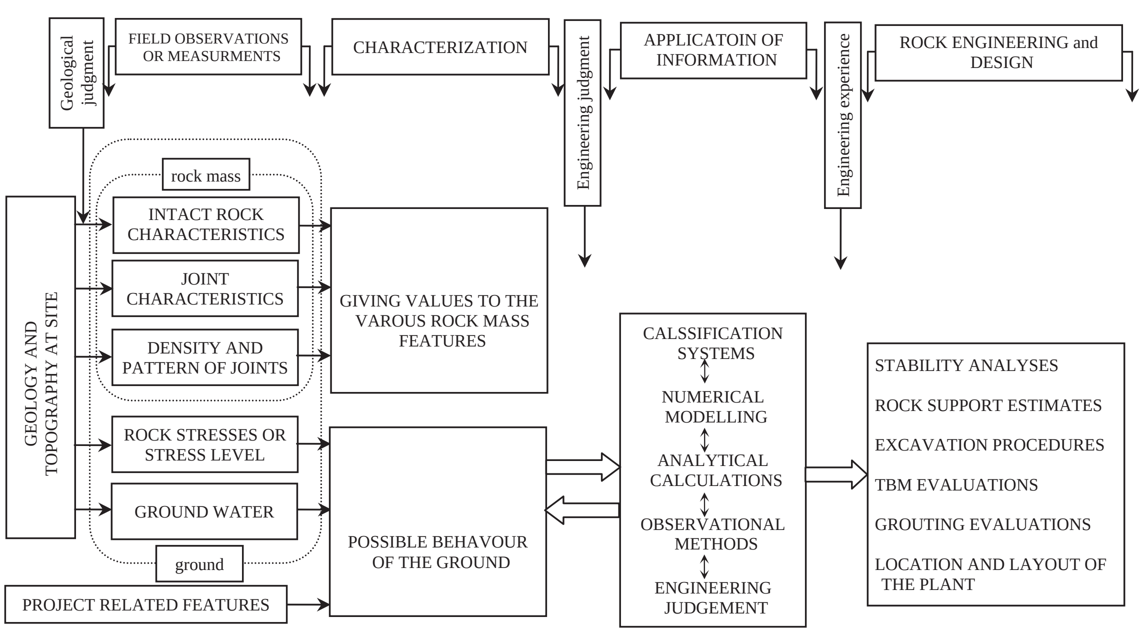

Fig. 3. The principle relationships between ground behavior and rock engineering and design (Palmstrom and Stille, 2007).

Table 1
The fitness of various engineering design tools (Palmstrom and Stille, 2007).

Ground behavior	Rock engineering and design tools							
	Classification systems			NATM	Numerical modeling(for continuous ground)	Analytical calculations	Observational methods	Engineering judgment
	RMR	Q	support RMi					
a: Stable	2	2	1–2	1	1	2	1	1
b: Fall of block(s) or fragment(s)	1–2	1–2	1–2	1–2	2	2	2	1
c: Cave-in	3	2–3	2	3	3	2	3	2
d: Running ground	4	4	4	4	4	4	3	2
e: Buckling	4	3	3	3	2	2	2	2
f: Rupturing from stresses	4	3	3	2	2	3	2	2
g: Slabbing, spalling	4	2	2	2–3	2	2	2	2
h: Rock burst	4	3–4	2	3	2	2	1–2	2
i: Plastic behavior (initial)	4	3–4	3	2–3	2	2	3	2
j: Squeezing ground	4	3	3	1–2	2	2	2	3
k: Raveling from slaking or friability	4	4	4	3	4	4	2	2
l: Swelling ground	4	3	3	3	3	3	2	2
m: Flowing ground	4	4	4	3–4	4	4	3	3
n: Water ingress	4	4	4	4	3	2	2	3

Fitness rating of the various tools: 1, suitable; 2, fair; 3, poor; 4, not applicable.

models, and also allow the incorporation of grouted dowels and shotcrete linings. Analyses of block stability can also be carried out with analytical solutions.

Observational methods rely on the review of the design during construction. Before excavation starts, an initial design is made, based on predictions of the rock mass behavior, and including plans for a monitoring system and contingency plans for incremental support works. Engineering judgment should always be applied in all types of engineering, as a check or verification.

One of the most important factors to consider for design is the relative degree of jointing. For rock engineering purposes, the continuity of the ground can be expressed by a continuity factor. For design purposes, ground continuity is described by continuity factor (CF). The amount of this factor is defined as the tunnel diameter divided by a mean value of a block diameter (Dt/Db). This factor shows the number of blocks located in the width of the tunnel. Continuity and discontinuity of rock mass can be determined by using the CF factor. Palmstrom and Stille have classified ground quality by means of the CF factor (Stille and Palmstrom, 2007):

(1) CF < 6, continuous-intact,
(2) 3 < CF < 30, discontinuous (blocky),
(3) CF > 15, continuous-blocky,
(4) 3 < CF < 6, continuous-intact to discontinuous (blocky),
(5) 15 < CF < 30, discontinuous (blocky) to continuous-blocky.

The purpose of the rock engineering process is to construct and complete the project. The design is a part of the rock engineering process. It is essential to understand that, as the design is a continuing process, decisions based on the design have to be taken gradually and in parallel with the progress of the scheme. Four steps are recommended for starting from the decision to be taken by researchers as follows (Palmstrom and Stille, 2007):

- Firstly, update all engineering geological data and project related information.
- Secondly, determine any uncertainties related to the information.

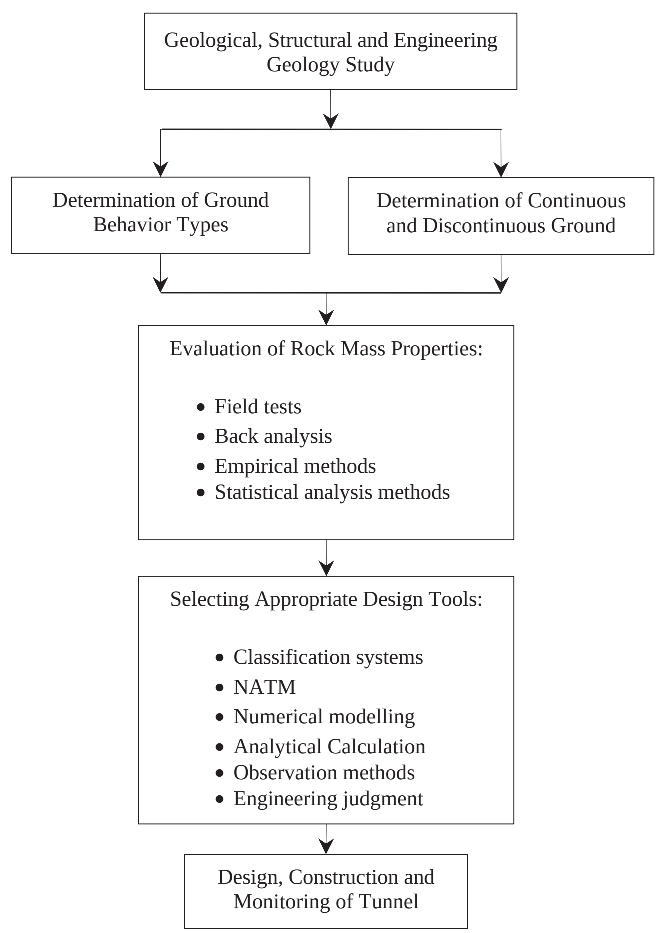

Fig. 4. Tunnel design procedure based on ground behavior and continuity factor.

- Thirdly, extensive explicit information enough to flow correctly through the project organization.

• Fourth, transfer the purpose of the engineer to the construction, with respect to any uncertainty in the parameters.

Tunnel design procedure based on ground behavior and continuity factor are presented in Fig. 4.

The procedure in Fig. 4 considers an approach for appropriate design methods using the following steps:

1. General, Structural and Engineering geology studies of site project.
2. Assessment the type of ground behavior for the ground surrounding the tunnel.
3. Determination of continuity factor, continuous and discontinuous of ground.
4. Estimation of rock mass properties and in situ stresses.
5. Application of statistical analysis methods for estimation of rock mass parameters and in situ stresses using empirical methods in order to obtain rational and reasonable results.
6. Fitness the suitable engineering design tools.
7. Design, construction and monitoring of tunnel.

The knowledge of the rock mass, which is fundamental for the tunnel design, is usually determined in engineering geological study. Monitoring measurements during the work are carried out before, during and even after the excavation of the tunnel, investigate a large series of parameters. In order to improve and make the first estimation of the geomechanical parameters of the rock obtained by the geomechanical characterization more reliable, one should proceed with the treatment of the results of the measurements through adequate back-analysis techniques .These results to be even more important in the construction of underground tunnels and voids, when a certain variability of the geomechanical characteristics of the rock mass is encountered along the section which was not possible to ascertain in detail during the preliminary analysis. Back-analysis therefore usually consists in the search for unknown parameters, of which one only has a preliminary estimation, that minimize the difference between the results of the calculation with the numerical model and the results of the performed measurements (Oggeri and Oreste, 2012).

4. Geology and engineering geology

The Qazvin–Rasht railway tunnel is located within the Western Alborz volcanic. The Geological formations mainly consist of the tuff and andesite–basalt rock masses of Eocene and Precambrian deposit. Andesite–basalt unit is main rock type along the tunnel alignment. Tuff and andesite–basalt units are moderately to highly weathered. Weathered faces of these rocks are brown to brownish-yellow in color and fresh parts are dark grey to grey in color. Andesite–basalt composed of mainly olivine, pyroxene, plagioclase, amphibole, and also mica minerals. Tuff contains mainly silica minerals and thin layers.

The thickness of andesite–basalt bedding is about 0.3–1 m. The thickness of tuff, which is above andesite bedding and makes the thickest part of overburden, is about 30 m. The alluvial and sedimentary deposits are located at the entrance and exit tunnel and its thickness is about 5–10 m. The particle size of alluvium varies from clay to pebble.

The tunnel alignment is divided into three different zones, each of which has different engineering geological properties.

1. The first zone (initial part) of the tunnel with the length of 150 m which is in Andesite layers and is called as Ta.
2. The second zone (middle part) with the length of 205 m, which consists of thin tuff layers in the higher level and thick andesite layers in the lower level, is identified as Tb.
3. The third zone (end part) or Tc is 340 m length and will be driven in the andesite layers.

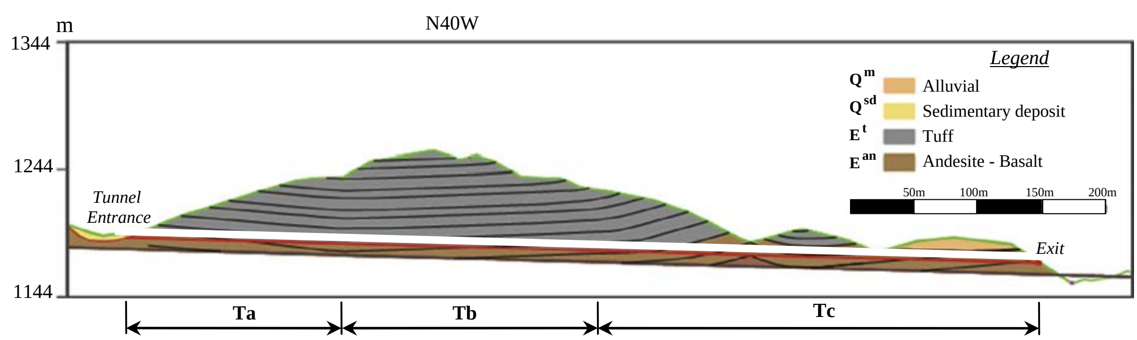

Fig. 5. Longitudinal geological cross-sections along tunnel.

Table 2
Engineering properties of discontinuities in first and second parts of the tunnel.

Joint sets	dip / dip direction	rang of dip direction / range of dip	Properties of joint sets and bedding surfaces: Length(m)	Spacing* (cm)	Aperture (mm)	Percent of infilling	Roughness	Weathering	Water condition
Bedding	039 / 17	±11 / ±8	>20	40 – 100 / 70	0.1–2	soft < 5	Slightly rough	Moderately to highly	Humid
J_1	084 / 83	±9 / ±7	10–20	10 – 60 / 35	0.1–1	soft < 5	Slightly rough	Moderately to highly	Humid
J_2	160 / 74	±20 / ±8	3–10	10 – 50 / 30	0.1–1	soft < 5	Slightly rough	Moderately to highly	Humid
J_3	309 / 63	±6 / ±6	3–10	30 – 70 / 50	0.1–1	soft < 5	Slightly rough	Moderately to highly	Humid

* $\frac{max-min}{avg}$.

Table 3
Engineering properties of discontinuities in third parts of the tunnel.

Joint sets	dip/dip direction	rang of dip direction/range of dip	Properties of joint sets and bedding surfaces						
			Length(m)	Spacing* (cm)	Aperture(mm)	Percent of infilling	Roughness	Weathering	Water condition
Bedding	014/18	±10/±8	3–10	70 – 150/100	0.1–5	Soft < 5	Slightly rough	Moderately to highly	Humid
J_1	105/83	±13/±6	3–15	30 – 60/40	0.1–3	Soft < 5	Slightly rough	Moderately to highly	Humid
J_2	199/71	±10/±9	3–10	30 – 60/40	0.1–2	Soft < 5	Slightly rough	Moderately to highly	Humid

* $\frac{max - min}{avg}$.

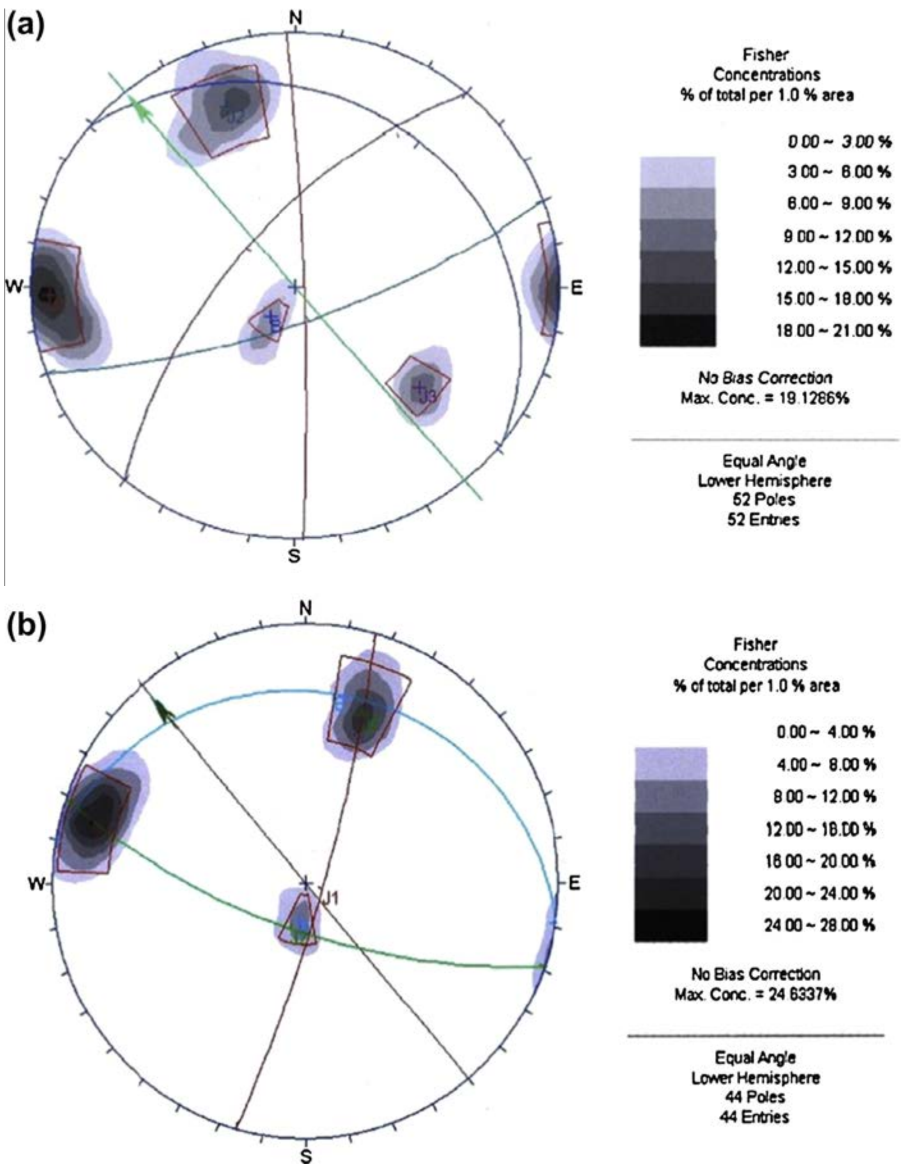

Fig. 6. Major discontinuity sets in Ta and Tb (a) and Tc (b) of the tunnel.

A longitudinal geological cross section along the tunnel is given in Fig. 5.

The engineering geological studies include both field and laboratory studies. The field studies consist of field observation and discontinuity surveys. Laboratory tests were conducted on samples, collected from the field and the boreholes. Discontinuities of the tunnel site were measured and the orientations of main discontinuities are processed utilizing a computer program based on the equal-area stereographic projection method. Results of engineering properties of discontinuities in all three parts of tunnel are given in Tables 2 and 3. The determined dominant discontinuity sets are illustrated in Fig. 6. Laboratory experiments were carried out to determine the physical and mechanical properties of rock material in all three zones of tunnel, including uniaxial com-

Table 4
Physical and mechanical properties of rocks obtained from the laboratory tests.

Properties, symbol (unit)	Maximum of overburden, H (m)	Poisson's ratio, v	Unit weight, γ (t/m^3)	Young modulus, E_i (GPa)	Uniaxial compressive strength, σ_c (MPa)
Ta	48	0.27	2.2	15	20
Tb	71	0.25	2.2	20	30
Tc	45	0.25	2.2	20	30

pressive strength (σ_c), Young modulus (E_i), Poisson's ratio (v) and unit weight (γ). Laboratory experiments were conducted on core specimens of NX size, 54 mm, taken from core drillings. As the specimens taken from the entrance of the tunnel show highly weathered structure, it was not appropriate to carry out all rock mechanic tests. The deformability parameters, Poison's ratio (v) and Young modulus (E_i) were obtained from deformability test. All laboratory tests were conducted in accordance with the ISRM suggested methods (ISRM, 1981) and the results are presented in Table 4. The average uniaxial compressive strength of Ta part is 20 MPa, Young's modulus is 15 GPa, Poisson's ratio is 0.27, unit weight is 2.2 t/m^3. The average uniaxial compressive strength of Tb and Tc parts is 30 MPa, Young's modulus is 20 GPa, Poisson's ratio is 0.25, unit weight is 2.2 t/m^3.

5. Using of rock mass classification systems in the tunnel

Rock mass classification evaluates the quality and expected behavior of rock masses based on the most important parameters that influence the rock mass quality. Rock mass classification systems are important as they provide a consistent means of describing quantitatively the rock mass quality. Many researchers have developed rock mass classification systems. In this research, rock mass are classified using RMR, Q, SRC, Support Weight and GSI. Since that RMR, Q, and GSI have been known, it is refused to description in their detailed. Here, the surface rock classification (SRC) and Support Weight is introduced briefly.

Table 5
Mapping of support categories into support weight (Tzamos and Sofianos, 2006).

Support category (Vector)	Code	Support weight (Scalar)
No support	NS	0
Spot bolting	SB	0.4
Systematic bolting	B	0.8
Bolts + shotcrete 5 cm	B S1	2.6
Bolts + shotcrete 10 cm	B S2	4.3
Bolts + shotcrete 15 cm	B S3	6.0
Bolts + shotcrete 20 cm	B S4	7.8
Bolts + shotcrete 20 cm + light steel sets	B S4 RRS1	8.2
Bolts + shotcrete 25 cm + medium sets	B S5 RRS2	10.5
Bolts + shotcrete 25 cm + heavy steel sets	B S5 RRS3	12.8
Cast concrete arches 30 cm	S6	10.2
Cast concrete arches 50 cm	CCA	15.5

The surface rock classification (SRC) system is more applicable for weak rocks and was developed from the RMR index to take into account the in situ stress, data from outcrops and tunnel construction conditions. In SRC classification system competence factor (σ_c/σ_1), tectonic events in near site, stress release factor and earthquake in the zones are used to assess the state of stress (Gonzalez de Vallejo, 2003). According to the SRC classification system, all three zones on the tunnel can be considered as poor rock mass. The SRC values for Ta, Tb and Tc are 25, 28 and 30, respectively.

In all rock mass classification systems the variable 'support' is expressed in vector terms. It is useful for our analysis to convert vector support quantities to scalar ones. A suitable variable is 'support weight' to be the approximate support pressure and dependent on the opening span. The meaning of support weight is the maximum equivalent pressure taken by the support elements. Support weight value is estimated by using Eq. (1) (Tzamos and Sofianos, 2006):

$$\text{support weight} = \frac{P_i D}{2} \tag{1}$$

where D is the span of the tunnel and P_i is the maximum pressure capacity of support components.

Support weight estimation based on the Q system and for a 10 m span can be calculated with Eq. (2):

$$\begin{aligned}\text{sup.weight} = &-0.034(\log Q)^4 + 0.117(\log Q)^3 + 0.72(\log Q)^2 \\ &- 3.67(\log Q) + 4.13\end{aligned} \tag{2}$$

Eq. (3) shows the relation between support weight with Q and span (Tzamos and Sofianos, 2006):

$$\begin{aligned}\text{sup.weight} = &-0.04\log Q^4 + 0.09\log Q^3 + 0.65\log Q^2 \\ &- 2Span^{0.27}(\log Q) + 1.5Span^{0.5}\end{aligned} \tag{3}$$

Support categories based on variable support weight (scalar) are given in Table 5. The support weight values for Ta, Tb and Tc are estimated 4.1, 4.5 and 5.6, respectively.

RMR, Q, SRC, GSI and support weight values for different rock masses along the tunnel alignment are given in Table 6. According to this results, the quality of rock mass in the tunnel are classified in the weak category.

6. Estimating rock mass properties using statistical analysis methods

The rock mass properties such as Hoek–Brown constants, deformation modulus (E_{mass}) and uniaxial compressive strength of rock mass (σ_{cmass}) the deformation modulus of a rock mass are an important input parameter in any analysis of rock mass, such as designing the primary support and final lining in a tunnel. The usual methods for determining rock mass properties and in situ stresses are empirical methods, back analysis, field tests and mathematical modeling. Field tests to determine these parameters directly are time consuming, expensive and the reliability of the results of these tests is sometimes questionable. Application of back analysis methods is not possible in the stage design and be-

Table 6
The estimated rock mass classification systems.

Parts of the tunnel	Rock mass classification (description, rate)				
	RMR	Q	SRC	GSI	Support weight
Ta	Weak, 40	Very weak, 0.55	Weak, 25	48–58	4.1
Tb	Good, 43	Weak, 1.21	Weak, 28	45–55	4.5
Tc	Good, 47	Weak, 1.65	Weak, 30	50–60	5.6

fore the tunnel construction. Several authors have proposed empirical relationships for estimating the value of an isotropic rock mass property on the basis of classification schemes such as RMR, *Q*, GSI and RMi. In most cases, estimation of rock mass parameters using empirical methods does not provide accurate enough. In this study, Statistical analysis methods are used to estimation of rock mass properties in order to obtain of rational and reasonable results and decrease uncertainties.

Statistical analysis is a branch of mathematics dealing with gathering, analyzing, and making inferences from data. This method is used to predict the characteristics of certain applicable real properties in all science. Statistical tools not only summarize past data through such indicators as the mean, medium, mode and the standard deviation but can predict future events using frequency distribution functions. Statistics provides ways to design efficient experiments that eliminate time-consuming trial and error.

In general case, the estimation of rock mass parameters using statistical analysis methods is carried out as following steps:

1. Selection of several empirical equation or classification system for estimation of rock mass properties. Note that some empirical equations are not applicable in every place and their use should be considered with condition tunnel.
2. Statistical analysis of obtained data from empirical equations. Generally, average, maximum, minimum, and standard deviation data are calculated. According to condition and requirement project may be calculated other statistical parameters.
3. Omit high deviation data.
4. Re-statistical analysis of data without high deviation data and estimation of rock mass properties.

6.1. Strength of rock masses (σ_{cmass})

Design of underground spaces depends on the accuracy estimate of stress and rock mass strength. Nowadays, the usual methods for determining this parameter are empirical failure criteria and classification systems, back analysis, Large-scale tests and mathematical modeling (Rahimi, 2008). In this study, empirical methods are used to estimate strength of rock mass. Different researchers have proposed different empirical equations to calculate the strength of rock mass (σ_{cmass}) based on rock mass classification systems. The most widely used equations and the calculated rock mass strength values for the present work are tabulated in Table 7. Estimation of rock mass strength for each parts of the tunnel was carried out by using of statistical analysis of these data and is presented in Table 8. For statistical analysis minimum, maximum, average, standard deviation and ration of ($\sigma_i/\sigma_{\text{cmass}}$) of data were calculated. In this method, the first step statistical parameters were calculated for all the data in Table 7 and the second step the strength values that are very different quantity rather than other data was not used in calculating of statistical analysis, such as equation values 5, 8 and 11. Since that can be seen in Table 8, the standard deviation in second step is less than first step.

6.2. Deformation modulus of rock mass (E_{mass})

Reliable estimate of the deformation modulus of rock masses are required for almost any form of analysis used for the design of slopes, foundations and underground excavations. In situ determination of the deformation modulus of rock mass (E_{mass}) is costly and often very difficult (Hoek, 2007). Using back analysis methods is not possible in the design stage and before the construction of tunnel. Furthermore, there were no similar projects in the near site of Qazvin–Rasht railway tunnel for estimation of E_m. Thus, empirical methods are generally used in estimating E_{mass}. By means of the empirical methods, E_{mass} can be easily acquired. The proposed equations by different researchers and the deformation modulus of rock masses values are given in Table 9. In this case, statistical analysis was used for determining deformation modulus of rock masses mass such as rock mass strength. Results of statistical analysis for the two states (first step for all data and second step with-

Table 7
Estimation of rock mass strength (σ_{cmass}) along tunnel using the proposed empirical equations (Sari and Pasamehmetoglu, 2004; Basarir, 2006; Genis et al., 2007; Palmstrom, 1996).

Researcher (year)	Equation	Equation number	Ta (MPa)	Tb (MPa)	Tc (MPa)
Rock-Lab software	$\sigma_{cmass} = \sigma_{ci} s^a (MPa)$	(4)	1.4	1.8	2.4
Singh et al. (1997)	$\sigma_{cmass} = 7\gamma Q^{1/3} (MPa), \sigma_{ci} > 2MPa, Q < 10$	(5)	12.60	16.40	18.2
Hoek and Brown (1980)	$\sigma_{cmass} = \sigma_{ci}\sqrt{e^{\left(\frac{RMR-100}{9}\right)}} (MPa)$	(6)	0.7	1.3	1.6
Yudhbir et al. (1983)	$\sigma_{cmass} = \sigma_{ci} e^{7.65\left(\frac{RMR-100}{100}\right)} (MPa)$	(7)	0.3	0.4	0.5
Ramamurthy (1985)	$\sigma_{cmass} = \sigma_{ci}\left[\frac{E_m}{E_i}\right]^{0.7} (MPa)$	(8)	10.2	14.2	16.3
Ramamurthy (1986)	$\sigma_{cmass} = \sigma_{ci} e^{\frac{RMR-100}{18/75}} (MPa)$	(9)	1.2	1.4	1.8
Goel (1994)	$\sigma_{cmass} = \frac{5.5\gamma Q_N^{1/3}}{\sigma_{ci} B^{0.1}}, Q_N = \left(\frac{RQD}{J_n}\right)\left(\frac{J_r}{J_a}\right) J_w$	(10)	–	–	–
Goel (1994)	$\sigma_{cmass} = \frac{5.5\gamma \acute{Q}^{1/3}}{B^{0.1}} (\mathrm{MPa}), Q = \left(\frac{RQD}{J_n}\right)\left(\frac{J_r}{J_a}\right)$	(11)	17.1	17.7	24.7
Kalamaris and Bieniawski (1995)	$\sigma_{cmass} = \sigma_{ci} e^{\frac{RMR-100}{24}} (MPa)$	(12)	2.5	2.8	3.3
Bhasin and Grimstad (1996)	$\sigma_{cmass} = \left(\frac{\sigma_{ci}}{100}\right) \times 7\gamma Q^{1/3}, \sigma_{ci} > 100MPa, Q > 10$	(13)	–	–	–
Singh et al. (1997)	$\sigma_{cmass} = \sigma_{ci} s_m^n (MPa)$	(14)	1.4	1.7	2.1
Sheorey (1997)	$\sigma_{cmass} = \sigma_{ci} e^{\frac{RMR-100}{20}} (MPa)$	(15)	1	1.7	2.1
Trueman (1998)	$\sigma_{cmass} = 0.5e^{0.06RMR}$	(16)	5.5	6.6	8.4
Aydan and Dalgic (1998)	$\sigma_{cmass} = \frac{RMR}{RMR+\beta(100-RMR)}\sigma_{ci} (MPa), \beta = 6$	(17)	1.9	3.4	3.9
Barton (2000)	$\sigma_{cmass} = 5\gamma\left(Q\frac{\sigma_{ci}}{100}\right)^{1/3} (MPa)$	(18)	5.3	7.8	8.7
Palmsrotm (2000)	$\sigma_{cmass} = RMi = \sigma_{ci} J_p (MPa)$	(19)	–	–	–
Hoek et al. (2002)	$\sigma_{cmass} = \frac{\sigma_{ci}(m_b+4s-a(m_b-8s))(m_b/4+s)^{a-1}}{2(1+a)(2+a)} (MPa)$	(20)	5.2	6.3	7.9
Barton (2002)	$\sigma_{cmass} = 5\gamma Q_c^{1/3}, Q_c = Q\frac{\sigma_c}{100}$	(21)	6	8.9	9.9

σ_{ci}: Uniaxial compressive strength of intact rock (MPa).
Jv: Coefficient of strength decrease in RMi.
E_i: deformation modulus of intact rock (MPa).
B: width tunnel (m).
a, s, m_b: Hoek and Brown constants for rock mass.
γ: Rock mass density (t/m^3).

Table 8
Statistical analysis results obtained from estimated rock mass strength (σ_{cmass}) along the tunnel.

	Parts of tunnel	Minimum	Maximum	Average	Standard deviation	Average with 95% confidence level	$\frac{\sigma_{ci}}{\sigma_{cmass}}$
First step: considering all data	Ta	0.3	17.10	4.82	4.96	4.82 ± 2.95	4.15
	Tb	0.4	17.70	6.16	5.8	6.16 ± 3	4.87
	Tc	0.5	24.7	7.45	7.21	7.45 ± 3.72	4.03
Second step: without considering of equation values 5, 8 and 11	Ta	0.3	6	2.7	2.15	2.7 ± 1.24	7.41
	Tb	0.4	8.9	3.68	2.91	3.68 ± 1.68	8.15
	Tc	0.5	9.9	4.38	3.34	4.38 ± 1.93	6.85

Table 9
Estimation of rock mass deformation modulus (E_{mass}) along tunnel using the proposed empirical equations (Sari and Pasamehmetoglu, 2004; Hoek, 2007; Barton, 2002; Basarir et al., 2005).

Researcher (year)	Equation	Equation number	Ta (GPa)	Tb (GPa)	Tc (GPa)
Bieniawski (1978)	$E_{mass} = 2RMR - 100(GPa), RMR > 50$	(22)	–	–	–
Serafim and Pereira (1983)	$E_{mass} = 10^{\left(\frac{RMR-10}{40}\right)}(GPa), RMR < 50$	(23)	5.6	6.7	8.4
Grimstad and Barton (1993)	$E_{mass} = 25\log Q(GPa), Q > 1$	(24)	–	2.1	5.4
Verman (1993)	$E_{mass} = 0.3H^{\alpha}10^{\left(\frac{RMR_{1979}-20}{38}\right)}(GPa), H > 50m$	(25)	–	–	–
Mitri et al. (1994)	$E_{mass} = E_i\left[0.5\left(1 - \{cos\pi\frac{RMR}{100}\}\right)\right](GPa)$	(26)	5.2	7.8	9.1
Palmstrom (1995)	$E_{mass} = 5.6RMi^{0.375}(GPa), RMi > 0.1$	(27)	–	–	–
Singh et al. (1997)	$E_{mass} = E_i(s_m)^{1/1.4}(GPa)$	(28)	0.3	0.3	0.4
Hoek and Brown (1998)	$E_{mass} = \sqrt{\frac{\sigma_{ci}}{100}}10^{\left(\frac{GSI-10}{40}\right)}(GPa), \sigma_{ci} < 100MPa)$	(29)	5.3	5.5	7.3
Read et al. (1999)	$E_{mass} = 0.1\left(\frac{RMR}{10}\right)^3(GPa)$	(30)	6.4	8	10.4
Ramamurthy (2001)	$E_{mass} = \frac{E_i\exp[(RMR-100)]}{17.4}(GPa)$	(31)	0.48	0.76	0.95
Ramamurthy (2001)	$E_{mass} = E_i\exp(0/8625\log Q - 2/875)(GPa)$	(32)	–	1.21	1.54
Hoek et al. (2002)	$E_{mass} = \left(1 - \frac{D}{2}\right)\sqrt{\frac{\sigma_{ci}}{100}}10^{\left(\frac{GSI-10}{40}\right)}(GPa)$	(33)	5.3	5.5	7.3
Barton (2002)	$E_{mass} = 10Q_c^{1/3}(GPa), Q_c = Q\frac{\sigma_c}{100}$	(34)	4.8	7.1	7.9
Barton (2002)	$E_{mass} = 10^{\left(\frac{15\log Q+40}{40}\right)}(GPa), Q < 1, RMR < 50$	(35)	8	10.7	11.8
Ramamurthy (2004)	$E_{mass} = E_i\exp -00035[5(100 - RMR)](GPa)$	(36)	5.3	7.4	7.9
Ramamurthy (2004)	$E_{mass} = E_i\exp -0.0035[250(1 - 0.3\log Q)](GPa)$	(37)	5.8	8.5	8.8
Hoek and Diederichs (2006)	$E_{mass} = E_i\left(0.02 + \frac{1}{1+e^{(60+15D-GSI)/11}}\right)(GPa)$	(38)	5.5	6.1	8.2

σ_{ci}: Uniaxial compressive strength of intact rock (MPa).
E_i: deformation modulus of intact rock (GPa).
GSi: ground strength index.
D: disturbance degree factor.
m_m: Hoek and Brown constant.
α: 0.16 for hard rocks and 0.35 for weak rocks.

Table 10
Statistical analysis results for determination of deformation modulus of rock mass (E_{mass}) in the tunnel.

	Parts of tunnel	Minimum	Maximum	Average	Standard deviation	Standard deviation	Average with 95% confidence level	$\frac{E_i}{E_{mass}}$
First step: considering all data	Ta	0.30	8.00	4.83	4.98	2.23	4.83 ± 1.28	3.10
	Tb	0.30	10.70	5.55	10.38	3.22	5.55 ± 1.72	3.60
	Tc	0.40	11.80	6.81	12.27	3.5	6.81 ± 1.87	2.94
Second step: without considering of equation values 28, 31 and 32	Ta	4.80	8.00	5.72	0.82	0.91	5.72 ± 0.58	2.62
	Tb	2.10	10.70	6.85	4.69	2.17	6.85 ± 1.3	2.92
	Tc	5.40	11.80	8.41	2.82	1.68	8.41 ± 1.00	2.38

out equation values 28, 31 and 32) are summarized in Table 10. Standard deviation without considering of equation values 28, 31 and 32 is obtained less than all data.

6.3. Hoek–Brown and Mohr–Coulomb constants of rock mass

Hoek–Brown and Mohr–Coulomb failure criterions are used for estimating the rock mass properties from geological data, such as rock mass strength and deformation modulus of rock mass, and rock mechanics analysis. Most of the analyses which are currently used for the evaluation of the stability of underground excavations or for slope stability calculations are formulated in terms of the Hoek–Brown and Mohr–Coulomb failure criterions. Consequently, it is necessary to determine equivalent Hoek–Brown constants (m_m, s_m, a) and Mohr–Coulomb constants (c, φ) for each rock mass. Several empirical equations have been suggested by different researchers for estimating these constants. The proposed equations by different researchers are presented in Table 11. The calculated Hoek–Brown and Mohr–Coulomb constants are listed in Table 12. According to the Table 12, estimation of Hook–Brown and Mohr–Coulomb constants is used by three methods: empirical equations, rock mass rating classification system (RMR) and Rock-lab software. The averages of these parameters are calculated as the estimation of Hoek–Brown and Mohr–Coulomb parameters value.

Table 11
The proposed empirical equations for calculation of Hoek–Brown constants of rock mass (Sari and Pasamehmetoglu, 2004; Genis et al., 2007; Basarir et al., 2005; Zulfu et al., 2007).

Researcher (year)	Equation	Equation number
Singh et al. (1997)	$s_m = 0.002Q_N, Q_N = \left(\frac{RQD}{J_n}\right)\left(\frac{J_r}{J_a}\right)J_w$	(39)
	$\frac{m_m}{m_i} = 0.135Q_N^{1/3}$	(40)
	$m_m = m_i exp\left(\frac{GSI-100}{28-14D}\right)$	(41)
Hoek et al. (2002)	$s_m = exp\left(\frac{GSI-100}{9-3D}\right)$	(42)
	$a = \frac{1}{2} + \frac{1}{6}\left(e^{-\frac{GSI}{15}} - e^{-\frac{20}{3}}\right)$	(43)
	$\frac{m_m}{m_i} = s_m^{1/3}, GSI > 25$	(44)
Singh et al. (1997)	$s_m^n = \frac{7\gamma Q^{1/3}}{\sigma_{ci}}, Q < 10, J_w = 1, \sigma_{ci} < 100MPa$ $\begin{cases} n = 0.5 & \text{, if } GSI \geqslant 25 \\ n = 0.65 - \frac{GSI}{200} \leqslant 0.6 & \text{, if } GSI < 25 \end{cases}$	(45)
Ramamurthy (1985)	$s_m = e^{\left(\frac{1}{40}(0.0564RMR-5.64)\right)}$	(46)
Palmstrom (1995)	$s_m = J_p^2$	(47)
	$m_m = m_i J_p^{0.64}$	(48)

GSi: ground strength index.
D: disturbance degree factor of rock mass the amount of which is between zero for intact rocks and is variable for different types of rock mass.
a, s_m and m_m: Hoek and Brown constant.
m_i: Hoek and Brown constant for intact rock.
Jp: coefficient of strength decrease in RMi.
γ: rock mass density (t/m3).

Table 12
Calculated Hoek–Brown and Mohr–Coulomb parameters values.

Method	Parameter	Ta	Tb	Tc
(1) empirical equations (based on Table 10)	m_m	4.6	2.73	3.90
	s_m	0.0047	0.0034	0.0048
	a	0.505	0.506	0.504
(2) rock mass rating classification (RMR)	c(MPa)	0.2–0.3	0.2–0.3	0.2–0.3
	φ (degree)	25–35	25–35	25–35
(3) Rock-lab software	m_m	3.733	2.515	4.009
	s_m	0.0054	0.0039	0.0067
	a	0.505	0.506	0.504
	c(MPa)	0.31	0.41	0.39
	φ (degree)	55	52	58
Estimation of Hoek–Brown and Mohr–Coulomb parameters values	m_m	4.17	2.62	3.95
	s_m	0.0051	0.0037	0.0058
	a	0.505	0.506	0.504
	c(MPa)	0.28	0.33	0.32
	φ (degree)	43	41	44

7. Determination in situ stresses

In situ stresses in rock have an important role in the design and construction of underground excavation. Any attempt to design engineering structures in rock mass requires knowledge of the common in situ stress field. It is always desirable to measure it, in whatever best way possible. There are various methods of determination of in situ stresses in rock mass (Kumar et al., 2004). Determination of in situ stresses is very difficult and expensive, for this reason, many projects are carried out in which the stress field has been estimated using compilations of measurement data from nearby or regional tunnels. In addition, typically the empirical methods are used to estimate for in situ stress. Several empirical equations have been suggested by researchers for estimating in situ stresses. The following equations, which are more relevant to tunnel design, have been selected for this study.

Table 13
Calculated in situ stress (σ_h, σ_v and *K*).

	Ta	Tb	Tc
σ_v (MPa)	1.06	1.56	0.99
σ_h (MPa)	1.52	1.91	1.65
K	1.43	1.22	1.67

The most widely accepted concept is that the vertical stress (σ_v) at any point in the rock mass is due to the weight of the overlying rock strata, i.e. $\sigma_v = \gamma H$ where γ is the unit weight of the overlying rock strata and *H* is the depth below surface. The horizontal stresses (σ_h) acting at a depth *H* below the surface are much more difficult to estimate than the vertical stress.

Normally the ratio of the average horizontal stress to the vertical stress is denoted by *K* so that $\sigma_h = K\sigma_v = K\gamma H$ (Ghosh, 2008). To take into account actions of tectonic forces, Sheorey (1994) developed an elasto-static thermal model which accounted for the crust curvature, changes in density, elastic constants and coefficients of thermal expansion. He suggested the following relationship for horizontal to vertical stress ratio *K* (Hoek, 2007):

$$K = 0.25 + 7E_h\left[0.001 + \frac{1}{H}\right] \tag{49}$$

where *H* is depth at the point of interest (m), E_h is Young's modulus of the rock mass measured in a horizontally (GPa).

Stephensson (1993) has suggested the following relation between horizontal stress and vertical stress based on hydraulic fracturing tests.

$$\sigma_h = 2.8 + 1.48\sigma_v \quad (H < 1000\text{ m}) \tag{50}$$

Sengupta (1998) used σ_v in his equation to calculate horizontal stress as follows.

$$\sigma_h = 1.5 + 1.2\sigma_v \tag{51}$$

The horizontal stress was determined from the following equation based on results of in situ tests in Canada, Australia, USA, Scandinavia, South Africa and other regions in the world (Rahimi, 2008).

$$\sigma_h = \frac{12.60}{\sqrt[3]{z}}\sigma_v \tag{52}$$

Sheorey et al. (2001) proposed the below equation for calculating σ_h:

$$\sigma_h = \frac{v}{1-v}\sigma_v + \frac{\beta E_{mass} G}{1-v}(H + 100) \tag{53}$$

where $\beta = 8 \times 10^{-6}$/°C is the coefficient of linear thermal, *G* = 0.024 °C/m that is geothermal gradient, *v* is Poisson's ratio and E_{mass} deformation modulus of rock mass (MPa).

The calculated σ_h, σ_v and *K* values from the above equations are presented in Table 13.

8. Selection suitable rock engineering and design tools for the tunnel

In the previous parts, the general, structural and engineering geological information was expressed for the tunnel. According to this information, different rock mass classification systems were used and rock mass properties and in situ stresses estimated to all three parts of tunnel.

Rock mass in the tunnel are frequently weathered near the earth's surface, and are sometimes altered by hydrothermal processes (Fig. 7). Both processes generally first affect the walls of discontinuities. Weathering is the natural process of disintegration

Fig. 7. Highly weathered rock mass near at the tunnel site.

and decomposition of the materials according with changing environments. The weathering is the major factors which decreased the strength and stiffness of the rock mass. The quality of rock mass in the tunnel is poor and somewhere is observed large joints with several centimeters disruption and minor faults with crushed zoned around them (Fig. 8).

Falling of blocks or wedges occurs due to discontinuities, highly alteration and low strength of the rock mass in the tunnel. An example of a wedge failure and collapse is shown in Fig. 9.

In this figure, collapse in the tunnel roof is shown. First, discontinuous surfaces were visible. However, falling continued as irregular due to being located in a fault zone, intense fracturing and weathering and also the presence moisture and humidity of the rock mass. Lithology, weathering of rock mass in the tunnel and influence of surface water in deep cause gradually changing from rock to form plastic and rock mass can easily be bent with hand force. It should be mentioned, the similar events along the first 100 m of tunnel construction has occurred seven times with approximately 1–5 cubic meters extension.

The ground water flow is very important factors which cause the underground structure unstable by decreasing the effective stress, by swelling and reveling of the ground, settlements of the ground surface due to consolidation from lowered ground water

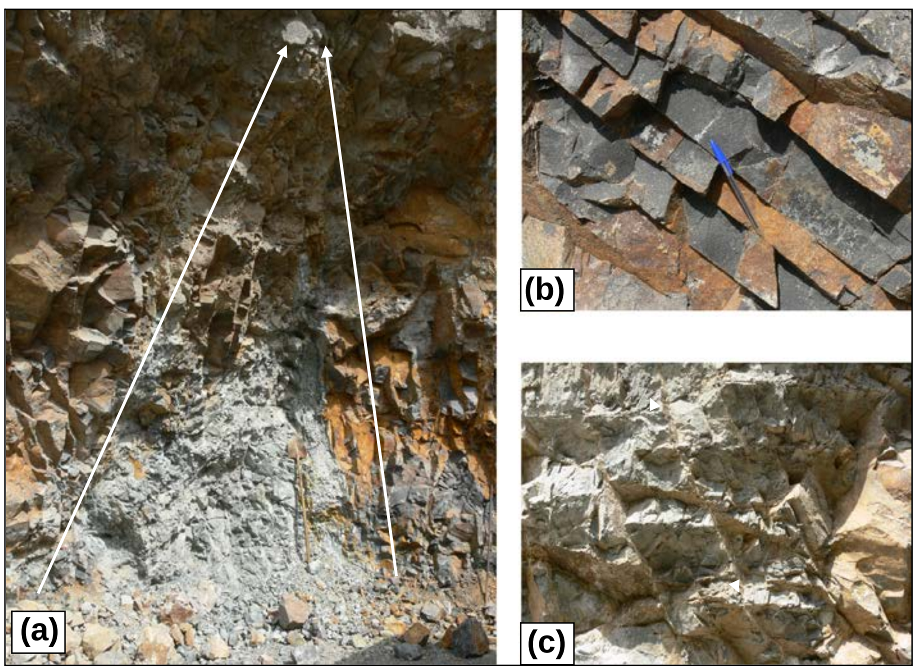

Fig. 8. Rock mass condition in the tunnel: (a) the fault zone, (b) bedding, and (c) joint sets.

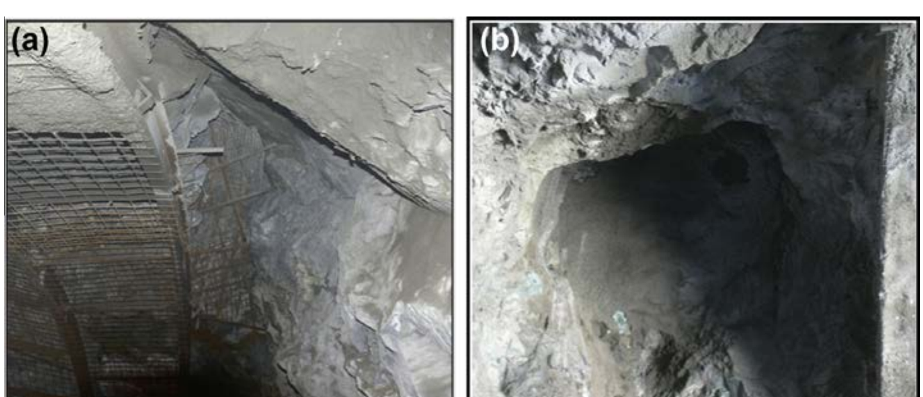

Fig. 9. (a) Wedge failure in the tunnel due to intersection of joints (approximately 2 cubic meters), (b) Collapse in the tunnel roof (approximately 4 cubic meters), which was initially wedge failure and then has continued irregular due to the intense fractures, weathering and the presence moisture and humidity of the rock mass as a result of rain fall.

level, drainage of existing wells, corrosion and deterioration of installation and rock support, toxic gases from ingress water. The groundwater pressure is generally reduced in the rock masses adjacent to the excavation caused by drainage along the joints. Relatively few block failures are clearly related to joint water pressure (Palmstrom and Stille, 2007).

The water in the tunnel is as humidity, moisture, or dripping (Fig. 10). The water flows is variable with rainfall and climate condition.

Therefore, types of ground behavior in the tunnel is stable with the potential of discontinuity controlled wedge failure, wedge failure(s) of several blocks, shallow shear failure, plastic behavior (initial), swelling of certain rocks and water ingress. At this stage, suitable design tools are selected for the tunnel support design based on ground behavior and according to Table 1.

Fig. 10. The water inflow to tunnel.

For stable with the potential of wedge failure(s) types of rock mass behavior in the tunnel, all of methods (classification systems, NATM, numerical modelling, observational methods and engineering judgment) are suitable tools except for analytical calculations. Numerical modelling, analytical calculation and engineering judgment methods can be used as design tools for shallow shear failure and plastic behaviors in the tunnel. In the case of swelling ground and water ingress, design tools for the tunnel can be analytical calculations, observational methods and engineering judgments, while fitness rating of these is poor. For all types of rock mass behavior, numerical modelling used in the design should be supported by engineering judgment. This requires experience, skill and understanding by those involved in the works. The classification systems work best in jointed rock where the behavior is dominated by wedge failure.

Therefore, classification systems, numerical modeling, engineering judgments and observational methods are suitable design tools for the tunnel support design. In this paper, classification systems and numerical modelling are used for design support tunnel, and engineering judgments and observational methods will be used during construction.

The tunnel of 12 m span is cut by many joints in roof, the properties of the joints mainly determine the stable and wedge failure (ground behavior). The risk for block fall due to deep reaching discontinuous and create a wedge, gravity induced falling and sliding of blocks, occasional local shear failure is obvious. In this case the continuity factor is more than 15. Therefore, the design has to be based on an analysis of continual blocks (a continuum mechanical approach).

8.1. Empirical support design

During initial design stages of a tunnel, when very few detailed information is available on the rock mass properties and its stress, the use of a rock mass classification system can be of important benefit. Empirical design method relates field experience gained on previous projects to the conditions predicted at a proposed site and requires experience as well as engineering judgment. Rock

Table 14
Empirical support recommendations for the tunnel.

Empirical methods	Ta	Tb	Tc
RMR	Excavation: 1.0–1.5 m advance in top heading, install support concurrently with excavation 10 m from the face Support: Systematic bolts, 4–5 m long, spaced 1.0–1.5 m in crown and walls with wire mesh and light ribs steel sets spaced 1.5 m where required, Shotcrete 0.1–0.15 m in crown and 0.1 m in sides	Excavation: top heading and bench 1.5–3.0 m advance in top heading, commence support after each blast, complete support 10 m from face Support: Systematic bolt 4 m long, spaced 1.5–2.0 m in crown and walls with wire mesh, Shotcrete 0.05–0.1 m in crown and 0.03 m in sides	Excavation: top heading and bench 1.5–3.0 m advance in top heading, commence support after each blast, complete support 10 m from face Support: Systematic bolt 4 m long, spaced 1.5–2.0 m in crown and walls with wire mesh, Shotcrete 0.05–0.1 m in crown and 0.03 m in sides
Q	Fibre reinforced Shotcrete 9–12 cm. Bolt, 3–5 m long and spaced 1.5–1.7 m.	Fibre reinforced Shotcrete 5–9 cm. Bolt, 3–5 m long and spaced 1.7–2.1 m.	Fibre reinforced Shotcrete 5–9 cm. Bolt, 3–5 m long and spaced 1.7–2.1 m.
Support weight	Bolts + shotcrete 15 cm	Bolts + shotcrete 10 cm	Bolts + shotcrete 15 cm
SRC	Excavation: 1.0–1.5 m advance in top heading, install support concurrently with excavation 10 m from the face Support: Systematic bolts, 4–5 m long, spaced 1.0–1.5 m in crown and walls with wire mesh and light ribs steel sets spaced 1.5 m where required, Shotcrete 0.1–0.15 m in crown and 0.1 m in sides.	Excavation: 1.0–1.5 m advance in top heading, install support concurrently with excavation 10 m from the face Support: Systematic bolts, 4–5 m long, spaced 1.0–1.5 m in crown and walls with wire mesh and light ribs steel sets spaced 1.5 m where required, Shotcrete 0.1–0.15 m in crown and 0.1 m in sides.	Excavation: 1.0–1.5 m advance in top heading, install support concurrently with excavation 10 m from the face Support: Systematic bolts, 4–5 m long, spaced 1.0–1.5 m in crown and walls with wire mesh and light ribs steel sets spaced 1.5 m where required, Shotcrete 0.1–0.15 m in crown and 0.1 m in sides
Support proposed for the tunnel based on empirical methods and engineering judgment	Excavation: Top & bench excavation method Support: Shortcrete 0.15–0.2 m with wire mesh and light ribs steel sets spaced 1–2 m	Excavation: Top & bench excavation method Support: Shortcrete 0.15–0.2 m with wire mesh and light ribs steel sets spaced 1–2 m	Excavation: Top & bench excavation method Support: Shotcrete 0.15–0.2 m with wire mesh and light ribs steel sets spaced 1–2 m

mass classification systems are an integral of empirical tunneling design and have been successfully applied throughout the world (Zulfu et al., 2007). In order to empirical support design of the tunnel was used to RMR, Q, support weight and SRC and the support recommendations for their are given in Table 14. According to empirical results and engineering judgment, shotcrete 0.15–0.2 m with wire mesh and light ribs steel sets spaced 1–2 m are proposed for support design for the tunnel propose for the tunnel preliminary support and excavation method suggests top heading and bench.

8.2. Numerical modeling

Although empirical methods are generally applied to carry out the support design of tunnels, they cannot give a quantitative description to a specific rock mass and they fail to predict interaction between the surrounding rock mass and supporting system, thus fail to give descriptions on the developments of the support and behavior of supported structures such as tunnel deformation and stress redistribution. The objective of using numerical modeling method is to verify and fortify stability and support recommendations from rock mass classification systems.

The computer software FLAC, an explicit 2D finite difference program suited to the modelling of geomechanical continuum problems that consist of several stages, such as sequential excavations, backfilling and loading, was used for calculating the stresses, the deformations and the thickness of the developed plastic zone around tunnel. In order to analyze tunnel stability and deformations in different rock masses and to explore the concept of rock support interaction, three models were generated using mesh and tunnel geometry and different material properties. These models are as follows:

Model I: tunnel runs through Ta part.
Model II: tunnel runs through Tb part.
Model III: tunnel runs through Tc part.

The rock mass properties assumed in this analysis were obtained from the estimated values presented in Section 4. The analysis includes two models; the first model was used to examine the conditions excavation without any support and the second model consist of support application to the excavation boundary. Hoek–Brown failure criterion was used to estimate yielded elements and plastic zone of rock masses in the vicinity of tunnel. According

Model I:
Ta part

Model II:
Tb part

Model III:
Tc part

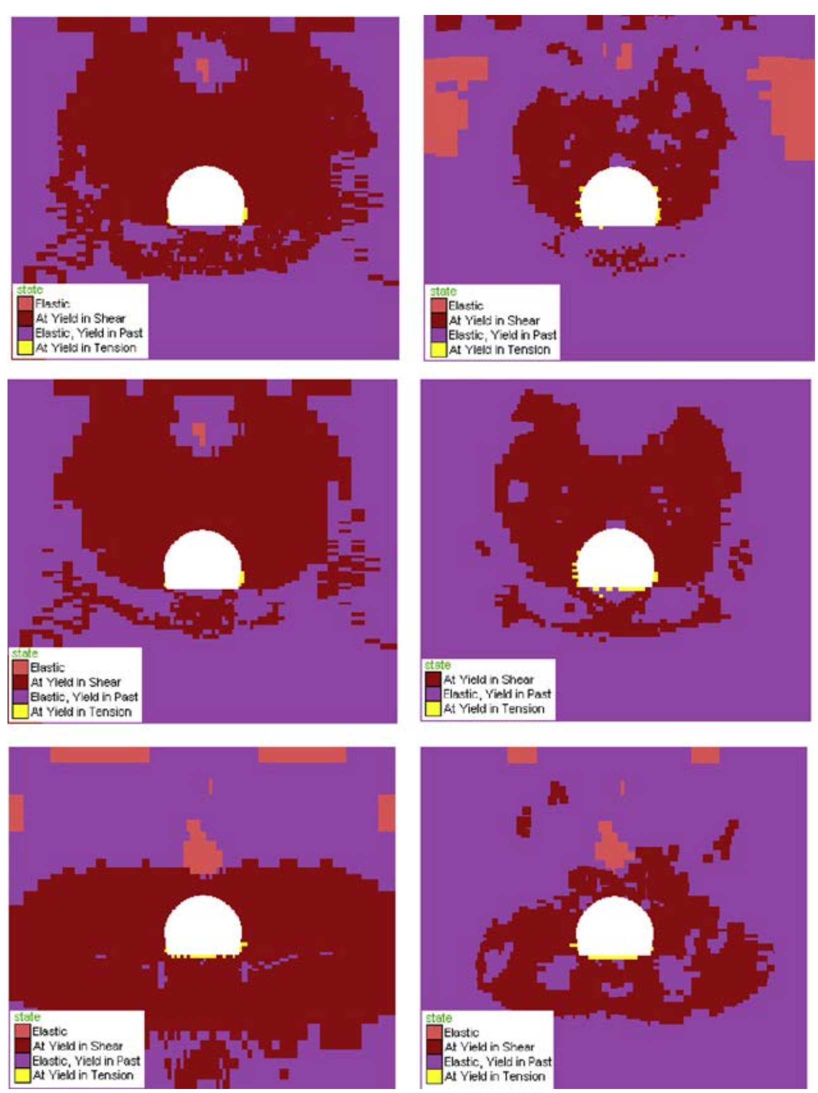

(a) before support (b) after support

Fig. 11. The extent of plastic zone around the tunnel before and after support.

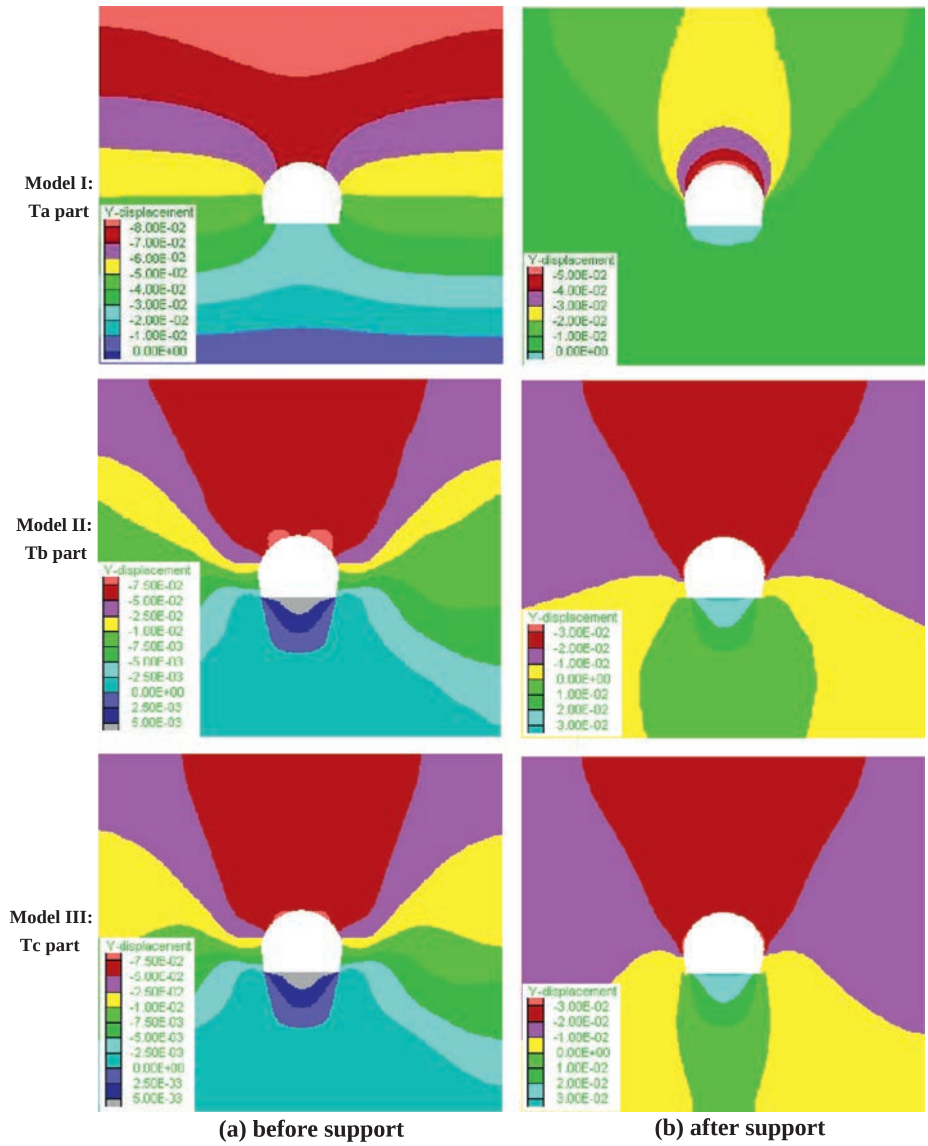

Fig. 12. The displacement behavior around the tunnel before and after support.

to plasticity theory, a plastic zone occurs around a tunnel after excavation when induced stresses exceed the rock mass strength.

The displacement behavior and extent of plastic zone before and after support for Ta, Tb and Tc are given in Figs. 11 and 12, respectively.

It can be seen from Figs. 11 and 12 that the extent of plastic zone and yielded elements suggest that there would be stability problem for the tunnel. The maximum displacement values for unsupported tunnel in Ta, Tb and Tc and are 8 cm, 7.5 cm and 7.5 cm, respectively. Support elements used are composed of shotcrete with wire mesh and light ribs steel sets as proposed by the empirical methods. The properties of support elements, such as thickness of shotcrete are similar to those proposed by the empirical methods. For tunnel in Ta, Tb and Tc parts, 0.15–0.2 m thick shotcrete with mess and light ribs steel sets spaced 1–2 m are proposed as support elements. After considering support measures in the numerical model, not only the number of yielded elements but also the extent of plastic zone decreased substantially, as shown in Fig. 11. The maximum displacement values for Ta, Tb and Tc parts decreased to 5 cm, 3 cm and 3 cm, respectively, as shown in Fig. 11. This indicates that the applied support systems were adequate to obtain tunnel stability.

8.3. Optimum support design of the tunnel

Rock mass classification systems indicate that stability problems exists for the rock mass along tunnel route and support measures are necessary. By considering the support recommendations of the empirical methods, support systems and excavation methods were proposed for the rock masses. Numerical modeling was utilized to evaluate the performance of recommended support system. The results obtained from the empirical and numerical approaches were fairly comparable. According to results of empirical and numerical methods and engineering judgment, shotcrete 0.15–0.2 m with wire mesh and light ribs steel sets (IPE160) are proposed as support elements for the tunnel. However, the measurements carried out during construction can be used to check the validity of the proposed support system or to adapt the design of support system.

9. Conclusions

An essential step in the tunnel design procedure is to assess the ground behavior and continuity factor. The ground behavior is related to mode of failure and continuity factor is one of the most important factors to consider for design is the relative degree of jointing. To help in selecting appropriate design methods of tunnel, a methodology based on ground behavior and continuity factor has been presented as a guide in the paper. Furthermore, statistical analysis methods, in order to obtain rational and reasonable results and decrease uncertainties, have been used to estimation of rock mass properties in the tunnel.

The behavior types assessed as stable with the potential of discontinuity controlled block fall, block fall(s) of several blocks, shallow shear failure, plastic behavior (initial), swelling of certain rocks and water ingress in the design tunnel. Prediction of the behavior types in the Qazvin–Rasht railway tunnel and comparison with the real conditions was compatible in the first 30 m length of stage tunnel construction. According to the ground behavior and continuity factor, appropriate design methods have been selected empirical methods, numerical modelling, observation methods, and engineering judgment.

Based on the collected information in the field and determination of rock material properties in the laboratory, rock masses were characterized by means of RMR, Q, support weight, SRC and GSI rock mass classification systems. The quality of rock mass in the tunnel has been classified in the weak category based on rock mass classification systems.

Rock mass properties and in situ stresses for each parts of the tunnel estimated from the empirical methods and carried out by using of statistical analysis. For statistical analysis, minimum, maximum, average, standard deviation of data calculated for all three parts of tunnel and their results used as input data for numerical modeling. The empirical methods and engineering judgments recommend the utilization of shotcrete 0.15–0.2 m with wire mesh and light ribs steel sets spaced 1–2 m as support elements for the tunnel.

The results proved that the empirical and numerical methods agree with each other. However, the validity of the proposed support system, obtained from combination of empirical and numerical modeling, should be verified by comparing predictions with actual monitoring results during construction, taking into account that technological aspects act also to spread the behavior of the first phase support, excavation duration, damage of surrounding rock, change of field stress due to particular rock behavior. We found that using proposed methodology the optimum support system could be designed.

References

Aydan, O., Dalgic, S., 1998. Prediction of deformation behaviour of 3 lanes Bolu tunnels through squeezing rocks of North Anotolian Fault Zone (NAFZ), Reg. Symp. on Sedimentary Rock Engineering, Taipei, pp. 228–233.

Barbero, M., Barpi, F., 2011. Quarry-induced slope instability at a broadcasting transmission plant near Valcava, Lombardia, Italy. Int. J. Geoeng. Case Hist. 2 (2), 163–181.

Barpi, F., Peila, D., 2012. Influence of the tunnel shape on shotcrete lining stresses. Comput. Aided Civil Infrastruct. Eng. 27, 260–275, ISSN 1093–9687.

Barpi, F., Barbero, M., Peila, D., 2011. Numerical modelling of ground-tunnel support interaction using bedded-beam-spring model with fuzzy parameters. Gospodarka Surowcami Mineralnymi 27 (4), 71–87.

Barton, N., 2000. TBM Tunnelling in Jointed and Faulted Rock, Balkema, Rotterdam, 169 pp.

Barton, N., 2002. Some new Q-value correlations to assist in site characterization and tunnel design. Int. J. Rock Mech. Mining Sci. 39, 185–216.

Basarir, H., 2006. Engineering geological studies and tunnel support design at Sulakyurt dam site, Turkey. Eng. Geol. 86, 225–237.

Basarir, H., Ozsan, A., Karakus, M., 2005. Analysis of support requirements for a shallow diversion tunnel at Guledar dam site, Turkey. Eng. Geol. 81, 131–145.

Bhasin, R., Grimstad, E., 1996. The use of stress–strength relationships in the assessment of tunnel stability. Tunnelling Underground Space Technol. 11 (1), 93–98.

Bieniawski, Z.T., 1978. Determining rock mass deformability: experience from case histories. Int. J. Rock. Mech. Min. Sci. Geomech. Abstr. 15, 237–247.

Genis, M., Basarir, H., Ozarslan, A., Bilir, E., Balaban, E., 2007. Engineering geological appraisal of the rock masses and preliminary support design, Dorukhan Tunnel, Zonguldak, Turkey. Eng. Geol. 92, 14–26.

Ghosh, A.K., 2008. Rock stress measurements for underground excavations. The 12th international conference of international association for computer methods and advances in geomechanics (IACMAG), 1–6 October, Goa, India.

Goel, R.K., 1994. Correlations for predicting support pressures and closures in tunnels, PhD. Thesis, Nagpur University, Nagpur, India, 308 p.

Gonzalez de Vallejo, L.I., 2003. SRC rock mass classification of tunnels under high tectonic stress, excavated in weak rocks. Eng. Geol. 69, 273–285.

Grimstad, E., Barton, N., 1993. Updating the Q-system for NMT. Proc. Int. Symp. on Sprayed Concrete, Fagernes, Norway, Norwegian Concrete Association, Oslo, vol. 1993. 20 pp.

Haraz Rah Consulting Company, 2006. General, structural and engineering geological report of Qazvin–Rasht railway tunnel, Rasht, Tehran, Iran.

Hoek, A., 2007. Practical Rock Engineering. Published. In: <www.rocscience.com>.

Hoek, E., Brown, E.T., 1980. Underground Excavations in Rock, Institute of Mining and Metallurgy, London, 527 pp.

Hoek, E., Brown, E.T., 1998. Practical estimates of rock mass strength. Int. J. Rock Mech. Min. Sci. 34 (8), 1165–1186.

Hoek, E., Carranza–Torres, C., Corkum, B., 2002. Hoek–Brown failure criterion– 2002 edition. In: Hammah, R., Bawden, W., Curran, J., Telesnicki, M. (Eds.), Proceedings of NARMSTAC 2002, Mining Innovation and Technology. Toronto – 10 July 2002, University of Toronto, pp. 267–273.

Hoek, E., Diederichs, M.S., 2006. Empirical estimation of rock mass modulus. Int. J. Rock Mech. Mining Sci. 43, 203–215.

Hudson, J.A., Feng, X.T., 2007. Updated flowcharts for rock mechanics modeling and rock engineering design. Int. J. Rock Mech. Mining Sci. 44, 174–195.

ISRM, 1981. Rock characterization, testing and monitoring. In: Brown, E.T. (Ed.), ISRM Suggested Methods. Pergamon Press, New York, p. 211.

Kalamaris, G.S., Bieniawski, Z.T., 1995. A rock mass strength concept for coal incorporating the effect of time. Proc. of 8th Int. Cong. Rock Mechanics. ISRM, 1. Balkema, Rotterdam, pp. 295–302.

Kumar, N., Varughese, A., Kapoor, V.K., Dhawan, A.K., 2004. In situ stress measurement and its application for hydro-electric projects – an INDIAN experience in the HIMALAYAS. Int. J. Rock Mech Min. Sci. 41 (3).

Mitri, H.S., Edrissi, R., Henning, J., 1994. Finite element modeling of cable-bolted slopes in hard rock underground mines, Presented at the SME Annual Meeting, SME, Albuquerque, 14–17 February, New Mexico, USA, pp. 94–116.

Oggeri, C., Oreste, P., 2012. Tunnel static behavior assessed by a probabilistic approach to the back-analysis. Am. J. Appl. Sci. 9 (7), 1137–1144.

Palmstrom, A., 1995. RMi – a rock mass characterization system for rock engineering purposes. PhD. Thesis, Oslo University, Norway, 400 p.

Palmstrom, A., 1996. Characterizing rock masses by RMi for use in practical rock Engineering. Tunneling Underground Space Technol. 11 (2), 173–188.

Palmstrom, A., 2000. Recent developments in rock support estimates by the RMi. J. Rock Mech. Tunn. Technol. 6 (1), 1–19.

Palmstrom, A., Stille, H., 2007. Ground behavior and rock engineering tools for underground excavations. Tunneling Underground Space Technol. 22, 363–376.

Rahimi, B., 2008. Stability analysis and support design Qazvin–Rasht railway Tunnel, M.Sc. Thesis, Department of Mining & Metallurgical Engineering, Amir Kabir University of Technology, Tehran, Iran.

Ramamurthy, T., 1985. Stability of rock mass, 8th Annual lecture. Indian Geotech. J. 1–74.

Ramamurthy, T., 1986. Stability of rock mass, 8th Annual lecture. Indian Geotech. J. 1–74.

Ramamurthy, T., 2001. Shear strength response of some geological materials in triaxial compression. Int. J. Rock Mech. Min. Sci. 38, 683–697.

Ramamurthy, T., 2004. A geo-engineering classification for rocks and rock masses. Int. J. Rock Mech. Min. Sci. 41, 89–101.

Read, S.A.L., Richards, L.R., Perrin, N.D., 1999. Applicability of the Hoek-Brown failure criterion to New Zealand greywacke rocks, Proceeding 9th International Society for Rock Mechanics Congress, vol. 2. Paris, pp. 655–660.

Sari, D., Pasamehmetoglu, A.G., 2004. Proposed support design, Kaletepe tunnel, Turkey. Engineering Geology 72, 201–216.

Sengupta, S., 1998. Influence of geological structures on in situ stresses, PhD. Thesis, Department of Civil Engineering, Indian Institute of Technology, New Delhi, p. 275.

Serafim, J.L., Pereira, J.P., 1983. Considerations of the geomechanics classification of Bieniawski, Proceedings International Symposium Engineering Geology and Underground Construction, vol. 1. Balkema, Rotterdam, pp. 1133–1142.

Shahriar, K., Sharifzadeh, M., Rahimi, B., 2009. General principles for the design of underground spaces-case study: Qazvin–Rasht railway tunnel, 8th tunnel conference, Tarbiat Modarres University of Tehran, Iran.

Sheorey, P.R., 1994. A theory for in situ stresses in isotropic and transversely isotropic rock. Int. J. Rock Mech. Min. Sci. & Geomech. Abstr. 31 (1), 23–34.

Sheorey, P.R., 1997. Empirical Rock Failure Criteria, Balkema, Rotterdam, 176 p.

Sheorey, P.R., Murali Mohan, G., Sinha, A., 2001. Influence of elastic constants on the horizontal in situ stress. Int. J. Rock Mech. Mining Sci. 38, 1211–1216.

Singh, B., Viladkar, M.N., Samadhiya, N.K., Mehrota, V.K., 1997. Rock mass strength parameters mobilized in tunnels. Tunnelling Underground Space Technol. 12 (1), 47–54.

Stephansson, O., 1993. Rock Stress in the Fennoscandian Shield in Comprehensive Rock Engineering, vol. 3. Pergamon Press Oxford, Chapter 17, pp. 445–459.

Stille, H., Palmstrom, A., 2007. Ground behavior and rock mass composition in underground excavations. Tunneling Underground Space Technol.. Article in press.

Trueman, R., 1998. An evaluation of strata support techniques in dual life gate roads, PhD. Thesis, University of Wales, Cardiff.
Tzamos, S., Sofianos, A.I., 2006. Extending the Q system's prediction of support in tunnels employing fuzzy logic and extra parameters. Int. J. Rock Mech. Mining Sci. 43, 938–949.
Verman, M., 1993. Rock mass-tunnel support interaction analysis, PhD. Thesis, University of Roorkee, Roorkee, India.
Yudhbir, Lemanza, W., Prinzl, F., 1983. An empirical failure criterion for rock masses. Proceedings of the 5th International Congress Society of Rock Mechanics Melbourne, vol. 1. pp. B1–B8.
Zulfu, G., Pranshoo, S., Musharraf, M.Z., 2007. Empirical and numerical analyses of support requirements for a diversion tunnel at the Boztepe dam site, eastern Turkey. Eng. Geol. 91, 194–208.

Shahrood University of Technology

Curtin University

Mostafa Sharifzadeh:
Western Australian School of Mines (WASM)

Comprehension of ground behaviour and selection of suitable design strategy,

1

Presentation Outline

2

2

Presentation Outline

3

3

Deep Underground Metal Mines common practice

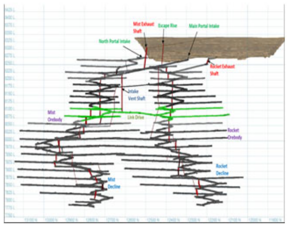

Frog's Leg Gold Mine, operated by Evolution Mining Western Australia (600m)

world largest open pit gold mine (Super pit) in WA

Underground Operations – Mt Charlotte shaft – KCGM – Western Australia (1200m)

4

4

Underground excavation Lifetime classification

- **Short-term excavations** (less than 1 year to 3 year), such as: crosscuts, ore drive, temporary openings, and exploration galleries.
- **Medium-term excavations** (more that 3–10 years), e.g. level accesses, ventilation drifts.
- **Long-term excavations** (Life of the mine) (more than 10 years), e.g. main accesses, decline, ramps, shaft.
- Civil projects could be categorised in long term excavations.

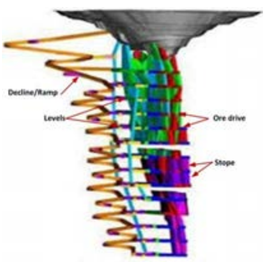

5

5

Simplified geotechnical Design methodology for deep underground mine excavation

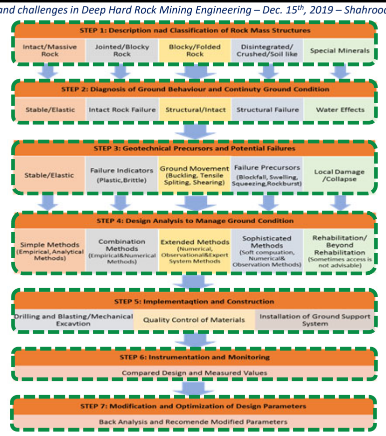

Rahimi, Sharifzadeh, Feng, 2019

6

6

Rock Engineering Design Approaches and challenges in Deep Hard Rock Mining Engineering – Dec. 15th, 2019 – Shahrood UT

Benefits of understanding design methodology:

Geomechanics Design tools considers the benefits of systematic utilization of Principles and Methodology in mining and underground construction Design. Understanding design methodology leads us to select correct analyses tools to solve engineering problems.

7

7

Rock Engineering Design Approaches and challenges in Deep Hard Rock Mining Engineering – Dec. 15th, 2019 – Shahrood UT

Rahimi B., Sharifzadeh M., Feng X-T., (2019) Ground Behaviour Analysis, Support System Design and Construction Strategies in Deep Hard Rock Mining–Justified in Western Australian's Mines, Journal of Rock Mechanics and Geotechnical Engineering,


Contents lists available at ScienceDirect
Journal of Rock Mechanics and Geotechnical Engineering
journal homepage: www.rockgeotech.org

Full Length Article

Ground behaviour analysis, support system design and construction strategies in deep hard rock mining — Justified in Western Australian's mines

Behrooz Rahimi [a,*], Mostafa Sharifzadeh [a], Xia-Ting Feng [b]

[a] Department of Mining and Metallurgical Engineering, Western Australian School of Mines: Minerals, Energy and Chemical Engineering (WASM-MECE), Curtin University, Kalgoorlie, WA, 6430, Australia
[b] Key Laboratory of Ministry of Education for Safe Mining of Deep Metal Mines, Northeastern University, Shenyang, 110819, China

ARTICLE INFO

Article history:
Received 25 September 2018
Received in revised form 29 November 2018
Accepted 9 January 2019
Available online xxx

Keywords:
Ground management
Support system design
Sequential excavation
Stress management
Geotechnical monitoring
Deep underground mines

ABSTRACT

Development of deep underground mining projects is crucial for optimum extraction of mineral deposits. The main challenges at great depth are high rock stress levels, seismic events, large-scale deformation, sudden failures and high temperatures that may cause abrupt and unpredictable instability and collapse over a large scale. In this paper, a ground control and management strategy was presented corresponding to the three stages of projects: strategic design, tactical design and operational design. Strategic design is results in preparing a broad plan and primary design for mining excavations. The tactical design is to provide detail design such as stabilisation methods. Operational design stage is related to monitoring and updating design parameters. The most effective ground control strategies in this stage are maintenance, rehabilitation, monitoring and contingency plan. Additionally, a new procedure for design of ground support systems for deep and hard rock was proposed. The main principles are: static and/or dynamic loading types, determination of loading sources, characterisation of geological conditions and the effects of orientation of major structures with openings, estimation of ground loading factor, identification of potential primary and secondary failures, utilisation of appropriate design analysis methods, estimation of depth failure, calculation of the static and/or dynamic demand ground support capacity, and selection of surface and reinforcement elements. Gravitational force is the dominant loading force in low-level stresses. In high stress level, failure mechanism becomes more complex in rock mass structures. In this condition, a variety of factors such as release of stored energy due to seismic events, stress concentration, and major structures influence on ground behaviour and judgement are very complicated.

8

8

Rock Engineering Design Approaches and challenges in Deep Hard Rock Mining Engineering – Dec. 15th, 2019 – Shahrood UT

Presentation Outline

1) Introduction

2) **Ground Characterization**

3) Diagnosis of Ground Behavior and Failure Mechanism

4) Ground Control and management strategies

5) Summary

6) References

9

9

Rock Engineering Design Approaches and challenges in Deep Hard Rock Mining Engineering – Dec. 15th, 2019 – Shahrood UT

Rock Mass Composition

- Rock mass characterisation is used to specify the inherent properties of the rock mass that involved measurement the intact rock strength, natural fracture and discontinuities and their condition to provide a context for rock mass classification and design procedure.
-
- Rock mass characterisation provide estimation of ore body geometry, rock mass properties which play key role to stope design, stope dilution and requirements of ground support.
- Data collection techniques with geological and geotechnical mapping, core logging methods can be used

10

10

Rock Engineering Design Approaches and challenges in Deep Hard Rock Mining Engineering – Dec. 15th, 2019 – Shahrood UT

Data processing procedure for ground characteristics

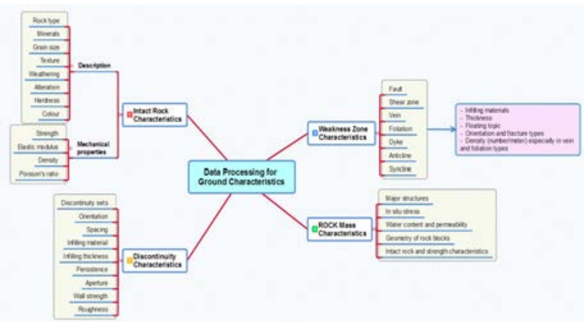

Rahimi, Sharifzadeh, Feng, 2019 11

11

Rock Engineering Design Approaches and challenges in Deep Hard Rock Mining Engineering – Dec. 15th, 2019 – Shahrood UT

The main features for characterising rock mass structure

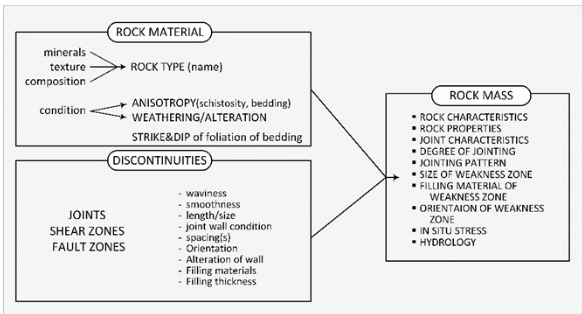

(Modified after Palmstrom and Stille (2015))

12

12

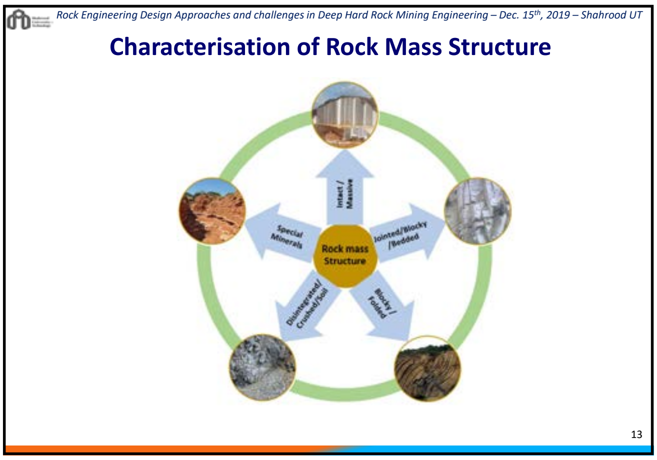

13

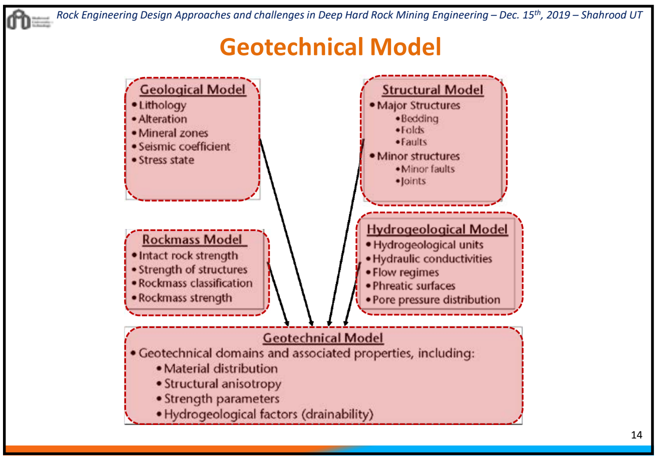

14

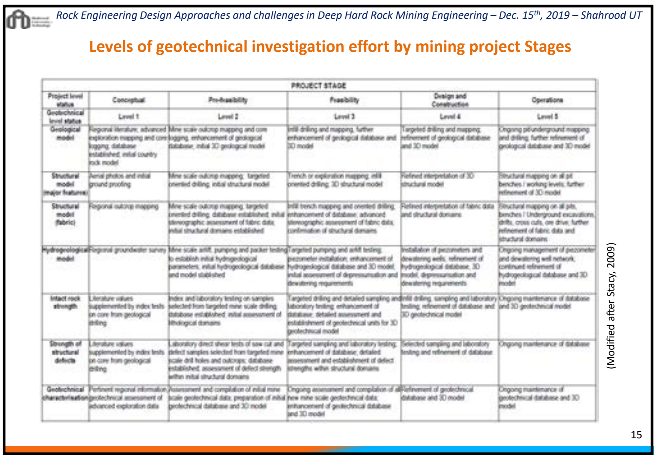

15

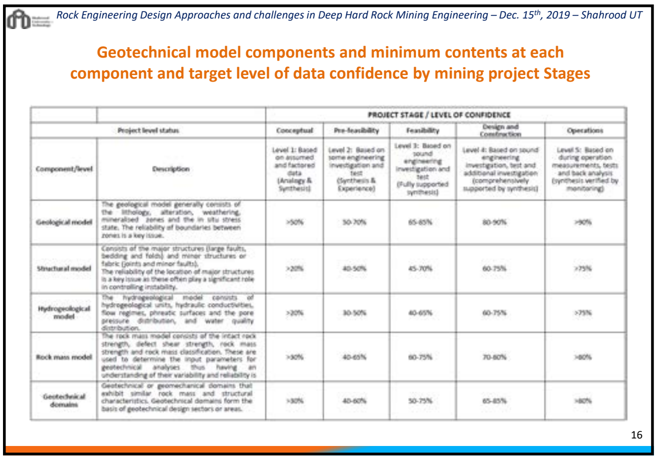

16

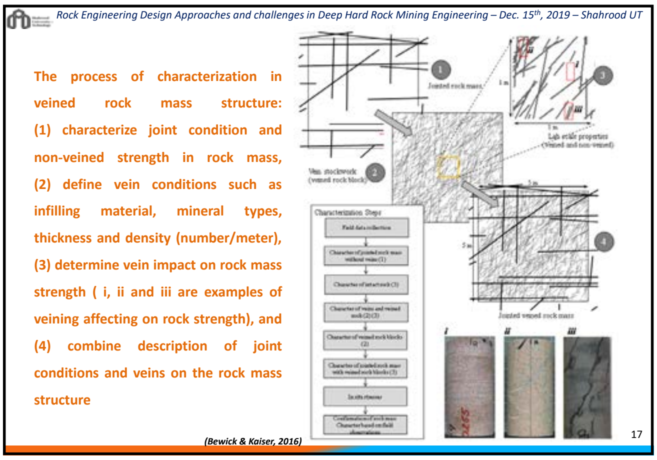

17

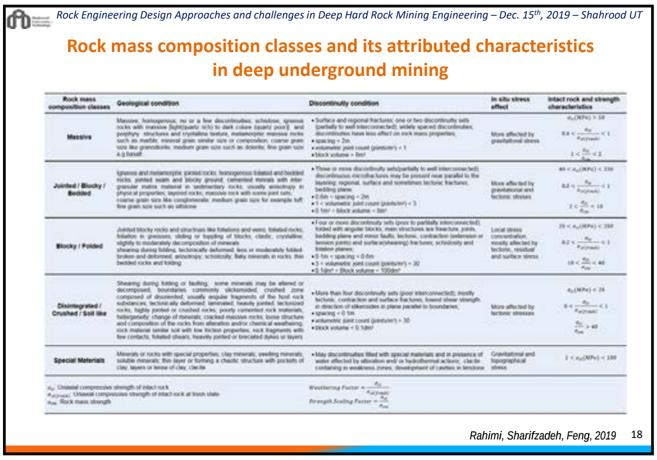

18

Factors influencing rockburst damage at deep underground excavtions

Seismic event	Geology	Geotechnical	Mining

• Event magnitude
• Rate of seismic energy release
• Distance to seismic source
• Fault mechanism
• Slip direction
• Blasts
	• In situ stress
	• Rock type
	• Beddings
	• Geological structures (dykes, faults and shears)
		• Rock strength
		• Joint fabric
		• Rock brittleness
		• Rock properties
			• Mining induced static stresses
			  • Excavation span
			  • Extraction ratio
			• Mine stiffness
			  • Excavation sequence (stress-path)
			• Production rate, blasting
			• seismically induced dynamic stresses
			• installed rock support
			• Backfill

(Modified after Cai and Kaiser, 2014) 19

19

Presentation Outline

20

20

Expected Ground Behaviour Modes

- **Ground behaviour modes not only depends on rock mass structures, but also depend on excavation geometry and construction methods.**
- **There are different modes of ground behaviour such as block falls, buckling, plastic behaviour and rockburst. Identification of main reasons of ground behaviour assist to distinguish types of rock failure.**
- **At great depth, when failure in ground conditions is not predicted or distinguished, rock mass may behave in unforeseen ways and sometimes the condition of good ground decreases in quality due to a variety of factors such as blasting quality.**

21

21

Diagnosis of Ground Behaviour

- **Making precise observation and careful interpretation of existence evidence in rock mass structures and environmental condition is first principal in diagnosis of ground behaviour.**
- **In great deep when the brittle failure in ground condition is not predicted or distinguished, rock mass may behave unforeseen mode and sometimes the good ground condition become bad ground due to variety of factors such as blasting quality.**

22

22

ROCK MASS BEHAVIOUR (RMB) IN MACRO-SCALE

$$\textit{Rock Mass Behaviour (RMB)} = \begin{cases} \textit{Rock Mass Composition (RMC)} \\ + \textit{Active Stress Condition (ASC)} \\ + \textit{Excavation Method, Size and} \\ \textit{Orientation (EMSO)} \end{cases}$$

RMC ⇨	Rock mass physical conditions such as; rock type, intact rock and discontinuities characteristics and geological structures, faults, folds and weak zones. ⇨	classify rock masses to: massive, blocky, heavily jointed, and special minerals.
ASC ⇨	Principle stresses resultant from: in-situ stresses, groundwater pressure, induced stresses, and seismic events. ⇨	Vertical stress: overburden, horizontal to vertical stress ratio: 0.5-4.Block interlocking
EMSO ⇨	underground opening: excavation method, sequence and orientation to rock mass condition ⇨	scale dependent rock mass behaviour (RMB) considering block and excavation size

More flexibility to input engineering experience and judgement using verbal equation rather than quantitative analysis

Sharifzadeh, 2017

23

23

Geotechnical input to determine rock mass response

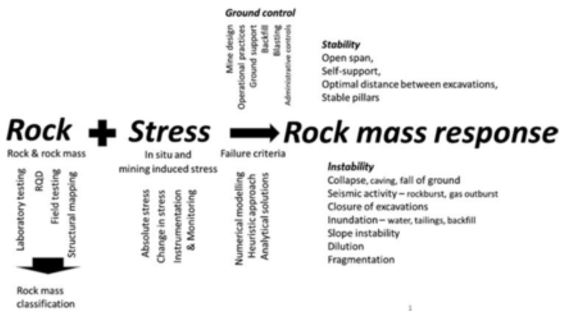

Szwedzicki, 2018 24

24

Mining factors affecting rock mass response (Szwedzicki et al., 2007)

Design and planning

- **Design**
  - Pillar / stope size
  - Opening (e.g. size, shape)
  - Layout (e.g. orientation, distance between levels)
  - Distance to production /caving line
- **Scheduling**
  - Optimised timing of development work (e.g. just-in-time)
  - Optimised time of opening rehabilitation

Development

- **Blasting**
  - Design (e.g. hole diameter and spacing, powder ratio, stemming)
  - Quality of drilling and blasting (e.g. hole direction, length
- **Ground support**
  - Selection of support elements
  - Design (e.g. bolt and cable bolt length, thickness of shotcrete, type of mesh)
  - Quality of ground support installation

Production

- **Production management**
  - Production blasting (e.g. design, sequence)
  - Quality of drilling and blasting (e.g. hanging wall overbreak, unblasted remnants)
  - Ore draw (e.g. rate, uniformity)
  - Ground control (e.g. backfill)

Szwedzicki, 2018 25

25

Ground behaviour modes in deep underground excavations

26

26

Sequences of geotechnical failures at great depth

- **The responses of the ground in the excavation is derived from change in loading, drawback natural support, and fluid flow.**
- **Sequences of geotechnical failures at great depth includes :**
  1) **Stable**
  2) **Failure indicators like faults, shear zones and moisture**
  3) **Ground movement such as crack opening, shear movement**
  4) **Failure precursors for example roof lowering and spalling**
  5) **Damage/collapse like cave in and rock burst**

27

27

SEQUENCE OF FIALURE

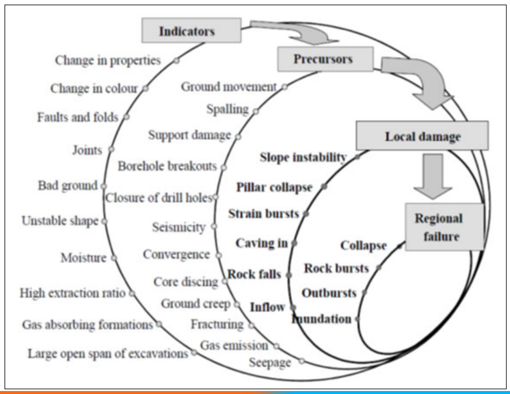

(Szwedzicki, 2003) 28

28

Rock mass – Excavation characteristics interaction: Scale – Construction dependent behaviour

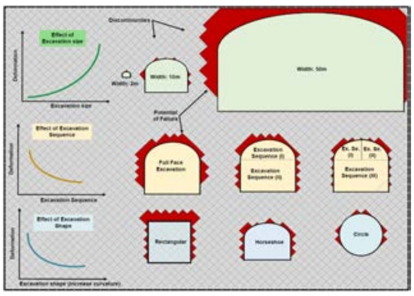

The relation between excavation size, sequence and shape with respect to the rock mass (Scale dependent behaviour) 29

29

Failure type modes in underground excavation

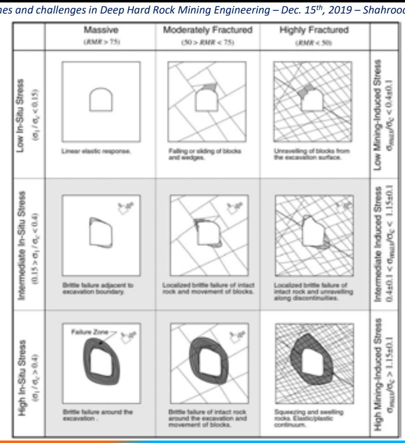

P.K. Kaiser & Kim, 2008 30

30

Some failure modes in deep underground mining in Western Australia

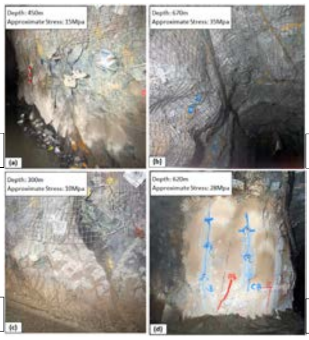

31

31

Rock Engineering Design Approaches and challenges in Deep Hard Rock Mining Engineering – Dec. 15th, 2019 – Shahrood UT

Hard Rock Sudden Failure Process

- Stress redistribution (Excavation, adjacent construction, seismic)
- Stress concentration around micro-cracks (Strain energy accumulation)
- Crack propagation (Energy dissipation)
- Crack coalescence (Spalling, chipping, Slabbing) (Minor energy release)
- Rock burst, ejection (Sudden high energy release) / Rock popping (Sudden medium energy release)

32

32

Rock Engineering Design Approaches and challenges in Deep Hard Rock Mining Engineering – Dec. 15th, 2019 – Shahrood UT

Underground deep and high stress excavations failure mechanisms due to induced stress and seismic events

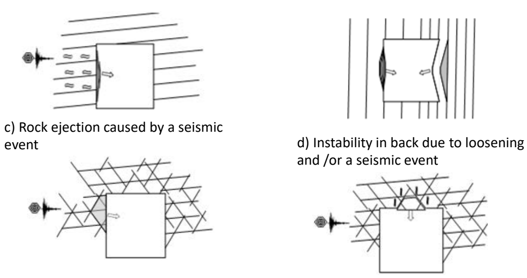

R. Masoudi & M. Sharifzadeh, 2018 33

33

Rock Engineering Design Approaches and challenges in Deep Hard Rock Mining Engineering – Dec. 15th, 2019 – Shahrood UT

Rockburst expectation based on intact rock property

	Index	Severity of potential Rockburst				
		Low		Strong		Violent
Index of strain energy* (Kwasniewski et al., 1994)	$F = \Phi_{sp} / \Phi_{st}$		2		5	
Potential energy of elastic strain (kJ/m³)(Kwasniewski, 2000)	$PES = \sigma^2_c / 2E_s$	50	100	150	200	250
Rock brittleness (Qiao and Tian, 1998)	$B = \sigma_C / \sigma_T$	40		26.7		14.5
Ratio of tangential stress to compressive strength (Wang et al., 1998)	$T_s = \sigma_\theta / \sigma_C$	0.3		0.5		0.7

* It has been done based on tests on coal specimen to provide the intensity of shocks or coal bombs

R. Masoudi & M. Sharifzadeh, 2018 34

34

Rock Engineering Design Approaches and challenges in Deep Hard Rock Mining Engineering – Dec. 15th, 2019 – Shahrood UT

Rockburst analysis methods

Rockburst Problem

- Analytical method
  - Catastrophe theory
  - Energy balance concept
  - Fracture mechanics
- Empirical method
- Data-based method
  - Statistical technique
  - Artificial intelligent method
- Numerical method
  - Continuum
  - Discontinuum
  - Hybrid
- Experimental method
  - Physical simulation
  - Lab test
  - In situ test

Manouchehrial, 2016 35

35

Rock Engineering Design Approaches and challenges in Deep Hard Rock Mining Engineering – Dec. 15th, 2019 – Shahrood UT

EXAMPLE: Sudden failure in deep underground Nickel mine in WA

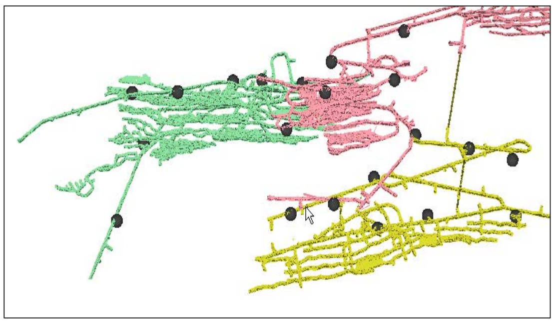

- **Seismic sensor locations around mine excavations**

36

36

EXAMPLE: Sudden failure in deep underground Nickel mine in WA

Stress Regime

Principal Stress	Magnitude at 800m depth (MPa)	Magnitude relationship to true depth (h in metres)	Bearing	Dip	Description
Major (σ_1)	56	0.058(h) + 10	150°	00°	Flat NNW-SSE
Intermediate (σ_2)	36	0.037(h) + 6	060°	15°	Shallow dip to ENE
Minor (σ_3)	22	0.020(h) + 6	240°	75°	Steep dip to WSW

Geological Structural model of the mine

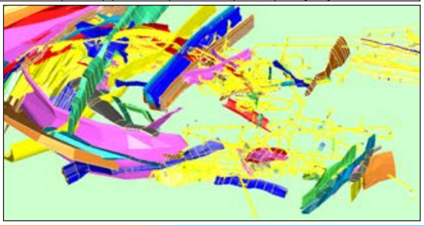

37

37

EXAMPLE: Sudden failure in deep underground Nickel mine in WA

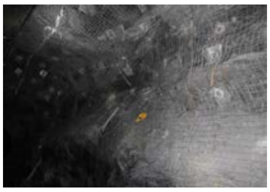


Block ejection, overbreak, and dilution in narrow vein stope (Depth about 700m)

38

38

EXAMPLE : Sudden failure in deep underground Nickel mine in WA


Low energy rock burst, in pillar at depth of 850m.

39

39

EXAMPLE : Sudden failure in deep underground Nickel mine in WA


Low energy rock burst, in pillar at depth of 850m.

40

40

EXAMPLE: Sudden failure in deep underground Nickel mine in WA


Chipping, Spalling

Low energy rock burst, in pillar at depth of 850m.

41

41

EXAMPLE: Sudden failure in deep underground Nickel mine in WA


Floor cracking and heave at the depth of 850m ore drives (Excavations).

42

42

Summary of mechanisms associated with large deformation

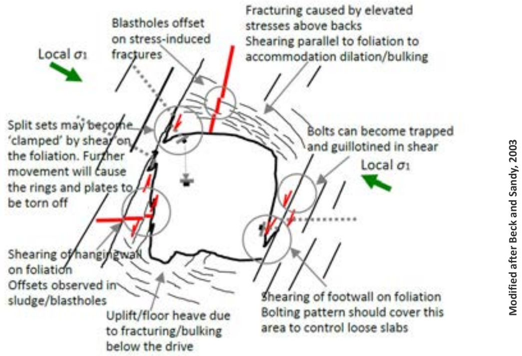

43

43

EXAMPLE : LARGE DEFORMATION IN DEEP UNDERGROUND MINE IN WESTERN AUSTRALIA

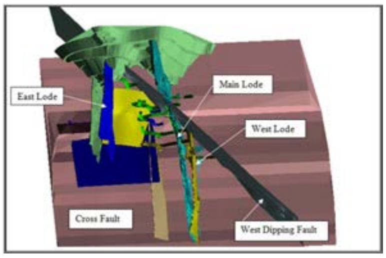

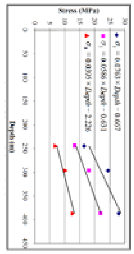

Main geological structures and principal stress magnitude

44

44

Case Example : Large Deformation In Deep Underground Mine In Western Australia

45

45

Case Example : Large Deformation In Deep Underground Mine In Western Australia

46

46

Examples Deep Underground Mine failure mechanisms

Foliated basaltic rocks bulking from side views (left) and front view (right)

47

47

Interaction of multiple sequences of matrix deformation in rocks

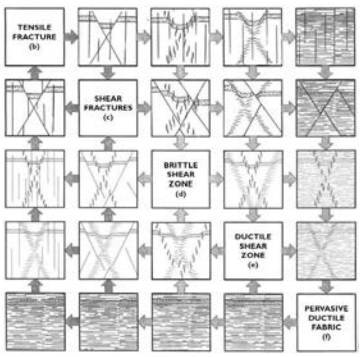

48

48

Rock Mass Condition at Macro-scale

- Geological structure at transition of surface to underground gold mine with mainly basaltic rocks

49

49

Rock Mass Condition at Macro-scale

- Geological structure at transition of surface to

inly b

50

50

TYPICAL FAILURE MECHANISMS IN UNDERGROUND MINES

- Failure modes involving only intact rock
  - Rockburst
  - Squeezing
  - Spalling

- Failure modes involving only discontinuity
  - Sliding
  - Rockfall
  - Sliding and Rockfall

- Failure modes involving intact rock and discontinuity
  - Bending
  - Bucking
  - Flexural topping

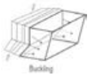

51

51

The main principle types of Ground Behaviour (Palmstrom, 2000).

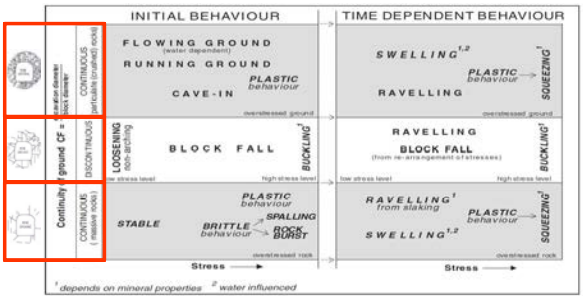

52

52

Identification of rockmass behaviour in underground excavations

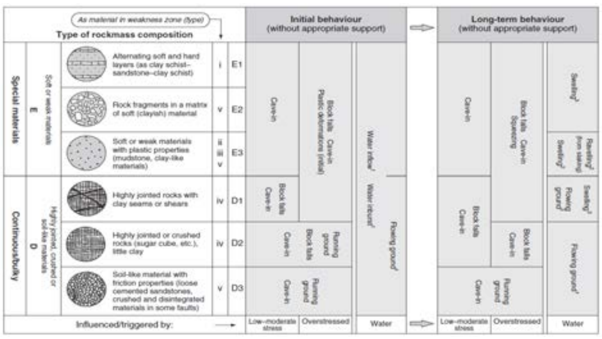

(Stille and Palmstrom, 2008)

53

53

Identification of rockmass behaviour in underground excavations

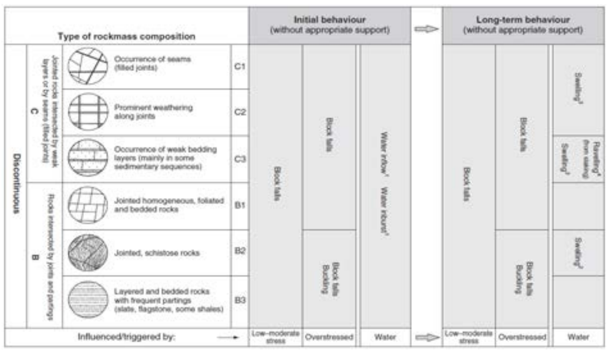

(Stille and Palmstrom, 2008)

54

54

Identification of rockmass behaviour in underground excavations

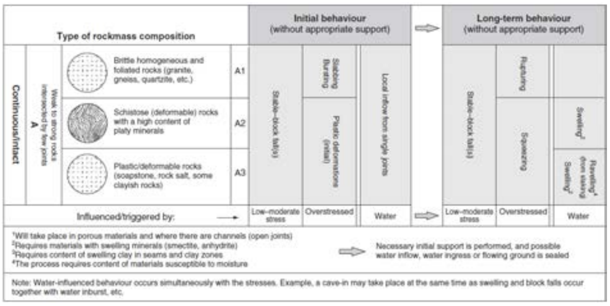

(Stille and Palmstrom, 2008)

TYPICAL FAILURE MECHANISMS IN UNDERGROUND MINES

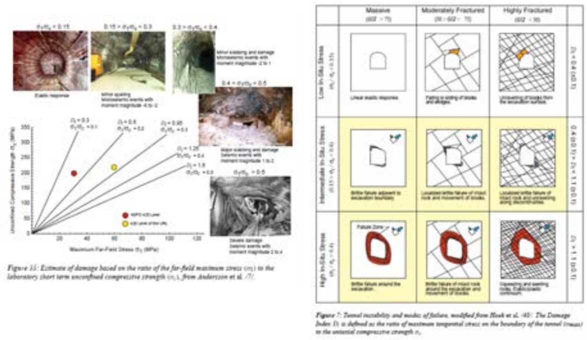

Behaviour type, based on Austrian guidelines for geomechanical planning(1)

Basic behaviour type	Description of potential failure modes/mechanics during excavation of the tunnel
1. Stable	Stable rockmass with the potential of small local gravity- induced falling or sliding of blocks
2. Stable discontinuity-controlled block fall	Deep-reaching, discontinuity-controlled, gravity-induced falling and sliding of blocks, occasional local shear failure
3. Shallow shear failure	Shallow stress-induced shear failures in combination with discontinuity- and gravity-controlled failure of the rockmass
4. Deep-seated shear failure	Deep-seated stress-induced shear failures and large deformation
5. Rock burst	Sudden and violent failure of the rockmass, caused by highly stressed, brittle rocks and the rapid release of accumulated strain energy
6. Buckling failure	Buckling of rocks with a narrowly spaced discontinuity set, frequently associated with shear failure

Behaviour type, based on Austrian guidelines for geomechanical planning(2)

Basic behaviour type	Description of potential failure modes/mechanics during excavation of the tunnel
7. Shear failure under low confining pressure	Potential for excessive overbreak and progressive shear failure with the development of chimney-type failure, caused mainly by a deficiency of side pressure
8. Ravelling ground	Flow of cohesionless dry or moist, intensely fractured rocks or soil
9. Flowing ground	Flow of intensely fractured rocks or soil with high water content
10. Swelling	Time-dependent volume increase of the rockmass caused by physico-chemical reaction of rock and water in combination with stress relief, leading to inward movement of the tunnel perimeter
11. Frequently changing behaviour	Rapid variation of stresses and deformations, caused by heterogeneous rockmass conditions or the block-in-matrix rock situation of a tectonic melange (brittle fault zone)

Behaviour types in underground excavations (Palmstrom&Stille,2015)

Behaviour type		Definition	Comments
Group 1. Gravity driven			
a. Stable		The surrounding ground will stand unsupported for several days or longer	Massive, durable rocks at low and moderate depths
b. Block fall(s)	of single blocks	Stable, with the potential fall of individual blocks	Discontinuity-controlled failure
	of several blocks	Stable, with the potential fall of several blocks (slide volume ,10 m3)	
c. Cave-in		Inward, quick movement of larger volumes (.10 m3) of rock fragments or pieces	Encountered in highly jointed or crushed rock
d. Running ground		A particulate material quickly invades the tunnel until a stable slope is formed at the face. The stand-up time is zero or nearly zero	Examples are clean medium to coarse sands and gravels above the groundwater level

Behaviour types in underground excavations (Palmstrom&Stille,2015)

Behaviour type	Definition	Comments
Group 2. Stress induced		
e. Buckling	Breaking out of fragments in tunnel surface	Occurs in anisotropic, hard, brittle rock under sufficiently high load due to deflection of the rock structure
f. Rupturing from stresses	Gradually breaking up into pieces, flakes or fragments in the tunnel surface	The time-dependent effect of slabbing or rock burst from redistribution of stresses
g. Slabbing	Sudden, violent detachment of thin rock slabs from the sides or roof	Moderate to high overstressing of massive hard, brittle rock. Includes popping or spallinga
h. Rock burst	Much more violent than slabbing, and involves considerably larger volumes	Very high overstressing of massive hard, brittle rock (heavy rock bursting often registers as a seismic event)
i. Plastic behaviour (initial)	Initial deformations caused by shear failures in combination with discontinuity and gravity- controlled failure	Takes place in plastic (deformable) rock from overstressing. Often the start of squeezing
j. Squeezing	Time-dependent deformation, essentially associated with creep caused by overstressing Deformations may terminate during construction or continue over a long period	Overstressed plastic, massive rocks and materials with a high percentage of micaceous minerals or of clay minerals with a low swelling capacity

Behaviour types in underground excavations (Palmstrom&Stille,2015)

Behaviour type		Definition	Comments
Group 3. Water influenced			
k. Ravelling from slaking		Ground gradually breaks up into pieces, flakes or fragments	Disintegration (slaking) of some moderately coherent and friable materials Examples: mudstones and stiff, fissured clays
l. Swelling	of certain rocks	Advance of surrounding ground into the tunnel due to expansion caused by water adsorption. The process may sometimes be mistaken for squeezing	Occurs in swelling of rocks, in which anhydrite, halite (rock salt) and swelling clay minerals, such as smectite (montmorillonite), constitute a significant portion
	of certain clay seams or fillings	Swelling of clay seams caused by adsorption of water. This leads to loosening of blocks and reduced shear strength of clay	The swelling takes place in seams having fillings of swelling clay minerals (smectite, montmorillonite)
m. Flowing ground		A mixture of water and solids quickly invades the tunnel from all sides, including the invert	May occur in tunnels below the groundwater table in particulate materials with little or no coherence
n. Water ingress		Pressurised water invades the excavation through channels or openings in rocks	May occur in porous and soluble rocks, or along significant openings or channels in fractures or joints

61

61

Rock Engineering Design Approaches and challenges in Deep Hard Rock Mining Engineering – Dec. 15th, 2019 – Shahrood UT

Variable Ground Response

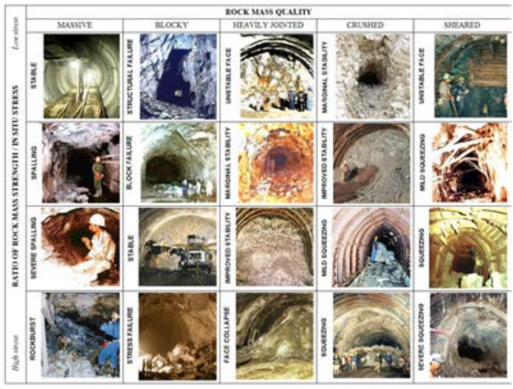

62

62

Rock Engineering Design Approaches and challenges in Deep Hard Rock Mining Engineering – Dec. 15th, 2019 – Shahrood UT

Detection of failure mechanisms through physical modelling

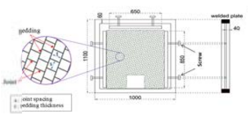

Classification of failure mechanisms

- Based on stress arch
  - 0 <dip < Φ
  - Φ <dip < (Ø/2)+(π/4)
  - ((Ø/2)+(π/4))<dip
- Dimensional ratio
  - Low jointing
  - Medium jointing
  - High jointing

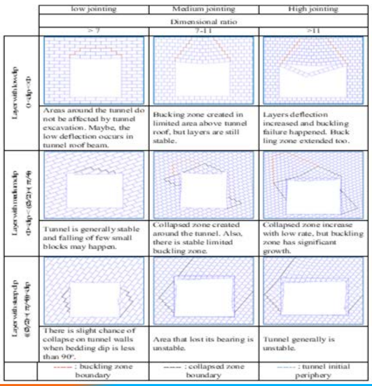

63

63

Rock Engineering Design Approaches and challenges in Deep Hard Rock Mining Engineering – Dec. 15th, 2019 – Shahrood UT

Presentation Outline

1) Introduction
2) Ground Characterization
3) Diagnosis of Ground Behavior and Failure Mechanism
4) **Ground Control and management strategies**
5) Summary
6) References

64

64

Rock Engineering Design Approaches and challenges in Deep Hard Rock Mining Engineering – Dec. 15th, 2019 – Shahrood UT

Design analysis methods in deep underground mines

- **Strategic design:** This is a type of primary design and preparing broad plan for the mines site such as the location of access and underground stopes,
- **Tactical design:** Tactical object is to provide the detail design of projects for example stability analysis of rock mass in underground excavations and selecting ground support system before operational stage at the mines, and
- **Operational design:** This is related to monitoring and updated design parameters through observational methods and monitoring system.

65

65

Rock Engineering Design Approaches and challeng ... d UT

Ground management strategies in deep underground excavations.

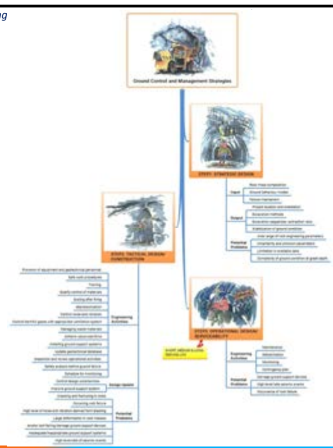

Rahimi, Sharifzadeh, Feng, 2019

66

66

The major steps for ground control and management at great depth

- Collect data from available evidences, observed features and seismic events,
- Identify potential geotechnical hazards,
- Analyse the hazards for ground management, and determine appropriate strategies such as smooth blasting method and install ground support system,
- Evaluate the effectiveness of multi-factor on ground conditions, especially time,
- Implement ground management strategies in hazardous areas,
- Conduct geotechnical monitoring and review the ground responses, and
- Update the strategies.

67

67

Ground control and management

- During the design phase of ground control and management, three following approaches significantly affect the type of ground behaviours and failure mechanisms in underground excavations.

1. Project location and orientation,
2. Sequential excavation/excavation method/extraction rate, and
3. Ground support selection method.

68

68

Project location and orientation

The angle between the orientation of an opening and major structures of rock masses influences the type of failure and mechanisms in underground mining activities.

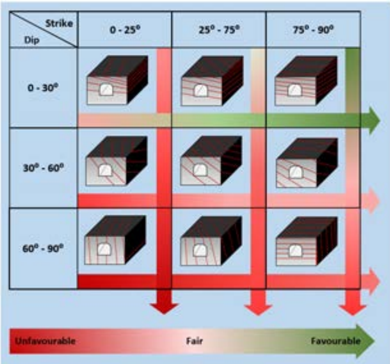

Rahimi, Sharifzadeh, Feng, 2019

69

69

Excavation method, sequences and extraction rate

- Excavation method has a significant influence on the engineering behaviour of rock masses.
- Sequences in underground operations can be divided into primary, secondary and tertiary priorities. The first priority of sequential panels or stopes is usually designed and extracted in high-grade regions of the orebody in consideration of target products in mine planning, field stresses, stability of rock masses, dimension of stopes, and backfilling methods. The primary panels or stopes are excavated and then filled with backfill materials for two vertical lifts before extracting secondary and tertiary priorities of stopes.

70

70

Sequential excavation in (a) a tunnel, (b) an underground mine with bottom-up and centre-out method, and (c) an underground mine with bottom-up sequences method (The number shows the sequences of excavations).

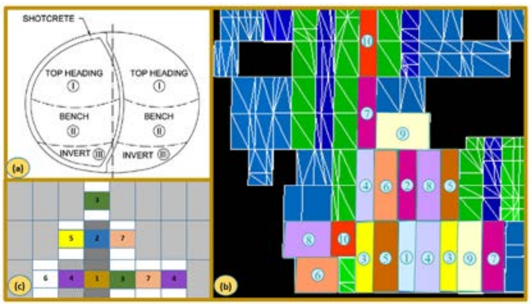

Rahimi, Sharifzadeh, Feng, 2019

71

71

Mining Sequences

Generally, the excavation sequence dimension varies between 5–30 m width, 15–50 m length and 15–100 m height in Australia. Sequential excavation in mining operations can be developed as top–down, bottom–up, centre–out and abutment–centre. The dimension of stopes in sequential excavation affects mining operation costs, stability of rock masses and failure mechanisms.

72

72

Ground supports in underground mines

- Determine project conditions and purposes,
- Identify major geotechnical defects and failure mechanisms in rocks,
- Identify main types of loading (static/dynamic) surrounding excavations and estimate their intensities,
- Analyse ground condition and estimate rock mass deformations,
- Select the type of ground support approaches: natural ground support and/or artificial ground support systems,
- Select the types of surface and reinforcement support devices, and
- Control the ground–support performance.

73

73

Different types of ground support devices in a failure zone

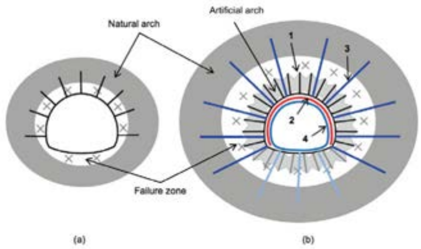

(a) Rock bolting in small damaged zone;

(a) Large damaged zone with (1) rock bolting, (2) retaining by inner surface support devices, (3) cable bolting, and (4) surface support devices

(Li, 2017)

74

74

Application of typical ground support system to control rock failure

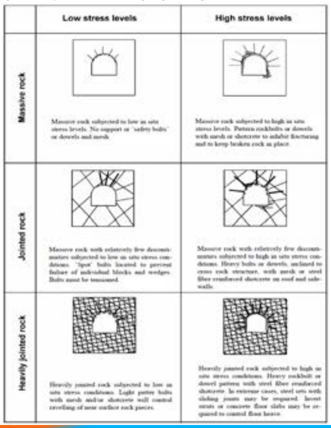

Hoek, Kaiser, & Bawden, 1995

75

75

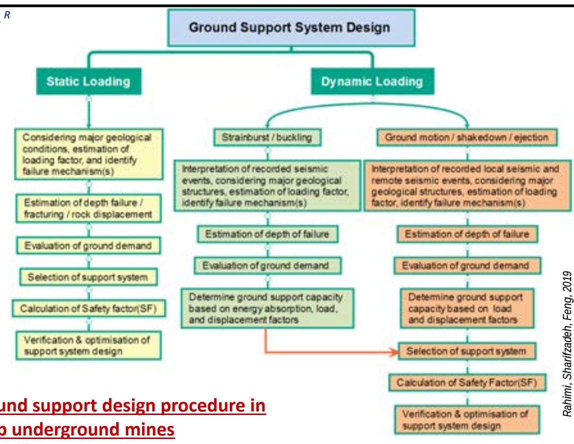

Ground support design procedure in deep underground mines

Rahimi, Sharifzadeh, Feng, 2019

76

76

Design principles for deep hard rock conditions under static loading

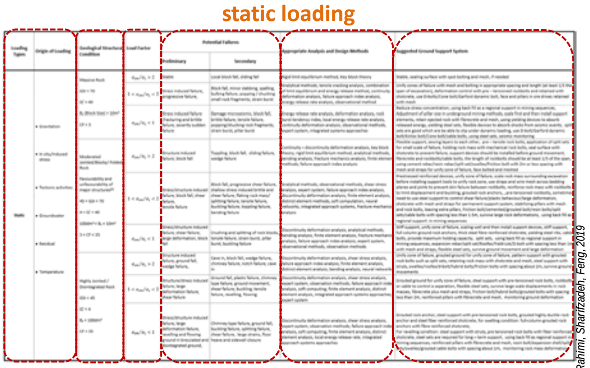

Rahimi, Sharifzadeh, Feng, 2019

77

77

Design principles for deep hard rock conditions under static loading

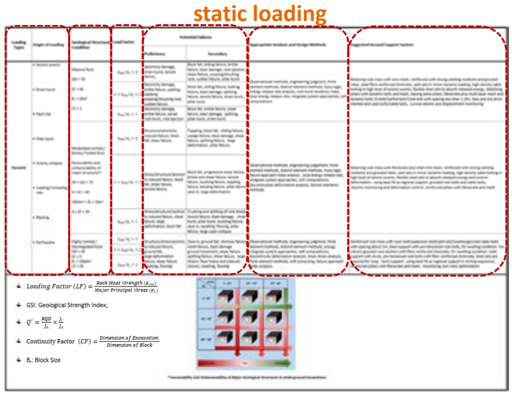

Rahimi, Sharifzadeh, Feng, 2019

78

78

Countermeasures to eliminate or reduce sudden failure risk

(i) Optimization of the project layout scheme,

(ii) Pre-conditioning of the rock mass,

(iii) Rock mass reinforcement and support.

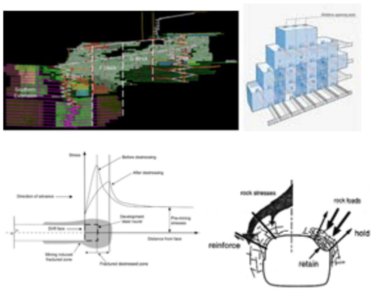

79

79

Rock Engineering Design Approaches and challenges in Deep Hard Rock Mining Engineering – Dec. 15th, 2019 – Shahrood UT

Countermeasures to eliminate or reduce sudden failure risk

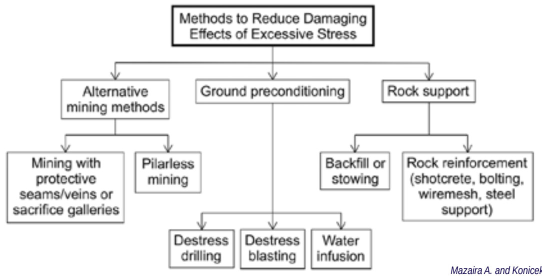

Mazaira A. and Konicek P., 2015

80

80

Rock Engineering Design Approaches and challenges in Deep Hard Rock Mining Engineering – Dec. 15th, 2019 – Shahrood UT

Mine Sequencing and backfilling

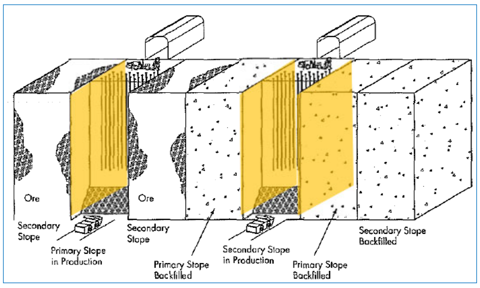

81

81

Rock Engineering Design Approaches and challenges in Deep Hard Rock Mining Engineering – Dec. 15th, 2019 – Shahrood UT

Mine Sequencing and backfilling

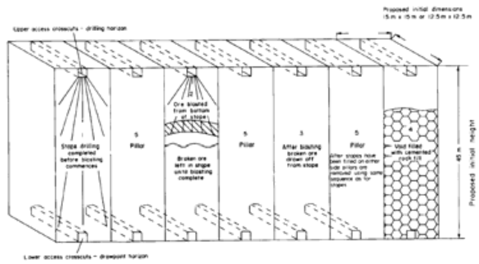

Figure 4 Vertical crater retreat with cemented rockfill

FERGUSON G. A. 1993

82

82

Rock Engineering Design Approaches and challenges in Deep Hard Rock Mining Engineering – Dec. 15th, 2019 – Shahrood UT

Mine Sequencing and backfilling

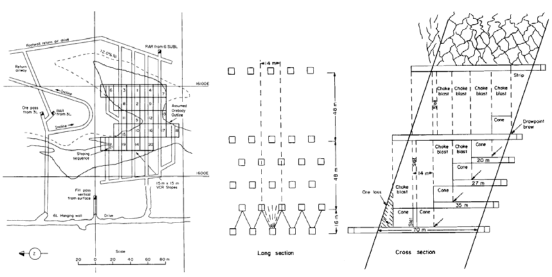

Figure 6 Vertical crater retreat stoping layout plan, 6 Level

Figure 7 Layout of choke mass blast caving method

FERGUSON G. A. 1993

83

83

Rock Engineering Design Approaches and challenges in Deep Hard Rock Mining Engineering – Dec. 15th, 2019 – Shahrood UT

Presentation Outline

1) Introduction
2) Ground Characterization
3) Diagnosis of Ground Behavior and Failure Mechanism
4) Ground Control and management strategies
5) **Summary**
6) References

84

84

Conclusion

- ✓ A developed design methodology based on ground behaviour and failure mechanism proposed for underground excavations.
- ✓ Rock mass structure, stress concentration and construction condition are main parameters to diagnose ground behaviour modes.
- ✓ The sequences of failure process at great depth specified as stable, indicator warnings, ground movement, failure precursors, and damage/collapse.
- ✓ In high stress situation, determination of energy absorption, cost, compatibility of external and internal support tools, efficiency, easy production and installation, and adaptable are assessed for design of ground support systems.
- ✓ Severe damage in rock mass structures and ground support systems may occur due to large magnitude seismic events, defects in rock mass structures, stress concentration, blasting damage and tectonic activities such as strike-slip faults.

Conclusion

- Utilisation of proper ground control and management strategy can avoid the risk of failure. A ground control and amendment strategy of deep hard rock was proposed in regard to the design, construction and serviceability stages of works.
- Collecting comprehensive data, diagnosis of hazard conditions and failure mechanisms, design analysis, and selecting stabilization methods were conducted in the design phase.
- Determination of safe work procedures, training personnel, identification of hazard conditions, quality control and quality assurance of materials, and safety analysis before ground failure are essential in construction stage.

Conclusion

- ✓ Control of the ground condition during serviceability (short-, medium- and long-term) is focused on monitoring (seismic events and load–deformations), maintenance, rehabilitation, seismic monitoring, and contingency planning.
- ✓ The critical factors in the design stage of deep underground mining projects are to establish suitable location and layout of openings; determination of suitable excavation method, sequential excavation and extraction ratio; and selection of proper ground support equipment for small- and/or large-scale deformation.
- ✓ Field observational methods utilise instrumentation, monitoring and back analysis to control the performance of the ground–support system in rock underground projects. The typical monitoring system in deep underground mining methods is seismic monitoring and measurement of rock deformation surrounding excavations.

Presentation Outline

1) Introduction
2) Ground Characterization
3) Diagnosis of Ground Behavior and Failure Mechanism
4) Ground Control and management strategies
5) Summary
6) **References**

References

- Atlas Copco. Mining methods in underground mining-Atlas Copco Rock Drills AB. Stockholm: Atlas Copco; 2007. p.33-45.
- Brady BHG, Brown ET. Rock Mechanics for underground mining. 3rd ed. Springer; 2006.
- Cai M, Kaiser PK. Rockburst Phenomenon and Support Characteristics, MIRARCO–Mining Innovation. In: Rockburst Support Reference Book. Sudbury, Canada; 2018.
- Diederichs MS, Martin CD. Measurement of Spalling Parameters From Laboratory Testing. In: Proceedings of the ISRM International Symposium-EUROCK, Lausanne, Switzerland. International Society for Rock Mechanics and Rock Engineering; 2010.
- Diederichs MS. Early assessment of dynamic rupture and rockburst hazard potential in deep tunnelling. In: Proceedings of the ISRM AfriRock-Rock Mechanics for Africa, Cape Town, South Africa. International Society for Rock Mechanics and Rock Engineering; 2017.
- Feng XT, Hudson JA. Rock engineering design. Leiden, The Netherlands: CRC Press; 2011.
- Ghasemi Y. Numerical studies of mining geometry and extraction sequencing in Lappberget, Garpenberg. MSc Thesis. Lulea University of Technology; 2012.
- Hudyma M, Potvin Y. Seismic hazard in Western Australian mines. Journal of the Southern African Institute of Mining and Metallurgy 2004; 104(5):265-75.
- Jacobsson L, Toyra J, Woldemedhin B, Krekula H. Rock support in the Kiirunavaara Mine. In: Proceedings of the 7th International Symposium on Ground Support in Mining and Underground Construction. Perth: Australian Centre for Geomechanics; 2013.

References

- Kaiser PK, MacCreath DR, Tannant DD. Canadian rockburst support handbook: prepared for sponsors of the Canadian rockburst research program 1990-1995. Geomechanics Research Centre; 1996.
- Kaiser PK, Cai M. Design of rock support system under rockburst condition. Journal of Rock Mechanics and Geotechnical Engineering 2012; 4(3), 215-27.
- KNOBBEN, C. Seismic hazard at the Rosebery mine. Proceedings of the Eighth International Conference on Deep and High Stress Mining, 2017. Australian Centre for Geomechanics, 53-59.
- Li CC. Parameters required for the design of rock support in high-stress masses. In: Proceedings of the ISRM AfriRock-Rock Mechanics for Africa, Cape Town, South Africa. International Society for Rock Mechanics and Rock Engineering; 2017.
- Louchnikov V, Sandy M. Selecting an optimal ground support system for rockbursting conditions. In: Proceedings of the 8th International Conference on Deep and High Stress Mining. Perth: Australian Centre for Geomechanics; 2017.
- Masoudi R, Sharifzadeh M. Reinforcement selection for deep and high-stress tunnels at preliminary design stages using ground demand and support capacity approach. International Journal of Mining Science and Technology 2018; 28(4):573-82.
- Mazaira A, Konicek P. Intense rockburst impacts in deep underground construction and their prevention. Canadian Geotechnical Journal 2015; 52(10):1426-39.
- Morissette P, Hadjigeorgiou J, Punkkinen AR, Chinnasane DR. The influence of change in mining and ground support practice on the frequency and severity of rockbursts. In: Proceedings of the 7th International Conference on Deep and High Stress Mining, Sudbury, Ontario, Canada. 2014.

References

- MOSHAB. Surface rock support for underground mines code of practice. Western Australia: Mines Occupational Safety and Health Advisory Board; 1999.
- Potvin Y, Wesseloo J, Heal D. An interpretation of ground support capacity submitted to dynamic loading. Mining Technology 2010; 119(4):233-45.
- Rahimi B, Shahriar K, Sharifzadeh M. Evaluation of rock mass engineering geological properties using statistical analysis and selecting proper tunnel design approach in Qazvin–Rasht railway tunnel. Tunnelling and Underground Space Technology 2014; 41:206-22.
- Rahimi B, Sharifzadeh M. Evaluation of ground management in underground excavation design. In: Proceedings of the 8th International Conference on Deep and High Stress Mining. Perth: Australian Centre for Geomechanics. 2017. p. 813-26.
- Saharan MR, Mitri H. Destress blasting as a mines safety tool: some fundamental challenges for successful applications. Procedia Engineering 2011; 26:37-47.
- Sharifzadeh M, Kolivand F, Ghorbani M, Yasrobi S. Design of sequential excavation method for large span urban tunnels in soft ground–Niayesh tunnel. Tunnelling and Underground Space Technology 2013; 35:178-88.
- Sharifzadeh M, Feng XT, Zhang X, Zhang Y. Challenges in Multi-Scale Hard Rock Behavior Evaluation at Deep Underground Excavations. In: Proceedings of the 12th Iranian and 3rd Regional Tunnelling Conference, Tunnelling and Climate Change, Tehran, Iran. 2017a.
- Sharifzadeh M, Ghorbani M, Yasrobi S. Observation-based design of geo-engineering projects with emphasis on optimization of tunnel support systems and excavation sequences. In: Feng XT, editor. Rock Mechanics and Engineering Volume 4: Excavation, Support and Monitoring. London, UK: CRC Press; 2017b.

References

- Stacey TR. Innovative and controversial support for rockbursting conditions. In: Proceeding of the 8th International Symposium on Ground Support in Mining and Underground Construction, Lulea, Sweden. 2016.
- Szwedzicki T. Quality assurance in mine ground control management. International Journal of Rock Mechanics and Mining Sciences 2003; 40(4):565-72.
- Talbot JF, Burke J. Practical improvements to the shotcreting process at Lisheen Mine with particular attention to the mix design and admixture usage. In: Proceedings of the 7th International Symposium on Ground Support in Mining and Underground Construction. Perth: Australian Centre for Geomechanics; 2013.
- Yokota Y, Yamamoto T, Date K, MORI T. Quality improvement of rockbolting. In: Proceedings of the 7th International Symposium on Ground Support in Mining and Underground Construction. Perth: Australian Centre for Geomechanics; 2013.
- Zhang P, Dineva S, Nordlund E, Hansen-Haug J, Woldemedhin B, Töyrä J, Boskovic M, Nyström A, Marklund PI, Mozaffari S. Establishment of experimental sites in three Swedish mines to monitor the in-situ performance of ground support systems associated with mining-induced seismicity. In: Proceeding of the 8th International Symposium on Ground Support in Mining and Underground Construction, Lulea, Sweden. 2016.

Presentation Outline

1) Introduction
2) Ground Characterization
3) Diagnosis of Ground Behavior and Failure Mechanism
4) Ground Control and management strategies
5) Summary
6) References

Geotechnical input to determine rock mass response

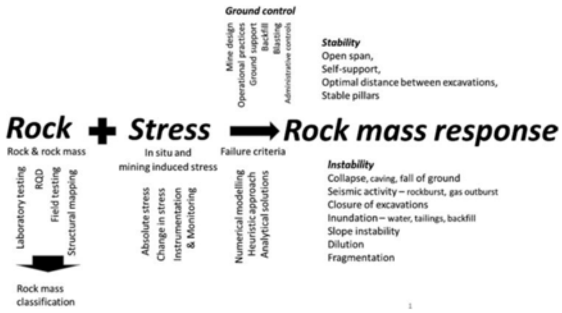

Szwedzicki, 2018

Mining factors affecting rock mass response (Szwedzicki et al., 2007)

Design and planning

- **Design**
  - Pillar / stope size
  - Opening (e.g. size, shape)
  - Layout (e.g. orientation, distance between levels)
  - Distance to production /caving line
- **Scheduling**
  - Optimised timing of development work (e.g. just-in-time)
  - Optimised time of opening rehabilitation

Development

- **Blasting**
  - Design (e.g. hole diameter and spacing, powder ratio, stemming)
  - Quality of drilling and blasting (e.g. hole direction, length
- **Ground support**
  - Selection of support elements
  - Design (e.g. bolt and cable bolt length, thickness of shotcrete, type of mesh)
  - Quality of ground support installation

Production

- **Production management**
  - Production blasting (e.g. design, sequence)
  - Quality of drilling and blasting (e.g. hanging wall overbreak, unblasted remnants)
  - Ore draw (e.g. rate, uniformity)
  - Ground control (e.g. backfill)

Szwedzicki, 2018

The main features for characterising rock mass structure

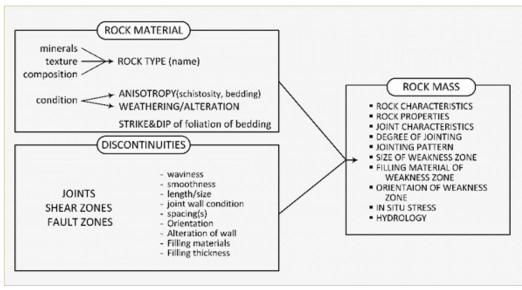

(Modified after Palmstrom and Stille (2015))

Accepted Manuscript

Ground behaviour analysis, support system design and construction strategies in deep hard rock mining – Justified in Western Australian's mines

Behrooz Rahimi, Mostafa Sharifzadeh, Xia-Ting Feng

PII: S1674-7755(18)30500-6

DOI: https://doi.org/10.1016/j.jrmge.2019.01.006

Reference: JRMGE 585

To appear in: *Journal of Rock Mechanics and Geotechnical Engineering*

Received Date: 25 September 2018

Revised Date: 29 November 2018

Accepted Date: 9 January 2019

Please cite this article as: Rahimi B, Sharifzadeh M, Feng X-T, Ground behaviour analysis, support system design and construction strategies in deep hard rock mining – Justified in Western Australian's mines, *Journal of Rock Mechanics and Geotechnical Engineering*, https://doi.org/10.1016/j.jrmge.2019.01.006.

Journal of Rock Mechanics and Geotechnical Engineering

Journal online: www.rockgeotech.org

Ground behaviour analysis, support system design and construction strategies in deep hard rock mining – Justified in Western Australian's mines

Behrooz Rahimi[a,*], Mostafa Sharifzadeh[a], Xia-Ting Feng[b]

[a] Department of Mining and Metallurgical Engineering, Western Australian School of Mines: Minerals, Energy and Chemical Engineering (WASM-MECE), Curtin University, Kalgoorlie, WA 6430, Australia

[b] Key Laboratory of Ministry of Education for Safe Mining of Deep Metal Mines, Northeastern University, Shenyang, 110819, China

Received 25 September 2018; received in revised form 29 November 2018; accepted 9 January 2019

Abstract: Development of deep underground mining projects is crucial for optimum extraction of mineral deposits. The main challenges at great depth are high rock stress levels, seismic events, large-scale deformation, sudden failures and high temperatures that may cause abrupt and unpredictable instability and collapse over a large scale. In this paper, a ground control and management strategy was presented corresponding to the three stages of projects: strategic design, tactical design and operational design. Strategic design is results in preparing a broad plan and primary design for mining excavations. The tactical design is to provide detail design such as stabilisation methods. Operational design stage is related to monitoring and updating design parameters. The most effective ground control strategies in this stage are maintenance, rehabilitation, monitoring and contingency plan. Additionally, a new procedure for design of ground support systems for deep and hard rock was proposed. The main principles are: static and/or dynamic loading types, determination of loading sources, characterisation of geological conditions and the effects of orientation of major structures with openings, estimation of ground loading factor, identification of potential primary and secondary failures, utilisation of appropriate design analysis methods, estimation of depth failure, calculation of the static and/or dynamic demand ground support capacity, and selection of surface and reinforcement elements. Gravitational force is the dominant loading force in low-level stresses. In high stress level, failure mechanism becomes more complex in rock mass structures. In this condition, a variety of factors such as release of stored energy due to seismic events, stress concentration, and major structures influence on ground behaviour and judgement are very complicated. The key rock engineering schemes to minimise the risk of failures in high-stress levels at great depth involve depressurisation and quality control of materials. Microseismic and blast monitoring throughout the mining operations are required to control sudden failures. Proper excavation sequences in underground stopes based on top-down, bottom-up, centre-out and abutment-centre were discussed. Also, the performance of a ground support system was examined by field observation monitoring systems for controlling and modifying ground support elements. The important outcome of the research is that the proposed procedure of selecting ground support systems for static and dynamic situations was applied in several deep underground mines in Western Australia. Ground behaviour modes and failure mechanism were identified and assessed. Ground demand for static and dynamic conditions was estimated and an appropriate ground support system was selected and evaluated in site-specific conditions according to proposed method for ground support design at great depth. The stability of rock masses was confirmed, and the reliability of the design methodology for great depth and hard rock conditions was also justified.

Keywords: ground management; support system design; sequential excavation; stress management; geotechnical monitoring; deep underground mines

1. Introduction

Underground mine development in a cost-effective manner at great depth poses some challenges for ground control and maintenance of stability of excavations. Distribution of field stresses and forces (static and dynamic) causes critically stressed rock, deformations and failures in the vicinity of the openings. The strength of rocks increases at great depth due to high confinement and it is removed with underground excavation, resulting in a considerable reduction in rock strength. Rapid change in rock strength, high field stress conditions, sources of static and dynamic loads and defects in geological structures can cause complex ground behaviours from the microscale, such as microcracks in rocks, to the large scale like a sudden failure (Sharifzadeh et al., 2017a). Deep mining is associated with geotechnical challenges related to sudden failure and large deformation in rock mass structures. The dominant factor of failure mechanism in deep mining is high induced stress/seismic events. Generally, depths more than 600 m are referred to as deep mining.

Stress concentration, seismicity, water pressure and temperature are the main hazards of fracturing in deep underground mines. These parameters can have influences on the behaviour of hard rock and cause violent failures such as rockburst, brittle failure, fault burst and spalling. Hazardous condition in the ground may lead to a delay in production, high-cost in rehabilitation, damage support and mining equipment, loss of ore reserves, and injury and fatalities of personnel.

The geotechnical challenges in underground excavations can be evaluated by collecting rock engineering data, considering site-specific conditions and determining uncertainty in parameters. Application of appropriate mining methods, sequential excavation and ground support system is needed in underground engineering projects (Morissette et al., 2014).

Designs of ground support systems using traditional methods are mostly based on restraining the gravity of rock blocks surrounding excavation face, but in modern design, support elements should endure static and/or dynamic loading and large deformations in rock mass structures during the whole life of excavations (Rahimi and Sharifzadeh, 2017). Ground support demand for stabilising rock mass structures in hard rock and high stresses requires an estimate of energy demand of the rock and energy dissipation of support elements, especially in dynamic loading conditions (Feng and Hudson, 2011). Ground control and management deal with all geotechnical activities related to hazard recognition, understanding of failure mechanisms, and design of ground

*Corresponding author. E-mail address: behrooz.rahimi@postgrad.curtin.edu.au

support systems to provide a safe environment economically in rock underground engineering projects.

Serviceability is utilised for underground openings where are used for service purposes such as mine access, ore drives and ventilation, and usually have medium-long term life. The most effective ground control strategy in this stage is maintenance, rehabilitation and monitoring.

The purpose of this article is to propose a practical geotechnical strategy for ground management in deep and hard rock conditions during the design, construction and serviceability stages of underground mining projects. Critical geotechnical steps for mitigation of risks and stabilisation of rock masses in deep underground excavations are as follows:

(1) Optimise layout of openings based on major geological structures and orientation of the principal stresses;
(2) Modify sequential excavation and extraction rate;
(3) Define ground control and management strategies for small/large deformation based on potential failure modes;
(4) Design natural ground as a local support system, such as pillars in underground mining methods;
(5) Design and utilise backfilling methods as a regional support system in mines; and
(6) Design and apply surface and reinforcement support devices for unstable rocks.

Additionally, a practical methodology for the design of ground support systems in deep, hard rock and high-stress conditions was proposed with regard to geological structural conditions, loading conditions (static and/or dynamic), loading factor (the ratio of rock mass strength to major field stress), and primary/secondary failure modes. Several deep underground mines in Western Australia were used as case studies and some results were presented in this paper.

2. Governing factors in ground behaviour and its management strategy

Ground control and management deal with techniques to solve geotechnical problems of instability in underground mining operations. The techniques include plan, design and method of operations to avoid workplace injuries and equipment damage due to the risk of rock failure. The geotechnical aims of a ground control and management plan in underground mining stopes are listed below:

(1) To define a hazard control program by evaluating, designing and monitoring rock mass structures;
(2) To extract mineral resources in a safe and economical manner; and
(3) To develop a process for hazard identification and failure mechanism diagnosis supported by a training program for personnel.

Diagnosis of failure modes and their mechanism is fundamental in ground control planning. Collected data from site investigations, engineering geological survey and laboratory/field tests are used for characterisation of rock mass structures and then the failure mechanism is diagnosed based on in situ rock stresses, hydrological and project conditions.

Fig. 1 presents a ground management strategy in deep underground mining projects. The main steps of the scheme are design, construction and serviceability. The design step of ground management is associated with input geological and geotechnical data from site investigations, engineering geological mapping and results of laboratory/field tests. Design analysis of an underground excavation is carried out based on ground behaviour, failure mechanisms and project conditions, and results in location and project orientation, excavation method, sequential excavation, extraction rate, and selecting ground support systems. The practical approach of ground control and management during the construction stage is determination of standard procedures for geotechnical activities, provision of required equipment with competent personnel, quality control of materials, identification of geotechnical hazards, safety analysis before ground failure occurs, and inspection/monitoring of ground support performance. The appropriate approach for the projects during serviceability is conducted by maintenance and rehabilitation of ground support failure, load deformation measurements and preparation of a contingency plan.

Deep underground mining projects are designed and developed in the following stages:

(1) Strategic design: This is a type of primary design and preparing broad plan for the mines site such as the location of access and underground stopes;
(2) Tactical design: Tactical object is to provide the detail design of projects for example stability analysis of rock mass in underground excavations and selecting ground support system before operational stage at the mines; and
(3) Operational design: This is related to monitoring and updated design parameters through observational methods and monitoring system.

A wide range of parameters in rock mass compositions, ground behaviours modes, failure mechanisms and in situ stresses make it complex and uncertain in estimation of rock engineering properties, especially in seismically-active mines at great depth. In design phase, visualisation, interpretation, assessment of the real orientation and geometry of rock mass structures are difficult from direct observations to prepare geological and geotechnical model. Therefore, uncertainty and confidence in characterising rock mass structures, diagnosis of ground behaviour, failure mechanism, and ground support design are assumed. The possible engineering disasters from design phase encountered in construction stage could be a complex failure mechanism such as sudden failure and large deformation, inadequate and inappropriate ground support systems. Hence, ground control and management strategies should be accomplished in accordance with knowledge, experience and management to address the problems in mining operations. In serviceability stage, seismic events, stress concentration and corrosion of ground support systems may lead to damage to support devices and rock failures. A contingency plan with a monitoring system is required for evaluation of ground problems.

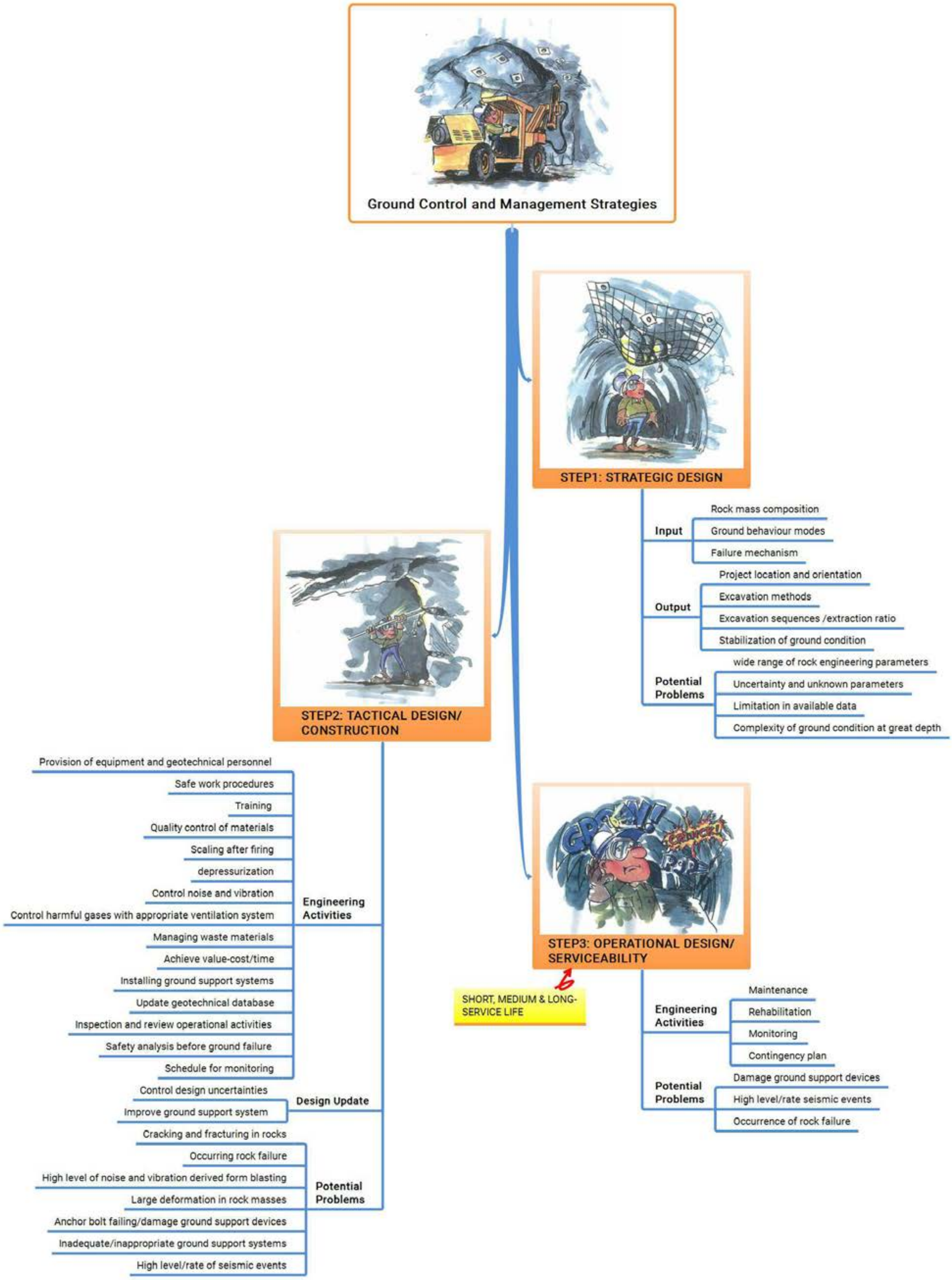

Fig. 1. Ground management strategies in deep underground excavations.

The major steps for ground control and management at great depth are listed as follows:

(1) Collect data from available evidences, observed features and seismic events;

(2) Identify potential geotechnical hazards;

(3) Analyse the hazards for ground management, and determine appropriate strategies such as smooth blasting method and install ground support system;

(4) Evaluate the effectiveness of multi-factor on ground conditions, especially time;
(5) Implement ground management strategies in hazard area;
(6) Conduct geotechnical monitoring and review the ground responses; and
(7) Update the strategies.

Geotechnical issues and ground control management should be considered during the whole lifetime of underground opening projects from the feasibility study stage to the final closure of a mine.

During the design phase of ground control and management, three approaches, i.e. project location and orientation, sequential excavation/excavation method/extraction rate, and ground support selection method, can significantly affect the type of ground behaviours and failure mechanisms in underground excavations. For example, suitable drill-and-blast design parameters can reduce damaged zones in rocks and result in satisfactory size fragmentation, cost-reduction in production and ground support equipment (Szwedzicki, 2003). These approaches will be briefly discussed in the following sections.

2.1. Project location and orientation

The layout of project location and orientation is situated based on the principal stress orientations, major structural defects in rock masses, excavation geometry, location of mineral resources, availability and accessibility of equipment, objective and purpose of projects, and location of mineral resources in mining projects. The angle between the orientation of an opening and major structures of rock masses influences the type of failure and mechanisms in underground mining activities (see Fig. 2). Theoretical results and practical implementations indicate that the perpendicular and parallel orientations of an opening with major structures are the most favourable and unfavourable in underground mining projects, respectively. Simple failure mechanisms, like tensile fracturing and shear failure, may combine and produce complex ground behaviours at different orientations of excavations, and the unfavourable orientation of discontinuities surrounds openings to reduce the bearing capacity of rock blocks and may lead to ground fall or sliding failure (Sharifzadeh et al., 2017a).

The axis of underground excavations also has influence on discontinuities inside rock masses and may affect fluid channels and flow rates in openings. Fluid flow can cause different types of ground behaviours and failure modes, for example, flowing and swelling phenomena.

The appropriate layout of location and orientation of excavations with regard to the orientation of dominant structures and principal stresses can reduce structural failure modes and consequently, the required ground support system for stabilising. As a result, an underground mining project is forecast to run at a low cost and have a high performance in such a situation.

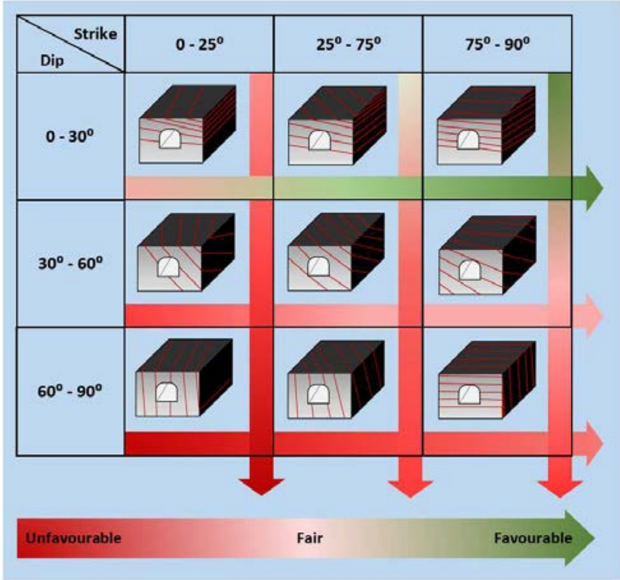

Fig. 2. The influence of discontinuity orientations and dips with the axis of excavations.

2.2. Excavation method, sequences and extraction ratio

Excavation method has a significant influence on the engineering behaviour of rock masses. For example, drill-and-blast methods can provide safe environments compared to mechanical excavation methods at great depth and in hard rock conditions, because of a destressing effect and dissipation of stress concentrations in a fractured rock mass following blasting (Mazaira and Konicek, 2015). Strain energy accumulation in rock masses can be released by blasting method in excavation boundaries, which assist to diminish occurrence of sudden failure in hard rock.

Underground works require some access for stopes, extraction of mineral resources, transport of ore and waste materials, water/power supply, ventilation of main and temporary accesses, drainage, transport of personnel and equipment. Typical underground mining access is shown in Fig. 3. Excavations in underground mining projects are divided into the following two parts (Brady and Brown, 2006):

- Underground excavations for service purposes include mine access, ore drives, ventilation, crusher chambers and spaces for underground workshops. These types of openings have mostly a medium- to long-term life; and
- Underground excavations for production purposes such as underground stopes, stop access, and service ways. They have mostly a short-term life and are temporary.

Mining projects at great depth are developed using various excavations such as vertical shafts, inclined ramps, horizontal drifts, fuel stores, explosive magazines, mining stopes, fuel stores and pump houses. The type and geometry of mining excavations have influences on the method and sequences of openings. The excavations for production purposes are usually in highly stress concentration areas, and they are typically a type of large span with short-term lifetime. Excavations for service purposes are usually small-medium span with medium- to long-term life. For example, the dimensions of drifts and ramps are selected based on equipment, ventilation, walkways and other facilities. The dimension can change from 2.2 m to 6 m, or 5 m^2 to 25 m^2 (Atlas Copco, 2007). These excavations are generally far from mining-induced zones. The challenges of excavation phase in openings for service purposes are generally less than production purposes.

Excavation sequence in a mining operation is described by the extraction of the orebody in an underground mining operation in order to achieve a high extraction rate of the orebody with minimal ground problems. Post-excavation stress can be reduced by applying an appropriate excavation method, sequence and extraction rate in underground openings (Sharifzadeh et al., 2013). A series of individual stopes is excavated in a safe and economical manner. Sequences in underground operations can be divided into primary, secondary and third priorities. The first priority of sequential panels or stopes is usually designed and extracted in high-grade regions of the orebody in consideration of target products in mine planning, field stresses, stability of rock masses, dimension of stopes, and backfilling methods. The primary panels or stopes are excavated and then filled with backfill materials for two vertical lifts before extracting secondary and third priorities of stopes. Fig. 4 shows a schematic of sequential excavations in underground stopping. The numbers on Fig. 4b and c show the sequences of excavations. According to the figure, sequential excavations are used in sublevel stopping mining method as vertical mining in steeply inclined deposits. The method is more common in deep underground mines in Western Australia.

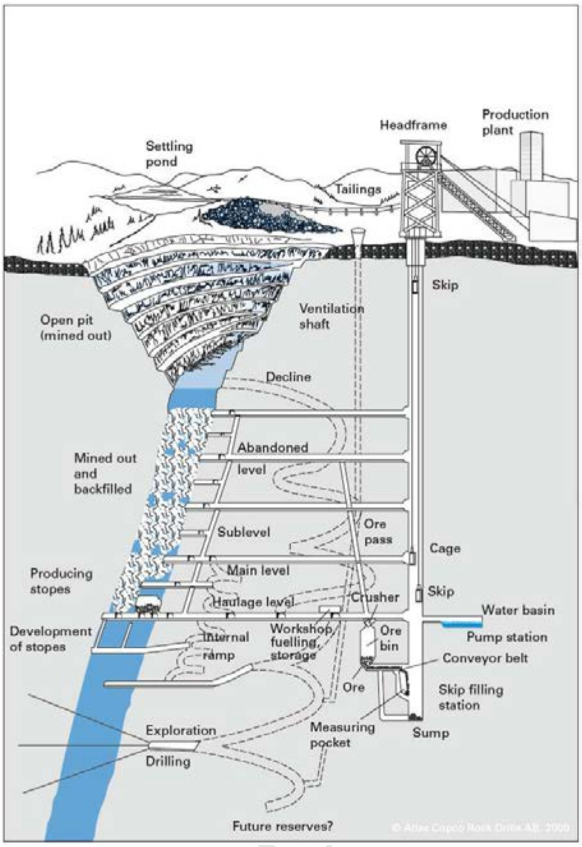

Fig. 3. Typical underground mine infrastructures and accesses (Atlas Copco, 2007).

Generally, the excavation sequence dimension varies between 5–30 m width, 15–50 m length and 15–100 m height in Australia. Sequential excavation in mining operations can be developed as top-down, bottom-up, centre-out and abutment-centre (Ghasemi, 2012). The dimension of stopes in sequential excavation affects mining operation costs, stability of rock masses and failure mechanisms.

2.3. Ground supports in underground mines

Ground supports provide a strong zone in unstable rocks and reduce a certain amount of rock deformation to avoid immature failure. Stabilisation of the ground in underground works can be accomplished by natural or artificial ground support methods. Natural ground support approaches like room-and-pillar methods are useful in medium-hard rock conditions, low-medium stress levels and short-medium term life in excavations. Artificial ground support devices are mainly divided into surface rock support and rock reinforcement elements. Surface support tools are applied on the surface and external parts of rock mass structures. Rock reinforcements are installed in the internal part of rock masses. The usual surface and reinforcement devices used in underground mining projects are rock bolts, cable bolts, shotcrete, concrete lining, strapping, mesh, timber sets, steel sets, hydraulic props, yielding sets and mesh (MOSHAB, 1999). Backfilling material method is a practical technique for sublevel stopping as a local support system in large-scale openings in mining projects. Stress level, density, particle size, porosity, strain level and proportion of cementation are assessed to design backfill materials.

Instability of rock masses is derived from geotechnical structural defects in rocks and static/dynamic loading conditions due to stress concentration, seismic events and released energy, drilling and blasting, gravitation, groundwater and temperature. The stabilisation process for rock mass structures in underground openings is as follows:

- Determine project conditions and purposes;
- Identify major geotechnical defects and failure mechanisms in rocks;
- Identify main types of loading (static/dynamic) surrounding excavations and estimate their intensities;
- Analyse ground condition and estimate rock mass deformations;
- Select the type of ground support approaches: natural ground support and/or artificial ground support systems;
- Select the types of surface and reinforcement support devices; and
- Control the ground–support performance.

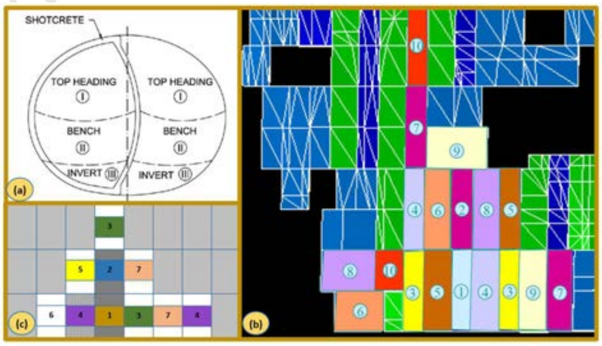

Fig. 4. Sequential excavation in (a) a tunnel, (b) an underground mine with bottom-up and centre-out method, and (c) an underground mine with bottom-up sequences method (The number shows the sequences of excavations).

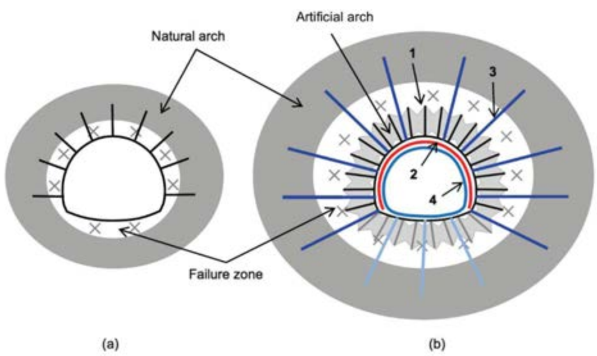

Fig. 5. Different types of ground support devices in a failure zone: (a) rock bolting in small damaged zone; and (b) large damaged zone with (1) rock bolting, (2) retaining by inner surface support devices, (3) cable bolting, and (4) outer surface support devices (Li, 2017).

The application of ground support and reinforcement systems has to provide stable conditions in rock mass structures through reinforcing, holding and retaining functions (Kaiser et al., 1996). Fig. 5 shows the use of support devices in different parts when encountering failure zones in an underground excavation. Installing rock bolts in a small damaged zone may provide stability in excavation. Large-scale damaged zones require the use of different layers of support systems as described below (dependent on the loading condition and failure modes) (Li, 2017):

- Part 1: installing rock bolts to reinforce and strengthen fractured rock by forcing rock blocks together;
- Part 2: using inner support systems (shotcrete, mesh, etc.) for retaining function;
- Part 3: cable bolting to provide an effective holding function in loosened blocks; and
- Part 4: implementation of outer surface support devices like steel sets and casting concrete, which is more applicable for long-term life excavations.

Ground support systems at great depth and high-stress conditions are evaluated and designed by practical, numerical and observational methods.

3. Ground support analyses and design strategies

The techniques for ground improvement by support elements are sewing rock blocks together, unifying the zone of failure, avoiding fracturing progression, controlling deformation and strengthening rock mass structures. A number of factors including availability, capacity, simplicity, cost-effectiveness, installation method, and energy absorption should be considered in the design.

Different loading conditions surrounding an excavation require different types of ground support systems (Rahimi et al., 2014). In general, the effective loads on an excavation surface are static, dynamic and a combination of them. The origins of static loading are gravity, in situ/induced stress, tectonic activities, groundwater, residual stresses, and temperature. Seismic events, strain burst, fault slip, pillar slip, gravity collapse, loading/unloading rate, and blasting are the main sources of dynamic loading in underground openings.

At great depth and high stress conditions, seismic hazard changes with mining and excavation sequence. Assessment of seismic events and risks can be carried out by collecting data from spatial seismic event clusters, magnitude–frequency of events, history of apparent stress–time, focal mechanism, estimating peak particle velocity, and decay rates of post firing event methods (Knobben, 2017). These methods need plenty of knowledge, experience and training in the seismic field. Table 1 presents a seismic hazard scale (SHS) for mines of Western Australia. This parameter considers quantification of seismic events recorded in geological structures, underground stopes and mining operations like blasting, based on the rate of magnitude events and *b*-value parameter from the Gutenburg–Richter relation (Hudyma, 2004). SHS is applicable for reflected seismic events, up to about Richter magnitude +3, from failures of rock structures at the mine site.

Support capacity depends on loading mode, loading rate, share of loads between different support elements, displacement of support system, and energy absorbing capacity (Kaiser and Cai, 2012). The capacity of ground support system is evaluated with regard to availability and combination of support elements to act as an integrated system, including the type and amount of loads, displacements and energy demand, especially in dynamic loading conditions (Cai and Kaiser, 2018). Fig. 6 shows the design procedure of ground support system in deep underground mining projects. The main factors in the design are an estimation of depth failure and fracturing, demand ground support in static and dynamic conditions, and evaluation of rock support system capacity based on the load, displacement and energy absorption factors.

Ground support design based on static loading conditions is used in underground mining projects where the risk of seismic events is low. The typical ground support devices for static loading conditions are fibre-reinforced shotcrete, rock bolts and cable bolts (Jacobsson et al., 2013). Ground support design in a ground with dynamic loading conditions should include an absorbing kinetic energy factor derived from seismic events (Kaiser et al., 1996). The results of drop-weight tests indicate that about 25% and 75% of absorption of energy demand, respectively, belong to surface support and rock bolt devices in hard rock conditions. In soft rock conditions, this proportion is divided into 30% for rock bolts and 70% for surface support systems (Louchnikov and Sandy, 2017). Transferring the load from the surface to reinforcement ground devices is not critical in static conditions, whilst this point is a fundamental requirement in dynamic conditions to ensure the performance of ground support systems.

3.1. Ground demand in static conditions

Ground support demand in static conditions is determined based on dead-weight and stress concentration in rock masses surrounding excavations and is estimated by Eq. (1) (Cai and Kaiser, 2018). Support elements increase the frictional forces of rock blocks, resistance to deformation of the fractured rock mass, and the support of the dead-weight surrounding an excavation.

$$\text{Ground demand (static condition)} = \rho g d_{\mathrm{f}} \tag{1}$$

where ρ is the density of rock (t/m^3), g is the gravitational acceleration (m/s^2), and d_{f} is the displacement of rock/depth of failure (m).

Table 1. Seismic hazard scale (SHS) in the mines of Western Australia (Hudyma, 2004).

		Mine seismicity frequency per day				
Qualitative description		Felt locally	Felt in a few parts of a mine, like a secondary blast	Often felt on surface, or like a development blast	Felt like a production mass blast	Detected by regional earthquake network
Approx. Richter magnitude		$M_L \geq -2$	$M_L \geq -1$	$M_L \geq 0$	$M_L \geq +1$	$M_L \geq +2$
Seismic hazard scale and qualitative description						
-2	Nil	>0.001 (once every few years)	0 (has never occurred)	0 (has never occurred)	0 (has never occurred)	0 (has never occurred)
-1	Very low	>0.01 (a few times per year)	>0.001 (once every few years)	0 (has never occurred)	0 (has never occurred)	0 (has never occurred)
0	Low	>0.1 (at least weekly)	>0.01 (a few times per year)	>0.001 (once every few years)	0 (has never occurred)	0 (has never occurred)
0.5	Low to moderate	>0.3 (a few times per week)	>0.03 (monthly)	>0.003 (yearly)	<0.001 (may have happened once)	0 (has never occurred)
1	Moderate	>1 (at least daily)	>0.1 (at least weekly)	>0.01 (a few times a year)	>0.001 (once every few years)	0 (has never occurred)
1.5	Moderate to high	>3 (a few a day)	>0.3 (a few times a week)	>0.03 (monthly)	>0.003 (yearly)	<0.001 (may have happened once)
2	High	> 10 (more than 30 a day)	>1 (at least daily)	>0.1 (at least weekly)	>0.01 (a few times a year)	>0.001 (once every few years)
2.5	High to very high	>30 (more than 30 a day)	>3 (a few a day)	>0.3 (a few times a week)	>0.03 (monthly)	>0.003 (yearly)
3	Very high	>100 (more than 100 a day)	>10 (more than 10 a day)	>1 (at least daily)	>0.1 (at least weekly)	>0.01 (a few times a year)
3.5	Very high to extreme	>300 (more than 300 a day)	>30 (more than 30 a day)	>3 (a few a day)	>0.3 (a few times a week)	>0.03 (monthly)
4	Extreme	>1000 (more than 1000 a day)	>100 (more than 100 a day)	>10 (more than 10 a day)	>1 (at least daily)	>0.1 (at least weekly)

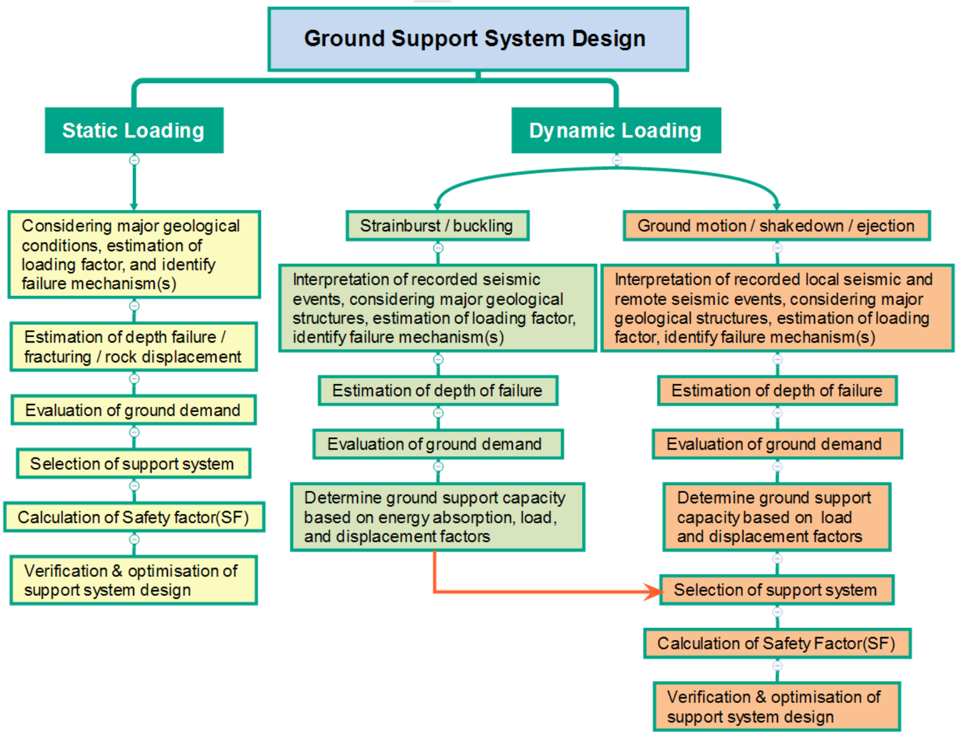

Fig. 6. Ground support design in deep underground mines.

3.2. Ground demand in dynamic conditions

Dynamic support demand stabilises a rock mass under dynamic loading conditions and dynamic failure mechanisms, and is estimated by (Kaiser et al., 1996):

$$\text{Ground demand (dynamic condition)} = \frac{1}{2}mv^2 + qmgd \tag{2}$$

where m is the mass of ejected rock materials (t), v is the velocity (m/s), q is the constant factor for the effect of gravity on the ejected rock materials (m/s) (-1: floor, 0: wall, and 1: back), and d is the distance of ejected rock blocks (m).

The velocity v (peak particle velocity, PPV) can be estimated from numerical modelling or seismicity event data using Eq. (3) (Potvin et al., 2010):

$$v\ (\text{PPV}) = \frac{C10^{\frac{1}{2}(m_{\mathrm{L}}+1.5)}}{R+R_0} \tag{3}$$

where C is the parameter with value about 0.2–0.3 for design purposes, R is the distance to the source, $R_0 = \alpha\ 10^{\frac{1}{3}(m_{\mathrm{L}}+1.5)}$, m_{L} is the magnitude event, and α is the parameter with value of 0.53–1.14.

Fig. 7 shows an estimation of failure depth in the dynamic rupture mechanism based on empirical data from previous projects. In Fig. 7, CI is the crack initiation threshold stress in rocks and is determined from laboratory tests. CI is about 0.4–0.5 UCS for crystalline rocks (Diederichs, 2017), and UCS is the uniaxial compressive stress.

The depth of failure where there is spalling behaviour and for a circular tunnel is estimated by (Diederichs, 2017):

$$\text{Depth of failure } (D_{\mathrm{f}}) = \left[1 + 0.4K^{-0.27}\left(\frac{3\sigma_1-\sigma_3}{\mathrm{CI}} - 1\right)^{0.65K^{0.14}}\right] R_{\mathrm{s}} \tag{4}$$

where K is the stress ratio; CI is the crack initiation stress (for the case where there is no data available, and $CI = 0.5UCS$); and R_{s} is the radius or half-span of an underground excavation.

The capacity of energy absorption of various surfaces and reinforcement support devices is shown in Table 2 and Fig. 8, respectively. The implication is that yielding support devices such as Durbar, Cone bolt, Garford bolt and D-bolt are effective in dynamic and tensile loading, rockburst, and squeezing behaviour. Installing further rock bolts at an acute angle (less than 30°) to the orientation of discontinuities is a solution to reducing shear failure (Stacey, 2016).

The factor of safety is a key for stability analysis and design of a ground support surrounding a rock mass in underground structures. This parameter estimates the load capacity of support devices under static and dynamic loading conditions. The factor of safety (F_{s}) is estimated by

$$F_{\mathrm{s}} = \left\{ \begin{array}{c} \dfrac{\text{Loading capacity of ground support system}}{\text{Total effective static loads on the ground surrounding excavation}} \\ \text{or} \\ \dfrac{\text{Critical discplacement } (u_{\mathrm{r}})}{\text{Rock displacement at equilibrium} (u_{\mathrm{eq}})} \\ \text{or} \\ \min\left(\dfrac{nE_{\mathrm{ab}}}{E_{\mathrm{ej}}}, \dfrac{u_{\max}}{u_{\mathrm{eq}}}, \dfrac{u_{\mathrm{ult}}}{u_{\mathrm{eq}}}\right) \end{array} \right\} > 1 \tag{5}$$

where $E_{\mathrm{ab}} = \frac{1}{2}mv^2$; n is the number of rock bolts; E_{ej} is the kinetic energy from ejected rocks; u_{eq} is the rock displacement at equilibrium; $u_{\max}$ is the maximum allowable displacement; and u_{ult} is the ultimate displacement.

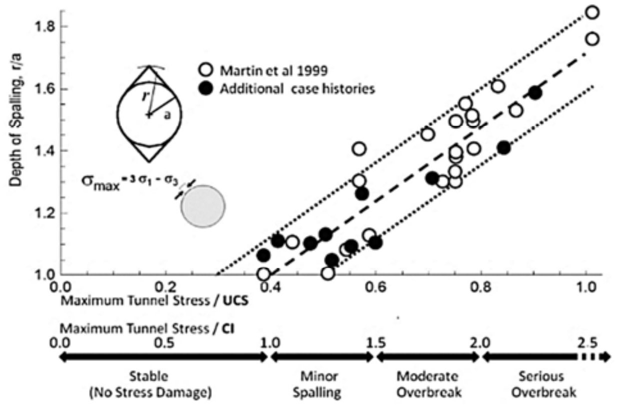

Fig. 7. The estimation of depth failure in a dynamic loading condition (Diederichs and Martin, 2010).

Table 2. The capacity for energy absorption of different surface support elements (Louchnikov and Sandy, 2017).

Surface support	Energy absorption (kJ/m²)	Maximum displacement at failure (mm)
FRS 60 mm, synthetic fibre	0.8	60
FRS 80 mm, synthetic fibre	2.2	80
FRS 110 mm, steel fibre and weld mesh embedded	7.0	120
Weld mesh 100 × 100 mm (5.6 mm wire)	1.3	210
FRS 60 mm + weld mesh over	2.1	210
FRS 80 mm + weld mesh over	3.5	210
M85/2.7 mesh (Minax high-tensile chain-link)	2.4	200
G80/4 mesh (Tecco high-tensile chain-link)	6.5	300
FRS 60 mm + M85/2.7	3.2	200
FRS 60 mm + G80/4	7.3	300
FRS 80 mm + M85/2.7	4.6	200
FRS 80 mm + G80/4	8.7	300
Woven mesh (6 mm wire) with welded double-wire on perimeter	2.0	300
HEA mesh	11.8	800
Woven mesh (10 mm wire)	22.5	600

Note: FRS = fibre reinforced shotcrete; HEA = high energy absorption.

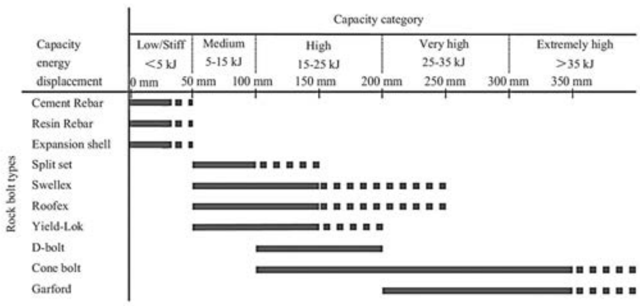

Fig. 8. Energy absorption capacity of various reinforcement devices (Masoudi and Sharifzadeh, 2018).

The required long-term factor of safety is between 1.5 and 3. At high-stress levels and soft-medium rock strength conditions, squeezing behaviour may occur with high-stress deformation. Critical displacement (u_{r}) is a suitable parameter to calculate the factor of safety where there is a squeezing behaviour. In addition, under dynamic loading conditions, the capacity of ground support devices for absorbing energy should be higher than the ejected kinetic energy of rock masses. The ratio of energy absorption capacity by ground support devices to the kinetic energy of ejected rocks in a dynamic loading condition is used as the factor of safety in burst-prone rocks (Li, 2017).

A factor of safety of more than one may provide stability under dynamic loading conditions. However, ground control and management should be accompanied with field measurements to update ground support systems with any significant changes in the ground condition like the rate of seismic events.

Table 3 presents the design principles and a procedure for ground support and reinforcement in deep and hard rock conditions. The most effective steps in the design of ground support systems are as follows:

(1) Identification of the loading types:
- Static loading, and
- Dynamic loading.

(2) Determination of the main source of loading:
- Origin of static loading: Gravity, in situ/induced stress, tectonic activities, groundwater, residual stresses and temperature; and
- Origin of dynamic loading: Seismic events, strain burst, fault slip, pillar burst, gravity collapse, loading/unloading rate, blasting and earthquake.

(3) Geological structural condition:
- Description of the majority of the geological structure: Massive rock, moderately jointed/blocky/folded rock, highly jointed/disintegrated rock;
- Favourability and unfavourability of major structures in openings;
- Estimation of the block size surrounding openings; and
- Determination of continuity factor (CF) in the ground.

(4) Estimation of the loading factor ($LF = \frac{\text{Rock mass strength } (\sigma_{\text{cm}})}{\text{Major principal stress } (\sigma_1)}$):
- $LF > 2$ (Low level),
- $1 < LF < 2$ (Medium level), and
- $LF < 1$ (High level).

(5) Identification of potential failure based on loading type, loading source, major geological structural condition and loading factor:
- Primary failures, and
- Secondary failures.

(6) Use of appropriate analysis and design methods based on failure modes in static and/or dynamic conditions.

(7) Selection of ground support systems (natural ground and/or artificial devices) in accordance with the required life term of excavations.

The lifespan of underground openings can be divided into three groups based on their service purposes and uses:

(1) Short-service life (less than 6 months), for example, mine stopes and temporary access;

(2) Medium-service life (more than 6 months and less than 3 years), such as ore drive access and exploration tunnel; and

(3) Long-service life (more than 3 years) like decline, road tunnel and underground cavern.

The ground support and reinforcement system should be selected with regard to durability and service life of underground excavations. Temporary support systems or natural ground are suitable for short-term service lifetime, and permanent support systems are used in medium- or long-term.

In deep and hard rock conditions where there is frequently changing behaviour, rapid variations of stress and deformation, energy accumulation in rock masses, and application of fibrecrete, yielding rock bolts, cable bolts and mesh are necessary to stabilise openings. Seismic and deformation monitoring could be a useful strategy to control ground behaviour during mining operations.

It should be mentioned that the proposed method in Table 3 is more applicable for strategic and tactical design of underground mine projects. Verification and optimisation of design parameters should be accomplished in operational design stage.

4. Underground mining and construction strategies

Underground mining excavations entail excavation methods, sequential excavation/extraction ratio, depressurisation, quality control of material, and installation of ground support systems. The main principles involved in the excavation or extraction phase are construction time, project conditions such as the geometry of stopes, and geological factors like faults and shear zones. Stress management and quality control of support elements considerably influence mining operations at great depth, which will be discussed in the following sections.

4.1. Stress management

Depressurisation or destressing is a typical method to control rock failures in deep and high-stress conditions. Ground stress and seismic events are inevitable in underground mining operations and may cause various failures at great depth, such as rockburst (Rahimi and Sharifzadeh, 2017). Fig. 9 shows different methods for reduction of rock failure due to excessive stresses. Destress blasting is used for fracturing rock zones to dissipate stored strain energy from rock masses in mining operations and underground constructions. The method is used to reduce the level of stress concentration, by creating fractures in the rock mass that cause a reduction in the elastic modulus of the rock mass, and enable the rock to carry high-stress conditions. Fig. 10 shows a relocation of stress concentration level by destress blasting method surrounding an excavation. The effect of the destress blasting method can be evaluated by measuring some rock engineering parameters such as deformation of rock mass, stress magnitude changes, seismic effects, and changes in the elastic modulus (Mazaira and Konicek, 2015). The technique is applied to manage rock hazards derived from high-stress conditions such as strain burst and rock ejection.

Table 3. Design principles and procedure of ground support and reinforcement systems in deep and hard rock conditions.

Loading types	**Origin of loading**	**Geological structural condition**	**Load factor**	**Potential failures**		**Appropriate analysis and design methods**	**Suggested ground support system**
				Preliminary	**Secondary**		
Static	• Gravitation • In situ/induced stress • Tectonic activities • Groundwater • Residual • Temperature	Massive rock *GSI* > 70 *Q′* > 40 B_s (block size) > 10 m^3 *CF* < 3	$\sigma_{cm}/\sigma_1 > 2$	Stable	Local block fall, sliding fall	Rigid limit equilibrium method, key block theory	Stable, sealing surface with spot bolting and mesh, if needed
			$1 < \sigma_{cm}/\sigma_1 < 2$	Stress induced failure, progressive failure	Block fall, minor slabbing, spalling, bulking failure, popping/shucking small rock fragments, strain burst	Analytical methods, tensile cracking analysis, combination of limit equilibrium and energy release method, continuity deformation analysis, failure approach index analysis, energy release rate analysis, observational method	Unify zones of failure with mesh and bolting in appropriate spacing and length (at least 1/3 the span of excavation), deformation control with pre-tensioned rockbolts and retained with shotcrete, use D-bolts/Cone bolt/Garford dynamic bolt, face and pillars in ore drives retained with mesh
			$\sigma_{cm}/\sigma_1 < 1$	Stress induced failure, fracturing and brittle failure, severity sudden failure	Damage microseismic, block fall, brittle failure, tensile failure, popping/shucking rock fragments, strain burst, pillar burst	Energy release rate analysis, deformation analysis, rock burst tendency index, local energy release rate analysis, continuity deformation analysis, observational methods, expert system, integrated systems approaches	Reduce stress concentration, using back fill as a regional support in mining sequences, Adjustment of pillar size in underground mining methods, scale first and then install support elements, retain ejected rock with fibrecrete and mesh, using yielding devices to absorb released energy, yielding steel sets, flexible devices to absorb shocks from seismic events, split sets are good which are be able to slip under dynamic loading, use D-bolt/Garford dynamic bolt/Kinloc bolt/Cone bolt/cable bolts, using steel sets, seismic monitoring
		Moderated jointed/blocky/folded rock Favourability and unfavourability of major structures (Fig. 2) 45 < *GSI* < 70 4 < *Q′* < 40 100 dm^3 < B_s < 10 m^3 3 < *CF* < 35	$\sigma_{cm}/\sigma_1 > 2$	Structure induced failure, block fall	Toppling, block fall, sliding failure, wedge failure	Continuity–discontinuity deformation analysis, key block theory, rigid limit equilibrium method, analytical methods, bending analysis, fracture mechanics analysis, finite element methods, failure approach index analysis	Flexible support, sewing layers to each other, pre-tensile rock bolts, application of split sets for small scale of failure, holding rock mass with mechanical rock bolts, seal surface with shotcrete to prevent failure, support devices should be installed before ground movement, fibrecrete and rockbolts/cable bolts, the length of rockbolts should be at least 1/3 of the span, using cement rebar/resin rebar/split set/swellex/friction bolt with 2 m or less spacing with mesh and straps for unify zone of failure, face bolted and meshed
			$1 < \sigma_{cm}/\sigma_1 < 2$	Stress/structure induced failure, block fall, shear failure, tensile failure	Block fall, progressive shear failure, shallow stress induced brittle and shear failure, flaking rock mass/splitting failure, tensile failure, buckling failure, toppling failure, bending failure	Analytical methods, observational methods, shear stress analysis, expert system, failure approach index analysis, discontinuity deformation analysis, finite element analysis, distinct element methods, soft computation, neural networks, integrated approach systems, fracture mechanics analysis	Prestressed reinforced devices, unify zone of failure, scale rock mass surrounding excavation before installing support tools to unify rock zone, use straps and wire mesh across bedding planes and joints to prevent skin failure between rockbolts, reinforce rock mass with rockbolts to limit displacement and buckling, grouted rock anchors, pre-tensioned rockbolts, sometimes need to use steel support to control shear failure/plastic behaviour/large deformation, shotcrete with mesh and straps for permanent support system, stabilizing pillars with mesh and rock bolts, leaving extra pillars, friction bolt/cemented/grouted bolt/resin bolts/split sets/cable bolts with spacing less than 1.5 m, survive large rock deformations, using back fill as regional support in mining sequences
			$\sigma_{cm}/\sigma_1 < 1$	Stress/structure induced failure, shear failure, large deformation, block fall	Crushing and splitting of rock blocks, tensile failure, strain burst, pillar burst, buckling failure	Discontinuity deformation analysis, analytical methods, bending analysis, finite element analysis, fracture mechanics analysis, failure approach index analysis, expert system, observational methods, observation methods	Stiff support, unify zone of failure, scaling well and then install support devices, stiff support, full column ground rock anchors, thick steel fibre reinforced shotcrete, yielding steel ribs, cable bolts, provide maximum holding capacity, split sets, using back fill as regional support in mining sequences, expansion rebar/split set/Roofex/Yield-Lok/D-bolt with spacing less than 1 m with mesh and straps, flexible steel sets, survive ground movement and large deformation
		Highly jointed/disintegrated rock *GSI* < 45 *Q′* < 4 B_s < 100 dm^3	$\sigma_{cm}/\sigma_1 > 2$	Structure induced failure, ground fall, wedge failure,	Cave in, block fall, wedge failure, chimney failure, notch failure, cave in	Discontinuity deformation analysis, shear stress analysis, failure approach index analysis, finite element analysis, distinct element analysis, bending analysis, neural networks	Unify zone of failure, grouted ground for unify zone of failure, pattern support with grouted rock bolts such as split sets, retaining rock mass with shotcrete and mesh, steel support with struts, swellex/roofex/d-bolt/hybrid bolts/friction bolts with spacing about 2 m, survive ground movements
			$1 < \sigma_{cm}/\sigma_1 < 2$	Structure/stress induced failure, large deformation failure, shear failure	Ground fall, plastic failure, chimney type failure, ground movement, shear failure, buckling, tensile failure, ravelling, flowing	Discontinuity deformation analysis, shear stress analysis, expert system, observation methods, failure approach index analysis, soft computing, finite element analysis, distinct element analysis, integrated approach systems	Grouted ground for unify zone of failure, steel support with pre-tensioned rock bolts, rockbolts or cable to control a separation, flexible steel sets, survive large scale displacements in rock masses, fibrecrete plus mesh and straps, friction bolt/hybrid bolts/grouted bolts with spacing less than 2 m,

		CF > 35				approaches, expert system	reinforced pillars with fibrecrete and mesh, monitoring ground deformation
			$\sigma_{\mathrm{cm}}/\sigma_1 < 1$	Stress/structure induced failure, large deformation failure, ravelling and flowing ground in brecciated and disintegrated ground	Chimney type failure, ground fall, buckling failure, splitting failure, shear failure, large strains, floor heave and sidewall closure	Discontinuity deformation analysis, shear stress analysis, expert system, observation methods, failure approach index analysis, soft computing, finite element analysis, distinct element analysis, local energy release rate, integrated approach systems approaches	Grouted rock anchor, steel support with pre-tensioned rock bolts, grouted highly ductile rock anchor and steel fiber reinforced shotcrete, for swelling condition: full-column grouted rock anchors with fibre reinforced shotcrete, For ravelling condition: steel support with struts, pre tensioned rock bolts with fiber reinforced shotcrete, steel sets are required for long-term support, using back fill as regional support in mining sequences, reinforced pillars with fibrecrete and mesh, resin bolt/expansion shell/split sets/swellex/grouted cable bolts with spacing about 1 m, monitoring rock mass deformation
Dynamic	• Seismic events • Strain burst • Fault slip • Pillar burst • Gravity collapse • Loading/unloading rate • Blasting • Earthquake	Massive rock *GSI* > 70 Q' > 40 B_s > 10 m^3 *CF* < 3	$\sigma_{\mathrm{cm}}/\sigma_1 > 2$	Seismicity damage, strain burst, tensile failure,	Block fall, sliding failure, brittle failure, blast damage, rock ejection, shear failure, pooping/shucking rock, sudden failure, pillar burst	Observational methods, engineering judgment, finite element methods, distinct element methods, fuzzy logic, energy release rate analysis, rock burst tendency index, local energy release rate, integrate system approaches, soft computations	Retaining rock mass with wire mesh, reinforced with strong yielding rockbolts and grouted rebar, steel fibre reinforced shotcrete, split sets in minor dynamic loading, high density cable bolting in high level of seismic events, flexible steel sets to absorb released energy, stabilizing pillars with dynamic bolts and mesh, leaving extra pillars, fibrecrete plus multi-layer mesh and dynamic bolts (D-bolt/Garfod bolt/Cone bolt with spacing less than 1-2 m), face and ore-drive meshed and used bolts/cable bolts, survive seismic and displacement monitoring
			$1 < \sigma_{\mathrm{cm}}/\sigma_1 < 2$	Seismicity damage, brittle failure, spalling, slabbing popping/shucking rock, sudden failure	Block fall, sliding failure, bulking failure, blast damage, splitting failure, tensile failure, strain burst, pillar burst		
			$\sigma_{\mathrm{cm}}/\sigma_1 < 1$	Seismicity damage, brittle failure, server rock burst, rock ejection	Block fall, brittle failure, shear failure, blast damage, splitting, pillar burst, strain burst		
		Moderated jointed/blocky/folded rock Favourability and unfavourability of major structures (Fig. 2) 45 < *GSI* < 70 4 < Q' < 40 100 dm^3 < B_s < 10 m^3 3 < *CF* < 35	$\sigma_{\mathrm{cm}}/\sigma_1 > 2$	Structure/seismicity induced failure, block fall, shear failure	Toppling, block fall, sliding failure, wedge failure, blast damage, shear failure, splitting failure, large deformation, pillar failure	Observational methods, engineering judgement, finite element methods, distinct element methods, fuzzy logic, failure approach index analysis , local energy release rate, integrate system approaches, soft computations, discontinuities deformation analysis, distinct elements methods	Retaining rock mass with fibrecrete plus chain link mesh, reinforced with strong yielding rockbolts and grouted rebar, split sets in minor dynamic loading, high density cable bolting in high level of seismic events, flexible steel sets to absorb released energy and control deformation, using back fill as regional support, grouted rock bolts and cable bolts, Seismic monitoring and deformation control, reinforced pillars with fibrecrete and mesh
			$1 < \sigma_{\mathrm{cm}}/\sigma_1 < 2$	Stress/structure/seismicity induced failure, block fall, shear failure, tensile failure	Block fall, progressive shear failure, brittle and shear failure, tensile failure, buckling failure, toppling failure, bending failure, pillar failure, cave in, large deformation		
			$\sigma_{\mathrm{cm}}/\sigma_1 < 1$	Stress/structure/seismicity induced failure, shear failure, large deformation, block fall	Crushing and splitting of rock blocks, tensile failure, blast damage, , strain burst, pillar burst, buckling failure, cave in, ravelling, flowing, pillar failure, large scale collapse		
		Highly jointed/disintegrated rock *GSI* < 45 Q' < 4 B_s < 100 dm^3 *CF* > 35	$\sigma_{\mathrm{cm}}/\sigma_1 > 2$	Structure/stress/seismicity induced failure, ground fall large deformation failure, shear failure ravelling, flowing	Cave in, ground fall, chimney failure, notch failure, blast damage ground movement, shear failure splitting failure, shear failure, large strains, floor heave and sidewall closure, ravelling, flowing	Observational methods, engineering judgment, finite element methods, distinct element methods, energy integrate system approaches, soft computations, discontinuity deformation analysis, shear stress analysis, finite element methods, soft computing, failure approach index analysis	Reinforced rock mass with resin bolt/expansion shell/split sets/swellex/grouted cable bolts with spacing about 1 m, steel support with pre-tensioned rock bolts, for swelling condition: full-column grouted rock anchors with fibre reinforced shotcrete, for ravelling condition: steel support with struts, pre tensioned rock bolts with fiber reinforced shotcrete, steel sets are required for long-term support, using back fill as regional support in mining sequences, reinforced pillars with fibrecrete and mesh, monitoring rock mass deformation
			$1 < \sigma_{\mathrm{cm}}/\sigma_1 < 2$				
			$\sigma_{\mathrm{cm}}/\sigma_1 < 1$				

Note: GSI: geological strength index; $Q' = \frac{RQD}{J_n} \times \frac{J_r}{J_a}$; Continuity factor $(CF) = \frac{\text{Dimension of underground excavation(m)}}{\text{Dimension of rock block(m)}}$.

4.2. Support elements quality control

Quality control and assessment of materials are determined by the necessary quality level and quality grade. The quality level is described as the difference between the required geotechnical techniques including specifications and actual implanting work. Quality grade is the difference between standards and specifications required of companies and the quality of manufactured products. Quality control is assessed through a systematic examination and quality assurance from geotechnical activities to achieve planned objectives. Quality assurance of ground control management in underground mining projects includes verifying that the construction is being done in accordance with the design, checking the availability of equipment, personnel facilities and general resources, which can be summarised by the following tasks (Szwedzicki, 2003):

(1) Discussion with managers about related activities for ground control;
(2) Inspection of geotechnical activities in underground mines;
(3) Review of procedures of operational activities, standards, documents and critical tasks;
(4) Consideration, discussion and review of geotechnical record and input data on the design;
(5) Observation and monitoring of drilling, blasting, rock mass behaviour and failure modes; and
(6) Discussion with supervisors and operators about the identified issues and development activities.

The common problems during the shotcreting process in underground mining projects are difficulty in achieving correct consistency (especially water/cement ratio, *W*/*C*), sprayability, proper storage and utilisation of admixtures, and use of the correct nozzle distance by operators (Talbot and Burke, 2013). Training of operators and supervisors is required to address these problems in projects. Also, there is a concern in using grouted rock bolts to fill pores in rock zones where there is groundwater which would lower the rock bolts' performance in the ground. Using recent technology, reflected ultrasonic wave signals can indicate any voids, and the quality of rock bolt installations can be improved (Yokota et al., 2013). Geotechnical quality control should be undertaken before installation to ensure that they are in accordance with the design parameters.

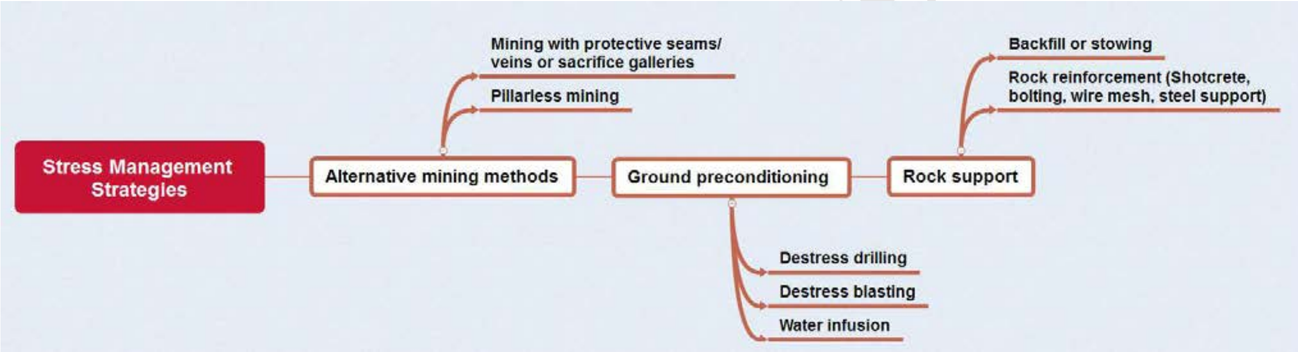

Fig. 9. Excessive stress management methods in rock damaged zone around excavation (Modified after Saharan and Mitri, 2011).

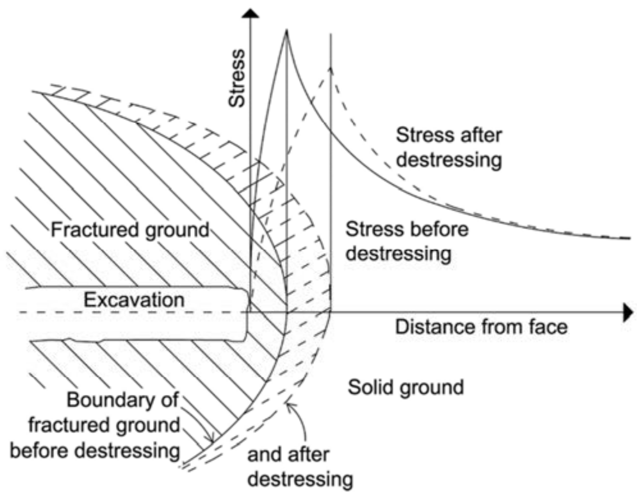

Fig. 10. The effect of destress blasting method on rock zone surrounding an excavation (Mazaira and Konicek, 2015).

5. Monitoring ground-support system performance

Rock mass structures in deep underground mines have conditions that range from stabilisation to collapse in the following four steps:

(1) Stabilisation;
(2) Failure warnings, such as major joints, weakness zones, blasting damage zones, noise in rocks, seismic events and tectonised structures in ground;
(3) Ground movements, for example, fracturing, cracking, opening rock bolts, and sliding rock blocks; and
(4) Rock failure, such as sudden failure, ground fall and spalling.

Rock mass behaviour and its change are not always recognisable as warnings of failure. A procedure to recognise pre-failure of a rock mass can be useful for rock engineers in prediction of geotechnical failure and collapse, in order to avoid a fundamental loss. Geotechnical indicators such as faults and folds show that a rock mass has a potential for failure. Observational methods and monitoring system at great depth should be accomplished by collection, interpretation and analysis of this information to evaluate ground-support performance.

The performances of the ground support system under static and dynamic loadings, field stress conditions and seismic events are assessed by monitoring systems. A good monitoring system is using all available information from seismic event sources, seismic loading, and available data in rock mass structures and induced stress in field measurements. Installing of different types of instruments at great depth and high-stress levels, where there is a great potential for damage of the devices due to seismic events, allows different measurements like excavation deformation and seismic events, in order to evaluate ground support performance (Zhang et al., 2016). The main components of geotechnical observational methods are instrumentation, monitoring and back analysis, as shown in Fig. 11. There are various types of instrument devices, like extensometer, pressure cell and electrical piezometer, which can be used to measure the performances of support devices and ground parameters. Measurement of deformations and forces are most common in monitoring systems.

The design of monitoring plan deals with project conditions and geotechnical objectives. The mechanism of behaviour control of support elements and ground conditions determines the type of instrument devices and the location of their installation. The monitoring is performed by collecting data, processing, interpretation and analysis. Collected data from monitoring are used in two ways. In the first way, for abnormal status, for example, an excessive deformation, an immediate action may be required to prevent failure. Secondly, data analysis and interpretation are undertaken to find reliable values of design parameters.

Back analysis methods are used for confirmation of field stress and rock engineering parameters. Generally, back analysis techniques use two approaches: deterministic and non-deterministic. Deterministic methods such as the direct approach, inverse approach and graphic method, are based on the difference between system and model to minimise variability of the (deterministic) signal between them. Non-deterministic methods, like probabilistic methods and genetic algorithms, are based on the discrepancy between model and systems, which is considered as a non-deterministic signal (Sharifzadeh et al., 2017b).

Observation and monitoring methods can be used during the early stages of development of underground mining projects to acquire real ground behaviour and modify design parameters. Some of the benefits of monitoring and site observations are control of design uncertainties, achieving value–cost/time, reducing hazard failure in rock mass structures, and improving ground support systems.

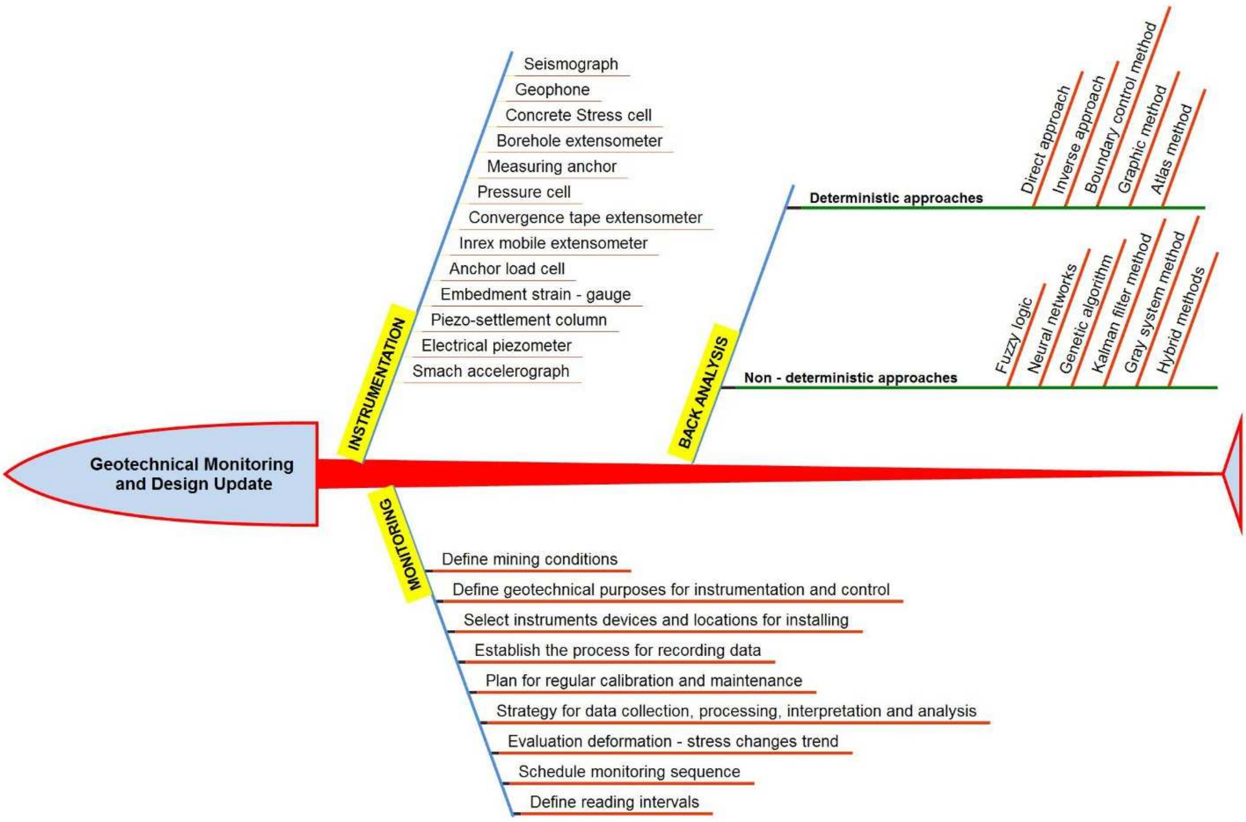

Fig. 11. Geotechnical monitoring and design update procedure in underground excavations (Modified after Sharifzadeh et al., 2017b).

6. Case examples from deep underground mines in Western Australia

6.1. Mine A

The Mine A geology consists of mafic to volcanic and volcanoclastic sedimentary, shale and conglomerate rocks. Major geological structures are western shear zone and eastern, horizontal fault and thrust fault. Sublevel stopping method is used for the extraction of mineral resources. Stope dimensions in the mine site are typically 30 m long and 20 m high. Pillars as natural ground support are implemented in low grade and uneconomic zones. Typical failure modes in the mine site are structural failures (ground fall and wedge failure) and stress-induced failure types (slabbing, pillar failure and squeezing failure).

6.2. Mine B

The gold mine is hosted in Devonian carbonaceous metasediment units. The mineralisation consists of pyrrhotite, arsenopyrite and chalcopyrite. The orebody is mined using the underground long-hole open stoping method. The main challenges associated with the mining operations are a high degree of jointing in the rock mass, several existing shear zones, instability of the rock mass and dilution of the ore body in stopes. The record of seismic events indicates that the mine area is in low to moderate levels of seismicity. The most failure modes are structural and induced stress failure modes.

6.3. Mine C

The gold mine deposit is hosted in mafic stratigraphical units, which are coarse grain and massive basalt units. Gold mineralisation is related to sphalerite, galena and scheelite mineralisation, and it is mostly hosted in laminated quartz veins. Three geotechnical domains at the mine site are hanging wall basalt, the ore body (dolerite, basalts and shear zones) and footwall basalts. The *Q*-value of the rock masses was estimated to be in the range of 4 to 30. Failure mechanisms in the rock masses include mining induced stress, gravity and blasting, and cause wedge failure, ground fall, slabbing, shear slip and pillar failure. The seismicity of the mine site is low to moderate.

6.4. Mine D

Nickel ore as the main resource is hosted in nickel-rich lava rivers and nickel placer deposits. The nickel ore contains a band of massive sulphide, overlain by matrix ore and disseminated ore. The main rock types are basalt, talc-chlorite ultramafic, antigorite ultramafic, porphyry-felsic and porphyry-intermediate. Mineral resources at the mine site are extracted by the long hole and cut-and-fill mining methods. There are several faults, shear zones and porphyry dykes in the mine area. There is a low rate of groundwater inflow (3-5 m^3/d) from the ore surface and hanging walls during the rainy seasons. Seismic events caused a sudden fracture, creating new joints and failures in rock zones surrounding excavations. Strain burst, pillar burst, fault slip, shear failure, floor heave, stress-induced failure and squeezing failure occurred during engineering operations.

6.5. Mine E

The gold deposit consists of multiple shallow dipping ore zones of gold mineralisation and is hosted by mafic and conglomerate. The main rock types are basalt, conglomerate, siltstone, sandstone and shale. Major structures at the mine site are discontinuity sets, fault zones and weakness zones. The quality of rock mass, based on the *Q*-system, was estimated to be between 2 and 19. Rock noise was recorded in underground stopes in some cases before the occurrence of rock failure. During mining operation, several rockfalls and rockbursts occurred. Failure modes at the mine site were classified into gravity, induced stress, and seismicity types. In some cases, unravelling occurred in rock zones with high degrees of jointing. Also, seismic events caused slabbing, strain bursts, rockbursts and ground falls.

The summary of geological information and geotechnical properties in the mines sites are presented in Tables 4 and 5. Also, some typical failure modes that occurred in deep underground mines in Western Australia are shown in Fig. 12. Typically, failure mechanisms at great depth could be classified into three groups: structural failure, induced stress/seismic failure, and operational failure mechanism. Ground fall (Fig. 12a) and wedge failure (Fig. 12c) are a type of structural failure mechanism that is associated with existence of structures in rock masses. The failure occurs due to gravity and sliding rock blocks between discontinuities surfaces. Rockburst failure (Fig. 12b), blocky undercutting failure (Fig. 12d), bulking failure (Fig. 12e), and pillar burst failure (Fig. 12f) are a type of induced stress/seismic failure mechanism. High stress concentration, seismic events and released stored energy from seismic events lead to rockburst failure. High stress level in ground condition results in occurrence of buckling failure.

The design of ground support systems for the case studies is evaluated based on the proposed method in Table 3. The main source of loading at the mine site was identified as gravity, tectonic activities, seismic events, fault slip, strain burst and blasting damage. The geological structural condition was mainly of moderately jointed/blocky rocks, and the GSI and *Q*-value were estimated in the range of 30–80 and 1–48, respectively. The results of the design of ground support system at some deep underground mines in Western Australia are summarised in Table 6. The loading factor (σ_{cm}/σ_1), where σ_{cm} is between 50 MPa and 120 MPa, and σ_1 is about 40-70 MPa, is between 0.9 and 2.3. Therefore, the rock mass structures have the potential to suddenly fail. Site investigations and observations indicate that the primary failure modes are mostly of block fall, wedge failure, induced stress failure, shear failure, slabbing and rockburst failure modes. In addition, during mining operation, secondary failure modes like squeezing failure and pillar failure occurred due to seismic events, induced stresses and blasting damage in rock zones surrounding excavations. Ground support elements were selected based on the estimation of static and dynamic ground support demands in each mine site. Fibrecrete with mesh as a surface support system, friction bolt, split sets, and grouted rebars and cable bolts as reinforcement tools, were selected as ground support systems for stabilising rock mass structures. Fig. 13 shows the results of numerical modelling of the main decline access with 5.2 m width and 5.7 m height in Mine C. Fig. 13b is the estimation of plastic zone (failure zone) surrounding excavation, which is about 1.5 m. The numerical results demonstrate the reliability of failure depth estimation compared with empirical methods (1–1.5 m) and observational methods (0.5–1.2 m). Also, the ratio of safety factor/loading factor (σ_{cm}/σ_1) is presented in Fig. 13c. The maximum displacement of rocks surrounding excavation was estimated 2.2 cm after installing ground support system (Fig. 13d). The numerical results demonstrate stability of rock masses surrounding excavation after installation of ground support systems.

Table 4. The summary of geological information of mine case studies.

Mine site	Mineral resources	Lithology	Mining method	Major geological structures
Mine A	Nickel	Mafic to felsic volcanic rocks, volcanoclastic sedimentary rocks, conglomerate, ultramafic rocks, massive sulphide mineralization	Downhole bench stopping method	Fault, shear zone, discontinuity sets
Mine B	Gold	Pyrite, arsenopyrite, chalcopyrite, coarse crystalline arsenopyrite	Long hole open stopping method	Discrete striking and dipping fault structures, shear zones
Mine C	Gold	Basalt, laminated quartz, sphalerite, galena,	Sublevel stop mining method	Anticline, faults, ductile structures, foliated zones
Mine D	Nickel	Basalt, talc-chlorite, ultramafic, antigorite, porphyry-felsic, and porphyry intermediate	Long hole and cut and fill mining method	Fault, shear zone, porphyry dykes, joint sets
Mine E	Gold	Basalt, conglomerate, siltstone, sandstone, and shale	Long hole open stopping method	Discontinuity sets, faults, shear zones,

Table 5. Rock engineering properties at deep underground mine case studies in Western Australia.

Mine site	Depth (m)	UCS (MPa)	*E* (GPa)	*v*	Dip/dip direction (°/°)			σ_1 (MPa)	σ_2 (MPa)	σ_3 (MPa)
					Joint set 1	Joint set 2	Joint set 3			
Mine A	650	120-160	50-70	0.3	65/85	80/175	51/263	40	32	7
Mine B	950	70-100	30-40	0.28	49/50	55/001	82/182	55	39	18
Mine C	1300	135-170	55-75	0.32	35/37	13/339	48/225	70	56	25
Mine D	800	130-220	45-80	0.34	67/304	74/140	83/86	56	37	21

Mine E	780	160-240	63-80	0.33	49/350	4/57	81/109	51	31	19

Table. 6. The results of design of ground support system in five deep underground mines in Western Australia.

Mine site	Source of loading	Geological structural condition	Load factor	Potential failures		Depth of failure/fracturing (m)		PPV (m/s)	Estimation of ground support demand		Ground support System
				Primary	Secondary	Estimation	Observation		Static (kN/m^2)	Dynamic (kJ/m^2)	
Mine A	Gravitation, field stress, tectonic activities, seismic events, pillar burst, blasting	Moderated jointed/blocky/folded rock $53 < GSI < 77$ $4.5 < Q'^{*} < 27$ $0.5 < B_s^{*} < 9$ $4 < CF < 10$	$1 < \sigma_{cm}/\sigma_1 < 1.3$	Wedge failure, block fall, induced stress failure, tensile failure	Pillar failure, slabbing, brittle failure, unravelling, squeezing failure	0.6-0.9	0.5-1.5	1.1	41	11	50 mm fibrecrete with mesh, 2.4 m Friction bolts (1.2 m × 1.2 m), 2.4 Resin bolts (1 m × 1 m), 6-9 m Cable bolts (2 m × 2 m) (where required), face meshed for drives
Mine B	Gravitation, induced stress, tectonic activities, fault slip, pillar burst, blasting	Moderated–Highly jointed $30 < GSI < 77$ $1 < Q' < 10$ $0.1 < B_s < 7$ $6 < CF < 19$	$0.6 < \sigma_{cm}/\sigma_1 < 1$	Shear failure, block fall, tensile failure, large deformation failure, unravelling, pillar failure	Plastic failure, squeezing failure, splitting failure, chimney failure	0.8-1.3	0.5-1.7	0.7	47	10.6	75-100 mm fibrecrete with mesh, 3 m Resin bolts (1.3 m × 1.3 m), 2.4 m D-bolts (1.3 m × 1.3 m), 8 m Cable bolts (where required), applied mesh and fibrecrete for pillars
Mine C	Gravitation, induced stress, tectonic activities, fault slip, blasting damage, strain burst	Massive–Moderated jointed/blocky rock $58 < GSI < 83$ $14 < Q' < 48$ $3.7 < B_s < 12.5$ $2 < CF < 6$	$0.9 < \sigma_{cm}/\sigma_1 < 1.2$	Large wedge failure, shear slip, slabbing, rock burst	Pillar burst, brittle failure, ground fall, popping rock fragments, strain burst	1-1.5	0.5-1.2	1.5	36	11.5	2.4 m galvanised friction bolt (1.2 m × 1.2 m), 2.4 m grouted split sets (1-1.3 m × 1-1.3 m), 9 m Garford cable (2 m × 2 m) and mesh, face bolted and mesh
Mine D	Strain burst, pillar burst, seismic events, gravitation, stress induced, ground water	Moderated jointed/blocky rock $47 < GSI < 75$ $3 < Q' < 27$ $1 < B_s < 9$ $5 < CF < 17$	$1.1 < \sigma_{cm}/\sigma_1 < 2$	Stress induced failure, wedge gravity failure, strain burst, shear failure, ground movement,	Floor heave failure, squeezing failure, crown pillar failure, blast damage rock, fault slip	0.7-1.1	0.3-1.4	1.8	39	14.4	2.4 m Grouted rebar (1.5 m × 1.5 m), 50 mm fibrecrete with mesh, 3 m and 2.4 m Grouted Split sets (1.5 m × 1.5 m), 6 m Cable bolts (1.5 m ×1.5 m), mesh
Mine E	Seismic events, stress induced, gravitation, tectonic activities	Moderated jointed/blocky rock $43 < GSI < 65$ $13 < Q' < 35$ $2 < B_s < 12$ $3 < CF < 14$	$1.5 < \sigma_{cm}/\sigma_1 < 2.3$	Gravity driven large wedge failure, shallow dipping wedge failure, slabbing, rock burst,	Ground fall, unravelling, strain burst cracking, seismically induced wedge failure, buckling, blast damage	0.5-0.9	0.4-1.3	1.4	37	11.2	50-100mm fibrecrete, mesh, 2.4 m Resin bolts (1.1 m × 1.1 m), 2.4 m Friction bolt (1.5 m × 1.5 m), 2.4 m split set (1.4 m × 1.4 m) where required, 5-8m Cable bolt (2 m × 2 m) where required)

Fig. 12. Some typical failures in deep underground mines in Western Australia: (a) ground fall, (b) rockburst, (c) wedge failure, (d) blocky undercutting, (e) bulking, and (f) pillar burst.

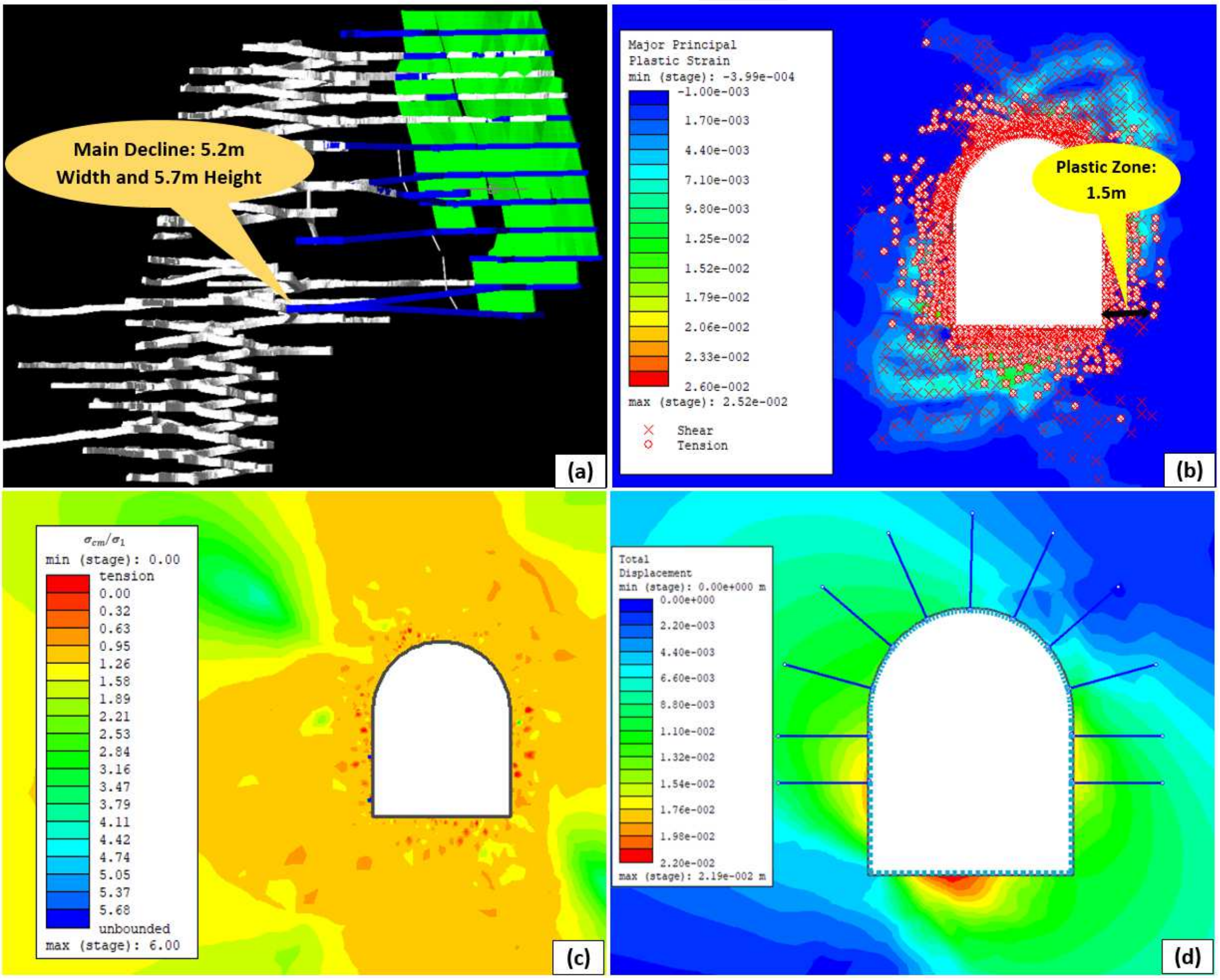

Fig. 13. Numerical modelling of main decline of Mine C: (a) main decline access, (b) plastic zone, (c)loading factor ($\boldsymbol{\sigma_{cm}/\sigma_1}$), and (d) total displacement after installing ground support system.

7. Discussion and conclusions

Deep rock underground excavations are usually associated with high-stress environments and seismic events. Severe damage in rock mass structures and ground support systems may occur due to large magnitude seismic events, defects in rock mass structures, stress concentration, blasting damage and tectonic activities such as strike-slip faults. Utilisation of proper ground control and management strategy can avoid the risk of failure. A ground control and amendment strategy of deep hard rock was proposed in regard to the design, construction and serviceability stages of works. Collecting comprehensive data, diagnosis of hazard conditions and failure mechanisms, design analysis, and selecting stabilisation methods were conducted in the design phase. Determination of safe work procedures, training personnel, identification of hazard conditions, quality control and quality assurance of materials, and safety analysis before ground failure are essential in construction stage. Control of the ground condition during serviceability (short-, medium- and long-term) is focused on monitoring (seismic events and load-deformations), maintenance, rehabilitation, seismic monitoring, and contingency planning.

The critical factors in the design stage of deep underground mining projects are to establish suitable location and layout of openings; determination of suitable excavation method, sequential excavation and extraction ratio; and selection of proper ground support equipment for small- and/or large-scale deformation. Microseismic and blast monitoring throughout the mining operations are required to control sudden failures. Sequential excavation for mining purposes utilises the top-down, bottom-up, centre-out and abutment-centre methods to deal with stress concentration and instability in large-scale mine stopes.

In addition, a procedure for ground support design in deep and hard rock is presented. The main principles in the proposed method are as follows:

(1) Ground loading types and sources,
(2) Characterisation of the major geological structural condition,
(3) Determination of ground load factor,
(4) Identification of primary and secondary potential failure,
(5) Selection of appropriate design analysis for static and/or dynamic loading conditions,
(6) Estimation of static and/or dynamic support demand, and
(7) Selection of surface and reinforcement support elements based on their capacity for energy absorption and safety factor.

At low-stress levels, the dominant loading source is the gravitational force, and ground support elements should be selected based on their capacity for energy dissipation. The behaviour of rock masses and failure mechanism are complex in high rock stresses and dynamic loading conditions due to the released strain energy from seismic events, strain burst, fault slip and pillar burst. The support elements are selected on the basis of their capacity for energy absorption factor in rock mass structures.

Furthermore, field observational methods utilise instrumentation, monitoring and back analysis to control the performance of the ground–support system in rock underground projects. The typical monitoring system in deep underground mining methods is seismic monitoring and measurement of rock deformation surrounding excavations.

A number of deep underground mining projects in Western Australia were studied in this context. The mine sites have hard rock and high field stress. For ground support design, the geological structures were characterised and the potential failure modes were identified. Wedge failure, block fall, squeezing, rockburst, ravelling, pillar burst, slabbing and blast damage are the common types of failure at the mine sites. Also, the depth of failure based on observational methods, empirical methods and numerical methods were estimated in the range of 0.3-1.7 m in the main decline access with 5.2 m width and 5.7 m height. Static and dynamic ground support demands were calculated to be about 40 kN/m^2 and 11 kJ/m^2, respectively. Fibrecrete with mesh was selected as a surface support system, and cable bolt, split sets, friction bolt and D-bolt were selected as reinforcement systems in the rock masses. The applied ground support systems at the mine sites provide stable rock mass structures and a safe environment during mining operations.

Conflict of interest

The authors wish to confirm that there are no known conflicts of interest associated with this publication and there has been no significant financial support for this work that could have influenced its outcome.

Acknowledgments

The research was supported by Curtin International Postgraduate Scholarship (CIPRS)/Department of Mining and Metallurgy Scholarship. This study is also partly supported by National Natural Science Foundation of China the 111 Project under grant Nos. 51839003 and B17009.

Reference

Atlas Copco. Mining methods in underground mining-Atlas Copco Rock Drills AB. Stockholm: Atlas Copco; 2007. p.33-45.

Brady BHG, Brown ET. Rock mechanics for underground mining. 3rd ed. Springer; 2006.

Cai M, Kaiser PK. Rockburst phenomenon and support characteristics, MIRARCO–Mining innovation. In: Rockburst Support Reference Book. Sudbury, Canada; 2018.

Diederichs MS, Martin CD. Measurement of spalling parameters from laboratory testing. In: Proceedings of the ISRM International Symposium-EUROCK, Lausanne, Switzerland. International Society for Rock Mechanics and Rock Engineering (ISRM); 2010.

Diederichs MS. Early assessment of dynamic rupture and rockburst hazard potential in deep tunnelling. In: Proceedings of the ISRM AfriRock-Rock Mechanics for Africa, Cape Town, South Africa. ISRM; 2017.

Feng XT, Hudson JA. Rock engineering design. Leiden, The Netherlands: CRC Press; 2011.

Ghasemi Y. Numerical studies of mining geometry and extraction sequencing in Lappberget, Garpenberg. MSc Thesis. Lulea University of Technology; 2012.

Hudyma M, Potvin Y. Seismic hazard in Western Australian mines. Journal of the Southern African Institute of Mining and Metallurgy 2004; 104(5):265-75.

Jacobsson L, Toyra J, Woldemedhin B, Krekula H. Rock support in the Kiirunavaara Mine. In: Proceedings of the 7th International Symposium on Ground Support in Mining and Underground Construction. Perth: Australian Centre for Geomechanics; 2013.

Kaiser PK, MacCreath DR, Tannant DD. Canadian rockburst support handbook: prepared for sponsors of the Canadian rockburst research program 1990-1995. Geomechanics Research Centre; 1996.

Kaiser PK, Cai M. Design of rock support system under rockburst condition. Journal of Rock Mechanics and Geotechnical Engineering 2012; 4(3), 215-27.

Knobben, C. Seismic hazard at the Rosebery mine. In: Proceedings of the 8th International Conference on Deep and High Stress Mining. Perth: Australian Centre for Geomechanics; 2017.

Li CC. Parameters required for the design of rock support in high-stress masses. In: Proceedings of the ISRM AfriRock-Rock Mechanics for Africa, Cape Town, South Africa. ISRM; 2017.

Louchnikov V, Sandy M. Selecting an optimal ground support system for rockbursting conditions. In: Proceedings of the 8th International Conference on Deep and High Stress Mining. Perth: Australian Centre for Geomechanics; 2017.

Masoudi R, Sharifzadeh M. Reinforcement selection for deep and high-stress tunnels at preliminary design stages using ground demand and support capacity approach. International Journal of Mining Science and Technology 2018; 28(4):573-82.

Mazaira A, Konicek P. Intense rockburst impacts in deep underground construction and their prevention. Canadian Geotechnical Journal 2015; 52(10):1426-39.

Morissette P, Hadjigeorgiou J, Punkkinen AR, Chinnasane DR. The influence of change in mining and ground support practice on the frequency and severity of rockbursts. In: Proceedings of the 7th International Conference on Deep and High Stress Mining, Sudbury, Ontario, Canada. 2014.

MOSHAB. Surface rock support for underground mines code of practice. Western Australia: Mines Occupational Safety and Health Advisory Board; 1999.

Potvin Y, Wesseloo J, Heal D. An interpretation of ground support capacity submitted to dynamic loading. Mining Technology 2010; 119(4):233-45.

Rahimi B, Shahriar K, Sharifzadeh M. Evaluation of rock mass engineering geological properties using statistical analysis and selecting proper tunnel design approach in Qazvin–Rasht railway tunnel. Tunnelling and Underground Space Technology 2014; 41:206-22.

Rahimi B, Sharifzadeh M. Evaluation of ground management in underground excavation design. In: Proceedings of the 8th International Conference on Deep and High Stress Mining. Perth: Australian Centre for Geomechanics. 2017. p. 813-26.

Saharan MR, Mitri H. Destress blasting as a mines safety tool: some fundamental challenges for successful applications. Procedia Engineering 2011; 26:37-47.

Sharifzadeh M, Kolivand F, Ghorbani M, Yasrobi S. Design of sequential excavation method for large span urban tunnels in soft ground–Niayesh tunnel. Tunnelling and Underground Space Technology 2013; 35:178-88.

Sharifzadeh M, Feng XT, Zhang X, Zhang Y. Challenges in Multi-Scale Hard Rock Behavior Evaluation at Deep Underground Excavations. In: Proceedings of the 12th Iranian and 3rd Regional Tunnelling Conference, Tunnelling and Climate Change, Tehran, Iran. 2017a.

Sharifzadeh M, Ghorbani M, Yasrobi S. Observation-based design of geo-engineering projects with emphasis on optimization of tunnel support systems and excavation sequences. In: Feng XT, editor. Rock Mechanics and Engineering Volume 4: Excavation, Support and Monitoring. London, UK: CRC Press; 2017b.

Stacey TR. Innovative and controversial support for rockbursting conditions. In: Proceeding of the 8th International Symposium on Ground Support in Mining and Underground Construction, Lulea, Sweden. 2016.

Szwedzicki T. Quality assurance in mine ground control management. International Journal of Rock Mechanics and Mining Sciences 2003; 40(4):565-72.

Talbot JF, Burke J. Practical improvements to the shotcreting process at Lisheen Mine with particular attention to the mix design and admixture usage. In: Proceedings of the 7th International Symposium on Ground Support in Mining and Underground Construction. Perth: Australian Centre for Geomechanics; 2013.

Yokota Y, Yamamoto T, Date K, MORI T. Quality improvement of rockbolting. In: Proceedings of the 7th International Symposium on Ground Support in Mining and Underground Construction. Perth: Australian Centre for Geomechanics; 2013.

Zhang P, Dineva S, Nordlund E, Hansen-Haug J, Woldemedhin B, Töyrä J, Boskovic M, Nyström A, Marklund PI, Mozaffari S. Establishment of experimental sites in three Swedish mines to monitor the in-situ performance of ground support systems associated with mining-induced seismicity. In: Proceeding of the 8th International Symposium on Ground Support in Mining and Underground Construction, Lulea, Sweden. 2016.

Behrooz Rahimi is Geotechnical Engineer in a deep underground gold mine in Evolution Mining–Australian Gold Company. His research field in PhD is ground support design in deep and hard rock underground mining excavations based on ground behaviour and failure mechanism. He has over 8 years' experience in mining industry and tunnelling projects in the field of mine design, ground support design, ground control and management, stability analysis and numerical modelling. He obtained a demonstrated experience with successful project work in a variety of team sizes including independent and large teams.

Dr Mostafa Sharifzadeh is specialized in fundamental and applied geotechnical and geomechanics engineering in resource and civil engineering. He received his B.Sc. in Mining Engineering in 1993, MSc. in Rock Mechanics Engineering in 1996 and PhD in Geotechnical Engineering in 2005. He has over 20 years of experience in construction companies, consulting engineering and academia. He has worked in over 30 mining, civil and energy projects in Iran, Japan, Australia and China using innovative approaches and contributed the outcome to professional development through numerous publications and invited presentations. Dr Sharifzadeh has produced over 300 publications including books, book chapters, refereed journal papers, peer-reviewed conference papers, guidelines and engineering design reports. He has supervised over 12 doctoral students and 80 master students. He is a member of the committee of design methodology in International Society for Rock Mechanics (ISRM), editorial board member of Tunnelling and Underground Space Technology Journal (TUST), Journal of Tunnelling and Underground Space Engineering (TUSE), and reviewer for numerous international journals and conferences on geomechanics, tunnelling and mining. Since 2013, he has worked on geomechanical aspects of deep underground hard rock mining-related research at Western Australian School of Mines (WASM), Curtin University.

Prof. Xia-Ting Feng received his PhD at Northeastern University of Technology (namely Northeastern University since 1992), China in 1992 and then took the position of lecturer, associate professor and professor at the same university. He joined Institute of Rock and Soil Mechanics, Chinese Academy of Sciences (CAS) in 1998 as a Professor of Hundred Talent Program of the CAS and as Deputy Director in Charge and Director in 2001-2005. He has worked as Director of State Key Laboratory of Geomechanics and Geotechnical Engineering since 2007. He works at Northeastern University, China as a Vice President since September 2017. He is President of Federation of International Geo-engineering Societies—FedIGS, President of ISRM Commission on Design Methodology, member of ISRM Commission on Testing Methods, and President of Chinese Society for Rock Mechanics and Engineering (CSRME). He was the past President of International Society for Rock Mechanics (ISRM) 2011-2015. He is also Editor-in-Chief of *Chinese Journal of Rock Mechanics and Engineering*, Associate Editor-in-Chief of *Chinese Journal of Theoretical and Applied Mechanics*, and Associate Editor-in-Chief of *Journal of Rock Mechanics and Geotechnical Engineering (JRMGE)*. He is members of Editorial Board of *International Journal of Rock Mechanics and Mining Sciences* (2003-present), *Rock Mechanics and Rock Engineering* (2010-present), *Geomechanics and Tunneling* (2008-present).

Highlight

- Proposed an innovative analysis of ground behaviour and ground management strategies in deep underground mining
- Developed ground support system design in static and dynamic conditions
- Evaluation of stress management and quality control and support elements during mining operations
- Analysis of ground – support system performance by geotechnical monitoring and design update
- Justified proposed approaches in Western Australian's mines

Support system, reinforcement and stabilisation design and verification

Mostafa Sharifzadeh
Western Australian School of Mines (WASM)

1

Rock Engineering Design Approaches and challenges in Deep Hard Rock Mining Engineering – Dec. 15th, 2019 – Shahrood UT

Presentation Outline

1) Introduction
2) Introducing Reinforcement Systems
3) Ground stabilization (Treatment) Design Fundamentals
4) Mine Opening Support Design Methods
5) Summary
6) References

2

2

Rock Engineering Design Approaches and challenges in Deep Hard Rock Mining Engineering – Dec. 15th, 2019 – Shahrood UT

Presentation Outline

1) **Introduction**
2) Introducing Reinforcement Systems
3) Ground stabilization (Treatment) Design Fundamentals
4) Mine Opening Support Design Methods
5) Summary
6) References

3

3

Rock Engineering Design Approaches ar...od UT

Simplified geotechnical Design methodology for deep underground mine excavation

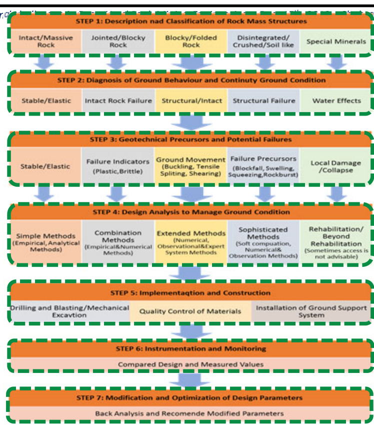

4

4

Rock Engineering Design Approaches and challenges in Deep Hard Rock Mining Engineering – Dec. 15th, 2019 – Shahrood UT

Main Failure mechanisms

1. Stress controlled failure in continuum medium:

Failure Mechanisms Spalling, popping and rock bursts of rock caused by high in situ stresses. This type of failure is stress induced failure, occur in highly stressed brittle rock.

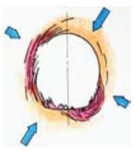

2. Structure controlled failure in discontinuum medium:

Failure Mechanisms Falling or sliding of wedges or blocks released by intersecting discontinuities. This type of failure is structurally controlled failure, generally occur in hard rock at relatively shallow depth.

5

5

Rock Engineering Design Approaches and challenges in Deep Hard Rock Mining Engineering – Dec. 15th, 2019 – Shahrood UT

Structure controlled failure

After Villaescusa 2014

6

6

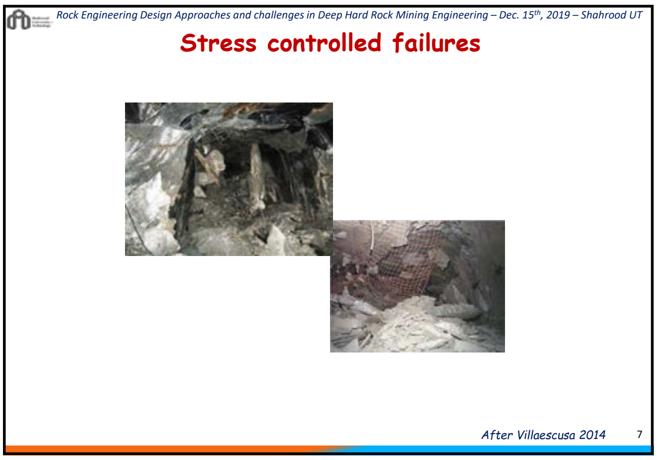
Rock Engineering Design Approaches and challenges in Deep Hard Rock Mining Engineering – Dec. 15th, 2019 – Shahrood UT
Stress controlled failures
After Villaescusa 2014
7

7

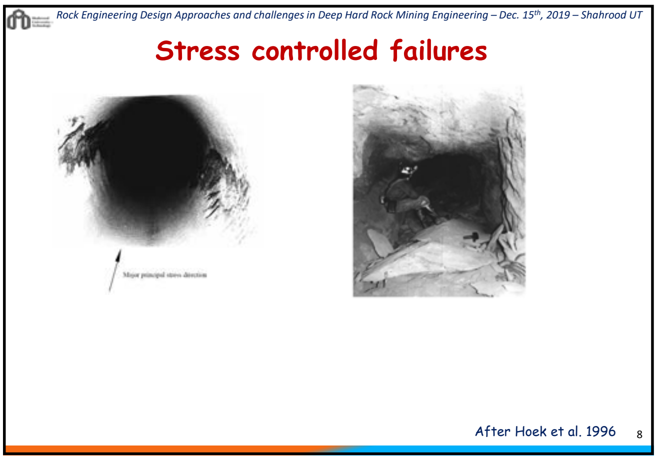
Rock Engineering Design Approaches and challenges in Deep Hard Rock Mining Engineering – Dec. 15th, 2019 – Shahrood UT
Stress controlled failures
Major principal stress direction
After Hoek et al. 1996
8

8

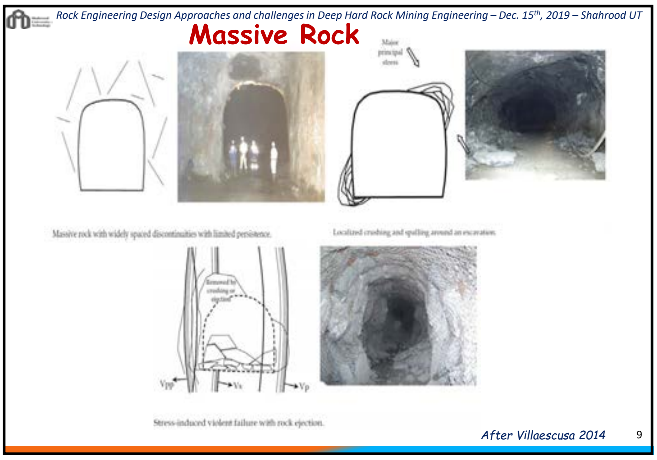
Rock Engineering Design Approaches and challenges in Deep Hard Rock Mining Engineering – Dec. 15th, 2019 – Shahrood UT
Massive Rock
Major principal stress
Massive rock with widely spaced discontinuities with limited persistence.
Localized crushing and spalling around an excavation.
Stress-induced violent failure with rock ejection.
After Villaescusa 2014
9

9

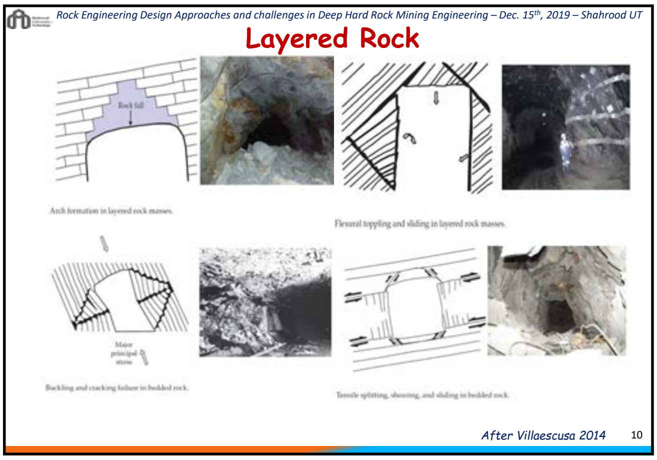
Rock Engineering Design Approaches and challenges in Deep Hard Rock Mining Engineering – Dec. 15th, 2019 – Shahrood UT
Layered Rock
Rock fall
Arch formation in layered rock masses.
Flexural toppling and sliding in layered rock masses.
Major principal stress
Buckling and cracking failure in bedded rock.
Tensile splitting, shearing, and sliding in bedded rock.
After Villaescusa 2014
10

10

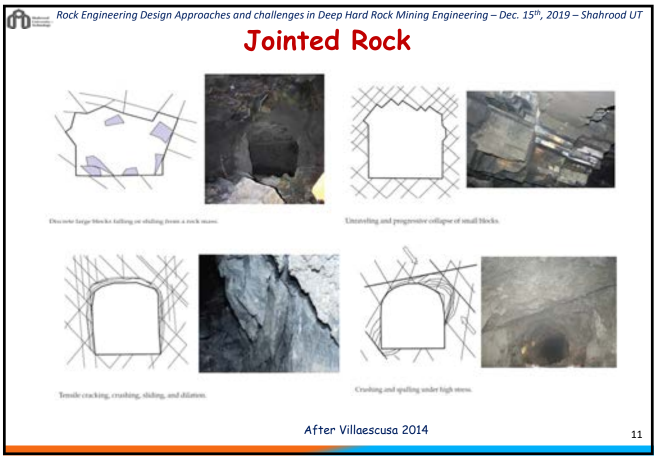
Rock Engineering Design Approaches and challenges in Deep Hard Rock Mining Engineering – Dec. 15th, 2019 – Shahrood UT
Jointed Rock
Discrete large blocks falling or sliding from a rock mass.
Unraveling and progressive collapse of small blocks.
Tensile cracking, crushing, sliding, and dilation.
Crushing and spalling under high stress.
After Villaescusa 2014
11

11

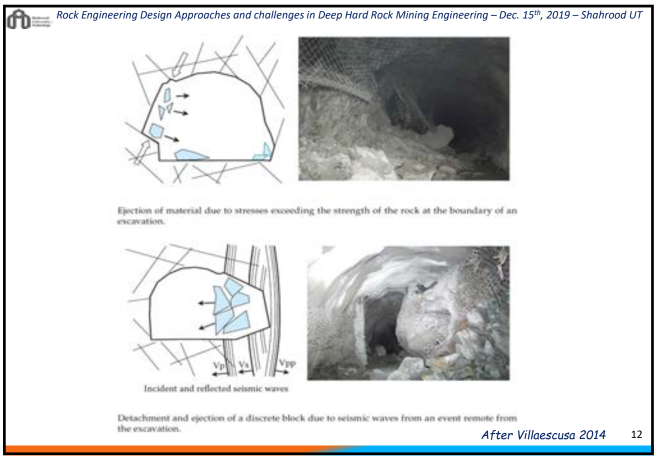
Rock Engineering Design Approaches and challenges in Deep Hard Rock Mining Engineering – Dec. 15th, 2019 – Shahrood UT
Ejection of material due to stresses exceeding the strength of the rock at the boundary of an excavation.
Incident and reflected seismic waves
Detachment and ejection of a discrete block due to seismic waves from an event remote from the excavation.
After Villaescusa 2014
12

12

Observed damage near the boundary of an excavation in hard rock under very high stress.

After Villaescusa 2014

Rock Engineering Design Approaches and challenges in Deep Hard Rock Mining Engineering – Dec. 15th, 2019 – Shahrood UT

Rock Reinforcement and Support

Two distinct techniques

Both can be used to control rock behaviour by minimizing displacements at the excavated walls

Reinforcement is used to improve the overall stability of the rock mass adjacent to an excavation

- E.g. Rock bolts, cable bolts, ground anchors

Support is used to provide a restraint at the excavation surface

- E.g. Timber, fill, shotcrete, mesh or steel or concrete sets or liners

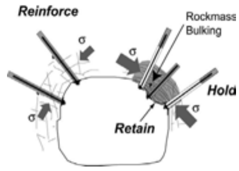

(After Kaiser et al, 2000)

Rock Engineering Design Approaches and challenges in Deep Hard Rock Mining Engineering – Dec. 15th, 2019 – Shahrood UT

How to prevent failure?

1. **Prevent stress concentration by suitable design of excavation size and orientation,**
2. **Grouting in rock mass to increase cohesion between blocks,**
3. **Rock anchor installation to increase frictional strength between blocks,**
4. **Installing support system (steel arc, shotcrete, faceplate) to increase confining stresses of rock mass,**
5. **Sealing, drainage, controlling water content and pressure,**
6. **Installing energy absorbing rock bolt to damp the dynamic loading,**
7. **Combination of above methods.**

Rock Engineering Design Approaches and challenges in Deep Hard Rock Mining Engineering – Dec. 15th, 2019 – Shahrood UT

Underground excavation Lifetime classification

- **Short-term excavations** (less than 1 year to 3 year), such as: crosscuts, ore drive, temporary openings, and exploration galleries.
- **Medium-term excavations** (more that 3–10 years), e.g. level accesses, ventilation drifts.
- **Long-term excavations** (Life of the mine) (more than 10 years), e.g. main accesses, decline, ramps, shaft.
- Civil projects could be categorised in long term excavations.

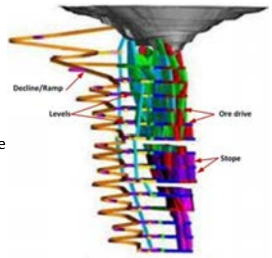

Therefore, support and reinforcement system design must be consistent with excavation service life and utilisation

Rock Engineering Design Approaches and challenges in Deep Hard Rock Mining Engineering – Dec. 15th, 2019 – Shahrood UT

Presentation Outline

1) Introduction
2) **Introducing Reinforcement Systems**
3) Ground stabilization (Treatment) Design Fundamentals
4) Mine Opening Support Design Methods
5) Summary
6) References

Rock Engineering Design Approaches and challenges in Deep Hard Rock Mining Engineering – Dec. 15th, 2019 – Shahrood UT

Ground Control

- Internal Reinforcement
  - Rock Bolts (typically less than 3 meters long)
  - Cable Bolts (typically greater than 5 meters long)
- Surface Support
  - Plates
  - Straps
  - Mesh
  - Sprayed Coatings
    - Concrete (Shotcrete)
    - Thin Sprayed Liners

Principles of (a) rock reinforcement and (b) rock support

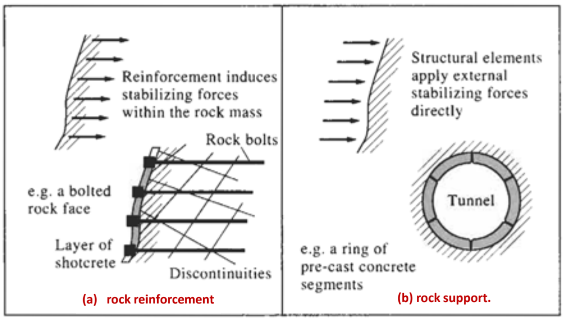

19

19

Rock Engineering Design Approaches and challenges in Deep Hard Rock Mining Engineering – Dec. 15th, 2019 – Shahrood UT

Load Transfer Mechanisms

- Rock – Internal Fixture
- Internal Fixture – Element
- Element – External Fixture
- External Fixture – Rock

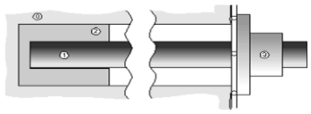

0 – Rock
1 – Element
2 – Internal Fixture
3 – External Fixture

After Villaescusa 2014

20

20

Rock Engineering Design Approaches and challenges in Deep Hard Rock Mining Engineering – Dec. 15th, 2019 – Shahrood UT

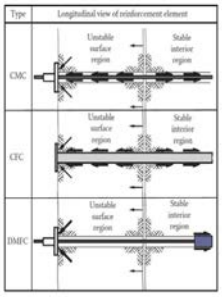

Classification of reinforcement action. (After Thompson, A.G. and Windsor, C.R., A classification system for reinforcement and its use in design, in T. Szwedzicki, G.R. Baird, and T.N. Little, eds., *Proceedings of the Western Australian Conference on Mining Geomechanics*, Kalgoorlie, Western Australia, Australia, June 8–10, 1992, pp. 115–125, Western Australian School of Mines, Kalgoorlie, Western Australia, Australia.)

Classification of Typical Reinforcement Devices

Type	Description
CMC	Full-column cement-/resin-grouted bars (grouted CT bolt, deformed bar, threaded bar, and fully grouted Posimix)
	Cement-grouted cables (plain strand and modified geometry)
CFC	Friction stabilizers (split-set bolt, friction bolt, and Swellex)
DMFC	Mechanical anchors (ungrouted CT and HGB bolts, expansion shell, and slot and wedge)
	Single cement/resin cartridge anchors (paddle bolt, deformed bar, and debonded Posimix)

Source: Thompson, A.G. and Windsor, C.R., A classification system for reinforcement and its use in design, in T. Szwedzicki, G.R. Baird, and T.N. Little, eds., *Proceedings of the Western Australian Conference on Mining Geomechanics*, Kalgoorlie, June 8–10, 1992, pp. 115–125, Western Australian School of Mines, Kalgoorlie, Western Australia, Australia.

21

21

Rock Engineering Design Approaches and challenges in Deep Hard Rock Mining Engineering – Dec. 15th, 2019 – Shahrood UT

Types of ground treatment systems:

1. **Bolts reinforcement:**
   1. **Rock bolts**
   2. **Cable bolts**
2. **Concrete support:**
   1. **Shotcrete**
   2. **Concrete in place casting**
   3. **Precast concrete segments**
3. **Steel arc support:**
   1. **Rigid steel arc**
   2. **Flexible steel arc**
   3. **Lattice girder**

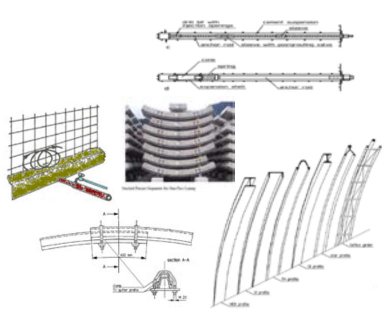

22

22

Rock Engineering Design Approaches and challenges in Deep Hard Rock Mining Engineering – Dec. 15th, 2019 – Shahrood UT

The three primary effects of excavation on the rock mass environment

1. Displacement and rock failure
2. Stress rotation such that normal and shear stress are zero at surface.
3. Water may cause failure or increased weathering or surface deterioration

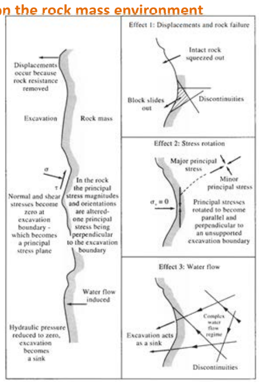

23

23

Rock Engineering Design Approaches and challenges in Deep Hard Rock Mining Engineering – Dec. 15th, 2019 – Shahrood UT

The stabilization strategy: Basic categorization of rock reinforcement and support.

Rock Stabilization

- **Rock Reinforcement** — Bars, rods or cables are inserted into the rock mass, such that the mass is stiffened and strengthened, with the result that it can 'support itself'
  - **Continuous medium** — Behaves as a reinforced composite material, analogous to reinforced concrete or glass fibre reinforced plastics
  - **Discontinuous medium** — Behaves as a discontinuous medium that is stiffer and stronger, because displacement on discontinuities is inhibited
- **Rock Support** — Structural elements are introduced into the excavation to inhibit rock mass displacement at the excavation boundaries e.g. steel arches
  - **Continuous medium** — Boundary conditions altered – structural elements apply forces or stresses which inhibit displacements of the continuum
  - **Discontinuous medium** — Boundary conditions altered – structural elements apply forces or stresses inhibiting displacements of individual blocks

(After Hudson & Harrison, 1997)

24

24

Reinforcement system

Reinforcement Devices	CMC	CFC	DMFC
Deformed bar	•		•
Hollow deformed bar	•		•
Ribbed bar	•		•
Forged Thread bar	•		•
Rolled Thread bar	•		•
Tubular Bolt	•		•
Yielding bolt	•		
Square twisted bolt	•		
Self drilling bolt	•		
Cone Bolt	•		
Injection polymer bolt	•		
Split Set		•	
Swellex bolt		•	
Wedge-Pipe bolt		•	
Cotter pin		•	
GD Rock Nail		•	
Plain bar			•
Pigtail or Wriggle bolt			•
Paddle bolt			•
Fibreglass bolt			•
Slot and wedge bolt			•
Expansion shell bolt			•

Friction Anchor (Split set): CFC / CMC

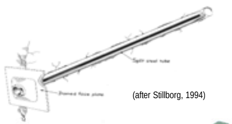

(after Stillborg, 1994)

CT Bolt: DMFC / CMC

(after Windsor & Thompson, 1998) 25

25

Rock Engineering Design Approaches and challenges in Deep Hard Rock Mining Engineering – Dec. 15th, 2019 – Shahrood UT

Rock bolt Function

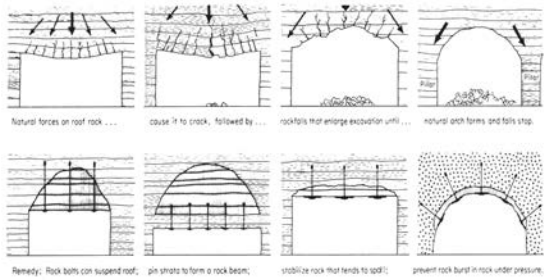

26

26

Rock Engineering Design Approaches and challenges in Deep Hard Rock Mining Engineering – Dec. 15th, 2019 – Shahrood UT

Cable bolt

- Used to stabilize large single blocks or wedges formed in the (Roof) back and walls of the excavations
- Provide effective reinforcement of very large spans where rock bolts geometrically inadequ
- Have a very high load bearing capacity (25 t/strand) as well as moderate corrosion resistance
- Plain and modified geometry twin or single installations
- Plated provides a high retention capacity
- Rely on good grouting practices

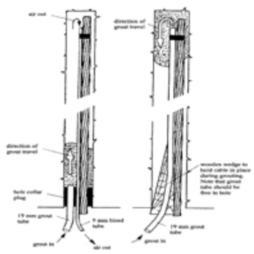

27

27

Rock Engineering Design Approaches and challenges in Deep Hard Rock Mining Engineering – Dec. 15th, 2019 – Shahrood UT

Cable Bolting

- Cables provide an alternative to leaving ore in pillars
- Twin cables that have an ultimate capacity of 50 tonnes are recommended for permanent back reinforcement
- Single strand can be used for hanginwall reinforcement
- Hole size (post grouted): single (57mm), double (64mm) strand
- Critical embedment length (bulbed) ranges from 1.0 to 2m
- Capacity partially depends on rock mass confinement (stress changes)

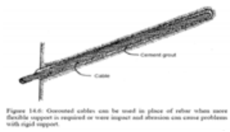

28

28

Rock Engineering Design Approaches and challenges in Deep Hard Rock Mining Engineering – Dec. 15th, 2019 – Shahrood UT

Cable Bolts

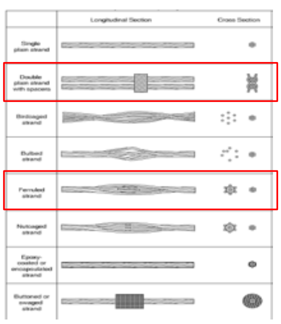

Cable bolts

Barrel and Wedges

29

29

Rock Engineering Design Approaches and challenges in Deep Hard Rock Mining Engineering – Dec. 15th, 2019 – Shahrood UT

Cablebolt Function

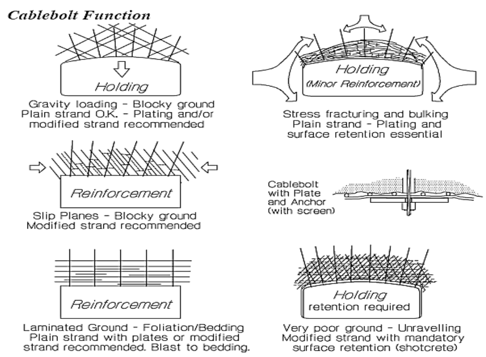

30

30

Common Cablebolt Applications

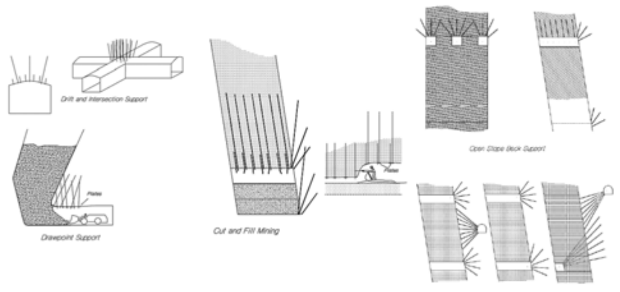

31

31

Schematic of dynamic loading due to seismic event

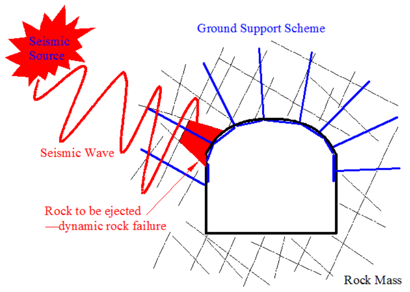

(a) ejection of unstable rock

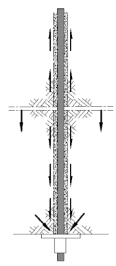

(b) pre-existing fracture opening

[Player et al., 2008]

32

32

Table Evolution of energy-absorbing bolts

Year	Bolts type/specification	Static		Dynamic	
		(kN)	(mm)	(kN)	(mm)
1987	Cone bolt(22mm)	200	200	196	118
2001	Durabar(16mm)	120	600	80	600
2008	Garford bolt(21.7mm)	215	500	100-125	400
2009	MCB38(17.2mm)	110	300-900	150	250
2009	D-bolt(22mm1500mm)	240	169	280	227
2010	Yield-Loc(17.2mm)	110	200	102	177
2010	Roofex(R20D,20mm)	200	150-800	80	275
2010	He-bolt(22mm)	160	00	168	925
2013	MP1 bolt(20mm2700mm)	229	170	285	174
2014	PA1 bolt(20mm2400mm)	210	185	225	230
2005	BHRB400(22mm2400mm)	207	369	220	378
2005	BHRB500(22mm2400mm)	270	308	N A	N A
2005	BHRB600(22mm2400mm)	285	255	N A	N A

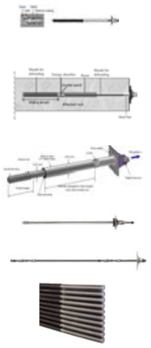

33

33

Categorization of energy-absorbing rockbolts

The existing bolts accommodate rock dilation and absorb energies via either utilizing plastic deformation of the shank(mode Ⅰ) in response to dynamic load or ploughing (slippage) through the encapsulation medium at predefined load levels (mode Ⅱ).

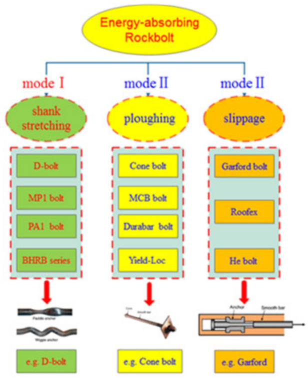

34

34

Reinforcement

Rebar

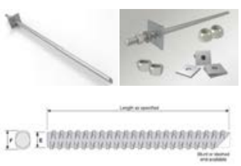

Frictional bolt (Split set and Swellex)

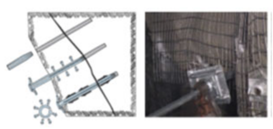

35

35

Reinforcement

Cone bolt

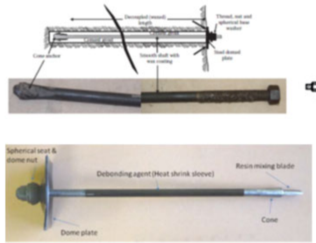

D-Bolt

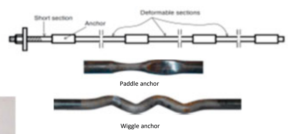

36

36

Reinforcement

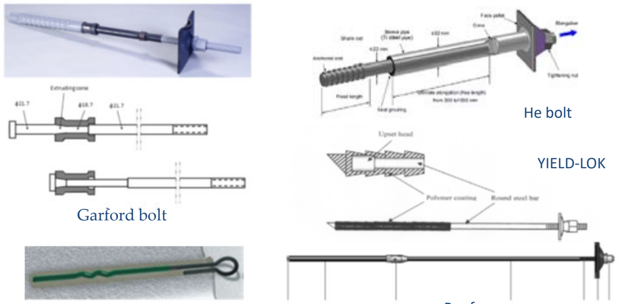

37

37

Rock Engineering Design Approaches and challenges in Deep Hard Rock Mining Engineering – Dec. 15th, 2019 – Shahrood UT

New Concept Mining (NCM) Yielding Rock Bolts

Yielding Roofbolts: Hybrid
- Vulcan

Yielding Roofbolts: Spin in Resin
- Par1 Resin and Helix Yielding

Yielding Roofbolts: Pre-tensioned, post-grouted
- MP1 (mechanised & handheld) and Par1 (handheld)

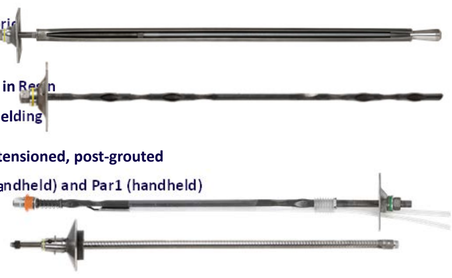

38

38

Rock Engineering Design Approaches and challenges in Deep Hard Rock Mining Engineering – Dec. 15th, 2019 – Shahrood UT

Surface Support

- **Plates**
  - Flat, domed
- **Straps**
  - Flat, W-Section
- **Steel Wire Mesh**
  - Welded grid, woven
- **Sprayed Coatings**
  - Shotcrete (sprayed concrete)
  - Liners (sprayed thin coatings)
- **Other support**
  - Props, fill

39

39

Rock Engineering Design Approaches and challenges in Deep Hard Rock Mining Engineering – Dec. 15th, 2019 – Shahrood UT

Surface Support

- **Plates**
  - Flat, domed
- **Straps**
  - Flat, W-Section
- **Steel Wire Mesh**
  - Welded grid, woven
- **Sprayed Coatings**
  - Shotcrete (sprayed concrete)
  - Liners (sprayed thin coatings)
- **Other support**
  - Props, fill

40

40

Rock Engineering Design Approaches and challenges in Deep Hard Rock Mining Engineering – Dec. 15th, 2019 – Shahrood UT

How Surface Support Works

Retains rock by transferring loads to the reinforcement or surrounding rock

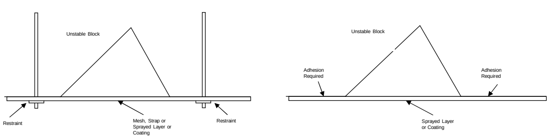

41

41

Rock Engineering Design Approaches and challenges in Deep Hard Rock Mining Engineering – Dec. 15th, 2019 – Shahrood UT

Objectives of support system design

1. To estimate energy accumulation in deep underground excavations
2. To assess the sudden failure potential, examine the critical energy, rock failure depth using suitable rock behaviour models and available analytical, numerical, and empirical methods
3. To determine ground energy demand
4. To select the suitable Rock support system to absorb ground energy.

42

42

Presentation Outline

1) Introduction
2) Introducing Reinforcement Systems
3) **Ground stabilization (Treatment) Design Fundamentals**
4) Mine Opening Support Design Methods
5) Summary
6) References

43

43

Rock Engineering Design Approaches and challenges in Deep Hard Rock Mining Engineering – Dec. 15th, 2019 – Shahrood UT

Design Fundamentals

1. Failure Mechanisms / Depth of Damage
2. Ground Deformation – Ground Reaction
3. Dynamic Loading

44

44

Rock Engineering Design Approaches and challenges in Deep Hard Rock Mining Engineering – Dec. 15th, 2019 – Shahrood UT

Stress path: changes of stress at different parts of tunnel

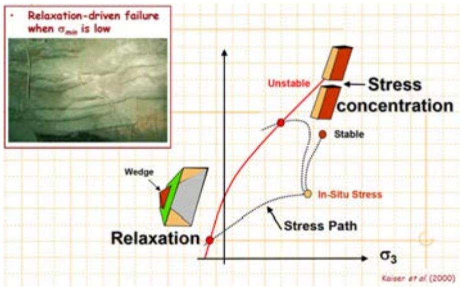

45

45

Rock Engineering Design Approaches and challenges in Deep Hard Rock Mining Engineering – Dec. 15th, 2019 – Shahrood UT

Deformation - Ground Reaction Curves

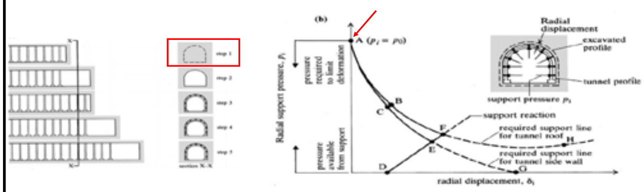

Step 1: Pre-mining state – rock provides support pressure

46

46

Rock Engineering Design Approaches and challenges in Deep Hard Rock Mining Engineering – Dec. 15th, 2019 – Shahrood UT

Deformation - Ground Reaction Curves

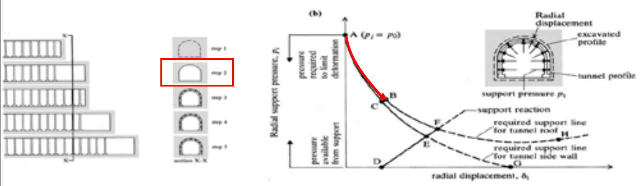

Step 2: Heading excavated

47

47

Rock Engineering Design Approaches and challenges in Deep Hard Rock Mining Engineering – Dec. 15th, 2019 – Shahrood UT

Deformation - Ground Reaction Curves

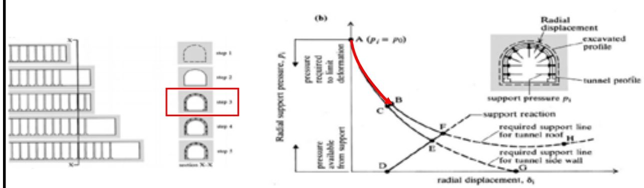

Step 3: Support Installed – no load on support.

48

48

Deformation - Ground Reaction Curves

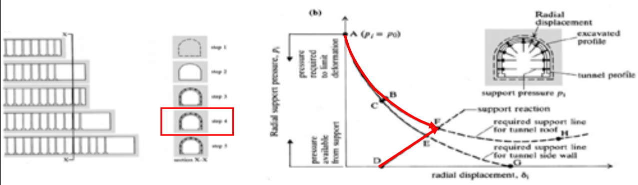

Step 4: Support Installed – headin advanced – support loaded

49

49

Rock Engineering Design Approaches and challenges in Deep Hard Rock Mining Engineering – Dec. 15th, 2019 – Shahrood UT

Deformation - Ground Reaction Curves

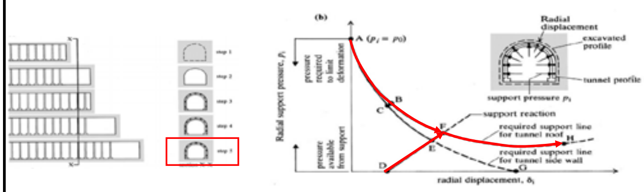

Step 4: Support Installed – more supported added - heading advanced – support loaded.

50

50

Rock Engineering Design Approaches and challenges in Deep Hard Rock Mining Engineering – Dec. 15th, 2019 – Shahrood UT

Load – Deformation Characteristics

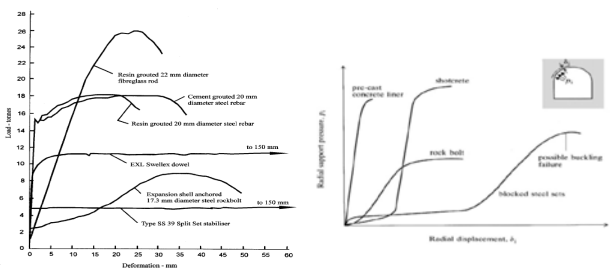

51

51

Rock Engineering Design Approaches and challenges in Deep Hard Rock Mining Engineering – Dec. 15th, 2019 – Shahrood UT

Recommendation of reinforcement and support for different ground conditions

	Low stress levels	High stress levels
Massive rock	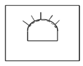 Massive rock subjected to low in situ stress levels. No permanent support. Light support may be required for construction safety.	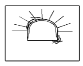 Massive rock subjected to high in situ stress levels. Pattern rockbolts or dowels with mesh or shotcrete to inhibit fracturing and to keep broken rock in place.
Jointed rock	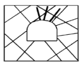 Massive rock with relatively few discontinuities subjected to low in situ stress conditions. 'Spot' bolts located to prevent failure of individual blocks and wedges. Bolts must be tensioned.	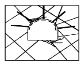 Massive rock with relatively few discontinuities subjected to high in situ stress conditions. Heavy bolts or dowels, inclined to cross rock structure, with mesh or steel fibre reinforced shotcrete on roof and sidewalls.
Heavily jointed rock	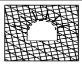 Heavily jointed rock subjected to low in situ stress conditions. Light pattern bolts with mesh and/or shotcrete will control ravelling of near surface rock pieces.	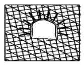 Heavily jointed rock subjected to high in situ stress conditions. Heavy rockbolt or dowel pattern with steel fibre reinforced shotcrete. In extreme cases, steel sets with sliding joints may be required. Invert struts or concrete floor slabs may be required to control floor heave.

(After Hoek et al., 1993, Hoek, 2000)

52

52

Rock Engineering Design Approaches and challenges in Deep Hard Rock Mining Engineering – Dec. 15th, 2019 – Shahrood UT

Ground support principle according to failure mechanisms

1. In non-seismic support design Static loading components must be considered such as :
   - Force / Weight
   - Length of embedment,
   - Yield / failure load
   - shear

2. In seismically active support design Static and Dynamic Loading factors must be considered such as:
   - Kinetic energy
   - Peak Particle Velocity (PPV),
   - Failure mode
   - Support dissipation capacity

53

53

Rock Engineering Design Approaches and challenges in Deep Hard Rock Mining Engineering – Dec. 15th, 2019 – Shahrood UT

Static Load Calculation approach for Underground Exc.

Static Load Case Calculation of Surface Support

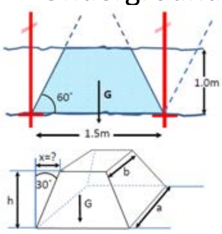

$V = \frac{1}{3}h(a^2+ab+b^2)$

$\tan 30^\circ = \frac{x}{h} \Rightarrow x = \tan 30 \cdot h$

$x = \tan 30 \cdot 1.0m$

$x = \underline{0.58m}$

$b = 1.5m - 2(0.58) = \underline{0.35m}$

$h = 1.0m$

$a = 1.50m$

$b = 0.35m$

$V = \frac{1}{3} \cdot 1.0(1.50^2 + 1.50 \cdot 0.35 + 0.35^2)$

$V = 0.97m^3$

$\rho = 2{,}800 kg/m^3$

$G = V \cdot g \cdot \rho \Rightarrow 0.97 \cdot 9.81 \cdot 2{,}800$

$G = 26.6kN \cdot 1.5$ (FOS)

$\underline{G = 39.9kN}$

54

54

Ground support principle according to failure mechanisms

$$\boxed{\text{Factor of Safety} = \frac{\text{Support Capacity}}{\text{Energy Demand}}}$$

$$\text{Factor of Safety} = \frac{\sum(\text{Load Capacity} \times \text{Displacement Capacity})_{\text{Support Elements}}}{\frac{1}{2}mv_e^{\,2} + qmgd}$$

- Where:
- m = the mass of the ejected block (kg);
- v_e = the ejection velocity of the block (m/s);
- g = acceleration due to gravity (m/s²);
- d = distance the ejected block has travelled (m); and
- q = 1, 0 or -1 for ejection from the back, wall or floor respectively.

55

55

Procedure for ground energy demand calculation:

1. Identify seismic sources
2. Assess seismic hazard of each source
3. Calculate velocity (near-field & far-field)
4. Calculate energy demand
   1. Intact Rock Property Approach
   2. Estimation of failure thickness and ejection velocity
   3. Rockburst Damage Potential Method

56

56

Surface Support Energy Absorption Capacities

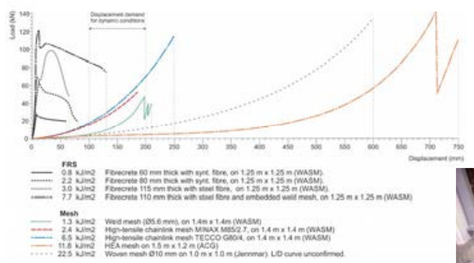

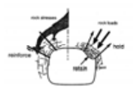

Louchnikov and Sandy (2017)

57

57

Concept of the ideal bolt and definitions of strength, ductile, and energy- absorbing rockbolts

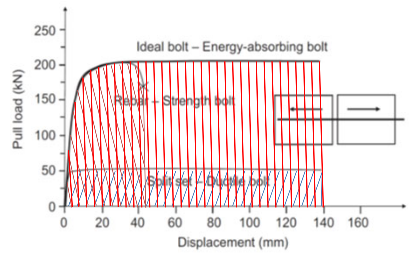

58

58

Load Displacement behaviour of different Rockbolt

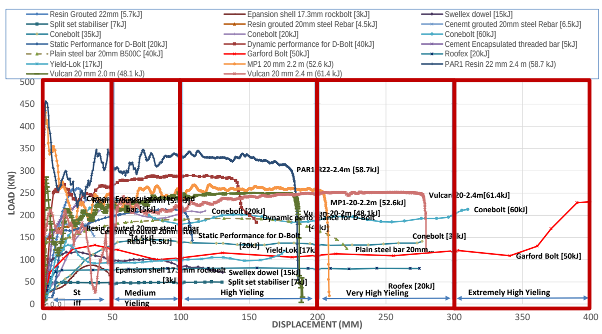

R. Masoudi & M. Sharifzadeh, 2018

59

59

Demand – Capacity based support selection

Ground Demand		Reinforcement Selection	
Surface Displacement (mm)	Energy (kJ/m2)	Recommended Reinforcement	Capacity Category
<50	<5	Expansion shell Rockbolt, Resin/Cement steel Rebar,	Low / Stiff
50–100	5–15	Split set, Swellex, Roofex, Yield-Lok, Modified Rebar	Medium
100–200	15–25	Swellex, D-Bolt, Conebolt, Roofex, Yield-Lok, PAR1, Vulcan (20 mm, 2 m)	High
200–300	25–35	Roofex, Conebolt, Garford, Vulcan (20 mm, 2.4 m), MP1	Very high
>300	>35	Conebolt ,Garford	Extremely high

R. Masoudi & M. Sharifzadeh, 2018

60

60

Energy dissipation capacity category of different types of reinforcement

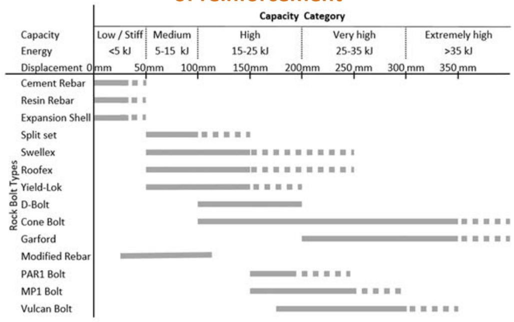

R. Masoudi & M. Sharifzadeh, 2018

61

61

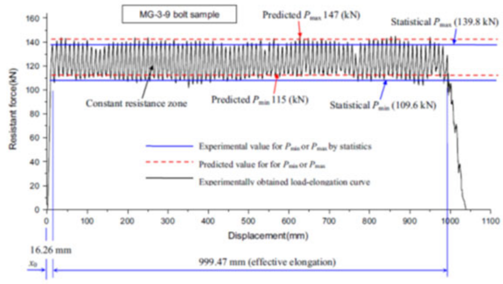

Pull-out test result of sample MG-3-9 (M HE, 2014)

62

62

Interpreting results of dynamic tests

- **Repeatability of results**

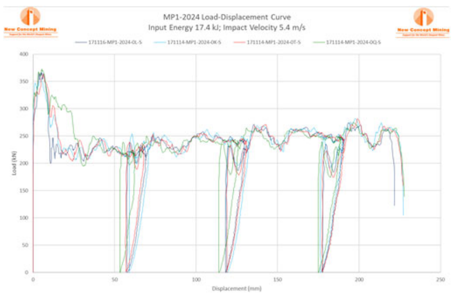

New concept Mining,2018

63

63

Effect of the Length of the bolts on energy absorption and deformation capacity

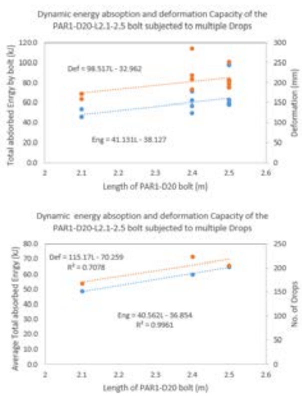

64

64

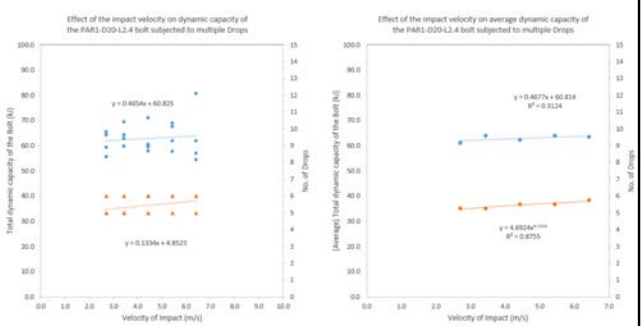

Effect of the velocity of the drops on energy absorption capacity

65

65

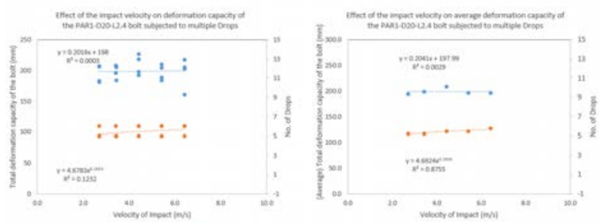

Effect of the velocity of the drops on deformation capacity

66

66

Role of surface support system

- **A surface support with high energy absorption takes a portion of the load and ensure a good load transfer to the reinforcing elements**

Potential savings in ground support costs

- **Mesh instead of shotcrete**
- **Shorter rock bolts**
- **Larger spacing between rock bolts**
- **Rock bolts of lower capacity**
- **Customised cablebolting patterns**

Underground mining and construction strategies- Stress Management

➢Depressurisation or destressing is a typical method to control rock failures in deep and high-stress conditions. Ground stress and seismic events are inevitable in underground mining operations and may cause various failures such as rockburst.

➢Destress blasting is used for fracturing rock zones to dissipate stored strain energy from rock masses in mining operations and underground constructions. The method is used to reduce the level of stress concentration, by creating fractures in the rock mass that cause a reduction in the elastic modulus of the rock mass, and enable the rock to carry high-stress conditions.

Excessive stress management methods in rock damaged zone around excavation

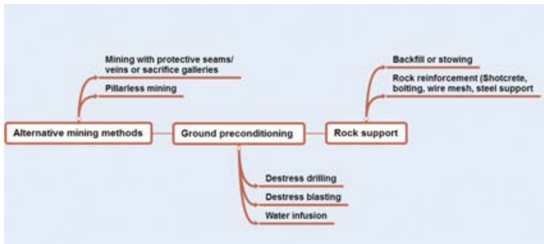

(Modified after Saharan and Mitri (2011))

Rahimi, Sharifzadeh, Feng, 2019

Underground mining and construction strategies- Support elements quality control

❑Quality control and assessment of materials are determined by the necessary quality level and quality grade.

❑Quality assurance of ground control management are:

1. Discussion with managers about related activities for ground control,
2. Inspection of geotechnical activities in underground mines,
3. Review of procedures of operational activities, standards, documents and critical tasks,
4. Consideration, discussion and review of geotechnical record and input data on the design,
5. Observation and monitoring of drilling, blasting, rock mass behaviour and failure modes, and
6. Discussion with supervisors and operators about the identified issues and development activities.

Presentation Outline

Ground Support Selection/ 'Design'– Commonly used approaches

- Analytical Approach
- Empirical Schemes
- Block fall / slide analysis
- Numerical Approach

Rock Engineering Design Approaches and challenges in Deep Hard Rock Mining Engineering – Dec. 15th, 2019 – Shahrood UT

Analytical Approach

1. Beam theory
2. Voussoir beam theory
3. Arching theory
4. Kirsch theory

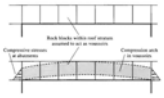

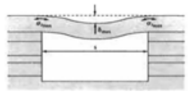

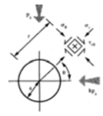

Rock Engineering Design Approaches and challenges in Deep Hard Rock Mining Engineering – Dec. 15th, 2019 – Shahrood UT

Stresses and displacements induced around a circular excavation in plane strain

In rock mechanics, the Kirsch equations are the most widely used suite of equations from the theory of elasticity. They allow the determination of stresses and displacements around a circular excavation.

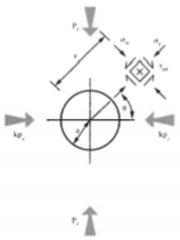

$$\sigma_r = \frac{1}{2}p_z\left\{(1+k)\left(1-\frac{a^2}{r^2}\right)-(1-k)\left(1-4\frac{a^2}{r^2}+3\frac{a^4}{r^4}\right)\cos 2\theta\right\}$$

$$\sigma_\theta = \frac{1}{2}p_z\left\{(1+k)\left(1+\frac{a^2}{r^2}\right)+(1-k)\left(1+3\frac{a^4}{r^4}\right)\cos 2\theta\right\}$$

$$\tau_{r\theta} = \frac{1}{2}p_z\left\{(1-k)\left(1+2\frac{a^2}{r^2}-3\frac{a^4}{r^4}\right)\sin 2\theta\right\}$$

$$u_r = -\frac{p_z a}{4G}\left\{(1+k)-(1-k)\left(4(1-\nu)-\frac{a^2}{r^2}\right)\cos 2\theta\right\}$$

$$u_\theta = -\frac{p_z a}{4G}\left\{(1-k)\left(2(1-2\nu)+\frac{a^2}{r^2}\right)\sin 2\theta\right\}$$

Rock Engineering Design Approaches and challenges in Deep Hard Rock Mining Engineering – Dec. 15th, 2019 – Shahrood UT

Stresses induced around a circular excavation

- With assuming r=a :

$\sigma_r = 0$
$\sigma_\theta = p_z[(1+k) + 2(1-k)\cos 2\theta]$
$\tau_{r\theta} = 0$

- Maximum tangential stress:

Max. Tangential Stress
$\sigma_{\theta max} = 3\sigma_1 - \sigma_3 = 3(k-1)\sigma_3$

- Minimum tangential stress:

Min. Tangential Stress
$\sigma_{\theta min} = 3\sigma_3 - \sigma_1 = 3(1-k)\sigma_3$

- If K=1

$\sigma_r = p_z\{1 - (a^2/r^2)\}$
$\sigma_\theta = p_z\{1 + (a^2/r^2)\}$

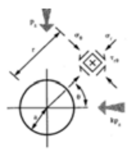

Rock Engineering Design Approaches and challenges in Deep Hard Rock Mining Engineering – Dec. 15th, 2019 – Shahrood UT

Stress concentration due to the excavation

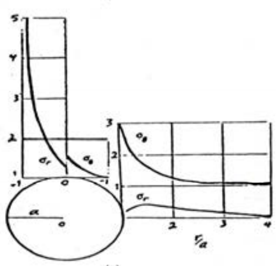

(a)

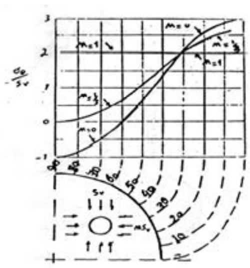

(b)

Rock Engineering Design Approaches and challenges in Deep Hard Rock Mining Engineering – Dec. 15th, 2019 – Shahrood UT

Empirical Systems

- Tunneling Index (Q or Q' system)
- Geomechanics Classification or Rock Mass Rating System (RMR) (or MRMR)

(Hoek, E (2000) Rock Engineering)

Rock mass classification RMR system

(a) Five basic rock mass classification parameters and their ratings

	Parameter								
1.	Strength of intact rock material	Point load strength index (MPa)	> 10	4 – 10	2 – 4	1 – 2			
		Uniaxial compressive strength (MPa)	> 250	100 – 250	50 – 100	25 – 50	5 – 25	1 – 5	< 1
	Rating		*15*	*12*	*7*	*4*	*2*	*1*	*0*
2.	RQD (%)		90 – 100	75 – 90	50 – 75	25 – 50	< 25		
	Rating		*20*	*17*	*13*	*8*	*3*		
3.	Joint spacing (m)		> 2	0.6 – 2	0.2 – 0.6	0.06 – 0.2	< 0.06		
	Rating		*20*	*15*	*10*	*8*	*5*		
4.	Condition of joints		not continuous, very rough surfaces, unweathered, no separation	slightly rough surfaces, slightly weathered, separation <1 mm	slightly rough surfaces, highly weathered, separation <1 mm	continuous, slickensided surfaces, or gouge <5 mm thick, or separation 1–5 mm	continuous joints, soft gouge >5 mm thick, or separation >5 mm		
	Rating		*30*	*25*	*20*	*10*	*0*		
5.	Groundwater	inflow per 10 m tunnel length (l /min), or joint water pressure/major in situ stress, or general conditions at excavation surface	none 0 completely dry	< 10 0 – 0.1 damp	10 – 25 0.1 – 0.2 wet	25 – 125 0.2 – 0.5 dripping	> 125 >0.5 flowing		
	Rating		*15*	*10*	*7*	*4*	*0*		

(b) Rating adjustment for joint orientations

Strike and dip orientation of joints		very favourable	favourable	fair	unfavourable	very unfavourable
Rating	tunnels	0	– 2	– 5	– 10	– 12
	foundations	0	– 2	– 7	– 15	– 25
	slopes	0	– 5	– 25	– 50	– 60

(c) Effects of joint orientation in tunnelling

Strike perpendicular to tunnel axis				Strike parallel to tunnel axis		Dip 0° – 20°
Drive with dip		Drive against dip				
Dip 45° – 90° very favourable	Dip 20° – 45° favourable	Dip 45° – 90° fair	Dip 20° – 45° unfavourable	Dip 45° – 90° very unfavourable	Dip 20° – 45° fair	irrespective of strike fair

Applications – Stand-up Time

- Application of RMR for estimation of tunnel stand-up time.
- Guidelines apply to a 10m span horseshoe shaped tunnel, in a rock mass subjected to σ_v <25 MPa.

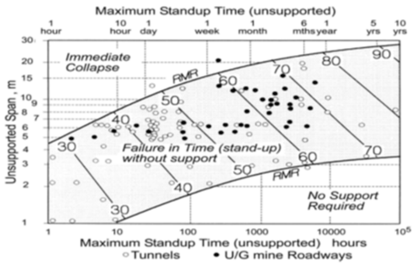

Applications – Stand-up Time RMR

Rock mass class	Excavation	Rock bolts (20 mm diameter, fully grouted)	Shotcrete	Steel sets
I - Very good rock *RMR*: 81-100	Full face, 3 m advance.	Generally no support required except spot bolting.		
II - Good rock *RMR*: 61-80	Full face , 1-1.5 m advance. Complete support 20 m from face.	Locally, bolts in crown 3 m long, spaced 2.5 m with occasional wire mesh.	50 mm in crown where required.	None.
III - Fair rock *RMR*: 41-60	Top heading and bench 1.5-3 m advance in top heading. Commence support after each blast. Complete support 10 m from face.	Systematic bolts 4 m long, spaced 1.5 - 2 m in crown and walls with wire mesh in crown.	50-100 mm in crown and 30 mm in sides.	None.
IV - Poor rock *RMR*: 21-40	Top heading and bench 1.0-1.5 m advance in top heading. Install support concurrently with excavation, 10 m from face.	Systematic bolts 4-5 m long, spaced 1-1.5 m in crown and walls with wire mesh.	100-150 mm in crown and 100 mm in sides.	Light to medium ribs spaced 1.5 m where required.
V – Very poor rock *RMR*: < 20	Multiple drifts 0.5-1.5 m advance in top heading. Install support concurrently with excavation. Shotcrete as soon as possible after blasting.	Systematic bolts 5-6 m long, spaced 1-1.5 m in crown and walls with wire mesh. Bolt invert.	150-200 mm in crown, 150 mm in sides, and 50 mm on face.	Medium to heavy ribs spaced 0.75 m with steel lagging and forepoling if required. Close invert.

STOPE SPAN DESIGN CURVE

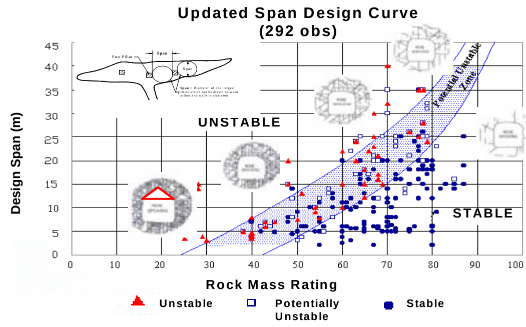

Empirical Systems - Rock Tunneling Quality Index, Q

- **Q Index**
  - Barton et al (1974) (Updated by Potvin to include SRF)
  - Via back analysis of large number of underground excavations

$$Q = \frac{RQD}{Jn} x \frac{Jr}{Ja} x \frac{Jw}{SRF}$$

- RQD – Rock Quality designation 100%
- Jn – Joint set number 3 Sets Jn = 9
- Jr – Joint Roughness number smooth Planar Jr =1.0
- Ja – Joint alteration number slightly altered Ja = 2
- Jw – Joint water reduction Number no water Jw = 1
- SRF – Stress reduction Factor SRF = 1
- Gives Q = 16

Excavation Support Analysis

	Excavation Category	ESR
A	Temporary mine openings	3-5
B	Permanent mine openings, water tunnels for hydro power excluding high pressure penstocks, pilot tunnels, drifts and headings for large excavations	1.6
C	Storage rooms, water treatment plants, minor road and railway tunnels, surge chambers, access tunnels	1.3
D	Power stations, major road and railway tunnels, civil defence chambers, portal excavations	1.0
E	Underground nuclear power stations, railway stations, sports and public facilities, factories	0.8

$$D_e = \frac{\text{Excavation Span, Diameter or Height (m)}}{\text{Excavation Support Ratio (ESR)}}$$

Excavation Support Analysis

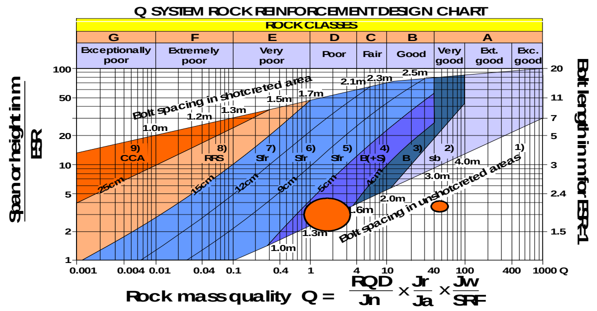

85

Rock Engineering Design Approaches and challenges in Deep Hard Rock Mining Engineering – Dec. 15th, 2019 – Shahrood UT

Q Application

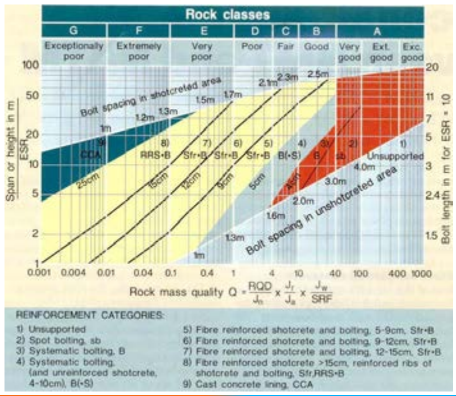

86

Rock Engineering Design Approaches and challenges in Deep Hard Rock Mining Engineering – Dec. 15th, 2019 – Shahrood UT

Q Classification Scheme

Roof pressure: $P_{roof} = \left(\frac{\sqrt{J_n}}{J_r}\right) Q^{-\frac{1}{3}}$ $\qquad P_{roof} = \left(\frac{0.2 \cdot \sqrt{J_n}}{3 \cdot J_r}\right) Q^{-\frac{1}{3}}$

Length of the bolts: (roof) $= 2 + \frac{0.15 \times H}{ESR}$ $\qquad$ (walls) $\frac{0.15 \times H}{ESR}$

Bhasin & Grimstad (1996): $P_{roof} = \left(\frac{40\, s}{J_r}\right) Q^{-\frac{1}{3}}$

Young's modulus: $E = 10^{3}\sqrt[3]{Q \frac{R_c}{3}}\ [MPa]$

Seismic wave velocity: $V_p = 3.5 + \log Q \frac{R_c}{100}\ [km/s]$

87

Rock Engineering Design Approaches and challenges in Deep Hard Rock Mining Engineering – Dec. 15th, 2019 – Shahrood UT

88

Rock Engineering Design Approaches and challenges in Deep Hard Rock Mining Engineering – Dec. 15th, 2019 – Shahrood UT

Correlation between Q - RMR

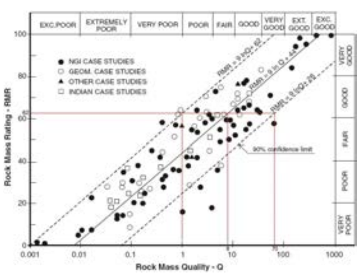

Correlation	Source
$RMR = 9 \ln Q + 44$	Bieniawski (1976)
$RMR = 13.5 \log Q + 43 = 5.9 \ln Q + 43$	Rutledge and Preston (1978)
$RMR = 5 \ln Q + 60.8$ (from in situ data)	Cameron-Clarke & Budavari (1981)
$RMR = 4.6 \ln Q + 55.5$ (from bore core data)	Cameron-Clarke & Budavari (1981)
$RMR = 12.5 \log Q + 55.2 = 5.4 \ln Q + 55.2$	Moreno Tallon (1982)
$RMR = 7.5 \ln Q + 42$	Baczynski (1983)
$RMR = 12.11 \log Q + 50.81 = 5.3 \ln Q + 50.81$	Udd and Wang (1985)
$RMR = 10 \ln Q + 39$	Choquet & Charette (1988)
$RMR = 6.3 \ln Q + 41.6$	Kaiser et al. (1986)
$RMR = 8.7 \ln Q + 38 \pm 18$ (probability theory)[a]	Kaiser et al. (1986)
$RMR = 6.8 \ln Q + 42$[b]	Sheorey (1993)
$RMR = 10.3 \ln Q + 49.3$ (when $Q \le 1$, $SRF = 1$)[c]	Rawlings et al. (1995)
$RMR = 6.2 \ln Q + 49.2$ (when $Q > 1$, $SRF = 1$)[c]	Rawlings et al. (1995)
$RMR = 6.6 \ln Q + 53$ (when $Q \le 0.65$)[c]	Rawlings et al. (1995)
$RMR = 5.7 \ln Q + 54.3$ (when $Q > 0.65$)[c]	Rawlings et al. (1995)
$RMR = 4.7 \ln Q + 56.8$	Kumar et al. (2004)
$RMR = 8.3 \ln Q + 42.5$ (with $SRF = 1$)	Kumar et al. (2004)
$RMR = 6.4 \ln Q + 49.6$ (with revised SRF values)	Kumar et al. (2004)
$RMR = 10.5 \ln Q + 41.8$	Abad et al. (1983)
$RMR = 7 \ln Q + 36$	Tugrul (1998)
$RMR = 5.97 \ln Q + 49.5$	Sunwoo & Hwang (2001)
$RMR = 3.7 \ln Q + 53.1$	Sari & Pasamehmetoglu (2004)
$RMR = 43.89 - 9.19 \ln Q$	Celada Tamames (1983)
$RMR = 9 \ln Q + 49$	Al Harthi (1993)
$RMR = 4.2 \ln Q + 50.6$	Asgari (2001)

[a] assuming RMR and ln Q are normal variates and satisfy the central limit theory of pr… [b] derived from the data presented by Sheorey (1993); [c] from bore core data

89

Rock Engineering Design Approaches and challenges in Deep Hard Rock Mining Engineering – Dec. 15th, 2019 – Shahrood UT

Geological Strength Index: GSI

Strength of jointed rockmass depends on:

- properties of intact rock pieces, and
- upon the freedom of these pieces to slide and rotate under different stress conditions,
- controlled by the geometrical shape of the intact rock pieces as well as the condition of the discontinuities separating the pieces

GSI Value	76 – 95	56 – 75	36 – 55	21 – 35	< 20
Rock Mass Quality	Very good	Good	Fair	Poor	Very poor

Hoek, 2000

90

Hoek – Brown failure criterion

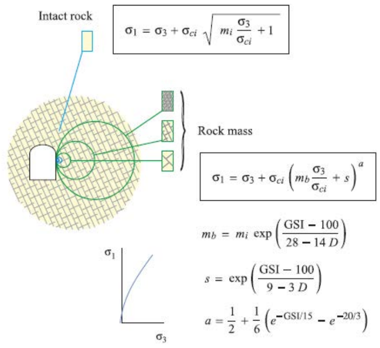

$$\sigma_1 = \sigma_3 + \sigma_{ci}\sqrt{m_i\frac{\sigma_3}{\sigma_{ci}} + 1}$$

$$\sigma_1 = \sigma_3 + \sigma_{ci}\left(m_b\frac{\sigma_3}{\sigma_{ci}} + s\right)^a$$

$$m_b = m_i \exp\left(\frac{\mathrm{GSI} - 100}{28 - 14D}\right)$$

$$s = \exp\left(\frac{\mathrm{GSI} - 100}{9 - 3D}\right)$$

$$a = \frac{1}{2} + \frac{1}{6}\left(e^{-\mathrm{GSI}/15} - e^{-20/3}\right)$$

91

91

Rock Engineering Design Approaches and challenges in Deep Hard Rock Mining Engineering – Dec. 15th, 2019 – Shahrood UT

GSI

$$m_b = m_i \exp\left(\frac{GSI - 100}{28 - 14D}\right)$$

For $GSI > 25$:

$$s = \exp\left(\frac{GSI - 100}{9 - 3D}\right)$$

and

$a = 0.5$

For $GSI < 25$:

$s = 0$

and

$$a = 0.65 - \frac{GSI}{200}$$

92

92

Rock Engineering Design Approaches and challenges in Deep Hard Rock Mining Engineering – Dec. 15th, 2019 – Shahrood UT

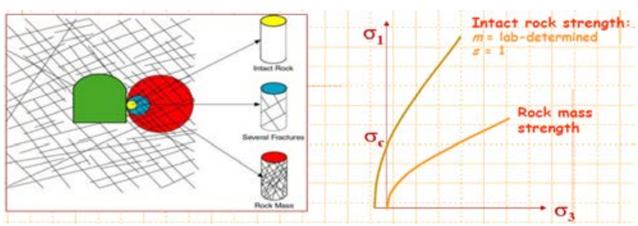

93

93

Rock Engineering Design Approaches and challenges in Deep Hard Rock Mining Engineering – Dec. 15th, 2019 – Shahrood UT

Block fall/slide analysis (Structurally controlled)

Structurally-controlled instability means that blocks formed by discontinuities either fall or slide from the excavation periphery as a result of the body forces (usually gravity) enabled by the process of excavation. To assess the likelihood of such failures, an analysis of the kinematic admissibility of potential wedges or planes that intersect the excavation face(s) can be performed.

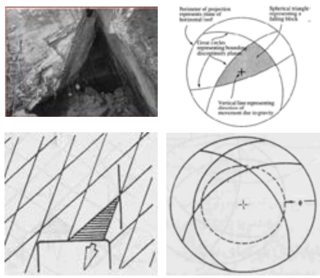

$$\tau = c + \sigma_n \tan\phi$$

94

94

Rock Engineering Design Approaches and challenges in Deep Hard Rock Mining Engineering – Dec. 15th, 2019 – Shahrood UT

Block analysis using limit equilibrium method (Unwedge)

Joint set	dip°	dip direction°
J1	70 ± 5	036 ± 12
J2	85 ±8	144 ± 10
J3	55 ± 6	262 ± 15

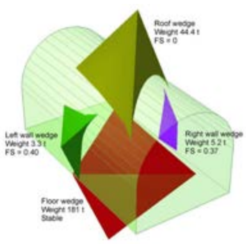

95

95

Rock Engineering Design Approaches and challenges in Deep Hard Rock Mining Engineering – Dec. 15th, 2019 – Shahrood UT

Block analysis using limit equilibrium method (Unwedge)

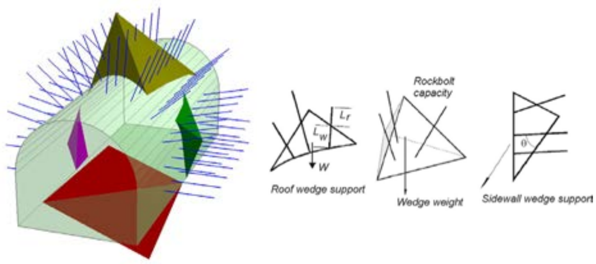

96

96

Numerical methods

- **Software:**
- *FEM* (Finite Element Method) → *PHASE²*
- *FDM* (Finite Difference Method) → *FLAC 2D and 3D*
- *BEM* (Boundery Element Method) → *MAP 3D , Examine*
- *DEM* (Distinct Element Method) → *UDEC*
- *3DEC*

97

Numerical methods

- Continuum analysis → • Phases, Examine,
- Discontinuum analysis → Map3d....

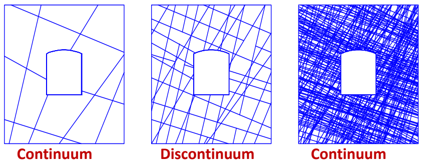

98

Numerical methods

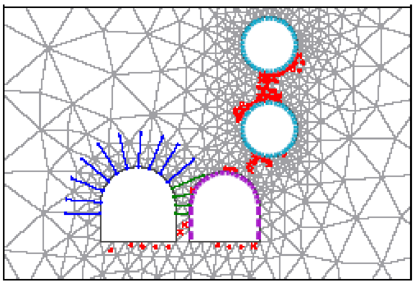

Design of Support System in FE Analysis (o: Yield in Tension, x: Yield in Compression)

99

Stress concentration due to excavation – Numerical analysis

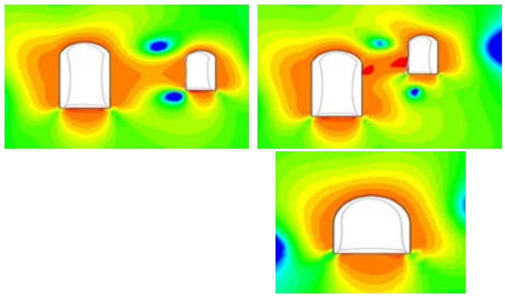

100

EMPIRICAL DESIGN METHOD

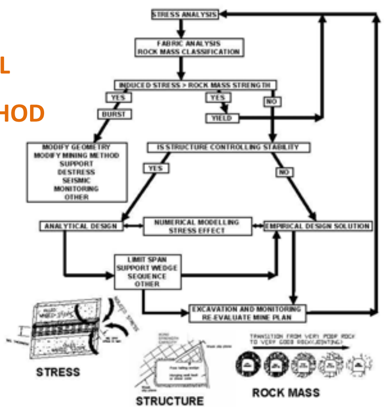

Rimas Pakalnis, 2014

101

EMPIRICAL DESIGN METHOD

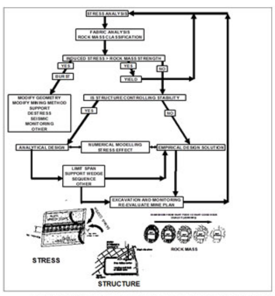

Fig. DESIGN METHODOLOGY INCORPORATING STRESS, STRUCTURE AND THE ROCK MASS

Empirical derivations have gained acceptance over the last thirty years largely due to their predictive capability since conventional methods of assessment have the difficulty of identifying the jointed nature of the rock material, assigning properties thereto and establishing input parameters for subsequent numerical evaluation. The process that the author has found to be of greatest value is to employ numerical codes, analytical tools and observational approaches as tools to the overall design process which will incorporate an empirical component towards the design. Individually each is only a tool that requires the designer to address the factors most critical to the stability of the overall underground structure which includes stress, structure and the rock mass as shown in Figure 1.

Rimas Pakalnis, 2014

102

Rock Engineering Design Approaches and challenges in Deep Hard Rock Mining Engineering – Dec. 15th, 2019 – Shahrood UT

Design Methodology Pakalnis (2008)

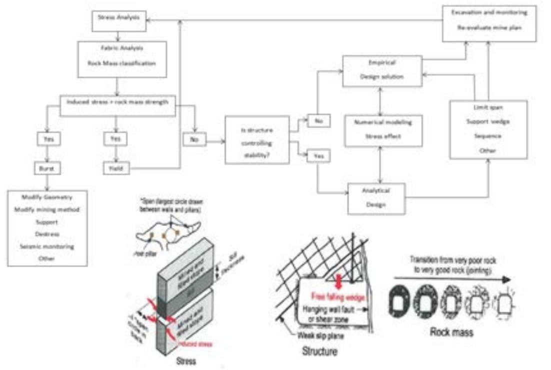

103

103

Rock Engineering Design Approaches and challenges in Deep Hard Rock Mining Engineering – Dec. 15th, 2019 – Shahrood UT

Stope stability assessment methods

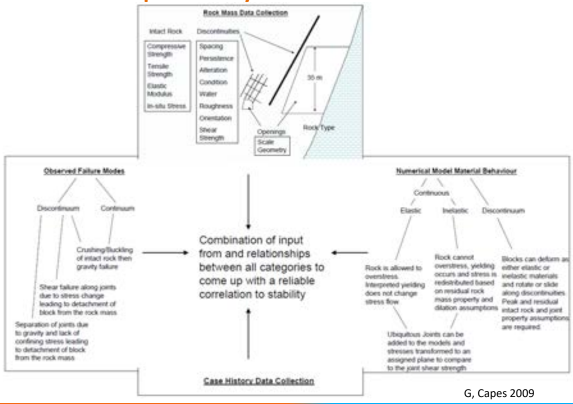

G, Capes 2009

104

104

Rock Engineering Design Approaches and challenges in Deep Hard Rock Mining Engineering – Dec. 15th, 2019 – Shahrood UT

Empirical Method of Design in Mining

A frequently used empirical method is one initially developed by Mathews et al. to the. in 1981, later modified by Potvin (1988) and Milne (1989).

The Mathews Stability Graph is a plot of **Stability Number (N)** against **Shape Factor or a Hydraulic Radius (RH).**

The hydraulic RADIUS is equal to the ratio of the area of a excavation face to the perimeter.

105

105

Rock Engineering Design Approaches and challenges in Deep Hard Rock Mining Engineering – Dec. 15th, 2019 – Shahrood UT

The stability number : N

The value of **N** is given by the following equation:

$$N = Q' \times A \times B \times C$$

Where:

Q' is the ***modified rock quality index*** where Jw/SRF = 1.

$$Q' = (RQD/Jn)\ (Jr/Ja)$$

- **A** is the rock ***stress factor.*** It replaces the SRF and varies from 0.1 and 1
- **B** is the ***joint orientation factor***. Varies between 0.3 /0.2 up to 1
- **C** is the ***factor of gravity*** **,** is related to the failure process by the rock block own weight. Varies from 2 to 8

106

106

Rock Engineering Design Approaches and challenges in Deep Hard Rock Mining Engineering – Dec. 15th, 2019 – Shahrood UT

Factor A, B, C

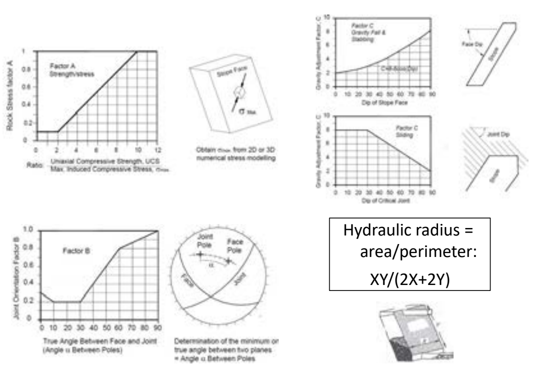

107

107

Rock Engineering Design Approaches and challenges in Deep Hard Rock Mining Engineering – Dec. 15th, 2019 – Shahrood UT

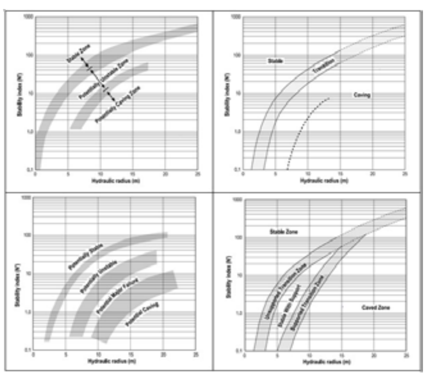

Stability index (N') versus the stope hydraulic radius.

Various authors, clock-wise from top left:

Mathews et al., 1981, Potvin, 1988, Nickson, 1992 and Stewart and Forsyth, 1993,

108

108

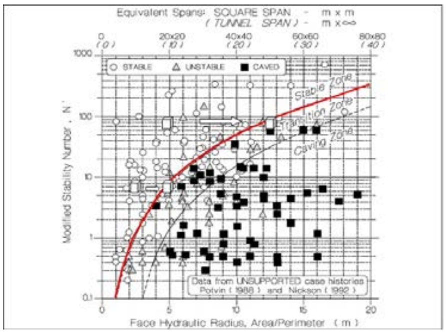

The Potvin, 1988 and Nickson, 1992 combined data base of unsupported case records. The 'cubes' correspond to caverns in civil works (added by NB). The red curve corresponds to an ESR of about 4.

109

109

AN EXPLANATION OF ESR(see left axis)

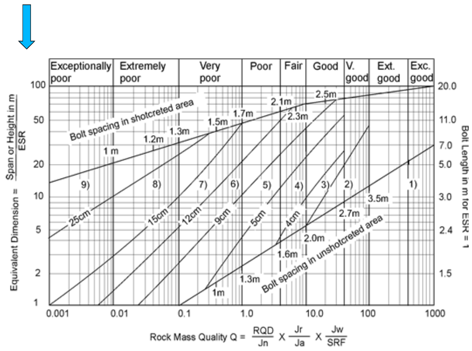

110

110

	Type of Excavation	ESR
A	Temporary mine openings, *etc.*	*ca* 2-5
B	Permanent mine openings, water tunnels for hydropower (exclude high pressure penstocks), pilot tunnels, drifts and headings for large openings, surge chambers	1.6-2.0
C	Storage caverns, water treatment plants, minor road and railway tunnels, access tunnels	1.2-1.3
D	Power stations, major road and railway tunnels, civil defence chambers, portals, intersections	0.9-1.1
E	Underground nuclear power stations, railway stations, sports and public facilities, factories, major gas pipeline tunnels	0.5-0.8

111

111

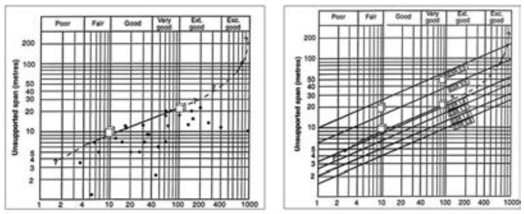

PERMANENTLY UNSUPPORTED TUNNELS AND CAVERNS, AND THE WORKINGS OF THE ESR (degree-of-safety) NUMBER.

General requirements for permanently unsupported openings

1. $Jn \leq 9$, $Jr \geq 1.0$, $Ja \leq 1.0$, $Jw = 1.0$, $SRF \leq 2.5$

Conditional requirements

2. If RQD ≤ 40, should have $J_n \leq 2$
3. If J_n = 9, should have $J_r \geq 1.5$ and RQD ≥ 90
4. If J_r = 1, should have $J_n < 4$
5. If SRF > 1, should have $J_r \geq 1.5$
6. If SPAN > 10 m, should have $J_n < 9$
7. If SPAN > 20 m, should have $J_n \leq 4$ and SRF ≤ 1

Note that the ESR = 1.6 line is closest to the 'envelope' drawn in the left-hand figure. This is too conservative for temporary-stope mining use. Some 'cross-plotting' cubes are shown: civil contra mining.

112

112

An attempt to relate civil (ESR) to mining

(Left: combined Potvin, 1988 and Nickson, 1992 data: Capes)

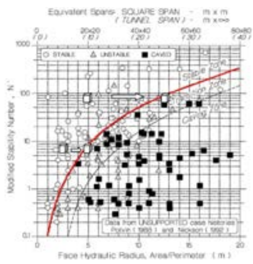

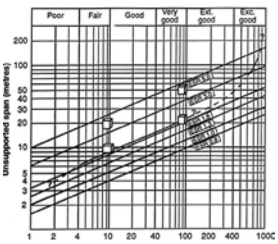

The 'cubes' showing 10 m increasing to 20 m, and 20 m increasing to 50 m span (approx.) in order to reach the red envelope.

113

113

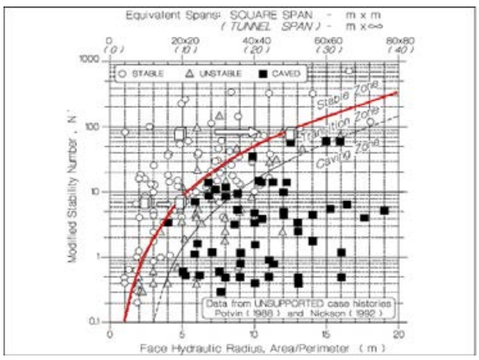

114

114

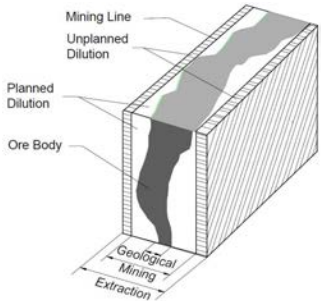

A simple definition of (average) dilution, beyond the planned and inevitable dilution.

Figure based on Scoble and Moss, 1995, but reproduced from Capes, 2009

115

115

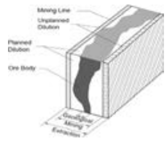

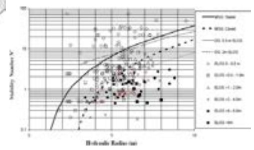

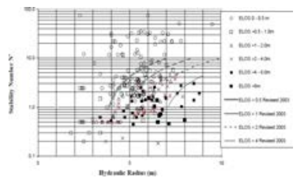

The 255 cases assembled by Capes, 2009, showing: a) the stable and caved Modified Stability Graph curves, and b) ELOS Dilution Graph curve.

116

116

"KNOW THY DATA BASE" AS EMPIRICAL DESIGN REQUIRES INTERPOLATION NOT EXTRAPOLATION!

- Use of empirical methods inherently made these systems more reliable as they are refined/verified.
- Empirical methods are evolving and application a t times confusing
- Methods in this talk have a strong analytical foun dation coupled with extensive field observation to arrive at a calibrated empirical ap proach towards the solution to a given problem.

117

117

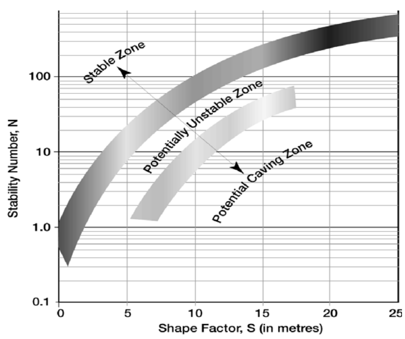

Three stability zones of original Mathews Stability graph.

118

118

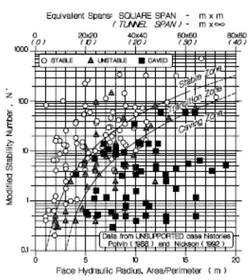

Database Potvin 1988 and Nickson 1992 Unsupported stopes

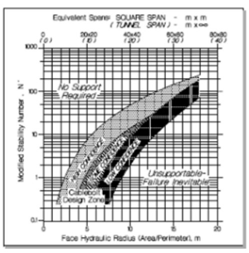

Design Zones for open stopes using Stability Graphs

119

119

The Stability Graph Method

The Stability Graph Method for open stope design was initially proposed by Mathews et al. (1980) and subsequently modified by Potvin (1988) and Nickson (1992) to arrive at the Modified Stability Graph. Stability was qualitatively assessed as either being stable, potentially unstable or caved. Research at the

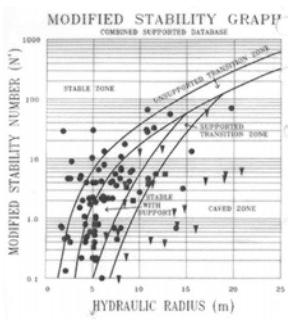

120

120

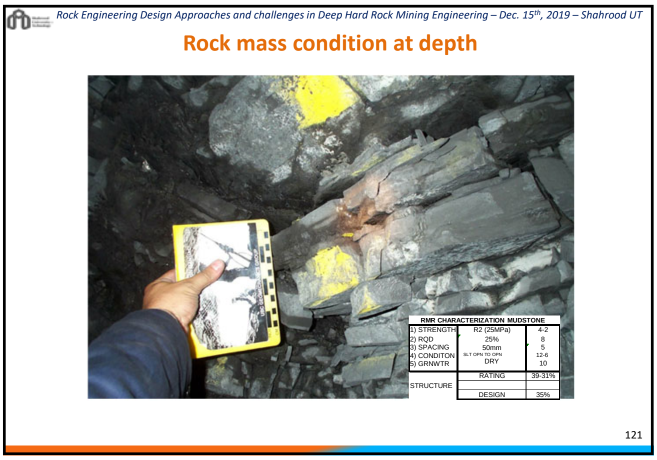

121

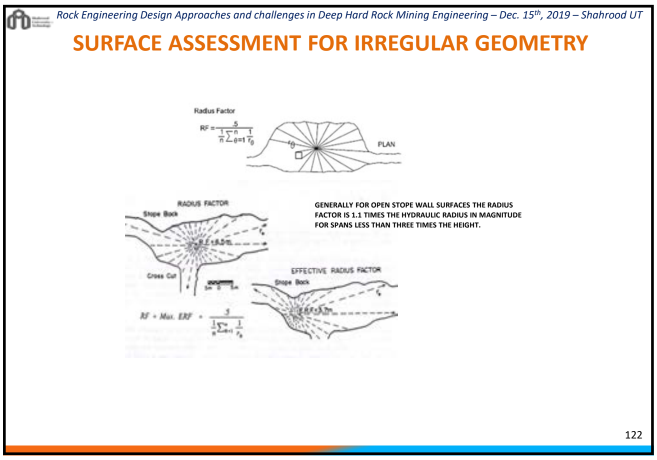

122

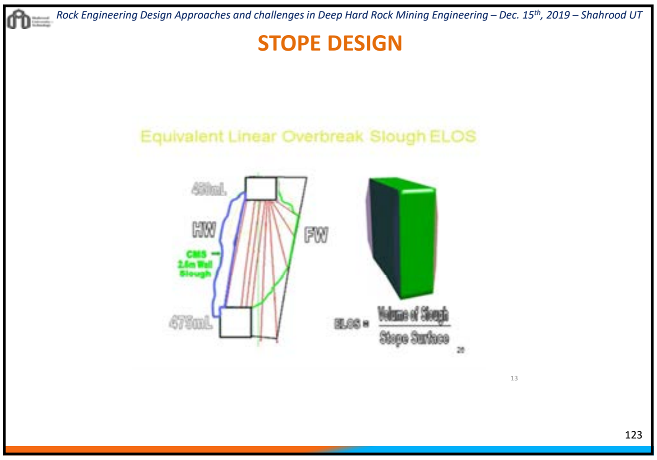

123

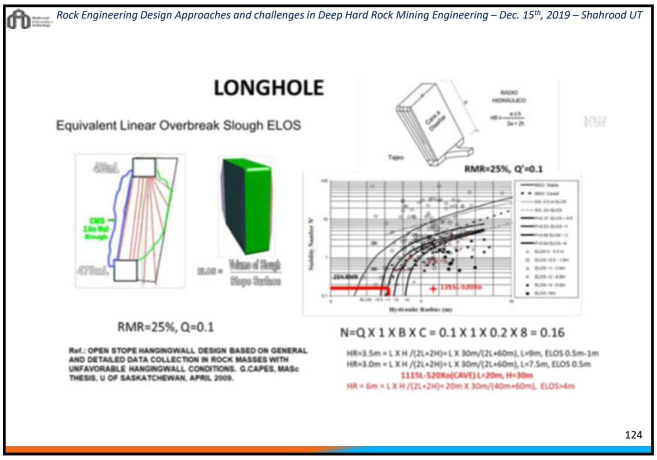

124

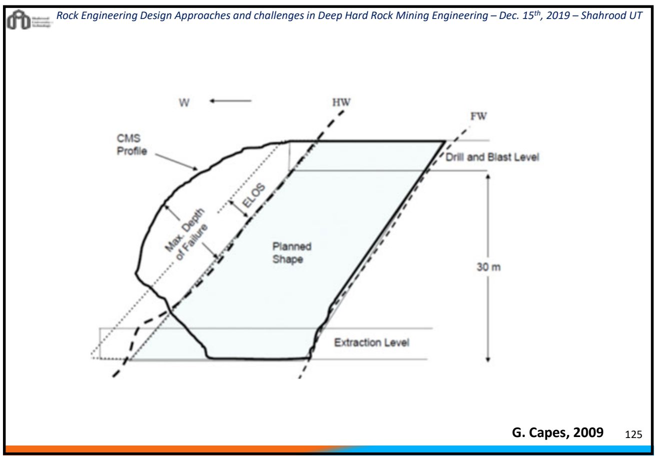

125

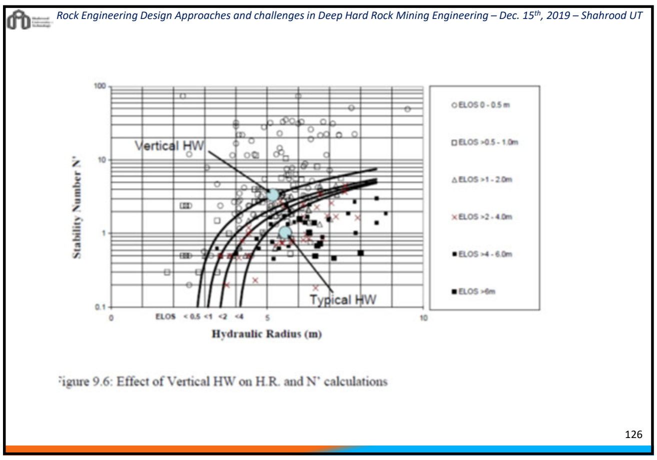

126

EMPIRICAL ESTIMATION OF WALL SLOUGH (ELOS) AFTER CLARK (1988).

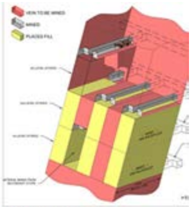

RELAXED HW
A = I
PARALLEL STRUCTURE
B=0.2,0.3
WALL DIP
C=8-6COS ϕ

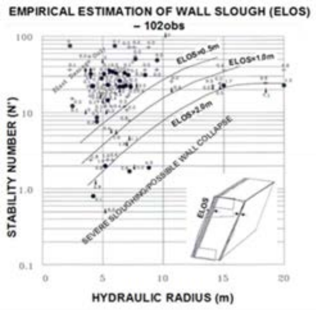

127

Rock Engineering Design Approaches and challenges in Deep Hard Rock Mining Engineering – Dec. 15th, 2019 – Shahrood UT

2.2 Span Design – Entry Methods

The Critical Span Curve (Lang, 1994) has been augmented to include 292 case histories of stable and unstable entry-type stope backs from six (6) different mines by Wang (2000). It expands on the original database to incorporate lower rock mass ratings. This is shown in Figure 3. The critical span is defined as the diameter of the largest circle that can be drawn within the boundaries of the exposed back as viewed in plan and shown in Figure 3. This exposed span is then related to the prevailing rock mass of the immediate back to arrive at a stability condition. The design span refers to spans which have used no support and/or spans which include pattern bolting (1.8m long bolts on 1.2m x 1.2m) for local support. The rock mass rating as proposed by Bieniawski (1976) is employed with corrections for the presence of shallow joints (under 30°) by reducing the RMR by "10". The stability of the excavation is classified into three categories:

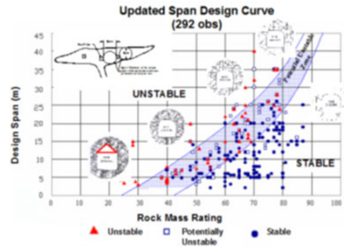

Figure 3. Critical span curve for mine entry methods employing local support only.

128

Rock Engineering Design Approaches and challenges in Deep Hard Rock Mining Engineering – Dec. 15th, 2019 – Shahrood UT

Empirical methods of design support systems

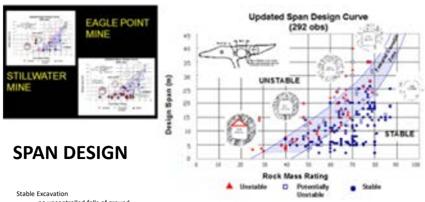

SPAN DESIGN

Stable Excavation
no uncontrolled falls of ground.
no movement of back observed
no extraordinary support measures have been implemented.

Potentially Unstable Excavation
extra ground support may have been installed to prevent potential falls of ground
movement within back
increased frequency of ground working

Unstable Excavation
the area has collapsed
failure above the back is approximately 0.5 x span in the absence of major structure
support was not effective to maintain stability.

CRITICAL SPAN CURVE FOR MINE ENTRY METHODS EMPLOYING LOCAL SUPPORT ONLY

16

129

Rock Engineering Design Approaches and challenges in Deep Hard Rock Mining Engineering – Dec. 15th, 2019 – Shahrood UT

PILLAR DESIGN

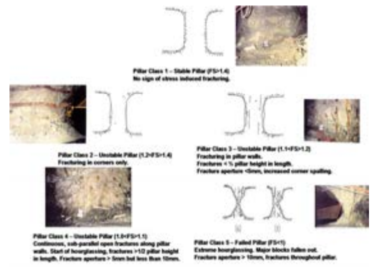

130

Rock Engineering Design Approaches and challenges in Deep Hard Rock Mining Engineering – Dec. 15th, 2019 – Shahrood UT

Graph for assessment of stability and geometry of pillars in mines (Pakalnis, 2014)

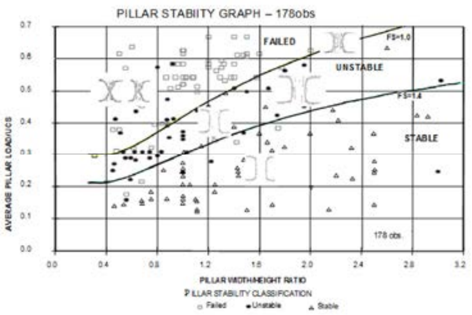

131

Rock Engineering Design Approaches and challenges in Deep Hard Rock Mining Engineering – Dec. 15th, 2019 – Shahrood UT

Outline of support properties in underground excavation (Pakalnis, 2014)

Rock Bolt Properties

Bolt Type	Yield Strength	Breaking Strength
	(tonnes)	(tonnes)
5/8 inch mechanical	6.1	10.2 (Grade 690MPa)
Split Set (SS-33)	8.5	10.6
Split Set (SS-39)	12.7	14
Standard Swellex	N/A	11
Yielding Swellex	N/A	9.5
Super Swellex	N/A	22
20mm rebar (#6)	12.4	18.5
22mm rebar (#7)	16	23
25mm rebar (#8)	20.5	30.8
#6 Dywidag	11.9	18
#7 Dywidag	16.3	24.5
#8 Dywidag	21.5	32.3
#9 Dywidag	27.2	40.9
#10 Dywidag	34.6	52
1/2 inch Cable Bolt	15.9	18.8
5/8 inch Cable Bolt	21.6	25.5
1/4" X 4" Strap (M.S)	25	39

#6 refers to 6/8", #7 refers to 7/8" diameter etc

SCREEN - BAG STRENGTH 4ft X 4ft PATTERN

4x4" Welded wire mesh (4 gauge)	Bag Strength = 3.6 tonne
4x4" Welded wire mesh (6 gauge)	Bag Strength = 3.3 tonne
4x4" Welded wire mesh (9 gauge)	Bag Strength = 1.9 tonne
4x2" Welded wire mesh (12 gauge)	Bag Strength = 1.4 tonne
2" chainlink (11 guage bare metal)	Bag Strength = 2.9 tonne
2" chainlink (11 guage galvanized)	Bag Strength = 1.7 tonne
2" chainlink (9 gauge bare metal)	Bag Strength = 3.7 tonne
2" chainlink (9 gauge galvanized)	Bag Strength = 3.2 tonne

4 gauge=.23" diam., 6gauge=0.20", 9 gauge=0.16" diam
11 gauge=0.125", 12 gauge=0.11" diam
shotcrete shear strength=2MPa=200tonnes/m^2

BOND STRENGTH

Bolt Type	Bond Strength
	(tonnes/m)
39mm Split Set Weak Ground(<45% RMR)	0.75-3.6
39mm Split Set Hard Ground (>55% RMR)	2.5-5
Standard Swellex Weak Ground(<45% RMR)	8.1-13.8
Standard Swellex Hard Ground(>55% RMR)	9-15
Cable Bolt Weak Ground(<45% RMR)	24
Cable Bolt Hard Ground(>55% RMR)	28
#6 Rebar Weak Ground(<45% RMR)	12-14
#6 Rebar Hard Ground(>55% RMR)	59

132

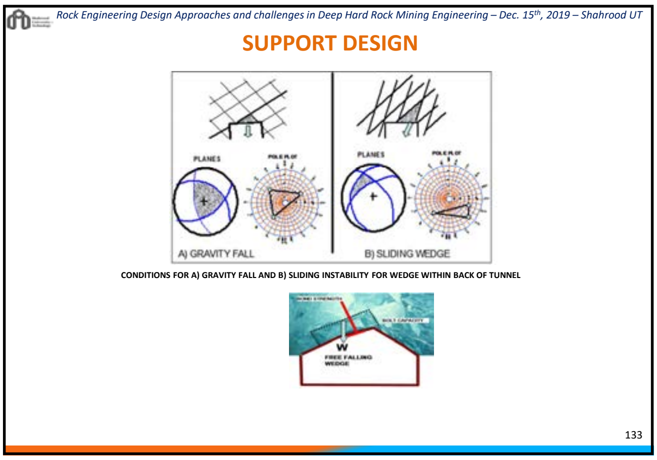

133

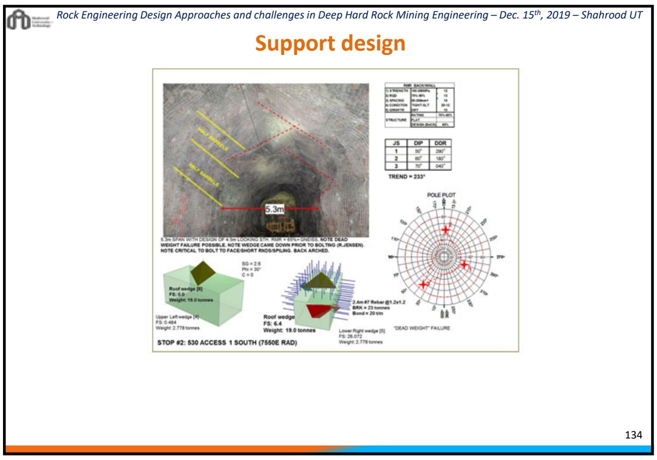

134

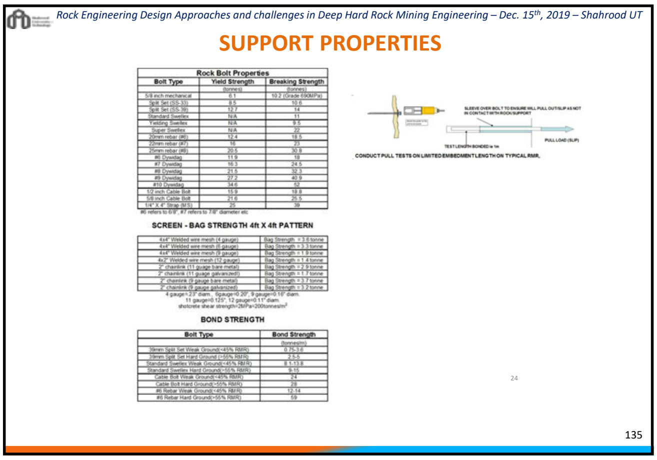

Rock Bolt Properties		
Bolt Type	Yield Strength	Breaking Strength
	(tonnes)	(tonnes)
5/8 inch mechanical	6.1	10.2 (Grade 690MPa)
Split Set (SS-33)	8.5	10.6
Split Set (SS-39)	12.7	14
Standard Swellex	N/A	11
Yielding Swellex	N/A	9.5
Super Swellex	N/A	22
20mm rebar (#6)	12.4	18.5
22mm rebar (#7)	16	23
25mm rebar (#8)	20.5	30.8
#6 Dywidag	11.9	18
#7 Dywidag	16.3	24.5
#8 Dywidag	21.5	32.3
#9 Dywidag	27.2	40.9
#10 Dywidag	34.6	52
1/2 inch Cable Bolt	15.9	18.8
5/8 inch Cable Bolt	21.6	25.5
1/4" X 4" Strap (M.S)	25	39

#6 refers to 6/8", #7 refers to 7/8" diameter etc

SCREEN - BAG STRENGTH 4ft X 4ft PATTERN

4x4" Welded wire mesh (4 gauge)	Bag Strength = 3.6 tonne
4x4" Welded wire mesh (6 gauge)	Bag Strength = 3.3 tonne
4x4" Welded wire mesh (9 gauge)	Bag Strength = 1.9 tonne
4x2" Welded wire mesh (12 gauge)	Bag Strength = 1.4 tonne
2" chainlink (11 guage bare metal)	Bag Strength = 2.9 tonne
2" chainlink (11 guage galvanized)	Bag Strength = 1.7 tonne
2" chainlink (9 gauge bare metal)	Bag Strength = 3.7 tonne
2" chainlink (9 gauge galvanized)	Bag Strength = 3.2 tonne

4 gauge=.23" diam., 6gauge=0.20", 9 gauge=0.16" diam.
11 gauge=0.125", 12 gauge=0.11" diam.
shotcrete shear strength=2MPa=200tonnes/m^2

BOND STRENGTH

Bolt Type	Bond Strength
	(tonnes/m)
39mm Split Set Weak Ground(<45% RMR)	0.75-3.6
39mm Split Set Hard Ground (>55% RMR)	2.5-5
Standard Swellex Weak Ground(<45% RMR)	8.1-13.8
Standard Swellex Hard Ground(>55% RMR)	9-15
Cable Bolt Weak Ground(<45% RMR)	24
Cable Bolt Hard Ground(>55% RMR)	28
#6 Rebar Weak Ground(<45% RMR)	12-14
#6 Rebar Hard Ground(>55% RMR)	59

135

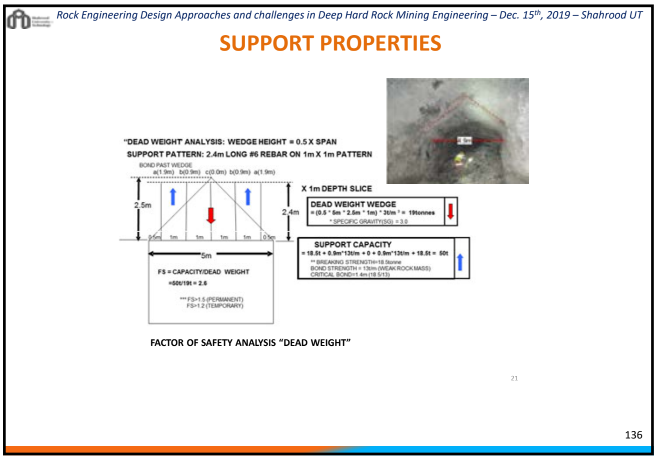

136

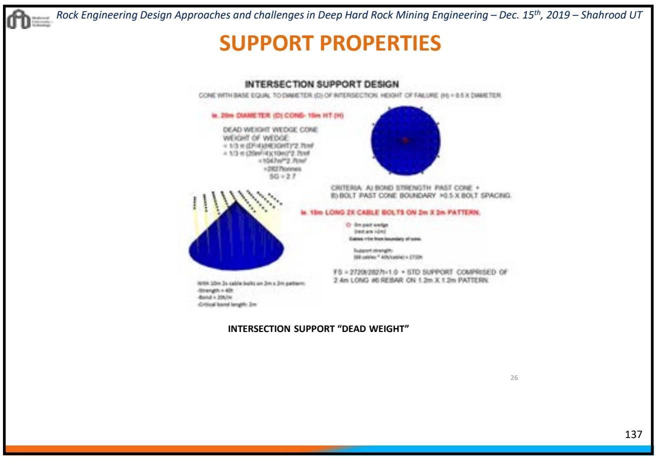

137

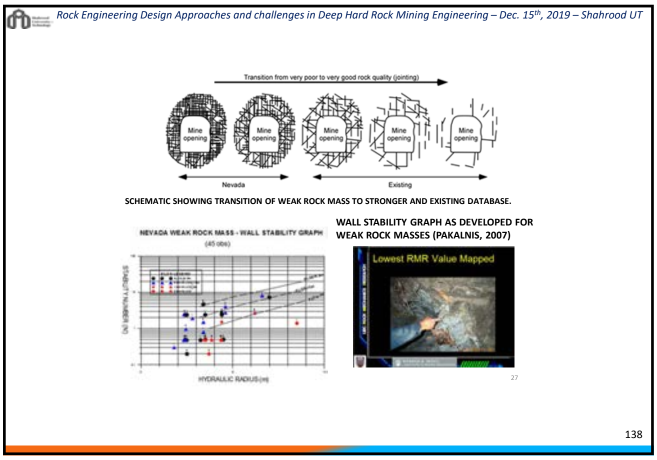

138

Cable Bolt Design

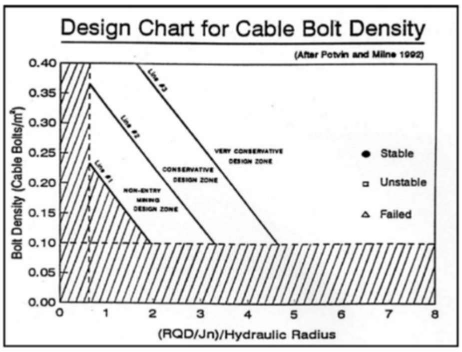

139

139

Presentation Outline

1) Introduction
2) Introducing Reinforcement Systems
3) Ground stabilization (Treatment) Design Fundamentals
4) Mine Opening Support Design Methods
5) **Summary**
6) References

140

140

THE OBJECTIVES OF GROUND STABLIZATION IN MINING

- Safe and economical excavation of ore
- Maximum recovery with minimum dilution
- For this purpose it is necessary to understand the:
- Ground condition consisting: Intact rock, discontinuities and rock mass behavior, geological structure, seismicity,…
- Ground behavior and probable failure mechanisms due to mining activities
- Reasonable countermeasure to control excavation instability and failure.

141

141

Main References:

1. ZHAO J., ROJAS R. Underground Construction Technology, Course Lectures 2008, EPFL.
2. Barton, N. 2002. Some new Q-value correlations to assist in site characterization and tunnel design. Int. Jnl Rock Mech Min Sc, 39, pp185-216
3. Barton, N., Lien, R., Lunde, J., 1974. Engineering classification of rock masses for the design of rock support. Rock Mech. 6, pp189-236.
4. Barton, N and Grimstad, E (1994). The Q-System following twenty years of application in NMT support selection, in Felsbau 12(6):428-436.
5. Bieniawski, Z.T.1988 The rock Mass Rating (RMR system (Geomechanics classification in Engineering Practice, in Rock Classification for Engineering Purposes, Kirkaldie L (Ed)
6. Grimstad, E and Barton, N (1993). Updating of the Q-system for NMT, in Proceedings of the International Symposium on Sprayed Concrete, 46-66. Norwegian Concrete Association, Oslo.
7. Hudson J A & Harrison J P (1997) Engineering Rock Mechanics, An Introduction to the principles, Pergamon.
8. Hutchinson, D.J., & Diederichs, M.S., 1996 Cablebolting in Underground Mines BiTech Publishers, Richmond
9. Hoek, E; Kaiser,P.K., and Bawden, W.F., 1995 Support of underground excavations in hard rock. Balkema, Rotterdam
10. Hoek, E. Rock Engineering. Course Notes. www.rocscience.com
11. Palmstrom, A, Milne, D & Peck, W. 2000. The reliability of rock mass classification used in underground excavation and support design. GeoEng Workshop www.ausmin.com.au
12. Peck, W. 2000 Determining the Stress Reduction Factor in Highly Stressed Jointed Rock. Australian Geomechanics, 35/2 pp57-60 www.ausmin.com.au
13. Stille H. & Palmstrom A. 2002 Classification as a tool for rock engineering, Tunnelling and Underground Space Technology, 18, pp331-345,
14. Villaescusa, Ernesto, (2014). Geotechnical Design for Sublevel Open Stoping, CRC Press, ISBN:9781482211887. http://link.library.curtin.edu.au/p?cur_aleph001151473

142

142

Presentation Outline

1) Introduction
2) Introducing Reinforcement Systems
3) Ground stabilization (Treatment) Design Fundamentals
4) Mine Opening Support Design Methods
5) Summary
6) **References**

143

143

Presentation Outline

1) Introduction
2) Introducing Reinforcement Systems
3) Ground stabilization (Treatment) Design Fundamentals
4) Mine Opening Support Design Methods
5) Summary
6) References

144

144

Introduction and motivation

✓Depleting surface resources and a tendency to use underground mines at great depth,

✓Development of urbanization construction of utilities such as power plant, gas storage and waste disposal in underground structures,

✓Great depth causes a growth potential of rock mass instabilities and risk of failures,

✓Application of appropriate design methodology is critical to overcome relevant challenges and problems and manage ground control.

145

145

Rock Engineering Design Approaches and challenges in Deep Hard Rock Mining Engineering – Dec. 15th, 2019 – Shahrood UT

References

Sharifzadeh M., Masoudi R., Ghorbani M. (2017) "Siah Bisheh Powerhouse Cavern Design Modification Using Observational Method and Back Analysis" Rock Mechanics And Engineering, Vol.5: Surface and Underground Projects, edited by Xia-Ting Feng, CRC press, Taylor and Francis Group, Pp.153-180.

Masoudi R., Sharifzadeh M., Ghorbani M. (2018). Partially decoupling and collar bonding of the encapsulated rebar rockbolts to improve their performance in seismic prone deep underground excavations, International Journal of Mining Science and Technology, In press, corrected proof, Available online 20 September 2018,

Li CC. Parameters required for the design of rock support in high-stress masses. In: Proceedings of the ISRM AfriRock-Rock Mechanics for Africa, Cape Town, South Africa. International Society for Rock Mechanics and Rock Engineering; 2017.

Louchnikov V, Sandy M. Selecting an optimal ground support system for rockbursting conditions. In: Proceedings of the 8th International Conference on Deep and High Stress Mining. Perth: Australian Centre for Geomechanics; 2017.

Masoudi R, Sharifzadeh M. Reinforcement selection for deep and high-stress tunnels at preliminary design stages using ground demand and support capacity approach. International Journal of Mining Science and Technology 2018; 28(4):573-82.

Morissette P, Hadjigeorgiou J, Punkkinen AR, Chinnasane DR. The influence of change in mining and ground support practice on the frequency and severity of rockbursts. In: Proceedings of the 7th International Conference on Deep and High Stress Mining, Sudbury, Ontario, Canada. 2014.

146

146

Rock Engineering Design Approaches and challenges in Deep Hard Rock Mining Engineering – Dec. 15th, 2019 – Shahrood UT

References

MOSHAB. Surface rock support for underground mines code of practice. Western Australia: Mines Occupational Safety and Health Advisory Board; 1999.

Potvin Y, Wesseloo J, Heal D. An interpretation of ground support capacity submitted to dynamic loading. Mining Technology 2010; 119(4):233-45.

Rahimi B, Shahriar K, Sharifzadeh M. Evaluation of rock mass engineering geological properties using statistical analysis and selecting proper tunnel design approach in Qazvin–Rasht railway tunnel. Tunnelling and Underground Space Technology 2014; 41:206-22.

Rahimi B, Sharifzadeh M. Evaluation of ground management in underground excavation design. In: Proceedings of the 8th International Conference on Deep and High Stress Mining. Perth: Australian Centre for Geomechanics. 2017. p. 813-26.

Saharan MR, Mitri H. Destress blasting as a mines safety tool: some fundamental challenges for successful applications. Procedia Engineering 2011; 26:37-47.

Sharifzadeh M, Kolivand F, Ghorbani M, Yasrobi S. Design of sequential excavation method for large span urban tunnels in soft ground–Niayesh tunnel. Tunnelling and Underground Space Technology 2013; 35:178-88.

Sharifzadeh M, Feng XT, Zhang X, Zhang Y. Challenges in Multi-Scale Hard Rock Behavior Evaluation at Deep Underground Excavations. In: Proceedings of the 12th Iranian and 3rd Regional Tunnelling Conference, Tunnelling and Climate Change, Tehran, Iran. 2017a.

Sharifzadeh M, Ghorbani M, Yasrobi S. Observation-based design of geo-engineering projects with emphasis on optimization of tunnel support systems and excavation sequences. In: Feng XT, editor. Rock Mechanics and Engineering Volume 4: Excavation, Support and Monitoring. London, UK: CRC Press; 2017b.

147

147

Rock Engineering Design Approaches and challenges in Deep Hard Rock Mining Engineering – Dec. 15th, 2019 – Shahrood UT

References

Stacey TR. Innovative and controversial support for rockbursting conditions. In: Proceeding of the 8th International Symposium on Ground Support in Mining and Underground Construction, Lulea, Sweden. 2016.

Szwedzicki T. Quality assurance in mine ground control management. International Journal of Rock Mechanics and Mining Sciences 2003; 40(4):565-72.

Talbot JF, Burke J. Practical improvements to the shotcreting process at Lisheen Mine with particular attention to the mix design and admixture usage. In: Proceedings of the 7th International Symposium on Ground Support in Mining and Underground Construction. Perth: Australian Centre for Geomechanics; 2013.

Yokota Y, Yamamoto T, Date K, MORI T. Quality improvement of rockbolting. In: Proceedings of the 7th International Symposium on Ground Support in Mining and Underground Construction. Perth: Australian Centre for Geomechanics; 2013.

Zhang P, Dineva S, Nordlund E, Hansen-Haug J, Woldemedhin B, Töyrä J, Boskovic M, Nyström A, Marklund PI, Mozaffari S. Establishment of experimental sites in three Swedish mines to monitor the in-situ performance of ground support systems associated with mining-induced seismicity. In: Proceeding of the 8th International Symposium on Ground Support in Mining and Underground Construction, Lulea, Sweden. 2016.

148

148

Rock Engineering Design Approaches and challenges in Deep Hard Rock Mining Engineering – Dec. 15th, 2019 – Shahrood UT

End of presentation:
Diagnosis of problem and selecting right tools to solve

149

149

ARTICLE IN PRESS

International Journal of Mining Science and Technology xxx (2018) xxx–xxx

Contents lists available at ScienceDirect

International Journal of Mining Science and Technology

journal homepage: www.elsevier.com/locate/ijmst

Reinforcement selection for deep and high-stress tunnels at preliminary design stages using ground demand and support capacity approach

Reza Masoudi *, Mostafa Sharifzadeh

Department of Mining & Metallurgical Engineering, Curtin University, Western Australian School of Mines (WASM), Perth 6102, Australia

A R T I C L E I N F O

Article history:
Received 25 October 2017
Received in revised form 19 January 2018
Accepted 29 January 2018
Available online xxxx

Keywords:
High-stress tunnels
Support system
Ground demand
Reinforcement capacity
Rockbolt

A B S T R A C T

Underground mining is going to be deeper gradually because near surface resources are going to be depleted. Therefore, risk of seismic events in underground mines is escalating. Additionally, existence of the large ratio of horizontal to vertical stress, could be a potential reason for high-stress condition and occurrence of dynamic activities. Depending on various parameters such as the level of induced stress, rock properties, etc., ground demand changes and it is difficult to estimate. On the other hand, under seismic condition, energy dissipation and deformation capacity of supports is the most important factors, however, rock support performance factors in dynamic conditions are still under investigation. Expanding the knowledge of reinforcement behaviour and capacity, specifically that of the rockbolt as a primary element in seismic conditions, would help to develop a suitable, safe and economic support design. This paper contains various methods to estimate ground demand including the intact rock properties approach, failure thickness and ejection velocity estimation, and rockburst damage potential method. It also covers measurement methods of rockbolts energy dissipation capacities such as drop test, blasting simulating, back calculation and momentum transfer measurement methods. A large-scale dynamic test rig is also explained. Based on the findings, a table and a graph to show the applicable range of each type of rockbolts were presented. Suitable rockbolt types for various ground energy demand and deformation capacity range were categorised in the table and the graph. The presented support selection method facilitates the selection of a suitable reinforcement system at the preliminary stages of design and guides the designer to adjust the support reinforcement system based on observed ground and support reaction.

1. Introduction

Deeper underground mining exploitation is increasing worldwide because near surface mineral resources become gradually depleted. In-situ stress increasing in rock is the main difference between rock stresses at depth compared to the rock near the surface, and dynamic activities are direct consequences of such a condition. Seismic events such as the rockburst might occur below 600–800 m depth and more likely passing 1000 m depth. Such phenomena are not limited only to deep mines as many shallow mines in Australia experience such events due to the presence of high horizontal to vertical stress ratios.

Hard rock mining is experienced at a depth of about 2 km in Australia, more than 3 km in Canada, and a depth of about 4 km in South Africa highlight the importance of ground stability at such depths. Finding a practical support design requires determining the rockmass energy demand and rock support energy dissipation capacity. Numerous unknowns, uncertainties in geomechanical parameters and randomness occurrence of seismic events increase the complexity of the rock demand determination and consequently extend the complication of an effective support design.

Though a significant amount of work has been done to estimate energy dissipation capacity of support elements, this subject is not much known. Additionally, the role played by other mechanisms of loading, like dynamic shear loading, in the support system is also not clearly understood.

To achieve stability and safety at deep and rockburst prone conditions, appropriate support and reinforcement design is necessary. The support system should not only be able to tolerate the static rock load and potential dynamic load due to induced stress, but it should also not lose strength over a wide range of deformation. It could be concluded that the energy dissipation capacity of support elements individually, as well as the ground support as an integrated system, needs to be found. Ground energy demand cannot accurately be determined or calculated, but some

* Corresponding author.
E-mail address: Reza.Masoudi@postgrad.curtin.edu.au (R. Masoudi).

https://doi.org/10.1016/j.ijmst.2018.01.004
2095-2686/© 2018 Published by Elsevier B.V. on behalf of China University of Mining & Technology.

Please cite this article in press as: Masoudi R, Sharifzadeh M. Reinforcement selection for deep and high-stress tunnels at preliminary design stages using ground demand and support capacity approach. Int J Min Sci Technol (2018), https://doi.org/10.1016/j.ijmst.2018.01.004

estimation might be achieved to help engineering judgment. Some of the methods, based on intact rock properties, have attempted to find a relationship between rockmass properties and their potential to burst, and the real condition of rockmass under stress [1,2]. Some other methods are based on the estimation of probable failure volume, ejection velocity and the travelling distance of ejected materials [3]. Another recent method relies on the definition of the effective parameters on the potential of rockburst and its likely damage [4]. On the other hand, some researchers believe that there is not a precise method to determine rockmass demand with any degree of confidence [5].

Along with ground demand during dynamic events, much effort has been expended in determining the rock support energy dissipation capacity. Rockbolt as the primary element to transfer the energy of the displaced volume of surface rock to the ground in depth has been the focus. Several approaches including the drop test, blast simulation, back calculation and momentum transfer method have been developed in order to examine rockbolt performance [4,6–10]. Another so-called large-scale dynamic test rig has been constructed in 2012 by Geobrugg in Switzerland in order to investigate the whole support system as an integrated system [11,12]. Despite several research studies on different ground types, support systems in a wide range of loading, rockbolt types, etc., there are limited comprehensive studies on this subject.

In this research, at first, a short explanation of different mechanisms of rockburst and rock ejection and various methods of ground demand estimation and rockbolt energy dissipation capacity, are illustrated. Then, suitable rockbolt type selection is recommended for different ground demand levels. The method is simply presented by table and graph which is easy to use in practice. The presented methods can assist the selection of appropriate rockbolt type at the preliminary stages of mine design. Additional to the rockbolt selection, some further considerations for the selection of other support elements is given as well.

2. Deep underground and high-stress mining

Seismically active underground mines are those which are prone to dynamic rockmass failure. As mining progresses, the natural stress equilibrium of the rockmass is disturbed. Stresses concentrate around the edges of an excavation or in pillars of rock between excavations left unmined for support, due to low grade or other reasons. Stress may also be increased or relaxed on preexisting planes of weakness such as faults, shears or lithological contacts. These stress changes cause the accumulation of potential energy in the unmined rock. This energy may be gradually dissipated, or it may be released suddenly during the process of inelastic deformation and radiates detectable seismic waves.

2.1. Ground behaviour in seismic conditions

Rockmass varies from massive, layered and jointed to heavily crushed conditions. In addition, dynamic loading has a broad range of frequency, amplitude, and wavelength. Therefore, ground behaviour varies widely considering the rockmass and dynamic loading conditions. The most common types of strain burst and seismic failure mechanisms in different ground types are categorised into four primary ejection types based on various factors as shown in Fig. 1.

Fig. 1a shows the mechanism of strain burst during ejection of a volume of rock due to stress concentrations or induced stresses. In this condition, discontinuities have a minor effect on ejection, so it is difficult to predict the volume of rock to be ejected and even sometimes the likelihood of an ejection.

Fig. 1b shows the ejection of a volume of rock by the mechanism of sudden buckling or spalling of rock in the wall or even in the face due to induced or concentrated stress on the boundaries of the opening where foliation of the rockmass is nearby vertical. This mechanism applies to strong to extremely strong rocks.

Fig. 1c shows the ejection of a volume of rock in the wall due to a seismic event near the boundaries of a stope or a tunnel which is due to slip or energy transfer on an adjacent discontinuity. Initial or secondary discontinuities can bound the volume of ejection so it can be estimated if the location of such an event is known.

Fig. 1d depicts the mechanism of instability in the back due to a combination of the effect of loosening of discontinuous blocks, gravity, and/or a seismic event. Loosening of the blocks in the back could be a result of the lack of enough confining stress or previous blasting. The seismic event can accelerate the phenomenon under the effect of available gravity.

Therefore, considering the wide range of rockmass and dynamic load conditions, various types of failures such as spalling, rock ejection and block fall can be expected.

2.2. Ground seismic energy demand

When a dynamic load propagates in the excavation, rock deformation occurs and cause an energy release. Estimating the magnitude of released energy is important to design a suitable reinforcement system. Although several methods have been developed to estimate the ground energy demand, they can be categorised into three groups namely, Intact rock property approach (IRPA), Estimation of failure volume and ejection velocity, Rockburst damage potential. A brief illustration of each method is given in the following subsections.

2.2.1. Intact rock property approach (IRPA)

When a volume of energy that should be tolerated within the rockmass exceeds its capacity (Strength), sudden failure happens, and energy is quickly released. Although all factors such as discontinuities and their infilling material properties, and the presence of underground water and its effects are important, intact rock properties have significant roles in this phenomenon. As a matter of fact, the intact rock energy absorption capacity could determine the upper limit of energy absorption capacity or in other words, the potential releasable energy of the rockmass. Some criteria have been defined to estimate the potential of rockburst based on intact rock properties including Index of strain energy, Potential energy of elastic strain [1,13], rock brittleness [14], and ratio of tangential stress to compressive strength [15].

An excess of energy during the post-peak deformation stage conclude in violent rock fracturing [16]. Energy release rate (ERR) has been developed as a basis for mining exploitation pattern design. Rock subjected to the compression process experiences elastic and plastic deformation. Elastic deformation (strain) of the rock can be recovered if unloading occurs before peak strength. At brittle failure, the elastic strain releases suddenly and causes a rockburst. Therefore, by applying a cyclic compressive strength test, the energy storage capacity of rock can be estimated. As it is shown in Fig. 2a, Φds is the portion of energy which is dissipated due to initiation and propagation of micro-cracks in the rock sample (plastic deformation). Φel is the portion of energy which is consumed for elastic deformation and stored in the rock. This portion of energy stored during the loading process up to point A could be released gradually by unloading or suddenly by failure. The ratio between elastic strain energy and dissipated energy (index of strain energy) could be used as a criterion or an indicator of rockburst potential.

$$F = \Phi el / \Phi ds \tag{1}$$

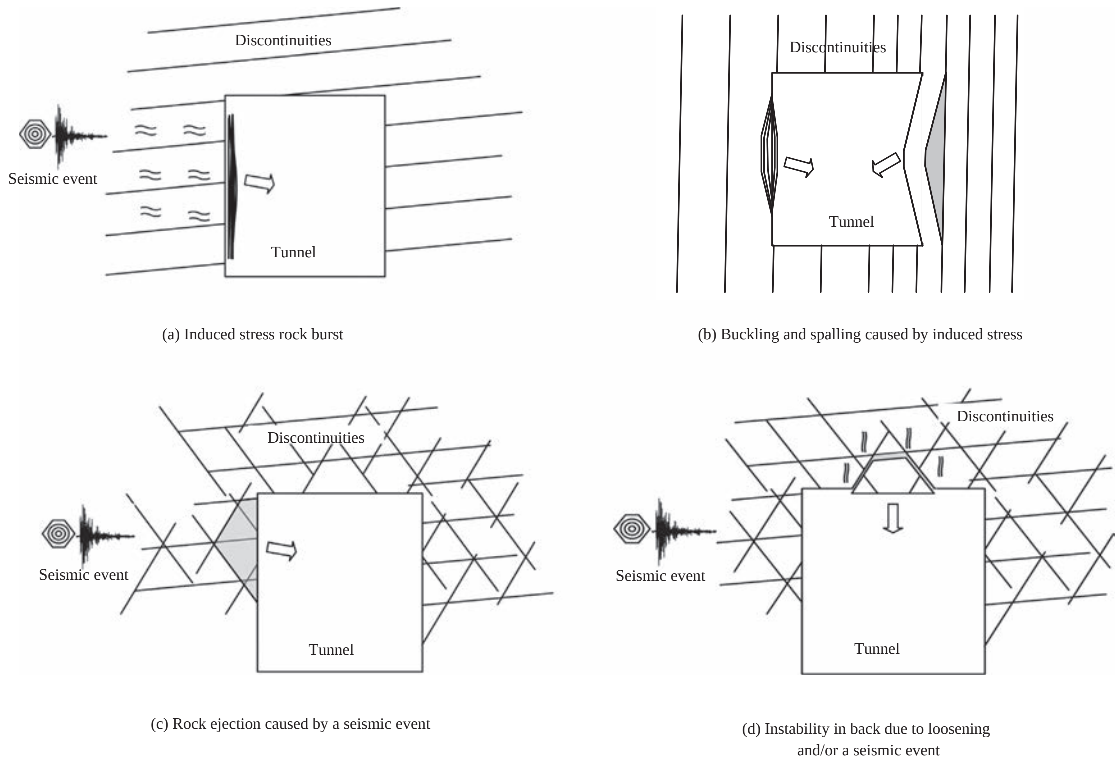

Fig. 1. Failure mechanisms for underground deep and high-stress tunnels due to induced stress and seismic events.

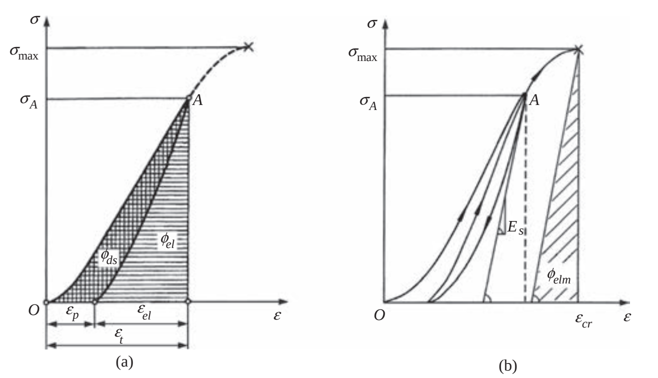

Fig. 2. Analytic calculation of energy in the rock sample cyclic loading of after Kwasniewski, Szutkowski) (a) [13] and calculation of potential elastic strain energy (b) [2].

Investigations demonstrate that the potential energy of elastic strain (PES), in other words, the elastic strain energy which is stored in a unit volume of rockmass, is another criterion that could scale the shock and rockburst occurrence [13]. As it is depicted in Fig. 2b, the maximum elastic strain energy which could be stored in a sample of rock before the peak strength is given by:

$$PES = \Phi_{elm} = \sigma_c^2/2E_s \tag{2}$$

where σ_c is the uniaxial compressive strength (MPa), and E_s is the unloading tangential modulus (MPa).

The third criterion is the index of rock brittleness which is defined as following:

$$B = \sigma_c/\sigma_T \tag{3}$$

In which σ_c is the uniaxial compressive strength (MPa), and σ_T is the tensile strength of the rock (MPa). Based on this criterion, the lesser index indicates the probability of the more violent rockburst.

The fourth criterion considers both the state of in-situ stress in the rockmass and the mechanical property of rock is expressed by:

$$T_s = \sigma_\theta/\sigma_c \tag{4}$$

In Eq. (4), σ_θ is the tangential stress in the rockmass surrounding the openings or stopes (MPa), and σ_c is the uniaxial compressive strength of rock (MPa). A larger *Ts* indicates a more violent probable rockburst [14].

A summary of these criteria is shown in Table 1.

Four indexes are available in this table indicating whether a rockburst event will be low, strong or violent based on estimated or calculated amount of each index. The indexes on the left side of the range indicate low potential, and on the right side of the range indicate strong or violent potential of rockburst.

2.2.2. Estimation of failure volume and ejection velocity

Estimation of failure thickness and ejection velocity will allow the estimation of ground demand by calculating the potential energy release (stored energy in flying rock) by the prospective volume of ejected rock and the estimated velocity of ejection.

The energy demand on ground support due to a block ejected from the backs, wall or floor could be calculated by the following Eq. [3]:

$$Energy\ Demand = 1/2mv_e^2 + qmgd \tag{5}$$

In this equation: m = the mass of the ejected block (kg); v_e = the ejection velocity of the block (m/s); g = acceleration due to gravity (m/s^2); d = distance the ejected block has travelled (m); and q = 1, 0 or -1 for ejection from the backs, wall or floor respectively.

The second term in Eq. (5) contributing to the energy demand ($qmgd$) represents the influence of gravity. Gravity adds potential energy to rocks ejected from the backs and reduces the energy of a block ejected from the floor, while not contributing to ejection from the wall [3].

Please cite this article in press as: Masoudi R, Sharifzadeh M. Reinforcement selection for deep and high-stress tunnels at preliminary design stages using ground demand and support capacity approach. Int J Min Sci Technol (2018), https://doi.org/10.1016/j.ijmst.2018.01.004

Table 1
Rockburst potential based on intact rock property.

	Description	Index	Potential of rockburst				
			Low		Strong		Violent
1	Index of strain energy[a] [13]	$F = \Phi_{el}/\Phi_{ds}$		2		5	
2	Potential energy of elastic strain (kJ/m^3) [13]	$PES = \sigma_C{}^2/2E_s$	50.0	100	150.0	200	250.0
3	Rock brittleness [14]	$B = \sigma_C/\sigma_T$	40.0		26.7		14.5
4	Ratio of tangential to compressive strength [15]	$T_s = \sigma_\theta/\sigma_C$	0.3		0.5		0.7

[a] Based on tests on coal specimens to provide the intensity of shocks or coal bombs.

If we consider the energy demand per square meter of excavation surface and substituting $t\rho$ for m, the equation becomes [3]:

$$Energy\ Demand\ per\ m^2 = \frac{1}{2}t\rho V_e^2 + qt\rho gd \tag{6}$$

In which: t = thickness of failed rock at the excavation surface (m); and ρ = rock density (kg/m^3).

Therefore, the critical factors required for energy demand are: peak particle velocity, which is assumed to equal the velocity of ejection (V_e); excavation closure or ejection distance (d), and the mass of ejected material, which is a function of the failure thickness (t) and the rock density (ρ).

The excavation closure (or ejection distance) "d" is used in the gravity component of the energy demand equation and is only applicable when the design is being undertaken for the backs. It represents the work done by the support system to halt the downward movement of the rockmass. An approach is to use the displacement capacity of the ground support elements in the backs as a guide. In practice, the displacement capacities of the support element that fails first in a rockburst can be used for "d". The results of drop weight dynamic testing of support elements can be used to assist in determining appropriate "d" values.

The fracturing due to induced stress, blast damage, geological structure or a combination of all these three factors can form the failure volume or mass of ejected rock which loads the support system. Failure volume can be estimated by various methods in an excavation. A borehole camera survey can help to find the potential discontinuities for ejection and hence the probable volume of rock. Numerical modelling also can be used for the estimation of the failure mass by measuring the overstressed zone surrounding an excavation, in other words, the zone around an excavation in which the stress exceeds the rock strength. Empirical estimation methods are also available.

Table 2 summarises the methods of estimating the failure volume for use in design calculations. The thickness should be calculated via as many possible as the mentioned methods in the table, and the maximum thickness should be used in the calculation.

2.2.3. Rockburst damage potential

Heal [4] has established a method for assessing the likelihood of rockburst damage occurring at particular excavations in seismically active underground mines. In this approach, five factors are combined into a single index for determining the potential for rockburst damage at a given location in an underground mine.

Excavation vulnerability potential (EVP) is proposed as an index to empirically quantify the effect of local site conditions on rockburst damage. It makes use of four of the five mentioned factors, those not related to the source of the seismic event:

- $E1$: The stress conditions (σ_{1T}/UCS);
- $E2$: The energy capacity of the installed ground support system (in kJ/m^2);
- $E3$: The excavation span (in m); and
- $E4$: The presence of seismically active major geological structure.

The empirical EVP index proposed makes use of these two components:

$$\text{EVP} = (\text{damage initiation factor}) \times (\text{depth of failure factor}) = (E1/E2) \times (E3/E4) \tag{10}$$

In order to consider the distance and magnitude of the seismic event involved in each case history, the EVP data was compared to the fifth factor, peak particle velocity (PPV) to create a single index called rockburst damage potential (RDP), as shown here:

$$\text{Rockburst damage potential(RDP)} = \text{EVP} \times \text{PPV} \tag{11}$$

The respective distributions of these factors show that, in general, an increasing level of rockburst damage is associated with:

- Increasing stress conditions ($E1$);
- Decreasing ground support system capacity ($E2$);
- Increasing excavation span ($E3$);
- Decreasing geology factor ($E4$); and
- Increasing peak particle velocity (PPV).

The above-explained procedure can be used to predict the level of rockburst potential. This method needs more experiments and practical feedback to prove or modify.

In most cases, it is difficult to carry out a specific design because the rockmass factors that define demand cannot be dependably evaluated. Therefore, the rockmass demand can be described qualitatively. As explained in Table 3, qualitative demand categories of rockmass could be defined in terms of low, medium, high, very high, and extremely high energy demand per square meter as well as surface displacement and reaction pressure. Similarly, such a rating can classify the reinforcement system in order to satisfy the rock demand [19].

3. Dynamic rock support and reinforcement classes and tests

The reinforcement and support system is a critical measure to prepare a safe workplace as well as increase the longevity of a stable opening. An effective support system influences the safety of workforces and equipment along with the economical mine extraction. Different sorts of reinforcement and support systems are required for a particular application rely on a few elements including: the geometry of the excavation, the strength of the rockmass, stresses present in the rock, corrosion and weathering processes, and blasting practices.

The primary method to lighten the impacts of mine seismicity is the design of a practical geometry and appropriate mining sequence. A rock support plan would be a complementary step intending to mitigate the rockburst impact. A ground demand-energy dissipation capacity approach is a vital step in such circumstances. Therefore, acquiring the knowledge of energy dissipation capabilities of elements of a support system including the reinforcement, surface support, connecting elements and faceplate & nut is necessary as well as a whole support system as an integrated system.

Please cite this article in press as: Masoudi R, Sharifzadeh M. Reinforcement selection for deep and high-stress tunnels at preliminary design stages using ground demand and support capacity approach. Int J Min Sci Technol (2018), https://doi.org/10.1016/j.ijmst.2018.01.004

Table 2
Failure thickness estimation [17,18] (after Heal [4]).

	Failure volume or thickness (t) can be estimated as the maximum of:
1	The potential volume of instability or probable active discontinuities can be observed at intersections around the site of interest
2	The volume surrounding the excavation, based on a calibrated numerical model, where the strength factor (SF) is less than 1[17]: $SF = \frac{(UCS+q\sigma_3)}{\sigma_1}$ (7) Where $q = tan^2(45 + \emptyset/2)$
3	Using the following empirical relationship to find the distance (R_f-a) [18]: $a = \frac{h\ (or\ w)}{\sqrt{2}}$ (8) $\frac{R_f}{a} = 1.34\ \frac{\sigma_{max}}{\sigma_c} + 0.43$ (9) 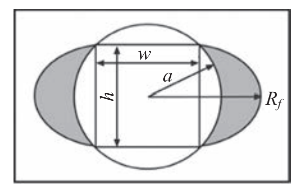 In which: σ_{max}=3σ_1-σ_3; σ_c is the unconfined compressive strength of the host rock; and the other terms in the equation are represented in the diagram
4	0.1 m for conventional blasting
5	0.05 m for controlled blasting
6	The volume of potential ejected mass based on pre-existing structural weaknesses in the rockmass up to h/2

Table 3
Typical rockmass demand for ground support design [19].

Demand category	Reaction pressure (kPa)	Surface displacement (mm)	Energy (kJ/m^2)
Low	<100	<50	<5
Medium	100–150	50–100	5–15
High	150–200	100–200	15–25
Very high	200–400	200–300	25–35
Extremely high	>400	>300	>35

3.1. Dynamic capacity of rockbolts

Implementation of a dynamic resistance support system is the most common method of stabilising an underground opening in mines. Rockbolts along with surface support comprised of mesh and shotcrete, play a crucial role as one of the main elements of a support system. A tunnel that experiences seismic activities like a rockburst needs to be supported by appropriate elements, capable of tolerating dynamic loading. This area in geotechnical engineering is still under development. In other words, the dynamic capacity or energy dissipation capacity of the rock support is under investigation by researchers [20]. The primary challenge in measuring the dynamic capacity of the ground support including the rockbolt is to prepare repeatable loading conditions similar to what is experienced at a supported face during a seismic event. Providing a good monitoring system and qualified data acquisition apparatus along with well-controlled equipment are requirements of a dynamic testing facility in order to acquire reliable data and meaningful analysis.

"Drop testing" has been under the attention of researchers to convey kinematic energy to ground support elements in order to measure energy dissipation capacity [3,9,21–27]. The momentum transfer concept has been utilised by some other researchers [6]. In this method, deceleration of a dropped reinforcement sample attached to a mass is measured and the amount of energy consumed particularly for deformation and failure of sample is calculated. Employing a simulated controlled blasting process as the dynamic load applied on a completely supported area along with a well-instrumented system is another category of measurement of dynamic performance of a support system as an integrated system [7,28]. In addition, back calculation of support capacity has also been performed by Heal [4] which can be assumed as another method to estimate the dynamic support capacity.

3.1.1. The 'drop test'

The drop test rig is a controlled laboratory facility to investigate the dynamic behaviour of ground support elements submitted to a seismic event simulated by sudden loading of a dropping mass from a predetermined height [3,9,21–27,29,30]. This test has experienced numerous amendments and has turned into a standard testing technique for laboratory assurance of rockbolt energy absorption or dissipation capacity. There are also various difficulties required with this test including slow instrumentation reaction, uncontrolled vibrations in the loading system, and other sources of unmeasured energy losses [31]. The advantage of this test facility is its repeatability and cost effectiveness as soon as it is assembled. A number of drop testing equipment has been constructed during the last twenty years in Canada, South Africa and recently in Australia to be able to perform dynamic performance assessment of ground support elements. Although a standard method of testing has been available, these rigs have been constructed with considerable dissimilarities which make the examination of their outcomes to some degree complicated or not comparable [20].

A rockbolt or cable bolt, cement or resin encapsulated in thick-wall steel pipe to replicate the rockmass, is frequently used in the drop testing experiments. Despite the fact that a specific thickness and measurement of steel tube were given to provide similar confinement of the in-situ rockmass with the same magnitude, the steel pipe cannot completely replicate the rockmass which may introduce an error of some degree into the estimation [8].

In spite of the fact that there have been critical enhancements made to the drop testing mechanical assembly, it is still not illustrative of in-situ conditions. The drop test technique has numerous presumptions that would influence the performance of the support elements contrasted with their genuine performance in the field. Moreover, the drop tests deliver results of individual support elements that need to be compiled and consolidated to design the support system. It is helpful to take the outcomes from the different reinforcement elements and the surface support and assemble them together. However, providing a cost effective, controlled and repeatable procedure for estimating the support elements' properties in a laboratory is its outstanding advantage.

3.1.2. Blast simulation

Blast simulation experiments have been performed in-situ trying to recreate the seismic event via the blasting to measure the consequences on most common ground support systems [7,32–37]. In-situ simulated blasting testing to investigate the rock support behaviour and performance was innovated by Ortlepp [38]. In comparison to drop testing, the simulation of rockbursts by blasting has a large level of difficulty. Performing such a destructive test in active mines during operation of other activities needs sophisticated coordination with operative units while the logistic of setting up and carrying out the tests is not straightforward, and the cost is also high. The positive points of the method is the testing of the support system as an integrated system which is completely installed in place as opposed to individual support elements. Issues, for example, installation procedures and the interaction with the rockmass were also investigated, and shortcomings of the whole system were underscored [20].

It is worth mentioning that the movement of ground in blasting is not similar to that of a rockburst because of seismic events. The gas pressure is not available in the rockburst condition while in blasting it is accompanied by the shock wave, as sometimes the generated gases quickly expand and may conclude to unpredictable results at the test location. On the other hand, the wave characteristics, including wavelength, amplitude and frequency created by blasting are different to those produced by large seismic events. Normally, the wavelengths in the seismic events are longer and frequencies are lower in comparison to those in blasting.

Obviously, to investigate and understand the behaviour of rockmass and ground support elements, a reproducible or repeatable simulated dynamic event would be a great success. Many researchers have tried to employ the blasting method for simulation of a rockburst, but there are few or small number of successful experiments. Distortion by gases and not enough generated energy to produce premeditated destruction have been the main reasons of ineffective experiments. Nevertheless, the behaviour of the whole support system as an integrated system can be investigated with this method.

3.1.3. Momentum transfer method

The momentum transfer concept has been employed by the Western Australian School of Mines (WASM) via a dynamic loading system in order to find out the energy dissipation capability of the ground support elements or system. This equipment utilises a sample of reinforcement attached to a mass to apply a dynamic impact to the sample by dropping them from a certain height and measurement of deceleration after impact. The testing facility is capable of testing different types of rockbolts, cable bolts, or reinforcement systems, prepared sample of surface support or a mixture of both, to be able to assess the mechanism of dissipation of the energy by a ground support system and interaction between the surface support and reinforcement and the mechanism of the transfer of the dynamic load [6].

The concept of this facility is illustrated in Fig. 3. Using a dropped mass of 2000 kg as the simulated ejected rock with an impact velocity of 6 m/s is a standard arrangement for testing of rock reinforcement. This arrangement provides a kinetic energy of 36 kJ applied to the test sample and must be dissipated by the support element. The buffers have to absorb the energy of the beam as well as a portion of the energy of the dropping mass. The excess energy is applied to the test sample following the impact because of the change in potential energy of the dropping mass. Making a radial cut artificially in steel pipe simulates the discontinuity in the rockmass typically situated 1.0 m beneath the bearing plate [39].

Characteristically, the investigation of a sample of reinforcement or support system has to be based on first impact loading that can be a single large dynamic impact. Therefore, the testing equipment has to have sufficient energy or enough capacity to be able to exceed the strength of the sample with a single impact.

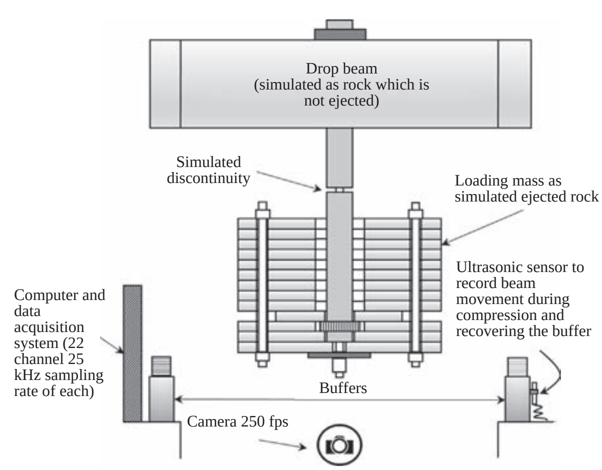

Fig. 3. Dynamic testing facility with momentum transfer concept (after player, Thompson [39]).

Based on previous experiments, it has been proved that the multiple loading cause the measured result to overestimate the capacity in comparison to the results of a single large impact. The WASM testing equipment is capable of applying 120 kJ of kinetic energy to the sample [39] which is more than the capacity of most common rock bolts.

It is practical to calculate the dynamic force-displacement diagram of the support element via a well instrumented and monitored system. The portion of the applied kinetic energy, which is dissipated by the prepared sample of support, would be determined by calculation of the area under the force-displacement graph. Another portion of energy that is absorbed by buffers can be calculated separately for every test. The accelerometers assist in evaluating and computing the deceleration response of the system. Alternatively, it can be calculated by a fast computerised video camera, measuring the relative displacement of a target by object tracking software.

Finally, the underground ejection velocity is considered as the relative velocity between the loading mass and the dropping beam. The ejection phenomenon happens and a block of rock, which was at rest or stationary under the stress at the wall or vault of the tunnel, quickly accelerates and reaches a peak velocity. The velocity returns to zero if the ground support system tolerates the dynamic impact. Compared to a strong ground support system, a weak or soft support system would be a reason for larger displacement and greater ejection velocity. The most important aspects of the ground support design that has to be considered in a mining operation is the maximum permissible deformation of the reinforcement system and ensuring that the surface support has enough toughness to tolerate the displacement [39].

3.1.4. Back-calculation

Back analyses of the actual rock ejection and the associated support system is potentially a way of estimation of the dynamic capacity of the ground support. The problem is predicting the location of an ejection due to its randomness and other uncertainties, and consequently lack of sufficient monitoring to collect enough data regarding the event, for example, velocity of the ejected mass. Therefore, back analyses of driven events like blasting would be an appropriate method to address this issue.

A comparison between the test results of simulated rockbursts with back analyses of absorbed energy in some case studies has been performed by Heal [4]. A correlation has been found between the back calculation of case studies and the simulated rockburst results, but the method has not been proved yet nor used by other researchers. It seems that this method with some modification can be an approach to calculating rock support dynamic dissipation capacity at the real scale.

3.1.5. Large-scale dynamic test rig for ground support

In order to examine the ground support as an integrated system, Geobrugg Company has constructed a dynamic test rig. Using this rig, it is possible to apply a dynamic load to a sample of a complete support system containing a 3.6 m $\times$ 3.6 m sample of surface support combined with four dynamic rockbolts. Because the large sample includes all support elements, it is capable of demonstrating the performance of the surface support and the reinforcement in combination together as well as the connecting and terminating elements [11,12]. Fig. 4 shows the test setup.

As it can be seen in the figure, a horizontal chain link mesh is connected to the main steel frame using lacing wire ropes, while the mesh is held by four dynamic rockbolts. Surface support simulated by shotcrete or concrete slab could be poured over the wire mesh engaged with the four rockbolts via terminating and connecting elements. Some natural rock boulders and gravel are placed on top of the slab sample to simulate broken rocks during a rockburst event contained by surface support. An impact platform made of steel is placed over the gravel to distribute and transfer the impact of a dropped block to the gravel layer, natural rock boulders, and simulated surface support. The mass of the dropped block is 6280 kg and it can be lifted and dropped from a maximum height of 3.25 m limited by a guiding rail. One of the four bolts is instrumented by two load cells at both ends. Two high-speed cameras are installed in front of the main frame, the upper one for the filming of the test block movement and impact and the lower one to monitor the support with several measuring targets on the mesh and bolts with a computer tracking program to evaluate the displacement, velocity and acceleration of the targets. Dissipated energy can be calculated by the difference in potential energy of the test block before and after the impact [11,12].

Testing a large scale of the support sample as an integrated system submitted to a dynamic impact is the strong point of this testing rig. Engineers, to some extent, can evaluate energy dissipation capability of a ground support system exposed to dynamic impact and compare the compatibility of the elements in the prepared sample. The result would help the designer to avoid leaving a weak link in a support system because the weakest link in a support system affects and limits the maximum capacity of the whole system.

One weak point of the system is that a single drop would not cause the support system to fail under test and multiple drops can conclude in an overestimation of the energy dissipation capacity of the rockbolts or even the whole support system.

There are not many published results of this testing facility and perhaps this is due to a limited number of support systems tested. Therefore, the performance of it can only be evaluated after publication of more test results and comparison to real case

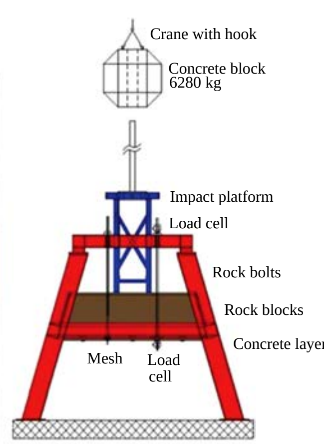

Fig. 4. The large-scale dynamic testing rig of geobrugg [11].

Please cite this article in press as: Masoudi R, Sharifzadeh M. Reinforcement selection for deep and high-stress tunnels at preliminary design stages using ground demand and support capacity approach. Int J Min Sci Technol (2018), https://doi.org/10.1016/j.ijmst.2018.01.004

studies. On the other hand, it seems that the monitoring data is not enough to calculate the portion of energy dissipated by a support sample because the steel frame absorbs a part of the potential energy of the testing block by deflection and vibration that cannot be measured or calculated by the predicted monitoring system. It is also worth mentioning that the testing facility does not completely replicate the seismic phenomenon that happens in the ground.

3.2. Rockbolts energy dissipation capacity

In this part, the most common types of rockbolts are discussed and divided into different capacity categories. It is assumed that the surface support system (including shotcrete, mesh and nut) are acting appropriately and transfer the load to the rockbolt. Then the rockbolt would be the central element absorbing and dissipating energy.

Typical load–deformation behaviours of different rockbolts under the loading test are collected and illustrated in Fig. 5. According to the load-deformation capacity, the rockbolts are classified into five groups namely, stiff, medium yielding, high yielding, very high yielding, and extremely high yielding rockbolts. As shown in the figure, a category of rockbolts, such as expansion shell and resin/grout encapsulated rebars, are concentrated on the left side of the plot and represent stiff rockbolts with less than 50 mm deformation capacity and less than 5 kJ energy absorption capacity. The second category such as Split set, Swellex, Roofex and Yield-Lok are the rockbolts which can tolerate deformations between 50 mm and 100 mm with an energy absorption capacity between 5 kJ and 15 kJ. The D-Bolt, Conebolt, Swellex, Roofex and Yield-Lok which are high yielding rockbolts could lie in the next category. For deformation capacity greater than 200 mm, Conebolt, Garford and Roofex (possibly with small spacing) fall into the very high yielding category, and just Conebolt and Garford are suitable for the extremely high yielding category.

An important fact related to high yielding rockbolts is that they show different behaviour depending on loading conditions and other environmental circumstances. Loading velocity is one factor that can change the load and deformation capacity of yielding bolts and the quality of installation is another important factor. As it can be seen in the graph, one of the Conebolts tolerates more than 300 mm deformation and absorbs or dissipates 60 kJ of the ground released energy. In comparison, two other Conebolts tolerate less than 150 mm and less than 300 mm and can dissipate 20 kJ and 35 kJ, respectively. Grout quality is a major factor for Conebolts because a strong cement grout could lead to higher initial loading and early rupture while soft cement grout leads the rockbolt to early sliding and not reaching its maximum load capacity. In both cases, energy absorption capacity of a rockbolt dramatically drops. So before starting to implement a ground support scheme, it would be necessary to plan a test program to determine the conditions for optimum performance of the rockbolts. Examples of influencing parameters include grout mix design, curing time and preloading. The result of the test program should be used to develop a quality control plan.

Considering rockbolts' energy absorption as shown in Fig. 5 and discussed above, suitable rockbolt type selection for various ground demand categories are proposed in Table 4. This table could be an initial guideline to narrow the choices, and it is evident that complementary studies such as dynamic tests are required for detail design. Although there are some newer types of rockbolt like Dynamic Omega-Bolt which can absorb 22–35 kJ in static and

Table 4
Demand–capacity based support selection.

Ground demand		Reinforcement selection	
Surface displacement (mm)	Energy (kJ/m^2)	Recommended reinforcement	Capacity category
<50	<5	Expansion shell rockbolt, Resin/cement steel rebar,	Low/stiff
50–100	5–15	Split set, Swellex, Roofex, Yield-Lok	Medium
100–200	15–25	Swellex, D-Bolt, Conebolt, Roofex, Yield-Lok	High
200–300	25–35	Roofex, Conebolt, Garford	Very high
>300	>35	Conebolt, Garford	Extremely high

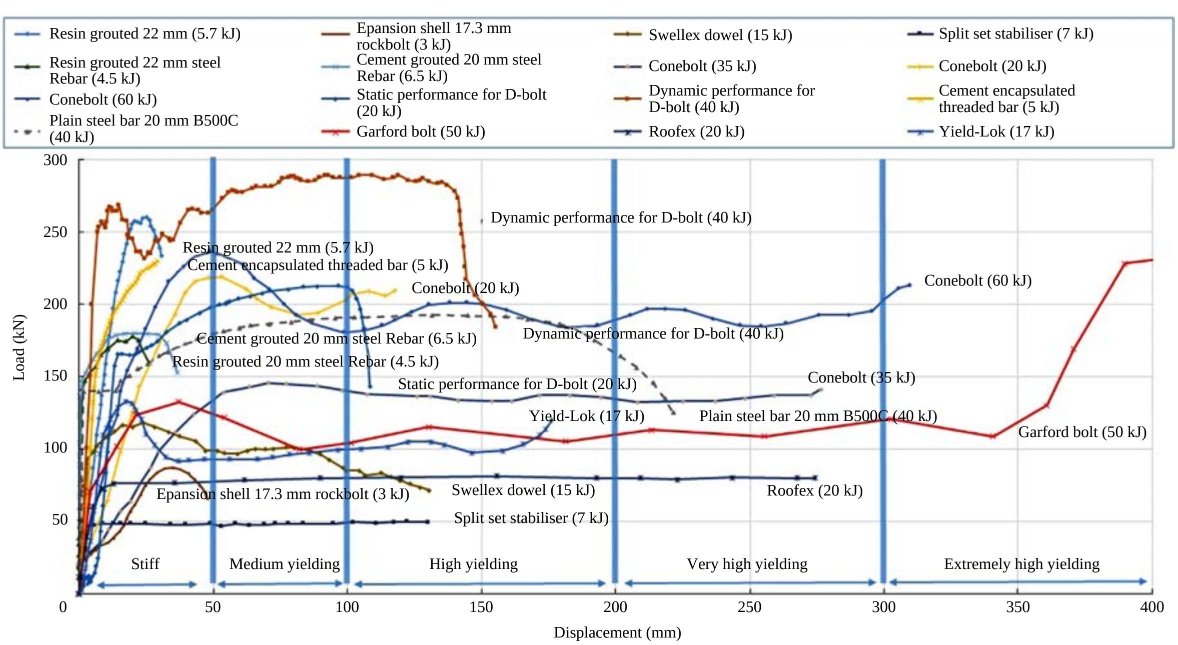

Fig. 5. Load-deformation behaviour of different rockbolts (modified after [29,30,39–41]).

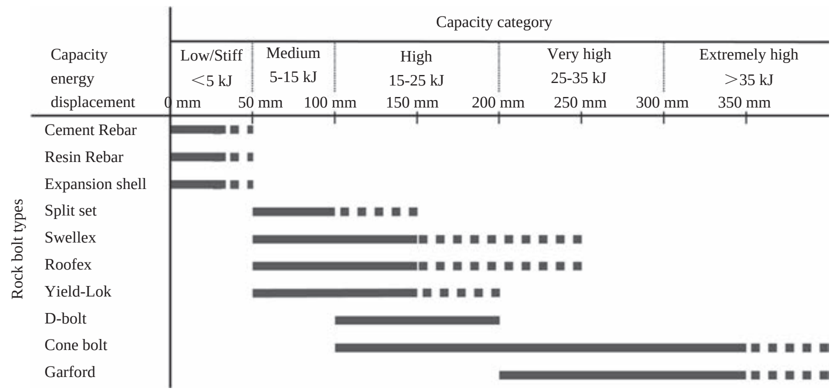

Fig. 6. Energy dissipation capacity category of different types of reinforcement.

dynamic conditions [42], they need more laboratory and industrial experimentation.

Fig. 6 shows the energy dissipation capacity of different types of reinforcement. Choosing a specific type of rock reinforcement, the figure shows the range of energy dissipation and deformation capacity under each named capacity category.

Based on the expectation of the deformation and energy demand of a location, the ground demand relates to the relevant categories in this table. The range of suitable reinforcement for the category is proposed in the "Rock Bolt Types" column. The expected deformation and ground demand are complicated though and come from the methods explained in Section 2.2 as well as previous experiences and engineering judgments.

3.3. Considerations of linking and terminating arrangements of reinforcements

The reinforcement connects to the surface support by linking and terminating arrangements like nuts and bearing plates, split set rings, or the sealing weld and soft ferrule on Swellex. The ejected mass applies the dynamic load to the surface support or containment support. The load needs to be passed via the linking and terminating arrangements and transferred to the ground through the reinforcement. Everyone of these elements have to be able to tolerate the applied dynamic load independently and if any of them failed, the load would no longer transmit to the ground and ejection would occur from in-between the rockbolts [3,4].

Some experiments show that the capacity of the bearing plate under a dynamic loading condition is much less than their nominal load capacity [43,44]. Therefore, in designating each ground support system, it is critical to be sure that the linking and terminating elements have adequate impact loading capacity to transfer the load to the reinforcement and avoid of local failure of the surface support.

4. Discussion

Ground support system design in a seismically active ground or rockburst prone area needs specific consideration regarding evaluation or estimation of the released or transferred energy to the surface of the opening on one hand, and knowing the energy absorption or dissipation capacity of the support system on the other hand. Design of a support system at a certain location underground requires an evaluation of both ground demand and support capacity, in order to design a reliable support system. The presented methods in the evaluation of ground demand have a large degree of uncertainty while the testing methods of the support system are not entirely capable of simulating the real conditions occurring in the ground.

Having an estimation of both factors, the ground demand and the support capacity, is essential, therefore, even with a large amount of uncertainty, designers can compare these two factors to define a factor of safety. In addition, the methods could be modified and calibrated in a certain area by the probable occurrence of seismic activities similar to observational methods. Comparison of the support systems tested by multiple facilities assists with promoting the design for the next step.

5. Conclusions

Under seismic conditions in mines, the idea of improving, conserving, and mobilising the inherent strength of the ground to be self-supported is not valid enough while energy dissipation capability and large deformation capacity of support system is the primary objective. In this research, the ground demand and likelihood of a dynamic event have been estimated using different methods. Despite the low accuracy of these estimation methods due to many assumptions, they can assist in the selection of a relatively appropriate support system at preliminary design stages. The design can be modified with observations during construction progress.

Stiff behaviour at the beginning of the loading, along with high strength and yielding capability by increasing deformation, are essential qualities of the support components under dynamic loading conditions in order to dissipate a sudden release of energy. To estimate the capacity of rock support systems exposed to seismic events, a number of estimation methods including laboratory drop tests, simulated rockbursts, back calculation, momentum transfer concept and large-scale dynamic test were discussed. Although various assumptions and interpretations are needed to employ the results of dynamic tests, more dynamic capacity measurement of support elements is required to cover the wide range of possible energy released and resulting deformation. On the other hand, ground support reacts in different ways under different circumstances. The velocity of ejection (dynamic loading velocity), quality of grouting of rockbolts and appropriate linking between all elements are some of the known factors that affect the performance of the ground support system. The arrangement of a test program before finalising the design is vital to ensure a successful design.

Ground demand is estimated using the methods discussed along with an associated degree of uncertainty. However, to begin with, the potential for rockburst could be assessed through laboratory tests on intact rocks. Estimation of failure thickness and velocity of ejection could support the assumptions and results of the laboratory tests. Using rockburst damage potential, the previous result could be cross-checked, and this could also be summarised

Please cite this article in press as: Masoudi R, Sharifzadeh M. Reinforcement selection for deep and high-stress tunnels at preliminary design stages using ground demand and support capacity approach. Int J Min Sci Technol (2018), https://doi.org/10.1016/j.ijmst.2018.01.004

into a qualitative description. Using ground demand – support energy dissipation capacity (Table 4 and Fig. 6), the rockbolt type selection was introduced. The selected rockbolt can be tested, verified, and modified by proper dynamic testing or observation of progress during construction. The reliability of the support elements would be monitored and back calculated after initial installation and following excavation progress. This will allow the support selection and details to be modified based on monitoring and back calculation, progressively and continuously.

References

[1] Kwasniewski M, Wang J. 3-D numerical modeling and study of mine tremors associated with coal mining in vicinity of major of faults. Pupls Inst Geophys 1999; 22: 351–64.
[2] Wang JA, Park HD. Comprehensive prediction of rockburst based on analysis of strain energy in rocks. Tunn Undergr Space Technol 2001;16:49–57.
[3] Kaiser PK, McCreath D, Tannant D. Canadian rockburst support handbook. Geomechanics Research Centre: Laurentian University, Sudbury; 1996. p. 314.
[4] Heal DP. Observations and analysis of incidences of rockburst damage in underground mines. Perth, Western Australia: University of Western Australia; 2010.
[5] Villaescusa E. Geotechnical design for sublevel open stoping. Boca Raton: CRC Press; 2014.
[6] Player JR, Villaescusa E, Thompson AG. Dynamic testing of rock reinforcement using the momentum transfer concept. In: Fifth international symposium on ground support in mining and underground construction. Perth; 2004. p. 327–40.
[7] Heal DP, Potvin Y. In-situ dynamic testing of ground support using simulated rockbursts. In: Deep mining. Perth; 2007. p. 373–94.
[8] Li L, Hagan P, Saydam S. A review of ground support systems performance subjected to dynamic loading. Int Soc Rock Mech; 2014.
[9] Plouffe M, Anderson T, Judge K. Rock bolts testing under dynamic conditions at CANMET-MMSL. In: Proc 6th int symp on ground support in mining and civil engineering construction, Cape Town, S Afr Inst Min Metall Symposium Series S; 2008. p. 581–95.
[10] Player J, Villaescusa E, Thompson A. An examination of dynamic test facilities. In: Australian mining technology conference; 2008. p. 349–79.
[11] Roth A, Cala M, Brändle R, Rorem E. Analysis and numerical modelling of dynamic ground support based on instrumented full-scale tests. In: proceedings of the seventh international conference on deep and high stress mining. Sudbury; 2014.
[12] Morissette PNR. A ground support design strategy for deep underground mines subjected to dynamic-loading conditions. Canada: University of Toronto; 2015.
[13] Kwasniewski M, Szutkowski I, Wang JA. Study of ability of coal from seam 510 for storing elastic energy in the aspect of assessment of hazard in Porabka-Klimontow Colliery. Sci Rept Silesian Technical University; 1994.
[14] Qiao CS, Tian ZY. Study of the possibility of rock burst in Dong-gua-shan Copper Mine. Chin J Rock Mech Eng 1998;17:917–21.
[15] Wang YH, Li WD, Li QG. Fuzzy estimation method of rock burst prediction. Chin J Rock Mech Eng 1998;17:493–501.
[16] Linkov AM. Rockbursts and the instability of rock masses. Int J Rock Mech Mining Sci & Geomech Abstr 1996;33:727–32.
[17] Wiles T. Reliability of numerical modelling predictions. Int J Rock Mech Min Sci 2006;43:454–72.
[18] Haile A, Grave D, Sevume C, Le Bron K. Strata control in tunnels and an evaluation of support units and systems currently used with a view to improving the effectiveness of support, stability and safety of tunnels; 1998.
[19] Thompson A, Villaescusa E, Windsor C. Ground support terminology and classification: an update. Geotech Geol Eng 2012;30:553–80.
[20] Potvin Y, Wesseloo J, Heal D. An interpretation of ground support capacity submitted to dynamic loading. Mining Technol 2010; 119: 233–45.
[21] Yi X, Kaiser P. Impact testing for rockbolt design in rockburst conditions. Int J Rock Mech Mining Sci & Geomech Abstr 1994;11:671–85.
[22] Ortlepp W, Stacey T. Testing of tunnel support: dynamic load testing of rockbolt elements to provide data for safer support design. Safety Mines Res Advis Committ 1998:1–49.
[23] Ortlepp WD. Rock fracture and rock bursts. In: Monograph Series M9. Johannesburg; 1997.
[24] Ortlepp WD, Stacey TR, Kirsten HAD. Containment support for large static and dynamic deformations in mines. In: international symposium-4th rock support and reinforcement practice in mining. Kalgoorlie; 1999. p. 359–66.
[25] Stacey TR, Ortlepp WD. Retainment support for dynamic events in mines. In: International symposium-4th Rock support and reinforcement practice in mining. Kalgoorlie; 1999. p. 329–33.
[26] Ortlepp W, Swart A. Extended use of the Savuka dynamic test facility to improve material and analytical technology in deep-level stope support. Safety Mines Res Advis Committ 2002:1–57.
[27] Gaudreau D, Aubertin M, Simon R. Performance assessment of tendon support systems submitted to dynamic loading: École polytechnique; 2004.
[28] Tannant DD, Brummer RK, Yi X. Rockbolt behaviour under dynamic loading: Field tests and modelling. Int J Rock Mech Mining Sci Geomech Abstr 1995;32:537–50.
[29] Li CC. A new energy-absorbing bolt for rock support in high stress rock masses. Int J Rock Mech Min Sci 2010;47:396–404.
[30] Li CC, Stjern G, Myrvang A. A review on the performance of conventional and energy-absorbing rockbolts. J Rock Mech Geotech Eng 2014;6:315–27.
[31] Soleimani SM, Banthia N. A novel drop weight impact setup for testing reinforced concrete beams. Exp Tech 2014;38:72–9.
[32] Archibald JF, Baidoe JP, Katsabanis PT. Rock burst damage mitigation benefits deriving from use of spray-on rock linings. In: Proceedings the 3rd international seminar on surface support liners: thin spray-on liners, shotcrete and mesh. Quebec City; 2003.
[33] Espley SJ, Heilig J, Moreau LH. Assessment of the dynamic capacity of liners for application in highly-stressed mining environments at Inco Limited. In: Surface support in Mining. Perth; 2002. p. 187–92.
[34] Hagan TO, Milev KB, Spottiswoode DM, Hildyard AM, Grodner SM, Rorke MW, et al. Simulated rockburst experiment - an overview. J S Afr Inst Min Metall 2001;101:217–22.
[35] Hildyard M, Milev A. Simulated rockburst experiment:numerical back-analysis of seismic wave interaction with the tunnel. J S Afr Inst Min Metall 2001;101:223–34.
[36] Hildyard M, Milev A. Simulated rockburst experiment: development of a numerical model for seismic wave propagation from the blast, and forward analysis. J S Afr Inst Min Metall 2001;101:235–46.
[37] Reddy N, Spottiswoode S. The influence of geology on a simulated rockburst. J South Afr Inst Min Metall 2001;101:267–74.
[38] Ortlepp WD. An empirical determination of the effectiveness of rockbolt support under impluse loading. In: Int symp on large permanent underground openings. Oslo; 1969. p. 197–205.
[39] Player J, Thompson A, Villaescusa E. Dynamic testing of reinforcement system. In: 6th international symposium on ground support in mining and civil and engineering construction. Cape Town; 2008. p. 597–622.
[40] Galler R, Gschwandtner G, Doucet C. Roofex bolt and its application in tunnelling by dealing with high stress ground conditions. In: ITA-AITES world tunnel congress Helsinki, Finland; 2011.
[41] Wu R, Oldsen J, Lamothe M. The Yield-Lok bolt for bursting and squeezing ground support. In: Proc 5th int seminar on deep and high stress mining, Santiago, Australian; 2010. p. 301–8.
[42] Scolari F, Brandon M, Krekula H. Dynamic inflatable, friction rockbolt for deep mining. In: Deep mining: eighth international conference on deep and high stress mining. Perth; 2017.
[43] Simser B, Potvin Y. The weakest link–ground support observations at some Canadian Shield hard rock mines. In: Deep mining—proceedings of the 4th international seminar on deep and high stress mining. Perth; 2007. p. 7–9.
[44] Jan VS, Palape M. Behaviour of steel plates during rockbursts. In: Deep mining. Perth, 2007.

Please cite this article in press as: Masoudi R, Sharifzadeh M. Reinforcement selection for deep and high-stress tunnels at preliminary design stages using ground demand and support capacity approach. Int J Min Sci Technol (2018), https://doi.org/10.1016/j.ijmst.2018.01.004


Vol. 28, March 2012
ISSN 0886-7798
ELSEVIER
Original research, innovations and case studies in the development of tunnelling, trenchless technology and underground space
Tunnelling and Underground Space Technology
incorporating Trenchless Technology Research
Editors: Chris Rogers (UK); Raymond Sterling (USA); Jian Zhao (Switzerland)
geo-investigation
underground mapping
planning
regulation
design
construction
operation
maintenance
www.elsevier.com
Available online at www.sciencedirect.com
SciVerse ScienceDirect

Tunnelling and Underground Space Technology 28 (2012) 41–48

Contents lists available at SciVerse ScienceDirect

Tunnelling and Underground Space Technology

journal homepage: www.elsevier.com/locate/tust

Displacement-based numerical back analysis for estimation of rock mass parameters in Siah Bisheh powerhouse cavern using continuum and discontinuum approach

M. Yazdani [a,*], M. Sharifzadeh [b,*], K. Kamrani [a], M. Ghorbani [b]

[a] Department of Civil Engineering, Tarbiat Modares University, Tehran, Iran
[b] Department of Mining and Metallurgical Engineering, Amirkabir University of Technology, Tehran, Iran

ARTICLE INFO

Article history:
Received 19 December 2010
Received in revised form 27 August 2011
Accepted 8 September 2011
Available online 26 October 2011

Keywords:
Continuum and discontinuum approach
Back analysis
Numerical modeling
Monitoring
Geomechanical parameters
Siah Bisheh cavern

ABSTRACT

Back analysis as a modern observational method is a helpful technique for evaluation of soil and rock mass parameters and prediction of their mechanical behavior. Most back analysis techniques in geotechnical engineering problems are based on the methods that utilize the monitored data of stresses, strain and displacements. This technique is one of the prominent processes in design and evaluation of the stability of caverns that reveals the shortcoming of supports design and in fact is essential for evaluation of design parameters. Siah Bisheh pumped storage project with complex geometry, changeable geological formations and diverse geotechnical properties of rocks, is under construction on the Chalus River at the north of Iran. The underground complex consists of three main caverns placed near each other. In this study displacement based direct back analysis using continuum and discontinuum numerical modeling were applied and geomechanical properties of rocks, stress ratio and joints parameters were identified and then calculated parameters were compared with the initial design parameters. Both continuum and discontinuum modeling results were in a good agreement with measured displacements which confirm the numerical modelings correctness and back analysis results.

1. Introduction

Siah Bisheh Pumped Storage project is located in 125 km north of Tehran, in the vicinity of Siah Bisheh village. This plant is designed to produce a rated capacity of 1040 MW peak energy. In this project, two concrete face rock fill dams are under construction in Chalus valley for the water storage. Siah Bisheh powerhouse cavern (PHC) with 24.5 m width, 46.5 m height and 131 m length is one of the largest underground power plants of its kind in Iran. Transformer cavern (TRC) with 16.1 m width, 28.4 m height and 160 m length and guard gate cavern (GGC) with 5.5 m width, 10.5 m height and 90.7 m length are the other main underground openings in this project. The powerhouse cavern was excavated at a depth of about 260 m (Fig. 1).

Back analysis techniques as a practical engineering tool are nowadays often used in geotechnical engineering problems for determining the unknown geomechanical parameters, system geometry and boundary or initial conditions using field measurements of displacements, strains or stresses performed during excavation or construction works.

From the mathematical point of view, displacement measurements are not greatly influenced by typical local effects. By comparison, stresses and strains are differential quantities, whose validity is limited to local regions (scale effect). Therefore, the observation at several successive points will be necessary to obtain a distribution over a sufficiently large area (Oreste, 2005). On the other hand, displacements of rock masses induced by excavation can be measured easily and reliably. Therefore, extensive studies have been conducted to develop different models of displacement-based back analysis (Sakurai and Takeuchi, 1983; Gioda and Locatelli, 1999; Swoboda et al., 1999; Feng et al., 2004; Zhang et al., 2006; Akutagawa et al., 2000; Sakurai, 2003). Back analysis techniques also have been used based on field measurements of strains or stresses (Kaiser et al., 1990; Zou and Kaiser, 1990).

The main purpose of this study is to use displacement-based direct back analysis approach in order to evaluate the geomechanical parameters of rock masses in Siah Bisheh PHC and compare them with adopted design parameters. The instruments used are inclusive extensometers, load cells, convergency pins and geodetic points. Rock mass parameters selected for design of powerhouse cavern have been based on laboratory tests and conventional rock mass classification methods (Lahmeyer Co., 2005a,b).

* Corresponding authors. Addresses: Geotechnical Engineering Group, Civil Engineering Department, Tarbiat Modares University, Tehran, Iran. Tel./fax:+98 82883343 (M. Yazdani), Department of Mining and Metallurgical Engineering, Amirkabir University of Technology, Hafez 424, Tehran 15875-4413, Iran. Tel.: +98 21 6454 2952; fax: +98 21 6640 5846 (M. Sharifzadeh).

E-mail addresses: myazdani@modares.ac.ir (M. Yazdani), sharifzadeh@aut.ac.ir, Most.sharif@gmail.com (M. Sharifzadeh).

0886-7798/$ - see front matter © 2011 Elsevier Ltd. All rights reserved.
doi:10.1016/j.tust.2011.09.002

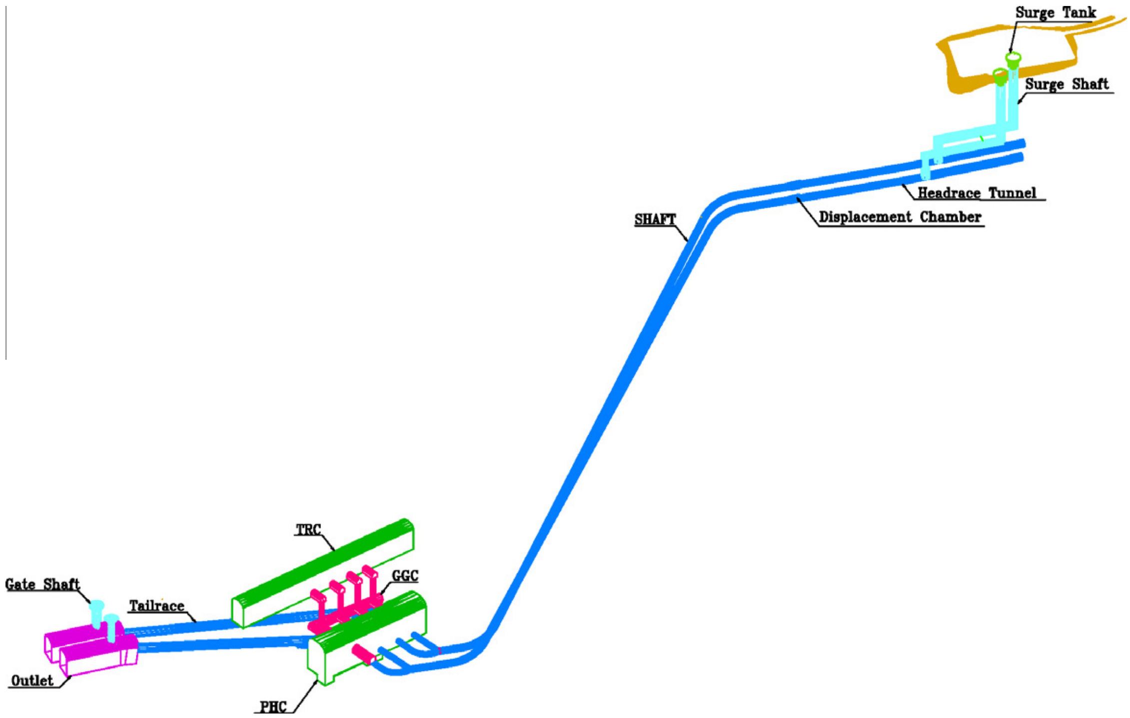

Fig. 1. A 3-D model of Siah Bisheh underground openings.

2. Project description

2.1. Geology and engineering geology

The Siah Bisheh pumped storage project is located at the Alborz Mountains, mainly folded and formed during the Alpine orogenic phase. Geomorphologically, Alborz is a young Mountain with deep and narrow valleys and active tectonics. The most important tectonic phenomenon of Siah Bisheh area are the fault called as the Main Thrust Fault (MTF), with a dip/dip direction of 78/028 and an almost *E–W* trend and the reverse fault of Chalus, which is parallel to the Chalus River in Siah Bisheh area, which must be taking into consideration in terms of seismicity. Powerhouse and transformer caverns are generally under construction at the Permian Formation. In this area, Permian formations mainly consist of quartzitic sandstone, siltstone and shaly siltstone, dark and red shale and igneous rocks. Thickness of these layers varies from some centimeters to 3.5 m (Lahmeyer Co., 2005a,b).

The influence of groundwater on the behavior of rock mass surrounding a tunnel is very important and has to be taken into account in the estimation of potential tunneling problems. When the water is not drained, it reduces the effective stresses and thus the shear strength along discontinuities and finally, in all cases, the strength of the rock mass. In addition, it is particularly important when dealing with shales, siltstones and similar rocks in which they are susceptible to changes in moisture content, which directly affect their strength.

There are uniform bedding layers throughout the powerhouse area with deep and dip direction of 55/195. It is noteworthy that during excavation of the powerhouse pilot at chain ages 40, 81 and 89 of the right wall, three shear zones, with an almost 40–50 cm thickness were encountered. All of these features are parallel to the bedding planes. The azimuth of powerhouse cavern is N152°E and all of the existing faults in the powerhouse area have an appropriate distance from cavern walls and without any intersection.

Rock mass consists of Bedding planes and 5 main joint sets in powerhouse area (Table 1). Based on surveying along the pilot tunnel at the center of powerhouse crown, the rock joints have different lengths of almost 3–10 m and their spacing is between 200 and 600 mm (Lahmeyer Co., 2005a,b).

Table 1
Discontinuities' orientations at powerhouse cavern [10].

Discontinuity	Dip direction (°)	Dip (°)
Bedding	191	55
Joint J1	030	56
Joint J1-1	018	81
Joint J1-2	009	66
Joint J1-3	305	80
Joint J2	078	82

2.2. Geotechnical parameters

Considering the large length of powerhouse cavern, various types of geological properties are present. Due to the fact that most of the geological properties could not be directly measured for this site, they had to be estimated by empirical and theoretical methods. For this purpose, generalized Hoek–Brown failure criterion was utilized. The results showed various geological zones at the power house cavern region and therefore, the area were initially divided into two zones. Likewise to determine the strength characteristics of the rock masses, the uniaxial compressive strength tests were carried out. Moreover, the large flat jack tests and dilatometer tests were performed to determine the deformability characteristics of the rock masses. Also using the field surveys, the RMR value at the related zones was obtained 45 with fair rock class IV. Table 2 shows the mechanical characteristics of different rock types adopted from rock mass classifications and in situ experiments (Lahmeyer Co., 2005a b).

A joint mapping program with 414 measurements was conducted in the exploratory vault adit indicating five major joint sets and one bedding plane.

The shear parameters of $\phi = 25°$ and $c = 0$ were assumed on bedding planes. Also, based on the assumption of 10 cm thick shear

Table 2
Rock mass shear strength according to Hoek and Brown, 2002 and flat jack tests.

				Disturbance factor = 0				Disturbance factor = 0.7				Flat jack test	
Rock Type	GSI	UCS (MPa)	m_i	E (GPa)	σ_{cm} (MPa)	C (MPa)	φ (°)	E (GPa)	σ_{cm} (MPa)	C (MPa)	φ (°)	E (GPa)	ν
Quartzitic sandstone	53	85	20	11	22	1.6	53	7.1	14	1.1	46	15	0.2
Red shale	48	50	9	6.3	7.9	0.98	41	4.7	0.66	0.66	32	7.5	0.25

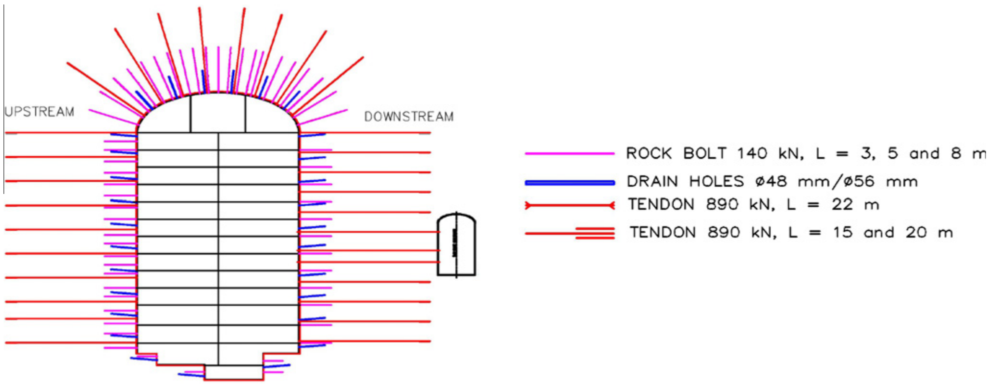

Fig. 2. Typical support system installed in the powerhouse cavern and excavation stages with drainage holes at roof and sidewalls.

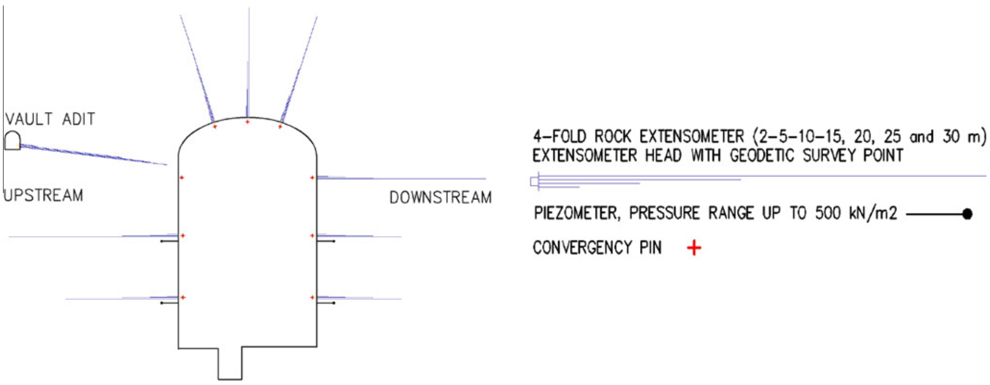

Fig. 3. Typical instrumentation array installed in the powerhouse cavern (chainage 67, Section 3).

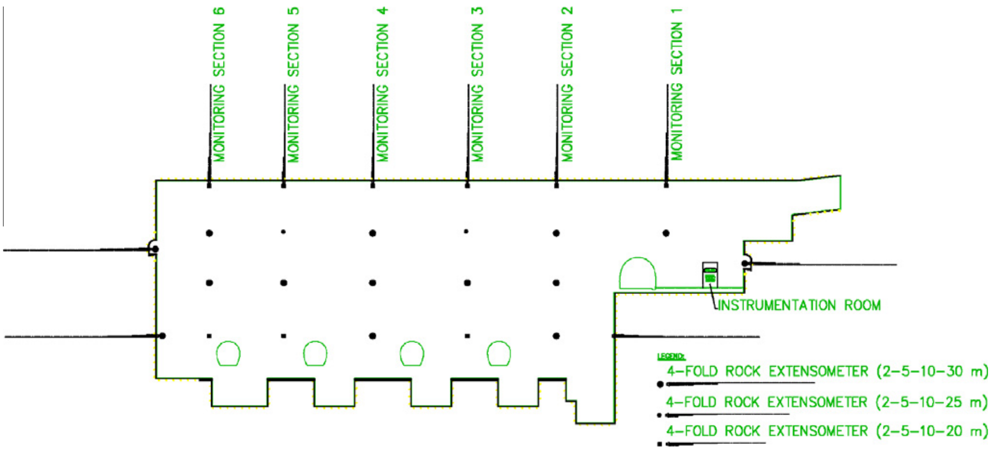

Fig. 4. A longitudinal section of monitoring system with rock extensometers in powerhouse cavern.

bands and the Young's Modulus of 2000 MP, the normal and shear stiffness parameters of rock joints were estimated 20,000 and 7692 MPa/m, respectively.

The value of stress ratio (k) was determined based on field investigation equals to 1.1.

2.3. Excavation, Support system and monitoring system

All caverns excavated using NATM method. For excavation of powerhouse cavern, at first a pilot was drilled at the center of crown and then slashing the crown were carried out. After that, benching was performed with 3 m depth in each stage toward powerhouse floor.

The support system in powerhouse cavern consists of shotcrete with wire mesh (20 cm in side walls and 25 cm in roof), grouted rock bolts (temporary support system) and double corrosion protection tendons (permanent support system). After each cycle of blasting, the exposed roof and walls were immediately shotcreted. Bolt installation had sometimes delay. Many drainage holes with 4 m length in a 4 × 4 m pattern have been performed at roof and side walls of powerhouse cavern (Fig. 2).

Monitoring is the systematic collection of the information as the project progresses. It is aimed at improving the efficiency and effectiveness of a project which can be an invaluable tool if done properly to provide a useful base for evaluation of parameters. Six instrumentation arrays were set up along the axis of the powerhouse cavern at chainages of 26, 49, 67, 87,105 and 121. These arrays consist of grouted rod extensometer in the roof and sidewalls, convergency pins, piezometer as well as cable anchor load cells on selected cables. Due to delay in installation of extensometers, some displacement data has been lost. The behavior of PHC and recorded values by instrumentations are largely depending on excavation sequence in the powerhouse cavern and adjacent underground openings (Lahmeyer Co., 2005a,b; Tablieh Construction Co., 2008). A typical instrumentation section and schematic presentation of monitoring system in powerhouse cavern are illustrated in Figs. 3 and 4.

3. Numerical modeling of powerhouse cavern

There are two different approaches available in modeling of jointed rock, one is continuum and the other is discontinuum approach. When considering a given rock mechanics problem, some regions of the rock mass could be treated as continuous, whilst discontinuum analysis would explicitly apply to other elements like discontinuities (Fakhimi, 2009). A continuum model would reflect mainly material deformation of the system, whilst a discontinuum model would reflect the component movement of the system. The concepts of continuum and discontinuum are, however, not absolute but relative and problem specific, depending on the problem scale (Elmo, 2006; Bobet, 2010). The use of continuum modeling in tunnel engineering makes it essential to simulate the rock mass response to excavation by introducing an equivalent continuum. The most common way to solve this problem is to scale the intact rock properties down to the rock mass properties by using empirically defined relationships such as those given by Hoek and Brown (1997).

Rock joints and discontinuities in a rock mass play a key role in the response of a tunnel to excavation, i.e. joints can create loose blocks near the tunnel profile and cause local instability; joints weaken the rock and enlarge the displacement zone caused by excavation; joints change the water flow system in the vicinity of excavation. The use of discontinuum modeling has been gaining progressive attention in tunnel engineering mainly through the use of UDEC and 3DEC codes, for 2D and 3D discontinuum modeling, respectively.

Siah Bisheh powerhouse cavern is located in discontinues media and due to low level in situ stress, the failure of rock mass is mainly controlled by the discontinuity distribution. In this study,

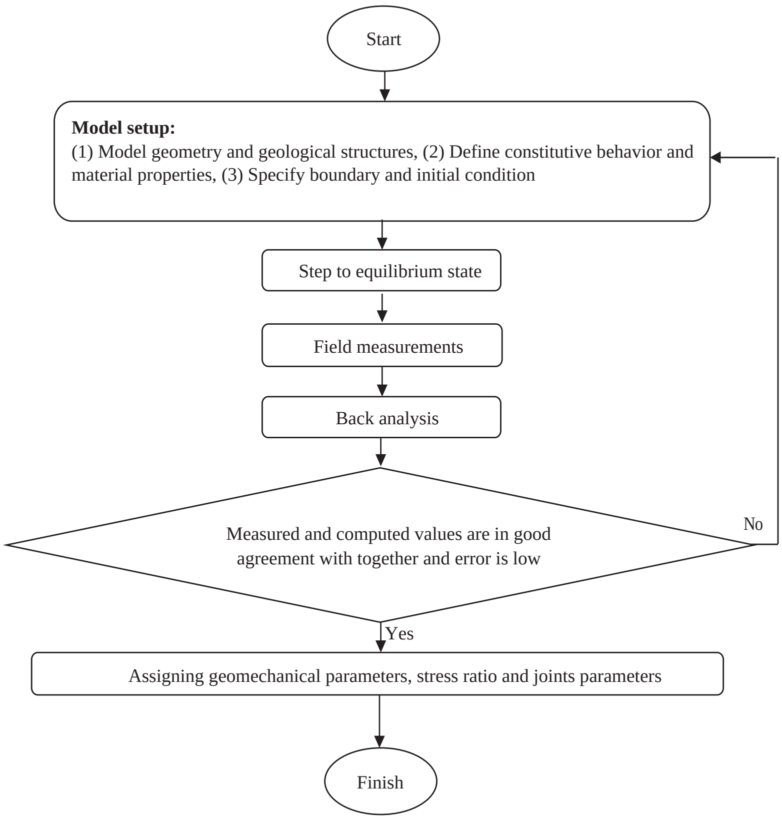

Fig. 5. Flowchart of back analysis under natural condition (Ghorbani and Sharifzadeh, 2009).

Table 3
Mechanical and physical properties of intact rocks (Lahmeyer Co., 2005a,b).

Parameters	Quartzitic sandstone	Red shale	Melaphyr
Dry density (kg/m^3)	2810	2630	2900
Saturated density (kg/m^3)	2970	2750	2920
Bulk modulus (GPa)	8.33	5	16.67
Shear modulus (GPa)	6.25	3	12.5
Compressive strength (MPa)	85	50	100
Tensile strength (MPa)	6	3	6
Friction angle (°)	50	40	50
GSI	53	48	55
mi	20	9	25

Table 4
Mechanical properties of rock joints (Lahmeyer Co., 2005a,b).

Item	Value
Normal stiffness (MPa/m)	20,000
Shear stiffness (MPa/m)	7692
Cohesion (MPa)	0.5
Friction angle (°)	30
Tensile strength (MPa)	0

considering blocks size, pattern and spacing of discontinuities, 3 dimensional distinct element analysis was performed. On the other hand, considering 5 joint sets, with joint spacing 12, 14 and 17 cm plus bedding planes, low overburden (maximum 250 m), uniformity of monitoring data and various lithology and also weak rock type in mostly monitoring sections, continuum function is likely to be more relevant. Therefore, it seems modeling in both continuum and discontinuum is essential. In order to numerical modeling of Siah Bisheh underground openings, PHASE^2 and 3DEC codes were utilized. At first, two 2-D models were prepared in the chainages, 49 m and 105 m of the powerhouse cavern using PHASE^2. Then, a 3D model was constructed through the 3DEC code. Fig. 5 shows the flowchart of back analysis of powerhouse cavern under natural condition.

Mechanical and physical properties assigned to both continuous and discontinuous models were determined from laboratory and field test (Table 3). Mechanical properties of rock joints are presented in Table 4. Physical properties of shotcrete and interface with the rock are presented in Table 5 and parameters of tendons are presented in Table 6.

The Mohr–Coulomb perfect plasticity model was assigned as constitutive model for both continuous and discontinuous analyses.

3.1. Continuum modeling

Due to the various geological conditions along the caverns an as-built geology model were made for two separate monitoring sections of the PHC. The model includes the final shape of caverns, the as-built excavation sequence, as-built support measures including their respective time of installation and installation time of monitoring equipments. In addition geological model had to be simplified, since a large number of thin layers, which changed partially in the decimeter range could not be taken over into the numerical model. Also, the contacts between different lithological units are assumed as joints (Yazdani and Kamrani, 2009), (Fig. 6).

Table 5
Physical properties of the shotcrete and the interface with the rock.

Shotcrete	
Density (kg/m^3)	2400
Elastic modulus (GPa)	21
Poisson's ratio	0.2
Compressive strength (MPa)	40
Tensile strength (MPa)	20
Interface between the shotcrete and the rock	
Cohesion (MPa)	2.5
Friction angle (°)	35
Dilation angle (°)	10
Normal stiffness (GPa/m)	10
Shear stiffness (GPa/m)	10

Table 6
Properties of tendons used in modeling.

Support type	Diameter (mm)	Young's modulus (GPa)	Ultimate yield load (KN)	Kbond (GN/m/m)	Sbond (MN/m)
Tendon	26.5	200	300	6.41	2.01
Tendon	47	200	890	6.03	3.77
Tendon	63.5	200	1540	6.79	4.59

3.2. Discontinuum modeling

For modeling of powerhouse complex, a block model with 210 m length, 220 m height and 270 m width including powerhouse, transformer and guard gate caverns were constructed (Fig. 7). Also, stages of excavation and support systems of underground openings were modeled based on real condition of construction. Critical joints and bedding planes were considered in the model.

Siah Bisheh underground openings are excavated in quartzite sandstone, red shale and igneous rocks (mainly classified as hard and competent rocks). Powerhouse cavern was constructed beneath underground water table. Therefore, for long term stability analysis, the effect of water was considered on these rocks and underground water table was applied in the discontinuum model. Water effect on such rocks is mainly mechanical and hence pore pressure in intact rock and uplift pressure in discontinuities should be considered. Water absorption in hard rocks does not change largely the strength parameters (cohesive strength and intrinsic friction angle). For these types of rocks, in all rock strength criteria, total stress should be replaced by effective stress and in rock joints, uplift pressure (u) is exerted to the joint surfaces, and uplift pressure subtracted from total normal stress (Ghorbani and Sharifzadeh, 2009).

After model setup and steps to equilibrium state, direct back analysis of powerhouse cavern using extensometers results was carried out and geomechanical properties of rocks, stress ratio and joints parameters were identified.

4. Back analysis of rock mass

In this study, displacement based direct back analysis using univariate optimization algorithm were applied. The direct approach employs the trial values of the unknown parameters as input data in the stress analysis algorithm, until the discrepancy between measurements and corresponding quantities obtained from a numerical analysis is minimized (Cividini et al., 1981). Direct formulation is very flexible and applying such a procedure for complex constitutive models is easier. Furthermore, development of the direct back analysis code is much less difficult than development of the code based on an inverse algorithm. The only work is appending an existing program with a module. For this reason a Fish function was written which minimizes the errors between measured and computed values as follows:

$$\varepsilon(p) = \sqrt{\frac{1}{n}\sum_{i=1}^{n}\left(\frac{u_i^m(p) - u_i}{u_i}\right)^2} \tag{1}$$

where u_i and $u_i^m(P), i = 1, 2, \ldots, n$ are the measured and corresponding numerical results, respectively. Obviously, $u_i^m(P)$ depends on the unknown model parameters collected in the vector P.

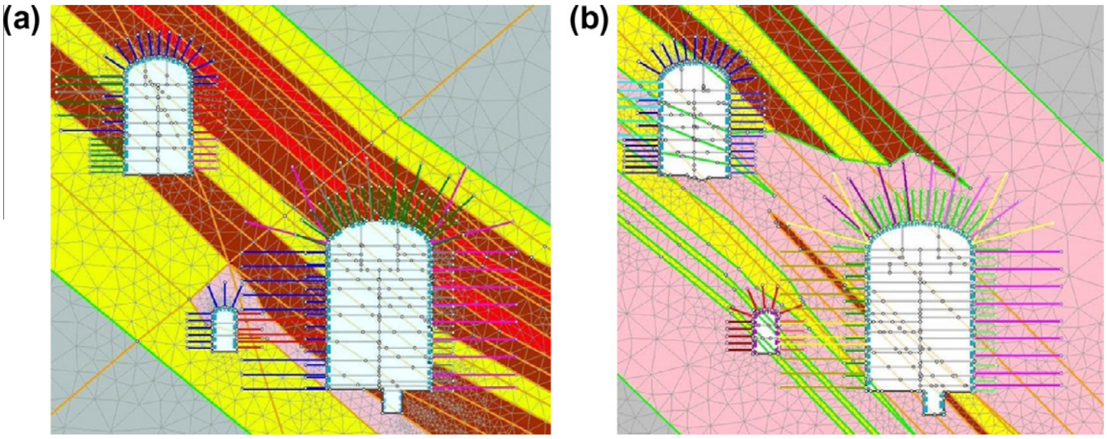

Fig. 6. (a) Continuum model for monitoring Section 2 (bedding area), and (b) continuum model for monitoring Section 5 (melaphyry area)- PHASE^2.

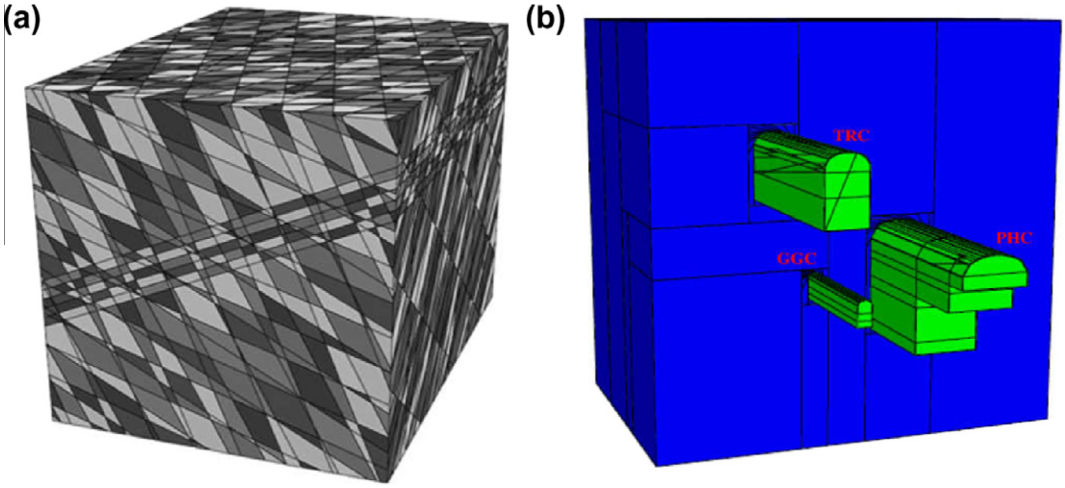

Fig. 7. (a) 3D Model geometry with discontinuities, bedding planes and underground water table; and (b) location of powerhouse, transformer and guard gate caverns in discontinuum model-3DEC.

Here, we used a normalized error function to decrease the effect of measurements error.

In univariate method, only one variable is changed at a time and the values of other $n-1$ variables are fixed. After optimization of one variable, in the next step the value of one variable which was fixed in previous step is changed and the values of other variables are fixed. This procedure is continued until the optimized values of all variables are determined.

About 40–50 m of the end of powerhouse cavern is igneous rock (Melaphyr) and the remaining is bedding part which is sequence of Quartzite Sandstone, Red Shale, mylonite and Melaphyr. For this reason, in order to back analysis of geomechanical properties of these parts, two different error functions based on formula (1) were developed in discontinuum model using the results of extensometers installed in each part. But, in continuum method, two different models in the chainages of 49 m (bedding part) and 105 m (melaphyry section) of the powerhouse cavern were prepared to perform back analysis separately for these two models.

It is better to process the measurements results before they can be used in back analysis. Wrong displacements due to reading error or inaccurate performance of instruments must be eliminating. Therefore, after the assessment of extensometers results, finally 150 points among 208 points of recorded displacements were selected for back analysis.

The minimization of the error function alone, does not always guarantee a correct back analysis. The qualitative trend of the displacements on the cavern walls should be the same in the calculation as in reality, as a confirmation of the validity of the calculation model and of the simplified assumed hypotheses.

In Table 7, final results of back analysis for Melaphyry section and bedding part are presented for both continuum and discontinuum models. The results of both models show that elastic modulus has highest effect and Poisson's ratio, friction angle and cohesion have respectively least effects on error function and thus on displacement values.

Relationship between the horizontal and vertical stresses in the rock mass (K) is difficult to be estimated from the preliminary investigations and hence rely heavily on back analysis results. For this reason, after geomechanical properties identified for Melaphyry section and bedding part in both models, the back analysis for stress ratio were carried out (Table 7). The results show that the stress ratio has a great effect on error function and by increasing it, the values of displacements in powerhouse walls have been increased.

In addition, back analysis were carried out to find joints strength and stiffness properties in both continuum and discontinuum models (Table 7). The results in continuum models indicate that friction angle have a major impact on deformations of the power house cavern. However, in discontinuum model it was obtained that joints parameters especially joints normal and shear stiffnesses have remarkable influences on error function values.

In Table 7, results of back analysis for geomechanical properties of melaphyry section and bedding part, stress ratio and joints

Table 7
Back analysis results for Siah Bisheh powerhouse cavern in continuum and discontinuum approach.

Geomechanical properties	Continuum approach		Discontinuum approach	
	Melaphyry section	Bedding part	Melaphyry section	Bedding part
Young's modulus (MPa)	10 ± 0.5	9 ± 0.5	16 ± 0.5	9 ± 0.5
Cohesion (MPa)	2 ± 0.25	1.5 ± 0.125	3 ± 0.25	1.75 ± 0.125
Friction angle (°)	44 ± 0.5	40 ± 0.5	41 ± 0.5	38 ± 0.5
Poisson's ratio	–	0.23	–	0.24
Stress ratio (k)	1.2	1.1	1.1	
Joints parameters				
Normal stiffness (GPa/m)	20	30	30	
Shear stiffness (GPa/m)	7.69	10	10	
Cohesion (MPa)	0.1 ± 0.05	0.2 ± 0.05	0.4 ± .05	
Friction angle (°)	15 ± 2.5	20 ± 2.5	30 ± 2.5	

Table 8
Comparison between computed values in both continuum and discontinuum models and measured values in 2rd instrumentation array.

	Position of extensometers	Measured values using extensometers (mm)	Computed values in continuum approach (mm)	Computed values in discontinuum approach (mm)
Upstream wall	EL. 1866 (EXT.1)	46.63	37.6	43.2
	EL. 1858 (EXT.2)	40.1	36.9	58.3
	EL. 1847 (EXT.3)	21.54	17.8	23.1
Roof	Upstream roof (EXT.4)	11.95	14.8	15.24
	Roof center (EXT.5)	36.78	36.4	18.23
	Downstream roof (EXT.6)	17.25	21.3	14.6
Downstream wall	EL. 1866 (EXT.7)	25.24	26.4	27.62
	EL. 1858 (EXT.8)	34.13	28.6	42.6
	EL. 1847 (EXT.9)	7.76	6.5	17.32

Table 9
Comparison between least square values of continuum and discontinuum models in 2rd instrumentation array.

Measured values using Extensometers (mm)	Least square method in continuum approach (d_c)	Computed values in discontinuum approach (mm) (d_d)	Least square method in discontinuum approach		Computed values in continuum approach (mm)	
			$A = \sum (d_c - d_m)^2/n$	LSM = $\sqrt{A}$	$A = \sum (d_c - d_m)^2/n$	LSM = $\sqrt{A}$
46.63	37.6	43.2	3.48	11.58	1.31	9.87
40.1	36.9	58.3	50.88		36.8	
21.54	17.8	23.1	3.12		0.27	
11.95	14.8	15.24	0.02		1.2	
36.78	36.4	18.23	36.68		38.23	
17.25	21.3	14.6	4.99		0.78	
25.24	26.4	27.62	0.17		0.63	
34.13	28.6	42.6	21.78		7.97	
7.76	6.5	17.32	13.01		10.15	

parameters in continuum and discontinuum approaches are presented. The best way to present final results of back analysis is to introduce them as a mean value and its amplitude.

In order to compare the results of continuum and discontinuum analysis with measured values, deformations are obtained in several locations of the powerhouse cavern where the extensometers of 2rd instrumentation array are installed (Table 8). This array is very important because there are many shear zones in this area. Instrumentation shows large values of displacement and load in this array. As seen in Table 8, computed values are in a good agreement with measured values in both models. Because of delay in the installation and reading of extensometers, the first part of deformations were lost, therefore in 3DEC model measured data exhibits the values lower than the analyzed results. However, in PHASE^2 model since as-built monitoring instruments, including their respective time of installation were considered, therefore, the analyzed results show lower values in comparison with measured data. Generally, numerical modeling results are close to reality. In the following, least square values of each approach were calculated and it became clear that results of both continuum and discontinuum approaches suits well with measured data. Table 9 provides a summary of the calculation results.

5. Discussion and conclusion

Back analysis is a practical engineering tool to evaluate geomechanical parameters of underground and surface structures based on field measurements of some key variables such as displacements, strains and stresses. These parameters are necessary for stability analysis and design of support system for geostructures.

Back analysis of Siah Bisheh powerhouse cavern during construction using the finite element method and distinct element method were carried out in the computer codes PHASE^2 and 3DEC. Initial values of input parameters required in the both models were based on results of geological and geotechnical investigations and estimated by empirical and theoretical methods.

The parametric studies were indicated that cavern response is strongly dependent on the rock mass modulus, horizontal to vertical stresses ratio and friction angle of joints. Based on results presented in Table 7, almost all rock mass parameters obtained from back analyses in both models are in good agreement with each other but the elasticity modulus of melaphyry section and friction angle of joint parameters in both models show discrepancy. This major difference between Young's modulus can be explained by adjacent excavation openings, shear zones and non-interference effect of rock layers in discontinuum model. It also seems that the difference between the values of friction angle of joint parameters is based on performance of softwares. This study clarifies that the back analyzed value of Young's modulus is more representative for mechanical behavior of rock masses in a large domain. Meanwhile, the results demonstrate very clearly that the default assumed rock mass parameters for design powerhouse cavern seem to be high. Finally, the least square values of each approach were calculated and it became clear that results of both continuum and discontinuum approaches suits well with measured data. 3 dimensional discontinuum modeling using 3DED software were difficult and time consuming, therefore we propose equivalent 2 dimensional continuum modeling using PHASE^2 software for numerical modeling of Siah Bisheh powerhouse complex.

Acknowledgements

The authors would like to express the appreciation and thanks for the managers and personnel of Tablieh Construction Co. for their contribution to this research.

References

Akutagawa, S., Takeuchi, K., Shimura, T., Sakurai, S., 2000. A comparative study on the performance of back analysis procedures for identification of nonlinear deformational behaviour of a rock mass around a large underground powerhouse cavern. In: Proceedings of the 4th NARMS, Pacific Rocks, Seattle, pp. 1035–1041.

Bobet, A., 2010. Numerical methods in geomechanics. The Arabian Journal for Science and Engineering 35 (1B), 27–48.

Cividini, A., Jurina, L., Gioda, G., 1981. Some aspects of characterization problems in geomechanics. International Journal of Rock Mechanics and Mining Sciences and Geomechanics Abstracts 18, 487–503.

Elmo, D., 2006. Evaluation of a hybrid FEM/DEM approach for determination of rock mass strength using a combination of discontinuity mapping and fracture mechanics modelling, with particular emphasis on modelling of jointed pillars, PHD thesis, p. 212, School of Geography Archaeology and Earth Resources, University of Exeter in Cornwall.

Fakhimi, Ali, 2009. A hybrid discrete–finite element model for numerical simulation of geomaterials. Computers and Geotechnics 36, 386–395.

Feng, X.T., Zhao, H., Li, S., 2004. A new displacement back analysis to identify mechanical geo-material parameters based on hybrid intelligent methodology. International Journal for Numerical and Analytical Methods in Geomechanics 28, 1141–1165.

Ghorbani, M., Sharifzadeh, M., 2009. Long term stability assessment of Siah Bisheh powerhouse cavern based on displacement back analysis method. Tunnelling and Underground Space Technology 574, 583.

Gioda, G., Locatelli, L., 1999. Back analysis of the measurements performed during the excavation of a shallow tunnel in sand. Numerical and Analytical Methods in Geomechanics 23, 1407–1425.

Hoek, E., Brown, E.T., 1997. Practical estimates or rock mass strength. International Journal of Rock Mechanics and Mining Sciences and Geomechanics Abstracts 34 (8), 1165–1186.

Kaiser, P.K., Zou, D., Lang, P.A., 1990. Stress determination by back analysis of excavation-induced stress changes–a case study. Rock Mechanics and Rock Engineering 23 (3), 185–200.

Lahmeyer Co., 2005a. Basic Design Criteria Report-Siah Bisheh Pumped Storage Powerhouse Cavern.

Lahmeyer Co., 2005b. Report on Geology and Engineering Geology of Powerhouse Cavern-Siah Bisheh Pumped Storage Powerhouse Cavern.

Oreste, P., 2005. Back-analysis techniques for the improvement of the understanding of rock in underground constructions. Tunnelling and Underground Space Technology 20 (1), 7–21.

Sakurai, S., 2003. Back analysis for tunnel engineering as a modern observational method. Tunnelling and Underground Space Technology 185, 196.

Sakurai, S., Takeuchi, K., 1983. Back analysis of measured displacements of tunnels. Rock Mechanics and Rock Engineering 16 (3), 173–180.

Swoboda, G., Ichikawa, Y., Dong, Q.X., Zaki, M., 1999. Back analysis of large geotechnical models. International Journal for Numerical and Analytical Methods in Geomechanics 23, 1455–1472.

Tablieh Constraction Co., 2008. Siah Bisheh Powerhouse Cavern Monitoring Results and Interpretation.

Yazdani, M., Kamrani, K., 2009. Numerical back analysis for estimation of rock mass parameters in Siah Bisheh powerhouse cavern. In: 2nd International Conference on Computational Methods in Tunneling, Ruhr University Bochum.

Zhang, L.Q., Yue, Z.Q., Yang, Z.F., Qi, J.X., Liu, F.C., 2006. A displacement-based back-analysis method for rock mass modulus and horizontal in situ stress in tunneling–illustrated with a case study. Tunnelling and Underground Space Technology 21 (6), 639–649.

Zou, D., Kaiser, P.K., 1990. Determination of in situ stresses from excavation-induced stress changes. Rock Mechanics and Rock Engineering 23 (3), 167–184.

Shahrood University of Technology

Curtin University

Real time monitoring (conventional – seismic) and design update (forensic study)

Mostafa Sharifzadeh
Western Australian School of Mines (WASM)

1

Presentation Layout

1. Introduction
2. Mine seismic source mechanisms
3. Seismic monitoring instruments and systems
4. Seismic monitoring procedure
5. Monitoring data analysis techniques
6. Monitoring data interpretation
7. Real time design using seismic monitoring results
8. Summary

2

2

Presentation Layout

1. **Introduction**
2. Mine seismic source mechanisms
3. Seismic monitoring instruments and systems
4. Seismic monitoring procedure
5. Monitoring data analysis techniques
6. Monitoring data interpretation
7. Real time design using seismic monitoring results
8. Summary

3

3

Why monitoring?

1. To record the real values of and variation in geotechnical parameters
2. To ensure safety during construction and operation
3. To check the validity of assumptions & conceptual models; and ground response.
4. To control and implementation of ground treatment and remedial works
5. Provide feedback to the design loop and regular design updates to optimise the project.

Brady and Brown (2004)

4

4

Real time Monitoring

- **Traditional monitoring**
  - Piezometer
  - Tiltmeters
  - Extensometers
  - Etc.
- **Seismic monitoring**
  - Sensors
  - Data acquisition instruments,
  - Data transfer units (cable, optical fiber, or wireless),
  - Centre server with processing software,
  - IMS, SINOSEISM

5

5

Conventional monitoring systems

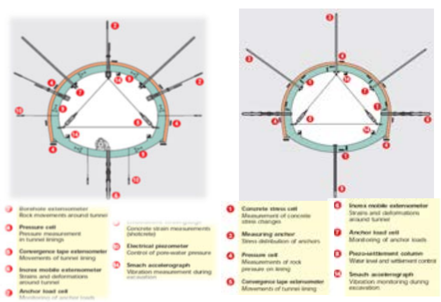

Underground Instrumentation tools

6

6

Rock Engineering Design Approaches and challenges in Deep Hard Rock Mining Engineering – Dec. 15th, 2019 – Shahrood UT

Modeling in forward analysis and back analysis

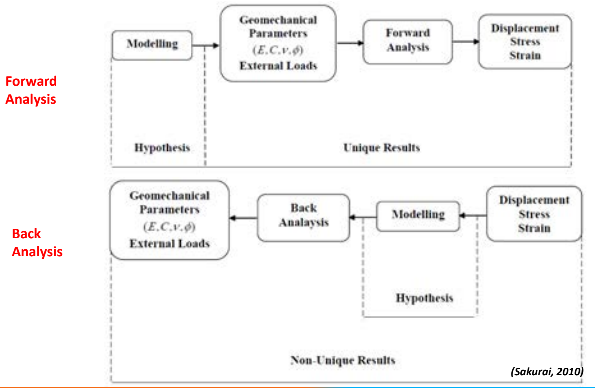

(Sakurai, 2010) 7

7

Rock Engineering Design Approaches and challenges in Deep Hard Rock Mining Engineering – Dec. 15th, 2019 – Shahrood UT

Observation-based design procedure

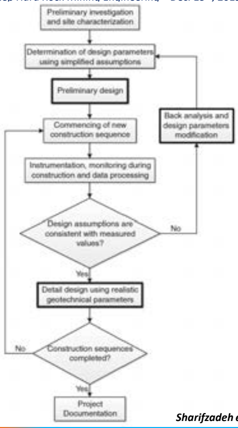

Sharifzadeh et al., 2017 8

8

Rock Engineering Design Approaches and challenges in Deep Hard Rock Mining Engineering – Dec. 15th, 2019 – Shahrood UT

How seismic monitoring assists mine design

1. Exploring whether the mine is seismically active,
2. Geo-structural investigation to detect seismic source mechanisms,
3. selection of seismic monitoring instruments and design of seismic monitoring network,
4. Seismic activity monitoring, acquisition, processing,
5. Prediction of ground behaviour based on seismic data analysis, and warning prior to rock burst.
6. Mitigation measures to prevent, reduce or manage seismic event consequence
7. Documentation of the event

9

9

Rock Engineering Design Approaches and challenges in Deep Hard Rock Mining Engineering – Dec. 15th, 2019 – Shahrood UT

Observational method procedure

- ✓ Exploration
- ✓ Most probable conditions and most unfavourable conceivable deviations
- ✓ Design based on a "working hypothesis" anticipated under most probable conditions
- ✓ Selection of quantities to be observed
- ✓ Calculation of values under most unfavourable conditions
- ✓ Selection in advance of course of action for every forseeable deviation
- ✓ Measurement
- ✓ Modification of design

10

10

Rock Engineering Design Approaches and challenges in Deep Hard Rock Mining Engineering – Dec. 15th, 2019 – Shahrood UT

Factors to be considered in designing an instrumentation project

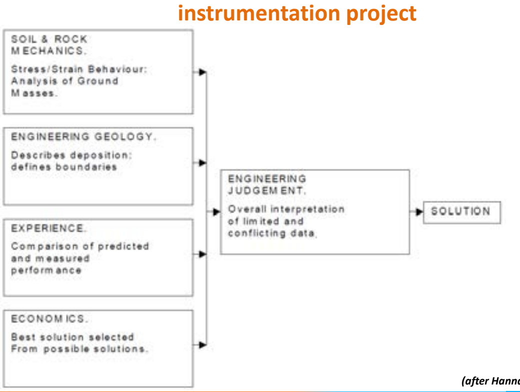

(after Hanna 1985). 11

11

Rock Engineering Design Approaches and challenges in Deep Hard Rock Mining Engineering – Dec. 15th, 2019 – Shahrood UT

Seismically originated backs of ore drive failure

12

12

Number of mine-wide microseismic monitoring systems implemented in Australia since 1994

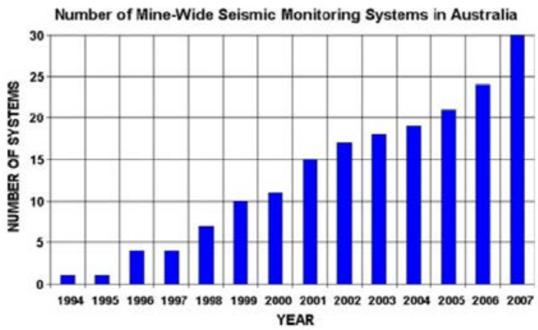

13

13

Rock Engineering Design Approaches and challenges in Deep Hard Rock Mining Engineering – Dec. 15th, 2019 – Shahrood UT

The advantages of applying monitoring and observational methods in underground mining

Modified after Rahimi and Sharifzadeh, 2017

14

14

Rock Engineering Design Approaches and challenges in Deep Hard Rock Mining Engineering – Dec. 15th, 2019 – Shahrood UT

Geotechnical monitoring and design update procedure in underground excavations

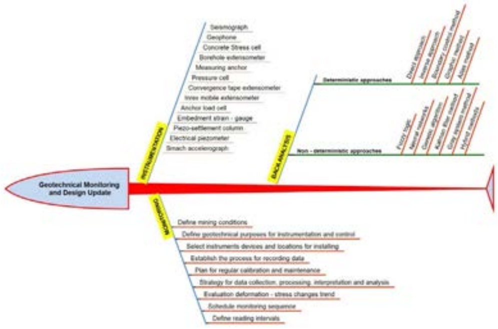

Modified after Rahimi and Sharifzadeh, 2017

15

15

Rock Engineering Design Approaches and challenges in Deep Hard Rock Mining Engineering – Dec. 15th, 2019 – Shahrood UT

The main process of geotechnical monitoring in underground mines

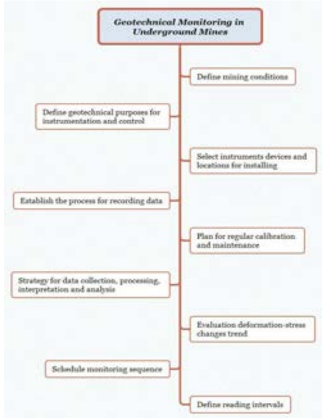

Modified after Rahimi and Sharifzadeh, 2017

16

16

Rock Engineering Design Approaches and challenges in Deep Hard Rock Mining Engineering – Dec. 15th, 2019 – Shahrood UT

Presentation Layout

1. Introduction
2. **Mine seismic source mechanisms**
3. Seismic monitoring instruments and systems
4. Seismic monitoring procedure
5. Monitoring data analysis techniques
6. Monitoring data interpretation
7. Real time design using seismic monitoring results
8. Summary

17

17

Rock Engineering Design Approaches and challenges in Deep Hard Rock Mining Engineering – Dec. 15th, 2019 – Shahrood UT

Rock Bursts associated with geological discontinuities

- **Stress redistribution from larger scale mining can lead to reactivation of faults in the area or violent formation of new fractures through intact rock.**
- **The most common type of large-scale seismic event is fault slip.**
- **The damage caused by these events can be very severe.**
- **They can affect a large area and even be felt on the surface**

18

18

Source Mechanisms of Seismicity

- **Fault Slip**
  Or the movement of a pre-existing geological structure, such as faults, shears, joints and even tight foliation
- **Strain bursting (violent ejection)**
  A condition which develops when local stresses exceeds the rock mass strength and the rock mass deforms instantaneously
- **Pillar bursting**
  The load of a pillar exceeds the strength of the pillar and the pillar fails in an unstable and violent manner
- **Gravity collapse**
  Sudden collapse of a large volume of rock material e.g. North Parkes

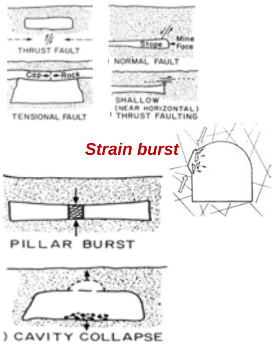

19

19

Source Mechanisms

- **Rockburst flow chart, after Ortlepp, 1997.**

Seismic event	Postulated source mechanism	First motion from seismic record	Richter magnitude M_L
Strain-bursting	Superficial spalling with violent ejection of fragments	Usually undetected, could be implosive	-0.2 to 0
Buckling	Outward expulsion of pre-existing larger slabs parallel to opening	Implosive	0 to 1.5
Face crush	Violent expulsion of rock from tunnel face	Implosive	1.0 to 2.5
Shear rupture	Violent propagation of shear fracture through intact rock mass	Double-couple shear	2.0 to 3.5
Fault slip	Violent renewed movement on existing fault	Double-couple shear	2.5 to 5.0

20

20

Typical Local Rockmass Failure Mechanisms

(b) stress change causing rockmass fracturing near excavations

(a) fault movement

(c) stope overbreak

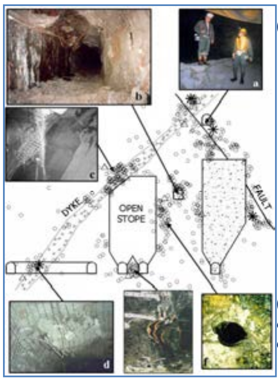

(d) contrast in rockmass material properties causing strainbursting

(f) stress increase causing rockmass deformation

(after Hudyma, 2007). (e) crushing of mine pillars

21

21

Five Mechanisms of Damaging Rock Bursts

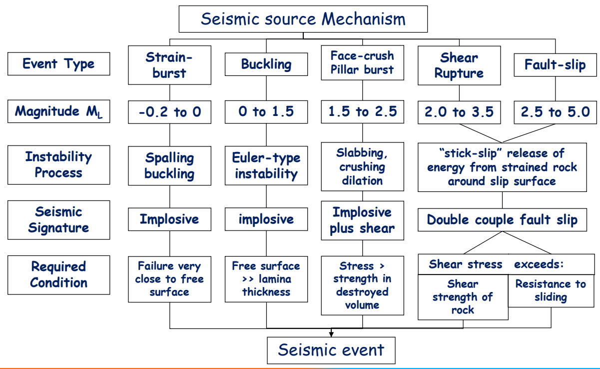

22

22

Damage Mechanisms

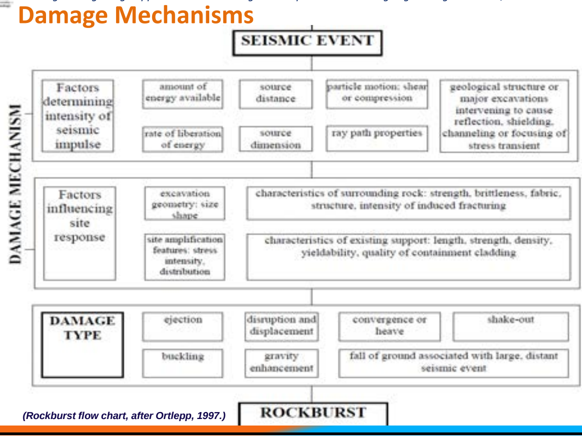

(Rockburst flow chart, after Ortlepp, 1997.)

23

23

Classification according to damage caused by seismic event

Author	Amount of damage				
Scott, 1990	Small seismic events		Large seismic events		
	bumps	knocks	strain burst	crush burst	
Scott et al., 1997	Microseismic events		Rockbursts		
			strain burst	crush burst	slip burst

24

24

Principles of seismic monitoring

When the stress is redistributed in the rock mass due to human activities such as mining, sudden slip or shear may occur along pre-existing zones of weakness, such as along faults or within fracturing networks. This movement or failure results in the release of energy in the form of seismic waves and is known as a seismic event. P- and S-waves (compressional and shear stress waves) radiate away from the rock mass fracturing source and, as these waves pass each sensor, a seismogram is recorded.

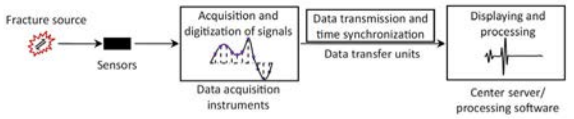

Xiao et al., 2016

25

25

Rock Engineering Design Approaches and challenges in Deep Hard Rock Mining Engineering – Dec. 15th, 2019 – Shahrood UT

Presentation Layout

26

26

Rock Engineering Design Approaches and challenges in Deep Hard Rock Mining Engineering – Dec. 15th, 2019 – Shahrood UT

Instrumentation - Key questions

- Which parameters will be the most appropriate indicators of excavation performance?
- What are the inherent complications during measurement of such parameters?
- What techniques and equipment are most appropriate for measuring such parameters?
- Where and when do we monitor?

(CORE USA 1997, Product Catalogue) 27

27

Rock Engineering Design Approaches and challenges in Deep Hard Rock Mining Engineering – Dec. 15th, 2019 – Shahrood UT

Geotechnical Monitoring in tunnels

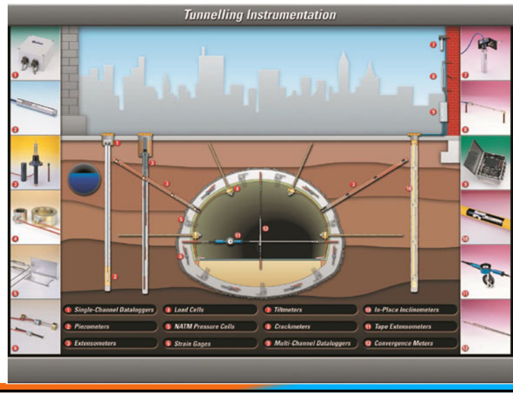

28

28

Rock Engineering Design Approaches and challenges in Deep Hard Rock Mining Engineering – Dec. 15th, 2019 – Shahrood UT

Geotechnical Monitoring in tunnels

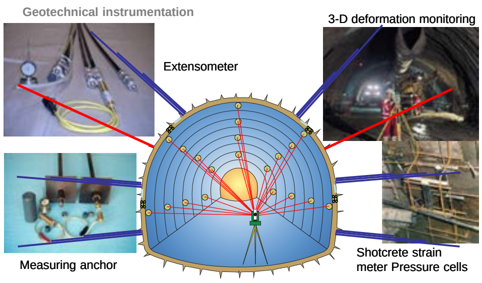

29

29

Rock Engineering Design Approaches and challenges in Deep Hard Rock Mining Engineering – Dec. 15th, 2019 – Shahrood UT

Auto-Warning Telltale Single Height Version – Model TTAW1

Close up of the information plate

➢ The Auto-Warning Telltale is based on a single height version of Golder RMT's standard TTW01S water diverting rockbolting telltale.

➢It has four bright Light Emitting Diodes fitted to the underside of the drip tray. The LEDs are configured to begin to flash if the movement on the visual indicator shows total roof dilation exceeding **5mm** (or other factory set trigger value).

Safety

The Auto-Warning Telltale has been designed and approved to be intrinsically safe to both IECEx and ATEX standards.

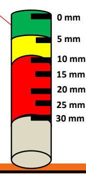

Warning Limits of Auto-warning T.T at Pinoura Mine CM Section

5mm : Setting of Roof dilation(Flashing LED Light)
15mm: Alert of all workmen at working place
20mm: Withdrawal of Men and Machinery

30

30

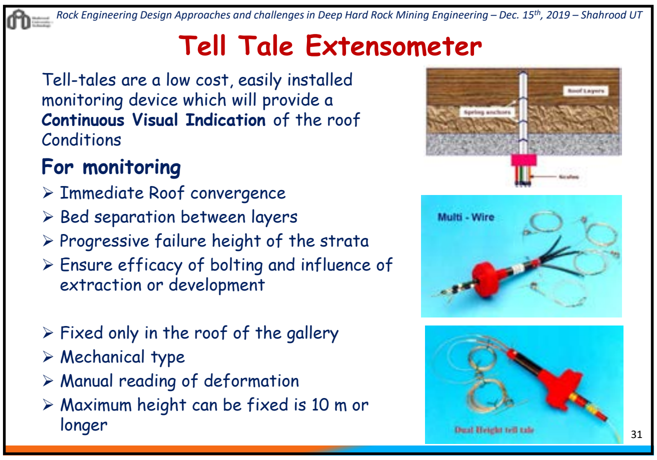

31

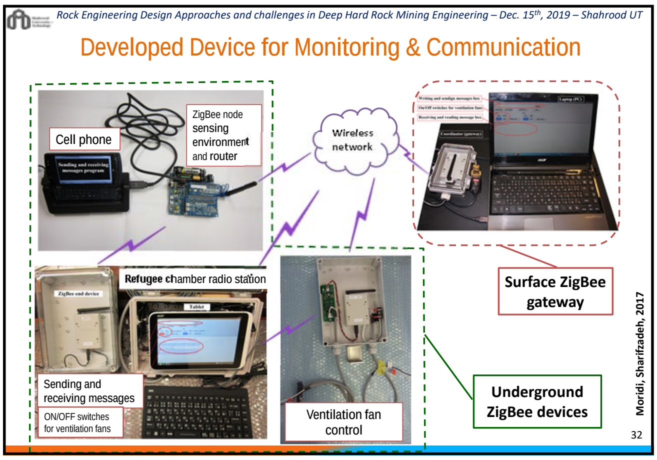

32

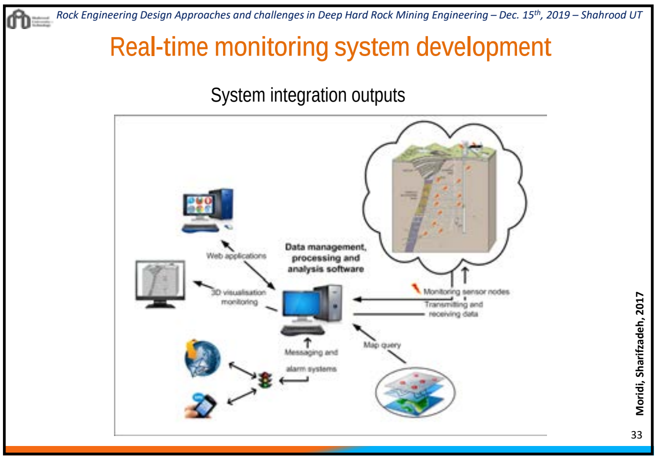

33

34

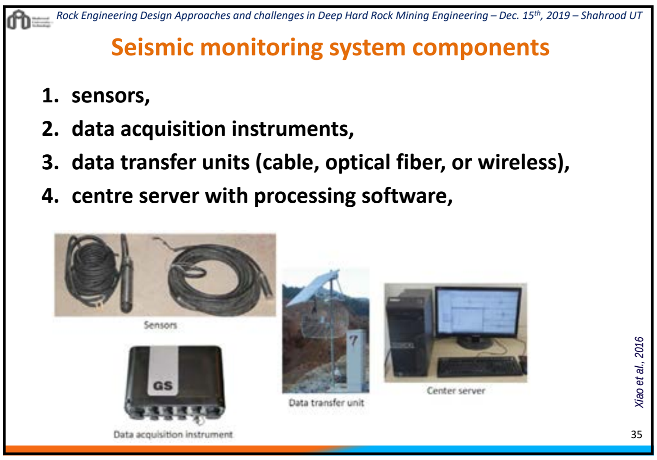

35

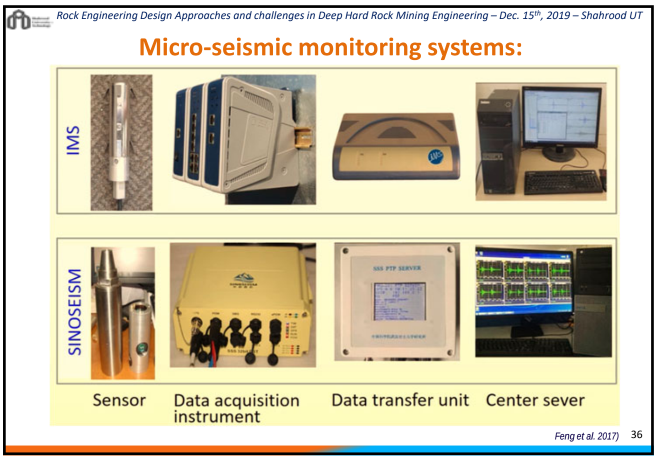

36

Seismic monitoring process

1. seismic waves (P- and S-waves) radiate from seismic sources,
2. seismic waves pass each sensor and recorded in seismogram sensor.
3. The recorded analog signals by sensors are sent to a data acquisition instrument for amplifying and digitizing.
4. the electric signals are transmitted to the centre server through a data transfer unit.
5. The electric signals shown through display software; also, the source parameters of the seismic event, such as origin time, three-dimensional location, radiated energy, and seismic moment, can be calculated and shown.
6. The space–time seismicity in the source mechanism process can be established and analyzed.

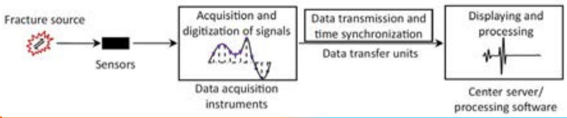

Xiao et al., 2016

37

37

Selection of Seismic Monitoring System

- **seismic monitoring systems are being developed for different purposes, e.g., stability assessment of large underground caverns, rockburst warning in tunnels and mines, and mapping of hydraulic fracturing.**
- **The microseismic monitoring system should be chosen with regard to the monitoring objective.**

Xiao et al., 2016

38

38

Monitoring systems

- **Geophone**
  - Transforms seismic energy into electrical voltage
  - Moving coil or moving magnet type
  - Moving coil:
  - Coil suspended in a magnetic field using springs.
  - Magnet fixed & integral with case.
  - Seismic wave causes magnet to move whilst the coil stationary
  - Relative movement of components generates a voltage.
  - Moving magnet:
  - Same principal - opposite components moving and stationary

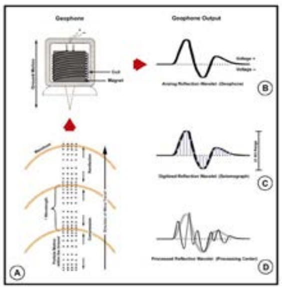

39

39

1- Sensors types

- The seismic sensors are the elements that can detect the elastic waves caused by rock mass fracturing and can convert the elastic wave into an analog signal.
- The types of sensors are divided into two main categories: namely, geophone and accelerometer. sensors can then be further divided into sub-categories for uniaxial and triaxial wave recording according to the number of sensing axes.

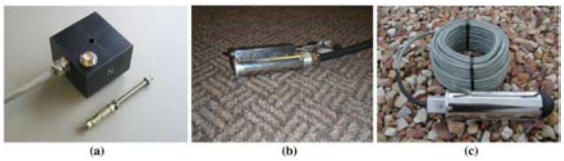

Sensors for seismic monitoring: a surface type, b borehole type of uniaxial geophone, and c borehole type of triaxial accelerometer

Xiao et al., 2016

40

40

Monitoring systems

- **Accelerometer**
  - Sensor output acceleration of the rock mass
  - Mass mounted on top of piezoelectric crystal element coupled to a supporting base
  - Seismic waves cause the mass to exert inertial force on the crystal proportional electric charge.
  - Charge acceleration measure acceleration of rock mass

41

41

Monitoring systems

- Velocity record of rock movement by **integrating** accelerometer results
- Velocity record of rock movement by **differentiating** geophone results
- Geophones better suited to low frequency, high amplitude seismic waveforms
- Accelerometers better suited to low amplitude, high frequency waveforms
- Both sensitive to ground motion in a single direction.
- Require 3 mutually perpendicular (example in image)

42

42

1- Sensors types selection

The types of sensors to be used are mainly determined by the scale of the monitoring project, the monitored objects, rock lithology, and the monitoring purpose. Table shows the project type, the monitored area, the linear dimension of the area, the type and number of sensors used, the frequency width of the sensors, and the moment magnitude range.

Table: Sensor selection referred to in the literature where seismic monitoring has been performed in tunnels, rock slopes, and caverns

References	Project types	Monitored Area	Seismic network	Typical distances	Bandwidth of sensors (Hz)	Moment magnitude
Young and Collins (2001)	Tunnels	Mine-by tunnel, Underground Research Laboratory, Canada	17 triaxial accelerometers	100 m	0.1–10,000	−4.5 to −1.5
Feng et al. (2013a)		Five parallel tunnels, Jinping II hydropower station, China (with frequent intensive rockbursts)	6 uniaxial and 2 triaxial geophones for each working face	70–150 m	7–2000	−2 to 2.5
Feng et al. (2013b)		Diversion tunnel, Baihetan hydropower station, China	6 uniaxial and 2 triaxial accelerometers	50 m	0.1–8000	−3 to 0
Lynch et al. (2005)	Rock slopes	Slope, Navachab mine, Namibia	8 triaxial geophones	200 m	7–2000	−2 to 0
Trifu et al. (2008)		Slope, Chuquicamata mine, Chile	9 uniaxial and 9 triaxial geophones	1 km	15–2000	−0.7 to 1.4
Xu et al. (2011)		Left bank slope, Jinping I hydropower station, China	28 uniaxial accelerometers	400 m	0.1–10,000	−2.5 to 0.2
Trifu et al. (1997)	Caverns	Strathcona mine, Sudbury, Canada	49 uniaxial and 5 triaxial accelerometers	200 m	0.1–10,000	0.5
Scott et al. (1997)		Sunshine mine, Kellogg, USA	Triaxial geophones	1 km	~500	0.5 to 2.5
Liu et al. (2013)		Hongtoushan copper mine, China	6 uniaxial and 1 triaxial geophones	300 m	7–2000	0.1

Xiao et al., 2016

43

43

2. Data Acquisition Instruments

- The data acquisition instrument, which encompasses devices responsible for the conversion of amplified analog signals into a digital format, is the core component of a seismic monitoring system.
- data acquisition instrument can be divided into three parts:
  1. the preamplifier: to amplify the analog electrical signals recorded by the triggered sensor,
  2. the analog–digital converter (A/D converter):transforms the continuous analog signal into a discrete digital signal.
  3. the embedded data acquisition computer (DAC) which provides time stamp marks for the recorded signals. It could be between 3 and 24, or even 48 channels.
- In order to avoid frequency aliasing, the sampling rate should be 5–10 times the maximum in the main frequency range of rock mass fracturing events.

Xiao et al., 2016

44

44

2. Data Acquisition Instruments

In order to avoid frequency aliasing, the sampling rate should be 5–10 times the maximum in the main frequency range of rock mass fracturing events.

Example of a frequency spectrum analysis for rock mass fracturing event

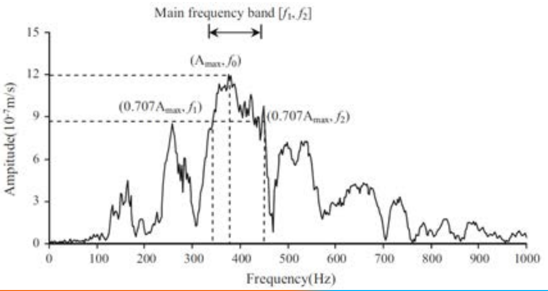

Xiao et al., 2016

45

45

3. Data Transfer Units

The data transfer units transmit the seismic data to a centre computer for storage and processing and provide time synchronization for each data acquisition instrument. The data transfer units can be divided into three parts: sensor to data acquisition instrument, data acquisition instrument to centre server, and centre server to departments of decision making and data processing. Typical data transfer units are shown in Figure.

Example of typical data transfer units in a seismic monitoring system: a the data transfer units between each component; and b the main form of data transfer units

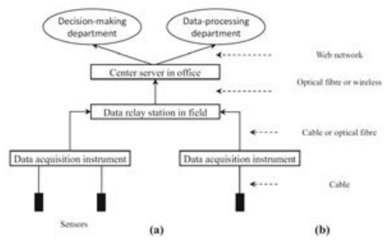

Xiao et al., 2016

46

46

4 – Centre Server and Processing Software

- The center server for setting and mastering the seismic monitoring system is needed for recording the seismogram data from the data acquisition instruments. The server must be adapted to work long hours, or even for several years. Therefore, the center server should be placed in a region which is dry, safe, and has a guaranteed power supply.
- the center server should have a double network card: one is for updating the monitoring data to the analysis location through the internet; the other is the communication interface of the monitoring system. System monitoring software is required for displaying the working condition of every device or component of the seismic monitoring system in real time.
- Some hardware filter rules are established as:
- trigger threshold to execute event detection by seismogram processing software, such as signal-to-noise ratio (SNR).
- recorded frequency width and minimum signal amplitude.
- Short Time Average/Long
- Time Average (STA/LTA), which is a measure of the SNR function,

Xiao et al., 2016

47

47

Seismic monitoring system layout

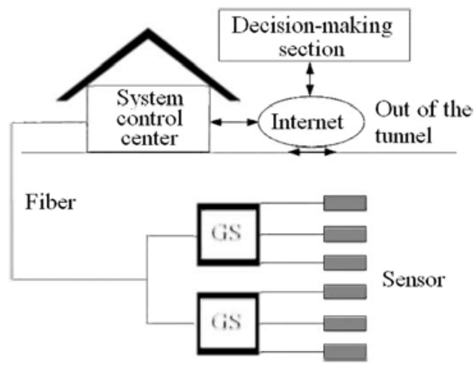

Chen et al. 2011

48

48

Monitoring systems

- **Guidelines for a *minewide* seismic monitoring**
  - **Number of sensors required**
    - A function of the volume of ground to be monitored
      - Intersensor spacing = 150 to 300m
    - Small array = 8 sensors; large array = 12 or more sensors
  - **Surround the volume of interest**
  - **Not all sensor are used for each event**
  - **Source Location**
  - **Sensor configurations:**
    - Uniaxial sensors: Location of seismic events
    - Triaxial sensors (3 uniaxial orthogonally mounted): for estimating parameters such as seismic energy, seismic moment and event magnitude
  - **$40 to $400K (Turner and Beck, 2002)**

49

49

Rock Engineering Design Approaches and challenges in Deep Hard Rock Mining Engineering – Dec. 15th, 2019 – Shahrood UT

Presentation Layout

1. Introduction
2. Mine seismic source mechanisms
3. Seismic monitoring instruments and systems
4. **Seismic monitoring procedure**
5. Monitoring data analysis techniques
6. Monitoring data interpretation
7. Real time design using seismic monitoring results
8. Summary

50

50

Rock Engineering Design Approaches and challenges in Deep Hard Rock Mining Engineering – Dec. 15th, 2019 – Shahrood UT

Seismic monitoring procedure

1. **Preparatory Investigations**
2. **Array Design for the Sensors**
3. **Installation**
4. **Calibration**
5. **Monitoring**

51

51

Rock Engineering Design Approaches and challenges in Deep Hard Rock Mining Engineering – Dec. 15th, 2019 – Shahrood UT

Array Design for the Sensors

Three types of spatial relations between seismic source and sensor array:

a. source a inside the sensor array,

b. at the edge of the sensor array, and

c. outside the sensor array

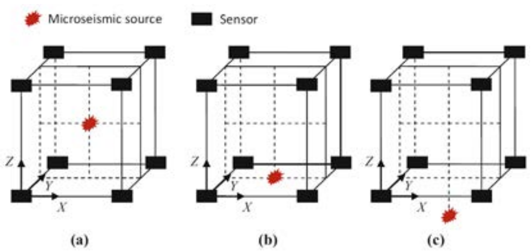

Xiao et al., 2016

52

52

Rock Engineering Design Approaches and challenges in Deep Hard Rock Mining Engineering – Dec. 15th, 2019 – Shahrood UT

Principles of sensor array layout design:

1. **The sensor array should surround the monitoring objects as far as possible to ensure the accuracy of source location.**
2. **sensor spacing will depend on sensor performance and required monitoring sensitivity; each position in the monitoring region should be covered effectively to satisfy the demand of event location accuracy.**
3. **For the critical locations and those with foreseeable potential instability, the density of layout sensors should be increased by increasing the number of sensors and reducing the sensor spacing.**
4. **The data transfer units depend on the sensors' layout and their convenience and security should be considered when designing the sensors layout to ensure continuous and accurate monitoring data.**
5. **During the entire monitoring process, the sensors should be supplemented in areas of adverse geological conditions and those regions with a risk of rock instability.**
6. **The influence of noise (such as from blasting, electrics, drilling, and construction vehicles) on the seismic signal should be reduced as far as possible.**
7. **The whole sensor network should have good 'self tolerance': when the sensors in a certain region do not work, sensors in other areas should still guarantee the basic monitoring in that region.**

Xiao et al., 2016

53

53

Rock Engineering Design Approaches and challenges in Deep Hard Rock Mining Engineering – Dec. 15th, 2019 – Shahrood UT

Approaches to sensor layout design

1. Semi-empirical method, such as the optimal design methods of C-optimality and D-optimality (Kijko 1977; Mendecki 1997). Firstly, a series of sensor layout schemes are prepared according to expertise. Then based on the spatial positions and minimum resolutions of peak particle velocity of sensors, the standard location error and monitoring sensitivity at each seismic source position can be evaluated.
2. Intelligent optimization algorithms, such as the DETMAX algorithm and genetic algorithms (GA) (Rabinowitz and Steinberg 1990; Gong et al. 2010; Maurer et al. 2010). The objective function should fit the demand of location accuracy and sensitivity. Then based on the given optimization algorithm and objective function, the optimal scheme can be determined through continuous search.

Xiao et al., 2016

54

54

Sensor layouts in tunnelling

- For tunnelling the sensors, in the form of 2–3 rows, are often placed behind the working face at a certain distance back and are moved forward repeatedly following the excavation process as shown in Figure.
- a) D&B construction and b) TBM construction

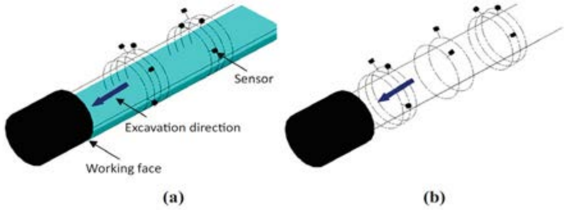

Xiao et al., 2016

55

55

Sensor layouts to monitor brittle sudden failure at Face and along excavation

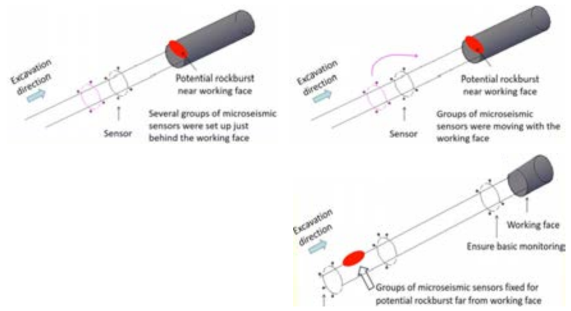

(Modified after Feng et al. 2017)

56

56

sensor layouts for seismic monitoring of rock mass fracturing in a large carven

Example of sensor layouts for seismic monitoring of rock mass fracturing in a large carven complex: sensors a located using pre-existing openings before excavation and b dynamically added via the excavated region during the excavation process

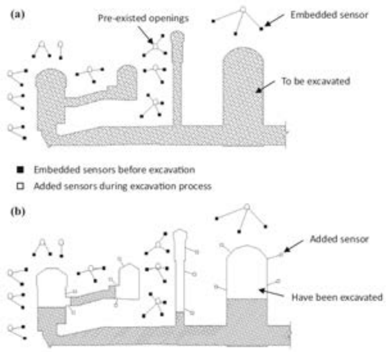

Xiao et al., 2016

57

57

Sensor layouts in Mining

- **For mining engineering, the sensor layout for largescale mining areas can be used for overall monitoring and local stope monitoring.**
- **For large-scale mining areas monitoring, sensors are arranged using pre-existing tunnels in each sub-levels.**
- **As the scale of mining areas can usually reach thousands of meters, the sensor array should cover the whole mining areas as far as possible.**
- **Therefore, enough sensors need to be arranged at each side of the stoped and caved volumes to meet the demand of event location accuracy.**

Xiao et al., 2016

58

58

Sensor layouts for seismic monitoring of a mine:

- Schematic of typical seismic monitoring system
- Sensors distributed in boreholes in 3D array throughout mine
- Sensors linked by digital or analog connection to central processing computer

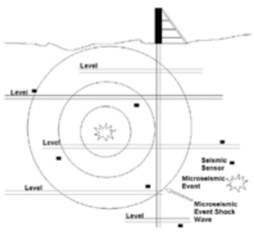

Hudyma et al, 2003

59

59

Typical ESG seismic monitoring system setup

In a typical ESG (Engineering Seismology Group) seismic network, sensors record the ground motion radiated by rock mass failure and it is transferred across copper cable to Paladins (digital seismic recorders). The signal is digitized and relayed to computers on surface through a fibre optic network. Figure 8 is an example of a typical ESG seismic monitoring system (Collins et al., 2014).

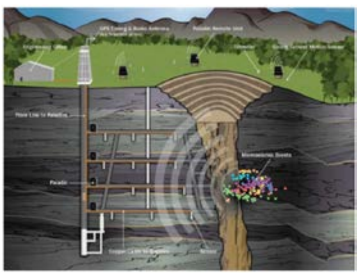

Brown L.G., 2015 60

60

Sensor layouts for seismic monitoring of a mine:

a-located using pre-existing tunnels in each sub-level for large-scale monitoring;

b-located for a typical stope before mining and

c-dynamically added in further tunnels during the mining process

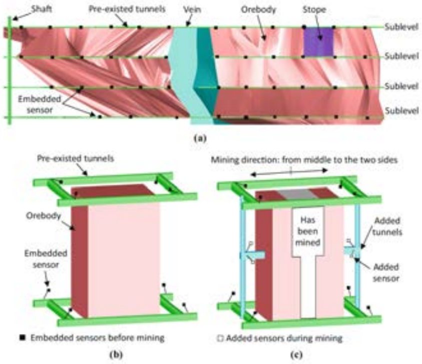

Xiao et al., 2016

61

61

Seismic Network system

- **Figure Top: Plan view of the Inter-Mountain Seismic Network broadband stations and accelerometers/short period stations (triangles) as well as the areal extents of the active stopes (rectangle).**
- **Figure Top: a section view of the in-mine seismic network (red cylinders), stopes (blue solids), and drifts (grey solids)**

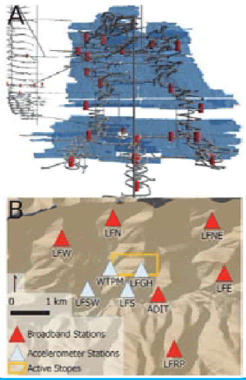

62

62

Sensor locations at Argo mine

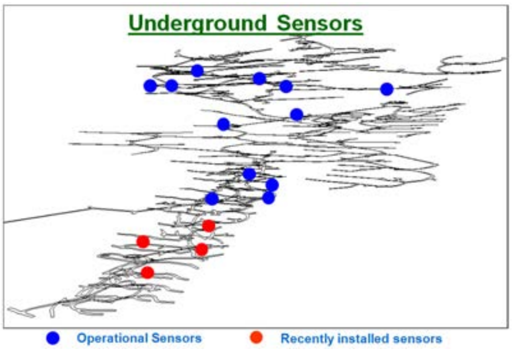

Sensor locations at Argo mine

63

63

Number of sensor per mine area

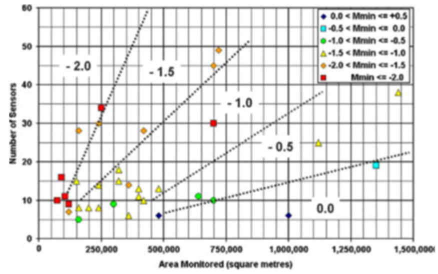

Comparison of the number of sensors in the array, the area monitored and the sensitivity (Mmin) of the microseismic monitoring system, from a compilation of data from 35 Canadian and Australian mines

(Hudyma 2008) 64

64

Installation procedure

1. **Drilling: Too small a borehole diameter will lead to the sensors not being able to be installed.**
2. **Cleaning: The gravels, water, and other residues in the hole caused by drilling should be cleaned.**
3. **Laying of sensor, grouting pipe, and exhaust: For horizontal and downwardly inclined holes, an installation beam is firstly used to place the sensor at the borehole bottom. Then the installation beam should be withdrawn, and the grouting and exhaust pipes are placed into the borehole.**
4. **Grouting: The borehole orifice should be sealed within a sufficient distance (e.g., 300 mm) before grouting.**

Xiao et al., 2016

65

65

Sensor installation process

a- tying the sensor and exhaust pipe together,

b- sensor is placed to the borehole bottom,

c- sealing of orifice, and

d- grouting

Xiao et al., 2016

66

66

Sensor Calibration

A calibration can be achieved with low-energy explosives, or a controlled point source and shear devices. The calibration shot (e.g., explosion) allows a check on sensor first motion polarities, and to see if all sensors are properly installed (rock/sensor contact surface). Relocating the calibration shot can serve as a first estimation of measurement and intrinsic errors involved in the hypocenter location algorithm.

Xiao et al., 2016

67

67

Rock Engineering Design Approaches and challenges in Deep Hard Rock Mining Engineering – Dec. 15th, 2019 – Shahrood UT

Monitoring process

1. Ensuring continuous monitoring is the first priority.
2. An on-the-spot survey should be executed daily by staff familiar with engineering geology and rock mechanics, and trained to recognize geological conditions and typical damage of the rock mass, such as different types of collapse, wall caving, and rockbursts.
3. Those analyzing the data should obtain the monitoring data initially and make an initial evaluation as soon as possible. By combining the seismicity and survey information, a proper interpretation for analysing the state of the rock mass can be given.
4. A database for storing the above-mentioned information is required. This database should include the information about the state of the system, geological conditions, construction events, damage of the rock mass, seismicity, and a comprehensive analysis with conclusions.

Xiao et al., 2016

Xiao et al., 2016

68

68

Rock Engineering Design Approaches and challenges in Deep Hard Rock Mining Engineering – Dec. 15th, 2019 – Shahrood UT

Data Calculations and Processing procedure

1. Diagnosing the Actual Rock Mass Fracturing Signals,
2. Location of Events and Velocity Calibration,
3. Calculation of Source Parameters,
4. Presentation of seismicity for a Rock Mass Fracturing Process.

Xiao et al., 2016

Xiao et al., 2016

69

69

Rock Engineering Design Approaches and challenges in Deep Hard Rock Mining Engineering – Dec. 15th, 2019 – Shahrood UT

Diagnosing the Actual Rock Mass Fracturing Signals

The diagnosis operation can be divided into four parts:

1. typical collection of signals for each seismic source,
2. Characteristics analysis for typical signals,
3. Choosing the method of recognizing a signal,
4. Choosing the digital filter.

Example of diagnosing a rock mass fracturing signal: a input information, waveforms recorded by the seismic monitoring system, and b output information, waveform of rock mass fracturing

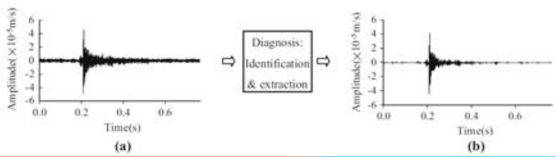

Xiao et al., 2016

70

70

Rock Engineering Design Approaches and challenges in Deep Hard Rock Mining Engineering – Dec. 15th, 2019 – Shahrood UT

Examples for typical time domain waveforms of seismic signals in tunnels:

a–c) different waveforms of rock mass fracturing signal,

d) electrical noise,

e) drilling,

f) blasting,

g) Mechanical vibration of TBM, and

h) vibration of a machine in a D&B tunnel, e.g., construction vehicle and blower

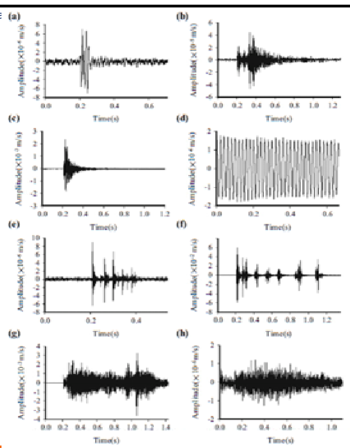

Xiao et al., 2016

71

71

Rock Engineering Design Approaches and challenges in Deep Hard Rock Mining Engineering – Dec. 15th, 2019 – Shahrood UT

Classification and characteristic descriptions of seismic signals

Signals types	Characteristic description
Rock mass facture	The fracturing signal of a rock mass generally has a duration of less than 1 s. The rock mass fracturing signal has a wide range of frequency, mainly concentrated in the range of 10–3000 Hz, with an amplitude magnitude of 10^{-2}–10^{-7} m/s. The waveforms of rock mass fracturing signals are various, as shown in Fig. 14a–c
Electrical	Electrical signals are mainly generated by the improper operation and connection of various electrical components, as well as ineffective cable grounding. The electrical signal generated due to ineffective cable grounding has very similar characteristics to the local AC power signal, which is the resonance wave with the same amplitude, very long duration, and a frequency of 50 Hz, as shown in Fig. 14d
Drilling	The drilling signal is mainly generated by the drilling of blast boreholes and rock bolt boreholes. This type of signal has a notable characteristic, i.e., its multiple wave nature. The waveform within the same signal has a clear periodicity with an occurrence period. The signal has a frequency mainly concentrated in the range of 100–2000 Hz, with an amplitude magnitude of 10^{-5}–10^{-6} m/s. The waveform characteristics of typical signals are shown in Fig. 14e
Blasting	The blast signal generally has a duration of more than 1 s, and the waveform in the same blast signal has a clear periodicity of 0.1– 0.2 s, which is longer than that of a drilling signal. The blast signal received by the geophone has a frequency mainly concentrated in the range of 100–500 Hz, with an amplitude magnitude of 10^{-2}–10^{-3} m/s. The waveform characteristics of typical blast signals are shown in Fig. 14f
Mechanical vibration	The mechanical vibration signals are mainly generated by the operation of construction equipment, such as TBM movement or heavy vehicles passing. The amplitude of this signal depends on the vibration strength, as shown in Fig. 14g, h
Unknown	In addition, there may be other signals with different waveform characteristics, but for which no clear signal sources have been found on site—which may be a result of the superimposition of various ambient noises, so these signals require further analysis

Xiao et al., 2016

72

72

Location of Events and Velocity Calibration

- Dependant on the P-wave to S-wave separation
- Dependant on velocities

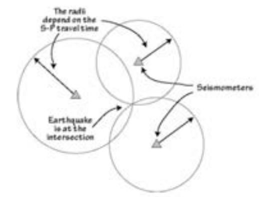

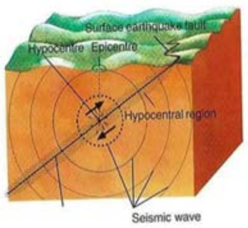

Brown L.G., 2015

73

73

Location of Events and Velocity Calibration

$$\Delta t_k = t_{k+1,P,S} - t_{k,P,S} = \frac{L_{k+1}-L_k}{v_{P,S}} = \frac{\Delta L_k}{v_{P,S}},$$

$$L_k = \sqrt{(x_k-x)^2+(y_k-y)^2+(z_k-z)^2},$$

The principle of source location. t_i is the moment when seismic wave arrives at the i-th sensor, t_0 is the occurrence of the fracturing source, V is the elastic propagation velocity in the rock mass media, x_i, y_i, and z_i are the coordinates of the i-th sensor, and x, y, and z are the location coordinates of the fracturing source

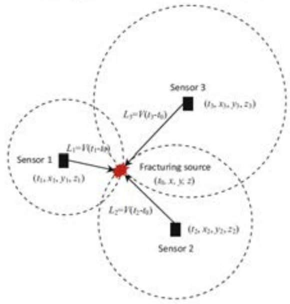

Xiao et al., 2016

74

74

The operation of rock mass fracturing source location can be divided into the following four steps:

1. Determining the arrival times of the P- and S-wave:
2. Calibration of the elastic wave velocity:
3. Choosing the location method of the fracturing source:
4. The representation of fracturing source location results:

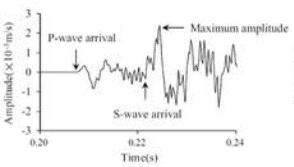

An example for picking the arrival times of the P- and S-waves

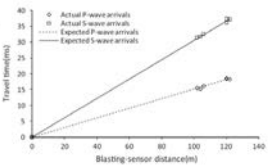

An example of velocity calibration

Xiao et al., 2016

75

75

Finding the location of trapped miner

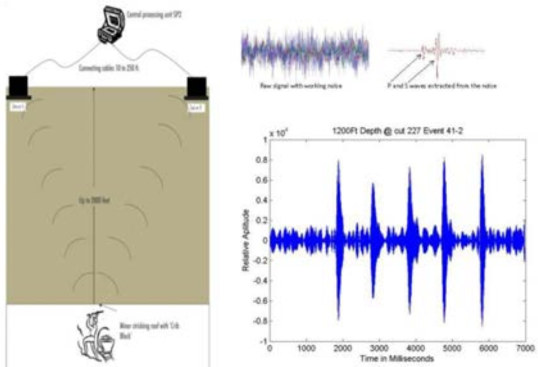

Brown L.G., 2015

76

76

Example of source location of seismic events in a rock mass fracturing process in a deep tunnel

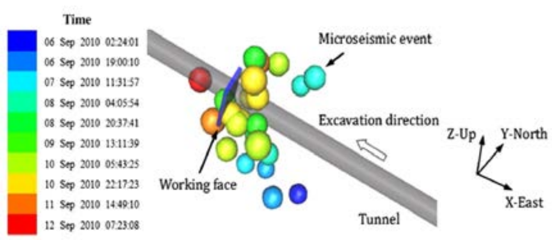

Xiao et al., 2016

Xiao et al., 2016

77

77

Challenges in effective Clustering of Microseismic Events

- **1. The noise in the data population.**
- **2. The accuracy of the hypocentral location.**
- **3. Choosing the appropriate cluster resolution.**
- **4. The static and dynamic nature of seismic sources in mines.**

78

78

Comprehensive Seismic Events Clustering (CSEC)

Plan view of a mine showing 193 CLINK clusters (top diagram) which have been re-grouped into 10 cluster groups (bottom diagram) using the SLINK clustering process

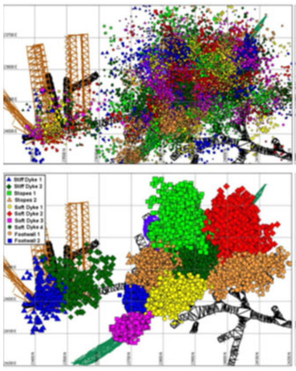

(Hudyma 2008)

79

79

Presentation Layout

1. Introduction
2. Mine seismic source mechanisms
3. Seismic monitoring instruments and systems
4. Seismic monitoring procedure
5. **Monitoring data analysis techniques**
6. Monitoring data interpretation
7. Real time design using seismic monitoring results
8. Summary

80

80

Calculation of Source Parameters

- Position in space (x, Y, Z) and Time
- Strength of the event
  - Magnitude and
  - Energy
- Source dimensions
  - Moment and
  - Source radii
- Stress release
  - Static stress drop and
  - Apparent stress

Brown L.G., 2015

81

81

Calculation of Source Parameters

- **A seismic event is considered to be described quantitatively when, apart from its timing, t, and location, x = (x, y, z), at least two independent parameters pertaining to the seismic source are determined reliably: namely, seismic potency, P, which measures coseismic inelastic deformation at the source, and radiated seismic energy, E.**
- **The mean ratio of displacements at near-field, intermediate-field, far-field, $U_N:U_I:U_F$, for the seismic moment having the ramp function of a sufficiently short rise time can be estimated as follows ignoring the radiation pattern**

Xiao et al., 2016

82

82

Calculation of Source Parameters

- **1. Seismic potency, P (m_3):** $P_{P,S} = 4\pi v_{P,S} R \frac{\Omega_{0,P,S}}{\omega_{P,S}},$
- X_0: amplitude of the low-frequency displacement spectra
- $x_{P,S}$ is the root-mean-square value for the radiation pattern of far-field amplitudes averaged over the focal sphere, and x_P = 0.516 for the P-wave and x_S = 0.632 for the S-wave,
- **2. Radiated energy (J):**

$$E = E_P + E_S. \qquad E_{P,S} = 4\pi\rho v_{P,S} R^2 \frac{J_{c,P,S}}{F^2_{c,P,S}},$$

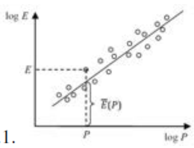

- **3. Seismic moment (Nm):**

$$m = 2/3 \log M - 6.1.$$

- $EI = \frac{E}{\bar{E}(P)} = \frac{E}{10^{d \log P + c}} = 10^{-c} \frac{E}{P^d},$

Xiao et al., 2016

83

83

Presentation of seismicity for Fracturing Process

Example of the evolution of seismic events versus time in tunnel monitoring. a A number of seismic events, and b the spatial distribution of accumulated seismic events

(The section of tunnel is arc-shaped and its size is 13 m 9 8 m)

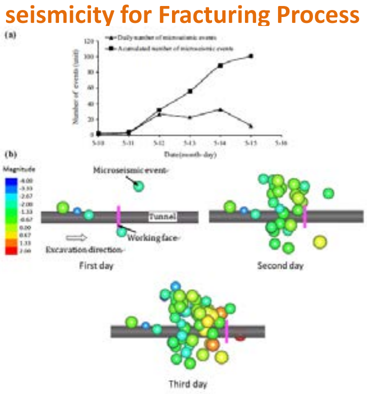

Xiao et al., 2016

84

84

Presentation of seismicity for Fracturing Process

Example of seismic energy versus time: a seismic energy; and b energy index on three consecutive days

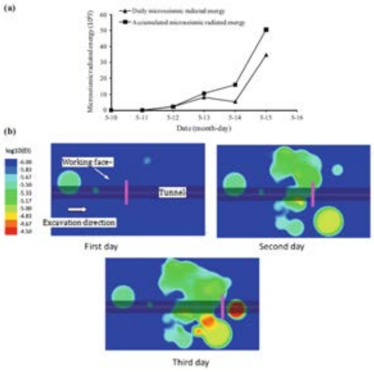

Xiao et al., 2016

85

85

Presentation of seismicity for Fracturing Process

Example of the evolution of seismic apparent volume versus time: a seismic apparent volume, and b the cloud of accumulated seismic apparent volume on three consecutive days

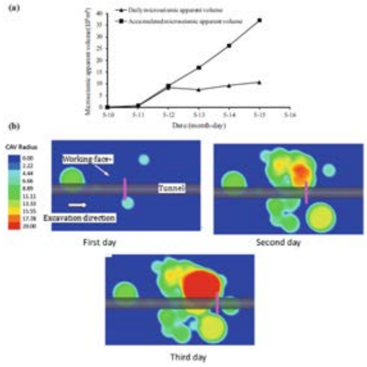

Xiao et al., 2016

86

86

Presentation of seismicity for Fracturing Process

- Example of evolution with local magnitude 1.2 occurred of EI and accumulated apparent volume versus time. The characteristic pattern of dropping energy index and accelerating cumulative apparent volume prior to a large seismic event (local magnitude 1.2 in this case), from seismic data recorded at the Jinping II hydropower station in China

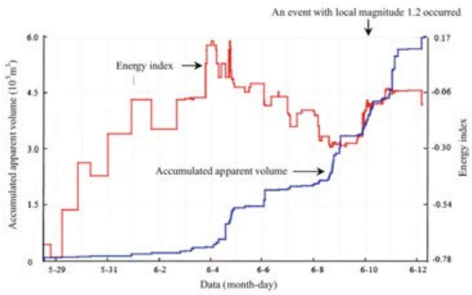

Xiao et al., 2016

87

87

Seismic Source Parameters

- In order to provide a meaningful description of a seismic event, the event time, location and two additional independent source parameters are required (Mendecki et al., 1999). Additional independent seismic source parameters include: energy, moment and size. These parameters can be further manipulated to generate secondary source parameters such as magnitude and apparent stress.

1. Time
2. Location
3. Event magnitude
4. Seismic Energy
5. Seismic Moment
6. Apparent Stress

Brown L.G., 2015

88

88

Seismic Analysis Techniques

Seismic analysis techniques allow for meaningful observations and conclusions to be drawn from seismic databases or subsets within the data. Various techniques provide insight into data integrity, seismic hazard, stress conditions and the general normal/abnormal rock mass response to mining.

1. Gutenberg-Richter Frequency-Magnitude Relation
2. Magnitude-Time History
3. Energy-Moment Relation
4. S:P Energy Ratio (ES:EP)
5. Apparent Stress Time History (ASTH)
6. Seismic Hazard Mapping

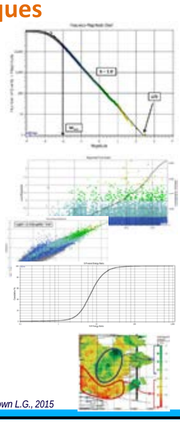

Brown L.G., 2015

89

89

Seismic parameters suitable for failure analysis

- The parameters that were found to best characterise the failure mechanism and hazard at a source include:
- The frequency-magnitude relation of events.
- The timing of events as a result of stress field changes (caused by mining or blasting).
- The timing of larger events versus smaller events.
- The ratio of S-wave to P-wave energy.
- The level of stress (Apparent Stress) associated with the failure process.

Brown L.G., 2015

90

90

Presentation Layout

91

Time dependent deformation mechanisms

1. **Elastic movements:**
   - Associated with stress and ground modulus
   - Reaction of rock mass to excavation unloading
2. **Creep movements:**
   - relatively slow time and stress dependent movements
3. **Cracking and dislocation**
4. **Collapse**

Need to differentiate between "cracking and dislocation" and "collapse" since slope may remain serviceable.

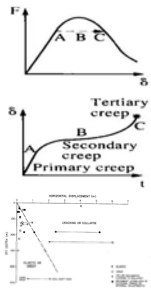

92

Movement characteristics

- **Regressive system:**
  - Common
  - Typical of simple control mechanisms
  - Points 1, 2 and 3 show a decelerating trend. Usually related to an external event (rainfall, blasting etc)
- **Progressive system:**
  - Shear stress greater than shear strength.
  - Positive exponential displacement.
  - Timeframes may be quite short (days rather than months).
- **Transitional system:**
  - Commence as regressive failures then move into progressive failures through a transitional period.
- **Stick-slip:**
  - Sudden movements followed by periods of little or no movement.
  - Usually movement caused by rainfall, blasting etc.

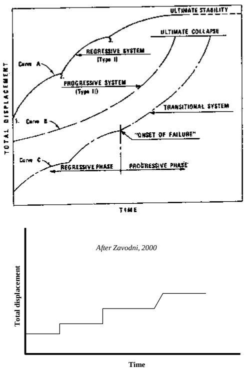

93

Trends in Slope monitoring results – Will it Fail?

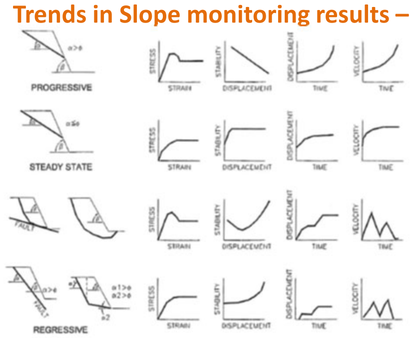

'Yes'

'No'

'Probably not, but keep watching'

'Probably not, but keep watching'

94

Final comments (Zavodni, 2000)

- Regressive and progressive slope movements are only expected after a period of initial response.
- The period of initial response and strain hardening may take several days to several years during which movements proceed at decreasing rates.
- Regressive and progressive slope failure in large slopes range from a few days to 700 days.

95

The frequency-magnitude relation of events

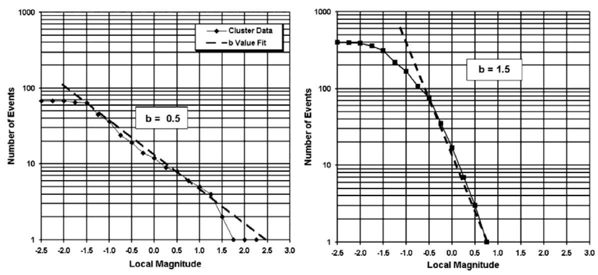

96

The Magnitude–Time History Analysis

Magnitude-time history charts of two different seismic sources. The top graph is indicative of a low hazard as the seismicity tends to respond to the blasting activity and is of low magnitude. The bottom graph is indicative of elevated hazard, as relatively large seismic events occur independently of blasting activities

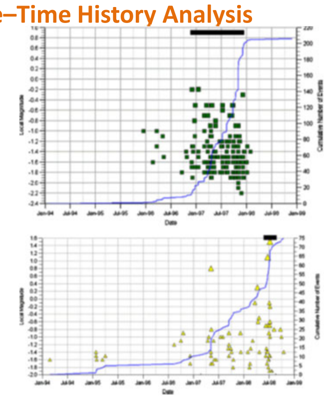

97

97

The Diurnal Chart

Two examples of diurnal charts. The top chart shows a case where seismicity is not dependant on blasting whilst in the bottom chart, the seismicity is highly responsive to blasting

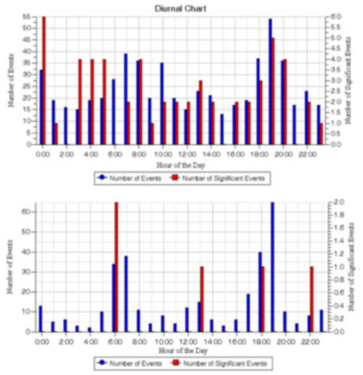

98

98

The S:P Energy Analysis

S wave to P wave energy ratio for two cluster groups (cluster 18 on the left and cluster 10 on the right). The distribution from cluster 18 shows a dominant shear mechanism whilst cluster 10 on the right shows a dominant non-shear (volumetric stress change) mechanism

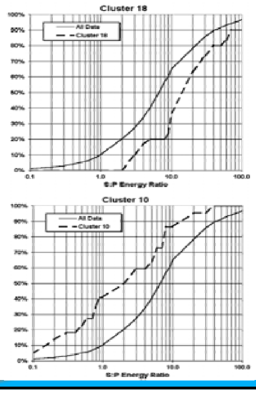

99

99

Apparent Stress

•

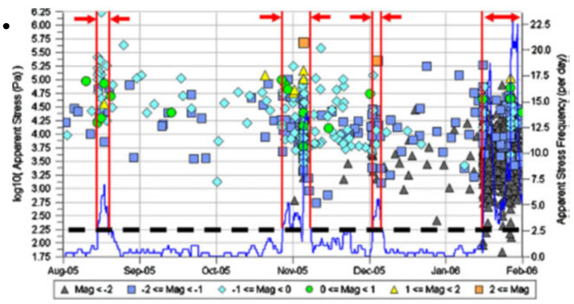

100

100

Location, time and sizes of seismic events

Location, time and sizes of events from the combined catalogue. Events are sized according to log P and coloured according to time. The existing and planned future mining are displayed by grey and pink wireframes respectively

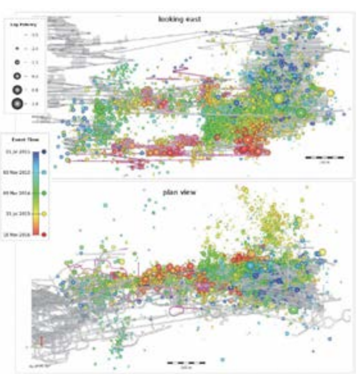

Chalmers et al., 2017

101

101

Recorded and modelled seismicity

Recorded seismicity (top) and modelled seismicity (bottom) for Renison mine after Malovichko and Basson (2014)

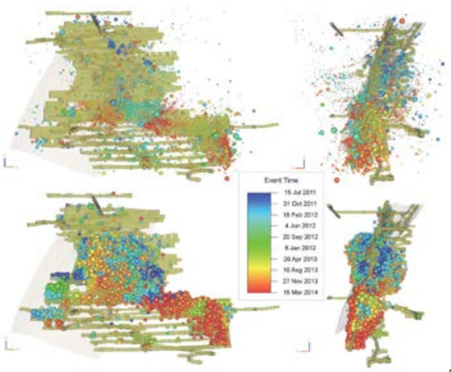

Chalmers et al., 2017

102

102

Rockburst damage scale

Fig. Empirical chart relating to ground motion (ppv), the excavation vulnerability (EVP) and the potential rockburst damage. Isoprobability lines of damage equal or exceeding R4 are given

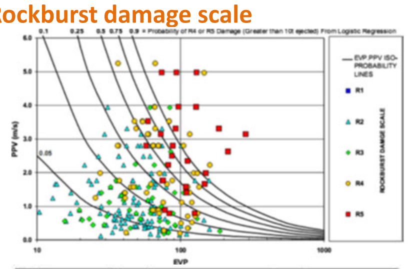

Rockburst damage scale	Rock mass damage	Support damage
R1	No rock mass damage or minor loose rock dislodged	No damage to the support system
R2	Minor damage, less than 1 t displaced	Support system is loaded, loose in mesh, plates deformed
R3	1–10 t displaced	Some broken bolts
R4	10–100 t displaced	Major damage to support system
R5	100+ t displaced	Complete failure of support system

103

103

Recorded seismicity (top) and modelled seismicity (bottom) for Renison mine after

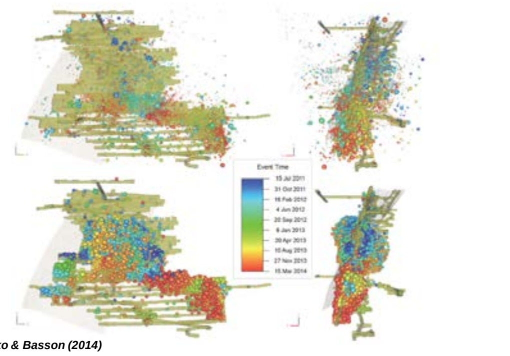

Malovichko & Basson (2014)

104

104

Ground motion hazard

The seismic hazard can be assessed using both recorded and modelled seismicity. The results are then converted to ground motion hazard by applying a ground motion prediction equation (GMPE) and a MC simulation taking the variability of the GMPE equation into consideration. Isosurfaces of PGV can be generated for different probabilities of exceedance.

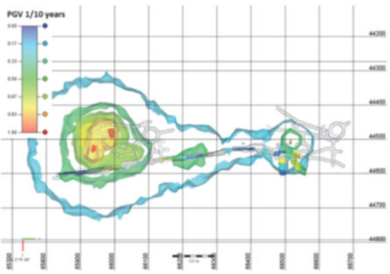

Malovichko 2017

105

105

Calibration of Numerical Models

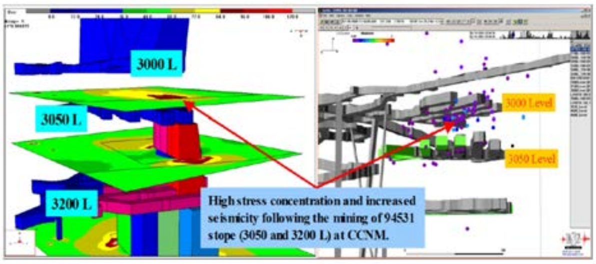

Trifu and Suorineni (2010)

106

106

Where is the Highest Risk?

Rehab!

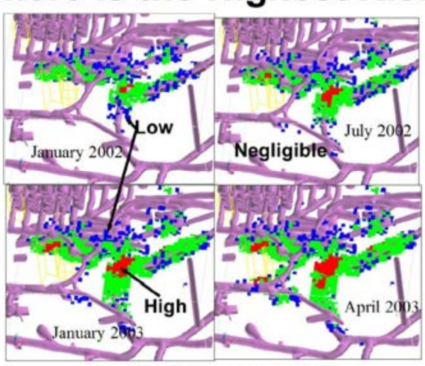

Kaiser, Vasak, Suorineni and Thibodeau (2005)

107

107

Plan view of a stoping area of a mine showing an example of 10 seismic cluster groups (top diagram), also expressed in terms of seismic hazard of individual sources (middle diagram), and shown as seismic hazard on mine drives (bottom diagram)

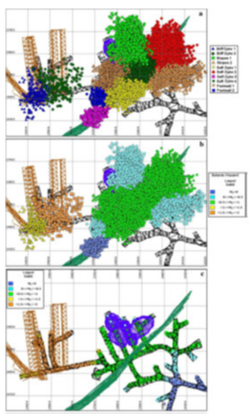

108

108

Presentation Layout

Sudden Brittle failure process

Sudden Brittle failure process

Stress redistribution (Excavation, adjacent construction, seismic)

Stress concentration around micro-cracks (Strain energy accumulation)

Crack propagation (Energy dissipation)

Crack coalescence (Spalling, chipping, Slabbing) (Minor energy release)

Rock burst, ejection (Sudden high energy release) | Rock popping (Sudden medium energy release)

Classification of sudden or unstable failure mechanisms

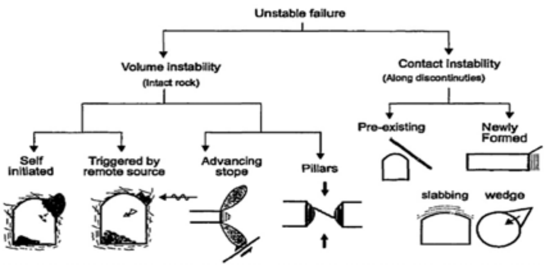

AgLawe, 1999

Prediction of rock sudden failure prone zones:

1. Comprehension of Structural geology, lithology and stress condition of the area, which infers to sudden failure prone hazards,
2. Experimental tests on intact rock samples which indicate brittleness,
3. Seismic monitoring during excavation and careful count of seismic events types and magnitude.

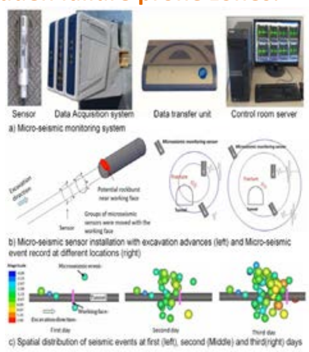

Real time warning and dynamic control of rockburst

- seismic activity represents the evolution of seismic sources and their potential trends so seismic monitoring provides an approach for indicating the real time rock mass behaviour during tunnelling, which can also be used as a tool for the real time warning of rockburst risks.
- In the tunnels, the seismic monitoring provided new information, so one of the important results was that rockburst risks and damage potential could be assessed from the seismic information or seismic parameters.
- Treatment to reduce rockburst damage or some approaches to control rockburst intensities could be adopted and used.
- Seismic monitoring can identify the effects and effectiveness of these treatments and control approaches.
- Adjustment of the treatments and control approaches may be employed based on the evaluation of the effects and effectiveness.
- In this way, the process can be dynamic and be related to 'dynamic excavation and dynamic support'.

Rockburst dynamic control process.

- (a)Warning and reduction of rockbu change in TBM excavation advance

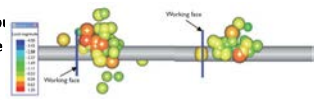

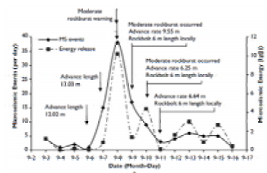

(b) Location of seismicity during September 6th–8th during which time rockburst risk was not controlled (left part) and during September 9th–11th during which time the rockburst risk was controlled successfully (right part),

Feng et al., 2013

Monitoring network of rock burst in tunnels

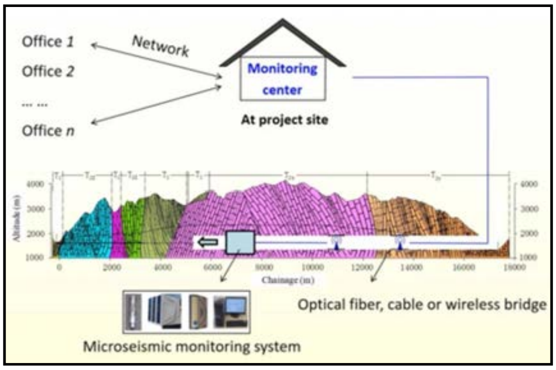

115

115

Monitoring results

Basic microseismic monitoring results used for rockburst warning after microseismic monitoring data analysis

1) Spatiotemporal distribution of microseismic events

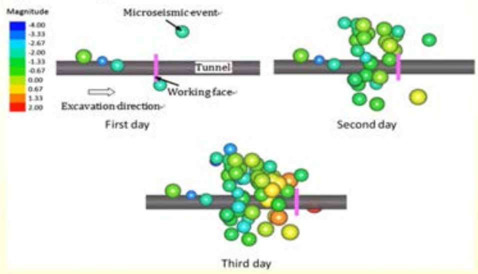

116

116

Monitoring results

2) Evolution of microseismic parameters with time

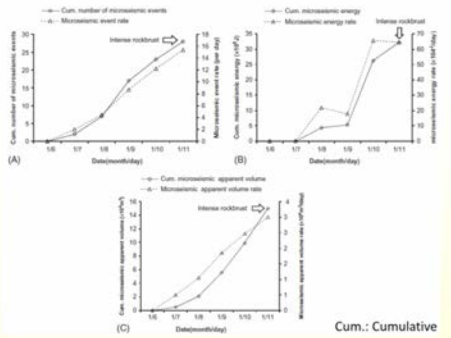

Cum.: Cumulative

117

117

Monitoring results

- **Warning result**

  Location, intensity, and probability of the rockburst

- **Warning purpose**

  According to the warning result, proper engineering measures can be taken to mitigate the rockburst risk

118

118

Monitoring results – warning

For most of the rockbursts in tunnels:

1. A series of fractures associated with the rockburst development process can be monitored *in situ* by microseismic monitoring technique
2. Microseismic events in spatial distribution approach nucleation with evolution of rockburst

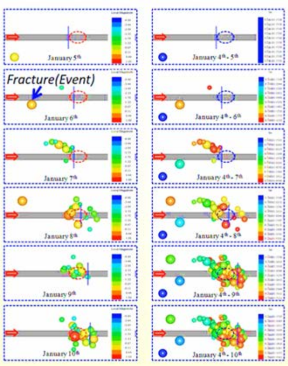

119

119

Monitoring results – energy distribution

3. Spatial distribution & energy of microseismic events, temporal distribution of the number of microseismic events during development processes of rockburst reveal fractal structures and self-similarity

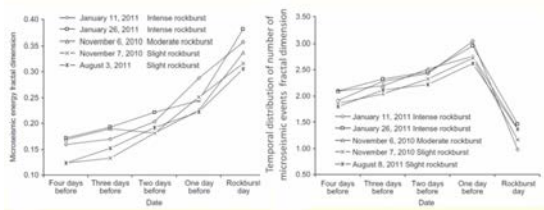

120

120

Monitoring results – warning

Therefore, in most cases, warning of the a rockburst in a given area can be issued by using the *in situ* monitored microseismicity in that area.

121

121

Monitoring results – Warning

Characteristics should be considered for rockburst warning in tunnels

1. The microseismicity associated with rockburst development process induced by different construction methods, TBM tunneling or drilling & blasting, are different

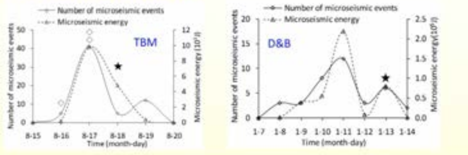

◇ – Slight rockburst, ☆ – Moderate rockburst, ★ – Intense rockburst

122

122

Monitoring results – Warning

2. Rockbursts can be divided into different types, with a different levels of microseismicity

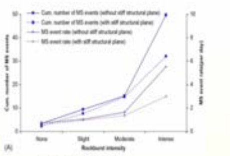

Case example at D&B tunnels

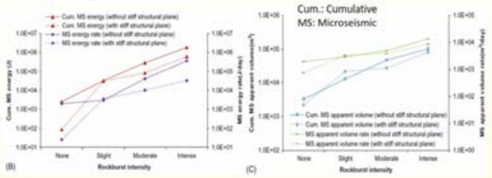

123

123

Monitoring results – Warning

A method for quantitative warning of rockburst at tunnels using the *in situ* microseismicity

$$P_i^{mr} = \sum_{j=1}^{n} w_j^{mr} P_{ji}^{mr}$$

m-**construction method:** *D&B, TBM*

r- **rockburst type:** *strainburst, fault slip rockburst, et al.*

i-**rockburst intensity:** *extremely intense, intense, moderate, slight, none*

j-the *j*th ***MS parameter:***

For D&B: *Cumulative number of MS events, Cumulative MS energy, Cumulative MS apparent volume, MS event rate, MS energy rate, and MS apparent volume rate;*

For TBM: *Cumulative number of MS events, Cumulative MS energy, Cumulative MS apparent volume, Number of MS events in real-time, MS energy in real-time, and MS apparent volume in real-time.*

P_i- ***probability of rockburst intensity i***

P_{ji}- ***relation between j and i***

w_j- ***weighting coefficient of j***

MS: Microseismic

124

124

Monitoring results – Warning

Relation between the number of microseismic events and strainburst in a TBM tunnel: Example

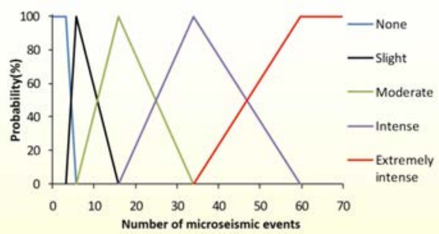

125

125

Monitoring results – Warning

Quantitative warning of a rockburst in a TBM tunnel

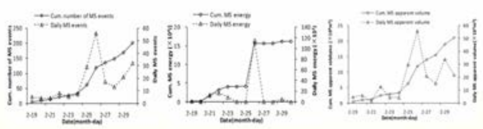

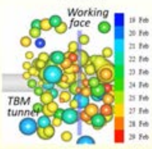

Rockburst warning

P(E. Intense)=0.0%

P(Intense)=49.2%

P(Moderate)=23.0%

P(Slight) =15.2%

P(None)=12.6%

Actual situation

TH beams deformed by the intense rockburst

Cum.: Cumulative; P: probability; E.: extremely

126

126

Monitoring results – Warning

Dynamic warning of rockbursts

Microseismicity changes with the variation of geological condition, *in situ* stresses, rockmass properties, excavation, and support

The change of excavation and/or support would result in a change of the rockburst development process

There should be a dynamic warning of rockbursts based on the variation of the microseismicity.

127

127

Rock Engineering Design Approaches and challenges in Deep Hard Rock Mining Engineering – Dec. 15th, 2019 – Shahrood UT

Monitoring results – Warning

Dynamic warning of rockbursts: Case example

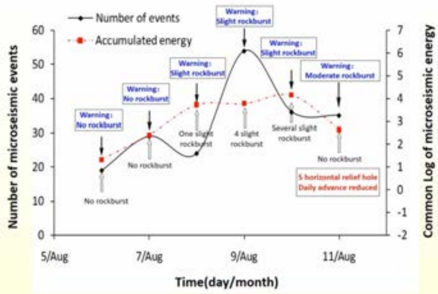

128

128

Rock Engineering Design Approaches and challenges in Deep Hard Rock Mining Engineering – Dec. 15th, 2019 – Shahrood UT

Distribution of rockburst and seismic activity

- Distribution of rockburst and seismic activity in the tunnel #3 withTBMexcavation.

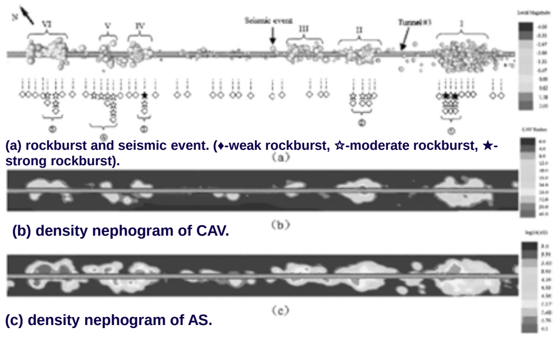

(a) rockburst and seismic event. (♦-weak rockburst, ☆-moderate rockburst, ★-strong rockburst).

(b) density nephogram of CAV.

(c) density nephogram of AS.

129

129

Rock Engineering Design Approaches and challenges in Deep Hard Rock Mining Engineering – Dec. 15th, 2019 – Shahrood UT

Countermeasures to eliminate or reduce sudden failure risk

(i) Optimization of the project layout scheme,

(ii) Pre-conditioning of the rock mass,

(iii) Rock mass reinforcement and support.

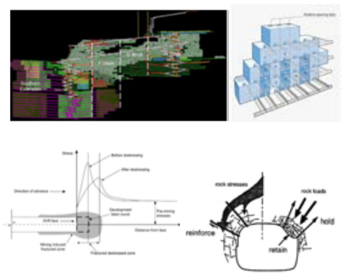

130

130

Rock Engineering Design Approaches and challenges in Deep Hard Rock Mining Engineering – Dec. 15th, 2019 – Shahrood UT

PREVENTION AND CONTROL OF ROCKBURST

- The cause of rockburst is (in many cases) a combination of stiffness of rock and stresses high enough to exceed the strength of the rock.
- The potential of violent failure is also higher in homogenous rock, i.e., rock with less natural discontinuities or with little variation in mineralogy.

- To Control Rockburst or Prevention need;
- Decrease in rock stiffness.
- Greater energy dissipation in rock.
- Changing layout of excavation to decrease the stresses.
- Changing Shape of Opening.

131

131

Rock Engineering Design Approaches and challenges in Deep Hard Rock Mining Engineering – Dec. 15th, 2019 – Shahrood UT

Countermeasures to eliminate or reduce sudden failure risk

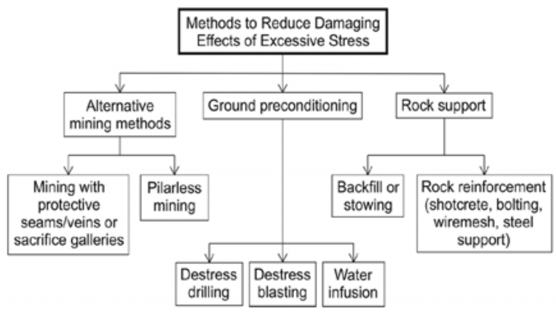

Mazaira A. and Konicek P., 2015

132

132

Seismic risk reduction strategy at the Mount Charlotte Mine

Seismic Strategy Item	Summary
Backfill	Use to add confinement, control loosening
Stiffness	Keep local stope stiffness low, regional stiffness high, avoid irregular lumps and mining front. Faults reduce stiffness.
Access	Do not mine accesses along faults. Avoid driving along any mining structure.
Unlock faults quickly	Start mining at faults so it can move early. Intersect structure early.
West dipper	Avoid undercutting or overcutting west dipping structure.
Stope end abutment access	Orient abutment development E–W.
Stress shadow the faults	Unclamp faults and encourage gradual movement.
Abutment stress	Use narrow E–W abutments. Avoid increased shear stress on clamped faults.
Pillars	Avoid diminishing pillars. Avoid stress increases in and around pillars.
Blasts	Small blasts generally cause small stress change, and are associated with small energy releases.
Preconditioning	Intentionally weaken ground to reduce its ability to carry stress, and encourage movement.
Destressing	Redirect locally high stresses.
Blast timing	Die-down exclusion time of two hours.
Reoccurrence	New events are less likely in ground distressed by previous large events.

133

133

Rock Engineering Design Approaches and challenges in Deep Hard Rock Mining Engineering – Dec. 15th, 2019 – Shahrood UT

Ground support benchmarking data for rockburst-prone mines

Mine location	Strength: stress ratio	Rating (seismicity)	Surface support	Rockbolts	Bolt spacing (m)	Other support
Australia (Mine A)	1.2–2.6	Moderate	75 mm fibrecrete and weld mesh to 1.8 m from floor	2.4 m D-bolt	1.0 × 1.5	Face meshed for drives sub-parallel to σ_1
Australia (Mine B)	0.5–1.4	Strong	75 mm fibrecrete plus weld mesh to floor	2.4 m Garford dynamic bolt	1.2 × 1.2	Face meshed
Australia (Mine C)	3.3–4.2	Strong	Mesh 1.8 m from floor	2.4 m Kinloc bolt	1.1 × 1.1	Closure pillar mining sequence
Australia (Mine D)	0.6–1.8	Strong	50–75 mm fibrecrete plus weld mesh to floor	2.4 m D-bolt	1.4 × 1.1	Face meshed, cable bolts and mesh straps
Australia (Mine E)	2.9–5.8	Minor	Weld mesh to 2 m from floor	2.4 m de-bonded resin bolts	1.3 × 1.2	–
Australia (Mine F)	1.8–5.3	–	60 mm fibrecrete plus weld mesh	2.4 m Garford dynamic bolts	1.5 × 1.4	–
Australia (Mine G)	1.4–1.9	Strong	75 mm fibrecrete plus mesh to floor	3 m de-bonded resin bolts	1.4 × 1.5	Face meshing where required

134

134

Rock Engineering Design Approaches and challenges in Deep Hard Rock Mining Engineering – Dec. 15th, 2019 – Shahrood UT

Presentation Layout

1. Introduction
2. Mine seismic source mechanisms
3. Seismic monitoring instruments and systems
4. Seismic monitoring procedure
5. Monitoring data analysis techniques
6. Monitoring data interpretation
7. Real time design using seismic monitoring results
8. **Summary**

135

135

Rock Engineering Design Approaches and challenges in Deep Hard Rock Mining Engineering – Dec. 15th, 2019 – Shahrood UT

The process of seismic monitoring system (Essrich, 2005)

Part A Seismic Data Collection	1. Seismic Systems • Monitoring objectives • Principal concepts/solutions • Sensors • Data transfer • Network design • Limitations	Outcome Ability to choose monitoring equipment best suited to defined needs; knowledge of technical and financial requirements of monitoring; knowledge of physical limitations of technology;
	2. Data Processing • Automatic processing • Manual processing • Basic parameters • Spectral domain • First motion • Moment Tensor	Outcome Knowledge of hard- and software requirements for seismic data processing; awareness of issues related to quality of seismic raw data; knowledge of seismic source quantification methods;
	3. Theoretical Seismology • Source types • Elastic waves • Radiation pattern • Oscillatory motion • Wave propagation • Interfaces • Real and idealised media	Outcome Knowledge of theoretical concepts of seismic sources, initiation and termination, strain energy storage and release; knowledge of simplified models of vibration and their mathematical description; properties of waves and physical principles of their propagation simplified media;
Part B Seismic Data Analysis	1. Descriptive Statistics • Classification • Histograms • Location • Variation • Correlation	Outcome Knowledge of statistical methods of data analysis and awareness of their limitations;
	2. Data manipulation • Smoothing • Compression • Regression • Probabilities	Outcome Knowledge of methods of data manipulation and their benefits in terms of trend and pattern identification;
	3. Seismological Tools • Time history • Gutenberg-Richter relation • Maximum size estimates • Recurrence time • Predictions & success rate • Energy-Moment Graph • Energy/Moment Index • Ground-Motion Relation • Seismic hazard assessment	Outcome Ability to choose from a wide selection of tools to create desired types of information; ability to direct service provider w.r.t. deliverables; ability to formulate relevant questions and seek comprehensive answers; familiarity with limitations of methods and common pitfalls;
Part C Seismic Data Interpretation	1. Application I: Single event • Source location • Source parameters • Failure mechanism • Damage mechanism • Zone of influence	Outcome Interpretation of basic source parameters as quantified by seismic monitoring equipment; physical interpretation of parameters and their significance for source interpretation; correlation between underground observations and source parameters (location, source dimension, source mechanism);
	2. Application II: Event clusters • Trends over time • Patterns in space • Seismically active • Rockburst prone • Instability concept • Mine design parameters	Outcome Ability to identify trends and trend changes in seismic data; ability to recognise patterns; correlation of observed changes with mining and geotechnical parameters; classification of working places and geotechnical areas into various seismic risk categories;
	3. Application III: Losses • Rockburst reports • Damage classification • Ground motion vs. damage • Threshold of relevance • Local rockburst scenario • (In)direct costs • Contingency planning	Outcome Ability to document rockbursts and associated damage; ability to estimate ground motion characteristics for support design and hazard classification; ability to quantify rockburst related losses and their financial implication; ability to utilise knowledge gained from rockburst report analysis to reduce seismic hazard and mitigate its consequences;
	4. Administration • Contract law • Quality management • Auditing • Mine Health & Safety Act • Other legal requirements	Outcome Knowledge of contract law; ability to evaluate data quality and aspects of seismic system performance; awareness of legal requirements in the field of health and safety.

136

136

Rock Engineering Design Approaches and challenges in Deep Hard Rock Mining Engineering – Dec. 15th, 2019 – Shahrood UT

Prediction of rock sudden failure prone zones:

1. Comprehension of Structural geology, lithology and stress condition of the area, which infers to sudden failure prone hazards,
2. Experimental tests on intact rock samples which indicate brittleness,
3. Seismic monitoring during excavation and careful count of seismic events types and magnitude.

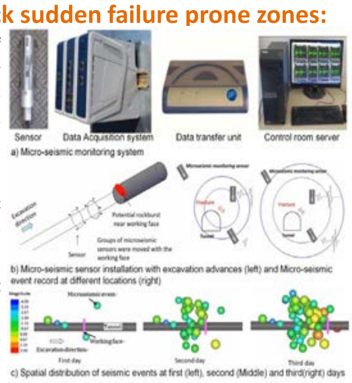

a) Micro-seismic monitoring system

b) Micro-seismic sensor installation with excavation advances (left) and Micro-seismic event record at different locations (right)

c) Spatial distribution of seismic events at first (left), second (Middle) and third(right) days

137

137

Rock Engineering Design Approaches and challenges in Deep Hard Rock Mining Engineering – Dec. 15th, 2019 – Shahrood UT

Dynamic Risk Assessment

Implementing procedures of dynamic risk assessment for rockburst in the process of tunnel construction.

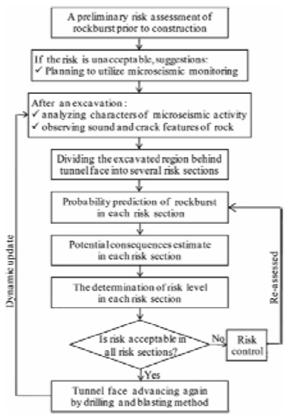

138

138

Final notes

- It should be stressed that seismic monitoring is a constantly evolving topic: equipment is being improved, new processing and analyzing techniques are being developed, and innovative applications are being tested. this presentation addresses the current state-of-the-art in seismic monitoring, it is possible that some aspects will be improved in the future.
- growing number of seismic monitoring systems are being developed for different purposes, e.g., stability assessment of rock slopes and large underground caverns, rockburst warning in tunnels and mines, and mapping of hydraulic fracturing.

139

139

Rock Engineering Design Approaches and challenges in Deep Hard Rock Mining Engineering – Dec. 15th, 2019 – Shahrood UT

Observations always win over models

Military approach

The variability and non-predictability of rock means we have a military style situation – we don't know exactly what the enemy could do

Therefore need data:

- back-analysis of individual adverse occurrences, and
- study of trends

Beware incompetence!

- **Too easy to be blind and biased.** Observations must be KING and always trump over models.
- Information will show correlations and trends that fit with geometry, mining history and geology

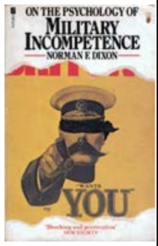

Modified after Mikula 140

140

Rock Engineering Design Approaches and challenges in Deep Hard Rock Mining Engineering – Dec. 15th, 2019 – Shahrood UT

Intelligence gathering

- The military collect intelligence
- So should we
- Changes underground are usually first noticed by the operators most familiar with the workplaces
- We need their reports

Modified after Mikula 141

141

Rock Engineering Design Approaches and challenges in Deep Hard Rock Mining Engineering – Dec. 15th, 2019 – Shahrood UT

Presentation Layout

142

142

Rock Engineering Design Approaches and challenges in Deep Hard Rock Mining Engineering – Dec. 15th, 2019 – Shahrood UT

References

1. *Sharifzadeh M., Ghorbani M., and Yasrobi S. (2017) "Observation – based design of geo-engineering projects with emphasis on optimization of tunnel support systems and excavation sequence" Rock Mechanics And Engineering, Vol.4: Excavation, Support and Monitoring, edited by Xia-Ting Feng, CRC press, Taylor and Francis Group, Pp.449-486.*
2. *Sharifzadeh M., Masoudi R., Ghorbani M. (2017) "Siah Bisheh Powerhouse Cavern Design Modification Using Observational Method and Back Analysis" Rock Mechanics And Engineering, Vol.5: Surface and Underground Projects, edited by Xia-Ting Feng, CRC press, Taylor and Francis Group, Pp.153-180.*
3. *Ghorbani M., Sharifzadeh M., Daiyan M., (2011) " Application of observational method in conventional tunnelling projects in urban areas- the case of Niayesh road tunnel project, Tehran, Iran", 8th International Symposium on Field Measurements in GeoMechanics Berlin, September 12-16, 2011.*
4. *Ya-Xun Xiao, Xia-Ting Feng, John A. Hudson, Bing-Rui Chen,Guang-Liang Feng, Jian-Po Liu, ISRM Suggested Method for In Situ seismic Monitoring of the Fracturing Process in Rock Masses, Rock Mech Rock Eng (2016) 49:843–869, DOI 10.1007/s00603-015-0859-y.*
5. *Jha P C, Chouhan R K S. Long range rockburst prediction : a seismological approach [J]. Int. J. Rock Mech. Min. Sci. & Geomech. Abstr., 1994, 31(1) : 71～74*

143

143

Rock Engineering Design Approaches and challenges in Deep Hard Rock Mining Engineering – Dec. 15th, 2019 – Shahrood UT

References

6. *Shang Z G. Preliminary study of rock burst for the diversion tunnel of Jinping II hydroelectric project [A]. In: CSRME ed. Proceedings of the, Third National Conference on Rock Dynamics[C]. Wuhan : Wuhan University of Mapping Technology Press, 1992, 523～537*
7. *Zhou D P, Hong K R. The rockburst features of Taipingyi tunnel and the prevention method [J]. Chinese J. Rock Mech. Eng., 1995, 14(2):171～178*
8. *Prediction of rockburst by artificial neutral network; Chinese Journal of Rock Mechanics and Engineering, May,2003. 762～768*
9. *W. D. Ortlepp and T. R. Stacey. Rockburst Mechanisms in Tunnels and Shafts.*
10. *Hudyma, M., Heal, D., Mikula, P, 2003, Seismic Monitoring in mines – old technology, new applications, Ground Control in Mining Technology and Practice, UNSW*
11. *Hudyma, M. 2004, Mining Induced Seismicity in underground, mechanised hardrock mines, Results of a worldwide survey, Australian Centre for Geomechanics, Perth*
12. *Turner, M H & Beck, D.A., 2002, Monitoring the onset of seismicity, Proceedings of the ACG International Seminar on Deep and High Stress Mining, Perth*

144

144

Rock Mech Rock Eng (2016) 49:843–869
DOI 10.1007/s00603-015-0859-y

ISRM SUGGESTED METHOD

ISRM Suggested Method for In Situ Microseismic Monitoring of the Fracturing Process in Rock Masses

Ya-Xun Xiao[1] · Xia-Ting Feng[1] · John A. Hudson[2] · Bing-Rui Chen[1] · Guang-Liang Feng[1] · Jian-Po Liu[3]

Received: 26 September 2015 / Accepted: 28 September 2015 / Published online: 16 October 2015

Abstract The purpose of this ISRM Suggested Method is to describe a methodology for in situ microseismic monitoring of the rock mass fracturing processes occurring as a result of excavations for rock slopes, tunnels, or large caverns in the fields of civil, hydraulic, or mining engineering. In this Suggested Method, the equipment that is required for a microseismic monitoring system is described; the procedures are outlined and illustrated, together with the methods for data acquisition and processing for improving the monitoring results. There is an explanation of the methods for presenting and interpreting the results, and recommendations are supported by several examples.

Keywords Suggested method · Fracturing process · In situ · Microseismic monitoring · Rock mechanics

Please send any written comments on this ISRM Suggested Method to Prof. Resat Ulusay, President of the ISRM Commission on Testing Methods, Hacettepe University, Department of Geological Engineering, 06800 Beytepe, Ankara, Turkey.

✉ Xia-Ting Feng
xtfeng@whrsm.ac.cn; xia.ting.feng@gmail.com

1 State Key Laboratory of Geomechanics and Geotechnical Engineering, Institute of Rock and Soil Mechanics, Chinese Academy of Sciences, Wuhan 430071, Hubei, China

2 Department of Earth Science and Engineering, Imperial College London, London SW7 2AZ, UK

3 Key Laboratory of Ministry of Education for Safe Mining of Deep Metal Mines, Northeastern University, Shenyang 110004, Liaoning, China

1 Introduction

Rock engineering activities, such as underground or surface excavations, and mining, induce stress redistributions that may trigger fracturing processes in the surrounding rock mass. These ruptures produce microseismic events, frequencies ranging from a few to thousands of Hz (Cai et al. 2007), which can be observed by microseismic monitoring systems and can provide a continuous stream of real-time information—enabling engineers to effectively monitor and guide production activities, such as the excavation operations, responses to warnings of hazardous regions and to establish fracture dynamic imaging. Therefore, microseismic monitoring is important for understanding the in situ fracturing process of rock masses and how the rock engineering responds to production activities.

Microseismic monitoring can be traced back to 1938 when the U.S. Bureau of Mines attempted to relate seismic wave velocity with pillar load. A noticeable increase in the seismic event rate prior to failure was observed during this research (Kaiser et al. 1996). The application of microseismic monitoring in understanding and investigating mining-induced seismicity became an important issue in 1961 when a seismic network was operated continuously between 2500 and 2800 m below surface for a period of 6 months at the East Rand Proprietary Mine (ERPM) in South Africa (Cook 1963, 1964). With the development of the technology relating to electronics, data storage, data remote transmission, and data processing, the microseismic monitoring system was improved from an analog signal type to a full digital type in the 1990s. The technology theory and application of microseismic monitoring were greatly improved based on the development of full digital technology in the last 20 years.

In situ microseismic monitoring of the rock mass fracturing process has been widely used in rock mechanics tests and rock engineering projects throughout the world, such as in the Underground Research Laboratory (URL) experiment (Gibowicz et al. 1991; Martin et al. 1997) and in the Science and Technology Research Partnership for Sustainable Development (SATREPS) experiment (Durrheim et al. 2012), in mines in South Africa, Canada, Australia, Poland, and China (Pattrick 1984; Scheepers 1984; Van Aswegen and Butler 1993; Mutke and Stec 1997; Luo et al. 2001; Potvin and Hudyma 2001; McGarr et al. 2009; Lesniak and Isakow 2009; Singh et al. 2009; Luo et al. 2010); for rock slopes (Vladut and Lepper 1985; Wesseloo and Sweby 2008; Xu et al. 2011; Occhiena et al. 2014); and in tunnels (Milev et al. 2001; Hirata et al. 2007; Tang et al. 2010; Feng et al. 2012, 2013a).

In China, the use of microseismic monitoring was introduced somewhat later, but there are now more than 50 microseismic monitoring systems in use for rock engineering projects. Feng et al. (2012, 2013a) used the microseismic technique for monitoring and early warning in the evolution process of rockbursts during the excavation of five parallel tunnels in the Jinping II hydropower station in China. These tunnels had a maximum overburden of 2525 m and each had a length of 17 km. Microseismic monitoring has also been applied to numerous mines with rockbursts, gas outbursts, and water inrushes (Li et al. 2013; Liu et al. 2013).

Based on the results of microseismic monitoring, a series of applications benefited significantly. For example, warnings of rockbursts in deep tunnels and mines were made and the rockbursts mitigated successfully (Bolstad 1990; Ogasawara et al. 2001; Durrheim et al. 2007; Durrheim 2010; Feng et al. 2013a). In addition, the stability of rock slopes and large caverns in hard rock with high stresses has been successfully estimated and the extent of the excavation damage zone (EDZ) has been outlined (Young and Collins 2001; Young et al. 2004). Also, information from microseismic monitoring has clarified the fracturing mechanism of monitored rock masses (Feignier and Young 1992; Cai et al. 1998; Feng et al. 2013a). Moreover, the microseismic monitoring is particularly appropriate for in situ experiments in underground research laboratories, and an example is given in Sect. 6.5.

2 Scope

The purpose of this ISRM Suggested Method is to describe a methodology for in situ microseismic monitoring of the rock mass fracturing processes occurring as a result of excavations for rock slopes, tunnels, or large caverns in the fields of civil, hydraulic, or mining engineering. In this Suggested Method, the equipment that is required for a microseismic monitoring system is described; the procedures are outlined and illustrated, together with the methods for data acquisition and processing for improving the monitoring results. There is an explanation of the methods for presenting and interpreting the results, and recommendations are supported by several examples.

It should be stressed that microseismic monitoring is a constantly evolving topic: equipment is being improved, new processing and analyzing techniques are being developed, and innovative applications are being tested. The equipment described in this SM is the 'best' at the time of publication, but in the future improvements should be expected. So although this SM addresses the current state-of-the-art in microseismic monitoring, it is possible that some aspects will be improved in the future. However, the general guidance, principles, suggestions, and recommendations will certainly hold and be useful for practitioners.

3 Equipment

A microseismic monitoring system comprises four main components: i.e., the sensors, the data acquisition instruments, the data transfer units, and the center server with processing software, as shown in Fig. 1. It should be noted that the data transfer units may be cable, optical fiber, or wireless.

3.1 Monitoring Principle

The basic principles of microseismic monitoring are described as follows. When the stress is redistributed in the rock mass due to human activities such as mining, sudden slip or shear may occur along pre-existing zones of weakness, such as along faults or within fracturing networks. This movement or failure results in the release of energy in the form of seismic waves and is known as a microseismic event. P- and S-waves (compressional and shear stress waves) radiate away from the rock mass fracturing source and, as these waves pass each sensor, a seismogram is recorded, as shown in Fig. 2. These analog signals recorded by sensors are sent to a data acquisition instrument for amplifying and digitizing. Then the electric signals are transmitted to the center server through a data transfer unit. The seismograms thus recorded can be shown through display software; also, the source parameters of the microseismic event, such as origin time, three-dimensional location, radiated energy, and seismic moment, can be calculated. Finally, the space–time microseismicity in the rock mass fracturing process can be established and analyzed.

Fig. 1 The components of a microseismic monitoring system

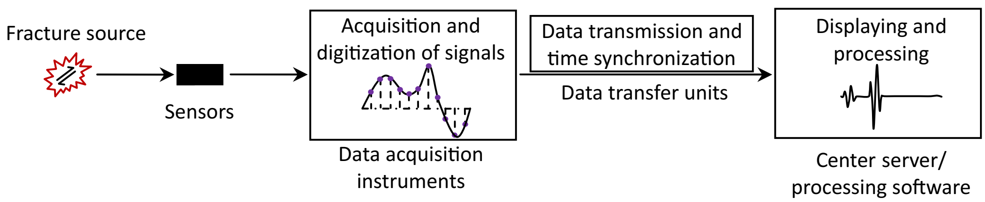

Fig. 2 The basic principle of microseismic monitoring

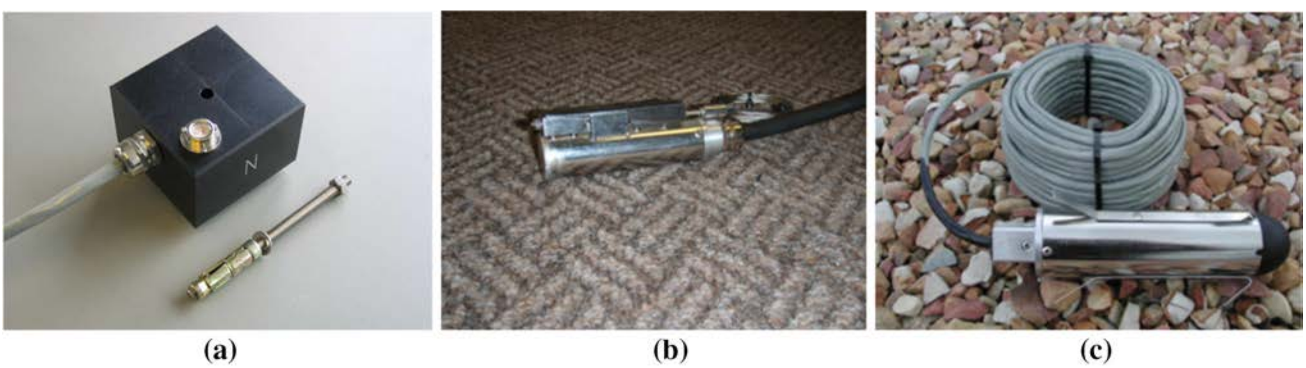

Fig. 3 Sensors for microseismic monitoring: **a** surface type, **b** borehole type of uniaxial geophone, and **c** borehole type of triaxial accelerometer

3.2 Selection of Microseismic Monitoring System

Currently, there are many microseismic monitoring organizations/firms all over the world. Also, a growing number of microseismic monitoring systems are being developed for different purposes, e.g., stability assessment of rock slopes and large underground caverns, rockburst warning in tunnels and mines, and mapping of hydraulic fracturing. The microseismic monitoring system should be chosen with regard to the monitoring objective. For example, a microseismic monitoring system which is specially designed for hydraulic fracturing would not be an appropriate choice for monitoring rockbursts or the stability of rock slopes. In addition, the parameters of microseismic monitoring systems must satisfy the several technical requirements (e.g., high sampling rate, flexible networking, and explosion proof) for adequate realization of the monitoring purpose. For instance, microseismic events resulting from excavation works in a hard, competent rock mass release high-frequency waves that require a microseismic monitoring system with a high sampling rate to prevent the distortion of the microseismic waveform.

3.3 Sensors

The microseismic sensors (see Fig. 3) are the elements that can detect the elastic waves caused by rock mass fracturing and can convert the elastic wave into an analog signal. The types of sensors are divided into two main categories: namely, geophone and accelerometer. These types of

Table 1 Sensor selection referred to in the literature where microseismic monitoring has been performed in tunnels, rock slopes, and caverns

References	Project types	Monitored Area	Seismic network	Typical distances	Bandwidth of sensors (Hz)	Moment magnitude
Young and Collins (2001)	Tunnels	Mine-by tunnel, Underground Research Laboratory, Canada	17 triaxial accelerometers	100 m	0.1–10,000	−4.5 to −1.5
Feng et al. (2013a)		Five parallel tunnels, Jinping II hydropower station, China (with frequent intensive rockbursts)	6 uniaxial and 2 triaxial geophones for each working face	70–150 m	7–2000	−2 to 2.5
Feng et al. (2013b)		Diversion tunnel, Baihetan hydropower station, China	6 uniaxial and 2 triaxial accelerometers	50 m	0.1–8000	−3 to 0
Lynch et al. (2005)	Rock slopes	Slope, Navachab mine, Namibia	8 triaxial geophones	200 m	7–2000	−2 to 0
Trifu et al. (2008)		Slope, Chuquicamata mine, Chile	9 uniaxial and 9 triaxial geophones	1 km	15–2000	−0.7 to 1.4
Xu et al. (2011)		Left bank slope, Jinping I hydropower station, China	28 uniaxial accelerometers	400 m	0.1–10,000	−2.5 to 0.2
Trifu et al. (1997)	Caverns	Strathcona mine, Sudbury, Canada	49 uniaxial and 5 triaxial accelerometers	200 m	0.1–10,000	0.5
Scott et al. (1997)		Sunshine mine, Kellogg, USA	Triaxial geophones	1 km	~500	0.5 to 2.5
Liu et al. (2013)		Hongtoushan copper mine, China	6 uniaxial and 1 triaxial geophones	300 m	7–2000	0.1

sensors can then be further divided into sub-categories for uniaxial and triaxial wave recording according to the number of sensing axes. In addition, the type of monitored surface or borehole can be chosen in accordance with the two kinds of installation method. It should be noted that the installation conditions for surface sensors can be harsh: for example, the installation site for surface sensors may need to be cleared of any loose ground cover until the solid bedrock is exposed and there may be water present and temperature fluctuations. Also, surface sensors often should be perfectly horizontal or vertical. Borehole sensors are usually more suitable for in situ microseismic monitoring. However, surface sensors are a better choice in some cases, such as boreholes which must withstand high temperature, pressures, and chemical issues.

The types of sensors to be used are mainly determined by the scale of the monitoring project, the monitored objects, rock lithology, and the monitoring purpose. Many examples of microseismic monitoring applications on rock slopes and around tunnels, and caverns, as found in the literature, are given in Table 1. This Table shows the project type, the monitored area, the linear dimension of the area, the type and number of sensors used, the frequency width of the sensors, and the moment magnitude range.

The microseismic monitoring for rock engineering can be roughly classified in the two scales of the construction region and the working face. The network radius of the construction region can be as much as several hundred meters to kilometers. The main monitoring frequency range varies from a few Hertz to several hundred Hertz (e.g., 5–200 Hz), and a geophone is an appropriate type for this monitoring scale (Manthei and Eisenblätter 2008). The network radius of the working face can also be large, e.g., in mines it can be hundreds of meters, or much less in the case of a tunnel. For this scale, the range of main monitoring frequency is several hundred Hz to thousands of Hz (e.g., 500–3000 Hz), and the accelerometer is the better type if the predominant frequencies are above 500–1000 Hz. For example, accelerometers are commonly used for monitoring the fracturing of rock masses with poor integrity in a small monitoring environment (Xu et al. 2011; Chen et al. 2014). For some cases, the accelerometers used are up to 10 kHz.

The trend for the development of microseismic monitoring for rock engineering is a combination of the two mentioned scales; accordingly, different types of sensors should be chosen to work together. It is important to note that the sensor spacing should be adjusted according to the performance of the adopted sensors on a specified project, together with the required monitoring sensitivity. A test for checking the suitability of sensors should be carried out before monitoring; the best type, bandwidth, and sensor spacing can then be determined according to the response of the sensors to rock mass fracturing. In addition, it is best to choose the sensitivity of the geophone and accelerometer to be no less than 80 V/m/s and 1 V/g ('g' stands for acceleration due to gravity, 1 g = 9.8 m/s^2).

As to whether the uniaxial or triaxial sensors should be chosen, several factors, e.g., monitoring purpose, monitoring range, and number of channels of microseismic monitoring system, need to be considered. Compared to uniaxial sensors, the triaxial sensors can provide a theoretically more comprehensive assessment of the rock mass fracturing. For example, the S-wave arrival can be determined precisely based on the polarization analysis of a three-component seismogram recorded by triaxial sensors, which will be beneficial to the estimation of event location and the calculation of source parameters. If the mechanism of rock mass movement and failure needs to be studied in detail, many triaxial sensors should be used instead of uniaxial sensors. In some engineering application cases, uniaxial sensors can be adopted when the rough spatial distribution and trend of microseismicity are of more concern as compared with the accuracy of source parameters (Tang et al. 2010; Xu et al. 2011). Also, uniaxial sensors are suitable for expanding the monitoring range when the microseismic monitoring system has a limited number of monitoring channels. For example, the monitoring range of a sensor array composed of 12 uniaxial sensors is much larger than that of four triaxial sensors.

3.4 Data Acquisition Instruments

The data acquisition instrument, which encompasses devices responsible for the conversion of amplified analog signals into a digital format, is the core component of a microseismic monitoring system. A data acquisition instrument can be divided into three parts: namely, the pre-amplifier, the analog–digital converter (A/D converter), and the embedded data acquisition computer (DAC). The pre-amplifier is used to amplify the analog electrical signals recorded by the triggered sensor. The A/D converter transforms the continuous analog signal into a discrete digital signal. Based on the specified collection mode, the DAC provides time stamp marks for the recorded signals. A portable data acquisition instrument usually spans between 3 and 24, or even 48 channels. A uniaxial and triaxial sensor requires one and three channels, respectively.

For a commercial microseismic monitoring system, it is often just required to set the appropriate sampling rate for the A/D converter. This work can be done during a trial period. Firstly, a high sampling frequency is set to collect the events of rock mass fracturing. Then based on the Discrete Fourier Transform (DFT), the frequency spectrum of microseismic waveforms from rock mass fracturing events can be analyzed. The main frequency band $[f_1, f_2]$ of a single rock mass fracturing waveform, which corresponds to the main distribution of amplitude, is the frequency width between the two frequency points with 0.707 times the maximum amplitude, as illustrated in Fig. 4. The main frequency range of rock mass fracturing events, which represents the frequency characteristic of the microseismic signals, can be obtained through analysis of the main frequency bands of the collection of typical rock mass fracturing waveforms. In order to avoid frequency aliasing, the sampling rate should be 5–10 times the maximum in the main frequency range of rock mass fracturing events. For example, the maximum of the main frequency range of rock mass fracturing events is about 1000 Hz in a rock slope; then a sampling rate of 6000 Hz is set for this monitoring program.

3.5 Data Transfer Units

The data transfer units transmit the seismic data to a center computer for storage and processing and provide time synchronization for each data acquisition instrument. The data transfer units can be divided into three parts: sensor to data acquisition instrument, data acquisition instrument to center server, and center server to departments of decision making and data processing. Typical data transfer units are shown in Fig. 5.

Various means of data communication should be employed to suit different system environments. Signal attenuation is a reduction of signal strength during transmission and depends on the distance and medium of transmission. As the transmission distance increases, the signal attenuation increases. Thus, the length of data transfer units should be less than the maximum distance that signal reduction affects the monitoring data. The data acquisition instrument should be close to its related sensors (e.g., be less than 300 m). For this communication component, twisted pair cable with copper conductor, 20 AWG (American Wire Gauge) and shielded aluminum coil is adopted commonly.

A data relay station is usually needed to be established between the data acquisition instruments and the center server, as shown in Fig. 5. This mode can reduce the monitoring cost and is beneficial for the maintenance of data transfer units. Between the data acquisition instruments and the data relay station, cable communication is appropriate for a work area with many construction vehicles and machinery. If the work area often has a large amount of electrical equipment and is subject to thunderstorms, which can easily produce high-voltage pulses, then optical fiber communication is the better choice. The distance between the data relay station and the center server

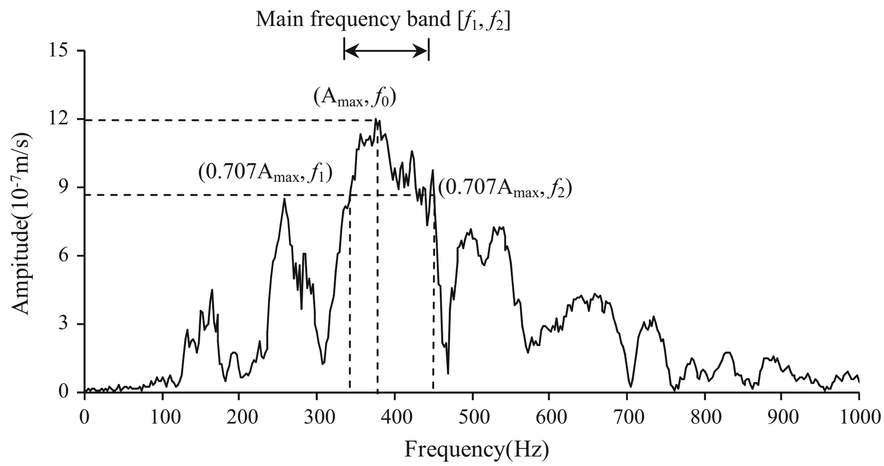

Fig. 4 Example of a frequency spectrum analysis for rock mass fracturing event

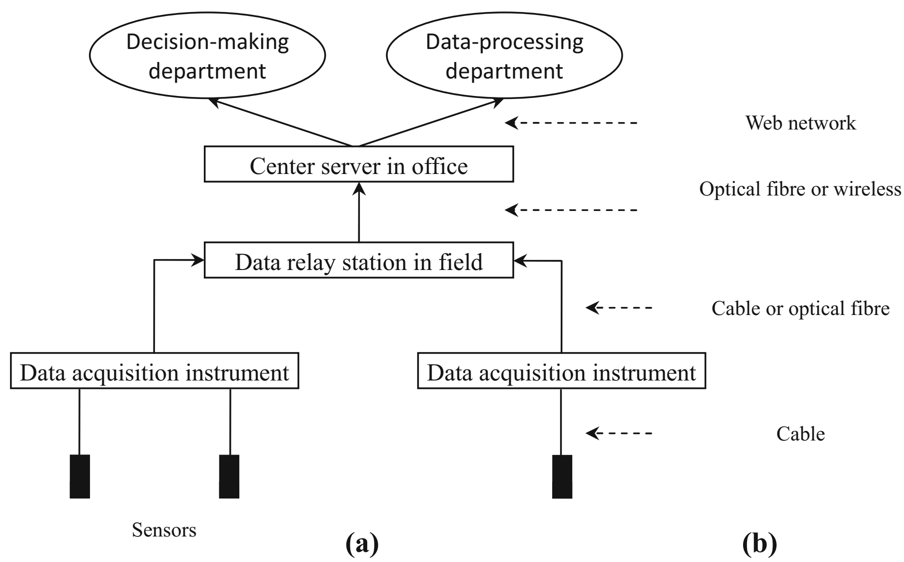

Fig. 5 Example of typical data transfer units in a microseismic monitoring system: **a** the data transfer units between each component; and **b** the main form of data transfer units

can reach some thousands of meters, and the single-mode optical fiber communication is a quiet adaptive option. If there is reduced electromagnetic interference and a wireless network exists in the construction area, then wireless communication can be advantageous.

The wireless communication and remote transmission, which are the trend in microseismic monitoring technology, can significantly save monitoring cost and improve the efficiency of data transmission. Between the center server and the location for data processing and decision making, web network communication can be used to establish the sharing of monitoring data in real time. Meanwhile, the manager can master the working condition of the microseismic monitoring system in any location through remote control.

In addition, time synchronization is a core requirement of a microseismic monitoring system with multiple acquisition instruments. The data from different acquisition instruments are deemed unusable if there is poor time synchronization. Therefore, the time synchronization between each acquisition instrument should be corrected at regular short intervals, such as a few minutes. The data transfer units for the time synchronization system and data transmission system are usually independent depending on the different communication modes and manufacturers.

3.6 Center Server and Processing Software

The center server for setting and mastering the microseismic monitoring system is needed for recording the seismogram data from the data acquisition instruments. The server must be adapted to work long hours, or even for several years. Therefore, the center server should be placed in a region which is dry, safe, and has a guaranteed power supply. In addition, the center server should have a double network card: one is for updating the monitoring data to the analysis location through the internet; the other is the communication interface of the monitoring system.

System monitoring software is required for displaying the working condition of every device or component of the microseismic monitoring system in real time. It is an effective tool for managers to establish any abnormal function of devices and/or communication malfunctions, and to ensure the normal working environment of the microseismic monitoring system. Seismogram processing software is used for displaying and processing seismogram data. The source parameters of rock mass fracturing can be calculated rapidly. Data interpretation software is also needed for visualizing and interpreting the space–time evolution and mechanism of rock mass fracturing.

Some hardware filter rules are established as a trigger threshold to execute event detection by seismogram processing software, such as signal-to-noise ratio (SNR) (Oye and Roth 2003), and recorded frequency width and minimum signal amplitude. The Short Time Average/Long Time Average (STA/LTA), which is a measure of the SNR function, is commonly used in commercial microseismic monitoring systems. The LTA represents the slow trend of signal energy, whereas the STA is more sensitive to a sudden increase in energy. If the STA/LTA of the microseismic wave exceeds a user-defined threshold, a detection time is assigned to this microseismic wave. Detailed information on the calculation and setting of STA/LTA can be found in a related paper (Trnkoczy 2009).

The format for the monitoring data usually depends on the manufacturer's type. Sometimes, the methods of location and diagnosing, which are selected for users to analyze data, are different from the provided methods of system software. Almost all seismogram processing software provided by manufacturers can export a data file for each microseismic event. This file contains the necessary information for signal analysis, such as the trigger time of each sensor, the value of each waveform sampling point, and so on.

4 Procedure

4.1 Preparatory Investigations

Firstly, the monitoring purposes should be determined according to the requirements of the rock engineering challenge and the applicability of microseismic monitoring. Then the whole region involved can be evaluated based on the monitoring purposes. The focus areas, where the instabilities of the rock mass are more likely to occur, can be estimated on the basis of the geo-engineering method, the engineering properties of the rock, predictive numerical simulations, and engineering analogies. The spread of sensitivity and location accuracy in the regions to be monitored depends on the probability and intensity of instability of the rock mass in each location. In regions where there is a greater probability of rock mass instability, the microseismic monitoring should have the more sensitive and the higher location accuracy.

The type of sensors should be selected according to the objective, purpose, and number of channels for monitoring, the selection rule having already been discussed above. An on-the-spot survey may be necessary for determining the monitoring environment and any limitations of the sensors' layout, and establishing feasible points for sensor installation. Also, the construction scheme should be known as far as possible for determining the communication circuits and the locations of all components in the microseismic monitoring system.

A coordinate system should be set up according to the monitoring objective. The coordinates of the sensors and anticipated locations of the rock mass failure events should be related to the established coordinate system. Then the three-dimensional geological model, which should include the monitoring area and macro-geological conditions, needs to be established for enabling the space–time evolution of rock mass fracturing in the monitoring region to be determined.

4.2 Array Design for the Sensors

The sensor array can be considered via the space geometry formed by all the sensors. The three types of spatial relations between microseismic source and sensor array are shown in Fig. 6. Commonly, a source inside the sensor array, as shown in Fig. 6a, should ensure high accuracy of source location. If the source is located outside the sensor array, as shown in Fig. 6b, c, then a poor source location may be the result.

The layout of the sensors will depend on the installation conditions determined by the monitoring environment and the purposes of microseismic monitoring. The general principles of sensor layout for rock engineering are summarized as follows:

1. The sensor array should surround the monitoring objects as far as possible to ensure the accuracy of source location, as shown in Fig. 6a.
2. The sensor spacing will depend on sensor performance and required monitoring sensitivity; each position in the monitoring region should be covered effectively to satisfy the demand of event location accuracy.
3. For the critical locations and those with foreseeable potential instability, the density of layout sensors should be increased by increasing the number of sensors and reducing the sensor spacing.

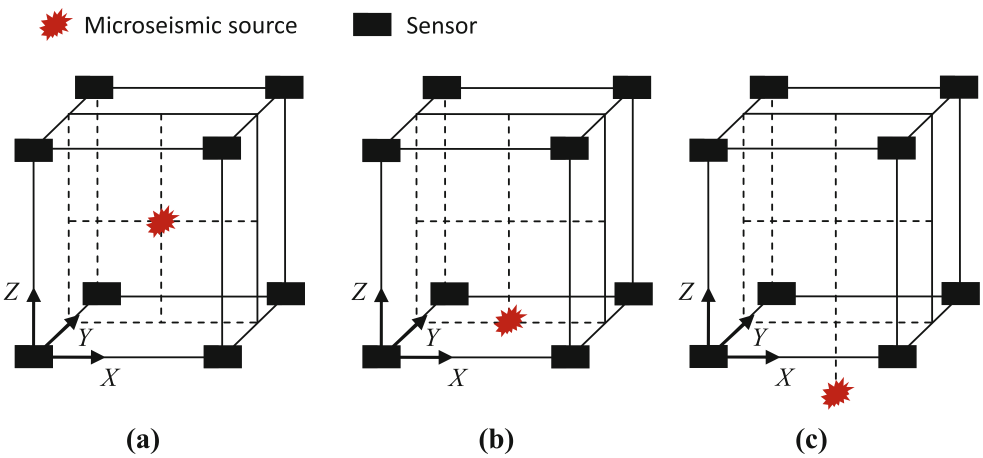

Fig. 6 Spatial relations between microseismic source and sensor array: source **a** inside the sensor array, **b** at the edge of the sensor array, and **c** outside the sensor array

4. The data transfer units depend on the sensors' layout and their convenience and security should be considered when designing the sensors layout to ensure continuous and accurate monitoring data. In addition, the feasibility of the sensors' installations should be confirmed through on-the-spot survey.
5. During the entire monitoring process, the sensors should be supplemented in areas of adverse geological conditions and those regions with a risk of rock instability.
6. The influence of noise (such as from blasting, electrics, drilling, and construction vehicles) on the seismic signal should be reduced as far as possible.
7. The whole sensor network should have good 'self tolerance': when the sensors in a certain region do not work, sensors in other areas should still guarantee the basic monitoring in that region.

Commonly, there are two approaches to such sensor layout design. One is the semi-empirical method, such as the optimal design methods of C-optimality and D-optimality (Kijko 1977; Mendecki 1997). Firstly, a series of sensor layout schemes are prepared according to expertise. Then based on the spatial positions and minimum resolutions of peak particle velocity of sensors, the standard location error and monitoring sensitivity at each microseismic source position can be evaluated. The two-dimensional contour map of location error and monitoring sensitivity from varied elevations can be drawn for each sensor layout scheme. The final scheme can be decided by comprehensively considering location accuracy, monitoring sensitivity, and cost. Another method is to plan the network of sensors through intelligent optimization algorithms, such as the DETMAX algorithm and genetic algorithms (GA) (Rabinowitz and Steinberg 1990; Gong et al. 2010; Maurer et al. 2010). The objective function should fit the demand of location accuracy and sensitivity. Then based on the given optimization algorithm and objective function, the optimal scheme can be determined through continuous search. Generally speaking, the semi-empirical method is suitable for small regional monitoring with the scale of a working face where fewer points of suitable sensor installation exist. The intelligent optimization method is suitable for large-scale monitoring where there are many feasible points for installing sensors.

However, constrained by the field monitoring conditions, it is often not possible to implement the ideal sensor layout scheme. The appropriate implementation plan should consider the various factors, such as monitoring condition, basic principles of sensor layout, monitoring object, and purpose. Typical layout schemes for some different kinds of rock engineering are described as follows.

For tunneling the sensors, in the form of 2–3 rows, are often placed behind the working face at a certain distance back and are moved forward repeatedly following the excavation process. The installation of sensors should adopt the method of 'recycling,' which will be described in Sect. 4.3. For the two different excavation methods (Tunnel Boring Machine, TBM, and Drilling and Blasting, D&B), typical sensor layout schemes are shown in Fig. 7. For D&B excavation, it is never allowed to install sensors within the blasting safety distances. For TBM excavation, the position of installation and recovery for sensors should consider the dimensional and operating characteristics of the TBM.

For slope engineering, sensors are installed directly into the slope body where there are concerns relating to slope surface, as shown in Fig. 8a. If there are pre-existing openings in the slope body, the sensors can be arranged using these openings, as shown in Fig. 8b. It should be remembered that, even if sensors are installed in the slope

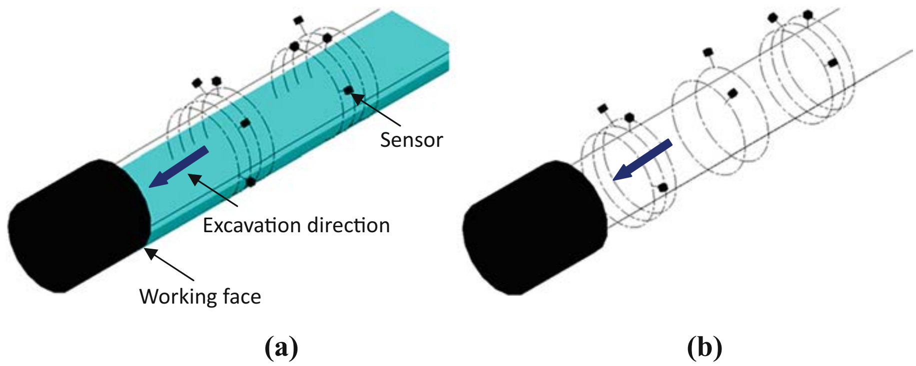

Fig. 7 Examples of sensor layouts for the microseismic monitoring of rock mass fracturing in a tunnel: **a** D&B construction and **b** TBM construction

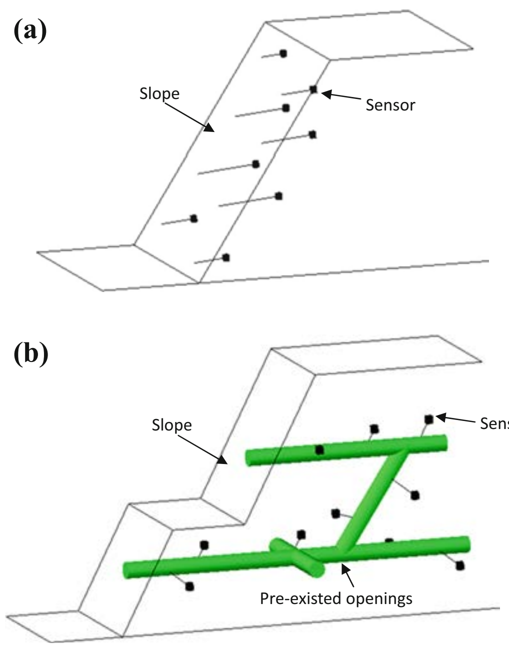

Fig. 8 Examples of sensor layouts for microseismic monitoring of rock mass fracturing in slope engineering: **a** layout directly into the slope body and **b** using pre-existed openings

body, particular care has to be addressed to verify that sensors do not lie on a pseudo-planar surface. In many cases, some sensors should be added according to the excavation situation.

For large cavern engineering, the majority of sensors are arranged using pre-existing openings before excavation and the additional sensors should be added as the excavation proceeds, as shown in Fig. 9.

For mining engineering, the sensor layout for large-scale mining areas can be used for overall monitoring and local stope monitoring. For large-scale mining areas monitoring, sensors are arranged using pre-existing tunnels in each sub-levels as shown in Fig. 10a. As the scale of mining areas can usually reach thousands of meters, the sensor array should cover the whole mining areas as far as possible. In addition, it should be noted that many stoped and caved volumes (areas where mining has already taken place) can be formed during the mining process, and the sensitivity and locational accuracy of the microseismic monitoring system will then be influenced when microseismic waves pass through these stoped and caved volumes. Therefore, enough sensors need to be arranged at each side of the stoped and caved volumes to meet the demand of event location accuracy. Meanwhile, an assumed 3-D velocity model, which will be described in Sect. 5.2, should be used for event location.

For local stope monitoring, many mining methods are used according to the orebody conditions. For one stope, it may be mined from top to bottom, from bottom to top, or from the middle to the two sides, etc. An example of sensor layouts for a stope mined from the middle to the two sides is shown in Fig. 10b, c. The majority of sensors are arranged using pre-existing openings before mining, and some sensors added as the mining proceeds, which is similar to the sensor layouts *for large cavern engineering*.

For open-pit mining monitoring, the sensors can be arranged near the surface of the slope in areas that are suspected of potential instability, as shown in Fig. 10d.

4.3 Installation

Installation plays a key role in the microseismic monitoring of rock mass fracturing. An installation contravening the instructions described below will lead to poor quality and discontinuities in the monitored data, causing difficulty in interpreting and characterizing the rock mass fracturing.

The installation of the components of a microseismic monitoring system, such as sensors, data acquisition instruments, and center server, can be concurrent. Surface sensors should be tightly fixed to the smooth wall according to the requirements of the installation angle. The boreholes for sensor installation may be upwardly inclined, horizontal, or downwardly inclined—but the respective installation methods are different. A typical grouting sensor installation process for an upwardly inclined borehole is

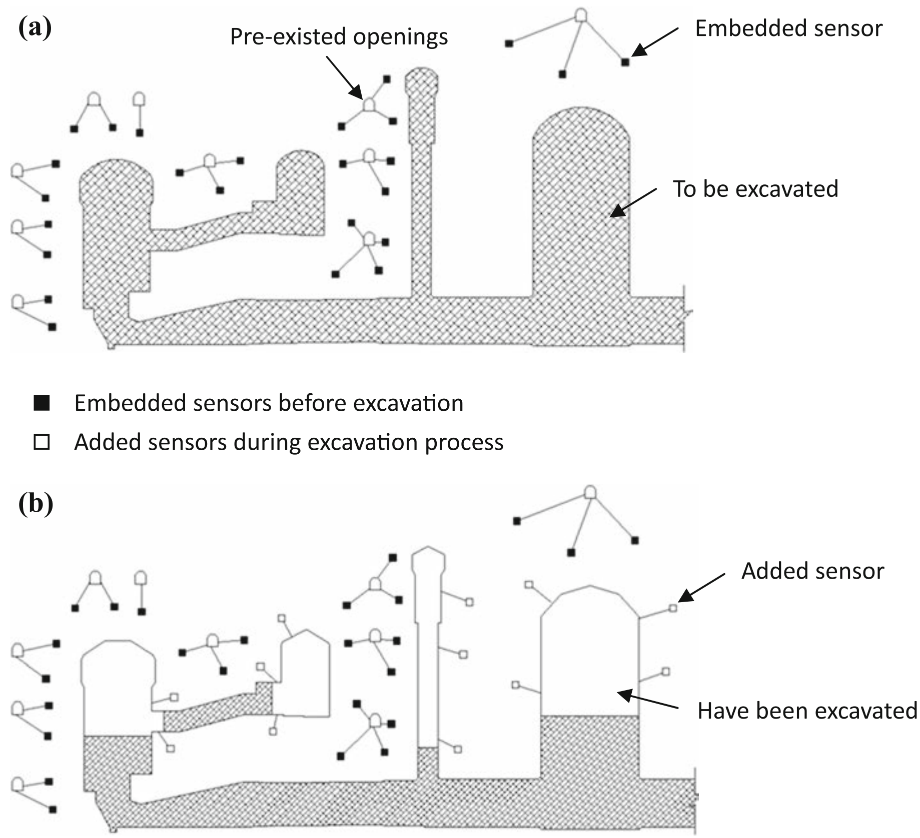

Fig. 9 Example of sensor layouts for microseismic monitoring of rock mass fracturing in a large carven complex: sensors **a** located using pre-existing openings before excavation and **b** dynamically added via the excavated region during the excavation process

shown in Fig. 11. An applicable installation procedure is listed as below.

1. *Drilling* Too small a borehole diameter will lead to the sensors not being able to be installed. In practice, the borehole diameter is commonly about 1.3–1.5 times the sensor diameter for the convenience of the sensor installation. In the case of a rock mass within the damage zone which is more fractured, there will be severe attenuation of microseismic waves. Thus, the lengths of boreholes should extend beyond the damage zone surrounding the excavation to ensure adequate events acquisition and data quality. Percussion drilling equipment is available, but diamond core drilling is much preferred and, in many cases, is essential for providing the reference elastic wave velocity. The location, length, and orientations of the boreholes should be recorded. Then the orientation and coordinates of the sensors can be calculated. In addition, knowledge of the orientation of the sensors provides additional information which is useful for location information and is vital for the calculation of the moment tensor.
2. *Cleaning* The gravels, water, and other residues in the hole caused by drilling should be cleaned. A blower device is needed to clean out the dirt at the bottom of horizontal and down-dip boreholes.
3. *Laying of sensor, grouting pipe, and exhaust* For horizontal and downwardly inclined holes, an installation beam is firstly used to place the sensor at the borehole bottom. Then the installation beam should be withdrawn, and the grouting and exhaust pipes are placed into the borehole. If the borehole is upwardly inclined, the sensor and exhaust pipe should be inserted to the borehole bottom together. The boreholes should be filled with grout to ensure the coupling quality between sensors and rock mass. To accomplish this, the grouting and exhaust pipes should be located near the bottom and orifice of borehole (e.g., 0.8 and 2 m, respectively, for a horizontal or downwardly inclined borehole). This is in contrast to the sensor installation in the upwardly inclined borehole.
4. *Grouting* The borehole orifice should be sealed within a sufficient distance (e.g., 300 mm) before grouting. The grouting can be operated at a constant and slow speed until the sealing material has mostly hardened. When the grout flows out of the exhaust pipe constantly, which means the borehole is already filled with grout, the grouting should be stopped. In addition, the grout should have similar acoustic impedance (i.e.,

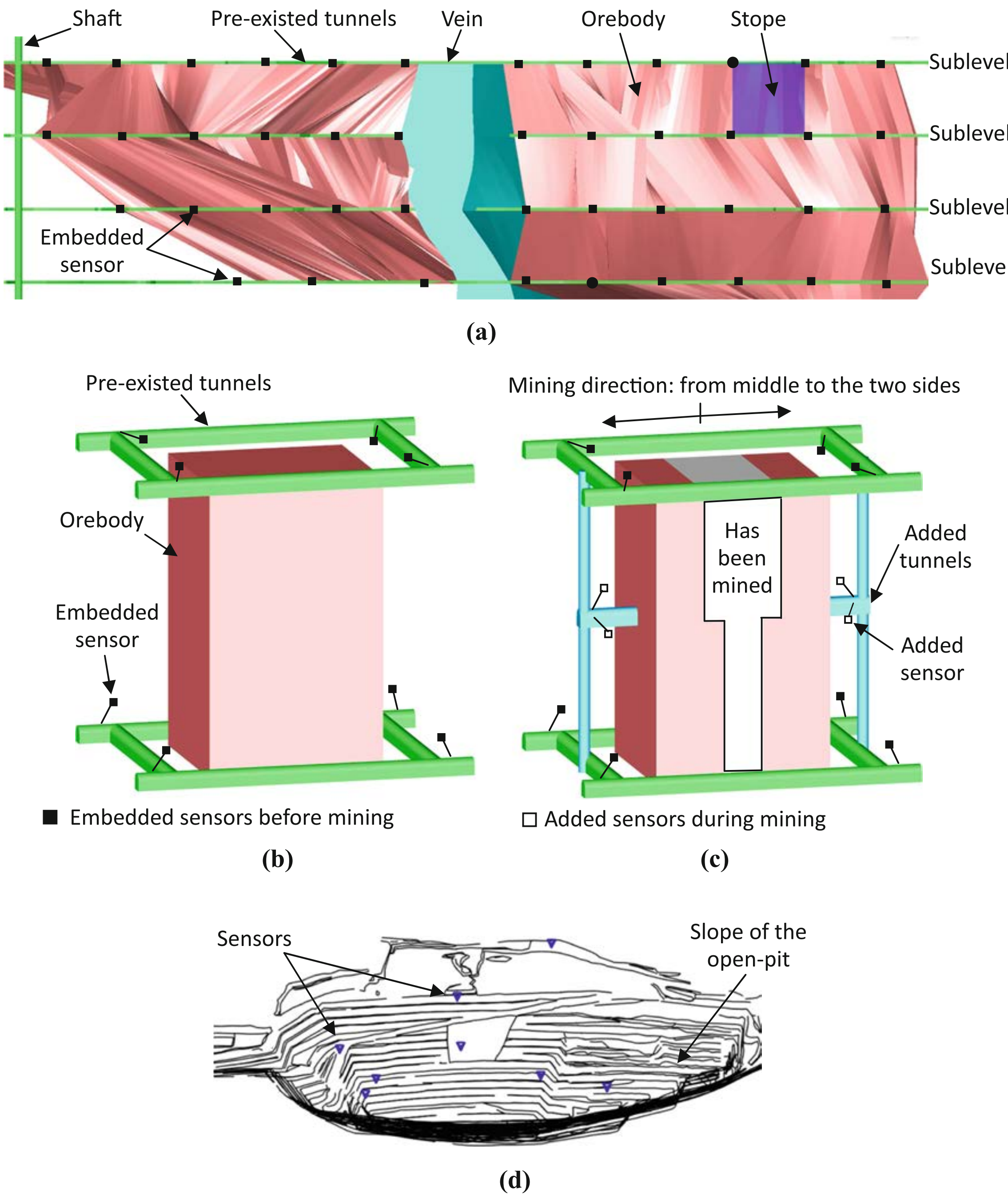

Fig. 10 Example of sensor layouts for microseismic monitoring of a mine: sensors **a** located using pre-existing tunnels in each sub-level for large-scale monitoring; **b** located for a typical stope before mining and **c** dynamically added in further tunnels during the mining process; **d** located near the surface of a slope in the areas that are suspected of potential instability (Lynch 2007)

the product of density and propagation velocity) as the rock.

For a rock mass with clear anisotropy (e.g., a layered rock mass or columnar jointed rock mass), the angle between the sensor installation location and the orientation with the greatest elastic wave velocity in the rock mass should be as small as is practically possible. If chemical corrosion is present in the monitoring environment, a protective jacket should be added to the sensors in the boreholes, and the sensor's cable should be coated with polyvinylchloride (PVC) pipes.

Sensors may be required to be recycled in a particular situation, such as monitoring in tunnels and rock slopes, and so a recovery package is needed. Typical feasible

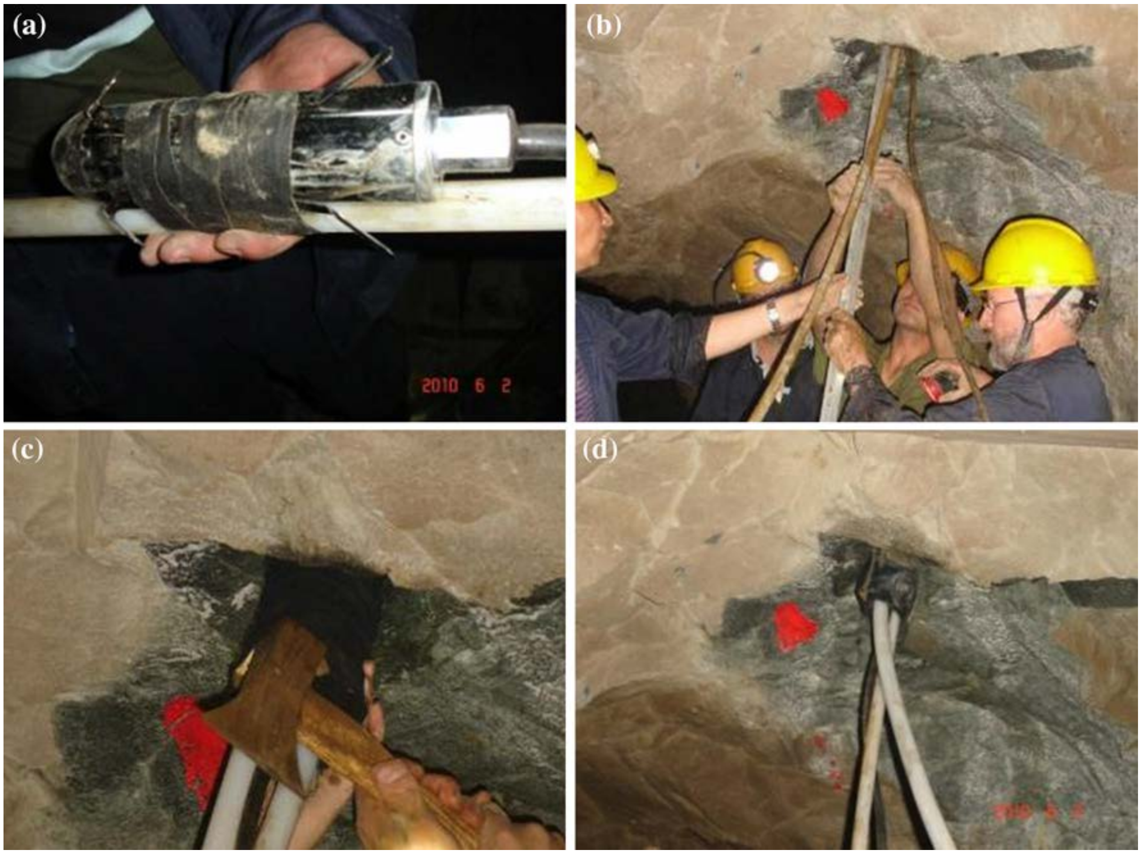

Fig. 11 The grouting installation process for a sensor in an upwardly inclined borehole: **a** tying the sensor and exhaust pipe together, **b** sensor is placed to the borehole bottom, **c** sealing of orifice, and **d** grouting

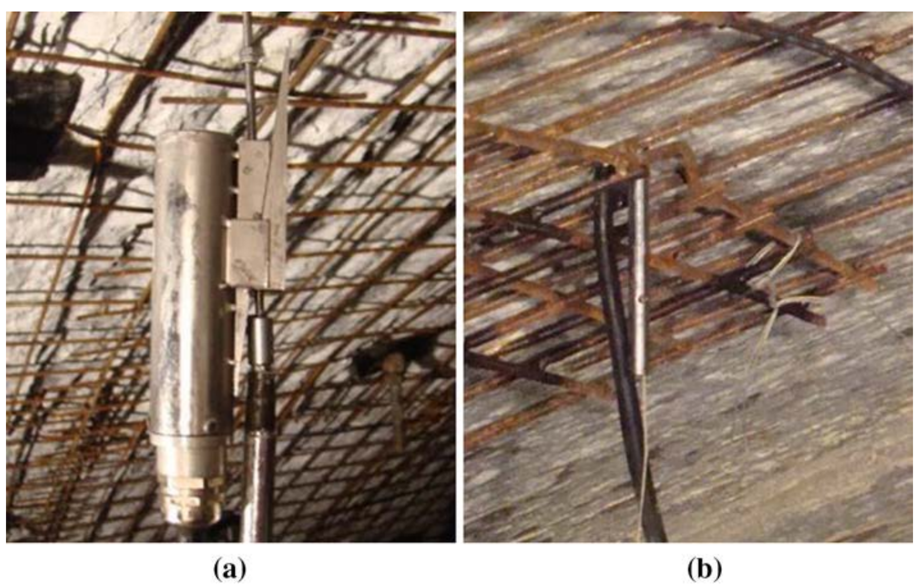

Fig. 12 An example of a sensor recycling installation: **a** Sensor and wedge sliding block, and **b** sensor is placed at borehole bottom

recycling equipment is shown in Fig. 12a. The removable wedge sliding block is fixed to the sensor. Firstly, the sensor is placed at the borehole bottom using the installation beam. Then the bolt of the sliding block is rotated through the beam, causing opening of the sliding block to ensure the sensors are tightly fixed against the borehole wall. Until the sensor is fully coupled with the borehole wall, the installation beam can be recycled.

The status of recycled sensors should be observed to check the coupling of the sensor to the borehole. If the data quality and trigger counts of the sensor show a continued slowdown day by day or are obviously less than other sensors, which means the coupling of the sensor to the borehole is probably questionable, the sensor should be installed again. When the sensors need to recycled, the installation beam can be used to rotate the bolt of the sliding block in the opposite direction. In the same way, the length of the borehole should be greater than the damaged zone surrounding the excavation.

In addition, the sensors are vulnerable components and so attention should be paid to protect the sensors during the process of installing, recycling, and moving, such as handling with care and avoiding impact with hard objects. The data transfer units must be protected by using shotcrete or U-shaped steel, etc., to avoid breakage caused by construction vehicles and other hazards. For applications in a strong chemical erosion environment, the sensors and the data transfer units must be protected using chemical-resistant coatings.

A surge protective device (SPD) should be added between the data acquisition instrument and each sensor to prevent surge impact from the sensor. As far as is practicable, data transfer units should be laid in a safety region, away from construction, to reduce discontinuous monitoring caused by damage to the lines. The data transfer units should avoid regions where many electrical appliances are present and high-voltage impulses can be easily generated. Warning measures should be adopted in regions where there is a risk of lines damage, such as spray painting and posting signs. In addition, all the lines need to be well grounded.

It is important to note that each part of the microseismic monitoring system should be configured for uninterrupted power supply (UPS) to ensure continuous monitoring. If the power supply in the area where the equipment is installed is unstable, a voltage stabilizer should also be added. The order of power supply is power, UPS, voltage stabilizer, and monitoring equipment. In addition, the components of the microseismic monitoring system, which are mostly weak current instruments, must have good electrical grounding cautions. The grounding resistance should be less than 4Ω for preventing interference of electromagnetic coupling on these instruments.

4.4 A Calibration Shot

A calibration shot is recommended. This can be achieved with low-energy explosives, or a controlled point source and shear devices. The calibration shot (e.g., explosion) allows a check on sensor first motion polarities, and to see if all sensors are properly installed (rock/sensor contact surface). Relocating the calibration shot can serve as a first estimation of measurement and intrinsic errors involved in the hypocenter location algorithm.

4.5 Monitoring

1. Ensuring continuous monitoring is the first priority. Monitoring should be conducted by a person acquainted with troubleshooting of the microseismic monitoring system. Moreover, a system of quick troubleshooting needs to be established. The manager should check the working condition of the monitoring system regularly, especially the state of each data acquisition instrument and sensor. Meanwhile, the data transfer units should be inspected periodically. Concatenated 8-h shifts should be adopted in the special periods when there is a high possibility of rock mass instability, such as intensive rockbursts, landslide, and so on.
2. An on-the-spot survey should be executed daily by staff familiar with engineering geology and rock mechanics, and trained to recognize geological conditions and typical damage of the rock mass, such as different types of collapse, wall caving, and rockbursts. The geological conditions, construction events, and any damage of the rock mass that follows excavation should be recorded. It is essential to take photographs for recording this information.
3. Those analyzing the data should obtain the monitoring data initially and make an initial evaluation as soon as possible. By combining the microseismicity and survey information, a proper interpretation for analyzing the state of the rock mass can be given.
4. A database for storing the above-mentioned information is required. This database should include the information about the state of the system, geological conditions, construction events, damage of the rock mass, microseismicity, and a comprehensive analysis with conclusions. The manager, survey staff, and analysts can update the database in real time according to the updating schedule that has been established.

5 Data Calculations and Processing

Unless otherwise specified, all data recorded by the microseismic monitoring system should be processed within 24 h of the readings being taken—so as to be able to respond immediately to any unusual microseismicity. The procedure for data processing can be divided into four steps: diagnosis of rock mass fracturing signals, source location of rock mass fracturing events, calculations of source parameters, and presentation of rock mass fracturing process—which are discussed in detail as follows.

5.1 Diagnosing the Actual Rock Mass Fracturing Signals

In the current context, the signals other than rock mass fracturing events can be termed 'noise.' In fact, usually most of the signals during real-time monitoring may be noise. Therefore, the most basic and important purpose of data processing is to filter out these noise signals quickly and efficiently. A single microseismic signal is composed of a set of microseismic waves. By analyzing the waveform characteristics of the microseismic waves, the essence of diagnosis is identifying the rock mass fracturing signals and filtering out the noise information in these rock mass fracturing signals, as illustrated in Fig. 13.

The diagnosis operation can be divided into four parts: typical collection of signals for each microseismic source, waveform characteristics analysis for these signals, signal type identification and filtering. The sequence of identification and filtering will rely on specific conditions during monitoring. Generally speaking, for the project, such as TBM tunnel construction and in metal mines, the source type and occurrence time of the noise are often known, and the rock mass fracturing signal is less disturbed by noise. The rock mass fracturing signal can firstly be recognized through the characteristics of the original waveform and then the noise information in the fracturing signals can be filtered. For other types of project, such as a tunnel using D&B excavation, rock slopes, and large caverns, the occurrence and types of most noise signals are unknown and the interference caused by the noise is often larger. In addition, various kinds of signals may be mixed. Thus, the recorded signals should be processed firstly to extract the waveform information which represents their main features. Then the fracturing signals can be identified according to the characteristics of the extracted waveform.

The procedure for diagnosis of microseismic signals is described in detail as follows:

1. Typical collections of signals for each microseismic source: a site survey of signals from all microseismic sources during the operation cycle of excavation is essential at the beginning of monitoring. The occurrence, position, and type of all microseismic signals (e.g., rock mass fracturing, electrical noise, blasting, drilling, and mechanical vibration) can be recorded against time. The typical time domain waveforms for various kinds of microseismic signals are shown in Fig. 14. It should be noted that the waveform characteristics of the same types of signals may differ under different monitoring conditions.
2. Characteristics analysis for typical signals: The characteristics of time, frequency, and time–frequency for all kinds of signal can be analyzed by signal processing methods, such as the fast Fourier transform (FFT) algorithm and wavelet transform (WT) (Mallet 1999). The feature parameters of a signal, such as amplitude, duration, main frequency, and arrival time can be obtained. The database, which records all kinds of signals and their feature parameters, should be established from the beginning and needs to be updated constantly during the whole monitoring process. The waveform characteristics for each signal are listed in Table 2.
3. Choosing the method of recognizing a signal: Commonly, there are often three approaches to signal recognition. Artificial identification for signal type can be done through observing the waveform in the display window of the system software. The advantage of this manual method is that it is easily mastered and operated. However, the effectiveness of the method relies on the data processing experience of the analysts and the complexity of the waveforms. Therefore, the manual method is mainly suitable for the monitoring project when there is a reduced level of noise

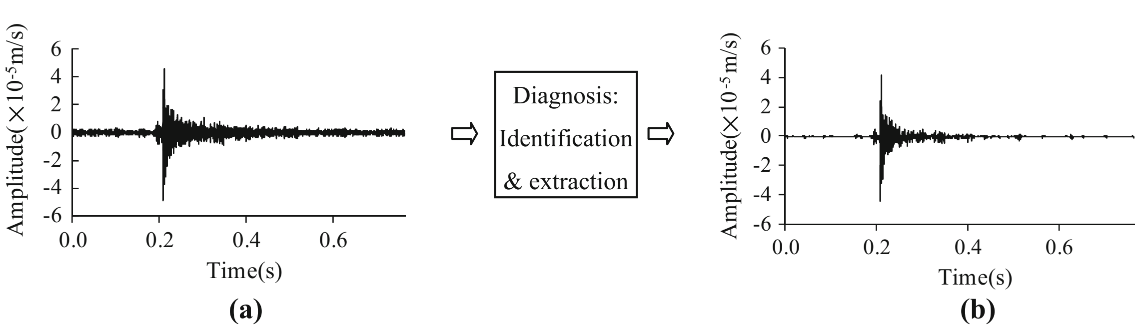

Fig. 13 An example of diagnosing a rock mass fracturing signal: **a** input information, waveforms recorded by the microseismic monitoring system, and **b** output information, waveform of rock mass fracturing

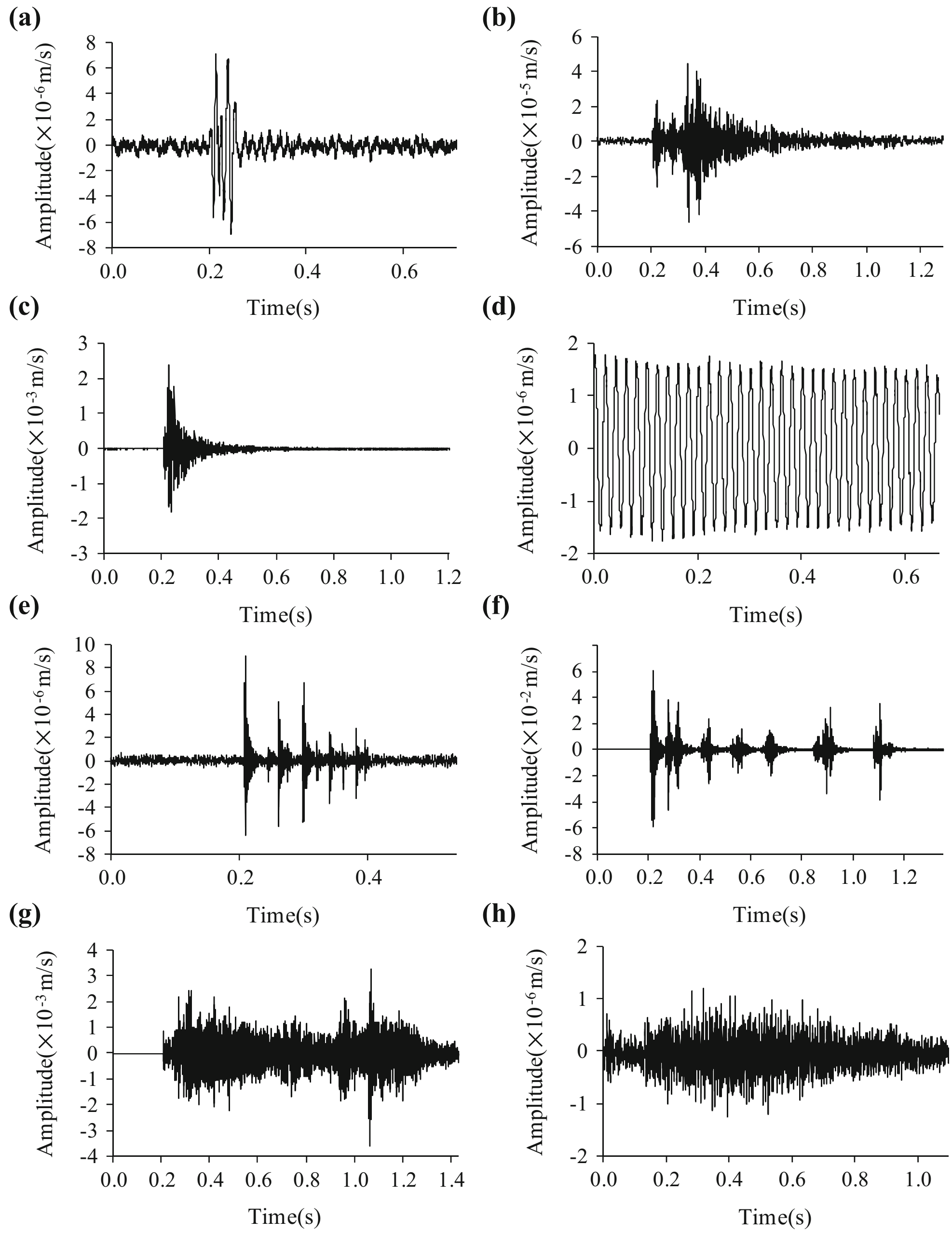

Fig. 14 Examples for typical time domain waveforms of microseismic signals in tunnels: **a**–**c** different waveforms of rock mass fracturing signal, **d** electrical noise, **e** drilling, **f** blasting, **g** mechanical vibration of TBM, and **h** vibration of a machine in a D&B tunnel, e.g., construction vehicle and blower

interference. The second method uses one parameter of the signal to identify the signal type. This single-index recognition method enables quick identification of the signal; but, it cannot be used for multi-type interlaced signals or in the case of multiple similar sources. In the case of a multi-parameter signal, the signal type can be identified using the multi-index method, such as the artificial neural network (ANN) method (Feng et al., 2013a). This method is appropriate for identifying signals with high complexity in a complicated environment, such as a tunnel being excavated by D&B or a large cavern.

4. Choosing the digital filter: the signals, which are acquired by the microseismic monitoring system, are sampled and in discrete time. A digital filter should be applied to these signals to reduce or enhance certain aspects of the signal based on a special filtering method. Digital filters can be divided into two types: the linear filter and the non-linear filter. The linear filters, such as low-pass filter, high-pass filter, and band-pass filter, only retain a certain frequency range of the signal components. Based on the idea that noise and effective signals are random, the non-linear filter estimates the signal itself by using the statistical

Table 2 Classification and characteristic descriptions of microseismic signals

Signals types	Characteristic description
Rock mass facture	The fracturing signal of a rock mass generally has a duration of less than 1 s. The rock mass fracturing signal has a wide range of frequency, mainly concentrated in the range of 10–3000 Hz, with an amplitude magnitude of 10^{-2}–10^{-7} m/s. The waveforms of rock mass fracturing signals are various, as shown in Fig. 14a–c
Electrical	Electrical signals are mainly generated by the improper operation and connection of various electrical components, as well as ineffective cable grounding. The electrical signal generated due to ineffective cable grounding has very similar characteristics to the local AC power signal, which is the resonance wave with the same amplitude, very long duration, and a frequency of 50 Hz, as shown in Fig. 14d
Drilling	The drilling signal is mainly generated by the drilling of blast boreholes and rock bolt boreholes. This type of signal has a notable characteristic, i.e., its multiple wave nature. The waveform within the same signal has a clear periodicity with an occurrence period. The signal has a frequency mainly concentrated in the range of 100–2000 Hz, with an amplitude magnitude of 10^{-5}–10^{-6} m/s. The waveform characteristics of typical signals are shown in Fig. 14e
Blasting	The blast signal generally has a duration of more than 1 s, and the waveform in the same blast signal has a clear periodicity of 0.1– 0.2 s, which is longer than that of a drilling signal. The blast signal received by the geophone has a frequency mainly concentrated in the range of 100–500 Hz, with an amplitude magnitude of 10^{-2}–10^{-3} m/s. The waveform characteristics of typical blast signals are shown in Fig. 14f
Mechanical vibration	The mechanical vibration signals are mainly generated by the operation of construction equipment, such as TBM movement or heavy vehicles passing. The amplitude of this signal depends on the vibration strength, as shown in Fig. 14g, h
Unknown	In addition, there may be other signals with different waveform characteristics, but for which no clear signal sources have been found on site—which may be a result of the superimposition of various ambient noises, so these signals require further analysis

characteristic of such signals. The median filter, particle filter, unscented Kalman filter, and wavelet filter are several typical non-linear filters. (The unscented Kalman filter is used to linearize a non-linear function of a random variable through a linear regression between n points drawn from the prior distribution of the random variable.) If the noise and rock mass fracturing signal are separate in the frequency domain, then the linear filter can be used; otherwise, the non-linear filter is more suitable. In addition, the characteristics of the filter should be in accordance with the characteristic differences between noise and rock mass fracturing signals. For example, if the frequency of the noise is low and that of the rock mass fracturing signal is high, then a high-pass filter can be chosen.

5.2 Location of Events and Velocity Calibration

According to the arrival time and propagation velocity of an elastic wave released by rock mass fracturing, the location of the rock mass fracturing can generally be determined. A rock cracking microseismic event means that localized cracking has given rise to the microseismicity. The principle of locating a microseismic event is shown in Fig. 15. In many cases, the event location can be processed automatically by seismogram processing software (Oye and Roth 2003). The errors of event location mainly depend on the following five factors: the spatial distribution of sensors with respect to the event to be located, inaccuracy in the sensor coordinates, errors in arrival time determination, inadequate knowledge of the

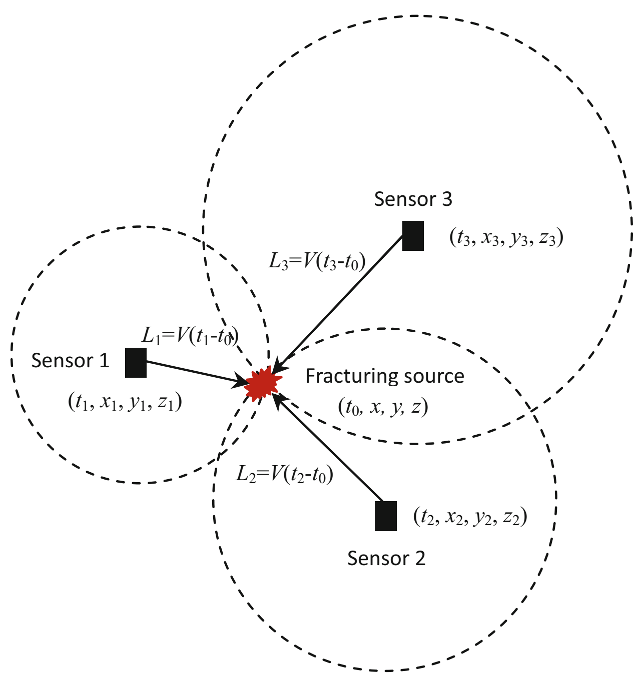

Fig. 15 The principle of source location. t_i is the moment when seismic wave arrives at the i-th sensor, t_0 is the occurrence of the fracturing source, V is the elastic propagation velocity in the rock mass media, x_i, y_i, and z_i are the coordinates of the i-th sensor, and x, y, and z are the location coordinates of the fracturing source

velocity model, and the method of location solution. The first two components of error are related to the sensor array and coordinate measures. The operations related to the remaining three parts are described below.

The operation of rock mass fracturing source location can be divided into the following four steps:

1. Determining the arrival times of the P- and S-wave: The velocity of a P-wave is higher than an S-wave, so the P-wave arrives at the trigger sensors earlier. The first pixels on the waveform diagram can generally be regarded as the onset time of the P-wave, as shown in Fig. 16. The arrival of the P-wave can be commonly picked out automatically. The point where the amplitude suddenly increases significantly can be regarded as the onset time of the S-wave, as shown in Fig. 16. However, it is not always easy to distinguish P- and S-waves; sometimes, only the P-wave arrivals are reliable and can be used for event location. The particle vibration of P- and S-waves is, respectively, parallel and perpendicular with the propagation direction of microseismic wave radiated from the rock mass fracturing source. Based on this different polarization characteristics of the P- and S-waves, the polarization analysis can be used to separate the P- and S- waves for triaxial sensors (Mendecki 1997).
2. Calibration of the elastic wave velocity: The propagation velocity of an elastic wave in rock mass media can be determined through fixed-point blasting. Several positions of blasting are selected first and the coordinates of these positions should be recorded. Then 'small dosage' instantaneous blasting with charges of 2–3 kg can be carried out at these positions and the blasting times should be recorded. According to the coordinates and arrival time at the trigger sensors and the coordinates and times of these blasting events, a series of velocities for the elastic waves (P- and S-waves) can be estimated by using Eq. 1. The constant velocity model was assumed here, also that the rock mass is homogeneous and the velocity of elastic waves (P- or S-wave) is the same in all directions, i.e., the rock mass is also isotropic. The velocity, which will be used in source location, is usually the mean of these calculated velocities. Since this is not always the case, it is important that the two events should be close to each other; less than 10 % of average hypocentral distance is a good rule of thumb. An example of velocity calibration according to blasting is shown in Fig. 17. The calibrated wave velocity is the inverse of the slope of the expected wave arrival. The blasting test results show that the mean velocity of the P-wave and S-wave are 6583 and 3259 m/s, respectively, which coincides with the testing results of wave velocities on site.

$$\Delta t_{\mathrm{k}} = t_{\mathrm{k+1,P,S}} - t_{\mathrm{k,P,S}} = \frac{L_{\mathrm{k+1}} - L_{\mathrm{k}}}{v_{\mathrm{P,S}}} = \frac{\Delta L_{\mathrm{k}}}{v_{\mathrm{P,S}}}, \tag{1}$$

where $t_{\mathrm{k,\,P,\,S}}$ is the arrival time of the P- or S-wave for *k-th* sensor, $v_{\mathrm{P,S}}$ is the velocity of the P- and S-wave, and L_k is the blasting sensor distance and can be expressed as follows:

$$L_{\mathrm{k}} = \sqrt{(x_{\mathrm{k}} - x)^2 + (y_{\mathrm{k}} - y)^2 + (z_{\mathrm{k}} - z)^2}, \tag{2}$$

where $(x_{\mathrm{k}}, y_{\mathrm{k}}, z_{\mathrm{k}})$ are the coordinates of the *k-th* sensor, and (x, y, z) is the position of the blasting.

It should be noted that the constant velocity model may be good enough for the scale of face monitoring, such as in tunneling and a small mining environment. But for the scale of construction area monitoring with complex geological conditions, e.g., large rock slopes and caverns, an anisotropic velocity model should be used in order to ensure the source location accuracy (Mendecki 1997). An assumed 3-D velocity model should be used to ensure the source location accuracy when there is a stoped and caved volume between the microseismic source and sensors. The location determined from standard straight-ray approximation may

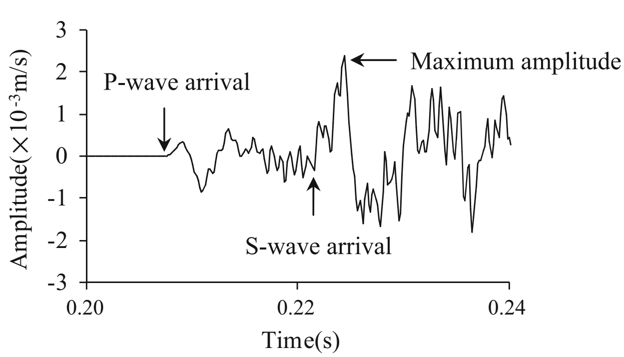

Fig. 16 An example for picking the arrival times of the P- and S-waves

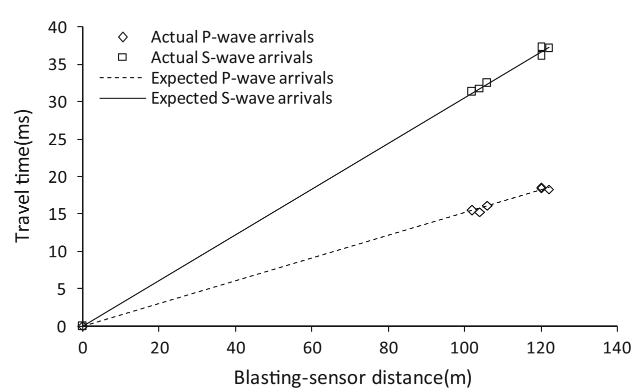

Fig. 17 An example of velocity calibration

have significant systematic errors. Several 3-D ray tracing methods can be used, such as bending method (Julian and Gubbins 1997), point-to-curve method (Hanyga 1991), finite difference method (Vidale 1988), wavefront construction method (Vinje et al. 1993).

If the span of the engineering is large and there are many sensors, a significant amount of memory is required to perform seismic event location with 3-D ray tracing. The test shots for velocity should be source located and can be used to determine source location accuracy when the actual locations are known.

3. Choosing the location method of the fracturing source: the crucial factor in the location method selection is the space relation between the sensor array and the fracturing source, as shown in Fig. 6. Based on the principle of least squares optimization, the local linear method constantly corrects the model parameters in the form of iteration until the arrival time of synthetic microseismic data can best fit the observed data within a certain error range. The methods of Geiger, conjugate gradient, the steepest descent, Gaussian, and FastHypo are the typical representatives of this approach. These methods, which are widely embedded in commercial software provided by manufacturers, have some advantageous properties—such as clear principles, simple methods, and convenient operation. If the sensors and monitoring object have a similar geometrical space relation, as shown in Fig. 6a, the location of the fracturing source can be quickly obtained by this method.

   However, if the geometrical space relation between sensors and monitoring object is changed to the situations shown in Fig. 6b, c, then the local linear method is not recommended—because of the convergence rate problem and divergent solution. The perfect non-linear method is a suitable way to solve this matter. This kind of method continually searches in the model space until the arrival time and location of synthetic microseismic data best fit the observed data within a certain error range. The Monte Carlo, artificial neural network (ANN), downhill simplex, and particle swarm optimization (PSO) (Zang et al. 1996, 1998; Ge 2005; Feng et al. 2013a) methods are attractive for this purpose. In some cases, these kinds of method may take a long time searching for a solution and caution should be observed in case of a local optimal solution.
4. The representation of fracturing source location results: the results of rock mass fracturing source location can be displayed in three-dimensional graphics for all directions. The fracturing source is generally expressed as a sphere. The color and size of the sphere represent the occurrence time and seismic energy of rock mass fracturing events, respectively, as shown in Fig. 18. The color and size can also be other source parameters according to the display purpose.

5.3 Calculation of Source Parameters

A seismic event is considered to be described quantitatively when, apart from its timing, t, and location, $x = (x, y, z)$, at least two independent parameters pertaining to the seismic source are determined reliably: namely, seismic potency, P, which measures coseismic inelastic deformation at the source, and radiated seismic energy, E.

The displacement field generated by the force of the microseismic source can be composed of three parts, i.e., components of the near-field, intermediate-field, and far-field. The mean ratio of displacements at near-field, intermediate-field, far-field, U_N:U_I:U_F, for the seismic moment having the ramp function of a sufficiently short rise time can be estimated as follows ignoring the radiation pattern (Fujii et al. 1997):

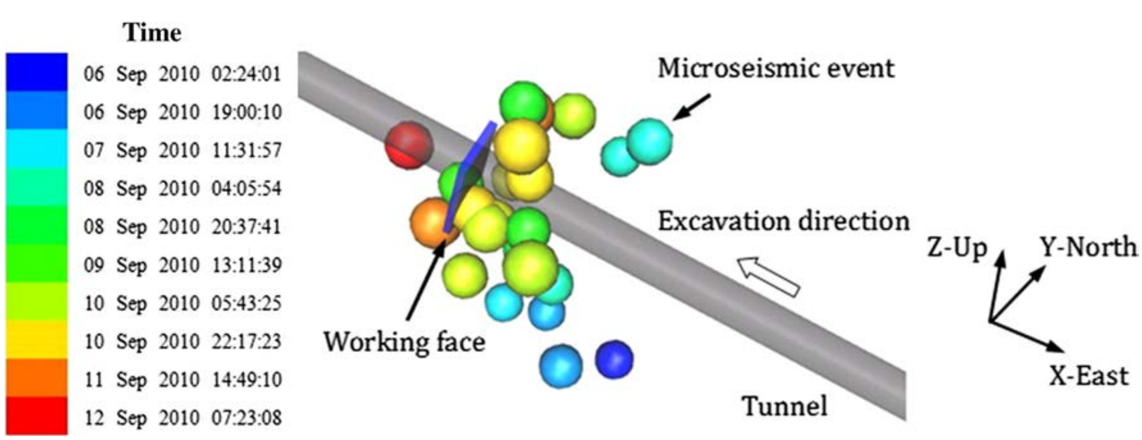

Fig. 18 Example of source location of microseismic events in a rock mass fracturing process in a deep tunnel

$$U_{\mathrm{N}} : U_{\mathrm{I}} : U_{\mathrm{F}} = 0.5R^{-2}(v_{\mathrm{S}}^{-2} - v_{\mathrm{P}}^{-2}) : (v_{\mathrm{P}}R)^{-2} : v_{\mathrm{P}}^{-3}R^{-1}\pi f_{\mathrm{c}}, \tag{3}$$

where R is the focal distance and f_c is the corner frequency.

Normally, the velocity of P-waves and S-waves in rock mass can be expressed as follows:

$$v_P = \sqrt{\frac{\lambda + 2\mu}{\rho}}, \tag{4}$$

$$v_S = \sqrt{\frac{\mu}{\rho}}, \tag{5}$$

where λ and μ are the Lamé constant and rigidity of the rock mass, and ρ is the rock density.

For most rock masses, the value of λ is equal to u approximately, so that $v_P/v_S \approx \sqrt{3}$, and formula (3) can be revised as follows:

$$U_N : U_I : U_F = 1 : 1 : v_P^{-1}R\pi f_c. \tag{6}$$

The calculation of source parameters in seismology is based on the seismic sources in the far-field.According to the Eq. (6), many microseismic sources may be near- or intermediate-field for the microseismic monitoring in rock engineering. For example, if $v_{\mathrm{P}} = 4500$ m/s and $f_{\mathrm{c}} = 75$ Hz, then U_{N}:U_{I}:$U_{\mathrm{F}} = 1$:1:0.05R. When the focal distance R is 10 m, U_{N}:U_{I}:$U_{\mathrm{F}} = 2$:2:1, then the displacements at near-field and intermediate-field dominate. This ratio becomes 1:1:5 as R increases to 100 m, the far-field displacement turning into the main displacement. When the R is increased to 200 m, the displacement of near-field and intermediate-field can be ignored. Therefore, the microseismic source should be estimated as to whether it is far-field firstly, and then the suitable calculation method of source parameters can be chosen.

1. Seismic potency, P (m^3): Seismic potency represents the volume of rock, of whatever shape, associated with coseismic inelastic deformation at the source (King 1978; Zhu and Ben-Zion 2013). According to the amplitude of the low-frequency displacement spectra Ω_0 of the recorded waveforms in the frequency domain, the seismic potency can be estimated (Keilis-Borok 1959) by the following:

$$P_{\mathrm{P,S}} = 4\pi v_{\mathrm{P,S}} R \frac{\Omega_{0,\mathrm{P,S}}}{\omega_{\mathrm{P,S}}}, \tag{7}$$

where $\omega_{\mathrm{P,S}}$ is the root-mean-square value for the radiation pattern of far-field amplitudes averaged over the focal sphere, and $\omega_{\mathrm{P}} = 0.516$ for the P-wave and $\omega_{\mathrm{S}} = 0.632$ for the S-wave (Aki and Richards 2002).

For near- or intermediate-field of microseismic sources, the estimation of Ω_0 should be dealt carefully. The estimation method based on the FFT with a multitaper window is applicative (Mendecki 1997).

2. Radiated energy (J): the portion of the energy released at the source that is radiated as seismic waves. Radiated energy is proportional to the integral of the squared velocity spectrum in the far-field and can be derived from recorded waveforms. In the time domain, the radiated seismic energy of the P- or S-wave is proportional to the integral of the radiation pattern corrected far-field velocity pulse squared of duration (Mendecki et al. 2007).

$$E_{\mathrm{P,S}} = \frac{8}{5}\pi\rho v_{\mathrm{P,S}} R^2 \int_0^{t_S} \dot{u}_{\mathrm{corr}}^2(t)\mathrm{d}t, \tag{8}$$

where t_s is the duration, and $\dot{u}_{\mathrm{corr}}^2(t)$ is the radiation pattern corrected far-field velocity pulse squared.

For a particular project, such as a tunnel or surface slope, the source should be regarded as near-field according to the short source–sensor distance. Then the seismic shock surface should be deemed to be a half sphere, and the seismic energy can be estimated as (Gibowicz and Kijko 1994) follows:

$$E_{\mathrm{P,S}} = 4\pi\rho v_{\mathrm{P,S}} R^2 \frac{J_{\mathrm{c,P,S}}}{F_{\mathrm{c,P,S}}^2}, \tag{9}$$

where $J_{\mathrm{c,P,S}}$ is the integral of the particle velocity, and $F_{\mathrm{c,P,S}}$ is the empirical coefficient of the seismic wave radiation type. It is noted that this calculation formula is largely reliant on the source model and may lead to a large error in the calculated results.

The total radiated seismic energy of a rock mass fracturing event is as follows:

$$E = E_{\mathrm{P}} + E_{\mathrm{S}}. \tag{10}$$

Then several important derived parameters can be calculated according to the seismic potency and radiated energy.

3. Seismic moment (Nm): a scalar that measures the coseismic inelastic deformation at the source can be calculated as follows:

$$M = \mu P. \tag{11}$$

In seismology, the seismic moment can be computed from the product of rigidity, fault area, and average slip displacement.

$$M = \mu\bar{u}A, \tag{12}$$

where $\bar{u}$ is a mean displacement (slip) over the source area A.

A relation that scales seismic moment into magnitude of a seismic event is termed moment magnitude (Hanks and Kanamori 1979).

$$m = 2/3 \log M - 6.1. \tag{13}$$

4. Apparent volume (m^3): the apparent volume scales the volume of rock with the coseismic inelastic strain of an order of apparent stress over rigidity (Mendecki 1993).

$$V_A = \frac{\mu P^2}{E}. \tag{14}$$

Apparent volume depends on seismic potency and radiated energy, and, because of its scalar nature, can easily be manipulated in the form of cumulative or contour plots.

5. Energy index, EI: the notion of comparing the radiated energies of seismic events of similar moments can be translated into a practical tool called the Energy Index (EI)—the ratio of the radiated energy of a given event (E) to the energy $\overline{E}(P)$ (derived from the regional log$E$ vs log$M$ relation for a given moment M, as shown in Fig. 19).

$$EI = \frac{E}{\overline{E}(P)} = \frac{E}{10^{d \log P + c}} = 10^{-c}\frac{E}{P^d}, \tag{15}$$

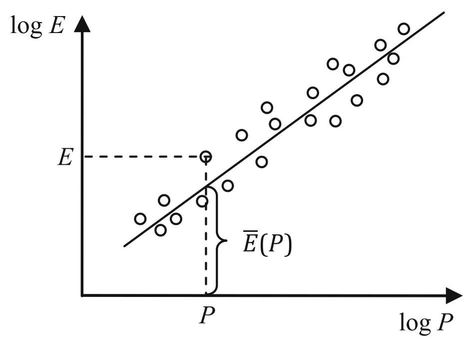

Fig. 19 Energy index concept (Mendecki 1997)

Table 3 Example of source parameters for a rock mass fracturing event that triggered ten sensors

Summary sheet of source parameters for events
Original time Jul 07 06:16:48:742765 2010
Location EAST = 10838 m, North = 3 m, Up = −34 m
Source:
1. Seismic potency $P = 9.66$ E-02 m^3; $P_P = 9.31$ E-02 m^3; $P_S = 9.73$ E-02 m^3
2. Seismic moment $M = 3.19E + 09$ Nm; $M_P = 3.08E + 09$ Nm; $M_S = 3.22E + 09$ Nm
3. Radiated energy $E = 9.81E + 03$ J; $E_P = 5.71E + 02$ J; $E_S = 9.24E + 03$ J
4. Corner frequency = 80.3 Hz
5. Apparent stress = 0.102 E + 06 Pa; apparent volume = 1.57E + 04 m^3
6. Moment magnitude = 0.3; local magnitude = −0.3
7. Static stress drop = 3.41E + 05 Pa; dynamic stress drop = 5.76E + 05 Pa
8. $E_S/E_P = 16.17$

Table 4 An example of measurements related to tunnel microseismicity

Microseismic monitoring					
Summary data sheet			Sensors network: Six uniaxial and two triaxial geophones		
Project: Diversion tunnels in Jinping II hydropower station, China					
Tunnel of monitoring No. 3 diversion tunnel					
Date acquisition instrument no. 100192 and 100086 (12 channels)					
Year of monitoring 2011					
Date (month-day)	Excavation (m)	Number of events (unit)	Radiated energy (J)	Apparent volume (m^3)	Notes
5-29	3	3	5.1 E + 03	6.8 E + 03	
5-30	5	27	2.3 E + 05	8.5 E + 04	
5-31	4	23	8.1 E + 05	7.6 E + 04	
6-01	5	33	5.4 E + 05	9.4 E + 04	
6-02	3	12	3.5 E + 06	1.1 E + 05	An intensive rockburst occurred
6-03	3	2	8.0 E + 02	2 E + 03	

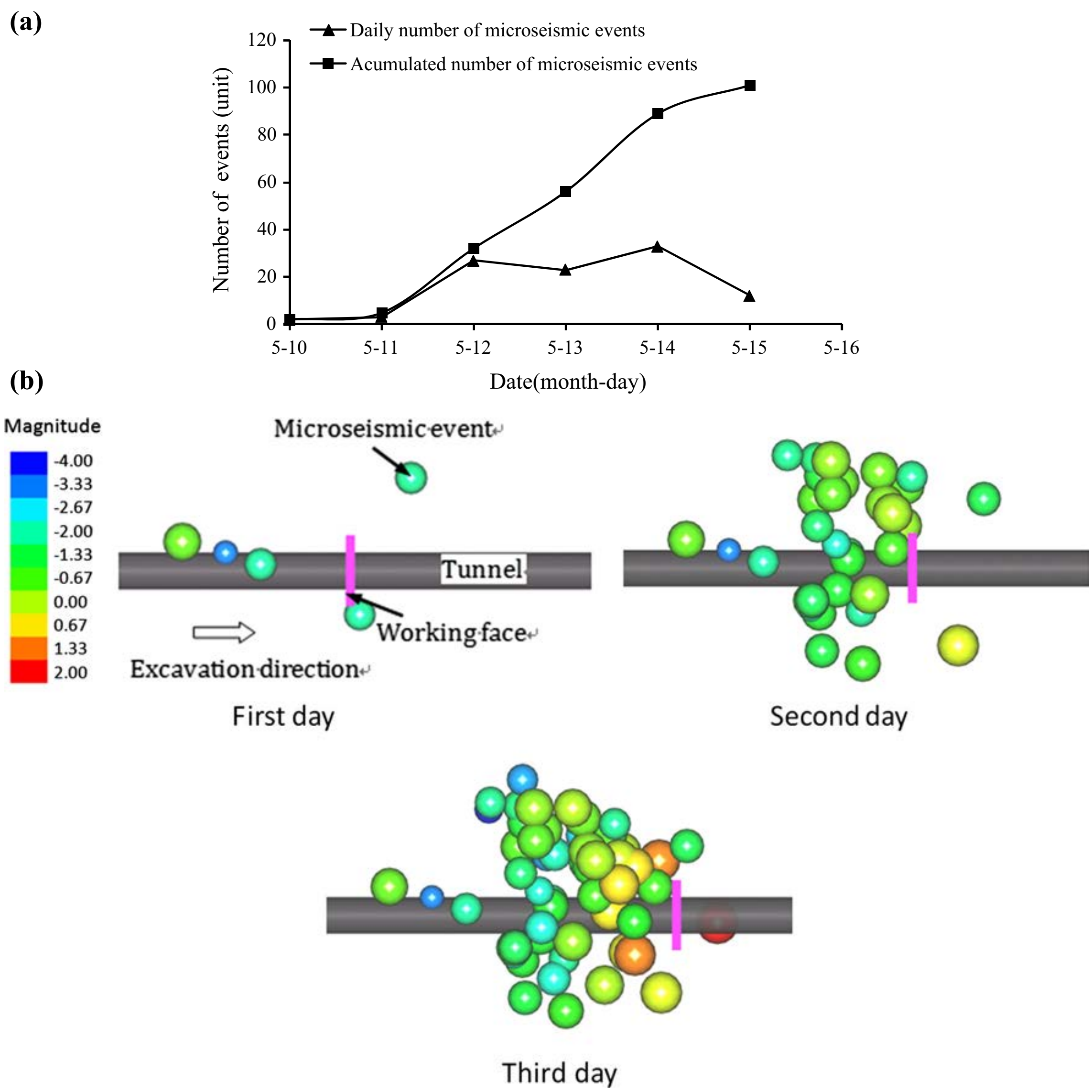

Fig. 20 Example of the evolution of microseismic events versus time in tunnel monitoring. **a** A number of microseismic events, and **b** the spatial distribution of accumulated microseismic events (The section of tunnel is arc-shaped and its size is 13 m × 8 m)

where d and c are the linear fitting parameters, $\log\overline{E}(P) = d\log P + c$. Generally, the d-value increases as the rock mass stiffness increases. For a given d, the c-value increases with stress.

A small or moderate event with EI > 1 indicates that the shear stress is higher than its mean value at this location. The opposite applies for the EI < 1 case.

In addition, other source parameters, such as the apparent stress, stress drop, source size, corner frequency, and local magnitude, etc., can be calculated as well. The detailed definitions and formulas for these source parameters (include those listed in Table 3) can be found in the related references (Gibowicz and Kijko 1994; Mendecki 1993, 1997). Often, just the wave arrivals and calibration of wave velocity for microseismic events are required, and then these source parameters can be quickly estimated by using seismogram processing software provided by commercial sources. As an example, the presentation of source parameters for a rock mass fracturing event that triggered ten sensors is listed in Table 3.

5.4 Presentation of Microseismicity for a Rock Mass Fracturing Process

The microseismicity characteristic parameters, such as number of microseismic events, sum of radiated energy, sum of apparent volume, etc., should be transferred to a

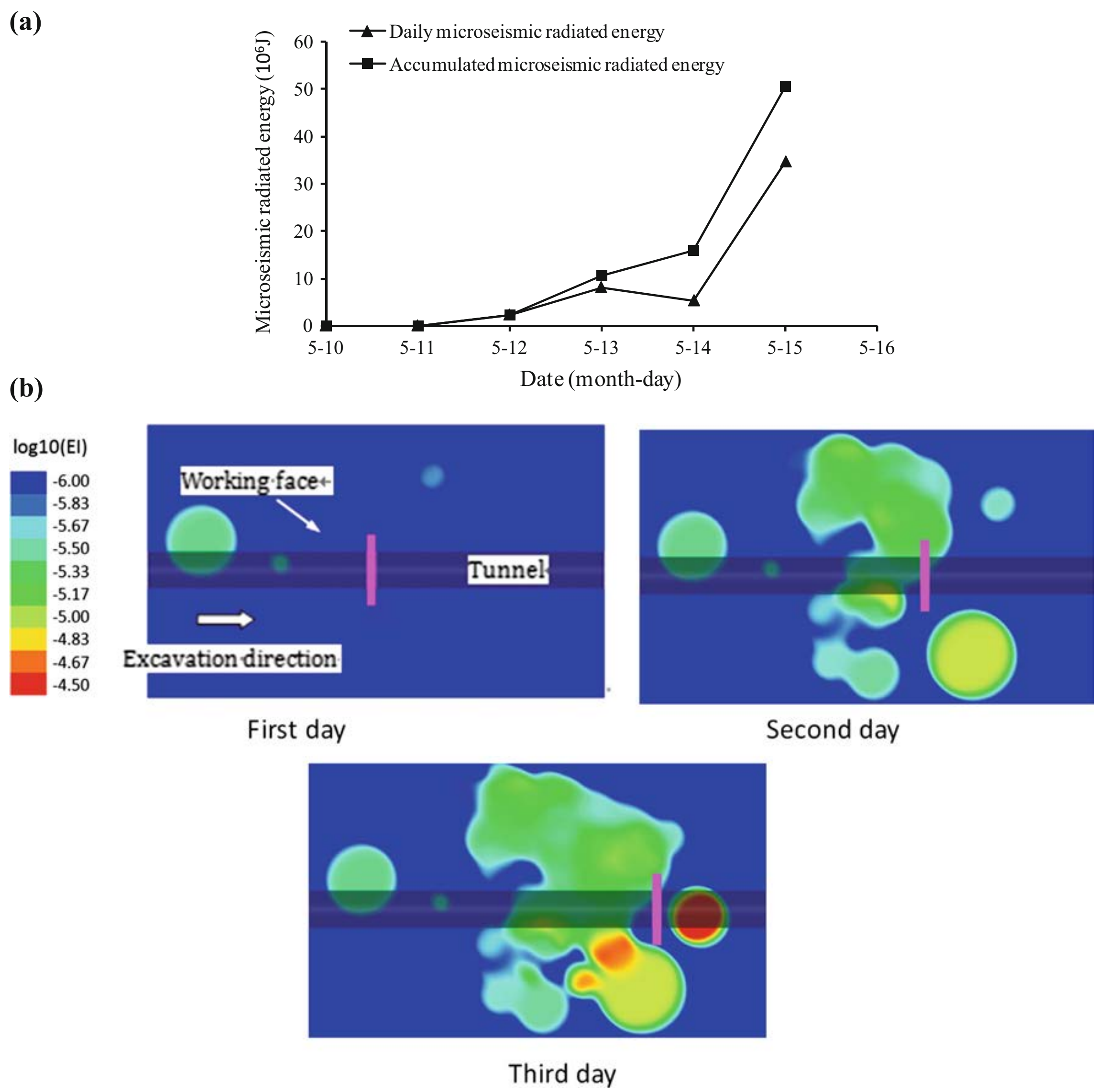

Fig. 21 Example of microseismic energy versus time: **a** microseismic energy; and **b** energy index on three consecutive days

computation and data summary sheet to represent the rock mass fracturing process. The data can be analyzed in terms of hours, days, or months. An example taken from a tunnel microseismic monitoring example is shown in Table 4.

A series of plots for microseismicity parameters versus time are the best means of summarizing current data and observing the trends of the monitoring data, and should be updated day by day. Figure 20 provides an example of the evolution of microseismic events versus time in a tunnel monitoring project. The number of events can be used to evaluate the activity and evolution trend of rock mass fracturing.

Figure 21 shows an example of the evolution of microseismic energy versus time in a tunnel monitoring project. The energy index (EI), which is a scalar quantity, can easily be manipulated in the form of cumulative or contour plots, as shown in Fig. 21b. Actually, the energy index of an event is proportional to its apparent stress. The higher this index, the more energy will be released per unit of inelastic deformation at the source.

An example of the evolution of microseismic apparent volume against time is shown in Fig. 22. This Figure can be used for estimation of the instability of a rock mass. For example, a continuous increase of cumulative apparent volume usually anticipates the potential instability of a rock mass.

Figure 23 provides an example of the relation of cumulative apparent volume vs. time and energy index vs. time. It can be used for estimation of the potential rock mass instability. For example, instability of the monitored rock mass may occur if there exists a period of increasing energy index with a normal rate of cumulative apparent volume (the stress hardening phase) following by a period

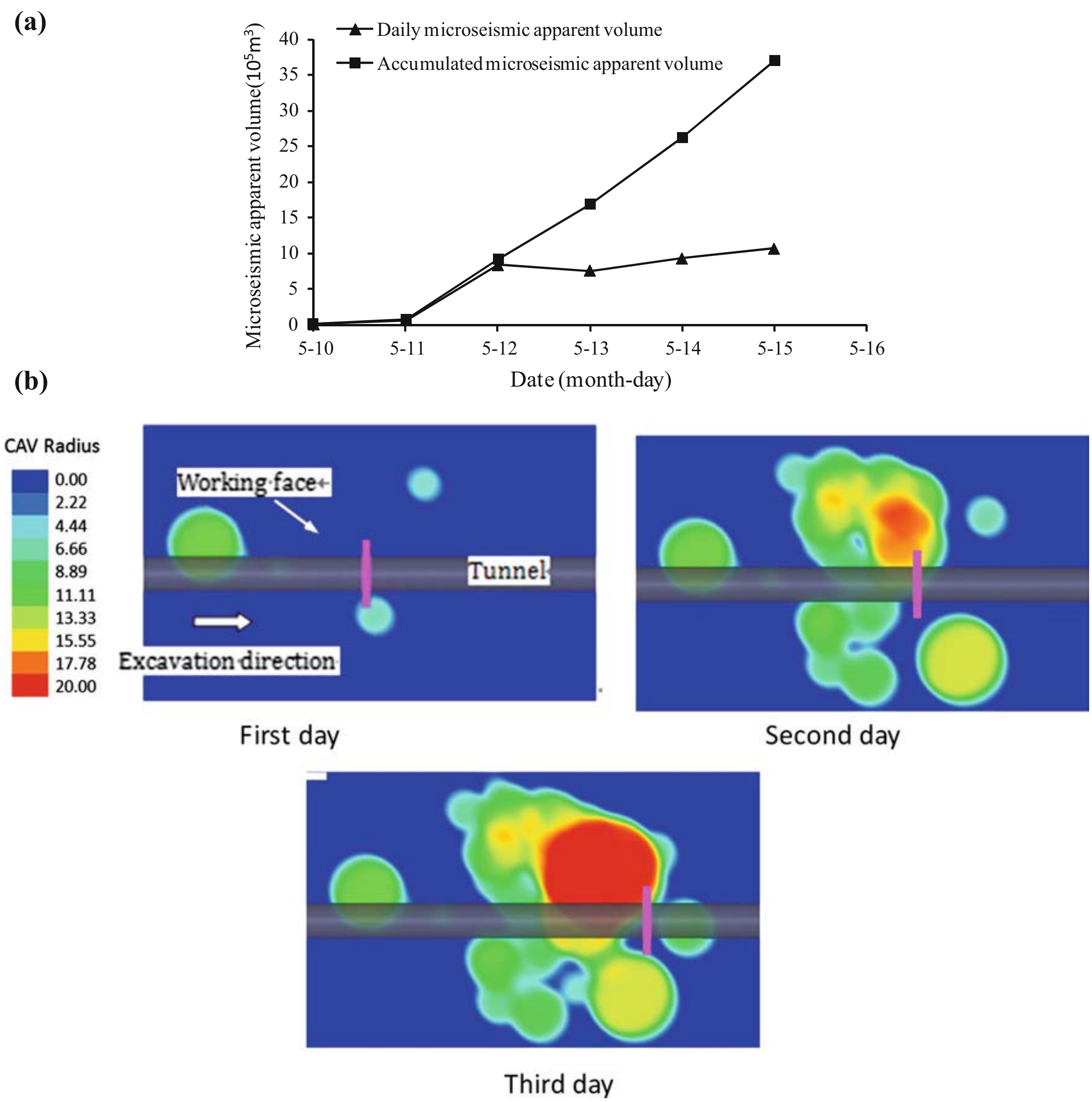

Fig. 22 Example of the evolution of microseismic apparent volume versus time: **a** microseismic apparent volume, and **b** the cloud of accumulated microseismic apparent volume on three consecutive days

of dropping energy index and simultaneously accelerating cumulative apparent volume (the stress softening phase). It should be noted that such patterns have quite low success rates in indicating the possibility of large events due to the low resolution of microseismic arrays.

If needed, evolution of other source parameters can be presented in a similar way.

6 Reports

Reports on microseismic monitoring are important for evaluating the quality of the rock mass fracturing process, for interpreting the monitoring results, and for accumulating experience. These reports, unless otherwise specified, include general data, installation, daily situation, and monitoring results.

6.1 General Data Reports

General data reports should contain the following items:

1. A brief description of the monitoring project, purpose of the monitoring, geological conditions, and rock lithology.
2. Engineering activities, such as method of excavation, support, and drilling during the entire monitoring process if undertaken.

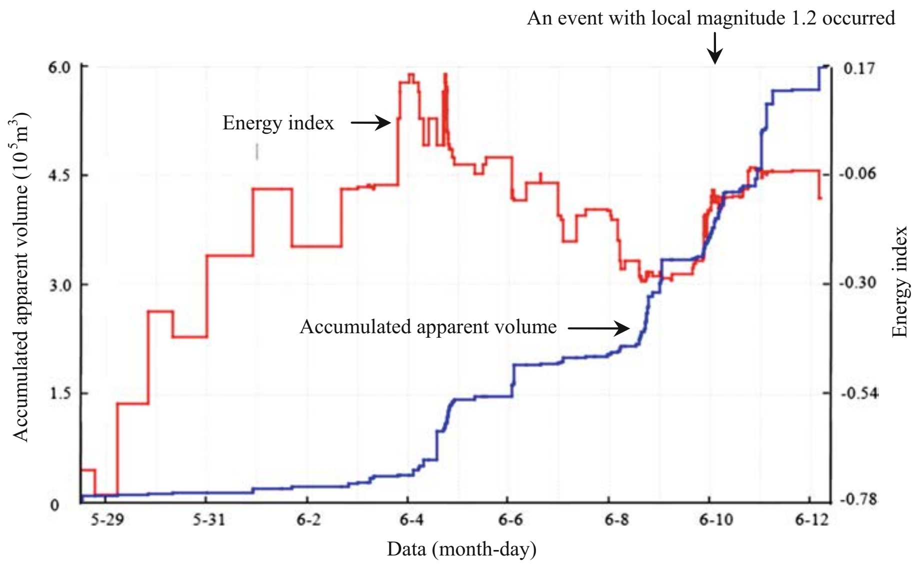

Fig. 23 Example of evolution of EI and accumulated apparent volume versus time. The characteristic pattern of dropping energy index and accelerating cumulative apparent volume prior to a large seismic event (local magnitude 1.2 in this case), from seismic data recorded at the Jinping II hydropower station in China (Feng et al. 2013a)

3. A brief description of the components of the microseismic monitoring system (see Fig. 1), the manufacturer, and main technical parameters.
4. Sensors (type, number, and main technical parameters, such as sensitivity, frequency, and bandwidth.).
5. A brief description of the equipment arrangement, data transfer units between each of the components of microseismic monitoring system (see Fig. 5).
6. Any additional comments.

6.2 Installation reports

1. A brief description of the coordinate system and three-dimensional model for displaying the rock mass fracturing process.
2. Details and methods for the installation of sensors (installation method, type, and details of drilling equipment, depth and dip of borehole, serial number and coordinates of sensors, etc.). Reference may be made to this ISRM Suggested Method, stating only departures from the recommended procedures.
3. The layout scheme of the sensors as shown in Figs. 7, 8, 9.
4. A brief description of the period, sequence, process, and method of installation, the difficulties involved, and solution, etc.
5. Any additional comments.

6.3 Daily situation reports

1. Log of the daily working condition of the monitoring system (especially the data acquisition instruments and sensors). The period and influences on the monitoring results of any malfunctioning equipment should be recorded clearly. The solutions in dealing with equipment failure should be described in detail.
2. Record of engineering activity information, such as excavation method, time and region of blasting, period of supporting, rock debris, drilling, supporting pattern, etc.
3. A brief description of the daily geological condition in the monitored area. Lithology and classification of the surrounding rock, occurrence of fractures, and the hydrogeology condition should be recorded in detail.
4. The failure, single or multiple, of the rock mass in the monitored area, such as collapse, rockburst, and water inrush, should be recorded in detail as appropriate. The information on the failure characteristics, occurrence, position, range, support in the failure area, loss, and treatment, is essential. Photographs should be taken of these failures as soon as possible.
5. Any additional comments.

6.4 Monitoring Results Report

This should include the following:

1. A detailed description of the procedure and method of signal identifying, filtering, and source locating.
2. The typical waveform characteristics of all known microseismic signals, as shown in Fig. 14 and listed in Table 2.
3. A set of monitoring result tabulations containing information, as shown in Table 4.
4. The evolution of microseismicity, as shown in Figs. 20, 21, 22, 23.
5. Any additional comments.

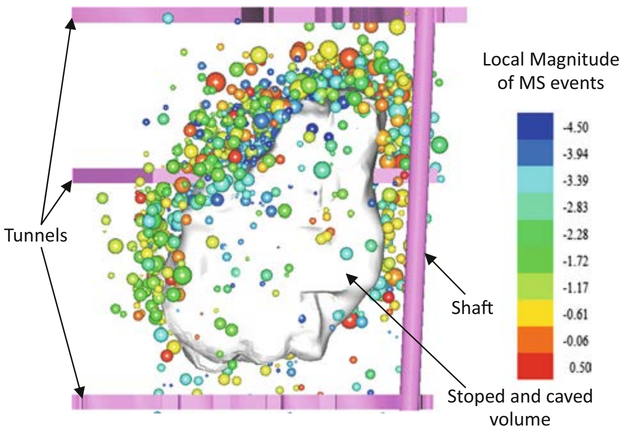

Fig. 24 Lateral view of shape of stoped and caved volume obtained by 3-D laser scanning and microseismic events distribution of a deep stope

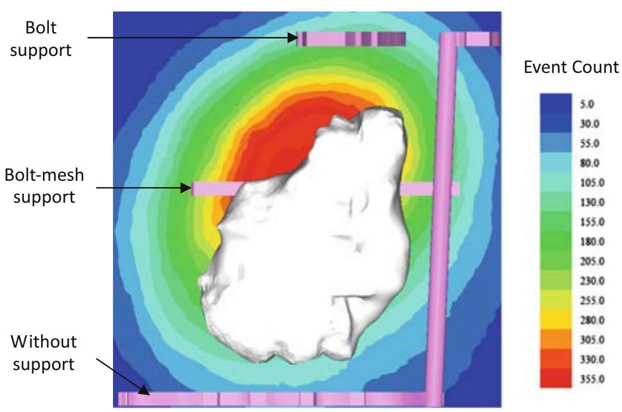

Fig. 25 Lateral view of microseismic events density and support scheme for tunnels

6.5 Presentation of Overall Conclusions

In addition to the reports described above, where applicable there should also be presentations of the overall conclusions to aid in the interpretation of the results. An example of these is shown in Figs. 24, 25. The two Figures illustrate the results of microseismic monitoring of a rock fracture around a stope that is at about 1100 m depth in the Hongtoushan copper mine, China. The purpose of the monitoring is to evaluate the damage and stability of the surrounding rock mass near the stope, which has been used to optimize support design and mining sequence. According to the microseismic events distribution, event density and shapes of stoped and caved volumes obtained by 3-D laser scanning, microseismic events are mainly located at the roof of the stoped and caved volume and have a higher event density. This indicates that the surrounding rock mass has a higher risk of hazards at the upside of stope than at the bottom. Therefore, bolt-mesh or bolt supports are used in tunnels at the roof, while tunnels at the floor are without support. In addition, the whole roof of the stope should not be early exposed. The mining process from the middle to the two side of the stope is recommended, rather than any other mining direction.

Figure 26 shows an example of microseismic monitoring results representation from an open-pit mine (Lynch 2007). From Fig. 26a, b, it seems that microseismic activity recorded in open-pit slopes is related to mining processes near the slopes. The microseismic monitoring provides a clear image where stresses are high enough to cause brittle fracturing within the rock mass, which is useful for evaluating the stability of the slope as mining progresses.

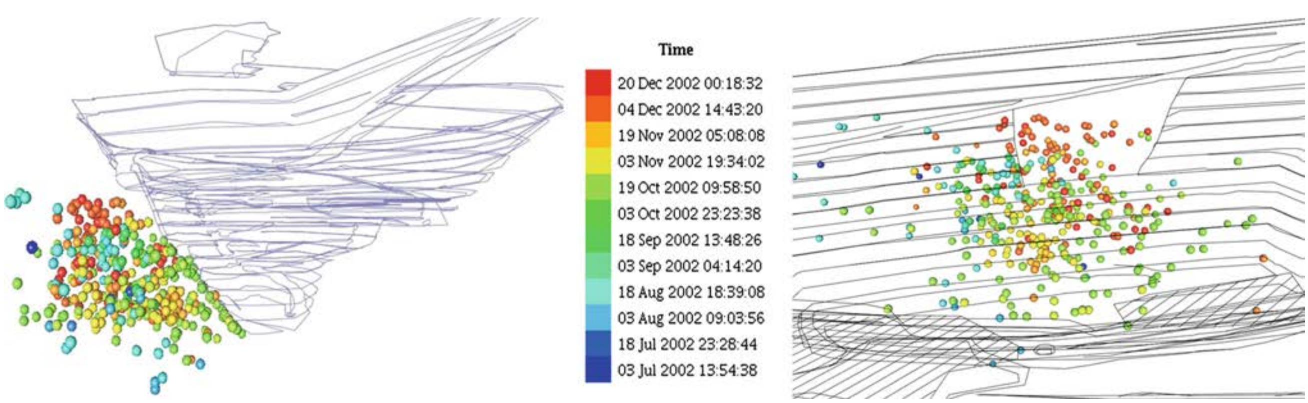

(a) Lateral view of microseismic events distribution **(b)** Inclined top view of microseismic events distribution

Fig. 26 Example of microseismic monitoring of an open-pit mine (Lynch 2007)

Such overall diagrams are most helpful in transmitting the overall results of a microseismic monitoring exercise and in enabling interested parties to understand how the relevant conclusions have been reached.

Acknowledgments This ISRM Suggested Method has been tested at four headrace tunnels and water drainage tunnel at Jinping II hydropower station, tunnels at Baihetan hydropower station, Shizhuyuan mine, and Hongtoushan Copper Mine, China. Review and comments from Professor Luo Xun, Professor Ray Durrheim, Professor Arno Zang, Professor Resat Ulusay, five anonymous reviewers, and members of the ISRM Board 2015–2019 are appreciated.

References

Aki K, Richards PG (2002) Quantitative Seismology. University Science Books, California

Bolstad DD (1990) Rockburst control research by the U.S. Bureau of Mines. Proc 2rd Int Symp on Rockbursts and Seismicity in Mines, A.A.Balkema, Rotterdam. pp 371-375

Cai M, Kaiser PK, Martin CD (1998) A tensile model for the interpretation of microseismic events near underground openings. Pure appl Geophys 153:67–92

Cai M, Kaiser PK, Morioka H, Minami M, Maejima T, Tasaka Y, Kurose H (2007) FLAC/PFC coupled numerical simulation of AE in large-scale underground excavations. Int J Rock Mech Min Sci 44:550–564

Chen BR, Li QP, Feng XT, Xiao YX, Feng GL, Hu LX (2014) Microseismic monitoring of columnar jointed basalt fracture activity: a trial at the Baihetan Hydropower Station, China. J Seismol 18:773–793

Cook NGW (1963) The seismic location of rockbursts. Pergamon Press, In Proc Fifth Symp Rock Mech, pp 493–516

Cook NGW (1964) The application of seismic techniques to problems in rock mechanics. Int J Rock Mech Min Sci 1:169–179

Durrheim RJ (2010) Mitigating the risk of rockbursts in the deep hard rock mines of South Africa: 100 years of research. In Extracting the Science: a century of mining research, Brune J (eds), Society for Mining, Metallurgy, and Exploration, Inc., pp 156–171

Durrheim RJ, Cichowicz A, Ebrahim-Trollope R, Essrich F, Goldbach O, Linzer LM, Spottiswoode SM, Stankiewicz T (2007) Guidelines, standards and best practice for seismic hazard assessment and rockburst risk management in South African mines. Proceeding of the 4th international seminar on deep and high stress mining, Perth, Australia. pp 249–261

Durrheim RJ, Ogasawara H, Nakatani M, Yabe Y, Kawakata H, Naoi M, Ward AK, Murpgh SK, Wienand J, Lenegan P, Milev AM, Murakami O, Yoshimitsu N, Kgarume T, Cichowicz A (2012) Establishment of SATREPS experimental sites in South African gold mines to monitor phenomena associated with earthquake nucleation and rupture. Deep Mining, Perth, pp 173–188

Feignier B, Young RP (1992) Moment tensor inversion of induced microseismic events: evidence of non-shear failures in the $-4 < M < -2$ moment magnitude range. Geophys Res Lett 19:1503–1506

Feng XT, Chen BR, Li SJ, Zhang CQ, Xiao YX, Feng GL, Zhou H, Qiu SL, Zhao ZN, Yu Y, Chen DF, Ming HJ (2012) Studies on the evolution process of rockbursts in deep tunnels. J Rock Mech Geo Eng 4:289–295

Feng XT, Chen BR, Zhang CQ, Li SJ, Wu SY (2013a) Mechanism, warning and dynamic control of rockbursts development processes. Science Press, Beijing (in Chinese)

Feng XT, Li SJ, Chen BR, Jiang Q (2013b) Report on comprehensive observation test and feedback analysis of the whole failure process of columnar joints basalt under excavation, in the diversion tunnel of Jinsha River hydropower station. Institute of Rock and Soil Mechanics, the Chinese Academy of Science, Wuhan (in Chinese)

Fujii Y, Ishijima Y, Deguchi G (1997) Prediction of coal face rockbursts and microseismicity in deep longwall coal mining. Int J Rock Mech Min Sci 34:85–96

Ge MC (2005) Efficient mine microseismic monitoring. Int J Coal Geol 64:44–56

Gibowicz SJ, Kijko A (1994) An introduction to mining seismology. Academic Press, New York

Gibowicz SJ, Young RP, Talebi S, Rawlence DJ (1991) Source parameters of seismic events at the Underground Research Laboratory in Manitoba, Canada: scaling relations for events with moment magnitude smaller than -2. Bull Seismol Soc Am 81:1157–1182

Gong SY, Dou LM, Cao AY, He H, Du TT, Jiang H (2010) Study on optimal configuration of seismological observation network for coal mine. Chin J Geophys 53:457–465 **(in Chinese)**

Hanks TC, Kanamori HA (1979) A moment magnitude scale. J Geophys Res 84:2348–2350

Hanyga A (1991) Implicit curve tracing and point-to-curve ray tracing. University of Bergen, Seismological Observatory

Hirata A, Kameoka Y, Hirano T (2007) Safety management based on detection of possible rock bursts by AE monitoring during tunnel excavation. Rock Mech Rock Eng 40:563–576

Julian B, Gubbins D (1997) Three-dimensional seismic ray tracing. J Geophy Res 43:95–114

Kaiser PK, Tannant DD, McCreath DR (1996) Canadian rockburst support hand book. Geomechanics Research Centre, Laurentian University, Sudbury, Ontario

Keilis-Borok VI (1959) On estimation of the displacement in an earthquake source and of source dimensions. Ann Geofis 12:205–214

Kijko A (1977) An algorithm for the optimum distribution of a regional seismic network-II:an analysis of the accuracy of location of local earthquakes depending on the number of seismic stations. Pageoph 115:1011–1021

King GCP (1978) Geological faults, fractures, creep and strain. Philosop Trans Royal Soc London Math Phy Sci 288:197–212

Lesniak A, Isakow Z (2009) Space–time clustering of seismic events and hazard assessment in the Zabrze-Bielszowice coal mine, Poland. Int J Rock Mech Min Sci 46:918–928

Li T, Mei TT, Sun XH, Lv YG, Sheng JQ, Cai M (2013) A study on a water-inrush incident at Laohutai coalmine. Int J Rock Mech Min Sci 59:151–159

Liu JP, Feng XT, Li YH, Xu SD, Sheng Y (2013) Studies on temporal and spatial variation of microseismic activities in a deep metal mine. Int J Rock Mech Min Sci 60:171–179

Luo X, Yu KJ, Hatherly P, Zhang X (2001) Microseismic monitoring of rock fracturing under aquifers in longwall coal mining. Proceedings of the 71st SEG Annual Meeting, St Antonio, USA. pp 1521–1524

Luo X, Creighton A, Gough J (2010) Passive seismic monitoring of minescale geothermal activity—a trial at Lihir Mine for mine risk management. Pure appl Geophys 167:119–129

Lynch RA (2007) Microseismic monitoring of open pit mines. ISS International Limited

Lynch RA, Wuite R, Smith BS, Cichowicz A (2005) Microseismic monitoring of open pit slopes. Proc 6th Int Symp on Rockbursts and Seismicity in Mines, 9–11 March 2005, Perth, Australian. pp 581–592

Mallet S (1999) A wavelet tour of signal processing, 2nd edn. Academic Press, Waltham

Manthei G, Eisenblätter J (2008) Acoustic Emission in Study of Rock Stability. In: Grosse CU, Ohtsu M (eds) Acoustic Emission Testing, Springer, Berlin. pp 239–310

Martin CD, Read RS, Martino JB (1997) Observation of brittle failure around a circular test tunnel. Int J Rock Mech Min Sci 34:1065–1073

Maurer H, Curtis A, Boerner DE (2010) Recent advances in optimized geophysical survey design. Geophys 75:75A177–75A194

McGarr A, Boettcher M, Fletcher JB, Johnston MJS, Durrheim RJ, Spottiswoode SM, Milev A (2009) A deployment of broadband seismic stations in two deep gold mines, South Africa. Bull Seism Soc Am 99:2815–2824

Mendecki AJ (1993) Real time quantitative seismology in mines. Proc 3rd Int Symp on Rockbursts and Seismicity in Mines, A. A. Balkema, Rotterdam. pp 287–295

Mendecki AJ (1997) Seismic monitoring in mines. Chapman and Hall, London

Mendecki AJ, Lynch RA, Malovichko DA (2007) Routine seismic monitoring in mines. VNIMI Seminar on seismic monitoring in Mines

Milev AM, Spottiswoode SM, Rorke AJ, Finnie GJ (2001) Seismic monitoring of a simulated rockburst on a wall of an underground tunnel. J S Afr I Min Metall 101:253–260

Mutke G, Stec K (1997) Seismicity in the upper Silesian Coal Basin, Poland: strong regional seismic events. Proc 4th Int Symp on Rockbursts and Seismicity in Mines, A. A. Balkema, Rotterdam. pp 213-217

Occhiena C, Pirulli M, Scavia C (2014) A microseismic-based procedure for the detection of rock slope instabilities. Int J Rock Mech Min Sci 69:67–79

Ogasawara H, Sato S, Nishii S, Sumitomo N, Ishii H, Lio Y, Nakao S, Ando M, Takano M, Nagai N, Ohkura T, Kawakata H, Satoh T, Kusunose K, Cho A, Mendecki AJ, Cichowicz A, Green RWE, Kataka MO (2001) Semi-controlled seismogenic experiments in South African deep gold mines. Proc 5th Int Symp on Rockbursts and Seismicity in Mines, The South African Institute of Mining and Metallurgy, Johannesburg. pp 287–292

Oye V, Roth M (2003) Automated seismic event location for hydrocarbon reservoirs. Comput Geosci 29:851–863

Pattrick KW (1984) The instrumentation of seismic networks at Doornfontein gold mine. Proc 1st Int Symp on Rockbursts and Seismicity in Mines, South African Institute of Mining Metallurgy, Johannesburg. pp 337–340

Potvin Y, Hudyma MR (2001) Keynote address: Seismic monitoring in highly mechanized hardrock mines in Canada and Australia. Proc 5th Int Symp on Rockbursts and Seismicity in Mines, The South African Institute of Mining and Metallurgy, Johannesburg. pp 267–280

Rabinowitz N, Steinberg DM (1990) Optimal configuration of a seismographic network: a statistical approach. Bull Seismol Soc Am 80:187–196

Scheepers JB (1984) The Klerksdorp seismic network—monitoring of seismic events and systems layout. Proc 1st Int Symp on Rockbursts and Seismicity in Mines, South African Institute of Mining Metallurgy, Johannesburg. pp 341–345

Scott DF, Williams TJ, Friedel MJ (1997) Investigation of a rockburst site, Sunshine Mine, Kellogg, Idaho. Proc 4th Int Symp on Rockbursts and Seismicity in Mines, A. A. Balkema, Rotterdam. pp 311–315

Singh M, Kijko A, Durrheim RJ (2009) Seismotectonic models for South Africa: synthesis of geoscientific information, problems and way forward. Seismol Res Lett 80:71–79

Tang CA, Wang JM, Zhang JJ (2010) Preliminary engineering application of microseismic monitoring technique to rockburst prediction in tunneling of Jinping II project. J Rock Mech Geo Eng 2:193–208

Trifu CI, Shumila V, Urbancic TI (1997) Space-time analysis of microseismicity and its potential for estimating seismic hazard in mines. Proc 4th Int Symp on Rockbursts and Seismicity in Mines, A.A Balkema, Rotterdam. pp 295–298

Trifu CI, Shumila V, Leslie I (2008) Application of joint seismic event location techniques at Chuquicamata open pit mine, Chile. Proceedings 5th International Conference and Exhibition on Mass Mining, 9–11 June 2008, Luleå, Sweden. pp 943–952

Trnkoczy A (2009) Understanding and parameter setting of STA/LTA trigger algorithm. In: Bormann P (ed) New Manual of Seismological Observatory Practice (NMSOP). Potsdam, Deutsches GFZ, pp 1–20

Van Aswegen G, Butler A (1993) Applications of quantitative seismology in South African gold mines. Proc 3rd Int Symp on Rockbursts and Seismicity in Mines, A.A. Balkema, Rotterdam. pp 261–266

Vidale J (1988) Finite-difference calculation of travetimes. Bull Seism Soc Am 78:2062–2076

Vinje V, Iversen E, Gjoystadl H (1993) Traveltime and amplitude estimation using wavefront construction. Geophysics 58:1157–1166

Vladut TL, Lepper CM (1985) Early warning of slope instabilities by microseismic monitoring. Proc 4th Conference on Acoustic Emission/Microseismic Activity in Geological Structures and Materials, 22–24 October 1985, Pennsylvania. pp 511–529

Wesseloo J, Sweby GJ (2008) Microseismic monitoring of hard rock mine slopes. SHIRMS, Australian Centre for Geomechanics, Perth, pp 433–450

Xu NW, Tang CA, Li LC, Zhou Z, Sha C, Liang ZZ, Yang JY (2011) Microseismic monitoring and stability analysis of the left bank slope in Jinping first stage hydropower station in southwestern China. Int J Rock Mech Min Sci 48:950–963

Young RP, Collins DS (2001) Seismic studies of rock fracture at the Underground Research Laboratory, Canada. Int J Rock Mech Min Sci 38:787–799

Young RP, Collins DS, Reyes-Montes JM, Baker C (2004) Quantification and interpretation of seismicity. Int J Rock Mech Min Sci 41:1317–1327

Zang A, Wagner CF, Dresen G (1996) Acoustic emission, microstructure, and damage model of dry and wet sandstone stressed to failure. Geophys J Int 101:17507–17521

Zang A, Wagner CF, Stanchits S, Dresen G, Andresen R, Haidekker MA (1998) Source analysis of acoustic emissions in Aue granite cores under symmetric and asymmetric compressive loads. Geophys J Int 135:1113–1130

Zhu LP, Ben-Zion Y (2013) Parametrization of general seismic potency and moment tensors for source inversion of seismic waveform data. Geophys J Int 194:839–843

Chapter 15

Observation-based design of geo-engineering projects with emphasis on optimization of tunnel support systems and excavation sequences

M. Sharifzadeh[1], *M. Ghorbani*[2] & *S. Yasrobi*[3]

[1]*Department of Mining Engineering, Western Australian School of Mines, Curtin University, Kalgoorlie, Western Australia, Australia*

[2]*Department of Mining & Metallurgical Engineering, Amirkabir University of Technology, Tehran, Iran*

[3]*Pazhoohesh Omran Rahvar (P.O.R.) Consulting Engineers Company, Tehran, Iran.*

Abstract: The geomaterial in engineering design rarely shows uniform distribution of its properties and behavior. Geotechnical investigation does not detect all possible design parameters accurately and some uncertainties always remain. In such conditions, preliminary design with simplifying assumptions, and detailed design using observational methods during construction, are recommended. Back analyses are very powerful tools for interpreting the results of field measurements. They should be used not only to determine material properties but also to generate a mechanical model of soils and rocks. A brief review of back analysis procedures is presented, including comparisons, problems, recent advances and further development. A classification of different back analysis methods, considering those deterministic and non-deterministic aspects applicable in geotechnical engineering problems, is proposed. The application of observational methods to a large urban tunneling project is illustrated as a case study. The importance of geotechnical/structural/geodetic instrumentation as a practical engineering tool for systematic monitoring of tunnels and buildings in urbanized areas is shown, together with details of how the Niayesh tunnel monitoring plan, taking into consideration all requirements, was created and implemented. Based on the monitoring results, probable alerts, possible countermeasures and several design optimizations were identified. In sequential excavation methods, for reasons of safety and cost, it is essential to fully understand the influence on tunneling performance of both a given excavation sequence, and the trailing distance and face-advancing sequences of different excavation stages in soft ground urban tunneling. Different excavation sequences employing the side drift method were planned and modeled using a three-dimensional finite element method and the optimal excavation sequence was selected. Finally, the trailing distance between different excavation stages was analyzed numerically and the optimal distance for minimum surface settlement was determined.

1 INTRODUCTION

Tunnel and underground excavations are increasingly used for civil, mining and energy purposes. From the civil point of view, because of the rapid development of urbanization, tunneling has become a preferred construction method for transportation and underground utility systems. From the mining point of view, because of limitations in surface resources, the development of underground mining has increased and existing underground mines are getting deeper and deeper.

Given the vast requirement for underground excavation, tunneling technology has significantly advanced in the past few decades. Previously, tunnels were designed in detail before construction. However, because of various ground-related uncertainties, construction methods in which detailed design was done before tunnel excavation could not cover all aspects of real ground conditions and several failures were reported in such design procedures. To minimize risks and uncertainties, observational approaches were introduced and applied. Based on the observational approach, tunnel design was firstly performed by preliminary geotechnical investigation and instrumentation, followed by the use of monitoring systems. By considering monitoring results from full-scale projects and back analysis, real ground behaviors were obtained. During the early stages of construction, the preliminary design could be modified and adjusted using the observed real-world ground behavior data obtained from back analysis. The potential benefits of such observational methods are illustrated in Figure 1.

In this chapter, first the tunnel design procedures involving observational methods are described, which illustrates the key roles of instrumentation, monitoring and back analysis in tunnel design, data update and subsequent design modification. Second, an

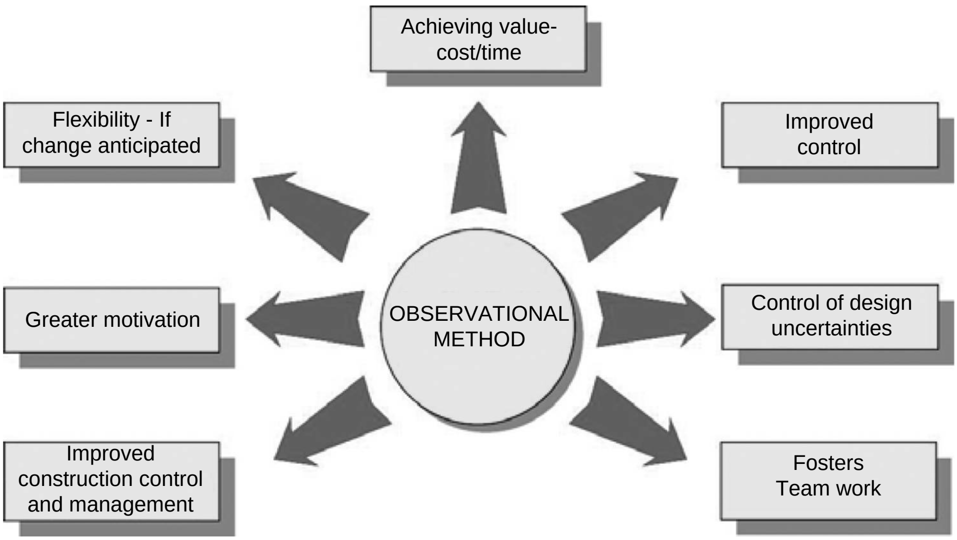

Figure 1 Some potential benefits of the observational methods in geotechnical engineering (Adapted from CIRIA, 1999).

insight into details of geotechnical instrumentation and the planning of monitoring in underground constructions is presented. Third, broad reviews of back analysis methods to derive ground mechanical parameters at full-scale are discussed. Then the applications of the observational approach in the special case of large urban tunnel project are illustrated and the benefits of such an approach in design optimization are explained. Finally, the efficiency of the observational approach is summarized and conclusions are discussed.

2 DESIGN UNCERTAINTIES AND OBSERVATION-BASED GEOTECHNICAL DESIGN PROCEDURE

2.1 Ground investigation and its uncertainties

Geomaterial rarely shows uniform distribution of its properties and, consequently, of behavior. This is because it is formed naturally and its materials are spatially distributed and vary from one point to another, yet only a limited number of geotechnical explorations can be conducted. The nature of its creation causes complexity and different material behavior at different locations – so-called site-specific factors. Geotechnical investigations such as field mapping, geophysical methods, boreholes and core logging, and field and laboratory tests cannot detect all possible variability in material properties and parameters. In most cases, therefore, obtaining the accurate geotechnical parameter values is extremely difficult or even impossible. This leads geotechnical design to explicitly involved assumptions and uncertainties in a project. Einstein and Baecher (1982) have been defined three main sources for uncertainties and errors in engineering geology and rock mechanics:

1. Innate, spatial variability of geological formations, where wrongly made interpretations of geological setting may be a significant consequence, as already described.
2. Errors introduced in the measurement and estimation of engineering properties, often related to sampling and measuring.
3. Inaccuracies caused by modeling physical behavior, including incorrect types of calculation or inappropriate models.

In any engineering study, one can never know what has been left out of an analysis. Thus, in addition to the three major uncertainties above, there is also uncertainty due to omission. The real world has variations and properties that cannot entirely be included in a characterization or an analysis. According to Einstein and Baecher (1982), most of the major failures of constructed facilities have been attributable to omissions.

The variation in material type and complexity in each site-specific case, and in project dimension and construction method on the neighboring ground disturbance, make it difficult to explore all uncertain parameters and conditions. Such high levels of uncertainty make it impossible to design in full detail prior to construction. Thus the development of investigations during construction using the observational method, and the updating of the design accordingly, remarkably enhance the project from both the technical and the economic point of view.

2.2 Observation-based geotechnical design procedure

In the process of designing an underground excavation, there are parameters with varying degrees of uncertainty that must be taken into account. These uncertainties are often related to subsurface conditions and other site-specific factors. Issues of safety and economy were key considerations when the basis for the observational method was formulated. The observational method approach is designated as active design. The basis of this approach is to establish a preliminary design, devise contingency actions for those cases in which the structural behavior deviates from the expected, select and execute relevant observations during construction, and conduct modification of design to suit the ground conditions encountered.

The geotechnical design procedure involving an observational approach is illustrated in Figure 2. As shown, each geotechnical engineering project first performs a preliminary geotechnical investigation and site characterization to identify ground conditions and associated hazards that may threaten the project. In this stage of geological and engineering investigation, engineering experiences and judgment can greatly facilitate the derivation of appropriate design parameters and the visualization of a ground geomechanical model using appropriate assumptions that reflect real-world conditions.

A preliminary design for the project is prepared, together with detailed instrumentation and monitoring plans for the various geotechnical units using limited data and existing norms and standards. Based on the preliminary design report, the construction sequences commence and are followed by excavation, instrument installation and the recording of monitoring data. During this stage, the measured data, such as displacement and stress, are processed and compared to those calculated during preliminary design. Considering the project is implemented at full scale, the ground's real behavior can be monitored and compared with the predictions of the early design stage. If big discrepancies between predicted and observed ground behavior are seen, then back analysis based on monitoring results and the practical evidence from construction can be engaged to derive more realistic ground parameters. Based on these newly calculated parameters, the design reports can be adjusted and updated, and the next construction sequences will be implemented using these updated reports. This cycle of parameter modification is repeated to achieve the most suitable design parameters for each geotechnical unit. Finally, the detailed or final design is established based on the most realistic ground behavior and design parameters. Further details regarding the acquisition of site investigation data can be found in several references (Bieniawski, 1984; Brady & Brown, 2004; Villaescusa, 2014).

3 GEOTECHNICAL INSTRUMENTATION AND MONITORING

3.1 Instrumentation and monitoring concepts

Instrumentation, monitoring and back analysis are the main components of the observational method. The main purpose of the instrumentation and monitoring is to monitor the performance of the geo-engineering projects and the behavior of the confining ground during the construction process, in order to provide safety and to optimize the ground parameters and design.

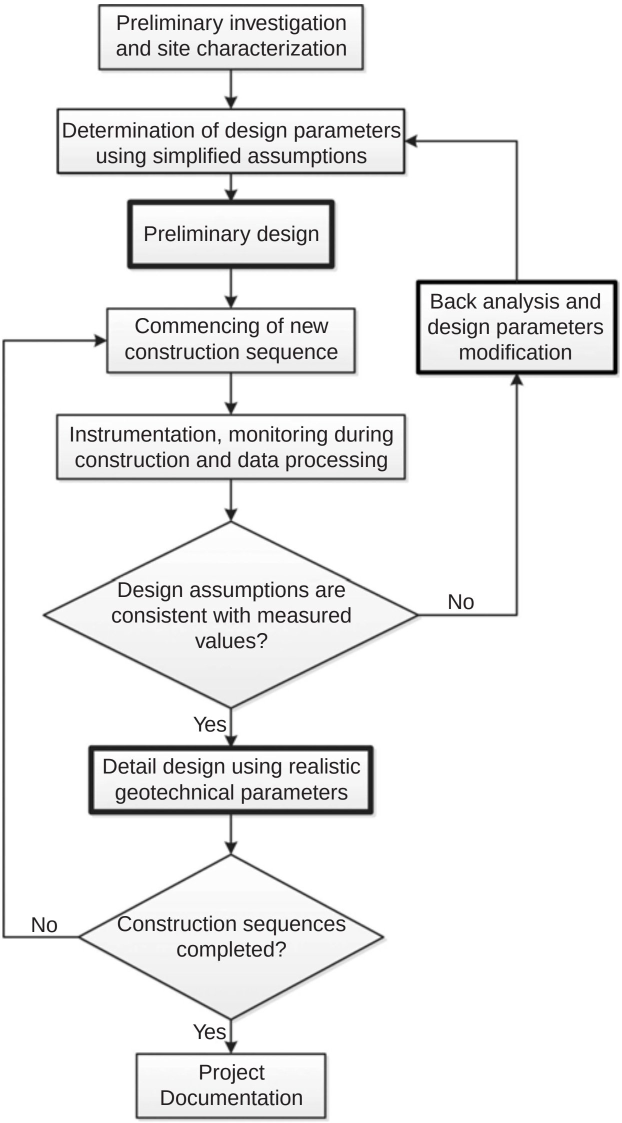

Figure 2 Observation-based design procedure for geotechnical projects.

Instrumentation involves the use of measuring devices to monitor both tunnel structure and its confining ground. The various types of instruments used for different parameter measurements in underground excavation are illustrated and annotated in Figure 3. The type of instrument is selected according to the parameter that must be measured. Force and displacement measurements make up the most popular monitoring applications in projects. The objectives of instrumentation during construction will change, depending on the size and type of construction, the geotechnical conditions and the project schedule. The use of geotechnical, structural or geodetic measurements – or a combination of them – depend

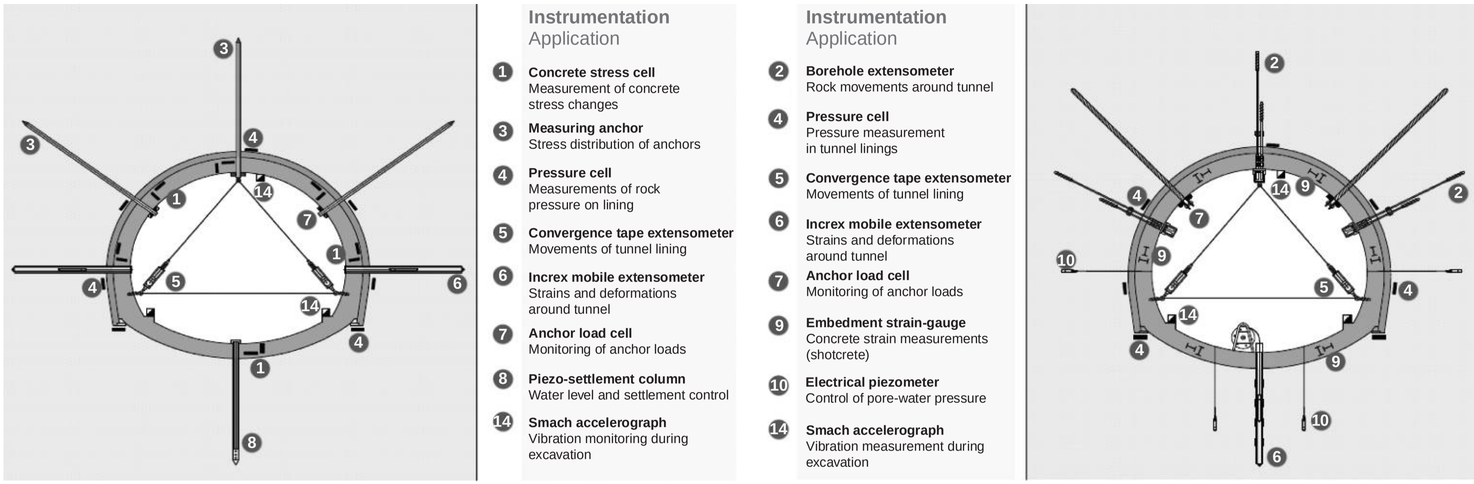

(a) (b)

Figure 3 Various instrumentation systems in an underground excavation (Adapted from Geokon, 2012).

on several factors, such as ground type, expected ground behavior, the importance of the tunneling influence zone, and the level of available measurement technologies.

The purpose of monitoring is to scrutinize and control the project through the collection of evidence such as instrument data and visual observation, followed by the processing and analysis of the evidence gathered. Data and evidence is collected using data acquisition systems and stored in appropriately designed databases. The data is manipulated, analyzed and presented in a technical way to represent the ground's response to project construction and enable the prevention of potential problems. By integrating the monitoring results in back analysis, the ground geotechnical parameters can be derived and used for design updates. The most important physical quantities to be monitored can be subdivided into deformations, stresses, piezometric levels and temperatures. The most common monitoring method is the measurement of displacements, for example, convergence of the underground openings or ground surface settlements. From a mathematical point of view, displacement measurements are not greatly influenced by typical local effects. By comparison, stresses and strains are differential quantities, whose validity is limited to local regions (Ghorbani & Sharifzadeh, 2009). It is therefore necessary to observe stress and strain at several successive points in order to obtain a distribution over a sufficiently large area.

3.2 Design monitoring plan

The task of planning a monitoring program should be a logical and comprehensive engineering process that begins with defining the objectives and ends with planning how the measurement data will be applied. Dunnicliff (1993) defines the steps involved in planning a monitoring program as follows:

1. Define the project conditions
2. Predict mechanisms that control behavior
3. Define the geotechnical questions that need to be answered
4. Define the purpose of the instrumentation
5. Select the parameters to be monitored
6. Predict magnitudes of change
7. Devise remedial actions
8. Assign tasks for design, construction, and operation phases
9. Select instruments
10. Select instrument locations
11. Plan recording of factors that may influence measured data
12. Establish procedures for ensuring reading correctness
13. List the specific purpose of each instrument
14. Prepare budget
15. Write instrument procurement specifications
16. Plan installation
17. Plan regular calibration and maintenance
18. Plan data collection, processing, presentation, interpretation, reporting and implementation
19. Write contractual arrangements for field instrumentation service
20. Update budget.

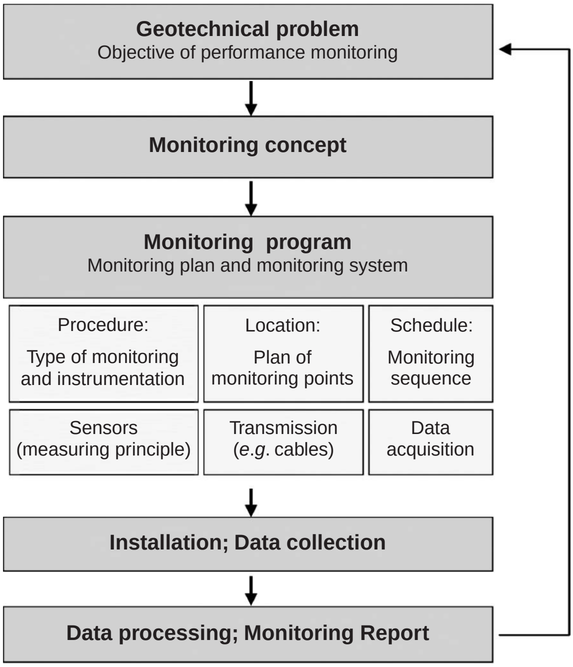

Figure 4 Content and course of a geotechnical monitoring program (Adapted from DIN, 2011).

Geotechnical monitoring should be planned, carried out and evaluated in conjunction with the geotechnical design. Geotechnical monitoring should take all features (both content and course of action) into consideration as shown in Figure 4.

3.3 Trigger criteria and trend rate

The comprehension and critical reading of the monitoring data has the same importance as the measure itself. Part of the comprehension process is the verification of the threshold values. These limits are defined with reference to the design values and, based on these, it is necessary to define some countermeasures. The threshold limits which are defined for each monitored quantity are as follows:

- Alert limit: the exceeding of this value requires an increase to the frequency of readings, both for underground instruments and those on the surface or in buildings, in order to better (and more rapidly) monitor the evolution of the unforeseen phenomenon so as to avoid potentially uncontrollable situations.
- Alarm limit: the exceeding of this value requires the immediate intervention of the engineer in order to apply appropriate countermeasures.

The countermeasures are necessary to bring the situation within acceptable limits or to reinforce the structure to increase its resistance. Countermeasures may include (but shall not necessarily be limited to) increased monitoring frequency, ground treatment, additional support measures, modifications to the excavation/support sequencing.

Monitoring is the basis of a flexible design approach in which the design hypotheses are systematically checked through monitoring results on site, and mitigation measures are those actions predefined at the design stage that form the reaction if and when the encountered conditions are different from the reference scenarios. Furthermore, the reference scenario of the section already excavated is systematically back analyzed to match it to the reality, which is then used to update the predictions of the reference scenario for the next tunnel section to be excavated. Mitigation measures to avoid the dangerous potential migration of the cavity to the surface are related to actions carried out from the surface or from inside the tunnel itself.

Tunneling-induced settlements in urban areas could affect buildings and other surface or subsurface structures. Thus, before constructing new underground structures in urban areas, an analysis of the possible induced effects and selection of appropriate mitigation measures – including the treatment of the ground, reinforcement of existing structures and changes to tunnel specifications – are necessary.

The collected monitoring data can be used in two ways. Initially, all observations and evidence is integrated into rapid diagnosis to prevent possible abnormal behavior, such as excessive displacement or load which may cause failure. In the case of an abnormal condition, immediate action such as changes in support patterns or excavation sequences may be required. At the second stage, the collected data are analyzed in detail: data trends are extracted and compared with the values predicted by the design. If there are big discrepancies between measured and predicted results, then back analysis to calculate the most realistic geotechnical parameters for the ground is recommended, followed by design review and modification with the updated parameters.

4 DESIGN REVIEW AND BACK ANALYSIS

The engineering design and construction of underground openings and surface structures requires *in situ* input parameters such as stress, rock and soil strength and deformation parameters, and porewater pressure. These parameters are essential for stability analysis and ground support system design for these geostructures. Without them, the process of engineering design is not possible.

Despite the availability of several experimental means for determining the parameters at the site, if the geological conditions are complex, it will be very difficult for the engineer to carry out the task in hand. In other words, because the mechanical parameters at various locations around the site vary greatly due to the complexity of the geological conditions, a large number of field tests may be required to describe the ground parameters adequately. In addition, if we conduct a large number of field tests at the site, then there is a large cost in money and time which is an intolerable burden for most projects. However, it is often not feasible to obtain a complete geotechnical characterization of the ground from the preliminary geological studies or from the geotechnical and geophysical explorations along the tunnel axis. Only during the construction of the tunnel itself, or of a pilot tunnel, is it possible to obtain a complete evaluation of the behavior of the ground. Thus, new approaches are needed to address these issues. One of these approaches, back analysis, was put forward in the 1970s and received much attention because of its obvious practical value.

Back analysis is generally defined as a procedure developed for solving system identification (or characterization, back calculation or calibration) problems, which can provide the controlling parameters of a system by analysis of its output behavior. The system is simulated in a model, and the input parameters of the model are identified through the output information. The term 'back analysis' well reflects the backward nature of this calibration procedure and, together with the basic concepts and methods of identification theory, it was introduced to geotechnical engineering in the design and construction of underground engineering, slope engineering, water conservancy and hydroelectric power engineering (Gioda & Maier, 1980; Cividini *et al.*, 1981; Sakurai, 1982; Gioda & Sakurai, 1987; Sakurai *et al.*, 2003).

In general terms, two 'tools' are necessary to perform a back analysis. The first is a stress analysis procedure using analytical or numerical methods, for determination of the stress, strain and displacement distributions for the problem at hand. The second is a suitable optimization algorithm that minimizes the discrepancy between the data measured in the field and the corresponding results obtained by the stress analysis (Cividini *et al.*, 1981). This discrepancy is commonly expressed as the error function and described below (Equation 1):

$$\varepsilon(P) = \left\{ \sum_{i=1}^{n} [u_i^* - u_i(P)]^2 \} \right\} \tag{1}$$

In this equation, u_i^* and $u_i(P)$, $i = 1, 2, ..., n$ are the normalized measured and corresponding analysis results, respectively. Obviously, $u_i(P)$ depends on the unknown model parameters collected in the vector P.

The various techniques for solving such a error minimization problem can be divided into two groups, comprising gradient-free and gradient-based parameter identification methods that are explained by Pichler *et al.* (2003) as follows:

- 'Gradient-free parameter identification methods' such as fuzzy logic, artificial neural network methods, genetic algorithms or probabilistic (stochastic) search techniques. In this type of method, the entire parameter space is searched for an optimal solution, and error function values are evaluated sequentially and compared for different parameter sets. This method requires a large amount of numerical analysis to find optimal parameters.
- 'Gradient-based parameter identification methods': these methods seem to be robust and efficient only if the error function shape is relatively smooth or if the chosen initial point is very close to the solution. They are, therefore, limited to the identification of a small number of parameters for which the influence on the error function will be important. Unfortunately, for geotechnical studies, problems are often complex and the solutions are not unique. To have information about the uniqueness of the solution, several minimizations need to be computed and compared. Gradient-based methods can then become an exhaustive process to identify parameters without a guarantee of reaching a good description of the solution set (Levasseur *et al.*, 2007). These methods employ the gradient of ε (*i.e.* the derivation of ε with respect to parameter vector P). In the case of elastic material behaviors, the gradient of ε can be computed analytically (Ohkami & Ichikawa, 1997; Ohkami & Swoboda, 1999). However, for other cases, especially non-linear or

elastoplastic problems, computation of the analytical expression of the gradient of ε is a challenging task, which makes major modifications of the analysis tool (*e.g.* finite element software) unavoidable (Mahnken & Stein, 1995). These methods are characterized by a local search for a minimum of the error function and do not search for optimal solutions in the entire parameter space. This local search starts from an initial choice for the unknown parameters. Since results depend highly on these initial choices, such algorithms may get trapped in a local minimum of the error function.

The back analysis method has been applied to: the identification of *in situ* stress fields (Cai & Chen, 1987; Kaiser *et al.*, 1990); the characterization of rock and soil parameters (deformation and strength characteristics) using field measurements in test galleries (Gioda & Maier, 1980; Sakurai & Takeuchi, 1983); rock mass hydraulic properties; rock mass zoning; boundary conditions (Tonon *et al.*, 2001); loads acting on tunnel linings; the predicted behavior of a geotechnical structure at an early stage of construction (Asaoka & Matsuo, 1984); evaluation of rock and soil mechanics field tests (Gioda & Maier, 1980; Cividini *et al.*, 1981); calibration of laboratory tests (Iding *et al.*, 1974; Imre, 1994). Application has involved closed-form solutions and numerical methods among others. Simultaneous evaluation of several parameters is achievable.

In the field of underground construction, the measurements that are most frequently carried out usually correspond to one of the following groups of parameters, according to the particular problem: strains, relative and absolute displacements, stresses in linings and in the surrounding material, support pressures (steel arches and rock bolts), forces in the rock anchors, and groundwater pressures. Preference is usually given to displacement measurements as they represent, from the mathematical point of view, parameters that are not greatly influenced by typical local effects. Stresses and strains are, by comparison, differential parameters that can result in values that are very different from point to point. Their mean value should therefore be calculated over a sufficiently large base of data to provide representative values (Oreste, 2005). On the other hand, because displacements of rock and soil induced by excavation can be measured easily and reliably, displacement-based back analysis techniques have been a hot research topic since the 1970s, and extensive studies have been conducted to develop different models of displacement-based back analysis (Kirsten, 1976; Jurina *et al.*, 1977; Sakurai & Abe, 1979; Gioda & Jurina, 1981; Sakurai & Takeuchi, 1983; Yang *et al.*, 1983, 2000; Wang *et al.*, 1987; Yang, 1990; Zhao & Lee, 1996; Sakurai, 1997; Gioda & Locatelli, 1999; Gioda & Swoboda, 1999; Swoboda *et al.*, 1999; Feng *et al.*, 2004; Zhang *et al.*, 2006). Back analysis based on field measurements of strains or stresses has also been used (Kaiser *et al.*, 1990; Zou & Kaiser, 1990). These models range from linear elastic to non-linear models – such as elastoplastic, viscoelastic (Ohkami & Swoboda, 1999) and viscoplastic models (Mahnken & Stein, 1995) – from two-dimensional to three-dimensional models (Swoboda *et al.*, 1999; Hisatake & Hieda, 2007), and from deterministic to non-deterministic (uncertain) models.

4.1 Back analysis techniques

Several back analysis techniques were developed in past few decades which is categorized and illustrated in Figure 5. In general, there are two fundamental approaches to the

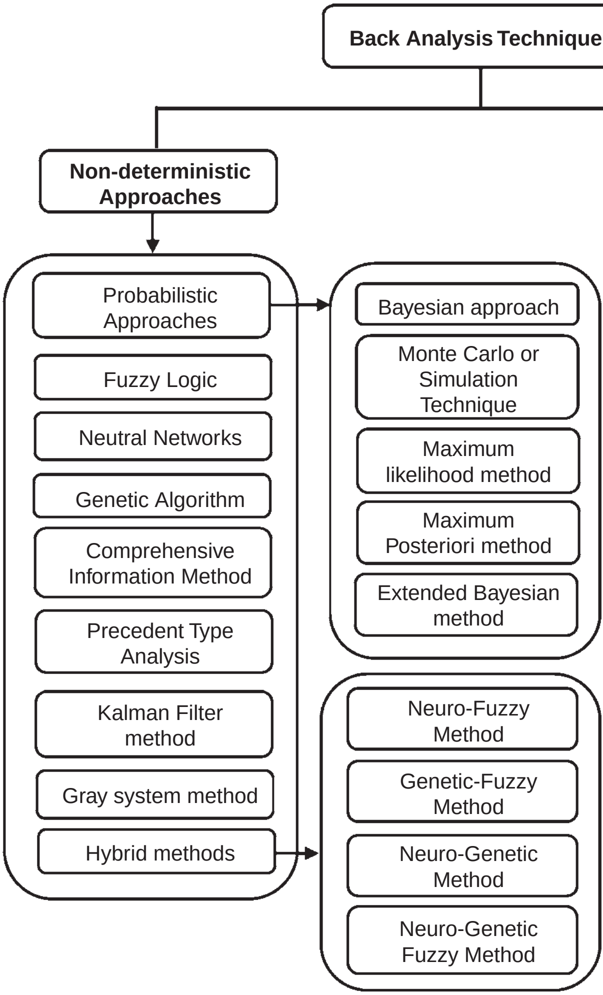

Figure 5 Classification of back analysis methods in geotechnical engineering.

back analysis problem, namely, deterministic and non-deterministic approaches. In deterministic identifications, the discrepancy between the system and the model variables is simply seen as a (deterministic) signal to be minimised according to a suitably defined loss function. Back analysis based on deterministic methods includes the inverse approach (Cividini *et al.*, 1981), the direct approach (Cividini *et al.*, 1981), the graphic method, the atlas method and the boundary control method (Ichikawa & Ohkami, 1992). In non-deterministic identification, the discrepancy between the system and the model is considered as a non-deterministic signal. Back analysis based on non-deterministic methods includes the probabilistic (statistical) methods, fuzzy logic (Liang *et al.*, 2003), artificial neural networks (Pichler *et al.*, 2003), genetic algorithms (Lavasseur *et al.*, 2007), the precedent type analysis method (Li *et al.*, 1998), the Kalman filter method (Kosmatopoulos *et al.*, 1995; Rubio & Yu, 2007), the grey system method, and the comprehensive information method. Probabilistic methods can be subclassified into the Bayesian method (Cividini *et al.*, 1981), Monte Carlo simulation techniques (Cividini *et al.*, 1981), the maximum likelihood method, the maximum a posteriori method and the extended Bayesian method. Today's hybrid of soft computing techniques (most of which incorporate fuzzy logic) – such as the neuro-fuzzy (Gokceoglu *et al.*, 2004), genetic fuzzy, neuro-genetic and neuro-fuzzy-genetic methods – are extensively used for parameter identification in geotechnical engineering problems.

4.1.1 Deterministic approaches

In relation to classical stress analysis problems, two alternative approaches for back analysis, referred to as 'inverse' and 'direct' approaches respectively, are described here in a deterministic context.

In the inverse approach, the system of equations governing the stress analysis problem is rewritten in such a way that material parameters appear as unknowns, and measured values (displacements or stresses) appear as input data. Since the number of available measurements usually exceeds the number of unknown parameters, the final system contains more equations than unknowns and the solution has to be based on a suitable optimization algorithm. The first inverse algorithm based on the finite element method (FEM) was proposed by Kavanagh & Clough (1971) for structural problems, and subsequently Jurina *et al.* (1977) developed the first inverse approach applicable to parameter identification in geotechnical problems. Gioda (1980) used this approach to search for elastic material parameters B (bulk modulus) and G (shear modulus), and it can be modified to calculate the earth pressure acting on a tunnel lining. Using the inverse algorithm suggested by Sakurai & Takeuchi (1983), it is possible to compute both Young's modulus and the initial state of stress simultaneously. Here, the Poisson's ratio and the initial vertical stress are assumed as known. An inverse algorithm for parameter identification of non-linear elastic solids was suggested by Iding *et al.* (1974).

The direct approach adopts the same numerical model used for stress analysis, within the framework of an iterative procedure; hence no formulation of the inverse problem is required. The direct approach employs the trial values of the unknown parameters as input data in the stress analysis algorithm, until the discrepancy between measurements and corresponding quantities obtained from a numerical analysis is minimised. Based on the error function described in Equation 1, back analysis aims at determination of the absolute minimum of ε, which provides the best agreement between measured and computed values.

In geotechnical engineering, most analyses are performed by means of the FEM. Unfortunately, the computational effort of such analyses is usually rather high. Moreover, realistic modeling of geotechnical problems requires consideration of different types of non-linearities. These arise from, for example, non-linear boundary conditions and/or non-linear material behavior. Consequently, the error function (Equation 1) may have several local minima, making back analysis a challenging task. In order to minimize this error function, which is highly non-linear and, in most cases, an analytical expression of its gradient cannot be determined easily, algorithms known in mathematical programming as direct search methods are used (Himmelblau, 1972). The simplex method, Rosenbrock's algorithm (Rosenbrock, 1960) and Powell's method (Powell, 1964), which are iterative procedures that perform the minimization process only by successive evaluation of the error function, were recommended by Gioda & Maier (1980) for this purpose.

An inverse back analysis procedure can demonstrate smooth, fast-converging and stable behavior, if measured data are well-selected (Gioda, 1985). This is because boundary control is built into the algorithm. Points where both the nodal forces and nodal displacements are known basically control the error minimizing procedure. This ensures quick convergence for data of good quality, but can cause divergence of the procedures in the case of ill-selected measurement data (Swoboda *et al.*, 1999).

Direct formulation is very flexible; applying such a procedure for complex constitutive models is easier, where the inverse relations cannot be derived in the simple direct way. Furthermore, development of the direct back analysis code is much less difficult than development of the code based on an inverse algorithm. The only work involved is appending a module to an existing program, which does the minimization of errors between measured and predicted data (Cividini *et al.*, 1981).

It is not straightforward to work out a general criterion for choosing the most convenient algorithm for back analysis. However, it should be observed that inverse techniques are particularly convenient when dealing with a relatively large number of unknown parameters and when the finite element mesh has a small number of nodal variables. On the other hand, the direct procedures are preferable when a few parameters are back analyzed using large finite element meshes (Cividini & Gioda, 2003). However, the course of convergence is highly dependent on the number of unknown parameters, the quality of their initial guess and on the optimization strategy chosen. The direct method can give an insufficient solution, especially in cases where Young's modulus and Poisson's ratio are to be identified simultaneously (Swoboda *et al.*, 1999).

The boundary control method suggested by Ichikawa and Ohkami (1992) combines the advantages of both approaches. In the inverse portion of this algorithm, the equilibrium equation is coupled together with observational boundary conditions and the direct part of the algorithm improves convergence of a Newton's iteration process.

When using a deterministic optimization strategy based on gradient evaluations, it is not guaranteed that the global minimum of the problem is obtained. However, a more systematic approach would be to use a hybrid method, that is, a combination of deterministic and stochastic strategies.

4.1.2 Non-deterministic approaches

Today, soft computing techniques (most of which incorporate fuzzy logic) are extensively used for parameter identification in rock and soil engineering problems. An interesting and, perhaps, the most attractive characteristic of fuzzy models compared with other conventional methods commonly used in geosciences, such as statistics, is that they are able to describe complex and non-linear multivariable problems in a transparent way (Setnes *et al.*, 1998). Moreover, fuzzy models can cope with non-probabilistic (*i.e.* semantic) uncertainties.

In the back analysis problem of rock engineering, in order to identify physical parameters, the displacements of the surrounding rock should be measured, but a particular precision of displacement may be required and sometimes may be beyond the available precision of measurement. Intricate experimental measurements or complicated numerical computations are often needed in conventional methods. This is time-consuming and costly. Therefore, a simple but sensitive analysis method for the identified parameters is needed. The neural network model is an ideal candidate to resolve this kind of identification problem. Neural network methods need only a few data measurements from any single place, provided that the data cover the area in which the physical parameters of interest are identified (Liang *et al.*, 2003).

In the engineering literature, genetic algorithms are well-known for their ability to solve complex optimization problems. The method is robust and highly efficient but does not guarantee an exact identification of the optimum solution. However, it does permit the localization of an optimum set of solutions close to this optimum (Gallagher & Sambridge, 1994). This property is interesting in relation to the idea of back analysis in geotechnical studies. The genetic algorithm is a new and efficient optimization method for geotechnical back analyses (Levasseur *et al.*, 2007).

The use of probabilistic (statistical) instruments for the calibration of numerical models is common in geotechnical contexts because of the large uncertainties in the initial estimation of the parameters of the rock mass, and because of the field measurements that represent the data of the back analysis, which are in general affected by errors that depend, for example, on the nature of the measured quantities, on the characteristics of the adopted devices, and on the field conditions. Various techniques have been proposed to evaluate the influence of these errors on the computed mechanical parameters. Some of them are described here.

A first approach is based on the so-called Monte Carlo simulation technique. In following this method, the influence of the measurement error, and of the number of input data, is evaluated through a series of numerical tests (Cividini *et al.*, 1981). Each of these consists of a set of back analyses based on suitable generated input measurements (*e.g.* displacements). The input data are obtained by adding a disturbance term, representing the experimental 'errors', to the 'exact' measurements. Independent random number generators, with chosen probability distributions and zero mean value, are used to work out these errors. The number of generators coincides with that of the input measurements. Their probability distributions depend on the characteristics of the measuring devices and of the measured quantities (Cividini & Gioda, 2003).

The 'exact' displacements can either be evaluated on the basis of actual field measurements or be simulated through a preliminary stress analysis of the problem at hand, in which reference values of the material parameters are introduced (Cividini *et al.*, 1981). This procedure permits establishment of a probabilistic correlation between the resolution of the measuring device, the number of measurements and the accuracy of the computed parameters characterizing the soil/rock mass.

The simulation technique offers the advantage of an extremely simple implementation, but requires a computational effort that rapidly increases according to the number of free variables in the numerical model and the number of unknown parameters.

A typical feature of the Bayesian approach is that a priori information on the unknown (uncertain) parameters can be introduced in the back analysis, together with the data deriving from *in situ* measurements. In most cases, the a priori information consists of an estimation of the unknown parameters based on the engineer's judgment or available general information. This leads to a numerical calibration procedure that combines the knowledge deriving from previous, similar problems with the results of the *in situ* investigation in order to obtain a mean value for the uncertain parameters and their variance. From this, it is possible to derive a final probabilistic distribution. It is worthwhile observing that the Bayesian approach is also applicable when the number of unknown parameters exceeds the number of *in situ* measurements, if a reliable initial guess on the parameters can be formulated (Cividini *et al.*, 1983).

Both approaches lead, in practical terms, to the same results, with regard to the relationship between the resolution of the measuring devices and the uncertainty of the estimated parameters. However, the computer time required by the (Monte Carlo) simulation process is much larger than that required by the Bayesian approach (Cividini & Gioda, 2003).

The Kalman filter (KF) was formulated in the 1960s as an algorithm for the analysis of linear discrete stochastic processes. The KF methodology is apt for solving parameter identification (inverse) problems in a statistical context, through a sequence of estimations, which starts from an a priori estimation by an 'expert' (Bayesian approach) and exploits a time-stepping flow of experimental data until convergence is empirically ascertained. The KF algorithm was incorporated into Gioda's inverse algorithm by Murakami and Hasegawa (1993). This probabilistic procedure allows us to use the measurement error information in the inverse calculation and to evaluate the influence of measurement error on the result of back analysis.

Grey system theory uses a black-grey-white color spectrum to describe a complex system whose characteristics are only partially known or known with uncertainty. White is used to denote a completely known system, and black represents a completely unknown system. Geotechnical systems are, by their nature, complex and usually heterogeneous, and it is very rare for such systems to be completely understood in all their complexity. Grey system theory generally includes: (a) grey incidence analysis, which compares and evaluates a system's factor behaviors; (b) system modeling, which predicts the behavior of the system (Deng, 1986).

4.2 Difference between parameter identification and back analysis

In much of the preceding discussion, the word 'identification' was used, rather than 'back analysis'. In parameter identification, the input data used in the computations are checked after the field measurement results have been analyzed, and can be modified if needed, but the model remains the same the whole time. In back analysis, the modeling should also be checked with field measurements as well as the material properties. Nevertheless, it is common that, in the observational methods, the input data used in the computation are usually checked during the excavation, with the modeling being fixed (Sakurai, 1997).

It is extremely important in any geotechnical engineering problem that the models should not be assumed, but rather should be determined by a back analysis. If a model is fixed all the time during observational procedures, the results are not only inadequate but also misleading in their interpretation, in that they provide incorrect information to the decision making in relation to modification of design and construction methods. In fact, after Sakurai (1997), the following three different procedures can be distinguished (Tonon *et al.*, 2001):

1. In a forward analysis, once a mechanical model is assumed, and the values of the mechanical parameters are determined, then displacements, stresses and strains can be calculated.
2. In an identification procedure, displacements, stresses and strains are measured, a mechanical model is assumed, and then the values of the mechanical parameters are calculated.
3. In a back analysis, displacements, stresses and strains are measured, and then the model as well as the values of the mechanical parameters are determined.

While the first two approaches are primarily inductive, the third approach is deductive. This means that the rules of thinking that we follow in the forward analysis and parameter identification are difficult to make explicit. By contrast, the mathematical theory of logic (completed with probability theory) seems to apply quite well to back analysis (inverse analysis) (Tarantola, 2005).

4.3 The main issues in back analysis

4.3.1 Uniqueness, identifiability and stability

The most significant problem of inverse analysis may be characterized by three key words: the uniqueness, identifiability and stability of the solution. The uniqueness of the solution relates to the idea that a given formulation of an inverse analysis has only one set of unique parameter values for a given observational data set. The identifiability, on the other hand, means a purely mathematical relationship, irrespective of any inverse analysis formulation, as to whether a distributed parameter system (*i.e.* a partial differential equation) is capable of mapping a unique set of parameter values from a set of observational data. The stability of the solution, in turn, is defined such that when an objective function converges at a point in a parameter hyperspace, a set of parameter values would also converge to a point at the same rate. One can easily imagine that the instability is associated with an objective function that is very flat near the optimum, so that most minimization algorithms converge slowly to this point (Honjo *et al.*, 1994).

4.3.2 Model identification

The other significant aspect that is often problematic in geotechnical inverse analysis is that of model identification. This relates to selection of the optimum model from many alternative models of varying sophistication and complexity. There are generally two types of error in inverse analysis: one is system modeling error, which can be evaluated by the goodness of fit of the calculated results to the observed data, and the other is the error associated with parameter uncertainty. An increase in parameter numbers generally improves the system modeling error, although the parameter uncertainty is increased, and vice versa. It should be recognized that an increase in the parameter uncertainty reduces the prediction reliability, which is the most important output of an inverse analysis. Therefore, a sophisticated model (*i.e.* a model with more parameters) may not give better prediction, and it all depends on the quantity and quality of the data. Apparently, there is a trade-off between these two components, and the best model is the one that balances these two, which is the essence of model identification (Honjo *et al.*, 1994).

4.4 Important considerations on the use of back analysis

To ensure the uniqueness of back analysis solutions and increase the speed of back analysis, Sakurai (1997) described a number of principles to follow in order to choose the parameters that must be identified:

1. Select parameters that are of greatest influence on the stability of underground openings;
2. Select parameters that are very difficult to obtain accurately enough by other methods;
3. Reduce the number of unknown parameters to be identified as much as possible.

The rock mass parameters that are most difficult to estimate from the preliminary investigations and that rely heavily on back analysis results include: (a) the relationship between the horizontal and vertical stresses in the rock mass; (b) the dilatancy of the rock mass; (c) the strength parameters of the rock mass in a plastic field (Oreste, 2005).

The minimization of the error function alone does not always guarantee a correct back analysis. The qualitative trend of the displacements on the wall of the excavations, for example, should be the same in the calculation as in reality, as a confirmation of the validity of the calculation model and of the simplified assumed hypotheses.

5 APPLICATION OF GEOTECHNICAL MONITORING IN THE CASE OF A LARGE URBAN TUNNEL (NIAYESH)

The Niayesh road tunnels were constructed in the urban area between the Niayesh and Sadr highways in Tehran, Iran. This project is one of the biggest tunneling projects in the Middle East, with a total length of over 8 km, and cross-sectional areas ranging from 87 to 470 m^2 (see Figure 6).

The major characteristics and limitations of the Niayesh road tunnel project include (Ghorbani *et al.*, 2012):

Figure 6 A plan of the Niayesh road tunnels in Tehran, Iran.

1. Heavy traffic along the highways and connecting roads above the tunnel
2. High building intensity in several areas of the tunnel alignment
3. Sewers and pipes above the tunnel route and old sewers with unknown locations
4. Highway bridges crossing the alignment of the tunnel
5. Low overburden in some areas with soft ground and man-made features with high water inflow in some regions
6. Passes beneath Mellat Park Lake
7. Many bifurcations with large cross sections along the tunnel route
8. Limitations on instrument installation along the tunnel route and on buildings and other surface structures
9. Inadequate site investigations due to a lack of permission, especially in residential areas.

5.1 Tunnel geology

According to the geology map of Tehran prepared by the Geological Survey of Iran – based on results from boreholes, test pits and trenches along the tunnels' routes and geological mapping during tunnel construction – the tunnels passed through A and B formations (Figure 7). The groundwater table was well below the tunnel level.

5.2 Construction procedure and emergency plan

The Niayesh tunnels were excavated according to the principles of the sequential excavation method (SEM), taking into consideration the following factors (after ITA, 2009):

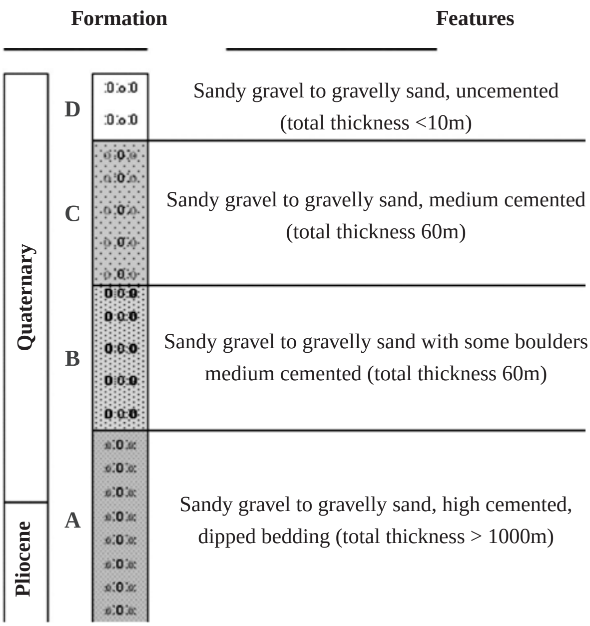

Figure 7 Stratigraphy of Tehran alluviums (Adapted from P.O.R., 2008).

1. Difficult and complex ground with changeable geological formations
2. Greater variability in the choice of excavation methods according to the ground conditions
3. Highly variable shapes of cross sections
4. Greater variability in the choice of excavation sequences according to the ground conditions (change from top-heading advance to side-heading advance and vice versa)
5. Easier optimization of the primary support using the observational method in special cases
6. Difficult access to the main tunnels (given that tunneling is in a densely populated urban area)
7. Many bifurcations and intersections with large cross sections along the tunnels' routes.

According to the SEM contract documents in the Niayesh road tunnel project, longitudinal profiles were defined along the tunnel's alignment, which was termed ground advance classification. In longitudinal profiles, the tunnels were divided into different sections based on depth of overburden, tunnel geometry and geotechnical specifications. Using this data, appropriate excavation class and support systems were defined for different sections and the values of tunnels' deformations and surface settlements were computed (Table 1).

The geometry, excavation classes and support elements for different cross sections of the Niayesh road tunnel project are presented in Table 2.

5.3 Monitoring system

Monitoring is an essential part of SEM (also known as the New Austrian Tunneling method (NATM)). Based on the special characteristics of the Niayesh tunnel, an extensive monitoring programmer was developed for this project, especially in residential areas and at junctions and bifurcations with large cross sections. The monitoring plan for the Niayesh tunnel project had the following objectives (Ghorbani *et al.*, 2012):

1. To prevent unexpected phenomena in order to avoid critical situations for tunnels, buildings, highways, roads and bridges in terms of safety. Monitoring enables appropriate mitigation measures to be taken as soon as measurements reflect a need for action.
2. To check the design assumptions and improve the design solutions through back analysis and further interpretation of the behavior of the ground during excavation.

A typical instrumentation array for a 3.5-lanes cross section is illustrated in Figure 8. As shown in Figure 6, the tunnels pass through densely populated urban areas with high-rise buildings with commercial, residential, governmental and political applications. Taking into account several factors of buildings, tunnels and ground conditions – such as buildings' characteristics, position of buildings relative to tunnels, and tunnel dimension – all the buildings at the tunnel route were classified into three categories: (a) critical buildings (red buildings – 29%); (b) buildings that needed more assessment (yellow buildings – 65%); (c) non-critical buildings that are not affected much by tunneling (green buildings – 6%). In Table 3, the type and total number of instruments

Table 1 Ground advance classification of 2.5-lanes cross section at Niayesh tunnel (P.O.R. Consulting, Iran & D2 Consult, Austria).

	Location	Main Tunnel											
	Lane Number	2+1											
	Type	2A				2B				2C			
	Ground Advance Classification	2AI	2AII	2AIII	2AIV	2BI	2BII	2BIII	2BIV	2CI	2CII	2CIII	2CIV
	Overburden [m]	8-15				15-30				>30			
	Total Length [m]	see Zoning Plan				see Zoning Plan				see Zoning Plan			
Geotechnic Specification	Description	High Cemented Clayey Sand or Gravel											
	Internal Friction	40	35	34.5	34	40	38	34,5	34	40	35,5	34,5	34
	Cohesion [kg/cm²]	55	42	38	35	55	45	40	30	55	45	40	30
	Permeability [cm/s]	1E-5--1E-4	1E-5--1E-4	1E-5--1E-4	1E-5--1E-4	1E-5--1E-4	1E-5--1E-4	1E-5--1E-4	1E-5--1E-4	1E-5--1E-4	1E-5--1E-4	1E-5--1E-4	1E-5--1E-4
	Density [gr/cm³]	1.7--2.4	1.7--2.4	1.7--2.4	1.7--2.4	1.7--2.4	1.7--2.4	1.7--2.4	1.7--2.4	1.7--2.4	1.7--2.4	1.7--2.4	1.7--2.4
Construction	Module	I	II	III	IV	I	II	III	IV	I	II	III	IV
	Initial Lining Thickness [cm]	30	30	30	30	30	30	30	35	35	35	35	40
	Temporary Initial Lining Thickness [cm]	-------	-------	15	15	-------	-------	15	20	-------	-------	20	30
	Temporary Invert Lining Thickness [cm]	-------	20	20	-------	-------	20	20	-------	-------	20	25	-------
	Sealing Thickness [cm]	2.0	2.0	2.0	2.0	2.0	2.0	2.0	2.0	2.0	2.0	2.0	2.0
	Invert Type	Arch	Arch	Arch	Arch	Arch	Arch	Arch	Arch	Arch	Arch	Arch	Arch
	Lattice Girder Spacing	1.7--2.2	1.3--1.7	1.3--1.7	1.0--1.3	1.7--2.2	1.3--1.7	1.3--1.7	1.0--1.3	1.7--2.2	1.3--1.7	1.3--1.7	1.0--1.3
	Length of Round TH	1.7--2.2	1.3--1.7	1.3--1.7	1.0--1.3	1.7--2.2	1.3--1.7	1.3--1.7	1.0--1.3	1.7--2.2	1.3--1.7	1.3--1.7	1.0--1.3
	Length of Round Bench (=F x TH) **)	2.0	2.0	2.0	2.0	2.0	2.0	2.0	2.0	2.0	2.0	2.0	2.0
	Length of Round Invert (=F x TH) **)	3.0	3.0	3.0	3.0	3.0	3.0	3.0	3.0	3.0	3.0	3.0	3.0
	Initial Lining Lattice Girder Bars	ϕ25 & 2•ϕ18	ϕ25 & 2•ϕ18	ϕ25 & 2•ϕ18	ϕ25 & 2•ϕ18	ϕ25 & 2•ϕ18	ϕ25 & 2•ϕ18	ϕ25 & 2•ϕ18	ϕ28 & 2•ϕ20	ϕ28 & 2•ϕ20	ϕ28 & 2•ϕ20	ϕ28 & 2•ϕ20	ϕ28 & 2•ϕ20
	Temporary Initial Lining Lattice Girder Bars	-------	ϕ20 & 2•ϕ18	ϕ20 & 2•ϕ18	ϕ20 & 2•ϕ18	-------	ϕ20 & 2•ϕ18	ϕ20 & 2•ϕ18	ϕ20 & 2•ϕ18	-------	-------	ϕ20 & 2•ϕ18	ϕ20 & 2•ϕ18
	Wire Mesh *)	ϕ8@200•200 (2 Layer)	ϕ8@200•200 (2 Layer)	ϕ8@200•200 (2 Layer)	ϕ8@200•200 (2 Layer)	ϕ8@200•200 (2 Layer)	ϕ8@200•200 (2 Layer)	ϕ8@200•200 (2 Layer)	ϕ8@200•200 (2 Layer)	ϕ8@200•200 (2 Layer)	ϕ8@200•200 (2 Layer)	ϕ8@200•200 (2 Layer)	ϕ8@200•200 (2 Layer)
Settlement	S1 Surface Settlement [mm]	-27	-28	-17	-16	-29	-31	-22	-19	-33	-35	-26	-23
	S2 Surface Settlement [mm]	-22	-22	-14	-13	-28	-28	-21	-18	-31	-34	-25	-23
Deflection	D1 First Excavated Side Drift [mm]	-18	-17	-13	-7	-30	-34	-29	-13	-45	-52	-41	-19
	D2 Second Excavated Side Drift [mm]	-18	-17	-3	-5	-30	-34	-5	-9	-45	-52	-7	-12
	D3 Middle Drift [mm]	-17	-17	-20	-6	-27	-28	-38	-9	-38	-41	-51	-11
	C1 First Excavated Side Drift [mm]	-5	-6	-13	-2	-11	-14	-29	-5	-15	-23	-46	-9
	C2 Second Excavated Side Drift [mm]	-------	-------	-------	-5	-------	-------	-------	-5	-------	-------	-------	-14

TH.....Top Heading
F.....Factor
Module means Excavation Concept
*).....2 Layers - 1 Layer earthside, 1 Layer airside
**).....In case of maximum settlement and ground deflection length of round bench and length of round invert shall be reduced.

Module I - Top Heading
Module II - Top Heading / Invert
Module III - Half Side
Module IV - Side Drift

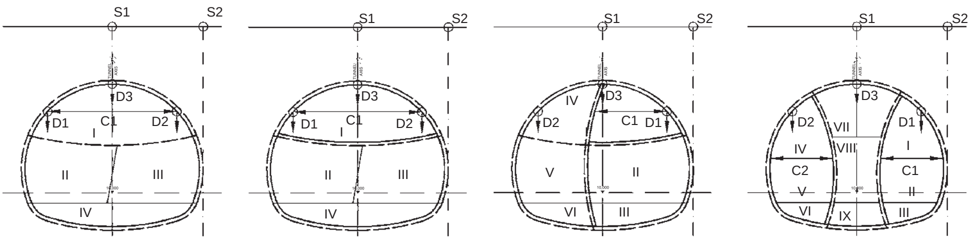

for the monitoring of tunnels, surrounding ground and buildings in the Niayesh tunnel are presented.

5.4 Design of sequential excavation method

The construction of tunnels in urban areas encounters many problems, such as face stability, ground surface settlement, tunneling-induced building damage and high

Table 2 Geometry, excavation classes and support elements of the Niayesh road tunnel project (Ghorbani *et al.*, 2012).

Excavation class	*1.5 lanes*	*2.5 lanes*	*3.5 lanes*	*Bifurcation*
Tunnel geometry				
Area (m^2)	87	136	186	470
Width/Height (m)	10.80/9.80	14.40/11.90	18/12.60	30.60/19.60
Number of traffic lanes	1	2	3	4
Total length of main tunnels (m)	8100			
The height of tunnel overburden	Maximum: 40m; Minimum: 4.7m; Average: 18m			
Maximum longitudinal slope (%)	4.5			
Transverse slope (%)	Maximum: 6%; Minimum: 1%			
Excavation and support				
Shotcrete (C25/30) (cm)				
Main wall	25	Based on ground advance classification (Table 1)	35	45–55
Temporary wall	–		25	25
Temporary invert	25		–	20
Main invert	25		35	45–55
Excavation round length in crown (m)	1–1.5		1–1.5	1
Excavation round length in bench (m)	3–4.5		3–4.5	2
Pre-support measures	Forepoling was arranged in the roof area of the tunnels in loose grounds in the form of a fan (Ls = 6 m and φ = 76 mm)			
Excavation method	Sequential excavation method (SEM) using mechanical tunnel excavator			
Tunnel shape	Modified horseshoe shape for 1.5- and 2.5-lanes cross sections, and mouth shape for 3.5- and 4- lanes cross sections			

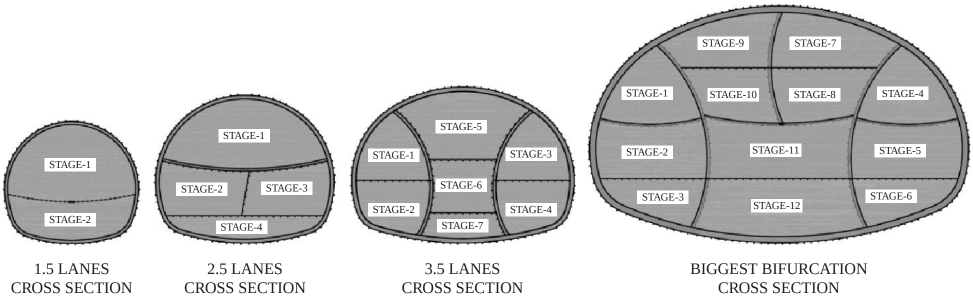

costs. In many countries, sequential excavation is currently applied where soft ground tunneling without a TBM is indicated (Romero, 2002). A great variety of excavation techniques have been developed (Geisler *et al.*, 1985; Pottler, 1992), which apply different methods to excavation and support. It is therefore important to investigate and compare the effect of these methods on ground disturbance and surface settlement. Given the low strength of the ground and the large span of the Niayesh tunnels, a full-face excavation was not possible. Therefore, SEM was selected for this project. This

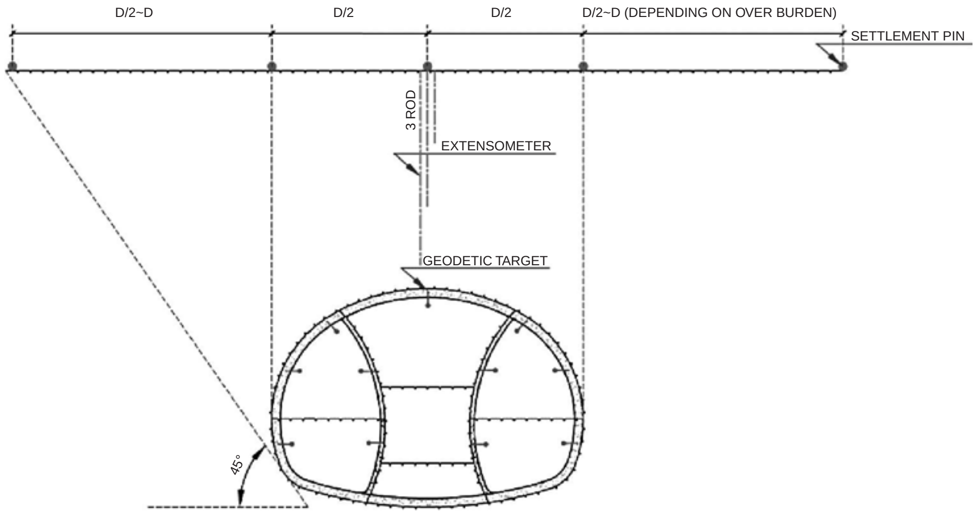

Figure 8 A typical instrumentation array for a 3.5-lanes cross section.

Table 3 The type and total number of instruments for monitoring the tunnels, surrounding ground and buildings in the Niayesh road tunnel project.

Instrument type	*Number*	*Instrument type*	*Number*
Total station (TM30, Leica 1201, …)	8	In-place MEMS bi-axial tiltmeter	107
Bi-reflex target	3,000	Portable tiltmeter	3
Digital convergence meter	4	Tilt plates	276
Tunnel convergence pin	1,500	Leveling instrument	7
Multiple Point Borehole Extensometer (MPBX)	8	Building settlement pins	396
Vibrating wire embedment strain gauge	81	Pavement settlement pins	1,000
Pressure cell	8	Deep settlement pins (2 m depth)	70
Crackmeter	75	Green field settlement pins	500

method is well-suited to tunneling in difficult, complex and rapidly changing geological formations.

5.4.1 *Finite element model of Niayesh tunnel*

The simulation of the SEM tunneling process for the Niayesh 3.5-lanes cross section tunnels started with the selection of the model geometry in three dimensions, and plane strain analysis was incorporated. Given the asymmetry of the excavation sequences in the assumed excavation methods, the entire domain was considered in the model (Figure 9). Given the constitutive modeling, the soil layers were assumed to be a Hardening Soil material, while the shotcrete lining was assumed to behave in a linear elastic manner. Table 4 summarizes the geotechnical properties used in the analyses. The shotcrete lining properties which were used in the modeling are presented in

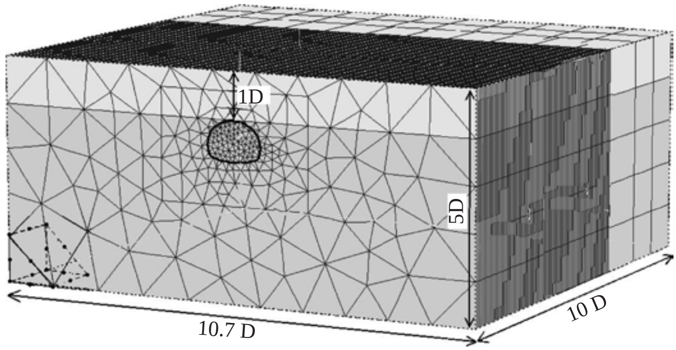

Figure 9 Finite element model of Niayesh 3.5-lane cross section tunnels (D = 15 m).

Table 4 Geotechnical properties of soil layers.

Depth (m)	*Unsaturated density γ_{unsat} (kN/m^3)*	*Saturated density γ_{sat} (kN/m^3)*	*Elasticity modulus unloading E_{ur}^{ref} (kN/m^2)*	*Elasticity modulus secant E_{50}^{ref} (kN/m^2)*	*Elasticity modulus oedometer E_{Oed}^{ref} (kN/m^2)*	*Cohesion C (kN/m^2)*	*Poisson ratio υ_{ur}*	*Internal friction angle φ (°)*	K_0^{nc}*
0–15	16	17	2.423×10^5	8.077×10^4	8.077×10^4	30	0.2	34	0.44
<15	18	19	2.827×10^5	9.423×10^4	9.423×10^4	40	0.2	36	0.41

* K_0 Value based on Jaky's formula for various layers of soil: ($K_0 = 1 - \sin \varphi$)

Table 5 Shotcrete lining properties used in modeling.

Lining type	*Poisson ratio (υ_{ur})*	*Weight W (kN/m/m)*	*Equivalent thickness d (m)*	*Element*	*Flexural rigidity EI (kNm^2/m)*	*Normal stiffness EA (kN/m)*
Temporary wall	0.2	5.35	0.25	Elastic	2.73×10^4	5.25×10^6
Permanent wall	0.2	7.5	0.35	Elastic	7.5×10^4	7.35×10^6

Table 5. Prior to the analysis, numerical models were developed and verified, based on the measured data from the Niayesh road tunnel.

5.4.2 Selection of tunnel excavation method

Tunnel design and construction requires the use of appropriate techniques and technologies during all phases of a tunnel project. In the main, a distinct rule does not exist to facilitate decision making about the selection of an appropriate excavation method.

This decision is mostly influenced by engineering experiences rather than theoretical calculations. The excavation method and sequencing schemes for a tunnel that is located in an urban area would typically be based on the complex interactions occurring between several factors, such as safety, cost and schedule (Hoek, 2001). Other significant factors that affect the selection of excavation method are the surrounding material properties (including geotechnical characteristics), the size and shape of the tunnel section, underground hydrology, in situ and induced stresses, regional geology, structural geology and weak-zone characteristics (Yu & Chern, 2007). Subdividing the excavation area is necessary for large-span tunnels in order to minimize ground disturbance and surface settlement. The structural integrity of the tunnel-surrounding material can thus be largely maintained.

After plotting the location of the Niayesh tunnel on the diagram proposed by Yu and Chern (2007) in Figure 10, side (or sidewall) drift (SD) and central diaphragm (CD) methods were shown to be the most suitable for the excavation. Thus, these excavation methods, based on the proposed excavation sequences shown in Figure 11, were

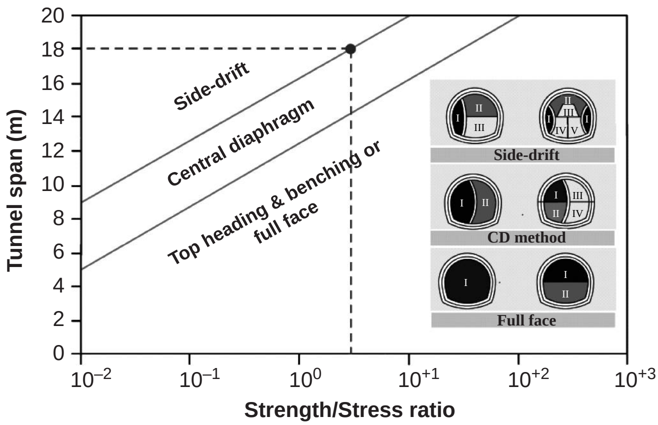

Figure 10 Empirical determination of excavation method based on three parameters of span size, compressive strength and vertical stress on tunnel.

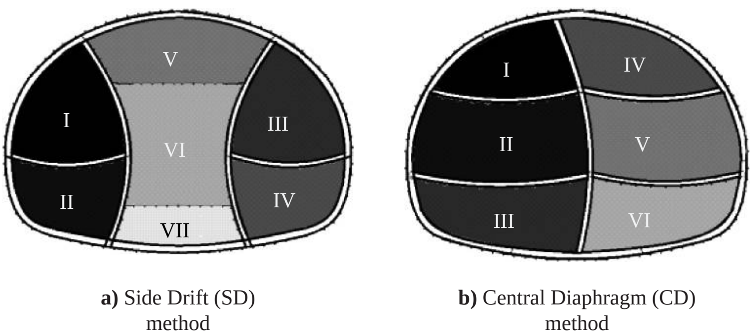

Figure 11 Excavation sequences of (a) the side drift method and (b) the central diaphragm method.

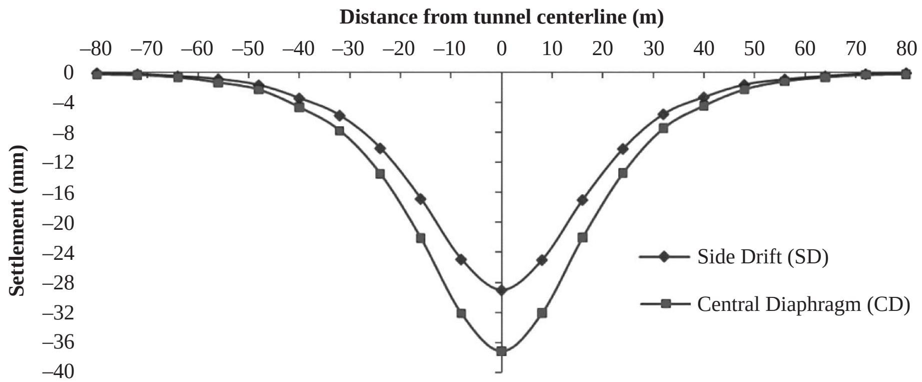

Figure 12 The computed transverse surface settlement profiles for CD and SD excavation methods.

simulated using a numerical FEM, in order to select the appropriate excavation method based on its potential for minimization of ground surface settlement. It was assumed that the final concrete lining would be placed at sufficient distance from the excavation face for it not to need consideration in the numerical simulations.

The results obtained from the 3D FEM models are relative to the final situation after completion of excavation and initial lining. In Figure 12, the computed surface settlement profiles for both CD and SD excavation methods are illustrated. As seen in Figure 12, for both SD and CD methods, the maximum value of surface settlements (about 29.4 mm and 37 mm respectively) were computed over the tunnel center line. Based on these modeling results, the CD method induces more surface settlement than the SD method. The SD method was, therefore, preferred over the CD method for the Niayesh urban tunnel excavation, given its better capability in limiting ground surface settlements as well as tunnel deformations. It should be noted that partitioning the face through staged excavation typically results in reduced face-advance rates, more stages of temporary support installation, and additional underpinning and delayed closure of the tunnel liner.

5.4.3 Optimal excavation sequence for side drift method

For economic execution of a SEM, it is essential to fully understand the influence of a given face-advancing sequence on the tunneling performance. The main factor in the selection of optimal excavation sequences is limitation of surface settlement values. The selection of excavation sequences depends, for example, on tunnel geometry, ground properties and the groundwater table. Limited research has been conducted in the field into the effects of different face-advancing methods on tunneling performance (Bowers, 1997; Karakus & Fowell, 2003; Farias *et al*., 2004). These studies have provided valuable information but they are limited to specific tunneling cases; the 3D effects of various face-advancing methods on tunneling performance have been considered in very few studies. As discussed more extensively by Szechy (1967), the arrangement of underground openings and their excavation sequences depend on the operations that must be conducted in them (excavation method, installation and

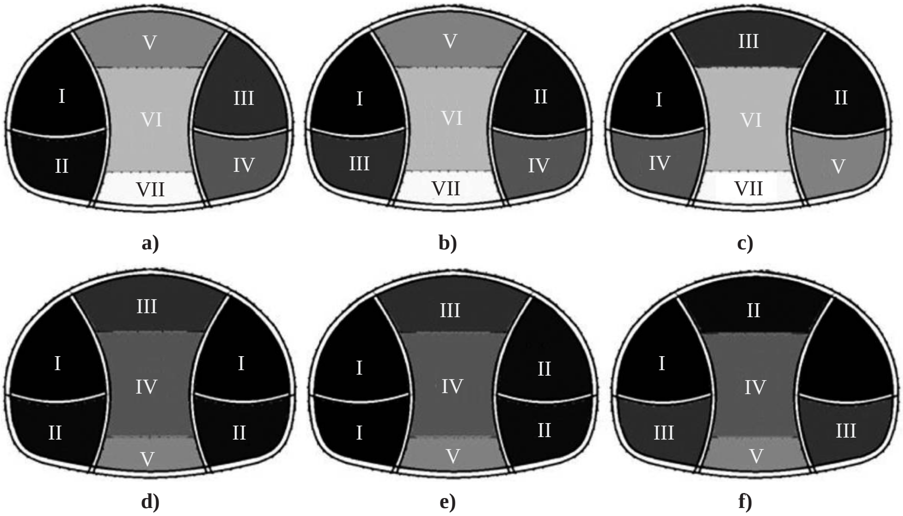

Figure 13 Proposed excavation sequences for the Niayesh tunnel using side drift method.

construction of temporary and permanent support, short-term and long-term use, etc.), the nature of the ground, and the in situ stress conditions encountered. There is, therefore, a practical need to simulate the different phases of tunnel construction and find the optimal construction procedure.

In order to find the optimal excavation sequences for the Niayesh tunnel, six excavation schemes based on the SD method were proposed and numerically analyzed, taking into consideration tunnel geometry and properties of soil layers (Figure 13). During selection of excavation sequences, principal factors such as ring closure time, number of excavation stages, subdividing area, and stage of central gallery excavation were considered.

Transverse surface settlement profiles for six excavation sequences are illustrated in Figure 14. Based on the numerical modeling results, the excavation scheme labeled (a) had the lowest surface settlement value and it was selected as the optimal scheme for the excavation of the Niayesh urban tunnel project. Results shows that rapid closure of the supporting ring and the excavation stage of the central gallery (middle drift) are the most important factors in controlling tunnel deformations and surface settlements in soft ground tunneling. Figure 12 indicates that conducting excavation of the central gallery in later stages reduces the extent of surface settlement.

The excavation volume of each stage has bilateral effects on surface settlement. A smaller excavation volume leads to less displacement and surface settlement. However, a smaller excavation volume also increases the number of excavation stages and delays support ring closure, which serves to increase surface settlement. Closing the support ring in soft ground must be done in fewer steps; delaying the ring closure results in large deformations and settlements. If face stability is adequately maintained, rapid ring closure through the adoption of a larger excavation volume is more effective than adopting a smaller excavation volume when it comes to limiting the

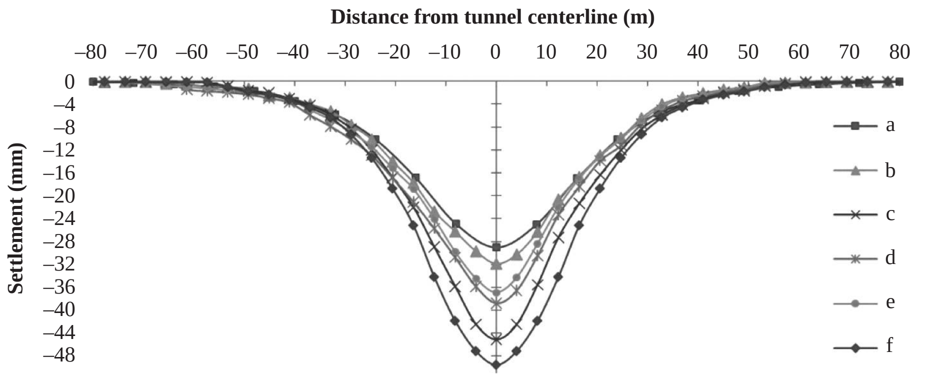

Figure 14 Transverse settlement profiles of the proposed excavation schemes (see) for the Niayesh tunnel.

tunnel crown and surface settlements in soft ground tunneling at shallow depths (Sharifzadeh *et al.*, 2013b).

5.4.4 Optimal trailing distance between excavation stages

Tunnel excavation causes a disturbance of the initial state of stress in the ground and creates a stress regime in the form of a bulb around the advancing tunnel face. The extent of the stress disturbance around an active heading depends mainly on ground conditions, distance between different excavation stages, and excavation round length. While a large disturbance zone will be produced when using a full-face excavation method, this zone can be reduced by adopting SEM and an appropriate trailing distance between different faces, thereby limiting surface settlement. Depending on the size of the opening and the quality of the ground, a tunnel cross section may be subdivided into multiple drifts (DTFHA, 2009). If the different excavation faces are close together, disturbance zones around faces will interfere with one another and lead to more displacement of the tunnel crown and greater surface settlement. Therefore, a trailing distance must be retained between different faces, so that critical disturbance zones will not interfere with or affect each other. During tunneling in soft ground conditions, the support ring closure behind the face should be executed as quickly as possible to create a load support ring, thus requiring the trailing distance between different faces to be kept as short as possible (Sharifzadeh *et al.*, 2013a).

In order to identify the optimal trailing distance between different faces, side galleries were simulated at distances of 6 m (0.4 D), 10 m (0.67 D), 15 m (1 D), 22 m (1.47 D) and 30 m (2 D) in front of the central gallery face (Figure 15). The excavations were simulated according to excavation scheme (a) (from Figure 13) in 1 m round length, with right and left side drifts excavated simultaneously.

Transverse surface settlement curves for different trailing distances between the central gallery and side drifts are illustrated in Figure 16, which shows that by increasing trailing distances, the disturbance zones of different stages do not

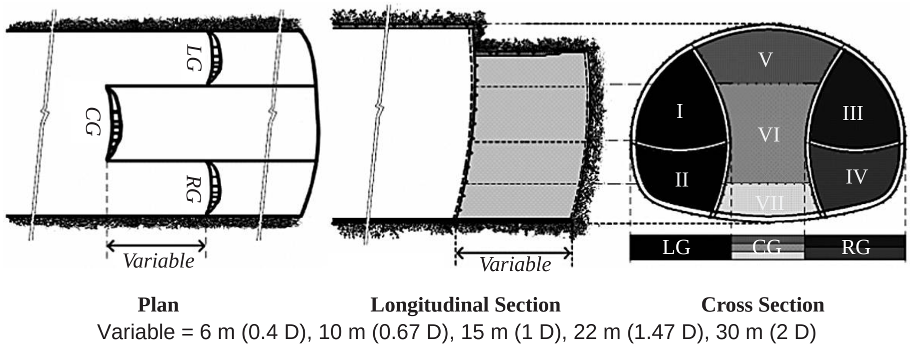

Figure 15 Plan view, longitudinal and transverse sections with variable distance between side drifts and middle drift faces.

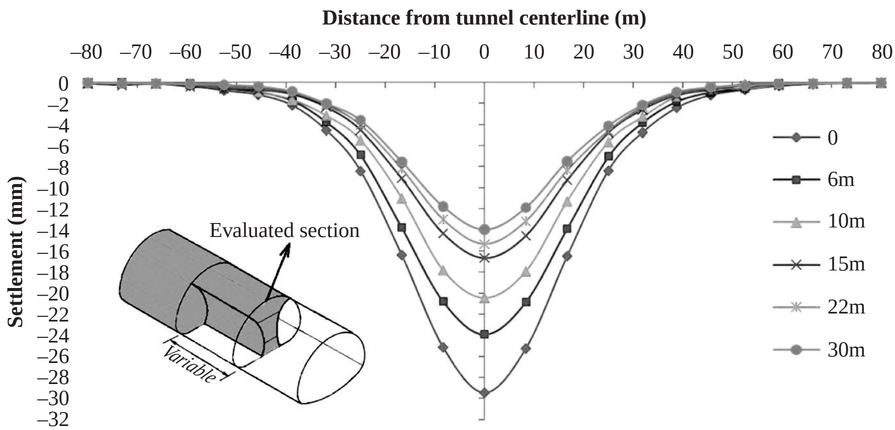

Figure 16 Transverse surface settlement curves for different trailing distances between side drifts and middle drift faces.

interfere with each other as much, leading to a reduction in the degree of surface settlement.

According to Figure 16, the optimum trailing distance was computed to be 15 m or more. This result is consistent with the statements of Yoo (2009), who reported that the best tunneling performance can be achieved by keeping the trailing distance greater than one tunnel diameter (D).

In the Niayesh project, given the urban environment, ground conditions, tunnel dimensions and value of the overburden in the tunnel route, the trailing distances between excavation faces were designed to be in the range 15–25 m, in order to reduce surface settlement. This example demonstrates that trailing distances derived using numerical simulation are in good accordance with operational results.

In order to minimize interference between disturbance zones and maintain efficient control of surface settlements, it is better to excavate side drifts separately. Thus, the

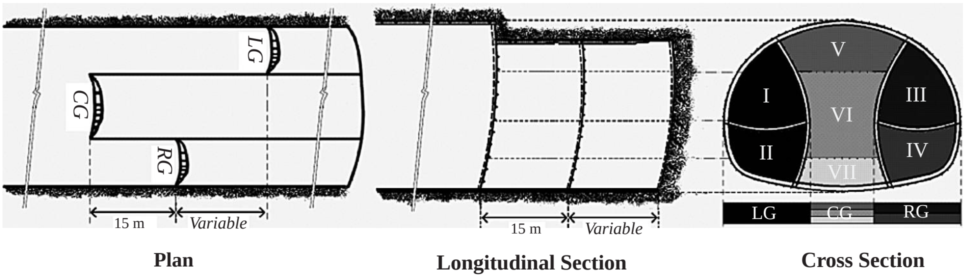

Figure 17 Plan view, longitudinal and transverse sections with variable distance between faces of side drifts.

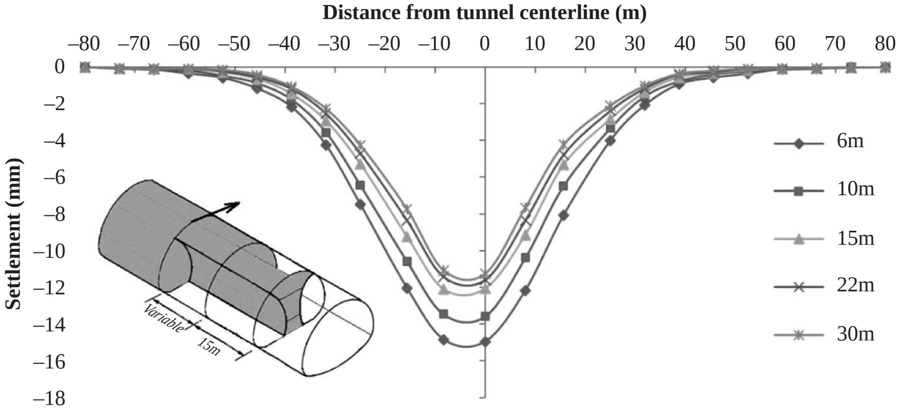

Figure 18 Transverse surface settlement curves for left gallery section at different trailing distances between side drifts.

excavations of three galleries (left, right and central) were simulated with different trailing distances from each other. Tunnel excavation procedures were simulated with trailing distances between the two side drifts of 6 m (0.4 D), 10 m (0.67 D), 15 m (1 D), 22 m (1.47 D) and 30 m (2 D), as shown in Figure 17. The minimum optimal trailing distance of 15 m between side drift faces and the middle drift face, derived in the previous step, was applied to all of the models.

Transverse surface settlement curves for left and right drift sections at different trailing distances between lateral galleries are illustrated in Figures 18 and 19 respectively. As expected, increasing the trailing distance between side drifts leads to a decrease in surface settlements.

As seen in Figures 18 and 19, surface settlement variations are larger as trailing distance increases from 6 m (0.4 D) to 15 m (1 D), but it has gentler variation once trailing distance is greater than 15 m (1 D). Based on these results, the optimal trailing distance between side drifts should be not less than 15 m (1 D).

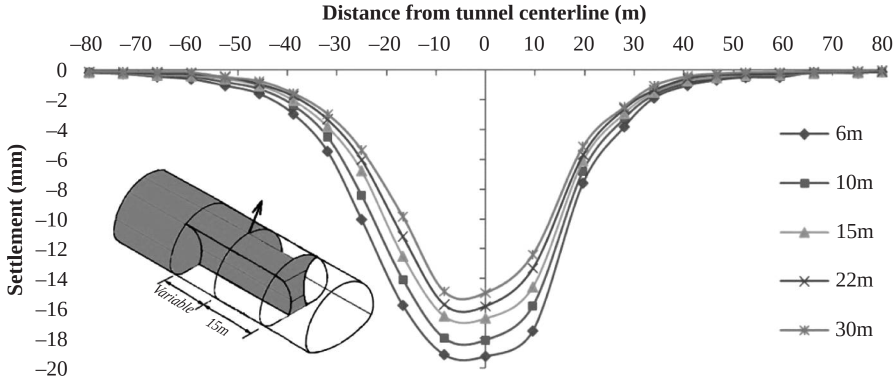

Figure 19 Transverse surface settlement curves for right gallery section at different trailing distances between side drifts.

5.5 Design optimization based on observational method

In the process of tunnel design, several parameters with varying degrees of uncertainty must be taken into account. These uncertainties are mostly related to tunnel-hosting ground conditions and tunnel construction performance. Thus, the real ground behavior around a tunnel's axis could not be accurately predicted at the design stage. This becomes even more important where a tunnel passes through an urban area and directly affects infrastructure and buildings. Therefore, for several reasons – such as safety, economy and understanding of the ground's real behavior – the use of the observational method as a practical engineering tool is necessary. A fundamental component of the observational method in tunneling is the use of monitoring data to assess the adequacy of the chosen design and the safety margins of the design.

In the Niayesh road tunnel project, given the technical and design requirements, the project's geological and geotechnical conditions, the results of monitoring, and the experiences gained during construction, the excavation activities and support elements were continuously adjusted to suit the ground conditions.

5.5.1 Modification of the excavation activities

During the preliminary design phase, excavation modules were selected for every section of the tunnels according to their longitudinal profile (ground advance classification). The real ground classes were defined on site, directly at the face, by mutual agreement between the geotechnical engineer and the resident engineer and based on the geotechnical monitoring results. Depending on the conditions of the ground encountered and these monitoring results, appropriate excavation modules were applied at different sections of the tunnels.

Modifications applied to the Niayesh tunnel excavation activities included: (a) modification of the pre-defined excavation modules; (b) modification of the length of excavation rounds for each stage; (c) modification of the trailing distance between excavation stages in different modules.

Table 6 Comparison of the costs of the designed and constructed modules for 2.5-lanes cross section in the Niayesh tunnel.

Designed module	*Constructed module*	*Cost ratio of constructed module to designed module*
Module A	Module A	1
Module B	Module A	0.71
Module C	Module A	0.62
	Module B	0.87
Module D	Module B	0.61
	Module C	0.70

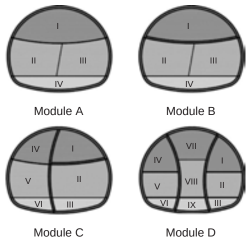

Note: The excavation rate of Module A is approximately 65 percent greater than Module B

Comparisons between the costs of the modules as designed and the modules as constructed are presented in Table 6.

5.5.2 Modification of the support elements

Based on the NATM concept, the ground around the tunnel not only acts as a load, but also as a load-bearing element. In the Niayesh tunnel, depending on the project conditions and monitoring results, the requirements for a specific support were determined. Contractual arrangements were flexible to ensure that the most economical type and amount of support was used.

Modifications applied to the Niayesh tunnel support elements included: (a) modification of the tunnel's initial support elements (*i.e.* the thickness of shotcrete and the distance between lattice girders); (b) modification of the pre-support elements (*i.e.* forepoling, pre-grouting); (c) modification of the initial support elements around the ramps and portals (*i.e.* number, diameter and depth of the reinforced piles, number and length of the soil nails).

In all of the design modifications described above, the major concern was limiting the ground settlements induced by tunneling and limiting any potential damage to the existing structures and utilities above the tunnel.

6 SUMMARY

We have presented a brief review of back analysis procedures, including comparisons, problems, recent advances and further development. Different back analysis methods according to those deterministic and non-deterministic aspects applicable in geotechnical engineering problems were introduced. Because back analysis is a practical engineering tool that can bridge field measurement, design and construction, further efforts are required to make the best use of developing technologies and also to raise the level of conceptual understanding of the back analysis procedures in current use. Back analysis is, and will continue to be, a key to achieving scientific tunnel construction in the future.

Back analyses are very powerful tools for interpreting the results of field measurements. Back analysis should not only be used to determine material properties but also to generate a mechanical model of soils and rocks.

Solutions of geotechnical inverse problems are neither identifiable nor unique in a strict sense. Furthermore, the limitations in quantity and quality of available data, together with the multicollinearity, tend to make solutions unstable. However, these issues do not prevent us from adopting the inverse analysis method to identify models and estimate parameters.

When constructing a system for a given purpose, our ultimate goal is to obtain a system that is as useful as possible for that purpose. This means, in turn, constructing a system that can handle a proper blend of the three most fundamental characteristics of systems: credibility, complexity and uncertainty. Ideally, we would like to obtain a system with high credibility, low complexity and low uncertainty. Unfortunately, these three criteria conflict with one another and to achieve a high level of usefulness from any system, we need to find the right trade-off among them.

There are many reasons why back analysis techniques are being used more frequently. The two most important are, first, the development of numerical calculation methods for the analysis of the stresses and strains in a rock mass, and second, the availability of quick and simple personal computers with which the large amounts of data – which are necessary to resolve the numerical modeling and error minimization (parametric analyses) – can be produced in the shortest possible time, at the lowest possible cost. However, the use of back analyses has not become as popular as previously expected. There are several reasons for this: (a) there are few engineers who can manage both on-site practice and the execution of back analyses in computer rooms; (b) back analyses are not included in the specifications of contracts for tunnel construction works; (c) practical methods for applying back analysis results to the design of tunnel supports and construction procedures have not been developed to a level that would be regarded as satisfactory for industry acceptance (Sakurai *et al.*, 2003).

Leroueil and Tavenas (1981) prepared guidelines for the correct use of back analysis techniques, the most important of which are:

- It is wrong to undertake back analysis of the same problem by carrying out uncoupled analysis on only a few limited phenomena – all of the uncertain parameters of the rock should be considered in the back analysis, and all of the physical phenomena should be simultaneously included;
- If the measurements carried out in situ are available, it is necessary to first of all look at their qualitative interpretation on the basis of known case histories in order to fully understand the physical phenomenon that governs the problem;
- Unrealistic conclusions of a back analysis should be rejected – if necessary, one should add the original hypotheses to the modification and the back analysis should be repeated with a new calculation model.

For economic execution of SEM, it is essential to fully understand the influence of a given face-advancing sequence on the tunneling performance. Improper selection of an excavation sequence could have a destabilizing effect on the tunnel, and the influence of excavation sequences on ground settlements must be taken into account, particularly in the case of large-span urban tunnels in shallow depths.

REFERENCES

Asaoka, A. & Matsuo, M. (1984). An inverse problem approach to the prediction of multi-dimensional consolidation behavior. *Soils and Foundations*, 24, 49–62.

Bieniawski, Z.T. (1984). *Rock Mechanics Design in Mining and Tunneling*. Rotterdam, Balkema.

Brady, B.H.G. & Brown, E.T. (2004). *Rock Mechanics for Underground Mining* (3rd edn). Netherlands, Springer.

Bowers, K.H. (1997). An Appraisal of the New Austrian Tunnelling Method in Soil and Weak Rock. PhD Thesis, The University of Leeds, 240p.

Cai, M. & Chen, X. (1987). Back-analysis of initial stress field in rocks by the simplex method. In: *Proceedings of First National Conference on Geomechanics*. pp. 217–222.

Cai, M., Morioka, H., Kaiser, P.K., Tasaka, Y., Kurose, H., Minami, M. & Maejima, T. (2007). Back-analysis of rock mass strength parameters using AE monitoring data. *International Journal of Rock Mechanics and Mining Sciences*, 44(4), 538–549.

CIRIA. (1999). *The observational method in ground engineering: Principles and applications, REP R 185*. London, Construction Industry Research and Information Association.

Cividini, A. & Gioda, G. (2003). Back analysis of geotechnical problems. In: Bull, J.W. (ed.) *Journal of Numerical Analysis and Modelling in Geomechanics*. London, Spon Press. pp. 165–196.

Cividini, A., Jurina, L. & Gioda, G. (1981). Some aspects of characterization problems in geomechanics. *International Journal of Rock Mechanics and Mining Sciences and Geomechanics*, 18, 487–503.

Cividini, A., Maier, G. & Nappi, A. (1983). Parameter estimation of a static geotechnical model using a Bayes' approach. *International Journal of Rock Mechanics and Mining Sciences and Geomechanics*, 20, 215–226.

Deng, J.L. (1986). *Grey Prediction and Decision Making*. Wuhan, China, Huazhong University Press.

DIN. (2011). *Geotechnical Measurements, DIN 1407*. Berlin, Beuth Verlag.

DTFHA. (2009). *Technical Manual for Design and Construction of Road Tunnels – Civil Elements*. Washington, DC, US Department of Transportation Federal Highway Administration.

Dunnicliff, J. (1993). *Geotechnical Instrumentation for Monitoring Field Performance*. New York, John Wiley.

Einstein, H.H. & Baecher, G.S. (1982). Probabilistic and statistical methods in engineering geology. 1. Problem statement and introduction to solution. *Rock Mechanics*, Supp. 12, 47–61.

Feng, X.T., Zhao, H. & Li, S. (2004). A new displacement back analysis to identify mechanical geo-material parameters based on hybrid intelligent methodology. *Numerical and Analytical Methods in Geomechanics*, 28(11), 1141–1165.

Farias, M.M., Moraes, A.H. & Assis, A.P. (2004). Displacement control in tunnels excavated by the NATM: 3-D numerical simulations. In: *Tunnelling and Underground Space Technology*, 19, 283–293.

Gallagher, K. & Sambridge, M. (1994). Genetic algorithms: A powerful tool for large-scale nonlinear optimization problems. *Computers and Geosciences*, 20(7/8), 1229–1236.

Geisler, H., Wagner, H., Zieger, O., Mertz, W. & Swoboda, G. Practical (1985). Theoretical aspects of the three dimensional analysis of finally lined intersections. In: *Proceedings of the 5th International Conference on Numerical Methods in Geomechanics*, Nagoya. pp. 1175–1183.

Geokon: http://www.geokon.com/content/posters/Tunnelling_Instrumentation.pdf.

Ghorbani, M. & Sharifzadeh, M. (2009). Long term stability assessment of Siah Bisheh power-house cavern based on displacement back analysis method. *Tunnelling and Underground Space Technology*, 24(5), 574–583.

Ghorbani, M., Sharifzadeh, M., Yasrobi, S. & Daiyan, M. (2012). Geotechnical, structural and geodetic measurements for conventional Tunnelling Hazards in Urban Areas – The case of Niayesh road tunnel project. *Tunnelling and Underground Space Technology*, 31, 1–8.

Gioda, G. (1980). Indirect identification of the average elastic characteristics of rock masses. In: Pells, P.J.N. (ed.) *International Conference on Structural Foundations on Rock, Sydney, Australia*. Rotterdam, Balkema. pp. 65–73.

Gioda, G. (1985). Some remarks on back analysis and characterization problems in geomechanics. In: Sakurai, S. & Ichikawa, T. (eds.) *Proceedings of the 5th International Conference on Numerical Methods in Geomechanics, Nagoya, Japan*. Rotterdam, Balkema. pp. 47–61.

Gioda, G. & Jurina, L. (1981). Numerical identification of soil structure. *Numerical and Analytical Methods in Geomechanics*, 5, 33–56.

Gioda, G. & Locatelli, L. (1999). Back analysis of the measurements performed during the excavation of a shallow tunnel in sand. *Numerical and Analytical Methods in Geomechanics*, 23, 1407–1425.

Gioda, G. & Maier, G. (1980). Direct search solution of an inverse problem in elastoplasticity: identification of cohesion, friction angle and in situ stress by pressure tunnel test. *International Journal for Numerical Methods in Engineering*, 15, 1832–1848.

Gioda, G. & Sakurai, S. (1987). Back analysis procedures for the interpretation of field measurements in geomechanics. *Numerical and Analytical Methods in Geomechanics*, 11, 555–583.

Gioda, G. & Swoboda, G. (1999). Developments and applications of the numerical analysis of tunnels in continuous media. *Numerical and Analytical Methods in Geomechanics*, 23, 1393–1405.

Gokceoglu, C., Yesilnacar, E., Sonmez, H. & Kayabasi, A. (2004). A neuro-fuzzy model for modulus of deformation of jointed rock masses. *Computers and Geotechnics*, 31, 375–383.

Himmelblau, D.M. (1972). *Applied nonlinear programming*. New York, McGraw-Hill.

Hisatake, M. & Hieda, Y. (2007). Three-dimensional back-analysis method for the mechanical parameters of the new ground ahead of a tunnel face. *Tunnelling and Underground Space Technology*, 23, 373–380.

Hoek, E. (2001). Big tunnel in bad rock. *Journal of Geotechnical and Geoenvironmental Engineering*, 127(9), 726–740.

Honjo, Y., Tsung, L.W. & Sakajo, S. (1994). Application of Akaike information criterion statistics to geotechnical inverse analysis: the extended Bayesian method. *Structural Safety*, 14, 5–29.

Ichikawa, Y. & Ohkami, T. (1992). A parameter identification procedure as a dual boundary control problem for linear elastic materials. *Soils and Foundations*, 32(2), 35–44.

Iding, R.H., Pister, K.S. & Taylor, R.L. (1974). Identification of nonlinear elastic solids by a finite element method. *Computer Methods in Applied Mechanics and Engineering*, 4, 121–142.

Imre, E. (1994). Model validation for the oedometric relaxation test. In: *Proceedings of the 13th International Conference on Soil Mechanics and Foundation Engineering, New Delhi, India*. Rotterdam, Balkema. pp. 1123–1126.

ITA. (2009). *General Report on Conventional Tunnelling Method*, ITA Report No. 002. Lausanne, Switzerland, International Tunnelling and Underground Space Association.

Jurina, L., Maier, G. & Podolak, K. (1977). On model identification problems in rock mechanics. In: *Proceedings of the International Symposium on the Geotechnics of Structurally Complex Formations, Capri*. Vol. 1. pp. 287–295.

Karakus, M. & Fowell, R.J. (2003). Effect of different tunnel face advance excavation on the settlement by FEM. *Tunnelling and Underground Space Technology*, 18, 513–523.

Kaiser, P.K., Zou, D. & Lang, P.A. (1990). Stress determination by back analysis of excavation-induced stress changes – A case study. *Rock Mechanics and Rock Engineering*, 23(3), 185–200.

Kavanagh, K.I. & Clough, R.W. (1971). Finite element application in the characterization of elastic solids. *International Journal of Solids and Structures*, 7, 11–23.
Kirsten, H.A.D. (1976). Determination of rock mass elastic moduli by back analysis of deformation measurement. In: Bieniawski, Z.T. (ed.) *Proceedings of Symposium on Exploration for Rock Engineering, Johannesburg*. Cape Town, Balkema. pp. 1154–1160.
Kosmatopoulos, E.B., Polycarpou, M.M., Christodoulou, M.A. & Ioannou, P.A. (1995). High-order neural network structures for identification of dynamical systems. *IEEE Transactions Neural Networks*, 6(2), 422–431.
Leroueil, S. & Tavenas, F. (1981). Pitfalls of back analyses. In: *Proceeding of the 10th International Conference On Soil Mechanics and Foundation Engineering*, Stockholm, pp. 185–190.
Levasseur, S., Malecot, Y., Boulon, M. & Flavigny, E. (2007). Soil parameter identification using a genetic algorithm. *Numerical and Analytical Methods in Geomechanics*, 32, 189–213.
Li, S.H., Wu, X.Y. & Ma, F.S. (1998). Application of precedent type analysis (PTA) in the construction of Ertan Hydroelectric Station, China. *International Journal of Rock Mechanics and Mining Science*, 35, 787–795.
Liang, Y.C., Zhang, D.P., Liu, G.R., Yang, X.W. & Han, X. (2003). Neural identification of rock parameters using fuzzy adaptive learning parameters. *Computers and Structures*, 81, 2373–2382.
Mahnken, R. & Stein, E. (1995). Parameter identification for viscoplastic models based on analytical derivatives of a least-squares functional and stability investigations. *International Journal of Plasticity*, 12(4), 451–479.
Murakami, A. & Hasegawa, T. (1993). Application of Kalman filtering to inverse problems. *Theoretical and Applied Mechanics*, 43, 3–14.
Ohkami, T. & Ichikawa, Y.A. (1997). Parameter identification procedure for visco-elastic materials. *Computers and Geotechnics*, 21(4), 255–275.
Ohkami, T. & Swoboda, G. (1999). Parameter identification of viscoelastic materials. *Computers and Geotechnics*, 24(4), 279–295.
Oreste, P. (2005). Back-analysis techniques for the improvement of the understanding of rock in underground constructions. *Tunnelling and Underground Space Technology*, 20(1), 7–21.
Pichler, B, Lackner, H. & Mang, H.A. (2003). Back analysis of model parameters in geotechnical engineering by means of soft computing. *International Journal for Numerical Methods in Engineering*, 57, 1943–1978.
Pottler, R. (1992). Three-dimensional modeling of junction at the channel tunnel project. *International Journal for Numerical and Analytical Methods in Geomechanics*, 16, 683–695.
POR. (2008). *Geotechnical Investigations & Foundation Report for Niayesh Tunnel Project*. Tehran, Pazhoohesh Omran Rahvar Consulting Engineers.
Powell, M.J.D. (1964). An efficient method of finding the minimum of a function of several variables without calculating derivatives. *The Computer Journal*, 7, 155–162.
Romero, V. (2002). NATM in soft-ground: A contradiction of terms. *World Tunnelling, NATM & Shotcreting Focus, Jacobs Associates, USA*, 338–343.
Rosenbrock, H.H. (1960). An automatic method for finding the greatest or least value of a function. *The Computer Journal*, 3, 175–184.
Rubio, J.D.J. & Yu, W. (2007). Nonlinear system identification with recurrent neural networks and dead-zone Kalman filter algorithm. *Neurocomputing Journal*, 70, 2460–2466.
Sakurai, S. (1982). Monitoring of caverns during construction period. In: Wittke, W. (ed.) *Rock Mechanics: Caverns and Pressure Shafts, Proceedings of the ISRM Symposium, Aachen*. Rotterdam, Balkema. pp. 433–441.
Sakurai, S. (1997). Lessons learned from field measurements in tunneling. *Tunnelling and Underground Space Technology*, 12, 453–460.
Sakurai, S. (1997). Monitoring and performance in tunneling. In: *Proceedings of the 14th International Conference on Soil Mechanics and Foundation Engineering, Hamburg, Germany*. Rotterdam, Balkema. pp. 2409–2412.

Sakurai, S. & Abe, S. (1979). A design approach to dimensioning underground opening. In: *Proceedings of the 3rd International Conference on Numerical Methods in Geomechanics, Aachen, Germany*. Balkema Publications, Rotterdam, The Netherlands. pp. 649–661.

Sakurai, S., Akutagawa, S., Takeuchi, K., Shinji, M. & Shimizu, N. (2003). Back-analysis for tunnel engineering as a modern observational method. *Tunnelling and Underground Space Technology*, 18(2–3), 185–196.

Sakurai, S. & Takeuchi, K. (1983). Back analysis of measured displacements of tunnels. *Rock Mechanics and Rock Engineering*, 16(3), 173–180.

Setnes, M., Babuška, R. & Verbruggen, H.B. (1998) Rule-based modeling: Precision and transparency. *IEEE Transactions on Systems, Man, and, Cybernetics Part C*, 28(1), 165–169.

Sharifzadeh, M., Ghorbani, M. & Masoudi, R. (2009). Displacement based back analysis of Siah Bisheh pumped storage powerhouse cavern by means of distinct element method. *Sharif: Engineering*, 47, 49–57.

Sharifzadeh, M., Darai, R. & Sharifi, M. (2011). Design of sequential excavation tunneling in weak rocks through findings obtained from displacements based back analysis. *Tunnelling and Underground Space Technology*, 28, 10–17. doi:10.1016/j.tust.2011.08.003

Sharifzadeh, M., Kolivand, F., Ghorbani, M. & Yasrobi, S. (2013a). Design of sequential excavation method for large span urban tunnels in soft ground – Niayesh tunnel. *Tunnelling and Underground Space Technology*, 35, 178–188.

Sharifzadeh, M., Tarifard, A. & Moridi, M.A. (2013b). Time-dependent behavior of tunnel lining in weak rock mass based on displacement back analysis method. *Tunnelling and Underground Space Technology*, 38, 348–356.

Swoboda, G., Ichikawa, Y., Dong, Q.X. & Zaki, M. (1999). Back analysis of large geotechnical models. *International Journal for Numerical and Analytical Methods in Geomechanics*, 23, 1455–1472.

Szechy, K. (1967). *The Art of Tunnelling*. Akademiai Kiado, Budapest.

Tarantola, A. (2005). *Inverse Problem Theory and Methods for Model Parameter Estimation*. Philadelphia, Society for Industrial and Applied Mathematics.

Tonon, F., Amadei, B., Pan, E. & Frangopol, D.M. (2001). Bayesian estimation of rock mass boundary conditions with applications to the AECL underground research laboratory. *International Journal of Rock Mechanics and Mining Sciences*, 38(7), 995–1027.

Villaescusa, E. (2014). *Geotechnical Design for Sublevel Open Stoping*. Boca Raton, FL, CRC Press.

Wang, S., Yang, Z. & Lin, X. (1987). The back-analysis method from displacements for visco-elastic rock mass. In: *Proceedings of the Second International Symposium on Field Measurements in Geomechanics, Kobe, Japan*. Rotterdam, Balkema. pp. 1059–1068.

Yang, L. (1990). Advance in back analysis approaches and application in engineering. In: *Engineering Application of Numerical Method in Rock Mechanics*. Shanghai, Tongji University Press. pp. 60–65.

Yang, Z.F., Liu, Z.H. & Wang, S.J. (1983). A practical back analysis's method from displacements to estimate some parameters of a rock mass for design of an underground opening. In: *Proceedings of International Symposium on Field Measurements in Geomechanics, Zurich, Switzerland*. Rotterdam, Balkema. pp. 1267–1276.

Yang, Z.F., Lee, C.F. & Wang, S.J. (2000). 3-D back analysis on one trial adit in three gorges, China. *International Journal of Rock Mechanics and Mining Science*, 37, 525–533.

Yoo, C. (2009). Performance of multi-faced tunnelling – A 3D numerical investigation. In: *Tunnelling and Underground Space Technology*, 24, 562–573.

Yu, C.W. & Chern, J.C. (2007). Expert system for D&B tunnel construction. In: *Underground Space the 4th Dimension of Metropolises*, London, England.

Zhang, L.Q., Yue, Z.Q., Yang, Z.F., Qi, J.X. & Liu, F.C. (2006). A displacement-based back-analysis method for rock mass modulus and horizontal in situ stress in tunneling – Illustrated with a case study. *Tunnelling and Underground Space Technology*, 21(6), 639–649.
Zhao, J. & Lee, K.W. (1996). Construction and utilization of rock caverns in Singapore, part C: planning and site selection. *Tunnelling and Underground Space Technology*, 11, 81–86.
Zou, D. & Kaiser, P.K. (1990). Determination of in situ stresses from excavation-induced stress changes. *Rock Mechanics and Rock Engineering*, 23(3), 167–184.

Rock Mechanics and Engineering

Volume 5: Surface and Underground Projects

Editor

Xia-Ting Feng
Institute of Rock and Soil Mechanics, Chinese Academy of Sciences,
State Key Laboratory of Geomechanics and Geotechnical Engineering,
Wuhan, China

CRC Press
Taylor & Francis Group
Boca Raton London New York Leiden

CRC Press is an imprint of the
Taylor & Francis Group, an **informa** business
A BALKEMA BOOK

CRC Press/Balkema is an imprint of the Taylor & Francis Group, an informa business

Typeset by Integra Software Services Private Ltd

Printed and bound in Great Britain by Antony Rowe (A CPI-group Company), Chippenham, Wiltshire

Library of Congress Cataloging-in-Publication Data

Names: Feng, Xia-Ting, editor.
Title: Rock mechanics and engineering / editor, Xia-Ting Feng, Institute of Rock and Soil Mechanics, Chinese Academy of Sciences, State Key Laboratory of Geomechanics and Geotechnical Engineering, Wuhan, China.
Description: Leiden, The Netherlands ; Boca Raton : CRC Press/Balkema, [2017]– | Includes bibliographical references and index. Contents: volume 1. Principles
Identifiers: LCCN 2016053708 (print) | LCCN 2017004736 (ebook) | ISBN 9781138027596 (hardcover : v. 1) | ISBN 9781315364261 (ebook : v. 1)
Subjects: LCSH: Rock mechanics.
Classification: LCC TA706 .R532 2017 (print) | LCC TA706 (ebook) | DDC 624.1/5132–dc23
LC record available at https://lccn.loc.gov/2016053708

Published by: CRC Press/Balkema
P.O. Box 11320, 2301 EH Leiden, The Netherlands
e-mail: Pub.NL@taylorandfrancis.com
www.crcpress.com – www.taylorandfrancis.com

ISBN: 978-1-138-02763-3 (Hardback)
ISBN: 978-1-315-36422-3 (eBook)

Cover photo: Mining equipment
Copyright: deadmeat243
Courtesy of: www.shutterstock.com

Contents

Chapter 6

Siah Bisheh powerhouse cavern design modification using observational method and back analysis

M. Sharifzadeh[1]*, R. Masoudi*[1] *& M. Ghorbani*[2]

[1]*Department of Mining Engineering, Curtin University, WASM Kalgoorlie, WA, Australia*

[2]*Department of Mining & Metallurgical Engineering, Amirkabir University of Technology, Tehran, Iran*

Abstract: The Siah Bisheh pumped storage powerhouse cavern with complex geometry, changeable geological formations and diverse geotechnical properties of rocks, is under construction on the Chalus River 125 km north of Tehran, Iran. The powerhouse cavern was located near the downstream (d/s) dam reservoir and its crown was more than 30 meters lower than the downstream (d/s) dam maximum lake level. After impounding of the d/s dam, the powerhouse region would be located under saturated conditions. Therefore long term stability assessment of the powerhouse cavern under saturated conditions was unavoidable. In this study displacement based direct back analysis using variable staggered grid optimization algorithm was applied and calibrated geomechanical properties of rocks, stress ratio and joints parameters were identified. The time dependent behavior of rock was tested at the laboratory and the creep test results were considered in the practical design. Numerical modeling results were in good agreement with measured displacements of extensometers which confirmed the numerical modeling accuracy and back analysis results. Then ordinary analysis of the powerhouse cavern under natural conditions using back analysis results were carried out. Results of the analysis showed that the powerhouse cavern was stable under natural conditions and existing support system had suitable efficiency and could effectively control displacements. Finally, the powerhouse cavern long term stability under saturated conditions was analyzed. Results of analysis showed that after d/s dam impounding, pore water pressure and uplift pressure in discontinuities around the powerhouse cavern would arise so the powerhouse cavern tended to have local failure around the region 2nd and 3rd instrumentation arrays in the middle of the powerhouse cavern. To obtain powerhouse long term stability, it was recommended to construct a cutoff curtain grouting around powerhouse cavern.

1 INTRODUCTION

The Siah Bisheh Pumped Storage project was located 125 km north of Tehran, Iran. The site can be reached in the vicinity of Siah Bisheh village on the main Chalus road, connecting Tehran with the Caspian Sea. Iran Water and Power Resources Development Company (IWPC) was the owner of the project. This plant was designed to produce a rated capacity of 4*260 = 1040 MW peak energy. In this project, two

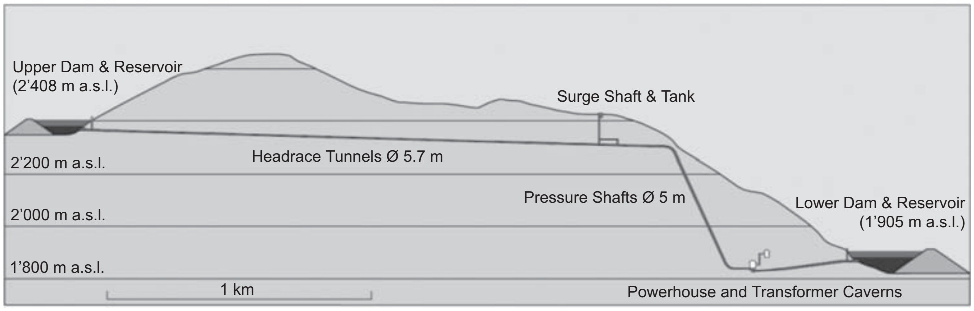

Figure 1 Schematic view of the Siah Bisheh CFRD dams and location of pumped storage powerhouse cavern (PHC) and transformer cavern (TRC).

concrete face rock fill dams (CFRD) were under construction in Chalus valley for the water storage. An underground power plant with complex geometry, changeable geological formations and diverse geotechnical properties of rocks, was under construction including powerhouse cavern, transformer cavern and guard gate cavern as well as an underground water way system in the mountain to accommodate all machinery and equipment for power generation and pumping (Figure 1).

The powerhouse cavern was located closed to the downstream (d/s) dam reservoir and its crown was more than 30 meters below the d/s dam maximum lake level. After impounding of the d/s dam, the underground powerhouse region would be located under saturated conditions. Therefore long term stability assessment of the powerhouse cavern under saturated conditions was unavoidable.

In order to do this assessment, displacement based direct back analysis using an optimization algorithm was applied and geomechanical properties of rocks, stress ratio and joints parameters were identified. Numerical modeling results were compared to actual measurements using extensometers and achieving good agreement between calculated displacements and measured displacements confirm the numerical modeling accuracy and back analysis results. Then direct analysis of the powerhouse cavern under natural conditions using back analysis results was carried out. Results of analysis showed that the powerhouse cavern was stable under natural conditions and predicted that the support system had suitable efficiency and could effectively control displacements. Finally, powerhouse cavern long term stability under saturated conditions was analyzed. Results of analysis showed that after d/s dam impounding, pore water pressure and uplift pressure in discontinuities around the powerhouse cavern would arise and had a tendency to local failure of powerhouse cavern in region 2nd and 3rd instrumentation arrays. To obtain powerhouse long term stability, it was recommended to construct a cutoff curtain (grouting) around the powerhouse cavern.

2 SIAH BISHEH POWERHOUSE CAVERN

Siah Bisheh powerhouse was constructed nearby Chalus River in the north part of Iran. The main purpose of the project was to compensate and stabilize the electricity in high and low electricity consumption period. The Powerhouse Cavern (PHC) with 131 m length, 24.5 m width and 46.5 m maximum height excavation and the Transformer Cavern (TRC) with 160.5 m length, 15.5 m width and 27 m height, were the main underground structures in this project. The other minor underground space which was constructed parallel to PHC was Guard Gate Cavern with 90.5 m length, 5.5 m width and 10.5 height. The powerhouse and transformer complex were constructed at a depth of approximately 250 m below surface. The total generating capacity of the scheme would be 1040 MW. The schematic three dimensional view of the Siah Bisheh project along with main caverns view was illustrated in Figure 2.

Siah Bisheh powerhouse cavern was located in fractured rock masses and the failure was mainly controlled by the discontinuity distribution. For cavern stability assessment, considering block size, pattern and spacing of discontinuities, three dimensional distinct element analysis was used.

3 GEOLOGY AND ENGINEERING GEOLOGY

3.1 Geology

The Siah Bisheh pumped storage project area lies in the southern part of the Paleozoic-Mesozoic Central Range of the alpine Alborz mountain chain, mainly folded and formed during the Alpine orogenic phase, with a NW-SE trend in the western parts and NE-SW in the eastern parts. Geomorphologically, Alborz is a young mountain range with deep and narrow valleys and active tectonics. The most important tectonic phenomenon of the Siah Bisheh area is the fault called the Main Thrust Fault (MTF), with a dip/dip direction of 78/028 and an almost E-W trend. The MTF has reverse mechanism. Meanwhile, the reverse fault of Chalus, which is parallel to the Chalus River in Siah Bisheh area, is another fault, which must be taken into consideration in terms of seismicity (Figure 3).

The rock sequences in the project area consist of massive limestones, detrital series (sandstones, shales) and volcanic rocks of Permian formations, Triassic dolomites and Jurassic (Lias) formations with black shales and sandstones. Several tectonic faults are crossing the project alignment. The Kandavan fault, a 15 km long and seismically active fault lies approx. 3 km south of the project area and builds the tectonic boundary between the Paleozoic-Mesozoic Central Range in the North and the Central Tertiary Zone in the South. The catchment areas of both reservoirs are of mountainous character with practically no vegetation. Based on the different strength of the geological formations, the slopes in the area of the upper dam and the headrace tunnel are generally smooth, while the lower project area lies within steep rock ridges built up by limestone and volcanic rocks.

Powerhouse and transformer caverns were constructed in the Permian Formation. Permian formations mainly consist of quartzitic sandstone, siltstone and shaly siltstone, dark and red shale and igneous rocks. Thickness of these layers varies from several centimeters to 3.5 meters (Lahmeyer & IWPC, 2005).

The attitude of the bedding planes had no considerable changes in dip and dip direction. There was uniform bedding throughout the powerhouse area with dip and dip direction of 55/195. It is noteworthy that during excavation of the powerhouse pilot gallery at chainages 40, 81 and 89 of the right wall, three shear zones, with an almost 40–50 centimeter thickness were encountered. All of these features were parallel

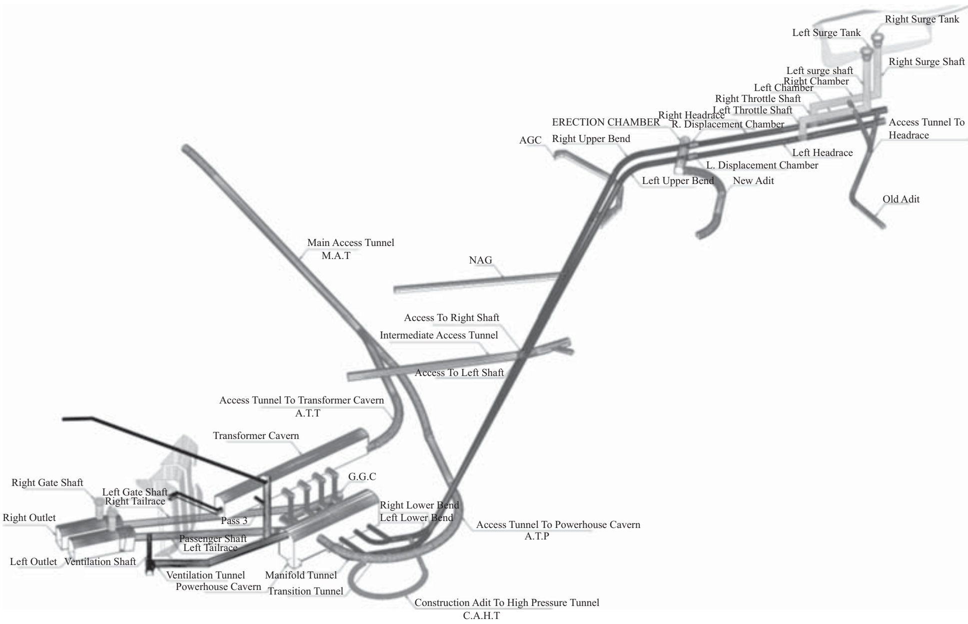

a) A 3-D model of Siah Bisheh underground excavations.

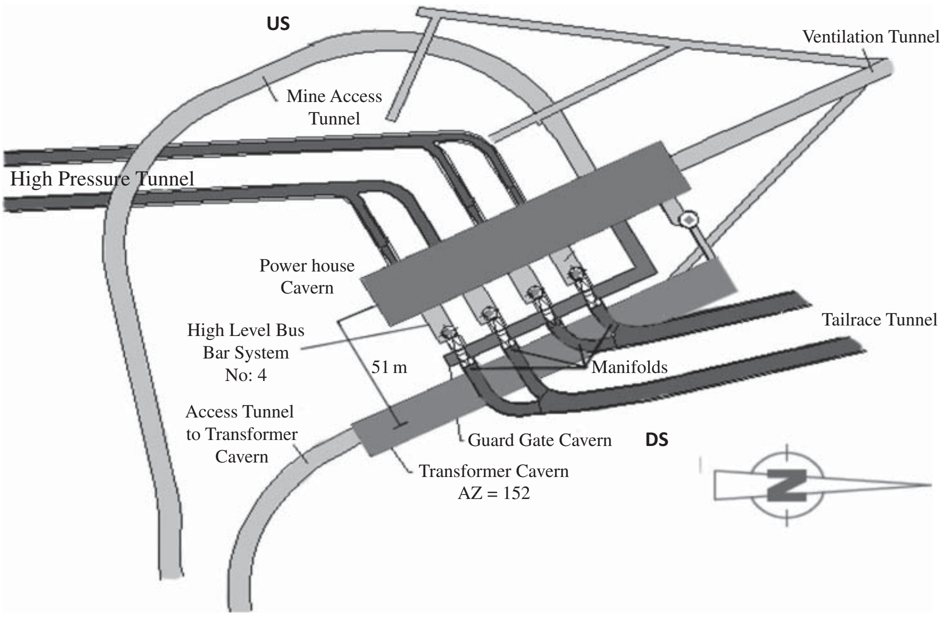

b) Plan view of the Siah Bisheh powerhouse caverns.

Figure 2 Schematic view of the Siah Bisheh pumped storage powerhouse, a) 3-D model of Siah Bisheh underground openings, b) Plan view of the Siah Bisheh powerhouse caverns.

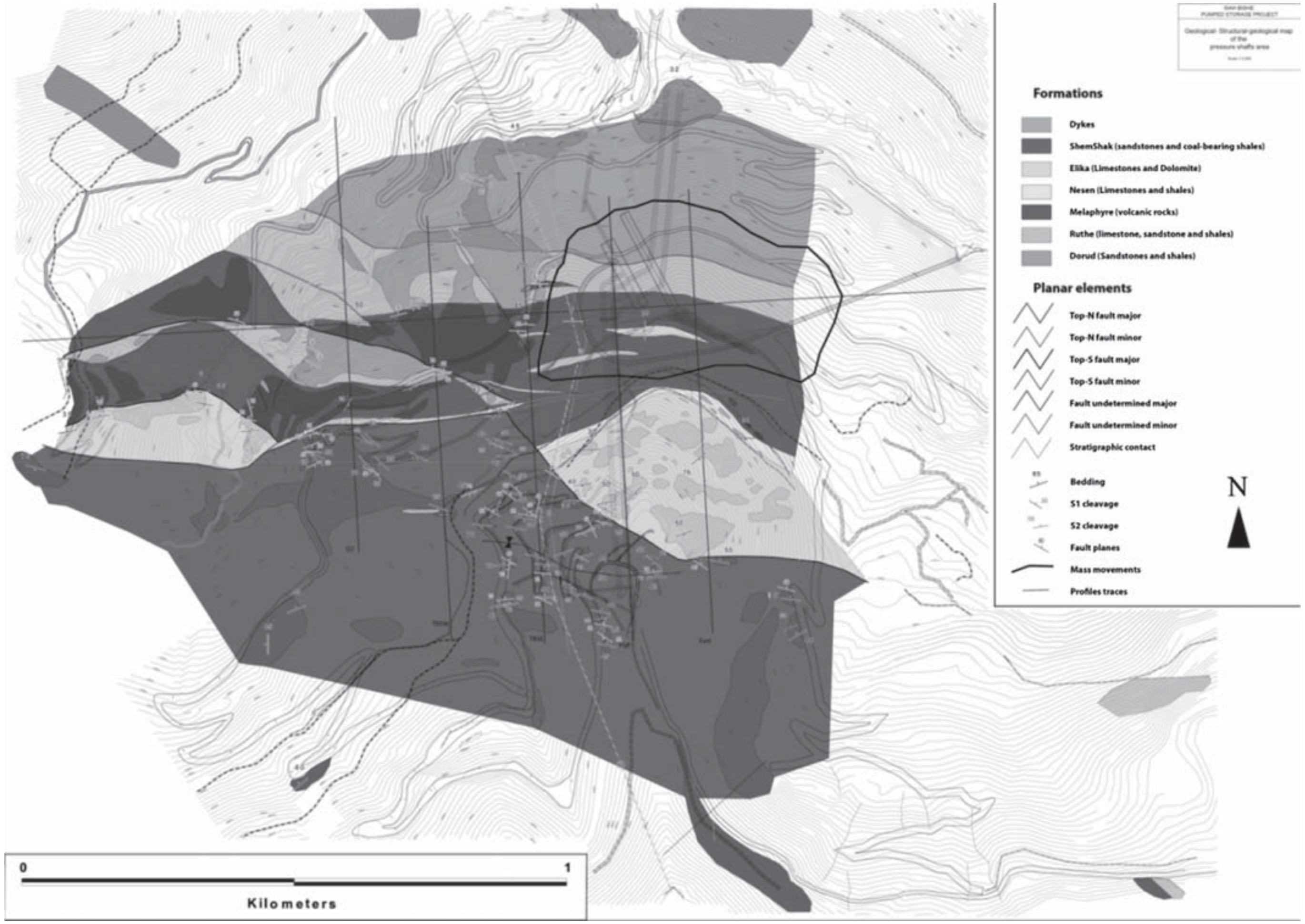

Figure 3 Geological map of Siah Bisheh Area (Lahmeyer & IWPC, 2005).

to the bedding planes. The azimuth of the powerhouse cavern was N152°E and none of the existing faults in the powerhouse area had crossed it and had an appropriate distance from it (Figure 3).

About 40 to 50 meters of the end of powerhouse cavern was completely made from igneous rock (Melaphyr) and the remaining part contained sedimentary rocks which was formed of a sequence of Quartzite Sandstone, Red Shale and Melaphyr. The influence of groundwater on the behavior of the rock mass surrounding a tunnel was very important and had to be taken into account in the estimation of potential tunneling problems. When the water is not drained it reduces the effective stresses and thus the shear strength along discontinuities and finally, in all cases, the strength of the rock mass. In addition, particularly important when dealing with shales, siltstones and similar rocks is that they are susceptible to changes in moisture content, which directly affect their strength. For long term stability analysis water effect is studied on rocks. Water effect on such rocks is mainly mechanical and pore pressure in intact rock and uplift pressure in discontinuities should be considered. Water absorption in hard rocks mainly doesn't change the strength parameters (cohesive strength and intrinsic friction angle). For these types of rocks, in all rock strength criteria, total stress should be replaced by effective stress and in rock joints, uplift pressure (u) is exerted to the joint surfaces, and uplift pressure should be subtracted from total normal stress (Sharifzadeh *et al.*, 2002).

3.2 Mechanical properties of rocks in the site

Considering the great length of the powerhouse cavern, a wide range and various types of geological properties were found as shown in the geological profile in Figure 4. Several laboratory and field tests and in situ measurements were performed to evaluate the mechanical properties of intact rock, rock joints and rock masses. The average results for mechanical and physical tests on intact rock are given in Table 1. The mechanical properties of rock joints based on test results are given in Table 2. Due to the fact that most of the geological properties could not be directly measured for this site, they had to be estimated by empirical and theoretical methods. For this purpose, the generalized Hoek-Brown failure criterion was utilized. The results showed various geological zones in the powerhouse cavern region and the area were initially divided into 2 zones. Likewise to determine the strength characteristics of the rock masses, the uniaxial compressive strength tests were carried out. Moreover the large flat jack tests and dilatometer tests were performed to determine the deformability characteristics of the rock masses. Using the field mapping the rock mass rating (RMR) value 45 at the related zones was obtained with fair rock class IV. The mechanical properties of different rock types adopted from rock mass classifications and in-situ experiments were illustrated in Table 3 (Lahmeyer & IWPC, 2005).

Discontinuity mapping program with 414 measurements was conducted in the exploratory vault adit indicating five major joint sets and one bedding plane. Rock mass consisted of bedding planes and 5 main joint sets in powerhouse area that were illustrated in Table 4. Based on surveying along the pilot, joints had different lengths of almost 3 to 10 meters and their spacings were between 200 and 600 millimeters (Lahmeyer & IWPC, 2005).

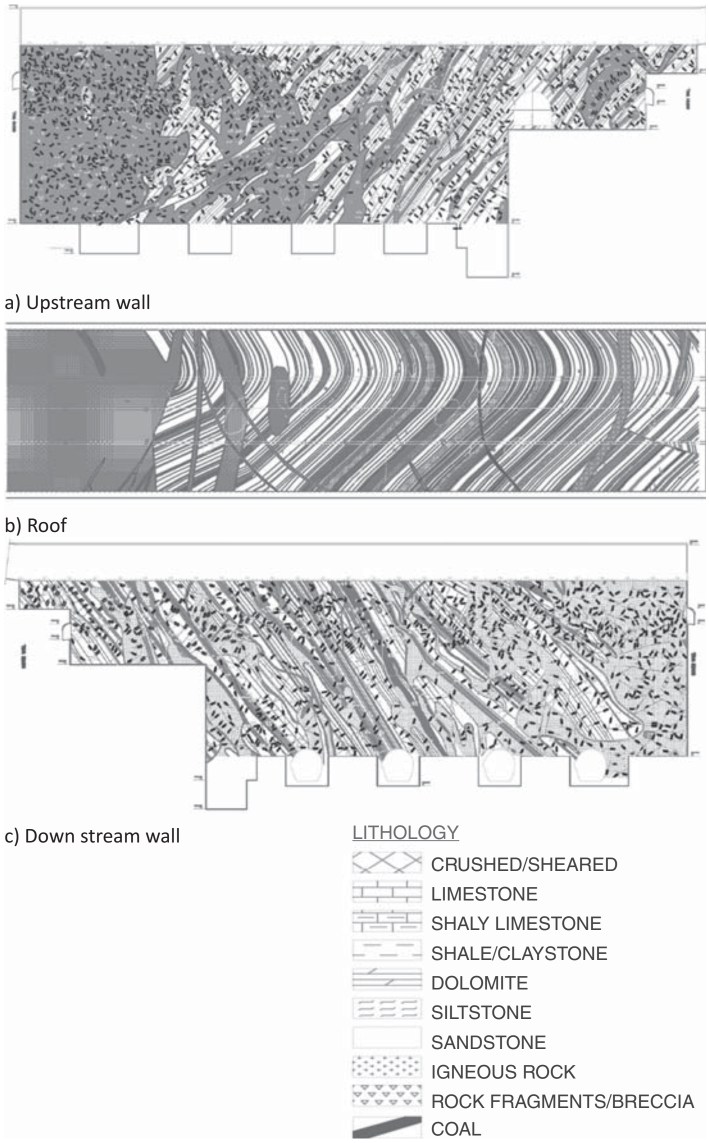

Figure 4 Geological profile of Siah Bisheh powerhouse cavern, a) Up stream wall, b) roof, and c) down-stream wall (Lahmeyer & IWPC, 2005).

The shear strength parameters of $\phi = 25°$ and $c = 0$ were assumed on bedding planes. Also based on the assumption of 10 cm thick shear bands and Young's Modulus of 2000 MP, the normal and shear stiffness of rock joints were estimated to be 20,000 and 7692 MPa/m, respectively.

The value of the horizontal to vertical stress ratio (k) was estimated equal to 1.1 based on field investigation.

Table 1 Mechanical and Physical properties of intact rocks (Lahmeyer & IWPC, 2005).

Parameters	*Quartzitic Sandstone*	*Red Shale*	*Melaphyr*
Dry Density (Kg/m3)	2810	2630	2900
Saturated Density (Kg/m3)	2970	2750	2920
Bulk Modulus (GPa)	8.33	5	16.67
Shear Modulus (GPa)	6.25	3	12.5
compressive strength (MPa)	85	50	100
Tensile Strength (MPa)	6	3	6
Friction Angle (°)	50	40	50
GSI	53	48	55
Mi	20	9	25

Table 2 Mechanical properties of rock joints (Lahmeyer & IWPC, 2005).

Item	*Value*
Normal Stiffness (MPa/m)	20000
Shear Stiffness (MPa/m)	7690
Cohesion (MPa)	0.5
Friction Angle (°)	30
Tensile Strength (MPa)	0

Table 3 Rock Mass Shear Strength according to Hoek and Brown 2001 and flat jack tests (Lahmeyer & IWPC, 2005).

Rock Type	*GSI*	*UCS (MPa)*	*mi*	*Disturbance Factor = 0*				*Disturbance Factor = 0.7*				*Flat Jack Test*	
				E (GPa)	*cmσ (MPa)*	*C (MPa)*	*φ (°)*	*E (GPa)*	*cmσ (MPa)*	*C (MPa)*	*φ (°)*	*E (GPa)*	*ν*
Quartzitic Sandstone Red	53	85	20	11	22	1.6	53	7.1	14	1.1	46	15	0.2
Shale	48	50	9	6.3	7.9	0.98	41	4.1	4.7	0.66	32	7.5	0.25

Table 4 Discontinuity orientations in the powerhouse cavern area (Lahmeyer & IWPC, 2005).

Discontinuity	*Dip Direction [°]*	*Dip [°]*
Bedding	195	55
Joint J1	030	56
Joint J1–1	018	81
Joint J1–2	009	66
Joint J1–3	305	80
Joint J2	078	82

3.3 Time dependent behavior of rocks

The understanding of time dependent effects or creep behavior of rocks adjacent to the cavern and its influence on long-term stability is extremely important. Increasing pressure on support system due to creep behavior of rock is one of the most important issues in underground structures with weak surrounding rock mass (Barla, 2001).

The time dependent deformation of rocks has significant impact on stability of underground structures, such as nuclear waste storage facilities, tunnels and powerhouse caverns. To evaluate the stability of the underground structures and design their support systems, time dependent deformations should be highly considered (Shalabi, 2004; Tsai, 2008; Sharifzadeh *et al.*, 2013). Therefore time dependent behavior of underground structures and predicting the long-term behavior of them is assumed in special places. Predicting the time dependent behavior of underground structures is not an easy task, because it needs a reliable constitutive model which can interpret creep phenomena (Boidy & Pellet, 2000). It is also well known that rock property measurements based on laboratory tests cannot be extrapolated directly to field scale without due precaution (Boidy, Bouvard & Pellet, 2002) because the mechanical properties of jointed rock mass are strongly dependent on the properties and geometry of joints. Therefore, it is essential to use numerical analysis for simulating time dependent behavior of rock mass and compare them with measurements obtained on the monitored cavern over a long period.

Several tri-axial creep tests were performed on rock specimens of the cavern site for estimating the time dependent behavior of rock around the cavern. The Axial strain – time curves under different deviatoric stress for a typical specimen (test 1) were shown in Figure 5. The creep tests and in situ measurements were used to estimate parameters of power constitutive creep model which was able to model the primary and secondary creep regions of rock masses (Nadimi *et al.*, 2010).

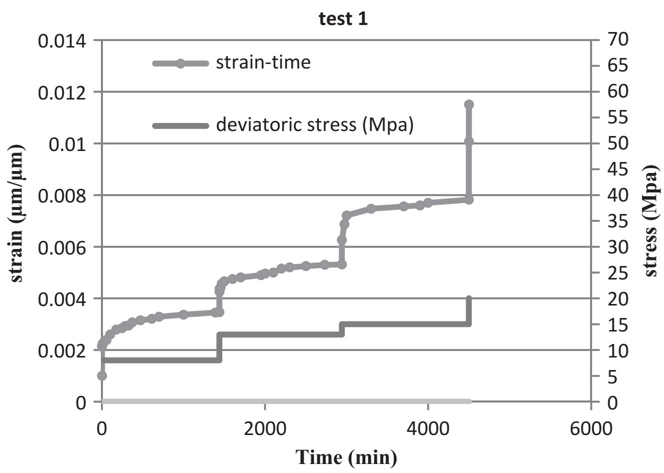

Figure 5 Axial strain – time plots of tri-axial creep test results under different deviatoric stress (Nadimi *et al.*, 2010).

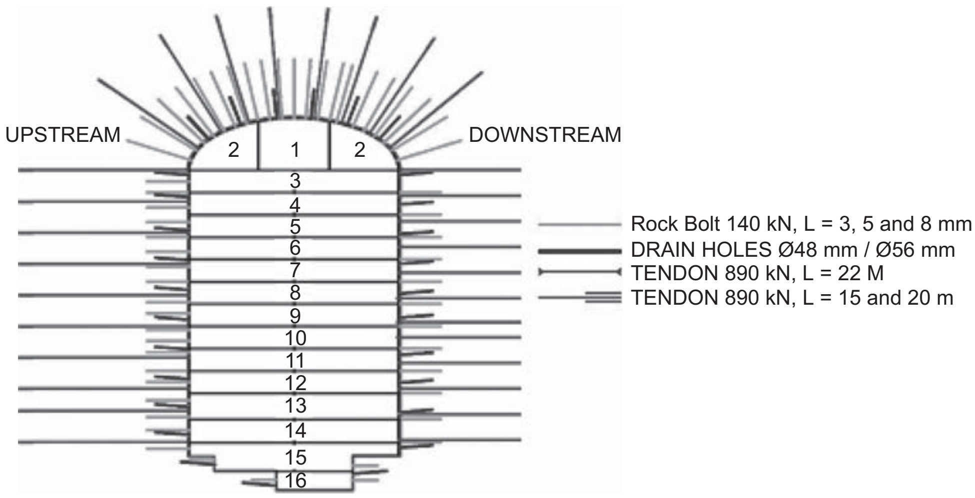

Figure 6 Excavation sequence and typical support system installed in the powerhouse cavern and excavation stages with drainage holes at roof and sidewalls (Sharifzadeh *et al.*, 2009).

4 EXCAVATION AND SUPPORT SYSTEM

All caverns were excavated using the New Austrian Tunneling Method (NATM). For excavation of the powerhouse cavern, at first a pilot was drilled at the center of the crown (sequence 1 in Figure 6) and then slashing of the crown was carried out (sequence 1 in Figure 6). After that, benching was performed with 3 meters' depth per stage which were excavated until the powerhouse floor (sequence 3 to 16 in Figure 6) (Ghorbani & Sharifzadeh, 2009).

The support system in the powerhouse cavern consists of shotcrete with wire mesh (20 cm in side walls and 25 cm in roof), fully grouted rock bolts (temporary support system) and double corrosion protected tendons (permanent support system). After each cycle of blasting, the exposed roof and walls were immediately shotcreted. Bolt installation was sometimes delayed. Systematically drainage holes 4 m in length and a 4 × 4 m spacing pattern were performed at roof and side walls of the powerhouse cavern (Figure 6) (Ghorbani & Sharifzadeh, 2009).

In Table 5 physical properties of shotcrete and interface with the rock and in Table 6 parameters of tendons were presented.

5 INSTRUMENTATION AND MONITORING SYSTEM OF CAVERN

Monitoring is the systematic collection of information as the project progresses. It is aimed at improving the safety, efficiency and design modification of a project which can be an invaluable tool to provide a useful base for parameter evaluation.

Six instrumentation arrays were set up along the axis of the powerhouse cavern at chainages of 26, 49, 67, 87,105 and 121. These arrays consist of multiple point borehole rod extensometers in the roof and sidewalls, convergence points, piezometers as

Table 5 Physical properties of the shotcrete and the interface with the rock (Ghorbani & Sharifzadeh, 2009).

Shotcrete	
Density (Kg/m3)	2400
Elastic modulus (GPa)	21
Poisson's ratio	0.2
compressive strength (MPa)	40
Tensile Strength (MPa)	20
Interface between the shotcrete and the rock	
Cohesion (MPa)	2.5
Friction Angle (°)	35
Dilation angle (°)	10
Normal Stiffness (GPa/m)	10
Shear Stiffness (GPa/m)	10

Table 6 Properties of tendons used in modeling (Ghorbani & Sharifzadeh, 2009).

Support type	*Diameter (mm)*	*Young's modulus (GPa)*	*Ultimate yield load (KN)*	*Kbond (GN/m/m)*	*Sbond (MN/m)*
Tendon	26.5	200	300	6.41	2.01
Tendon	47	200	890	6.03	3.77
Tendon	63.5	200	1540	6.79	4.59

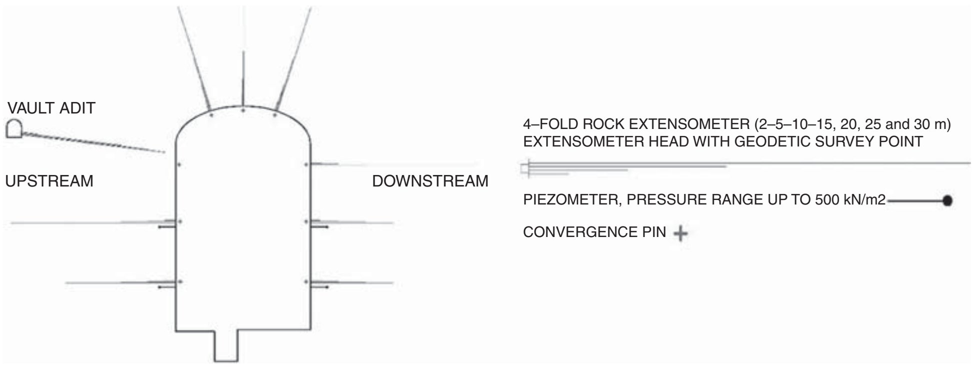

Figure 7 Typical instrumentation array installed in the powerhouse cavern (chainage 67) (Sharifzadeh *et al.*, 2009).

well as load cells on selected cable tendons. It is worth mentioning that due to delay in installation of extensometers, some part of displacement data was lost and should be considered in the calculation. A typical instrumentation section of the powerhouse cavern is illustrated in Figure 7 (Sharifzadeh *et al.*, 2009).

6 CONTINUUM-DISCONTINUUM NUMERICAL MODELING OF CAVERN

6.1 Numerical modeling of powerhouse cavern

There are two approaches available in jointed rock modeling, one is the continuum and the other is the discontinuum approach. The use of continuum modeling in tunnel engineering makes it essential to simulate the rock mass response to excavation by introducing an equivalent continuum.

The most common way to solve this problem is to scale the intact rock properties down to the rock mass properties by using empirically defined relationships such as those given by Brady and Brown (2004).

Rock joints and discontinuities in rock mass play a key role in the response of a tunnel to excavation, *i.e.* joints can create loose blocks near the tunnel profile and cause local instability; joints weaken the rock and enlarge the displacement zone caused by excavation; joints change the water flow system in the vicinity of the excavation. The use of discontinuum modeling has been gaining progressive attention in tunnel engineering mainly through the use of the UDEC and 3DEC codes, for 2D and 3D discontinuum modeling respectively (Itasca, 2007).

The Siah Bisheh powerhouse cavern was located in discontinuous media and considering low level in situ stress, the failure of rock mass was mainly controlled by the discontinuity distribution. In this study considering block size, pattern and spacing of discontinuities, three-dimensional distinct element analysis was performed.

Considering 5 joint sets, with joint spacing 12, 14 and 17cm plus bedding planes, low overburden (maximum 250 m), uniformity in monitoring data and various lithology and also bad type rock in most monitoring sections, continuum function is likely. Therefore it seemed modeling in both continuum and discontinuum was essential. In order to numerically model the Siah Bisheh underground openings, PHASE2 and 3DEC codes were utilized. At first two 2-D models were prepared in the chainages 49m and 105m of the powerhouse cavern using PHASE2. Then a 3D model was constructed through the 3DEC code. Figure 8 shows the flowchart of back analysis of the powerhouse cavern under natural conditions.

The Mohr-Coulomb plasticity model was assigned as constitutive model for both continuum and discontinuum analysis as constitutive mechanical model. The value of stress ratio (k) was determined based on field investigation to equal 1.1.

The minimization of the error function alone, does not always guarantee a correct back analysis. The qualitative trend of the displacements on the wall of the excavations should be the same in the calculation as in reality, as a confirmation of the validity of the calculation model and of the simplified assumed hypotheses. Then direct analysis of the powerhouse cavern under natural conditions (underground water table 1880 m) using these optimized parameters was implemented and stability of the powerhouse and its support system was assessed. Finally, for long term stability assessment of the powerhouse cavern under saturated conditions, the underground water table in the model was raised gradually to final elevation (1905 m). Considering instability problems especially in the area of 2nd and 3rd instrumentation array in saturated conditions, a cut-off curtain as an efficient method to guarantee long term stability was proposed.

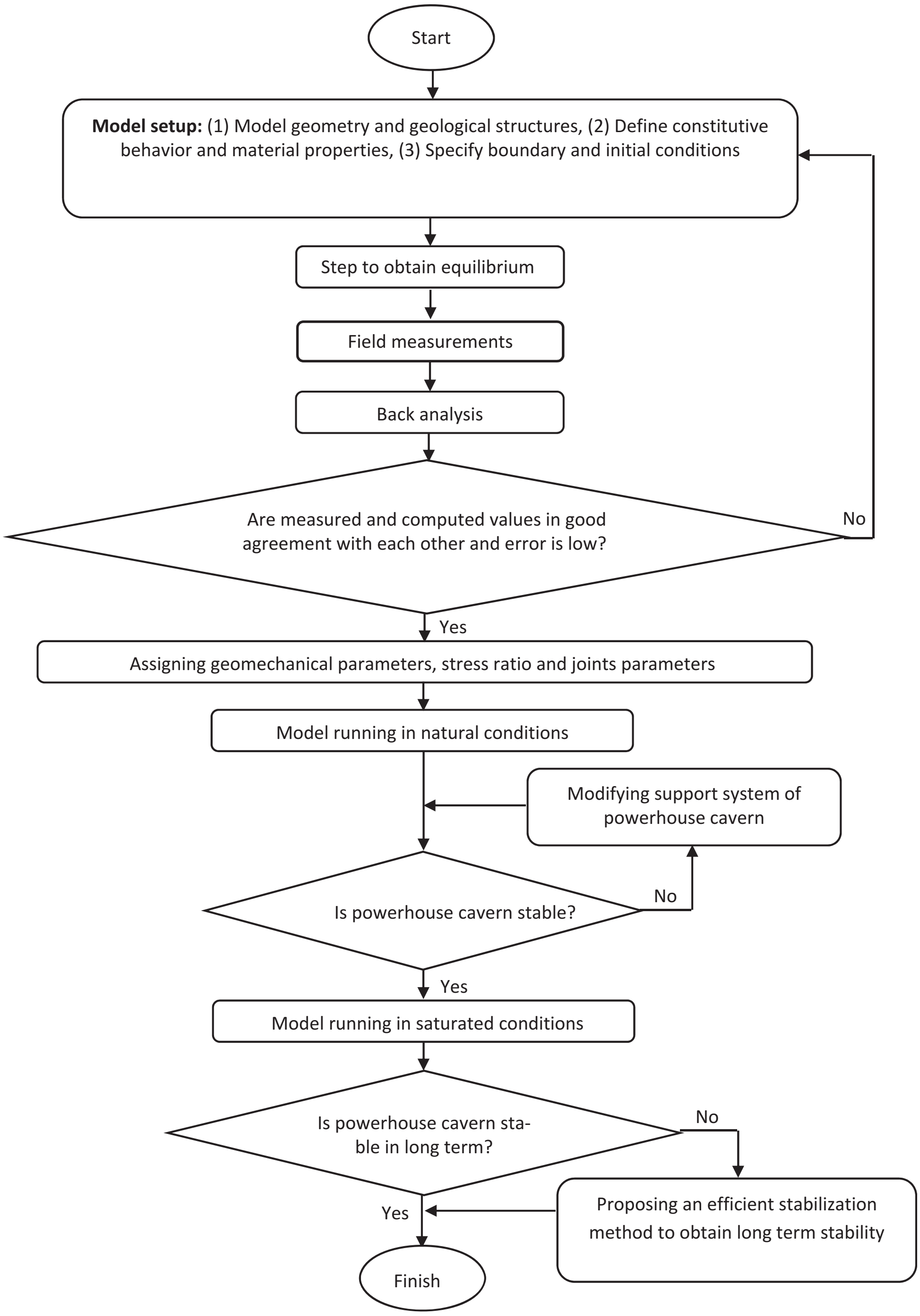

Figure 8 Flow chart of back analysis and stability analysis under natural and saturated conditions (Ghorbani & Sharifzadeh, 2009).

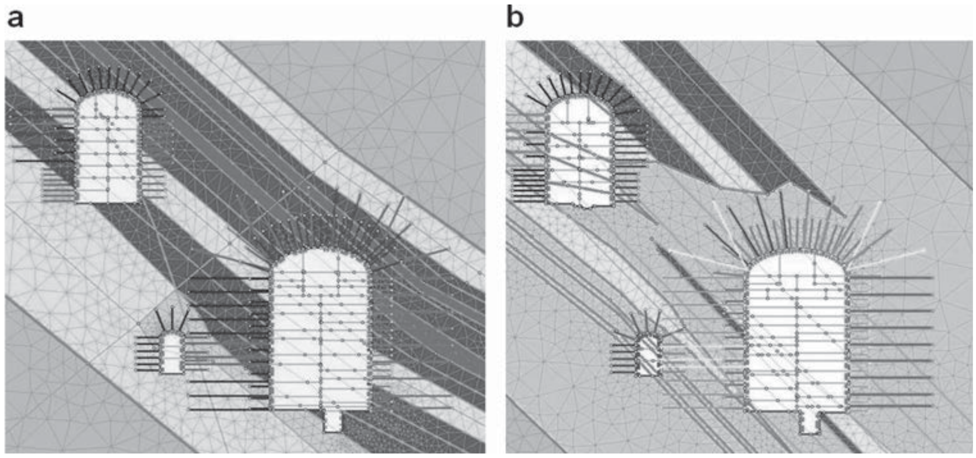

Figure 9 (a) Continuum model for monitoring section 2 (sedimentary area), and (b) Continuum model for monitoring section 5 (melaphyry area) – PHASE2 (Yazdani *et al.*, 2011).

6.2 Continuum modeling

The geological condition along the caverns was different so as built geology models for two separate monitoring sections of the PHC were made. The models include the final shape of caverns, the as-built excavation sequence, as-built support measures inclusive of their respective time of installation and installation time of monitoring instruments. Also geological model had to be simplified, considering the great number of thin layers, which changed partially in the decimeter range could not be taken over into the numerical model. Also the contacts between different lithological units were assumed, as joints (Yazdani *et al.*, 2011) (Figure 9).

6.3 Discontinuum modeling

The Siah Bisheh powerhouse cavern is located in discontinuous media and the failure of rock mass is mainly controlled by the discontinuity distribution. In this study considering block size, pattern and spacing of discontinuities, three-dimensional distinct element analysis was performed.

Siah Bisheh underground openings were under construction in rocks which are formed mainly from quartzite sandstone, red shale and igneous rocks (mainly classified as hard and competent rocks). The powerhouse cavern was constructed beneath the underground water table. Therefore for long term stability analysis the water effect was studied on these rocks and underground water table was exerted in the discontinuum model. Water's effect on such rocks is mainly mechanical and pore pressure in intact rock and uplift pressure in discontinuities should be considered. Water absorption in hard rocks mainly doesn't change the strength parameters (cohesive strength and intrinsic friction angle). For these types of rocks, in all rock strength criteria, total stress should be replaced by effective stress and in rock joints,

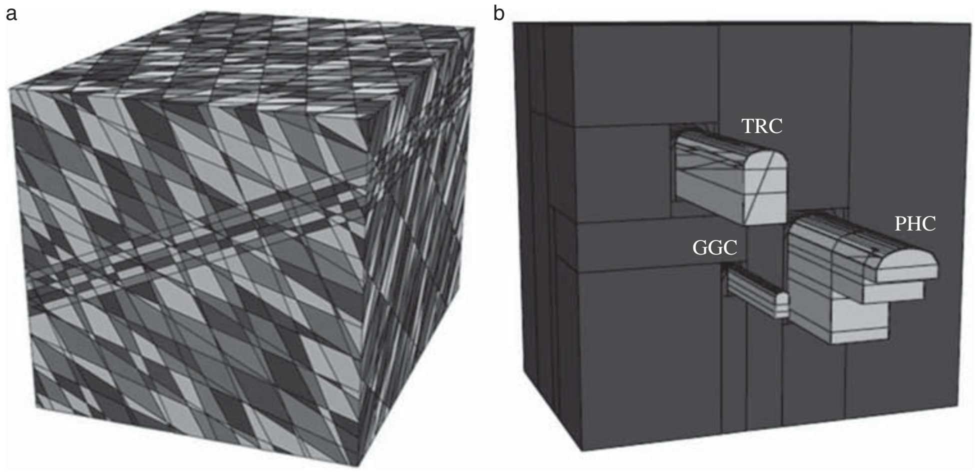

Figure 10 (a) 3D Model geometry with discontinuities, bedding planes and underground water table; and (b) location of powerhouse, transformer and guard gate caverns in discontinuum model-3DEC (Sharifzadeh *et al.*, 2007).

uplift pressure (u) was exerted on the joint surfaces, and uplift pressure was subtracted from total normal stress (Sharifzadeh, 2002) (Figure 10).

After model setup and steps to equilibrium state, direct back analysis of the powerhouse cavern using extensometer results was carried out and calibrated geomechanical properties of rocks, stress ratio and joints parameters were identified.

6.4 Time dependent numerical modeling

There are eight power models in 3DEC software for simulating time dependent behavior of structures. Based on the creep tests and in situ measurements power model was used for simulating the time dependent behavior of the cavern. The standard form of this law in 3DEC is as follow:

$$\dot{\varepsilon}_{cr} = A\overline{\sigma}^{n} \tag{1}$$

Where $\dot{\varepsilon}_{cr}$ is the creep rate, A and n are material properties, $\overline{\sigma} = \left(\frac{3}{2}\right)^{1/2}(\sigma_{ij}^{d}\ \sigma_{ij}^{d})^{1/2}$ with σ_{ij}^{d} being the deviatoric part of σ_{ij}. The deviatoric stress increments are given by;

$$\Delta\sigma_{ij}^{d} = 2G(\dot{\sigma}_{ij}^{d} - \dot{\sigma}_{ij}^{c})\Delta t \tag{2}$$

Where G is shear modulus, and $\dot{\sigma}_{ij}^{d}$ is the deviatoric part of the strain-rate tensor.

For time dependent analysis the system is required to be always in mechanical equilibrium, the time-dependent stress increment must not be too large compared to strain-dependent stress increment; otherwise, out of balance force will rapidly become large, and inertial effects may affect the solution. For the power law, the viscosity may be estimated as the ratio of stress magnitude $\overline{\sigma}$ to the creep rate, $\dot{\varepsilon}_{cr}$. Using Equation 1, the maximum creep timestep is;

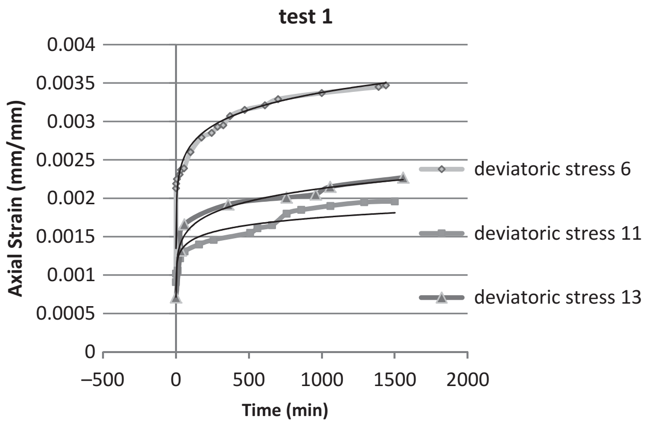

Figure 11 Axial strain – time plots for tri-axial creep tests and fitting curves for specimen 1 (Nadimi *et al.*, 2010).

$$\Delta t_{Max}^{cr} = \frac{\overline{\sigma}^{-1-n}}{AG} \tag{3}$$

Where A is power law constant; and G is elastic shear modulus (Itasca, 2007).

Triaxial creep tests were conducted on rock samples which were prepared from extensometer boreholes. The samples were red shale and quartzite sandstone and they were dry with 54 mm diameter and 110–120 mm high. The quartzite sandstone samples had high compression strength and very little creep strain; therefore triaxial creep tests of shale samples with more creep prone were used to determine power model parameters. As shown in Figure 11, the creep tests were conducted in several steps and different deviatoric stresses (Nadimi *et al.*, 2010).

7 BACK ANALYSIS OF ROCK MASS AND DISCONTINUITY PROPERTIES

Back analysis techniques as a practical engineering tool are nowadays often used in geotechnical engineering problems for determining the unknown geomechanical parameters, system geometry and boundary or initial conditions using field measurements of displacements, strains or stresses performed during excavation or construction works (Sakurai, 1993).

The direct approach employs the trial values of the unknown parameters as input data in the stress analysis algorithm, until the discrepancy between measurements and corresponding quantities obtained from a numerical analysis is minimized (Cividini *et al.*, 1981; Feng & Zhao, 2004). Trial values should be defined based on an algorithm which follows all combinations of different parameters until the optimum values of all variables are determined. This classic approach is relatively simple and suitable for parameters that are independent. While application of this method for parameters that influence or interact with one another is restricted. This method could successfully search the optimal values of parameters regardless of their initial values. Obviously it is better that variation of parameters take in a valid interval which has obtained from laboratory and field testing combined to experimental relations (Gioda & Locatelli, 1999; Oreste, 2005).

In this study displacement based direct back analysis using variable staggered grid optimization algorithm was applied. Direct formulation was very flexible and applying such a procedure for complex constitutive models was appropriate. Furthermore, development of the direct back analysis code was much less difficult than development of the code based on an inverse algorithm. The only work is appending an existing program with a module. For this purpose a Fish function was written to do the minimization of errors between measured and computed values as follows:

$$\varepsilon(p) = \sum_{i=0}^{n} \left(\frac{u_i^m(p) - u_i}{u_i} \right)^2 \tag{4}$$

Where u_i and $u_i^m(P)$, $i = 1, 2, ..., n$ were the measured and corresponding numerical results, respectively and n was the number of measured points. Obviously, $u_i^m(P)$ depends on the unknown model parameters collected in the vector P. Here we used a normalized error function to decrease the effect of measurement error.

As was mentioned before, the end part of cavern consisted of igneous rocks and for this reason to back analysis geomechanical properties of these parts two different error functions based on an equation (Swoboda *et al.*, 1999) using results of extensometers at each part were developed. The measurement results were processed before using them in back analysis. Wrong displacements due to error in installation, reading and recording of data or inaccurate performance of instruments were eliminated. Therefore after assessment of extensometer results, finally 150 displacement data among 208 displacement data were selected for back analysis. The results of back analysis for the Melaphyry section and sedimentary part are presented in Tables 7 and 8, respectively. Results showed that elastic modulus has the highest effect and Poisson's ratio, friction angle and cohesion had respectively the least effect on error function and thus on displacement values.

The relationship between the horizontal and vertical stresses in the rock mass (k) was more difficult to estimate from the preliminary investigations and it relied closely on

Table 7 Results of back analysis for Melaphyry section (Ghorbani & Sharifzadeh, 2009).

Constant Parameters	C = 2.5 MPa, ϕ = 43°, υ = 0.22, K = 1.1, β = 0°			
Young's modulus (MPa)	14	15	16	17
Error (%)	2.4410	2.1289	1.6571	1.9964
Constant Parameters	E = 16 GPa, ϕ = 43°, υ = 0.22, K = 1.1, β = 0°			
Cohesion (MPa)	2	2.5	3	3.5
Error (%)	1.7583	1.6571	1.5137	1.6852
Constant Parameters	E = 16 GPa, C = 3 MPa, υ = 0.22, K = 1.1, β = 0°			
Friction Angle (°)	40	41	42	43
Error (%)	1.3874	1.261	1.4023	1.5137

Table 8 Results of back analysis in sedimentary part (Ghorbani & Sharifzadeh, 2009).

Constant Parameters	C = 1.5 MPa, ϕ = 40°, υ = 0.25, K = 1.1, β = 0°				
Young's modulus (MPa)	6	7	8	9	10
Error (%)	5.5103	4.8061	4.3677	3.9664	4.4739
Constant Parameters	E = 9 GPa, ϕ = 40°, υ = 0.25, K = 1.1, β = 0°				
Cohesion (MPa)	1.25	1.5	1.75	2	2.25
Error (%)	4.2154	3.9664	3.6532	3.8912	4.2079
Constant Parameters	E = 9 GPa, C = 1.75 MPa, υ = 0.25, K = 1.1, β = 0°				
Friction Angle (°)	37	38	39	40	–
Error (%)	3.4277	3.2238	3.4816	3.6532	–
Constant Parameters	E = 9 GPa, C = 1.75 MPa, ϕ = 38°, K = 1.1, β = 0°				
Poisson's ratio	0.23	0.24	0.25	–	–
Error (%)	3.2351	3.1907	3.2238	–	–

Table 9 Results of stress ratio back analysis (Ghorbani & Sharifzadeh, 2009).

Melaphyry section parameters	E = 16 GPa, υ = 0.22, C = 3 MPa, ϕ = 41°, β = 0°		
Sedimentary part parameters	E = 9 GPa, υ = 0.24, C = 1.75 MPa, ϕ = 38°, β = 0°		
Stress ratio (k)	1.1	1.15	1.2
Total percent (%)	3.4238	3.7993	4.3486

back analysis results. For this purpose after identification of geomechanical properties for the Melaphyry section and sedimentary part, back analysis for stress ratio was carried out and results are shown in Table 9. Results also showed that stress ratio had a great effect on error function and by increasing it, values of displacements in the powerhouse wall had been increased.

Considering discontinuum modeling of powerhouse caverns and the effect of discontinuities parameters on numerical modeling results, back analysis was carried out to find strength of discontinuities and stiffness properties (Table 10). Results show that the parameters of discontinuities especially joints' normal and shear stiffness have a remarkable influence on the value of error function.

About 40 to 50 meters of the end of powerhouse cavern was igneous rock (Melaphyr) and the remainder was the sedimentary part which comprised a the sequence of Quartzite Sandstone, Red Shale, Mylonite and Melaphyr. For this reason to obtain back analysis geomechanical properties of these parts two different error functions based on formula (1) using results of extensometers installed in each part were developed in discontinuum model. But in the continuum method two different models in the chainages of 49m (sedimentary part) and 105m (melaphyry section) of the powerhouse cavern were prepared and back analysis was performed separately for these two models.

The minimization of the error function alone, does not always guarantee a correct back analysis. The qualitative trend of the displacements on the wall and vault of the

Table 10 Results of back analysis for joints parameters (Ghorbani & Sharifzadeh, 2009).

Melaphyr parameters	E = 16 GPa, υ = 0.22, C = 3 MPa, ϕ = 41°, β = 0°, K = 1.1			
Sedimentary part parameters	E = 9 GPa, υ = 0.24, C = 1.75 MPa, ϕ = 38°, β = 0°, K = 1.1			
Joint parameters	C = 0.5 MPa, ϕ = 30°			
Normal Stiffness (GPa/m)	10	20	30	40
Shear Stiffness (GPa/m)	2	7.69	10	30
Total percent (%)	5.6222	3.4238	3.0992	5.3968
Joint parameters	JKn = 30 GPa/m, JKs = 10 GPa/m, ϕ = 30°			
Cohesion (MPa)	0.4	0.5	0.6	–
Total percent (%)	2.7533	3.0992	3.6049	–
Joint parameters	JKn = 30 GPa/m, JKs = 10 GPa/m, C = 0.4 MPa			
Friction Angle (°)	25	30	35	–
Total percent (%)	2.9527	2.7533	3.1161	–

excavations should be similarly the same in the calculation as in reality, as a confirmation of the validity of the calculation model and of the simplified assumed hypotheses.

In tables 7 and 8, final results of back analysis for Melaphyry section and sedimentary part for both continuum and discontinuum models are presented. In both continuum and discontinuum models results show that elastic modulus has the highest effect and Poisson's ratio, friction angle and cohesion have respectively the least effect on error function and thus on displacement values.

Considering continuum and discontinuum modeling of powerhouse caverns and the effect of joint parameters on numerical modeling results, back analysis was carried out to find joint strength and stiffness properties (Table 8). Results in continuum models showed that friction angle had a major impact on deformations of the powerhouse cavern. Also results in the discontinuum model showed that joint parameters especially joints' normal and shear stiffness had a remarkable influence on error function values.

8 DIRECT STABILITY ANALYSIS OF POWERHOUSE CAVERN UNDER DIFFERENT CONDITIONS

8.1 Natural conditions

After finding calibrated model values for geomechanical properties of rocks, stress ratio and discontinuity parameters, direct analysis of the powerhouse cavern under natural conditions with existing underground water table (1880 m) were carried out.

In order to compare the results of analysis with measured values, deformations were utilized in several locations of the powerhouse cavern which were adjacent to extensometers of 3rd instrumentation array (Table 11). This array was very important due to presence of many shear zones in this region. Instrumentation showed large displacement and increase in the load of load cells in this array. As shown in Table 11, computed results

Table 11 Comparison between computed and measured values of displacements in 3rd instrumentation array (millimeter) (Ghorbani & Sharifzadeh, 2009).

		Measured values using Extensometers	*Computed values in natural conditions*
Upstream wall	Installed from Vault Adit (EXT.1)	18	21.2
	EL. 1858 (EXT.2)	59.06	64.2
	EL. 1847 (EXT.3)	24.5	23.17
Roof	Upstream roof (EXT.4)	11.73	16.23
	Roof center (EXT.5)	17.22	17.4
	Downstream roof (EXT.6)	4.7	14.68
Downstream wall	EL. 1858 (EXT.7)	11.3	21.18
	EL. 1858 (EXT.8)	45.6	48.1
	EL. 1858 (EXT.9)	16.98	23.26

were in good agreement with measured values. Because of delay in the installation and reading of extensometers, the first part of the deformations was lost; therefore measured data showed lower values compared to calculated results. Generally numerical modeling showed better consistency with reality. Figure 12 shows a cross section of displacement vectors in natural conditions. As seen in Figure 12, the powerhouse was stable and the existing support system had a good efficiency to control displacements. The maximum displacement of the powerhouse cavern which would occur in upstream wall equaled 6.51 cm. Transformer and guard gate caverns were both in stable condition. It is

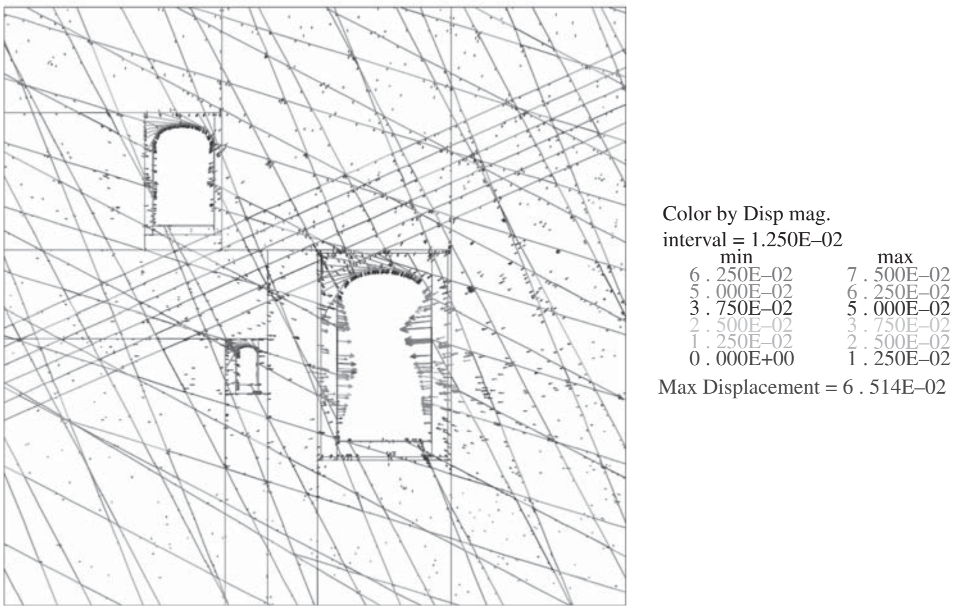

Figure 12 A cross section of displacement vectors (in m) in natural conditions (groundwater level 1880) (Ghorbani & Sharifzadeh, 2009).

noteworthy that the drainage system around the powerhouse cavern was not considered in the analysis and considering it would guarantee its stability under natural conditions.

To verify numerical simulation, displacements obtained by numerical method were compared with those obtained from direct measurements. Displacement measurements within the rock mass had been recorded in borehole extensometers installed over the periphery of the cavern. There were three types of extensometers installed in the cavern; the extensometers 30m in length, gave the displacement inside rock at 2 m, 5 m, 10 m and 30 m, the extensometers 25m in length, gave the displacement inside rock at 2 m, 5 m, 10 m and 25 m, and the extensometers 20m in length, gave the displacement inside rock at 2 m, 5 m, 10 m and 20 m from the crown of the cavern. The comparison of the measured and computed displacement-time curves showed that the power law model parameters of the data set No. 1(b) in Tab. 11 had better simulation results than another set of parameters (see Figure 11).

Figure 13 shows the failure zone around the powerhouse cavern in natural conditions. Proportionate to induced stress due to cavern excavations and rock strength, rock mass in some areas around the powerhouse cavern was in a failure condition. As seen in Figure 13, the type of failure in the powerhouse cavern was tension and the most critical situation was in the upstream wall. Depths of failure zone in upstream and downstream walls were respectively 6 m and 5 m. All design activities must be taken to prevent tension failure zone development. As shown in Figure 13, the pillars between the powerhouse and guard gate caverns were stable and their stress fields would not influence each other.

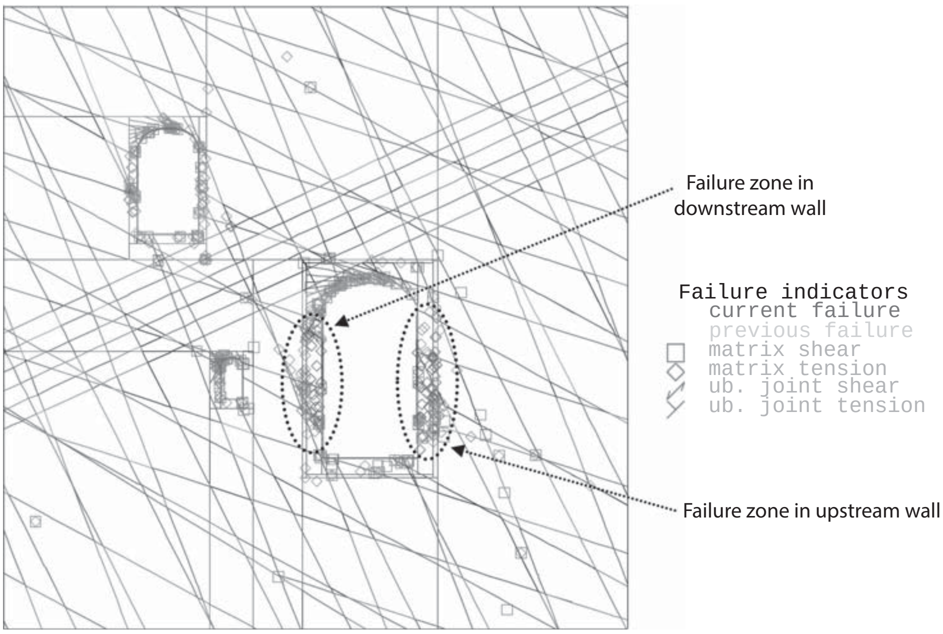

Figure 13 A cross section of failure zone around caverns in natural conditions (Ghorbani & Sharifzadeh, 2009).

8.2 Saturated conditions

After d/s dam impounding and increasing the level of the underground water table, the powerhouse cavern would be 30 m below the maximum lake level of the d/s dam. For stability analysis under such conditions the underground water table was raised gradually in five steps with 5 m intervals up to maximum level and results of analysis under fully saturated conditions were used to predict rate of displacements and efficiency of the support system. To calculate the value of uplift pressure in joints around the 3rd instrumentation array in the powerhouse cavern a Fish function was developed. This program found the nearest zone to the joint surface considering introduced points which were corresponded to extensometer installation points in the crown center, upstream and downstream walls and then draws the uplift pressure graphs based on solving time step for the model.

Figure 14 shows a cross section of displacement vectors in saturated conditions. As seen in Figure 14, powerhouse cavern walls in the chainage of the 2nd and 3rd instrumentation arrays were unstable and displacements were higher than permissible values. Powerhouse cavern roof displacements were in reasonable range and transformer and guard gate caverns were in good stable condition. The values of displacements in the downstream wall were higher than upstream wall. There were 3 reasons for this issue. First, the attitude of joints to the powerhouse cavern made some unstable blocks in the downstream wall. Second, the value of pore water pressure in the upstream wall was higher than of the downstream wall due to higher underground water table in the upstream wall. Then the value of effective stress which was the cause of displacements was higher in the downstream wall. Third, as shown in Figure 14, uplift pressure was

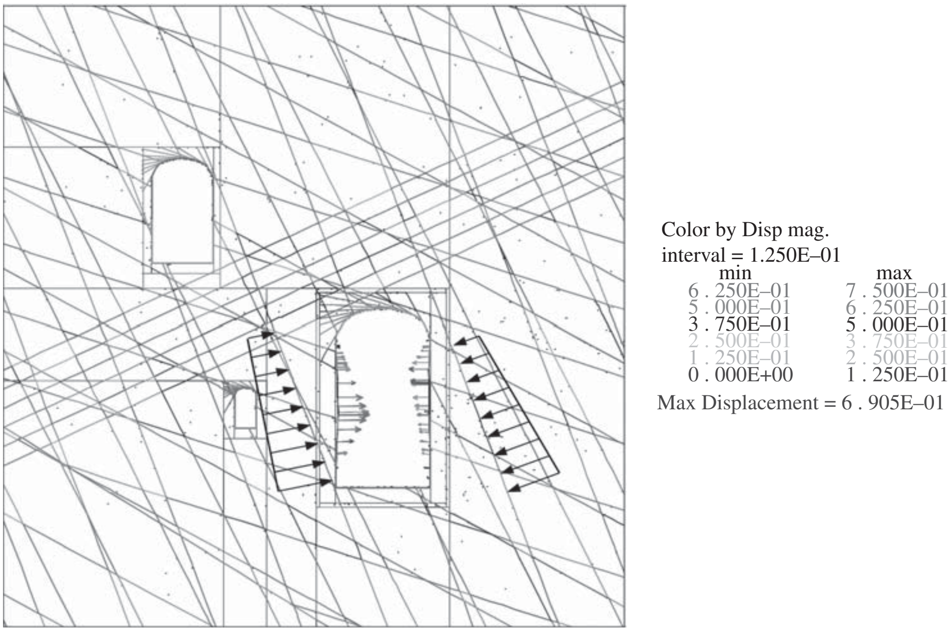

Figure 14 A cross section of displacement vectors (in m) in saturated conditions (groundwater level 1905) (Sharifzadeh *et al.*, 2008).

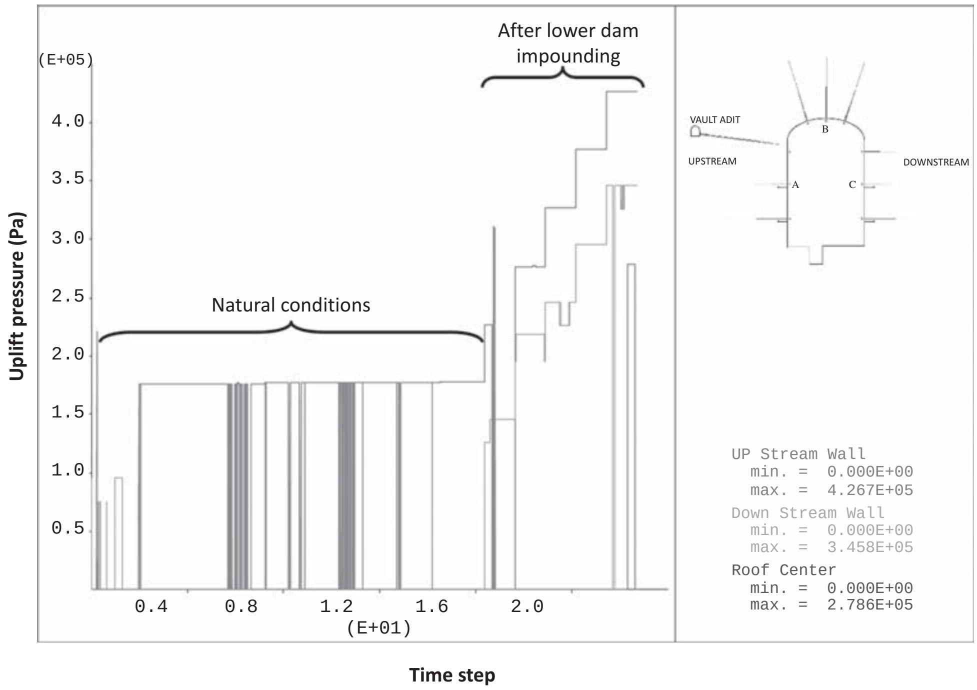

Figure 15 Histories of uplift pressure in PHC upstream wall (A), crown (B) and downstream wall (C) with increasing underground water table (Ghorbani & Sharifzadeh, 2009).

exerted on the rock mass in upstream wall joints and tended to stability but uplift pressure in downstream wall joints acted towards instability of the powerhouse cavern.

In Figure 15, the history of uplift pressures in joints surfaces of the crown center, upstream and downstream walls of the powerhouse cavern is illustrated. This figure shows increasing of uplift pressure in blocks interface correspond to 3 joints which cut the powerhouse cavern. As seen in Figure 15, with increasing of the underground water table from 1875 m (natural conditions) to 1905 m (saturated conditions) the values of uplift pressure increased in block interfaces. This is due to increasing of hydraulic pressure considering d/s dam impounding and rising underground water table.

The pressure exerted on discontinuity surfaces and called uplift pressure was computed as follows:

$$U = \gamma_w . Z \tag{5}$$

Where U is uplift pressure (Pa), γw is unit weight of water (N/m3) and z is the height of water above discontinuity surfaces (m).

With increasing uplift pressure in discontinuities, pressure on support systems would increase which tends to convergence of PHC walls and increasing the value of rock block displacements. This issue finally tends to powerhouse cavern failure in the area of the 2nd and 3rd instrumentation arrays. Therefore it was necessary to control the water pressure by an efficient stabilization method to guarantee long term stability of the powerhouse cavern.

As shown in Figure 14, the displacement plots had a similar tendency evolution; there were only some instantaneous displacements in computed plots due to shear deformation of joints or plane of layers. In addition, there were instantaneous increases of computed displacement after excavating the lower levels of the cavern. The total displacement contour after one year is shown in Figure 15. It should be implied that, by increasing the run time, the displacement in walls would be increased more than the crown.

At the time of analysis excavation of the powerhouse cavern was completed and it was impossible to modify the support system. Therefore to guarantee long term stability of the powerhouse cavern under saturated conditions, a cutoff curtain was proposed. Results of analysis under natural and saturated conditions showed that the powerhouse cavern roof was stable and there was no need to perform a cutoff curtain in the PHC roof. PHC floor concrete slab more than 5 m in height would be carried out in the future which would guarantee long term stability of this part under saturated conditions. So there was no need for a cutoff curtain for the floor of the PHC too. To perform cutoff curtain in the upstream wall of the PHC it was proposed to use vault adit which was excavated in this part of the PHC. It was recommended to perform the downstream wall's cutoff curtain from the transformer cavern (Figure 16). To perform cutoff curtain for the north wall and south wall of the PHC it was proposed to use a ventilation tunnel and transformer cavern respectively (Figure 17).

9 DISCUSSION

Back analysis is a practical engineering tool to evaluate geomechanical parameters of underground and surface structures based on field measurements of some key variables such as displacements, strains and stresses. These parameters are necessary for stability analysis and design of support system for geostructures.

Back analysis of Siah Bisheh powerhouse cavern during construction using the finite element method and distinct element method were carried out in the computer codes PHASE2 and 3DEC. Initial values of input parameters required in the both models

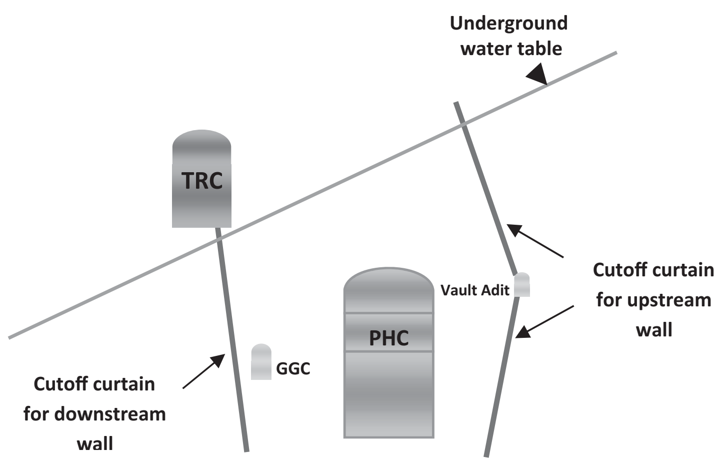

Figure 16 Proposed locations for cutoff curtain in PHC upstream and downstream walls (Ghorbani & Sharifzadeh, 2009).

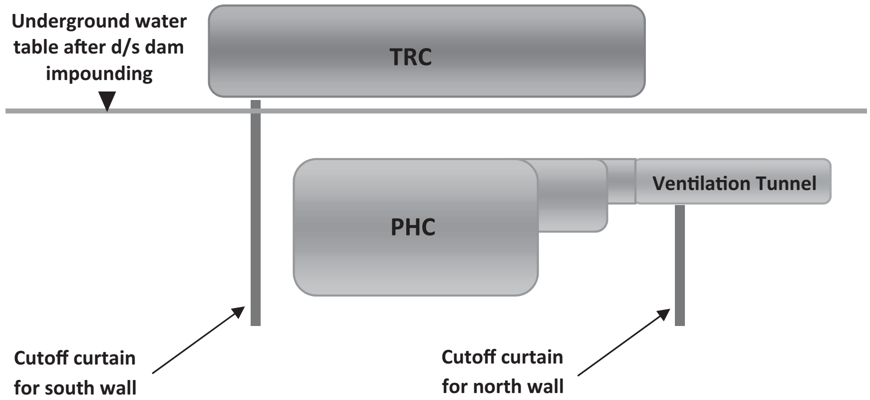

Figure 17 Proposed locations for cutoff curtain in PHC north and south walls (Sharifzadeh *et al*., 2008).

were based on the results of geological and geotechnical investigations and estimated by empirical and theoretical methods.

The parametric studies indicated that cavern response was strongly dependent on the rock mass modulus, ratio between horizontal and vertical stresses and friction angle of joints. As could be observed from Table 7, almost all rock mass parameters resulting from back analyses in both models were in good agreement together but the elasticity module of melaphyry section and friction angle of joint parameters in both models showed discrepancy. This major difference between Young's modulus could be explained by adjacent excavation openings, shear zones and non-interference efect of rocks layers in the discontinuum model. It also seems that the difference between the values of friction angle of joint parameters was based on software performance. This study clarified that the back calculated value of Young's modulus was more representative for mechanical behavior of rock masses in a large domain. Meanwhile the results demonstrated clearly that the default assumed rock mass parameters for design powerhouse cavern were high. Eventually with reference to modeling in this practice, it seems the interest has been placed on the adoption of discontinuum models which give a more realistic and representative picture of rock mass behavior than equivalent continuum models.

It is normally considered that the creep of rock masses in situ is governed primarily by the behavior of discontinuities, *i.e*. the bedding planes, faults and joints.

Numerical simulation of time dependent behavior of the Siah Bisheh powerhouse cavern showed that the power creep model was relevant on an enlarged scale. The parameters of this model were determined on the basis of triaxial creep tests and monitoring data. Crown inward displacement increased as the time increased with decreasing rate. Although there was a scale effect on the power model parameters, the creep behavior of the small rock samples had the same character as the rock mass around the cavern. It was considered that the creep of in situ rock mass was governed by the behavior of discontinuities.

In addition, by increasing the span or scale of the cavern, the rate of the displacement increased in the first days. Also, some instantaneous displacement occurred by drilling the second and third excavation sequences but the excavation of the 4th stage had

Table 12 Final results for back analysis of Siah Bisheh powerhouse cavern (Sharifzadeh, 2008).

Geomechanical properties	*Melaphyry section*	*Sedimentary part*
Young's modulus (MPa)	16 ± 0.5	9 ± 0.5
Cohesion (MPa)	3 ± 0.25	1.75 ± 0.125
Friction Angle (°)	41 ± 0.5	38 ± 0.5
Poisson's ratio	–	0.24
Stress ratio (k)	1.1	
Joints parameters		
Normal Stiffness (GPa/m)	30	
Shear Stiffness (GPa/m)	10	
Cohesion (MPa)	0.4 ± .05	
Friction Angle (°)	30 ± 2.5	

vanishingly small effect on the strain-time curve of the crown. However, the results of power model were fairly consistent.

10 CONCLUSION

In Table 12, results of back analysis for geomechanical properties for melaphyry section and sedimentary part, stress ratio and discontinuities parameters are presented. The best way to present the final results of the back analysis is to introduce them as a mean value and its amplitude.

Results of analysis showed that powerhouse, transformer and guard gate caverns were stable under natural conditions and the existing support system had suitable efficiency and could effectively control displacements. Powerhouse cavern long term stability under saturated conditions was analyzed. Results of analysis showed that after d/s dam impounding, considering the vicinity of powerhouse cavern to d/s dam reservoir, pore water pressure and uplift pressure in discontinuities around the powerhouse cavern would arise and tend to local failure of the powerhouse cavern. The values of displacements in downstream wall under saturated conditions were higher than upstream wall values. This was due to high effective stress in this region and forming some unstable blocks considering attitude of discontinuities to powerhouse cavern. To prevent powerhouse failure and assure its long term stability, a cutoff curtain corresponding to the introduced layout was proposed.

REFERENCES

Barla, G. 2001. Tunnelling under squeezing conditions. In *Tunnelling Mechanics, Euro summer school, Innsbruck*, pp. 169–268.

Boidy, E., Pellet, F., 2000. Identification of mechanical parameters for modeling time-dependent behaviour of shales, ANDRA Workshop, Behaviour *of deep argillaceous rocks: Theory and experiment, Proc. Int. Workshop on Geomech.*, Paris, October 11–12, 2000, p. 13.

Boidy, E., Bouvard, A., Pellet, F., 2002. Back analysis of time-dependent behaviour of a test gallery in claystone. *Tunneling and Underground Space Technology*, Vol. 17, pp. 415–425.

Brady, B.H.G., Brown, E.T., 2004. *Rock Mechanics for Underground Mining* (3rd Ed.), Springer, Netherlands. ISBN 10-1-4020-2064-3 (PB).

Cividini, A., Jurina, L., Gioda, G., 1981. Some aspects of characterization problems in geomechanics. *International Journal of Rock Mechanics and Mining Sciences and Geomechanics Abstracts*, Vol. 18, pp. 487–503.

Feng, X.T., Zhao, H., Li, S., 2004. A new displacement back analysis to identify mechanical geomaterial parameters based on hybrid intelligent methodology. *International Journal for Numerical and Analytical Methods in Geomechanics*, Vol. 28, pp. 1141–1165.

Gioda, G., Locatelli, L., 1999. Back analysis of the measurements performed during the excavation of a shallow tunnel in sand. *Numerical and Analytical Methods in Geomechanics*, Vol. 23, pp. 1407–1425.

Ghorbani, M., Sharifzadeh, M., 2009. Long term stability assessment of Siah Bisheh powerhouse cavern based on displacement back analysis method. *Tunnelling and Underground Space Technology*, Vol. 24, Issue 5, September, pp. 574–583.

Hoek, E., 2001. Rock mass properties for underground mines. *Underground Mining Methods: Engineering Fundamentals and International Case Studies*. Hustrulid, W.A., Bullock, R.L. (eds), Litleton, Colorado: Society for Mining, Metallurgy, and Exploration (SME).

Itasca Consulting Group, Inc. 2007. 3DEC (3 Dimensional Distinct Element Code Manual), Version 4.1. Minneapolis: ICG.

Lahmeyer, and Iran Water & Power Resources Development Co (IWPC). 2005. Report on geology and engineering geology of powerhouse cavern.

Nadimi, S., Shahriar, K., Sharifzadeh, M., Moarefvand, P., 2010. Triaxial creep tests and back analysis of time-dependent behavior of Siah Bisheh Cavern by 3-Dimensional distinct element method. *Tunnelling and Underground Space Technology*, Vol. 24, Issue 5, September 2009, pp. 574–583.

Oreste, P., 2005. Back-analysis techniques for the improvement of the understanding of rock in underground constructions. *Tunnelling and Underground Space Technology*, Vol. 20, Issue 1, pp. 7–21.

Sakurai, S., 1993. Back analysis in rock engineering. *Comprehensive Rock Engineering*, Vol.4, pp. 543–568.

Sharifzadeh, M., Fahimifar, A., Shahkarami, A. A., Esaki, T., 2002. Classification system for evaluation of water effect on mechanical behavior of intact and jointed rocks with case study, pp. 194–204, *Proceedings of the 3rd Iranian International Conference on Geotechnical Engineering and Soil Mechanics*, December 9–11, Tehran, Iran.

Sharifzadeh, M., Ghorbani, M. Nateghi, R. Masoudi, R., 2007. Long term stability assessment of a large underground opening under saturated condition, pp. 947–950, *11th ISRM Congress*, July 9–13, 2007, Sousa, L.R., Olalla, C., Grossmann, N.F. (eds), Lisbon, Portugal.

Sharifzadeh, M., Ghorbani, M., Masoudi, R., Eslami M., 2008. Performance prediction of support system of Siah Bisheh Pumped storage Cavern under saturated condition using numerical Analysis, p. 94, *2nd National Conference of Dam and Hydro-power plants*, May 2008, Tehran, Iran.

Sharifzadeh, M., Ghorbani, M., Masoudi, R., 2009. Displacement based back analysis of Siah Bisheh pumped storage powerhouse Cavern by means of distinct element method. Sharif Journal of Science and Technology; Transaction on: *Material Science and Engineering, University Journal*, April-May 2009, Issue 47, pp. 49–57.

Sharifzadeh, M., Tarifard, A., Moridi, M. A., 2013. Time-dependent behavior of tunnel lining in weak rock mass based on displacement back analysis method. *Tunnelling and Underground Space Technology*, Vol. 38, pp. 348–356. http://dx.doi.org/10.1016/j.tust.

Shalabi, F.I., 2004. FE analysis of time-dependent behavior of tunneling in squeezing ground using two different creep models. *Tunneling and Underground Space Technology*, Vol. 20, pp. 271–279.

Swoboda, G, Ichikawa, Y, Dong, Q.X., Zaki, M., 1999. Back analysis of large geotechnical models. *International Journal for Numerical and Analytical Methods in Geomechanics*, Vol. 23, 1455–1472.

Tsai, L.S., Hsieh, Y.M., Weng, M.C., Huang, T.H., Jeng, F.S., 2008. Time-dependent deformation behaviors of weak sandstones. *International Journal of Rock Mechanics and Mining Sciences*, Vol. 45, pp. 144–154.

Yazdani, M., Sharifzadeh, M., Kamrani, K., Ghorbani, M., 2011. Displacement-based numerical back analysis for estimation of rock mass parameters in Siah Bisheh powerhouse cavern using continuum and discontinuum approach. *Tunnelling and Underground Space Technology*, Vol. 28, pp. 41–48. doi:10.1016/j.tust.2011.09.002.

Journal of Rock Mechanics and Geotechnical Engineering 11 (2019) 511–526

Contents lists available at ScienceDirect

Journal of Rock Mechanics and Geotechnical Engineering

journal homepage: www.rockgeotech.org

Review

Rock mechanics contributions to recent hydroelectric developments in China

Xia-Ting Feng [a,*], Yang-Yi Zhou [a], Quan Jiang [b]

[a] Key Laboratory of Ministry of Education on Safe Mining of Deep Metal Mines, Northeastern University, Shenyang, 110819, China
[b] State Key Laboratory of Geomechanics and Geotechnical Engineering, Institute of Rock and Soil Mechanics, Chinese Academy of Sciences, Wuhan, 430071, China

ARTICLE INFO

Article history:
Received 14 August 2018
Received in revised form
31 August 2018
Accepted 4 September 2018
Available online 5 February 2019

Keywords:
Headrace tunnels
Cavern groups
Dam foundation
Rock spalling
Rockburst
Deep cracking

ABSTRACT

Rock mechanics plays a critical role in the design and construction of hydroelectric projects including large caverns under high in situ stress, deep tunnels with overburden more than 2500 m, and excavated rock slopes of 700 m in height. For this, this paper conducts a review on the rock mechanics contributions to recent hydroelectric developments in China. It includes the development of new testing facilities, mechanical models, recognition methods for mechanical parameters of rock masses, design flowchart and modeling approaches, cracking-restraint method, governing flowchart of rock engineering risk factors enabling the development of risk-reduced design and risk-reduced construction, and initial and dynamic design methods. As an example, the optimal design of underground powerhouses at the Baihetan hydroelectric plant, China, is given. This includes determination of in situ stresses, prediction of deformation and failure depth of surrounding rock masses, development of the optimal excavation scheme and support design. In situ monitoring results of the displacements and excavation damaged zones (EDZs) have verified the rationality of the design methodology.

1. Introduction

In order to meet the increasing requirements for energy consumption in China, a large number of hydroelectric engineering projects have been, and are being, or will be developed. There are totaling more than 20 large-scale hydroelectric power plants along Yangtze River, Jinsha River, Yalong River, and Dadu River. However, there are great challenges for the development of these hydroelectric projects. The first one is the complicated geological conditions encountered during construction. For example, columnar jointed basalt and several interlayer shear zones are observed in the Baihetan high-slope dam foundation (see Fig. 1). The second is the high in situ stresses. For example, the overburden of the Jinping II diversion tunnels is more than 2000 m (maximum depth of 2525 m), and the maximum in situ stress measured is about 70 MPa (Wu and Wang, 2011). The third is the large-scale dimensions. For example, the Baihetan underground cavern group is currently the largest in the world. The dimensions of each main powerhouse (Fig. 2) are 453 m (length) × 34/31 m (span) × 88.7 m (height). These difficult conditions introduce higher risk of rock mass failure in terms of large volumetric collapses, rockbursts, deep rock cracking, and large deformation of hard rocks. For example, a severe collapse of more than 3000 m^3 rock volume occurred in the Dagangshan powerhouse when excavating layer I (see Fig. 3). During tunnel boring machine (TBM) excavation of the drainage tunnel at Jinping II project, extremely severe rockbursts occurred (Fig. 4). Deep rock cracking has also been observed in the Jinping I powerhouse, in which the measured depths of excavation damaged zone (EDZ) on high sidewalls are 12–15 m (Fig. 5). Besides, large deformation of hard rock masses is also experienced in the same hydropower station, with the maximum displacement of 201.94 mm observed on the sidewall of the transformer chamber (Wei et al., 2010).

A significant effort has been made to guarantee the safe construction of these large-scale hydroelectric projects. Rock mechanics studies have been systemically carried out over the past half century, for example the Three Gorges Project (Dong et al., 2008). Some new models and methods have been developed and applied to the field by many scholars, which are of great contributions to the rock mechanics research community. One of the pioneers is the internationally high-acclaimed Professor Ted

* Corresponding author.
E-mail address: xia.ting.feng@gmail.com (X.-T. Feng).
Peer review under responsibility of Institute of Rock and Soil Mechanics, Chinese Academy of Sciences.

https://doi.org/10.1016/j.jrmge.2018.09.006

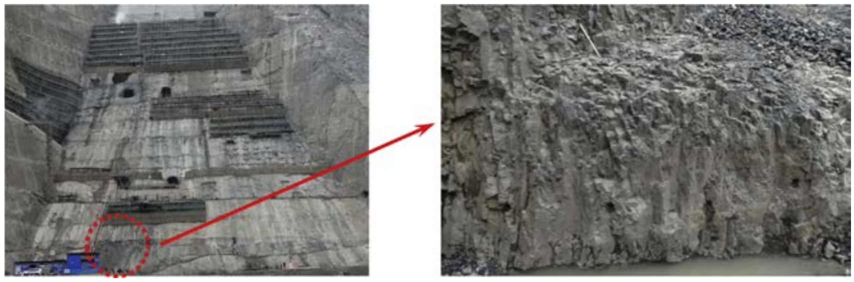

Fig. 1. Baihetan hydroelectric dam foundation (The marked area is the columnar jointed rock mass).

Fig. 2. Baihetan hydroelectric underground powerhouse.

Brown, from who the Chinese colleagues have learned a lot from his works (e.g. Brown, 1980, 2012a; b; 2015a; b; 2017, 2018; Hoek and Brown, 1980, 1997; 2019; Brady and Brown, 2004; Contreras et al., 2018; Contreras and Brown, 2019). He has given various rock mechanics advices for the Pulang copper mine and associated consulting projects, and also the keynote lectures in the 12th International Society for Rock Mechanics and Rock Engineering (ISRM) Congress in Beijing in 2011. The proposed Hoek-Brown criterion, one of his major achievements during his career life, has been widely accepted and used across the world (see Fig. 6). In Fig. 6, the data sources are mainly from China's database searched in China National Knowledge Infrastructure (CNKI), in which all the papers written in Chinese and some in English can be tracked. The category "English papers by foreign authors" is calculated as the difference between all the English papers related to the Hoek-Brown criterion and those with first author of China's affiliation. However, the article number is in fact underestimated since the CNKI database fails to include all the English papers related to the Hoek-Brown criterion published globally. With the generous encouragements and helps from Professor Ted Brown, the dynamic design method for deep tunnels and caverns has been improved and applied to hydroelectric projects recently in China. This paper is written, especially acknowledging Professor Ted Brown, due to his personal influence on the authors' research career in rock mass engineering.

2. Progress of recent hydroelectric developments in China

2.1. Underground powerhouses

China's hydroelectric developments have witnessed a rapid growth in the 21st century. There were 15 major hydropower bases in total, over 6000 hydropower stations, with a total installed capacity of 341 GW in 2017. Most of the hydropower stations adopt underground cavern groups as power generating facilities. The dimensions of the underground powerhouses for several hydropower stations in China are listed in Table 1. The lengths of the powerhouses are mostly in the range of 270–400 m, among which the largest one is 453 m (Baihetan). The spans of the powerhouses are

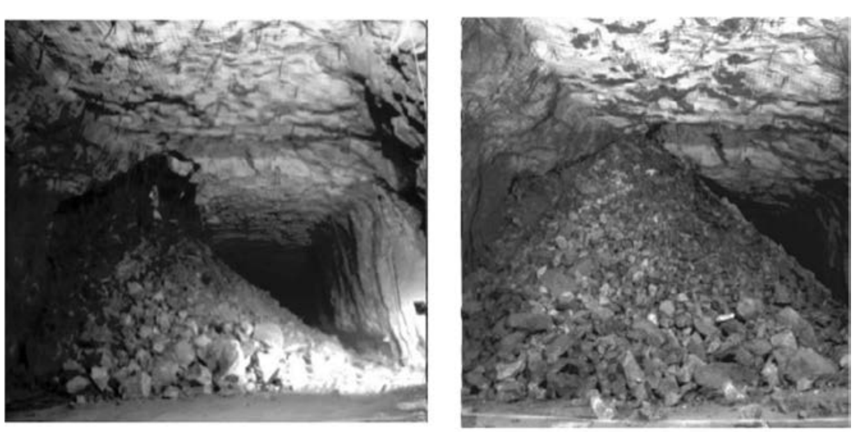

(a) Early stage. (b) Final state.

Fig. 3. Collapse in the Dagangshan underground powerhouse (Zhang, 2010).

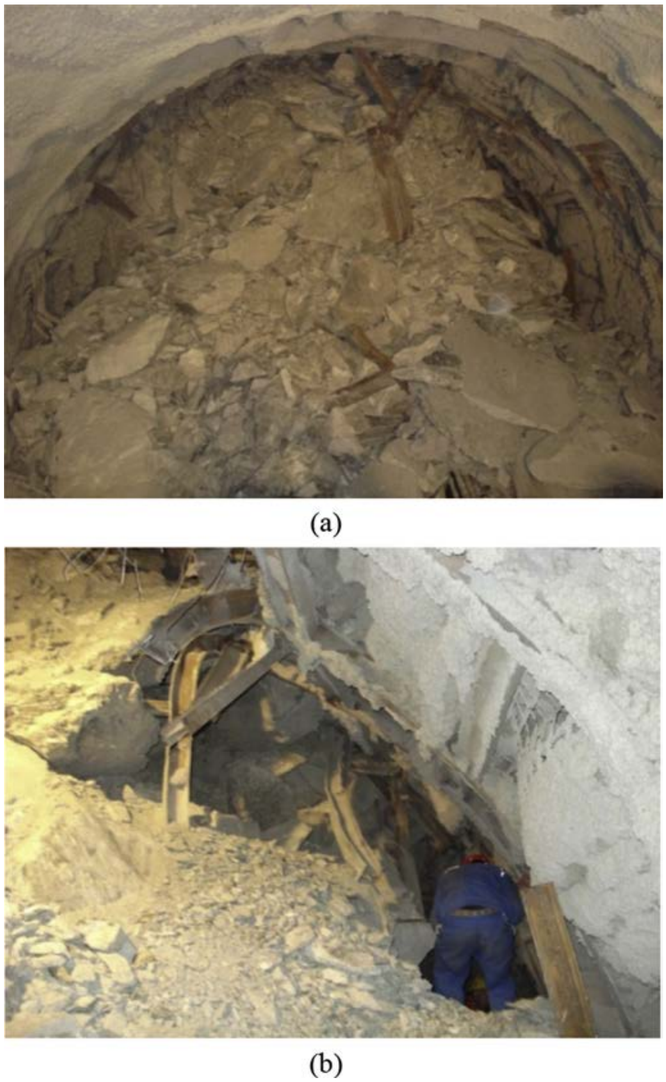

Fig. 4. Rockburst occurring during the TBM excavation of the drainage tunnel at Jinping II hydroelectric project.

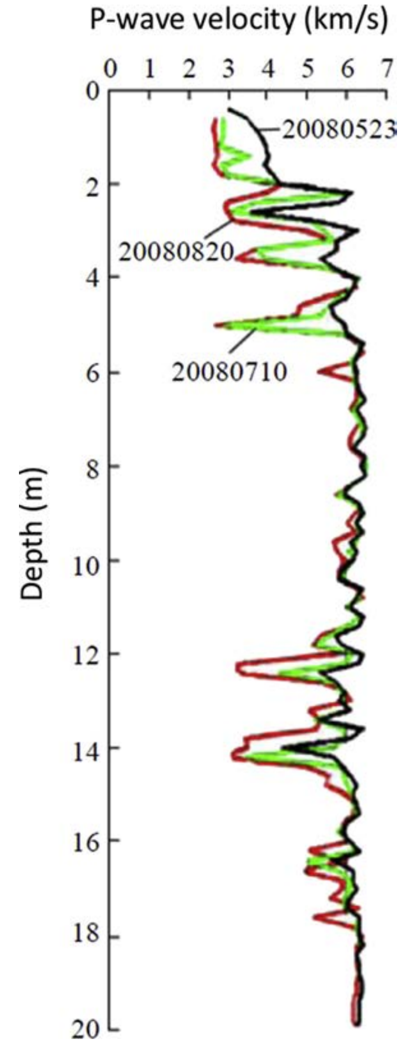

Fig. 5. The EDZ test by P-wave velocity in the Jinping I underground powerhouse (Li et al., 2009).

basically within the range of 26–32 m, among which the widest is 34 m (Baihetan). The heights of the powerhouses are generally in the range of 60–80 m, with the highest of 89.8 m (Wudongde). All these data demonstrate that the main features of these powerhouses are their large dimensions and the complex geological conditions. For this, various rock mechanics challenges should be well addressed during and after construction (Wu et al., 2011, 2016).

2.2. Tunnels

The headrace tunnels of Jinping II hydropower station are typical of large-scale tunnel group, which is characterized with large overburden, high in situ stresses, and high water pressure. Four tunnels are excavated in marble strata in parallel by TBM and drill-and-blast methods (Fig. 7). The average lengths and diameters are 16.67 km and 13 m, respectively. The average overburden is more than 2000 m, with a maximum depth of 2525 m. The maximum in situ stress measured is about 70 MPa, and the induced maximum stress estimated by back analysis is more than 70 MPa. The maximum external water pressure may exceed 10 MPa. Severe rockburst and spalling events have been frequently reported during excavation.

2.3. Slopes and abutments

Some of the slopes of over 300 m in height are listed in Table 2. The Jinping I left bank dam abutment slope is 530 m high, with the maximum horizontal depth of 130 m and the maximum width of 350 m; it is to date the largest rock slope excavations (Fig. 8) (Song et al., 2011). The Xiaowan slope is the highest slope at present in China, with height of 695 m. The geological conditions are generally very complicated in the slopes. Folds, large-scale faults and other rock mass structures render it difficult to predict the slope stability and to maintain its safety during and after excavation. These high slopes pose new challenges on rock mechanics research community due to the lack of sufficient experiences and it promotes the occurrence of new developments of engineering technologies.

Some of the representative high dams in China are listed in Table 3. These dams are mostly 200–300 m high, and are all double-curvature arch types. Among these dams, the Jinping I arch dam is the highest (305 m) in the world at present. The stabilities of the listed dam foundations are more or less affected by the faults

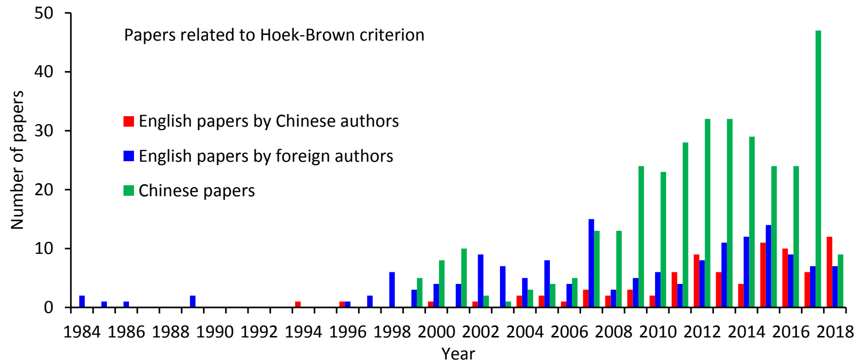

Fig. 6. Papers related to the Hoek-Brown criterion searched in China National Knowledge Infrastructure (CNKI).

and other discontinuities. No previous experiences and/or guidance can be followed. Therefore, new design methodologies have to be developed.

3. Developments and applications of design and modeling methods

3.1. The design flow chart and modeling approaches

The flowchart of rock mechanics modeling and rock engineering design approaches shown in Fig. 9 was developed by Feng and Hudson (2004, 2011). An updated flowchart for rock engineering design processes shown in Fig. 10 has also been provided by Feng and Hudson (2011). These flowcharts have been applied to recent hydroelectric developments in China, and the study of life-cycle safety control on high-steep rock slopes in hydroelectric engineering has also been considered (Zhou, 2013).

3.2. Identification of the features and constraints of the site, rock mass and project

Site investigation has been conducted to understand the site-specific geological conditions. Some methods have been developed for these purposes. For example:

(1) Three-dimensional (3D) laser scanning and surveying in geological investigation of high rock slope (Huang and Dong, 2008);
(2) Automated tunnel rock classification using rock engineering systems (Huang et al., 2013a,b); and

Table 1
Dimensions of underground powerhouses for several hydropower stations in China.

Name	Dimensions of underground powerhouses (length (m) × span (m) × height (m))	Geological condition
Three Gorges (right bank)	329.5 × 32.6 × 86.24	Granite and diorite, fine-grained granite dykes and pegmatite veins intruded, unstable wedges
Longtan	398.9 × 30.7/28.9 × 77.6	Triassic thick-layered sandstone, siltstone and argillaceous slate, dip angle = 55°–63°, intact and fresh, steeply-dipping joints and faults developed
Ertan	280.29 × 30.7/25.5 × 65.38	Syenite and gabbro, local-altered basalt, intact and high-strength, high in situ stress, spalling and rock burst occurred
Laxiwa	311.75 × 30/27.8 × 73.84	Blocky granite, intact and high-strength, high in situ stress, spalling and rockburst occurred, spalling and rockburst occurred
Xiaowan	298.4 × 30.6/28.3 × 86.43	Biotite granitic gneiss, schist lens, 3 small-scale faults and other discontinuities developed, fresh to slightly weathered rocks, medium to high in situ stress
Jinping I	276.99 × 28.9/25.6 × 68.8	Marble and green schist, mainly class III (BQ), 3 faults, 1 lamprophyre vein, 4 joint sets, high in situ stress, large deformation, deep fracturing
Jinping II	352.44 × 28.3/25.8 × 72.2	Steeply-dipping, medium to thick layered marble, mainly class III (BQ), small angle between bedding strike and cavern axis, medium to high in situ stress
Houziyan	219.5 × 29.2 × 68.7	Devonian medium to thick layered limestone and metamorphic limestone, dip angle = 25°–50°, intact rock mass with small-scale faults, fractured zones and joints. High in situ stress, high intermediate principal stress, spalling and rockburst occurred
Xiluodu	439.74 × 31.9/28.4 × 75.6	Permian blocky basalt, formed by multi-period volcanic eruptions. Fresh and intact and high-strength, mainly class II (BQ), gently dipping, interlayer shear zone developed, low to moderate in situ stress
Xiangjiaba	245 × 33/31 × 82.5	Triassic grey medium to thick layered sandstone, siltstone and mudstone, gently dipping. Main discontinuities are bedding planes and interlayer joints.
Nuozadu	418 × 31/29 × 81.6	Blocky granite, slightly weathered to fresh, 3 small-scale faults and 3 joint sets, low to moderate in situ stress
Dagangshan	226.58 × 30.8/27.3 × 74.6	Grey medium-grained biotite adamellite, multiple diabase dykes, fractured zones, faults and joints are developed along dykes, medium to high in situ stress
Baihetan	453 × 34/31 × 88.7	Cryptocrystalline basalt, porphyritic basalt, amygdaloidal basalt, breccia lava, etc. Three steeply-inclined faults, multiple inter- and interlayer shear zones, high in situ stress, spalling and large deformation of shear zones occurred
Wudongde	333 × 32.5/30.5 × 89.8	Steeply dipping medium to thick layered limestone, dolostone and marble, small angle between bedding strike and cavern axis, low to moderate in situ stress

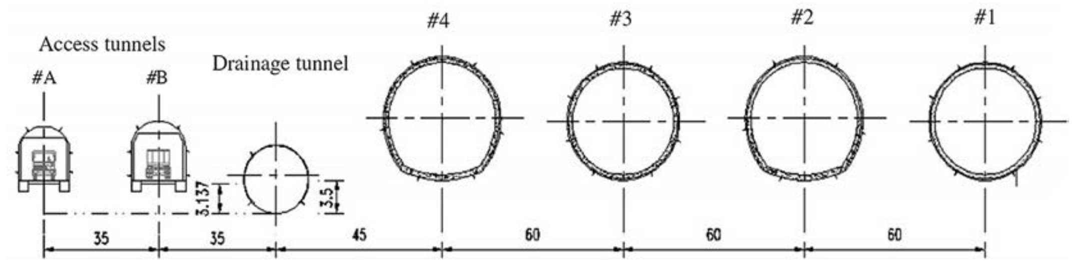

Fig. 7. Jinping II headrace tunnels (Zhang et al., 2012). Dimensions in m.

Table 2
Slopes for several major hydropower stations in China.

Name	Height (m)	Characterization
Xiaowan left bank Yinshuigou accumulation body slope	695	The highest slope is featured with large overburden, and creep and tensile deformation occurred during excavation
Jinping I left bank dam abutment slope	530	Situated at the left abutment of the world highest arch dam – Jinping I arch dam, complicated deformation and failure modes
Dagangshan right bank dam abutment slope	422	The stability of the slope is controlled by fault and unloading fractures
Longtan water inlet slope	420	Anti-dip layered rock mass is prone to toppling
Tianshengqiao II powerhouse syncline-oriented slope	380	Typical layered rock slope, and the stability is controlled by a syncline
Wudongde left bank dam abutment slope	350	Steeply-dipping layered rock slope, and the bedding strike forms at a large angle with the slope
Three Gorges Lianziya rock body slope	320	The hard rocks on the soft basement failed, forming a dangerous rock body with volume of 3.62×10^6 m^3
Baihetan left bank dam abutment slope	300	Large-scale columnar jointed basalt and multiple intralayer shear zones

Fig. 8. The left abutment slopes of Jinping I hydropower station (Song et al., 2011).

(3) The standard of engineering classification of rock masses (Wu and Liu, 2012).

Rock mass properties have been tested using rock samples and physical modeling in the laboratory, and in exploration tunnels and an underground laboratory. Tests on hard rocks under triaxial

Table 3
Dam foundations for several major hydroelectric stations in China.

Name	Dam height (m)	Geological condition
Jinping I	305	The world highest arch dam, complicated geological condition at dam abutments including faults, altered dykes, interlayer compressive zone, deep fractures and other discontinuities, and soft rocks and green schist lens. High in situ stress, high seismic intensity and high water load
Xiaowan	294.5	The dam foundation mainly consists of biotite granitic gneiss. Faults, alteration zone and small-scale discontinuities are distributed on the foundation
Baihetan	289	The dam foundation mainly consists of basalt. Inter- and intralayer shear zones, as well as the columnar joints are developed
Xiluodu	285.5	Blocky, high-strength basalt formed by multi-period volcanic eruptions. Interlayer and intralayer shear zones are developed
Wudongde	265	The dam foundation mainly consists of thick layer limestone and marble. Bedding planes and several other discontinuities are developed
Laxiwa	250	The rock of the dam foundation is comprised of mesozoic competent granite
Ertan	240	The dam foundation mainly consists of syenite and basalt. A fault is found at the right bank abutment
Dagangshan	210	Medium-grain biotite adamellite. Dykes, mainly the diabase dykes, and other large-scale fractures are developed. Faults are distributed mainly along dykes

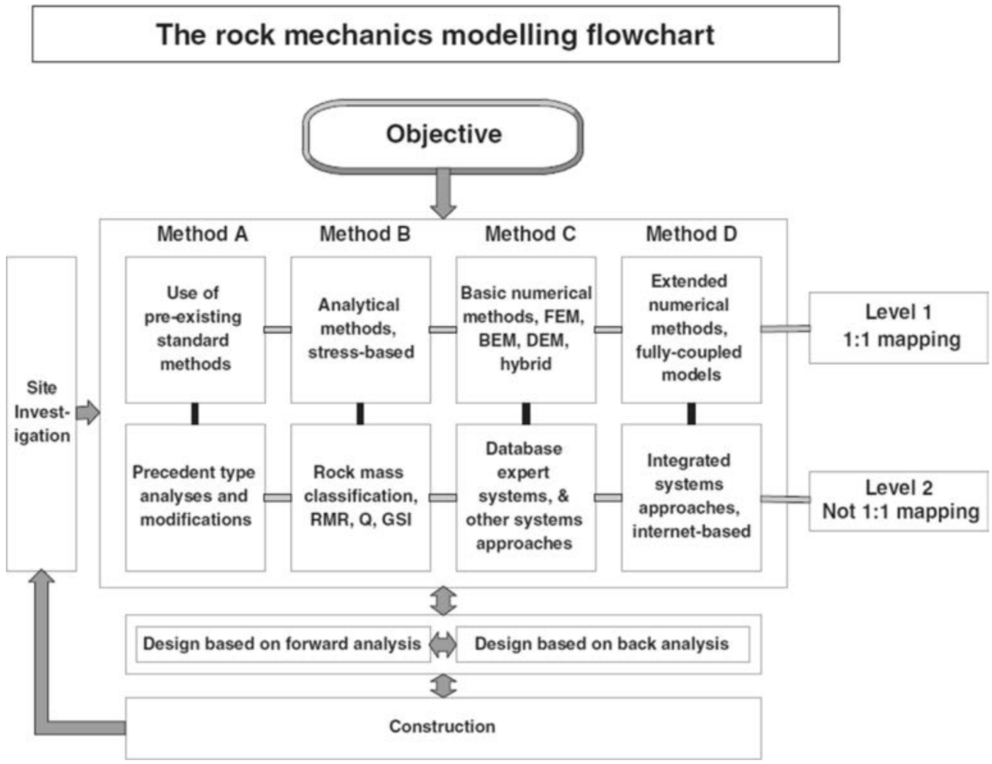

Fig. 9. Flowchart of rock mechanics modeling for rock engineering design approaches (Feng and Hudson, 2004, 2011).

compressive stresses and true triaxial compressive stresses have been conducted by loading and unloading testing conditions. The size effect of unloaded rock mass has been studied (Li and Wang, 2003). Some true triaxial compressive testing machines have been developed to understand the properties of rock masses at high stresses.

(1) A novel Mogi type true triaxial testing apparatus to obtain complete stress–strain curves of hard rocks (Feng et al., 2016b);
(2) A novel true triaxial apparatus for studying the time-dependent behavior of hard rocks under high stress (Feng et al., 2018);
(3) Development of a triaxial rheological testing machine with high pressure confinement in rock mechanics (Wu et al., 2006);
(4) Tests on the influence of unloading rates on the mechanical properties of Jinping marble under high geostress (Huang and Huang, 2010);
(5) Shaking table test on strong earthquake response of stratified rock slopes (Huang et al., 2013b);
(6) Quasi 3D physical model tests on a cavern complex under high in situ stresses (Zhu et al., 2011);
(7) Comprehensive field monitoring of deep tunnels at the Jinping underground laboratory (CJPL-II) (Feng et al., 2016d);
(8) In situ monitoring of rockburst nucleation and evolution in the deep tunnels of the Jinping II hydropower station (Li et al., 2012a);
(9) Evolution of fractures in the EDZ of a deep tunnel during TBM construction (Li et al., 2012b);
(10) In situ observation of the spalling process of intact rock mass at a large cavern excavation (Liu et al., 2017);
(11) In situ observation of failure mechanisms controlled by rock masses with weak interlayer zones in large underground cavern excavations under high geostress (Duan et al., 2017); and
(12) Deep fracturing of the hard rock surrounding a large underground cavern subjected to high geostress: in situ observation and mechanism analysis (Feng et al., 2017).

The in situ stresses are measured using hydraulic fracturing and overcoring methods. The techniques for measuring in situ stresses at large overburden depth have been improved. A back analysis method has been developed to understand 3D stress distributions in deep valley regions by considering tectonic history of rock masses with brittle failure features. For example:

(1) Hollow inclusion triaxial strain gauge for geostress measurement (Liu et al., 2001);
(2) Borehole wall stress relief method (BWSRM) and development of geostress measuring instrument (Ge and Hou, 2011);
(3) In situ stress measurement in the Jinping underground laboratory with overburden of 2400 m (Zhong et al., 2018);
(4) Nonlinear inversion of 3D initial geostress field in a hydropower station (Jiang et al., 2008a);
(5) Estimating in situ rock stress from spalling veins (Jiang et al., 2012); and
(6) A new hydraulic fracturing method for rock stress measurement based on double pressure tubes internally installed in the wire-line core drilling pipes (Wu et al., 2018).

Risk factors are identified and discussed within the governing framework for identification, assessment and management of rock engineering risk developed by Hudson and Feng (2015) (see Fig. 11). The potential failure risks of rock masses under high stress conditions such as collapse, rockburst, spalling, deep cracking, large deformation, and cracking of shotcrete are identified. The mechanisms for these geo-disasters have been investigated.

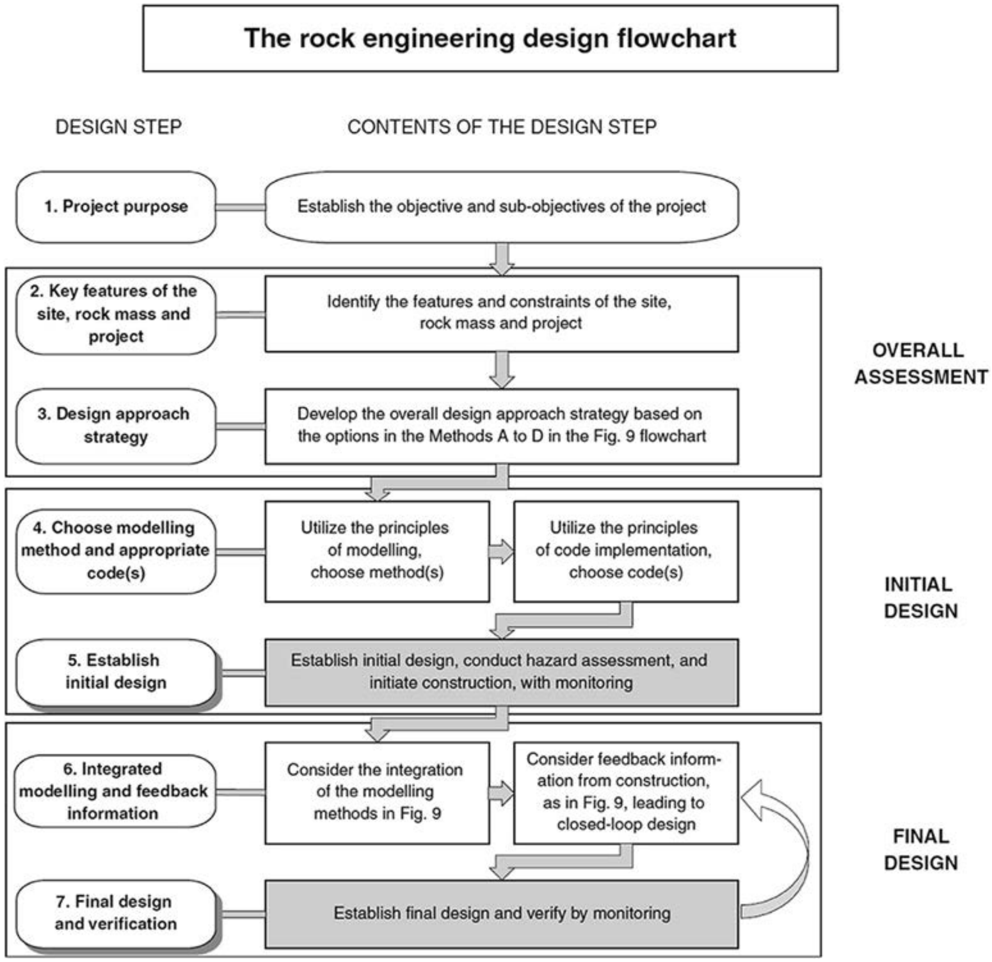

Fig. 10. Updated flowchart for rock engineering design processes (Feng and Hudson, 2011).

(1) Safety risk management of underground engineering in China (Qian and Lin, 2016);
(2) Assessing EDZ of a rock mass in a dam foundation (Wu et al., 2009);
(3) Geodynamical process and stability control of high rock slope development (Huang, 2008);
(4) Mechanism of deep cracks in the left bank slope of Jinping I hydroelectric station (Qi et al., 2004); and
(5) Geomechanics mechanism and characteristics of surrounding rock mass deformation failure in the construction phase for the underground powerhouse of the Jinping I hydroelectric station (Huang et al., 2011).

3.3. Development and application of modeling methods and software

In order to meet the requirements of the complicated hydroelectric projects, Methods C and D in the Level 1 (1:1 mapping) and Methods A-D at level 2 (not 1:1 mapping) of Fig. 9 are developed and applied. The Hoek-Brown criterion (Hoek and Brown, 1997, 2019) has been widely used to estimate the rock mass parameters. The codes adopting finite element method (FEM), fast Lagrangian analysis of continua (FLAC), 3D distinct element code (3DEC), discontinuous deformation analysis (DDA), and numerical manifold method (NMM) have been used in numerical analyses of the slopes, caverns and tunnels. Some new mechanical models and numerical analysis methods have been developed for recent hydroelectric projects. For example:

(1) A new generalized polyaxial strain energy strength criterion of brittle rock (Huang et al., 2008);
(2) A constitutive model considering surrounding hard rock deterioration under high geostresses (Jiang et al., 2008b);
(3) A mobilized dilation angle model for rocks (Zhao and Cai, 2010);
(4) A simple shear strength model for interlayer shear weakness zones (Xu et al., 2012);
(5) Multi-joint constitutive model of layered rock mass and experimental verification (Huang et al., 2012);
(6) An enhanced equivalent continuum model for layered rock mass incorporating bedding structure and stress dependence (Zhou et al., 2017);
(7) An elasto-plastic-brittle-ductile cellular automaton approach for numerical analysis of the fracturing process of heterogeneous rock masses (Feng et al., 2006a);
(8) DDA to analyze tunnel reinforcement and rockbursts (Hatzor et al., 2015, 2017);
(9) A generalized multi-field coupling approach for stability and deformation control of a high slope (Zhou et al., 2011);
(10) Zonal disintegration analysis method for tunnels (Qian et al., 2009);

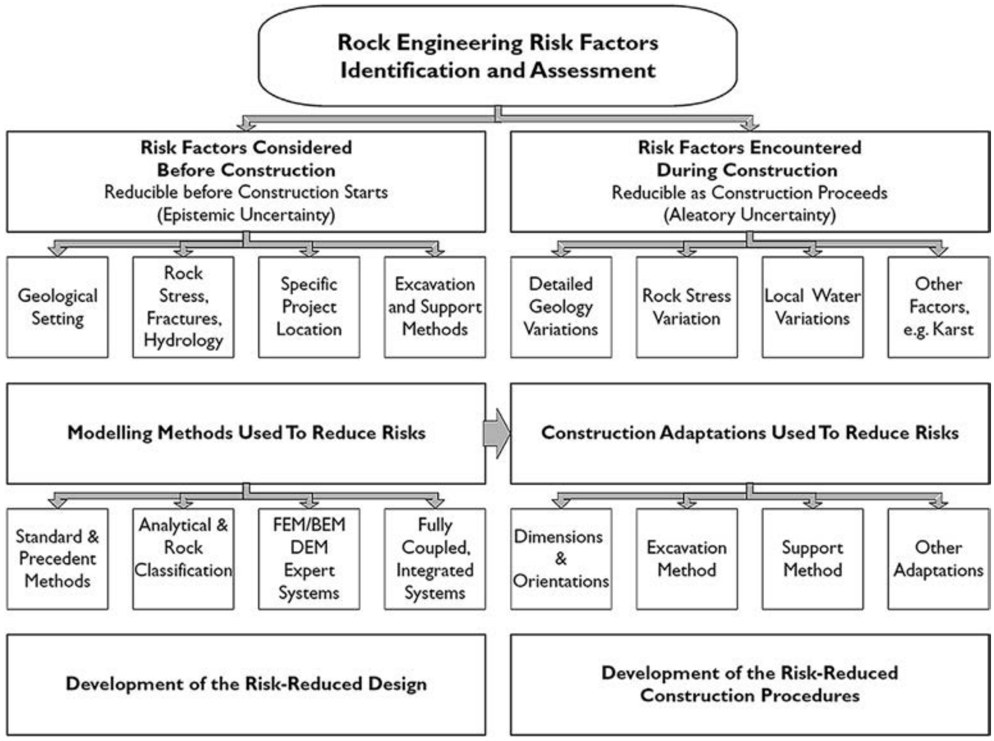

Fig. 11. Governing flowchart of rock engineering risk factors enabling the development of risk-reduced design and risk-reduced construction (Hudson and Feng, 2015).

(11) Internal state variable theory for stability analysis of slopes and tunnels (Zhang et al., 2016a,b,c; Lü et al., 2017);
(12) A 3D slope stability analysis method using the upper bound theorem (Chen et al., 2001a,b); and
(13) Stochastic response surface method for reliability analysis of rock slopes involving correlated non-normal variables (Li et al., 2011).

3.4. Initial design

A principle for determining the axes of tunnels and caverns (underground powerhouses) has been identified. Generally, the axes of tunnels and caverns (underground powerhouses) shall make an angle of less than 30° with the direction of the maximum principal stress. The angle between the axes of tunnels and caverns

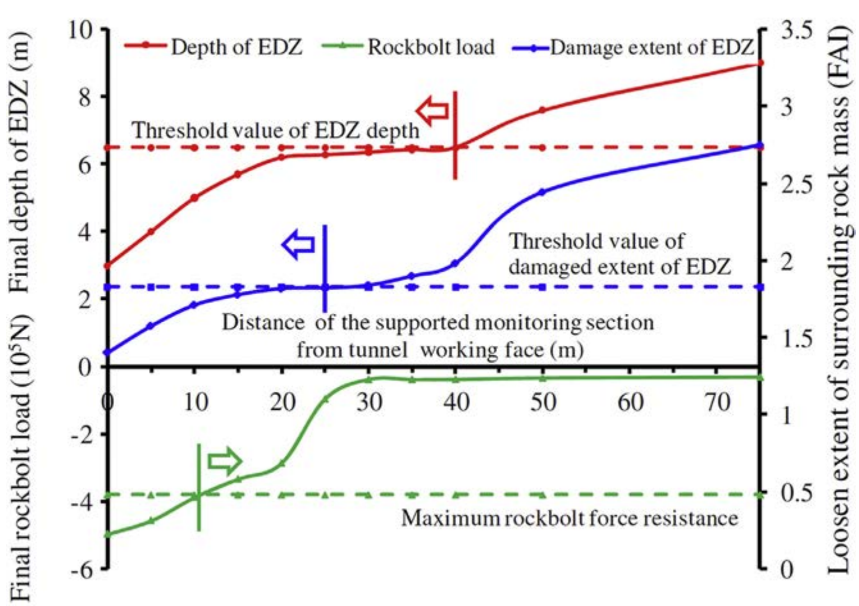

Fig. 12. Depth of the EDZ, load on rockbolts, and damage extent of EDZ for different locations from the support monitoring section to the tunnel working face (Feng et al., 2016c).

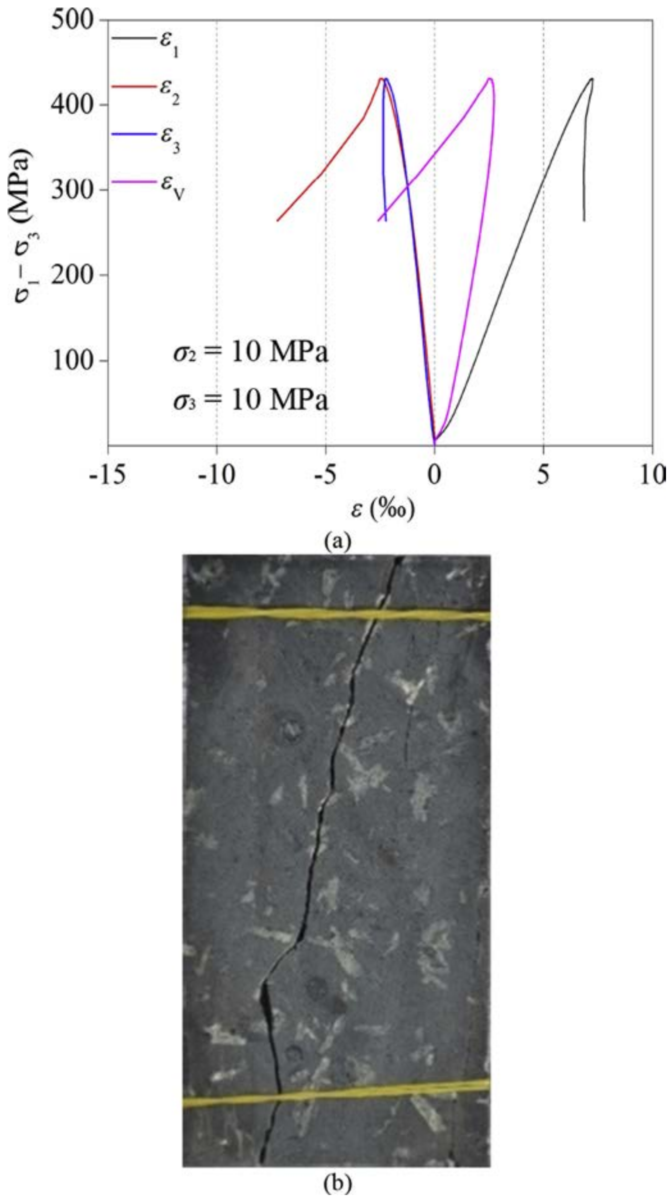

Fig. 13. True triaxial test result of porphyritic basalt. (a) Stress–strain curve, and (b) Failure mode. σ_1 is the maximum principal stress, σ_2 is the intermediate principal stress, σ_3 is the minimum principal stress, ε_1 is the strain along σ_1 direction, ε_2 is the strain along σ_2 direction, ε_3 is the strain along σ_3 direction, and ε_V is the volumetric strain.

(underground powerhouses) shall not be larger than 50° approximately with the direction of the intermediate principal stress when the intermediate principal stress is close to the maximum principal stress.

An intelligent optimal algorithm has been proposed to optimize the excavation process of rock masses under high stress conditions. This is to optimize (H, S, R) and minimize the EDZ, where H is the excavation bench height, S is the excavation sequence, and R is the excavation advance rate.

A cracking-restraint method has been proposed to optimize support design for rock masses under high stress conditions (Feng et al., 2016c). This is to optimize (ST, D, T), and minimize the EDZ and damage extent of the EDZ, where ST is the support type, D is the length of rock bolts/cable anchors, and T is the support time.

The cracking-restraint method involves limiting the evolution of cracking in the surrounding rock mass by optimizing the parameters and installation time of the support system. The support system should have a suitable stiffness and installation time so as to restrain the evolution of the depth and damage extent of the EDZ within the surrounding rocks. Therefore, the depth and damage extent of the EDZ, as well as the axial stress in the anchor bolts, are calculated at different distances between the support location and the tunnel working face to find out the appropriate stiffness and installation time of the support system (Fig. 12).

3.5. Monitoring and early warning

Some ISRM suggested methods have been developed. In situ monitoring has been widely performed to evaluate the deformation and microfracturing processes of the rock mass. For example:

(1) ISRM suggested method for measuring rock mass displacement using a sliding micrometer (Li et al., 2013a);
(2) ISRM suggested method for rock mass fracture observations using a borehole digital optical televiewer (Li et al., 2013b);
(3) ISRM suggested method for in situ microseismic monitoring of the fracturing process in rock masses (Xiao et al., 2016);
(4) The evolution of displacement, wave velocity and cracking in rock mass have been monitored to evaluate the stability of caverns, tunnels and slopes (Song et al., 2011, 2013, 2016; Li et al., 2012a, b; Feng et al., 2016a, 2017; Liu et al., 2017);
(5) Micoseismicity monitoring in slopes, caverns and tunnels (Tang et al., 2010, 2015; Feng et al., 2012; Xu et al., 2015);
(6) Acoustic emission monitoring in surrounding rock masses excavated by TBM and drill-and-blast methods (Feng et al., 2012);
(7) Water pressure in rock masses (Song et al., 2011);

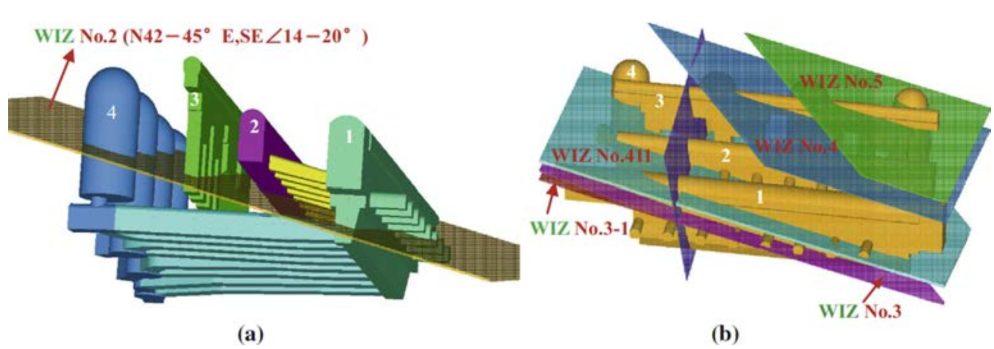

Fig. 14. Weak interlayer shear zones in the area of cavern groups. (a) Left bank, and (b) right bank (Duan et al., 2017). WIZ is the weak interlayer shear zone, 1 is the main powerhouse, 2 is the main transformer chamber, 3 is the tailrace gate chamber, and 4 is the tailrace surge chamber.

Table 4
Back analysis results of the in situ stress field for the Baihetan power plant.

Principal stress	Magnitude (MPa)	Trend (°)	Plunge (°)
Maximum	22–26	14–35	7–22
Intermediate	16–18	110–125	20–35
Minimum	10–15	80–100	−40–−65

(8) Forces on rockbolts and cable anchors in rock masses (Song et al., 2011);
(9) The in situ observation of failure mechanisms controlled by rock masses with weak interlayer zones in large underground cavern excavations under high geostress (Duan et al., 2017); and
(10) 3D visualization of safety monitoring for complicated high rock slope engineering (Meng et al., 2010).

Methods to warn the instability, failure and rockburst risk of rock masses have been established. For example:

(1) Early warning of deformation during the construction of underground powerhouses (Jiang et al., 2008c; Feng et al., 2011); and
(2) Formulae for early warning of rockbursts during tunneling by drill-and-blast method and by TBM have been developed (Feng et al., 2012, 2015; Feng, 2017).

3.6. Feedback analysis

The mechanical parameters of rock masses are estimated based on back analysis by using the in situ monitored deformation and wave velocity data. Two typical intelligent back-analysis methods have been proposed for this purpose:

(1) Intelligent displacement back analysis for deformation parameters of rock masses (Feng et al., 2000);
(2) Intelligent back analysis for visco–elastic parameters of rock masses (Feng et al., 2006b); and
(3) Intelligent back analysis of the in situ monitored displacement and depth of the EDZ for deformation and strength parameters of rock masses at high stresses (Jiang et al., 2007).

The estimated mechanical parameters with the revealed geological conditions after excavation are used as inputs in numerical analyses, so as to predict the deformation and failure behaviors of rock masses in the future or next excavations, and to evaluate the reasonableness of support design or to optimize support design, for example the dynamic feedback analysis and engineering control of surrounding rock local instability in underground powerhouse of Jinping II hydropower station (Jiang et al., 2008c).

3.7. Dynamic optimization of excavation and support design and establishment of final design

The design of excavation and support is modified or dynamically optimized according to the actual behavior of rock masses and the revealed geological conditions. If the actual mechanical behavior of the excavated rock mass is poor as estimated, the excavation shall be controlled to reduce the damage to the rock mass and the support shall be enhanced consequently. If the revealed geological conditions are poor, the support system shall be enhanced either, using dynamic design method (see Feng and Hudson, 2011; Hudson and Feng, 2015).

For intensive rockburst cases, the excavation advance rate can be adjusted according to the potential risks of rockburst occurrence. Stress release measures can be taken according to the predicted rockburst locations if excavation and support are reasonable. The support system can be modified according to the risk of rockbursts. A dynamic design method to control rockburst risk has been established (see Feng, 2017).

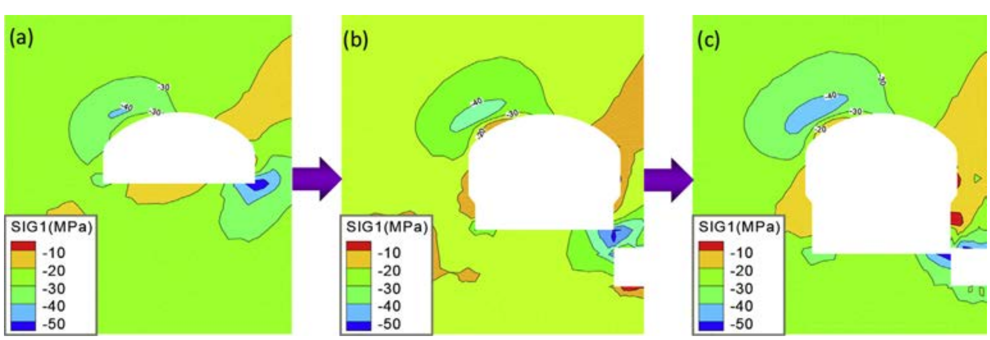

Fig. 15. Evolution of the stress concentration zone at the upstream roof. (a) After the 1st bench excavation, (b) after the 3rd bench excavation, and (c) after the 4th bench excavation.

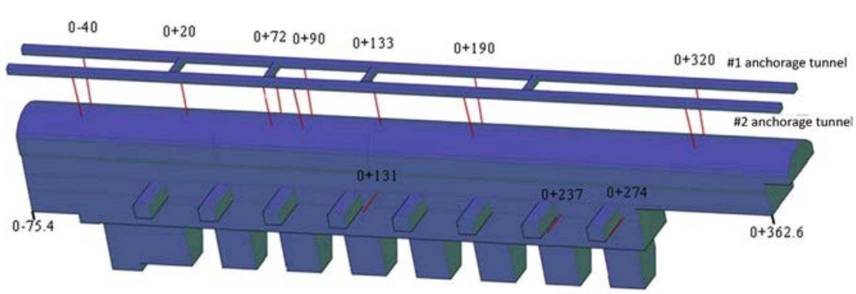

Fig. 16. Observational boreholes on the roof and sidewalls of powerhouse.

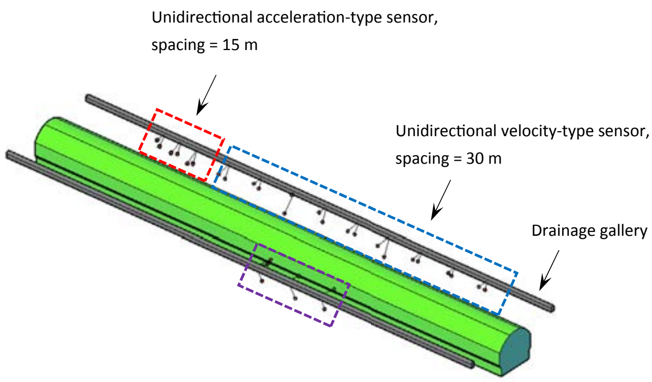

Fig. 17. Distribution of the microseismicity recording sensor.

4. Case study

In this section, an example of the optimal design of underground powerhouses at the Baihetan hydroelectric power plant is given. In this project, seven steps proposed by the updated flowchart for rock engineering design processes were strictly followed, in order to show how this design methodology is applied to the initial and final designs of a large-scale underground powerhouse.

4.1. Step 1: project purpose

The Baihetan hydroelectric power plant is located on the Jinsha River between Sichuan and Yunnan provinces (Jiang et al., 2017). There are 16 turbine generators, each of which has the generating capacity of 1000 MW. It has the largest underground cavern group to date in the world. The dimensions of the tailrace surge chamber are 43–48 m (diameter) × 93 m (height). The stability for the Baihetan underground caverns should be guaranteed in order to avoid excessive deformation and failure during their construction.

4.2. Step 2: key features of the site, rock mass and project

Key features of this project are: (1) large overburden (300–500 m) and high in situ stress (maximum value > 30 MPa); (2)

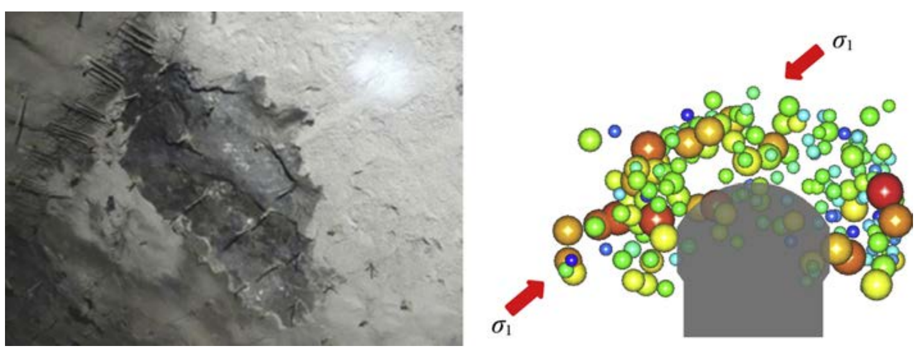

Fig. 18. Spalling in the upstream roof and microseismic monitoring result.

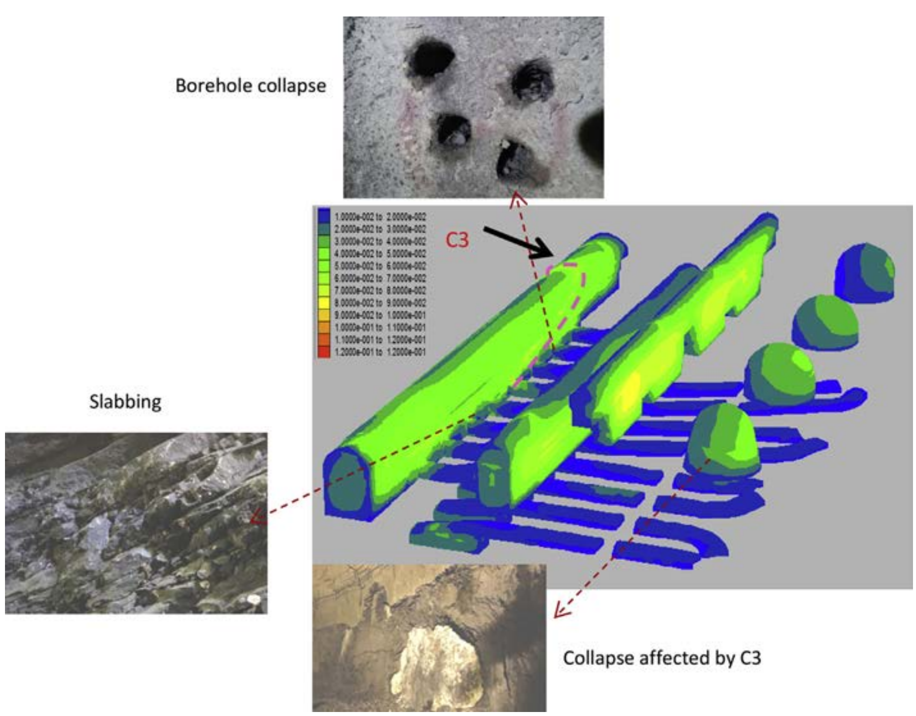

Fig. 19. Failure modes occurrence in different parts of cavern group. C3 is a major weak interlayer shear zone cutting through the entire cavern group region, and different colors represent different displacement magnitudes (unit in m).

Fig. 20. Spalling in the upstream roof of the left bank powerhouse during excavation of layer I (Liu et al., 2017).

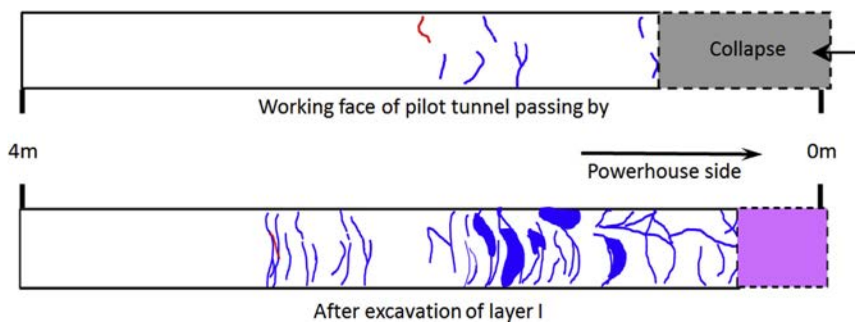

Fig. 21. Increasing depth of the EDZ in the spalling area during excavation of layer I and subsequent excavation. Blue line represents previously observed cracks, and red line represents newly identified cracks.

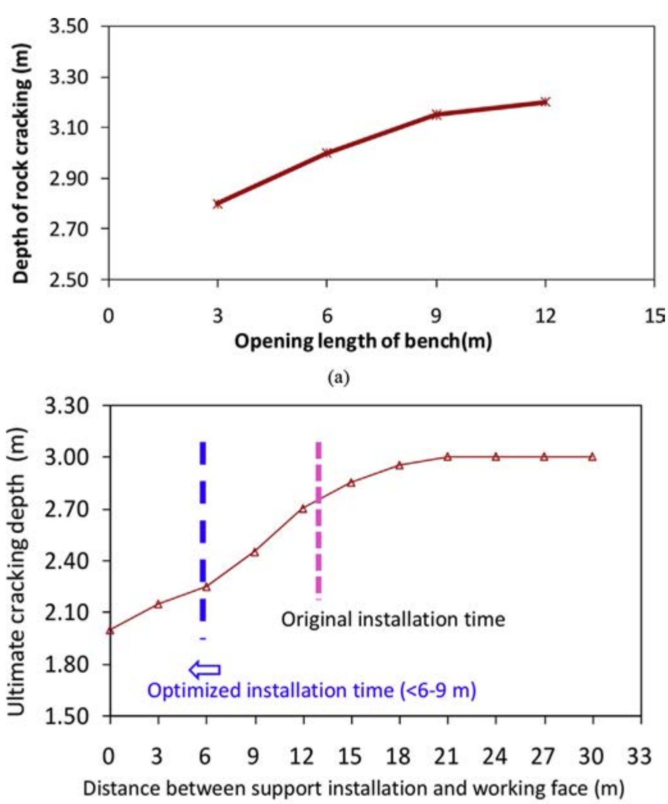

Fig. 22. Optimization of round length of excavation and support installation time. (a) EDZ depth with respect to different round lengths, and (b) EDZ depth with respect to different support installation time periods.

basalt (cryptocrystalline basalt, porphyritic basalt, amygdaloidal basalt) has the uniaxial compressive strength over 170 MPa, with typical brittle failure behavior (see Fig. 13); (3) six large-scale gently-dipping weak interlayer shear zones explored in the cavern group (Fig. 14); and (4) high risks of spalling, deep cracking and large deformation of interlayer shear zones.

4.3. Step 3: design approach strategy

By using the cracking-restraint method as discussed previously, the excavation and support scheme can be adjusted and optimized dynamically during the construction process, in order to minimize or avoid deeper transfer of the EDZ and fully utilize the self-bearing capacity of the surrounding rocks.

4.4. Step 4: modeling method

An elastoplastic model was employed for hard rock under true triaxial stress state based on true triaxial test results. In this model, we used a true triaxial failure criterion for hard rock and a non-associated flow rule. In this criterion, failure mechanism, effect of the intermediate principal stress, and difference between tensile and compressive strengths can be incorporated. As per the different post-peak curves, we defined different parameter evolution laws to characterize the post-peak behaviors of hard rock. Also, the anisotropy properties were taken into account by modifying the stiffness matrix of rocks after yielding. This model can reflect the elasto-plastic-brittle behavior of basalt. Based on the true triaxial failure criterion, an index named rock mass fractured degree (RFD) is proposed to reflect the failure degree of hard rock masses. At the pre-peak stage, RFD is defined by stress components; and at the post-peak stage, it is defined by the combination of two plastic strain components. $RFD = 1$ means that the current stress state lies at the peak strength, while $RFD = 2$ means that the current stress state enters the residual strength stage.

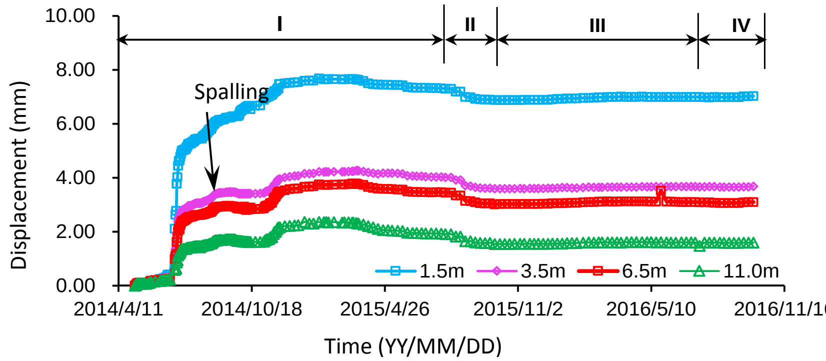

(a)

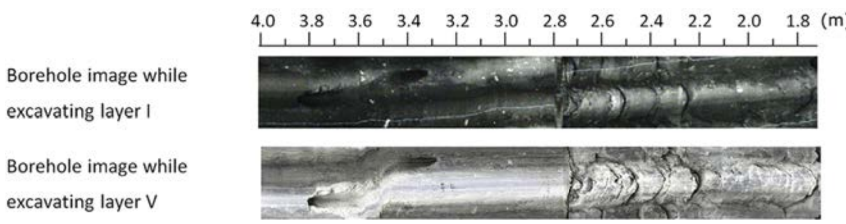

(b)

Fig. 23. Verifications of the proposed excavation and support measures. (a) Monitoring results of a multipoint extensometer, and (b) borehole images with respect to different layers (dimensions in m). Different lengths in (a) represent the depths of different measuring points, and the Roman numerals represent different excavation stages during the sequential excavation of the powerhouse.

4.5. Step 5: initial design

By back analyzing the in situ stress field of the Baihetan underground cavern group based on the measured results, the magnitudes and directions of the three principal stresses in the studied region are obtained and are listed in Table 4. The results show that the direction of the maximum principal stress is NNE and near horizontal. The axes of the main caverns therefore should form a small angle with this direction while choosing the appropriate position and direction of the main caverns. The final axis direction of the main powerhouse on the right bank changed from N20°W/N40°W (feasibility study) to N10°W.

4.6. Step 6: integrated modeling and feedback information

4.6.1. Numerical prediction of the stability of the right bank cavern group

By 3D modeling of the excavation process, the deformation and stress distributions as well as the failure degree of the surrounding rocks are obtained. According to the simulation results, a further increase in the roof deformation is anticipated in subsequent excavations. Increments of deformation of the concrete crane girder and sidewalls are evident. Areas affected by a weak interlayer shear zone on the sidewalls exhibit larger deformation. Stress concentrations are distinct in the upstream roof of the powerhouse and transformer chamber, with the maximum value reaching up to 50 MPa (Fig. 15). This indicates that stress-induced failure (e.g. spalling and slabbing) may occur in these locations. Stress unloading is more severe on the sidewalls of the powerhouse and transformer chamber, the entrances of the busbar tunnels, and the area affected by a weak interlayer shear zone. The average EDZ depth in the surrounding rock is 3–4 m after excavation. A deeper EDZ is observed in the upstream roof, the concrete crane girder, and the areas where a weak interlayer shear zone intersects the excavation directions. The maximum EDZ depth can reach up to 5–6 m. In other words, the weak interlayer shear zones have significant impact on the stability of the powerhouse.

4.6.2. Monitoring

P-wave test method is used to determine the EDZ depth and rock mass classification, and borehole camera is employed to observe the induced fracturing inside the rock mass, and microseismic monitoring is adopted to capture the micro-fracturing inside the rock mass. The monitoring scheme was proposed based on the predicted results as mentioned above. More than 30 observational boreholes were drilled on the sidewalls and in the anchorage tunnels above the powerhouse (see Fig. 16), and boreholes for microseismicity sensor installation were drilled in a drainage gallery (Fig. 17).

4.6.3. Back analysis

A mechanical parameter inversion method was proposed based on multivariate information fusion (Feng et al., 2000). In this method, the monitored displacements and EDZ depths (input) are used to back-analyze the mechanical parameters of the rock mass (output). Software incorporating a genetic algorithm (GA) and an artificial neural network (ANN) is adopted to establish the neural network model between the inputs and outputs. This method has a wider adaptability and is superior to other alternatives.

Back analysis of the in situ stress field and failure prediction shows that the upstream roof is a stress-elevating area characterized by higher risk of stress-driven failures. During excavation of the powerhouse, severe spalling occurred in the upstream roof (Fig. 18), suggesting that the predicted results of situ stress field obtained by back analysis are reasonable. Microseismicity monitoring results also show that micro-cracking scenario appeared more frequently in the upstream roof (Fig. 18). Additional evidence from borehole breakout analysis using vertical boreholes on the roof of the powerhouse clearly exhibited the breakouts. This shows that the direction of the local maximum horizontal stress deduced from the direction of breakouts is consistent with the back analysis results. Furthermore, instability and rock mass failure occurred in different parts of the powerhouse, which matched with our predictions (Fig. 19).

4.7. Step 7: final design and verification

The final design and verification are exemplified in terms of the spalling scenario and the corresponding treatments at section 0 + 330 of the left bank powerhouse. During excavation of layer I, serious spalling occurred in the upstream roof of the left bank powerhouse, exhibiting typical progressive and intermittent cracking of the surface rock (Fig. 20), under the condition of regular support design. Continuous observations of a borehole in the roof recorded the transfer process of the whole EDZ regime where spalling occurred (Fig. 21). Using the cracking-restraint method, the EDZ depths for different round lengths of excavation and for different support installation time periods were computed (Fig. 22). Based on this analysis, it suggests that the excavation length can be reduced from 5 to 6 m per round to 3 m per round, and that the support installation time can be reduced from the distance of 13 m to 6–9 m behind the working face. Herein we evaluate the appropriate support installation time by different distances behind working face just for the sake of convenience in tunneling. Subsequent monitoring results (Fig. 23) confirmed the effectiveness of the proposed excavation scheme and support measures.

5. Conclusions

Rock mechanics problems are the key to the successful engineering practice of recent hydroelectric projects in China, which are characterized by large scales, complex geological conditions, and high stresses.

(1) Some new devices and methods have been developed to measure in situ stresses at great depth and the properties of hard rocks and rock masses under high in situ stresses.
(2) Test tunnels and underground laboratories have been established to understand the behaviors of rock masses around large-scale excavations under high stresses. The unloading behaviors of rocks and rock masses have been considered.
(3) New models and numerical methods have been developed to predict the behaviors of rock masses in various large-scale hydroelectric projects, for which the continuous-discontinuous numerical methods have been used. The Hoek-Brown criterion, rock mass classification, and intelligent back analysis have become the main methods used to estimate the mechanical parameters of rock masses.
(4) In situ monitoring of displacement, digital boreholes, wave velocity, and microseismicity in rock masses has been conducted in high slopes, large underground caverns, and deep tunnels. The monitoring information is also helpful in understanding the failure mechanisms of rock masses. Back analysis of mechanical parameters and dynamic design of the excavation and support schemes also contribute to our understanding the failure mechanisms of rock masses.
(5) The intelligent and dynamic design method and the cracking-restraint method have been developed for the optimal design of large cavern groups, deep tunnels and high slopes. The deep cracking of rock masses is a key issue in terms of prediction and control. The cracking-restraint method has been successfully applied to recent hydroelectric projects under high in situ stresses in China including the underground powerhouse and headrace tunnels at the Jinping II hydroelectric project, and the left bank and right bank underground powerhouses at the Baihetan hydroelectric project where columnar joints, interlayer weak zones, and high in situ stresses are reported.
(6) Techniques for monitoring, early warning and dynamic control of rockbursts by TBM and drill-and-blast methods have been developed and successfully applied to the headrace tunnels and the drainage tunnel at the Jinping II hydroelectric project, the Jinping Underground Laboratories, the Bayu tunnels in the Lhasa-Nyingchi railway, and the headrace tunnels at the Neelum-Jhelum hydroelectric project in Pakistan.

Conflict of interest

The authors wish to confirm that there are no known conflicts of interest associated with this publication and there has been no significant financial support for this work that could have influenced its outcome.

Acknowledgement

The authors gratefully acknowledge financial support from the National Natural Science Foundation of China (Grant No. 51621006). The authors thank Prof. Shaojun Li, Dr. Guofeng Liu, Dr. Shuqian Duan, Mr. Shufeng Pei, and Mr. Jinshuai Zhao for their help in the in situ testing and numerical simulation for the Baihetan hydroelectric project, and we also thank Prof. Yilin Fan, Prof. Dachuan Ren, Prof. Jianrong Xu for their help in providing related monitoring data and geological information.

References

Brady BHG, Brown ET. Rock mechanics for underground mining. Kluwer Academic Publisher; 2004.
Brown ET. Recent advances in the application of rock mechanics to mining excavation design. Non-Ferrous Metals 1980;32(2):18–24. 28-30.
Brown ET. Book review: rock engineering design by Xia-Ting Feng and John A. Hudson. CRC Press/Balkema, Taylor & Francis Group (2011). 488 pages. ISBN: 978-0-415-60356-0 (Hbk), 978-0-203-09337-5 (eBook). Journal of Rock Mechanics and Geotechnical Engineering 2012a;4(1):III–IV.
Brown ET. Risk assessment and management in underground rock engineering – an overview. Journal of Rock Mechanics and Geotechnical Engineering 2012b;4(3):193–204.
Brown ET. Rock engineering design of post-tensioned anchors for dams – a review. Journal of Rock Mechanics and Geotechnical Engineering 2015a;7(1):1–13.
Brown ET. Book review: rock engineering risk by John A. Hudson and Xia-Ting Feng. CRC Press/Balkema, Taylor & Francis Group; 2015b. 572 pages. ISBN: 978-1-138-02701-5 (Hbk), 978-1-315-73857-4 (eBook PDF). Journal of Rock Mechanics and Geotechnical Engineering 2015b; 7(4):479-80.
Brown ET. Reducing risks in the investigation design and construction of large concrete dams. Journal of Rock Mechanics and Geotechnical Engineering 2017;9(2):197–209.
Brown ET. Book review: back Analysis in rock engineering by Shunsuke Sakurai. ISRM book series, Vol. 4. CRC Press/Balkema (2017); 2018. ISBN: 9781138028623 (Hbk), 9781315375168 (ebook). Journal of Rock Mechanics and Geotechnical Engineering 10(3):611-612.
Chen ZY, Wang XG, Haberfield C, Yin JH, Wang YJ. A three-dimensional slope stability analysis method using the upper bound theorem: Part I: theory and methods. International Journal of Rock Mechanics and Mining Sciences 2001a;38(3):369–78.
Chen ZY, Wang J, Wang YJ, Yin JH, Haberfield C. A three-dimensional slope stability analysis method using the upper bound theorem Part II: numerical approaches, applications and extensions. International Journal of Rock Mechanics and Mining Sciences 2001b;38(3):379–97.
Contreras LF, Brown ET. Slope reliability and back analysis of failure with geotechnical parameters estimated using Bayesian inference. Journal of Rock Mechanics and Geotechnical Engineering 2019;11(3):628–43.
Contreras LF, Brown ET, Ruest M. Bayesian data analysis to quantify the uncertainty of intact rock strength. Journal of Rock Mechanics and Geotechnical Engineering 2018;10(1):11–31.
Dong XS, Wu AQ, Guo XL. Rock mechanics study for three gorges project over 50 years. Chinese Journal of Rock Mechanics and Engineering 2008;27(10):1945–57 (in Chinese).

Duan SQ, Feng XT, Jiang Q, Liu GF, Pei SF, Fan YL. In situ observation of failure mechanisms controlled by rock masses with weak interlayer zones in large underground cavern excavations under high geostress. Rock Mechanics and Rock Engineering 2017;50(9):2465–93.

Feng XT. Rockburst: mechanisms, monitoring, waning and mitigation. Elsevier; 2017.

Feng XT, Hudson JA. The ways ahead for rock engineering design methodologies. International Journal of Rock Mechanics and Mining Sciences 2004;41(2):255–73.

Feng XT, Hudson JA. Rock engineering design. Leiden: CRC Press; 2011.

Feng XT, Zhang ZQ, Sheng Q. Estimating mechanical rock mass parameters relating to the Three Gorges Project permanent shiplock using an intelligent displacement back analysis method. International Journal of Rock Mechanics and Mining Sciences 2000;37(7):1039–54.

Feng XT, Chen BR, Yang CX, Zhou H, Ding XL. Identification of visco-elastic models for rocks using genetic programming coupled with the modified particle swarm optimization algorithm. International Journal of Rock Mechanics and Mining Sciences 2006a;43(5):789–801.

Feng XT, Pan PZ, Zhou H. Simulation of the rock microfracturing process under uniaxial compression using an elasto-plastic cellular automaton. International Journal of Rock Mechanics and Mining Sciences 2006b;43(7):1091–108.

Feng XT, Jiang Q, Xiang TB, Zhang CS, Wu SY. Intelligent and dynamic design method of large cavern group and its practice. Chinese Journal of Rock Mechanics and Engineering 2011;30(3):433–48 (in Chinese).

Feng XT, Chen BR, Li SJ, Zhang CQ, Xiao YX, Feng GL, Zhou H, Qiu SL, Zhao ZN, Yu Y, Chen DF, Ming HJ. Studies on the evolution process of rockbursts in deep tunnels. Journal of Rock Mechanics and Geotechnical Engineering 2012;4(4): 289–95.

Feng GL, Feng XT, Chen BR, Xiao YX, Yu Y. A microseismic method for dynamic warning of rockburst development processes in tunnels. Rock Mechanics and Rock Engineering 2015;48(5):2061–76.

Feng XT, Zhang CQ, Qiu SL, Zhou H, Jiang Q, Li SJ. Dynamic design method for deep hard rock tunnels and its application. Journal of Rock Mechanics and Geotechnical Engineering 2016a;8(4):443–61.

Feng XT, Zhang XW, Kong R, Wang G. A novel Mogi type true triaxial testing apparatus and its use to obtain complete stress-strain curves of hard rocks. Rock Mechanics and Rock Engineering 2016b;49(5):1649–62.

Feng XT, Hao XJ, Jiang Q, Li SJ, Hudson JA. Rock cracking indices for improved tunnel support design: a case study for columnar jointed rock masses. Rock Mechanics and Rock Engineering 2016c;49(6):2115–30.

Feng XT, Wu SY, Li SJ, Qiu SL, Xiao YX, Feng GL, Shen MB, Zeng XH. Comprehensive field monitoring of deep tunnels at Jinping underground laboratory (CJPL-II) in China. Chinese Journal of Rock Mechanics and Engineering 2016d;35(4):649–57 (in Chinese).

Feng XT, Pei SF, Jiang Q, Zhou YY, Li SJ, Yao ZB. Deep fracturing of the hard rock surrounding a large underground cavern subjected to high geostress: in situ observation and mechanism analysis. Rock Mechanics and Rock Engineering 2017;50(8):2155–75.

Feng XT, Zhao J, Zhang XW, Kong R. A novel true triaxial apparatus for studying the time-dependent behaviour of hard rocks under high stress. Rock Mechanics and Rock Engineering 2018;51(9):2653–67.

Ge XR, Hou MX. A new 3D in-situ rock stress measuring method: borehole wall stress relief method (BWSRM) and development of geostress measuring instrument based on BWSRM and its primary applications to engineering. Chinese Journal of Rock Mechanics and Engineering 2011;30(11):2161–80 (in Chinese).

Hatzor YH, Feng XT, Li SJ, Yagoda-Biran G, Jiang Q, Hu LX. Tunnel reinforcement in columnar jointed basalts: the role of rock mass anisotropy. Tunnelling and Underground Space Technology 2015;46:1–11.

Hatzor YH, He BG, Feng XT. Scaling rockburst hazard using the DDA and GSI methods. Tunnelling and Underground Space Technology 2017;70:343–62.

Hoek E, Brown ET. Underground excavations in rock. London, UK: The Institution of Mining and Metallurgy; 1980.

Hoek E, Brown ET. Practical estimates of rock mass strength. International Journal of Rock Mechanics and Mining Sciences 1997;34(8):1165–86.

Hoek E, Brown ET. The Hoek-Brown failure criterion and GSI – 2018 edition. Journal of Rock Mechanics and Geotechnical Engineering 2019;11(3):445–63.

Huang RQ. Geodynamical process and stability control of high rock slope development. Chinese Journal of Rock Mechanics and Engineering 2008;27(8):1525–44 (in Chinese).

Huang RQ, Dong XJ. Application of three-dimensional laser scanning and surveying in geological investigation of high rock slope. Journal of China University of Geosciences 2008;19(2):184–90.

Huang RQ, Huang D. Experimental research on affection laws of unloading rates on mechanical properties of Jinping marble under high geostress. Chinese Journal of Rock Mechanics and Engineering 2010;29(1):21–33 (in Chinese).

Huang SL, Feng XT, Zhang CQ. A new generalized polyaxial strain energy strength criterion of brittle rock and polyaxial test validation. Chinese Journal of Rock Mechanics and Engineering 2008;27(7):124–34 (in Chinese).

Huang RQ, Huang D, Duan SH, Wu Q. Geomechanics mechanism and characteristics of surrounding rock mass deformation failure in construction phase for underground powerhouse of Jinping I hydropower station. Chinese Journal of Rock Mechanics and Engineering 2011;30(1):23–35 (in Chinese).

Huang SL, Ding XL, Wu AQ, Lu B, Zhang YH. Study of multi-joint constitutive model of layered rockmass and experimental verification. Chinese Journal of Rock Mechanics and Engineering 2012;31(8):1627–35 (in Chinese).

Huang RQ, Huang J, Ju NP, Li YR. Automated tunnel rock classification using rock engineering systems. Engineering Geology 2013a;156(2):20–7.

Huang RQ, Li G, Ju NP. Shaking table test on strong earthquake response of stratified rock slopes. Chinese Journal of Rock Mechanics and Engineering 2013b;32(5): 865–75 (in Chinese).

Hudson JA, Feng XT. Rock engineering risk. CRC Press; 2015.

Jiang Q, Feng XT, Su GS, Chen GQ. Intelligent back analysis of rockmass parameters for large underground caverns under high earth stresses based on EDZ and increased displacement. Chinese Journal of Rock Mechanics and Engineering 2007;26(Supp.1):2654–62 (in Chinese).

Jiang Q, Feng XT, Chen JL, Zhang CS, Huang SL. Nonlinear inversion of 3D initial geostress field in Jinping II Hydropower Station region. Rock and Soil Mechanics 2008a;29(11):3003–10 (in Chinese).

Jiang Q, Feng XT, Chen GQ. Study on constitutive model of hard rock considering surrounding rock deterioration under high geostresses. Chinese Journal of Rock Mechanics and Engineering 2008b;27(1):144–52 (in Chinese).

Jiang Q, Hou J, Feng XT, Zhang CS, Chen JL, Xiang TB. Dynamic feedback analysis and engineering control of surrounding rock local instability in underground powerhouse of Jinping II hydropower station. Chinese Journal of Rock Mechanics and Engineering 2008c;27(9):1899–907 (in Chinese).

Jiang Q, Feng XT, Chen J, Huang K, Jiang YL. Estimating in-situ rock stress from spalling veins: a case study. Engineering Geology 2012;152(1):38–47.

Jiang Q, Fan Y, Feng X, Li Y. Unloading break of hard rock under high geo-stress condition: inner cracking observation for the basalt in the Baihetan's underground powerhouse. Chinese Journal of Rock Mechanics and Engineering 2017;36(5):1076–87 (in Chinese).

Li JL, Wang LH. Study on size effect of unloaded rock mass. Chinese Journal of Rock Mechanics and Engineering 2003;22(12):2032–6 (in Chinese).

Li ZK, Zhou Z, Tang XF, Liao CG, Hou DQ, Xing XL, Zhang ZZ, Liu ZG, Chen QH. Stability analysis and considerations of underground powerhouse caverns group of Jinping I hydropower station. Chinese Journal of Rock Mechanics and Engineering 2009;28(11):2167–75 (in Chinese).

Li DQ, Chen YF, Lu WB, Zhou CB. Stochastic response surface method for reliability analysis of rock slopes involving correlated non-normal variables. Computers and Geotechnics 2011;38(1):58–68.

Li SJ, Feng XT, Li ZH, Chen BR, Zhang CQ, Zhou H. In situ monitoring of rockburst nucleation and evolution in the deeply buried tunnels of Jinping II hydropower station. Engineering Geology 2012a;137:85–96.

Li SJ, Feng XT, Li ZH, Zhang CQ, Chen BR. Evolution of fractures in the excavation damaged zone of a deeply buried tunnel during TBM construction. International Journal of Rock Mechanics and Mining Sciences 2012b;55:125–38.

Li SJ, Feng XT, Hudson JA. ISRM Suggested Method for measuring rock mass displacement using a sliding micrometer. Rock Mechanics and Rock Engineering 2013a;46:645–53.

Li SJ, Feng XT, Wang CY, Hudson JA. ISRM Suggested Method for rock mass fractures observations using a borehole digital optical televiewer. Rock Mechanics and Rock Engineering 2013b;46:635–44.

Liu YF, Zhu JB, Liu YK. Research on hollow inclusion triaxial strain gauge for geostress measurement. Chinese Journal of Rock Mechanics and Engineering 2001;20(4):448–53 (in Chinese).

Liu GF, Feng XT, Jiang Q, Yao ZB, Li SJ. In situ observation of spalling process of intact rock mass at large cavern excavation. Engineering Geology 2017;226:52–69.

Lü QC, Liu YR, Yang Q. Stability analysis of earthquake-induced rock slope based on back analysis of shear strength parameters of rock mass. Engineering Geology 2017;228:39–49.

Meng YD, Xu WY, Liu ZB, Liu DW, Cai DW. Analysis of 3D visualization of safety monitoring for complicated high rock slope engineering. Chinese Journal of Rock Mechanics and Engineering 2010;29(12):2500–9 (in Chinese).

Qi SW, Wu FQ, Yan FZ, Lan HX. Mechanism of deep cracks in the left bank slope of Jinping first stage hydropower station. Engineering Geology 2004;73:129–44.

Qian QH, Lin P. Safety risk management of underground engineering in China: progress, challenges and strategies. Journal of Rock Mechanics and Geotechnical Engineering 2016;8(4):423–42.

Qian QH, Zhou XP, Yang HQ, Zhang YX, Li XH. Zonal disintegration of surrounding rock mass around the diversion tunnels in Jinping II Hydropower Station, Southwestern China. Theoretical and Applied Fracture Mechanics 2009;51(2): 129–38.

Song SW, Cai DW, Feng XM, Chen XP, Wang DK. Safety monitoring and stability analysis of left abutment slope of Jinping I hydropower station. Journal of Rock Mechanics and Geotechnical Engineering 2011;3(2):117–30.

Song SW, Feng XM, Rao HL, Zheng HH. Treatment design of geological defects in dam foundation of Jinping I hydropower station. Journal of Rock Mechanics and Geotechnical Engineering 2013;5(5):342–9.

Song SW, Feng XM, Liao CG, Cai DW, Liu ZX, Yang YH. Measures for controlling large deformations of underground caverns under high in-situ stress condition - a case study of Jinping I hydropower station. Journal of Rock Mechanics and Geotechnical Engineering 2016;8(5):605–18.

Tang CA, Wang JM, Zhang JJ. Preliminary engineering application of microseismic monitoring technique to rockburst prediction in tunneling of Jinping II project. Journal of Rock Mechanics and Geotechnical Engineering 2010;2(3):193–208.

Tang CA, Li LC, Xu NW, Ma K. Microseismic monitoring and numerical simulation on the stability of high-steep rock slopes in hydropower engineering. Journal of Rock Mechanics and Geotechnical Engineering 2015;7(5):493–508.
Wei JB, Deng JH, Wang DK, Cai DW, Hu JZ. Characterization of deformation and fracture for rock mass in underground powerhouse of Jinping I hydropower station. Chinese Journal of Rock Mechanics and Engineering 2010;29(6):1198–205 (in Chinese).
Wu AQ, Liu FZ. Advancement and application of the standard of engineering classification of rock masses. Chinese Journal of Rock Mechanics and Engineering 2012;31(8):1513–23 (in Chinese).
Wu SY, Wang G. Rock mechanical problems and optimization for the long and deep diversion tunnels at Jinping II hydropower station. Journal of Rock Mechanics and Geotechnical Engineering 2011;3(4):314–28.
Wu AQ, Zhou HM, Hu JM, Zhong ZW, Zhu JB, Chen HZ, Hao QZ. Development of a triaxial rheological testing machine with high pressure confinement in rock mechanics. Journal of Yangtze River Scientific Research Institute 2006;23(4): 28–31 (in Chinese).
Wu FQ, Liu JY, Liu T, Zhuang HZ, Yan CG. A method for assessment of excavation damaged zone (EDZ) of a rock mass and its application to a dam foundation case. Engineering Geology 2009;104:254–62.
Wu AQ, Yang QG, Ding XL, Zhou HM, Lu B. Key rock mechanical problems of underground powerhouse in Shuibuya hydropower station. Journal of Rock Mechanics and Geotechnical Engineering 2011;3(1):64–72.
Wu AQ, Wang JM, Zhou Z, Huang SL, Ding XL, Dong ZH, Zhang YT. Engineering rock mechanics practices in the underground powerhouse at Jinping I hydropower station. Journal of Rock Mechanics and Geotechnical Engineering 2016;8(5): 640–50.
Wu AQ, Han XY, Yin JM, Liu YK. A new hydraulic fracturing method for rock stress measurement based on double pressure tubes internally installed in the wireline core drilling pipes and its application. Chinese Journal of Rock Mechanics and Engineering 2018;37(5):1127–33 (in Chinese).
Xiao YX, Feng XT, Hudson JA, Chen BR, Feng GL, Liu JP. ISRM suggested method for in situ microseismic monitoring of the fracturing process in rock masses. Rock Mechanics and Rock Engineering 2016;49(1):343–69.
Xu DP, Feng XT, Cui YJ. A simple shear strength model for interlayer shear weakness zone. Engineering Geology 2012;147–148:114–23.
Xu NW, Li TB, Dai F, Li B, Zhu YG, Yang DS. Microseismic monitoring and stability evaluation for the large scale underground caverns at the Houziyan hydropower station in Southwest China. Engineering Geology 2015;188:48–67.
Zhang XB. Research and practice dealing with the roof collapse in Dagangshan hydropower station powerhouse. Sichuan Water Power 2010;29(6):55–9 (in Chinese).
Zhang CQ, Feng XT, Zhou H. Estimation of in situ stress along deep tunnels buried in complex geological conditions. International Journal of Rock Mechanics and Mining Sciences 2012;52(3):139–62.
Zhang CS, Liu N, Chu WJ. Key technologies and risk management of deep tunnel construction at Jinping II hydropower station. Journal of Rock Mechanics and Geotechnical Engineering 2016a;8(4):499–512.
Zhang L, Yang Q, Liu YR. Long-term stability analysis of the left bank abutment slope at Jinping I hydropower station. Journal of Rock Mechanics and Geotechnical Engineering 2016b;8(3):398–404.
Zhang L, Liu YR, Yang Q. Study on time-dependent behavior and stability assessment of deep-buried tunnels based on internal state variable theory. Tunnelling and Underground Space Technology 2016c;51:164–74.
Zhao XG, Cai M. A mobilized dilation angle model for rocks. International Journal of Rock Mechanics and Mining Sciences 2010;47(3):368–84.
Zhong S, Jiang Q, Feng XT, Liu JG, Li SJ, Qiu SL, Wu SY. A case of in-situ stress measurement in Chinese Jinping underground laboratory. Rock and Soil Mechanics 2018;39(1):356–66 (in Chinese).
Zhou CB. A prospect of researches on life-cycle safety control on high-steep rock slopes in hydropower engineering. Chinese Journal of Rock Mechanics and Engineering 2013;32(6):1081–93 (in Chinese).
Zhou CB, Chen YF, Jiang QH, Lu WB. A generalized multi-field coupling approach and its application to stability and deformation control of a high slope. Journal of Rock Mechanics and Geotechnical Engineering 2011;3(3):193–206.
Zhou YY, Feng XT, Xu DP, Fan QX. An enhanced equivalent continuum model for layered rock mass incorporating bedding structure and stress dependence. International Journal of Rock Mechanics and Mining Sciences 2017;97:75–98.
Zhu WS, Li Y, Li SC, Wang SG, Zhang QB. Quasi-three-dimensional physical model tests on a cavern complex under high in-situ stresses. International Journal of Rock Mechanics and Mining Sciences 2011;48(2):199–209.

Prof. Xia-Ting Feng received his PhD at Northeastern University of Technology (namely Northeastern University since 1992), China in 1992 and then took the position of lecturer, associate professor and professor at the same university. He joined Institute of Rock and Soil Mechanics, Chinese Academy of Sciences (CAS) in 1998 as a Professor of Hundred Talent Program of the CAS and as Deputy Director in Charge and Director in 2001–2005. He has worked as Director of State Key Laboratory of Geomechanics and Geotechnical Engineering since 2007. He works at Northeastern University, China as a Vice President since September 2017. He is President of Federation of International Geo-engineering Societies - FedIGS, President of ISRM Commission on Design Methodology, member of ISRM Commission on Testing Methods, and President of Chinese Society for Rock Mechanics and Engineering (CSRME). He was the past President of International Society for Rock Mechanics (ISRM) 2011–2015. He is also Editor-in-Chief of *Chinese Journal of Rock Mechanics and Engineering*, Associate Editor-in-Chief of *Chinese Journal of Theoretical and Applied Mechanics*, and Associate Editor-in-Chief of *Journal of Rock Mechanics and Geotechnical Engineering* (JRMGE). He is members of Editorial Board of *International Journal of Rock Mechanics and Mining Sciences* (2003-present), *Rock Mechanics and Rock Engineering* (2010-present), *Geomechanics and Tunneling* (2008-present). His research interests cover rock mechanics for deep rock engineering. He published more than 170 technical papers and the English book “Rock Engineering Design” and “Rock Engineering Risk” with Professor John Hudson. He has edited five volumes of the book “Rock Mechanics and Rock Engineering” (CRC Press) and the book Rockburst (Elsevier).